NASA CR 71491

SPACECRAFT DEPARTMENT

MISSILE AND SPACE DIVISION

N66-21083

(ACCESSION NUMBER)	(THRU)
469	1
(PAGES)	(CODE)
CR 71491	07
(NASA CR OR TMX OR AD NUMBER)	(CATEGORY)

FACILITY FORM 602

GPO PRICE $ _____

CFSTI PRICE(S) $ _____

Hard copy (HC) 7.69

Microfiche (MF) 2.25

ff 653 July 65

GENERAL ELECTRIC

NASA CR71491

JULY 30, 1965

DIN: 65SD4388

VOYAGER SPACECRAFT SYSTEM
PRELIMINARY DESIGN

ALTERNATE DESIGNS CONSIDERED

Telecommunications

VOLUME B (Book 2 of 3)

PERFORMED UNDER
CONTRACT NO. 951112 NAS-7-100

for

CALIFORNIA INSTITUTE OF TECHNOLOGY
JET PROPULSION LABORATORY
4800 OAK GROVE DRIVE
PASADENA, CALIFORNIA

GENERAL ELECTRIC
SPACECRAFT DEPARTMENT
A Department of the Missile and Space Division
Valley Forge Space Technology Center
P. O. Box 8555 • Philadelphia, Penna. 19101

TABLE OF CONTENTS

VOLUME B

(Book 2 of 3)

ALTERNATE DESIGNS CONSIDERED

Section		CII NO.
IV	ALTERNATE SUBSYSTEM MECHANIZATIONS CONSIDERED (TELECOMMUNICATIONS)	
	Telecommunications Subsystem	VB233AA101
	Radio Subsystem	VB233AA102
	Command Subsystem	VB233AA103
	Relay Radio Subsystem	VB233AA104
	Data Handling and Storage Subsystem	VB233AA105
	Data Encoder	VB233AA106
	Data Storage	VB233AA107

CII - VB233AA101

ALTERNATE SUBSYSTEM MECHANIZATIONS CONSIDERED

TELECOMMUNICATIONS SUBSYSTEM

Index

1 Scope
2 Applicable Documents
3 System Design
4 Command Function Trade-Offs
5 Telemetry Function Trade-Offs
6 Radio Function Trade-Offs
7 System Block Redundancy Trade-Offs
8 Telecommunications Equipment Trade-Offs
9 Bibliography

Appendix I. Mariner C Antenna Performance
Appendix II. Ranging
Appendix III. Signal Design
Appendix IV. Sample Reliability Calculation

1.0 SCOPE

This study covers trade-offs between the various subsystems comprising the telecommunications system, and between the telecommunications system and other spacecraft systems and the mission operation system. Insofar as practicable, equipment implementation and design trade-offs, which are confined within a particular subsystem, are treated separately in following subsystem trade-off studies.

This study contains sufficient detail to support the conclusions. In some cases, complicated analysis and supporting work are relegated to appendices, with results tabulated in this study. This study directly supports Voyager Functional Description VB233FD101.

2.0 APPLICABLE DOCUMENTS

The following documents are listed as being primary support documents for this study. Additional documents used for reference are listed at the end of the study in a bibliography.

2.1 JET PROPULSION LABORATORY DOCUMENTS

Engineering Planning Document 283	DSN, Planned Capability for the Period 1965-1980
MC-4-310	Functional Specification Mariner C Flight Equipment Telecommunication System
MC-4-320	Functional Specification Mariner C Flight Equipment Spacecraft Radio Subsystem
MC-4-321	Functional Specification Mariner C Flight Equipment Spacecraft Telemetry Subsystem
MC-4-322	Functional Specification Mariner C Flight Equipment Flight Command Subsystem
DOR-1002-FNC	Functional Specifications, DSIF, Ground Receiving Subsystem
DOT-1003-FNC	Functional Specification, DSIF, Ground Transmitting Subsystem

DON-1004-FNC	Functional Specification, DSIF, Ground Ranging Subsystem
DOI-1006-FNC	Functional Specification DSIF, Ground Instrumentation Subsystem
DON-1013-FNC	Functional Specification, DSIF, Ground Recording Subsystem

2.2 GENERAL ELECTRIC DOCUMENTS

VB220SR101	Design Characteristics
VB220SR102	Design Restraints
VB220FD107	DSN Interface
VB220FD109	Telemetry Criteria
VB220FD110	Telemetry Channel Assignment
VB220FD112	Flight Sequence
VB220FD113	Layout and Configuration
VB234FD101	Guidance and Control Subsystem
VB234FD102	Spacecraft Attitude Control Subsystem
VB236FD101	Spacecraft Power Subsystem
VB234FD107	Control and Sequence Subsystem
VB235FD102	Spacecraft Structure
VB235FD105	Determination of Weight, etc.
VB235FD112	Antenna Deployment and Gimbal
VB220FD101	Space Flight Trajectories

3.0 SYSTEM DESIGN

This section lists and explains the mission goals, ground rules, and design criteria which pertain to the design of the telecommunication system. Various telecommunications trade-offs are treated qualitatively and sequentially, according to mission phase. Following the narrative is a set of design constraints.

As a conceptual aid, a block diagram of the telecommunications system is given in Figure 3-1. This diagram is functional only and does not indicate redundance. Various interfaces are shown.

3.1 MISSION GOALS

The overall goals of Voyager '71 in terms of telecommunications are to successfully return engineering and scientific telemetry to Earth, to track and range the spacecraft, and to command the spacecraft, during a nominal six-month cruise, for a minimum period of one month in Mars orbit and as long thereafter as possible. In the event of conflicting technical requirements, the proper operation of the down-link telemetry has a priority second only to the requirement for maintaining planetary quarantine. The proper operation of the up-link command has a lesser priority.

3.2 GROUND RULES

a. The system design shall be simple and conservative, employing redundancy where possible. Functional redundancy and parallel redundancy shall be applied.

b. The system design shall be adaptable to the acceptance of subsequent mission requirements and subsequent improvements in technology, with minimum redesign.

c. Adequate system design margins shall be established.

d. Maximum advantage shall be taken of the knowledge and experience of system design, equipment design, and other techniques gained in the Ranger and Mariner programs.

e. The system design shall insure partial mission success in the event of system or component failure. Critical circuitry shall be independent of a single component failure.

f. The system design shall recognize the "long-life" requirements of the mission.

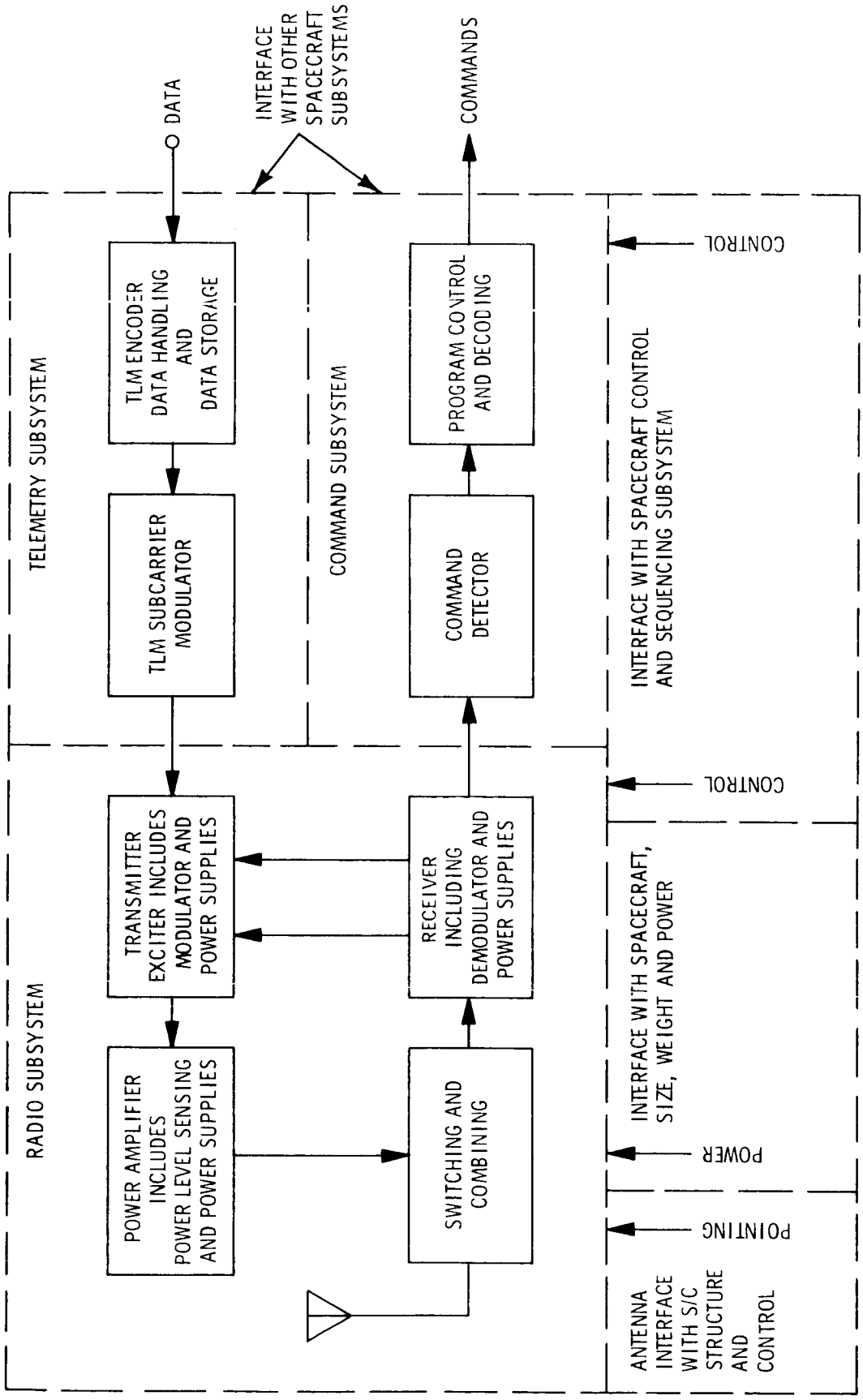

Figure 3-1. Telecommunications System Boundaries, Excluding Relay Radio Subsystem

g. The system design shall recognize the mission requirement for Earth-based control, and the requirement to minimize the number and complexity of Earth-based commands.

h. The system design shall recognize the need to advance the state of the art for Voyager '71. However, use of parts, materials, or processes which cannot demonstrate a history of reliability shall be, in general, prohibited.

3.3 DESIGN CRITERIA

a. To as great an extent as possible, the telecommunication system is designed to fulfill the mission goals using proven subsystem and element designs and techniques and presently existing DSN capabilities.

b. The system design criterion for block redundancy (multiple receivers, transmitters, etc.) is to maximize the ratio of incremental reliability to incremental weight, or incremental reliability to incremental power, when adding redundant subsystem elements. The maximization is carried to the limits of available system weight and power. The maximization is performed such that the minimum design reliabilities, as apportioned in Table 3-1, are met or exceeded.

c. The system design criterion for internal redundancy (multiple switches, etc.) is to insure that no single component failure causes failure of a system function, in light of existing block redundancy. Also, internal redundancy is used to equalize, as much as possible, the ratio of subsystem component (e.g. command detector) reliability to subsystem component weight or power.

d. The maximization of system reliability above the minimum reliability apportionment is tempered by the maximization of mission operation flexibility. This is in line with the requirement for adaptability of the system to subsequent missions and new technology.

e. To as great an extent as possible, the system is designed such that multiple component failures result in degraded system functions rather than failure of system functions.

3.4 SYSTEM TRADE-OFF NARRATIVE SUMMARY

3.4.1 GENERAL

This section sets down various trade-offs in a narrative fashion, according to mission phase.

3.4.2 MISSION PHASE DISCUSSION

3.4.2.1 LAUNCH PHASE

In order to provide telemetry during the launch phase, the telemetry data signal from the DH&S is sent to the launch vehicle telemeter through the in-flight disconnect. The telemetry signal is also transmitted directly to DSIF 71.

Because the launch vehicle systems provide the primary tracking and telemetry routes, the provision of direct spacecraft communications prior to separation does not warrant adding significant equipment. The antenna for the launch system is usable until separation, when the main spacecraft antennas to be used for the interplanetary cruise phase provide best coverage. While the launch vehicle shroud is in place, the launch antenna is coupled to the parasitic antenna on the shroud.

After shroud ejection, the launch antenna itself provides radiation in the direction of earth. The appropriate location is normally at the same clock angle as the shroud parasitic antenna, so that only a short cable run is required from the hat coupler on the shroud to the parasitic.

Either the primary or secondary low-gain antenna can be employed as the launch antenna. However, a switch is needed to utilize them as the power amplifiers are not energized during launch. Since there is no basic reliability degradation, a 3-db coupler is used in preference to a switch. The addition of a small, lightweight antenna is worth the improved reliability and performance. Also, a more optimum pattern coverage can be obtained during launch.

The transmitter to be used during launch may be a portion of the normal equipment required later in the mission. To provide margin for the coupling loss to the shroud parasitic, and launch vehicle exhaust attenuation, the Mariner C spacecraft employs a transmitter power of one watt. For Voyager, the capability of DSIF 71 is expected to be improved by the installation of a 10 to 30-foot antenna. Although the Voyager data rate is 3 times higher than for Mariner requiring a 5 db increase in transmitter power for the same performance, the improved capability of DSIF 71 can be at least 4db with the 10-foot dish and 14db with the 30-foot dish. Further improvement can be obtained by reducing the receiving system effective temperature to take advantage of the increased rejection of local r-f interference by the higher gain antennas.

The transmitter power is limited by the possibility of r-f and d-c breakdown as the spacecraft passes through the altitude range corresponding to critical pressure. The power amplifiers to be used in Voyager are most likely to be traveling wave tubes or electrostatically focused klystrons. On Mariner, the one-watt launch transmitter power is obtained by reducing the triode plate voltage to 100 volts, a level well below breakdown.

Of the probable Voyager tubes, the esfk affords the simplest means of switching power level. If twt's are used, the switching functions are more complex because both the helix and collector voltages must be changed.

The use of a solid state transmitter to provide about one watt is an attractive alternative possibility to switching tube power. The Mark I transponder provides 0.5 watt and may be used. With the potential improvement in DSIF 71 performance, a small portion of this power provides satisfactory performance. Therefore, the preferred approach couples 100 mw of the output of one of the main transponders to the launch antenna. The remaining power drives the main power amplifiers.

The use of a directional coupler prevents reception of command through the launch system, except through a very large attenuation, while the shroud is in place. Depending on the hat coupler configuration, it is possible that the leakage from the parasitic antenna to the other vehicle antennas and thence to the command receivers can be high enough to enable command in an emergency even if the shroud is not ejected. It is unlikely that commands to the spacecraft do much good in this situation anyway, so the lack of command capability is not regarded as a significant penalty. The advantage of having a separate isolated launch system is considered to outweigh this penalty.

3.4.2.2 INJECTION PHASE

From the time the launch shroud is removed, through injection, and until acquisition by the DSIF, there is no certainty that the spacecraft is visible from a ground station. Furthermore, there is no requirement for either two-way lock or command during this period. However, launch-phase telemetry is still available using the low-power exciter output and the launch low-gain antenna.

The trade-off in this phase is again between which antenna and power output to use. High power amplifiers may be used, since at injection altitude atmospheric pressure is below 10^{-4} mm Hg and outgassing is terminated by the time of injection. However, since the main antennas are not deployed until after injection and separation, and the link margin is adequate, launch telemetry is used during injection.

3.4.2.3 ACQUISITION PHASE

After injection of the vehicle into the transfer trajectory, the spacecraft initiates and completes a maneuver to "acquire" the sun, and high power is available for the telecommunications equipment. As the spacecraft climbs above the Earth's surface it becomes visible to a DSIF station (if not visible at the time of injection). Engineering telemetry, command, Doppler tracking, and/or ranging are required.

From a telecommunications standpoint this mission phase is very similar to later maneuver phases of the mission, since the spacecraft is maneuvering in its search for the Sun and Canopus. The telecommunication channels used during later maneuvers are appropriate at this time also. This implies that the cruise or maneuver bit rates for telemetry and command be used.

Due to the proximity of the Earth during this phase, normal cruise bit rates for command and telemetry are supportable using relatively low antenna gain and a power amplifier. As in the launch phase it is not desirable to implement special systems for the acquisition phase. Therefore, the normal mission low-gain antenna and the power amplifier normally used during maneuvers are employed to support the acquisition phase.

3.4.2.4 INTERPLANETARY TRAJECTORY CORRECTION PHASE

Shortly after acquisition and at selected times during the mission, the spacecraft performs maneuvers to modify its trajectory. These maneuvers imply a loss of Sun orientation with loss of orientation of the high-gain directional spacecraft antenna. The telecommunication requirement during this phase is to telemeter spacecraft attitude parameters and to accept commands.

During early maneuver phases, engineering telemetry, at the normal cruise bit rate, is supportable using a 20-watt amplifier and a low-gain antenna. A trade-off between antenna gain pattern, location of the antenna on the vehicle, and mission operational constraints indicates that by utilizing roll control of the vehicle about its thrust axis, reasonable antenna gain may be obtained between spacecraft and Earth for arbitrary orientation of the vehicle thrust axis.

During late maneuver phases, normal cruise rate telemetry is supportable using a 20-watt amplifier and the spacecraft high-gain directional antenna. A trade-off between antenna deployment, gimbaling, and mission operation, indicates the feasibility of using the directional antenna during maneuvers. As a back-up to use of the directional antenna during maneuvers, a minimal back-up telemetry rate is available for use with the 20-watt amplifier and low-gain antennas. The low-rate telemetry is also useful in case of loss of spacecraft attitude stabilization, for failure documentation purposes.

3.4.2.5 INTERPLANETARY CRUISE PHASE

During the transfer of the vehicle from the vicinity of Earth to the vicinity of Mars, the spacecraft is oriented to Sun and Canopus most of the time. During this phase the telecommunications requirements are for telemetry, command, two-way Doppler tracking, and ranging. The telemetry consists of Flight Spacecraft Engineering Data, Flight Capsule Engineering Data, and Scientific Data.

The major trade-offs concern selection of the "cruise-normal" bit rates for telemetry and command. These are trade-offs between mission operation requirements and spacecraft size, weight, power, and complexity. The availability of the spacecraft directional antenna and high-power amplifier, which are sized according to orbital operations requirements and spacecraft power and structure considerations, make possible very high cruise rates. However, the required data can be accommodated with a rate of about 100 bps.

The exact bit rates are also a trade-off against the allowable number of different bit rates, being a best compromise to support the entire mission with the allowable number of rates. The command rates are selected in a following study to be 1/2 and 15 information bits per second. The telemetry rates are selected to be 8533 1/3, 4266 2/3, 2133 1/3, and 533 1/3 bits per second, for the orbital phase, 106 2/3 bits per second for the cruise phase and 3 1/3 bits per second for a back-up capability.

In general, the cruise telecommunications are supported with a 20-watt amplifier and low-gain antenna until such time as decreasing circuit margins dictate employment of the high-gain antenna and/or higher power amplifier. A trade-off against mission operation indicates that the cruise channel power amplifier should be programmable by command from 20 to 50 watts. This satisfies the need for higher power without the use of radio frequency switching to employ the higher power amplifier. Control and switching of the spacecraft radio subsystem is treated in detail in a following study.

3.4.2.6 SPACECRAFT-CAPSULE SEPARATION PHASE

From a telecommunications standpoint, this phase appears to the flight spacecraft as cruise followed by a maneuver. Prior to the maneuver, telemetry and command are required. During the maneuver period, while the flight spacecraft is not Sun oriented, a requirement exists for telemetry and command. After separation, a requirement exists for telemetry relay from the flight capsule through the flight spacecraft.

The two portions of this phase will be accomplished as outlined in sections 3.4.2.4 and 3.4.2.5 with the addition of capsule relay telemetry. No special telecommunications implementations are required to support this phase.

3.4.2.7 FLIGHT CAPSULE TRAJECTORY DEFLECTION PHASE

During this phase the flight spacecraft is in cruise and/or maneuver configuration prior to orbit insertion. Relay telemetry is required. Telecommunications are as outlined in paragraphs 3.4.2.4, 3.4.2.5, and 3.4.2.6

3.4.2.8 FLIGHT SPACECRAFT ORBITAL INSERTION PHASE

During this phase the flight spacecraft is in a maneuver configuration. Telecommunication will be as outlined in paragraph 3.4.2.4.

3.4.2.9 FLIGHT CAPSULE ENTRY PHASE

The telecommunications impact on the flight spacecraft is essentially the same as in paragraph 3.4.2.7.

3.4.2.10 ORBITAL OPERATIONS PHASE

After orbit insertion, the flight spacecraft re-acquires the Sun and Canopus and embarks on the gathering and transmitting of scientific data. This phase is the

culmination of the mission, and the configuration of the spacecraft is essentially that of the cruise phase insofar as telecommunications is concerned, with the addition of high-rate scientific telemetry. The capabilities to re-program the data handling equipment by ground command at a command rate substantially greater than that for cruise phase, is provided.

The trade-offs for this phase are essentially between the scientific data rates, high-power amplifier size, directional antenna size, scientific data storage capacity, and total telecommunications reliability.

Trade-offs between scientific data rate and storage capacity yield a high bit rate of 8533 1/3 bits per second. Trade-offs between antenna size, power amplifier size, spacecraft structure, and spacecraft available power yield a power amplifier size of 50-watts and an antenna size of 7.5 feet (diameter of the parabolic reflector). Mission operation considerations (increasing range) yield two reduced scientific data rates of 4266 1/3 and 2133 1/3 bits per second. Failure consideration trade-offs show the desirability of implementing a further reduced scientific telemetry rate of 533 1/3 bits per second, compatible with a fixed medium-gain antenna of the Mariner C high-gain type, to be used as back-up for the directional antenna in the transmission of scientific data.

Trade-offs between mission operation requirements (probabilities of success) and spacecraft weight and power result in the level of redundancy and control configuration of the recommended telecommunications system.

3.5 CONSTRAINTS

The following is a list of constraints on the telecommunications system design.

3.5.1 MISSION OPERATION CONSTRAINTS

a. Telemetry verification of spacecraft attitude is required prior to thrusting.

b. Telemetry verification of correct receipt of certain critical commands is required.

c. Telemetry of spacecraft receiver agc voltage and static phase error is required.

d. Telemetry bit error rate (P_e) shall be less than 5×10^{-3}.

e. Nominal system operation time shall be six months in transit and six months in orbit.

f. The reliability apportionment per subsystem mission phase will be no less than that shown in Table 3-1.

Table 3-1. Reliability Apportionment-Per Subsystem-Per Mission Phase

Phase	I	II	III	IV	Mission
Time	2 hrs	178 days	2 days	30 days	210 days
Radio	0.99978	0.9816	0.99978	0.9969	0.9781
Command	0.99957	0.9653	0.99957	0.9942	0.9590
TLM	0.99978	0.9814	0.99978	0.9969	0.9779
Telecomm	0.99913	0.9298	0.99913	0.9911	0.9171

Assumed Mission Profile

Phase	Mission Event	Mission Time
1	Launch	T + 0
	Cruise Mode Acquisition	T + 2 hrs
2	Early Mid-Course*	T + 2-5 days
	Second Mid-Course*	T + 165 days
	Pre-Encounter Checkout	T + 176 days
	Lander Separation	T + 178 days
3	Third Mid-Course*	T + 179 days
	Orbit Injection*	T + 180 days
4	Mars Orbit	T + 180 to + 210 days, minimum

*Assumed 3-hour duration for maneuvering, confirmation, engine firing and reacquisition.

g. For purposes of system design, the nominal trajectory parameters for spacecraft - Earth station telecommunications as a function of mission time will be those shown in VB220FD101 (Trajectories).

h. Command bit error rate (P_e) shall be less than 10^{-5}.

i. The spacecraft shall be stabilized to Sun-Canopus during all but maneuver phases of the mission.

3.5.2 DEEP SPACE NETWORK CONSTRAINTS

The spacecraft telecommunication system design shall be compatible with the Deep Space Network as it presently exists and as it is planned to exist as described in JPL Document EPD-283. This broad constraint may be broken down into the following detailed constraints:

a. The spacecraft system design will be compatible with those DSN parameters tabulated in Section 5.1, Principal Parameters, VB233FD101, Functional Description, Voyager Telecommunication System.

b. The radio frequency signals to and from the spacecraft will be phase modulated.

c. The spacecraft transmitter will be capable of producing a signal with a stable residual carrier component, which is either phase coherent with the received residual carrier component or independent of the received carrier.

d. The command subsystem will be compatible with the DSN command verification equipment.

e. The command subsystem will use pseudo-random-code synchronization.

f. The radio subsystem will use a "turnaround" ranging channel.

4.0 COMMAND FUNCTION TRADE-OFFS

4.1 FUNCTIONAL BOUNDARY CONSIDERATIONS

This section gives a resume of the external factors governing command function trade-offs. These external factors, or boundaries, influence the design of the command subsystem. In some cases, these boundaries dictate a portion of the subsystem design. The boundaries, or interfaces, are broken down into particular areas given below.

4.1.1 MISSION OPERATION BOUNDARIES

4.1.1.1 COMMAND RELIABILITY

The design of the command subsystem will be such as to meet or exceed the reliability apportionments per mission phase. The reliability apportionments for the radio subsystem also reflect on the design of the command subsystem, since the transmission path for command is through the radio subsystem.

4.1.1.2 COMMAND FLEXIBILITY AND GROWTH POTENTIAL

The design of the command subsystem will be such as to insure flexibility in performing presently known mission operations. Also, the design will be such that the subsystem operation will be readily adaptable to advances in technology which may influence interfacing subsystems or mission operations.

4.1.2 DSIF BOUNDARIES

The design of the command subsystem shall be compatible with the nonmission-oriented portions of the DSIF.

4.1.3 RADIO SUBSYSTEM BOUNDARIES

The design of the command subsystem will insure compatibility between the command subsystem and the spacecraft radio equipment. In particular, the command signal structure, command detector capabilities, and characteristics of the radio receiver will be jointly compatible.

4.1.4 TELEMETRY SUBSYSTEM BOUNDARIES

The design of the command subsystem will insure compatibility between the command subsystem and the telemetry subsystem.

4.2 BIT RATE TRADE-OFFS

For the purposes of this section, the term "bit" rate is defined as the rate at which binary information is detected within the command detector.

The Mariner C one bit per second command detector requires +19.5 db SNR (normalized to 1 cps) with the power in the sync signal twice that in the data signal. The two-channel command detector can be improved to operate at +16 db SNR (1 cps). Use of an improved two-channel command detector, operating at one bit per second, satisfies mission requirements for command at maximum range, even with the low-gain antenna.

A high command rate is required to transmit long stored command programs. The number of consecutive quantitative commands is estimated to be 100. With the recommended Manchester coding, the transmission of 100 quantititive commands (assuming an

average 40 bits per word) takes approximately 2.2 hours at a one-half bit per second information rate. A high data rate is desirable to simplify operations, and, if it is an order of magnitude faster than the low rate, will reduce the transmission time for the assumed message to less than 15 minutes.

It is necessary to insure compatibility of the command signal structure with the spacecraft transponder receiver. Since the received command signal is taken from the carrier tracking loop error point, upper and lower bounds are set on the spectral envelope of the command signal. The upper bound is set by the carrier tracking loop predetection filter bandwidth, which should be narrow from a sensitivitiy standpoint. The lower bound is set by the carrier tracking loop noise bandwidth, which should be narrow, but increases adaptively with increasing SNR. A data rate of 15 command bits per second (30 sub-bits per second) was chosen. The PN bit rate is approximately the same as for the one-half bit per second system, and the PN sequence length is approximately 1/30 as long. The transmission time for 100 QC commands is thus approximately five minutes, using the 30 bit per second rate. The sync acquisition time is approximately five seconds compared to about five minutes for the one-half bit per second system.

4.3 SYNCHRONIZATION TECHNIQUE

4.3.1 GENERAL

There are two basic PN synchronization techniques: the two-channel system which requires sync and data to be transmitted separately, and the single channel system in which data and sync are embodied in a single channel. In the analysis which follows, the performance of the single channel system is compared with a two channel system which employs an adaptive phase lock loop.

The single-channel system has a potentially greater detection efficiency than the double-channel system; however, the overall advantage is small at both 1 bps and 30 bps. At 1 bps, the required RF carrier power predominates, and at 30 bps, the required data power predominates, so that the fraction of power allocated for the sync subcarrier in the double channel system is not significant in the overall system (order of 1 db). The single channel detector is more complex than the two channel detector which has been flight proven. For these reasons, the two channel system was chosen.

4.3.2 COMPARISON OF SINGLE CHANNEL AND DOUBLE CHANNEL WITH RESPECT TO REQUIRED NORMALIZED RECEIVED SIGNAL POWER

"The design of a PM link should begin with a specification as to the fraction of total power which must remain in the carrier channel to ensure the proper carrier threshold performance. Ideally, the carrier channel should perform as well, or slightly better than, the subcarrier system, or the power placed in the subcarriers will be wasted".*

---

*JPL Technical Report No. 32-215, "The Pioneer IV Lunar Probe, a Minimum-Power FM/PM System Design", Benn D. Martin, March 15, 1962.

For proper command operation an +8 db carrier SNR is required, computed in the transponder tracking loop two-sided noise bandwidth, 2 B_{Lo}.*

Table 4-1 shows the transponder loop threshold optimization points which were considered.

Table 4-1. Transponder Loop Optimization Points

Loop $2B_{Lo}$	Loop Threshold SNR	Required Carrier SNR for Proper Command Operation, Normalized to 1 cps
Case 1 20 cps	0 db	P_c/Φ = 20.5 db, (1 cps)
Case 2 20 cps	5 db	P_c/Φ = 18 db
Case 3 10 cps	0 db	P_c/Φ = 17.5 db
Case 4 10 cps	5 db	P_c/Φ = 15 db

The modulation loss due to a sine wave subcarrier and the carrier suppression loss is given by the following Bessel function equations.**

$$L_m = 2\ J_1^2\ (\Delta\varphi)\ ;\ \text{subcarrier} \tag{1}$$

$$L_c = J_o^2\ (\Delta\varphi)\ ;\ \text{carrier} \tag{2}$$

where $\Delta\varphi$ is the phase deviation in radians.

The above equations apply directly to the single-channel system which has a bi-phase modulated subcarrier for command. The double-channel Mariner C type command detector utilizes a square wave sync signal summed with a sine wave command signal. The modulation loss equations for this type of signal are given below; where the sync to command power ratio is equal to 1.

$$L_m = \text{Sin}^2\ (\Delta\varphi)\ J_o^2\ (\sqrt{2}\Delta\varphi);\ \text{square wave subcarrier} \tag{3}$$

$$L_m = 2\ \text{Cos}^2\ (\Delta\varphi)\ J_1^2\ (\sqrt{2}\Delta\varphi)\ ;\ \text{sine wave subcarrier} \tag{4}$$

---

*JPL Func. Spec., Mariner C Telecomm. System, MC-4-310A Table 5.1-6, 10 Dec. 1963.

**Appendix III, "Signal Design for Voyager," VB330TA001

The carrier suppression is:

$$L_c = J_o^2 (\sqrt{2}\Delta\varphi) \cos^2 (\Delta\varphi) \tag{5}$$

where $\Delta\varphi$ is the square wave modulation index in radians.

4.3.2.1 SINGLE CHANNEL

Under the assumption that the single channel 1 bit/sec system can be built as indicated in EPD 139* for a 13 db threshold condition, Table 4-2 shows the calculations made for a 1 bit/sec command system with $P_e = 1 \times 10^{-5}$.

Table 4-2. Optimum Phase Deviation (Single Channel)

	$\Delta\varphi$ rad	$J_o \Delta\varphi$	$J_1 \Delta\varphi$	$J_o^2 \Delta\varphi$	$J_1^2 \Delta\varphi$	$2J_1^2 \Delta\varphi$
Case 1	0.55	0.9258	0.2647	0.86	0.07	0.14
Case 2	0.75	0.8642	0.3492	0.747	0.122	0.244
Case 3	0.75	0.8642	0.3492	0.747	0.122	0.244
Case 4	0.95	0.7868	0.4234	0.619	0.1792	0.3585

The required normalized power at the transponder is then the sum of modulation loss and the required power for proper command operation. The four cases are shown in Table 4-3.

$$\frac{P_T}{\Phi} = \frac{P_c}{\Phi} - L_c \tag{6}$$

or

$$\frac{P_T}{\Phi} = \frac{P_{(sc)}}{\Phi} - L_m \tag{7}$$

* See Para. 2.1.1, JPL Documents

Table 4-3. Required Normalized Received Power at Transponder (Single Channel)

	$P_T/\Phi = P_c/\Phi - L_c$	$P_T/\Phi = P_{(sc)}/\Phi - L_m$
Case 1	21.1 db	20.5 db
Case 2	19.3 db	19.1 db
Case 3	18.8 db	18.6 db
Case 4	17.1 db	17.5 db

Theoretically, the two calculated required powers of Table 4-3 should be equal; however, the above data is within the required accuracy for comparison.

4.3.2.2 DOUBLE CHANNEL

The double-channel 1 bit/sec Mariner C detector has been built and tested for a 15 db threshold condition to give a probability of a bit error of 1×10^{-5} under laboratory conditions. The following calculations were made using the same ground rules for the transponder, and equal power in the sine and square wave modulating signals. Table 4-4 shows the calculations.

Using equations (3), (4), and (5) the modulation losses and carrier suppression were calculated and are presented in Table 4-5.

With equal power in the sync and command, the equations for total normalized received power at the transponder are as follows:

$$\frac{P_T}{\Phi} = \frac{P_{sq}}{\Phi} - L_m \text{ (sq)} = 12 \text{ db} - L_m\text{(sq)} \tag{8}$$

$$\frac{P_T}{\Phi} = \frac{P_{sine}}{\Phi} - L_m \text{ (sine)} = 12 \text{ db} - L_m\text{(sine)} \tag{9}$$

$$\frac{P_T}{\Phi} = \frac{P_{carr}}{\Phi} - L_c \tag{10}$$

A composite of the required normalized received power at the transponder for proper 1 BPS double channel operation is presented in Table 4-6.

Table 4-4. Optimum Phase Deviation
(Double Channel)

	$\Delta\varphi$	$\sqrt{2}\,\Delta\varphi$	$J_o\sqrt{2}\,\Delta\varphi$	$J_1\sqrt{2}\,\Delta\varphi$	$\cos^2\Delta\varphi$	$\sin^2\Delta\varphi$	$2J_1^2\sqrt{2}\,\Delta\varphi$	$J_o^2\sqrt{2}\,\Delta\varphi$
Case 1	0.35	0.495	0.94	0.24	0.883	0.11698	0.1151	0.885
Case 2	0.45	0.637	0.901	0.2926	0.8106	0.18943	0.1712	0.812
Case 3	0.47	0.665	0.8924	0.3145	0.7953	0.2047	0.198	0.796
Case 4	0.60	0.85	0.8274	0.3878	0.6808	0.3192	0.301	0.685

Table 4-5. Double-Channel Modulation Losses

	L_m (sine) = $2\cos^2\Delta\varphi J_1^2\sqrt{2}\Delta\varphi$	L_m (sq) = $\sin^2\Delta\varphi J_o^2\sqrt{2}\Delta\varphi$	L_c (car) = $\cos^2\Delta\varphi J_o^2\sqrt{2}\Delta\varphi$
Case 1	0.1018 = -9.9 db	0.102 = -9.1 db	0.781 = -1.1 db
Case 2	0.139 = -8.5 db	0.153 = -8.2 db	0.658 = -1.8 db
Case 3	0.1575 = -8.0 db	0.162 = -7.9 db	0.632 = -2.0 db
Case 4	0.2045 = -6.9 db	0.219 = -6.6 db	0.466 = -3.3 db

Table 4-6. Required Normalized Receiver Power at the Transponder for Proper Double Channel Operation

	$\frac{P_T}{\Phi} = \frac{P_{sq}}{\Phi} - L_{m(sq)}$	$\frac{P_T}{\Phi} = \frac{P_{sine}}{\Phi} - L_{m(sine)}$	$\frac{P_T}{\Phi} = \frac{P_{carr}}{\Phi} - L_c$
Case 1	12 + 9.9 = 21.9 db	12 + 9.9 = 21.9 db	20.5 + 1.1 = 21.6 db
Case 2	12 + 8.2 = 20.2 db	12 + 8.5 = 20.5 db	18 + 1.8 = 19.8 db
Case 3	12 + 7.9 = 19.9 db	12 + 8 = 20.0 db	17.5 + 2 = 19.5 db
Case 4	12 + 6.6 = 18.6 db	12 + 6.9 = 18.9 db	15 + 3.3 = 18.3 db

For comparison, the worst case required normalized received power at the transponder are considered for both the double-channel and single-channel command detectors. These are presented in Table 4-7.

Table 4-7 shows that the single-channel system possesses an advantage of approximately 1 db in required carrier power. However, the single-channel system is a more complex one whose flight performance is, as yet, unproven. In light of the above and the ground rules concerning the utilization of experience and proven designs, the single-channel system is not recommended at this time.

Table 4-7. Required Normalized Received Power for a 1 BPS Command System

Transponder	A = Double Channel	B = Single Channel	A-B
Case 1 20 cps, 0 db loop	21.9 db	21.1 db	0.8 db
Case 2 20 cps, 5 db loop	20.5 db	19.3 db	1.2 db
Case 3 10 cps, 0 db loop	20 db	18.8 db	1.2 db
Case 4 10 cps, 5 db loop	18.9 db	17.5 db	1.4 db

4.4 CODING

In order to evaluate the relative merits of coding the command transmissions, a review of the Mariner B and Mariner C command subsystems was conducted* and may be summarized as follows:

The utilization of the Manchester code in which an information bit is coded into two sub-bits, 01 = information bit "1" and 10 = information bit "0", provides a convenient method for implementing error rejection, unambiguous word synchronization, and variable length words without added weight or complexity. The problem of word sync without coding necessitates the transmission of a word sync pattern at least as long as the command word. The establishment of word sync at every command word transmission is desirable in order to insure that command data is not lost due to spurious detector out-of-lock indications, transponder and detector degradations, etc. Using Manchester coding also allows the out-of-lock threshold to be set well below that of the probability of a sub-bit error, and the system will operate successfully well below threshold as long as the sub-bit detector remains in lock.

*VB322TA001, Trade-Off Study, Voyager Flight Command Subsystem.

5.0 TELEMETRY FUNCTION TRADE-OFFS

In this section, the reasons for the selection of telemetry data rates and storage capacity are given. The choice of coherent vs non-coherent techniques for the transmission of 3 1/3 bps telemetry is discussed. Consideration given to the use of error control coding is also summarized.

5.1 ORBIT DATA RATE AND STORAGE CAPACITY

One of the principal performance goals of the telecommunications system design was the maximization of the capability to return scientific data throughout the mission. The principal parameters of the spacecraft system which affect the transmission capability are the antenna gain and transmitter power. One of the principal limitations on the amount of data that can be returned is the bulk data storage capacity.

The upper bound on the transmission capability is set by the selection of the 7 1/2 foot antenna and the 50 watt power amplifier. These values of the parameters provide a data rate capability (for the performance margin equal to the sum of the negative tolerances) of 8533 1/3 bps at 250 x 10^6 km, which is reached about three months after the latest 1971 encounter. By providing reduced bit rates of 4266 2/3 and 2133 1/3 bps, the data rate may be selected to maximize the information return out to the maximum range of 400 x 10^6 km.

The minimum bulk data storage capacity requirement is established by the high data rate primary planetary observation instruments. Sensors produce data rates as high as 100,000 bps, and the "hypothetical Spacecraft Science Payload" described in the Mission Guidelines is estimated to provide sensor output rates of 50,000 bits per second. The majority of the data from the high rate sensors will be obtained while the spacecraft passes over the sunlit portion of the planet near periapsis. This period is nominally two hours, during which the total data accumulation would be as high as 3.6 x 10^8 bits if the primary sensors produced 50,000 bits per second continuously during this period. This would correspond to 360 cycles of 10^6 bits each. Practically the total orbital period may be used for the transmission of stored data. The total transmission capability is 6 x 10^8 bits for the 19.3 hour orbit at the 8533 1/3 bps rate.

A tape recorder capacity of 2 x 10^8 bits was selected as the desired configuration. This size requires an extension of the capacity of recorders which have already been developed, including the Gemini recorder developed by RCA which has a capacity of 1.2 x 10^8 bits, and a JPL development* of a 10^8 bit transport. The provision of two 2 x 10^8 bit recorders would satisfy the expected maximum data collection requirement. However, in order to allow for a possible expansion of the capability of the planetary

---

*W. Storer, "A Family of Tape Recorder-Reproducer Mechanisms Employing a Novel Drive Technique", JPL Space Programs Summary No. 37-25, Vol. IV, p. 217-226, 29 February 1964.

observation instruments to match the link transmission capability, and to provide a back-up so that the full mission requirement could be met even in the event of a failure of one of the units, three recorders are provided in the system.

A data transmission rate of 533 1/3 bps is also provided to be compatible with the capability of the medium-gain antenna. This back-up system would enable a total data recovery of about 4×10^7 bits per orbit in the event that the high-gain antenna is not usable.

5.2 CRUISE DATA RATES

The cruise data rate requirement to accommodate capsule, engineering and interplanetary science data is considerably lower than the orbital rate. A rate of 106 2/3 bits per second is provided. This rate may be supported by the low-gain antennas to a range of approximately 25×10^6 km with the 85-foot antenna.

A low data rate capability is also provided. The high-gain antenna is normally used to transmit data during maneuvers to confirm that the vehicle has achieved the correct attitude for trajectory corrections, capsule separation and orbit insertion. Even though the high-gain antenna pointing capability has failed, a useful orbital scientific mission can be achieved through the medium-gain antenna, but alternate means must be provided to accomplish the high-gain antenna functions during maneuvers. The secondary low-gain antenna provides the correct coverage to accommodate all maneuver attitudes, but the system can only support a low data rate at long ranges. With a data rate of 3 1/3 bits per second, telemetry may be obtained to a range of about 150×10^6 km with the 50-watt transmitter and the 210-foot antenna. This is beyond the 1971 maximem encounter range of about 125×10^6 km.

5.3 LOW DATA RATE COMMUNICATIONS

The low data rate communication technique selected is the coherent PCM-PSK-PM single-channel technique operating at 3 1/3 bps and utilizing the presently available 12 cps carrier loop bandwidth of the DSIF receivers. It can provide data slightly beyond encounter range through the low-gain antennas. However, 50 watts of transmitted power is required and spacecraft orientation is restricted such that the earth is within the higher gain regions of the antennas.

To extend the transmission range and/or reduce the power requirements of the link using the selected modulation and detection technique, reduction of the carrier loop bandwidth and/or data rate is required.

Carrier loop bandwidth can be reduced only at the expense of increased acquisition time (proportional to inverse of bandwidth squared) and decreased automatic frequency tracking rate (proportional to bandwidth squared). In addition, oscillator phase jitter will tend to degrade detection efficiency as bandwidth is reduced. The extent of these penalties depend on the long and short term stability characteristics of the oscillators and the doppler

characteristics of the link. A preliminary analysis of these characteristics indicate that the 12 cps bandwidth is acceptable under most conditions and could perhaps be reduced; however, a complete investigation is required before the minimum acceptable bandwidth can be determined accurately.

Since the carrier contains 70 percent of the total transmitted power in the selected coherent system, reduction of data rate alone does not offer a significant overall power advantage.

Another approach which can potentially extend transmission range or reduce power requirements is the utilization of multi-level FSK. Goldstein* and Kendall's analysis of a noncoherent detection technique based on that used for the JPL Venus radar experiments indicates that transmission of the order of 1/2 bps from a range of 1 A.U. places minimal requirements on the spacecraft (1 watt transmitted through omni). Degradation of this capability resulting from oscillator instability and doppler is not indicated in the analysis.

Since adequate information is not available for reliable prediction of the performance of either a noncoherent system or a coherent system with reduced carrier loop bandwidth for a Voyager orbiter mission, neither could be recommended; however, further investigation of these techniques is recommended.

5.4 ERROR CONTROL CODING

The primary objective in considering error control coding for use in Voyager is the possible S/N improvement. This improvement can be translated into other parameters such as:

a. Data rate increase for a fixed transmitter power.

b. Reduced power for a fixed data rate.

c. Improved bit error rate for a fixed transmitter power and fixed data rate.

In certain marginal operational circumstances it is possible that the improved efficiency due to error control coding may provide the critical additional gain required to change an unsatisfactory operation into a satisfactory one.

The primary design constraints are : (1) the added complexity (and, hence size, weight, power and unreliability) of the error control encoder and synchronizer aboard the spacecraft, and (2) implications of the increased bandwidth.

From the standpoint of the DSN, any additional requirement for mission dependent equipment would be a design constraint, especially if such equipment had to be developed. Forward-acting error correcting coding places most of the equipment

*"Low Data Rate Telemetry", AAS Symposium on Unmanned Exploration of Space, Denver, Colorado, February, 1965.

burden and complexity at the receiving terminal which is the only alternative when considering deep space missions; nevertheless, cost and technical risk of developing a mission dependent error control decoder of adequate efficiency must be considered.

An intial selection narrowed the promising coding schemes to Bose-Chandhuri (15,7) and bi-transorthogonal (15,5).

The (15,7) code was selected because of its short word size which makes it compatible with the 24 bit word size of the SOS 900 series computer used for decommutation at the DSIF. In addition the seven information bits corresponds to the selected telemetry word length.

The (15,5) bi-transorthogonal code was selected as representative of the category of optimum correlation codes. Also the two sets of cyclic shifts of a pseudo-random maximal length sequence and its complement are readily decoded on a relatively simple hybrid correlator.

These codes were evaluated at the bit error rate (decoded) of 5×10^{-3}. At this bit error rate the maximum improvement possible with these codes is 1.7 db.

Since the 1.7 db is the theoretical maximum, and recognizing that losses occur in the demodulater and decoder, it was felt that the achievable S/N improvement did not justify the increased complexity required in the spacecraft. In addition to the complexity disadvantage the development of the spacecraft encoder represents a risk in the overall spacecraft development program. If the error control encoder development is dropped during the program, it will generate changes in the data encoder timing and synchronization as well as the ground demodulator and decommutator.

The cost of the encoder/decoder is also a factor in ruling out error control coding.

6.0 RADIO FUNCTION TRADE-OFFS

6.1 FUNCTIONAL BOUNDARY CONSIDERATIONS

This section sets down a resumé of the external factors governing radio function trade-offs. These external factors, or boundaries, influence the design of the radio subsystem. In some cases these boundaries dictate a portion of the subsystem design. The boundaries, or interfaces, are broken down into particular areas below.

6.1.1 MISSION OPERATION BOUNDARIES

6.1.1.1 RADIO RELIABILITY

The design of the radio subsystem will be such as to meet or exceed the reliability apportionments per mission phase of Table 3-1. It should be noted that the reliability apportionments for command and telemetry also reflect on the design of the radio subsystem, since the transmission paths for command and telemetry are through the radio subsystem.

6.1.1.2 RADIO FLEXIBILITY AND GROWTH POTENTIAL

The design of the radio subsystem will be such as to insure flexibility in performing presently known mission operations. Also the design will be such that the subsystem operation will be readily adaptable to advances in technology which may influence interfacing subsystems or mission operations.

6.1.1.3 TRAJECTORY DYNAMICS

The design of the radio subsystem will be compatible with the dynamics of the Voyager trajectory as given in VB220FD101.

6.1.2 DSIF BOUNDARIES

The radio subsystem shall be compatible with the DSIF.

6.1.3 COMMAND SUBSYSTEM BOUNDARIES

The design of the radio subsystem will insure joint compatibility between the spacecraft radio equipment and the command subsystem. In particular, the characteristics of the radio receiver will be compatible with both the command signal structure and the command detector capabilities.

6.1.4 TELEMETRY SUBSYSTEM BOUNDARIES

The design of the radio subsystem will ensure joint compatibility between the spacecraft radio equipment and the telemetry subsystem. In particular, the characteristics of the radio transmitter will be compatible with the telemetry signal structure.

6.1.5 SPACECRAFT SYSTEM BOUNDARIES

The design of the radio subsystem will be compatible with the upper limits on spacecraft size, weight, power, and environment, as listed in Paragraph 3.5.3.

6.2 RECEIVER TRADE-OFFS

6.2.1 GENERAL

The totality of the various design constraints, ground rules, etc., cited in Sections 3 and 6.1, imply a phase-tracking spacecraft receiver conceptually similar to these used in previous space missions (Mariner, Ranger, etc.). The ground rules concerning utilization of Mariner experience and maximization of data channel capacity within the bounds of reliability, weight, and power, strongly imply a Mariner-type receiver with, perhaps, increases in capability that are strongly justified in terms of current state-of-the-art feasibility. In other words, unproven design changes from the basic

Mariner receiver design are not contemplated unless completely justifiable as feasible from a reliability standpoint, and required from a mission operation standpoint. The trade-offs are derived in the above frame of reference.

Reliability claims for the Mark I S-Band Transponder are supported by life testing and actual performance in space environment on Mariner spacecraft. This reliability will be tested again on the Lunar Orbiter spacecraft which uses the same basic design. This record is unmatched by similar equipments.

Minor changes extend the capability of the Mark I unit so that command via the low-gain antennas is possible through the end of the mission. This performance is adequate but not unique; since other receiver designs can obtain the same performance.

Size does not appear to be the governing consideration for Voyager. Mechanical layouts of the radio subsystems shown in the Functional Descriptions reveal available room for expansion (using three transponders). Selection of a smaller, unproven design is unjustifiable.

Arguments concerning weight are essentially the same as for size. Lighter weight transponders can be designed, but there is no apparent requirement for further weight reduction. Selection of an unproven design on a weight basis is unjustifiable.

6.2.2 CARRIER LOOP TRADE-OFFS

At weak signals the Voyager transponder is adjusted for unity SNR for a received signal level of -153 dbm. This sensitivity, combined with an appropriate selection of carrier suppression versus command subcarrier power, allows the carrier and low rate command link to reach operational threshold simultaneously. This signal level also corresponds to operation at maximum distances using the low-gain spacecraft antenna. The following discussion points out the trade-off considerations concerning the carrier loop threshold bandwidth. The Mariner C bandwidth of 18 cps is chosen.

The following assumptions are made; (1) the transponder tracks at its "rest" frequency. That is, the ground transmitter is adjusted to a frequency such that no long term tracking stress is required at the transponder, (2) the average transponder acceleration tracking requirements are approximately 6 meter/second^2 deceleration at Mars encounter for a time duration of 365 seconds and (3) the maximum deceleration is about 10 meter/sec^2. The ground station is assumed to not make open loop corrections for this maneuver.

Using these assumptions, together with the calculated loop gain and bandwidths of the transponder at the Mars intercept carrier level, we find:

The received carrier power is:

$$P_c \cong -144 \text{ dbm} \quad (85 \text{ foot antenna, } 10 \text{ kw}) \tag{1}$$

The effective maximum loop gain is:

$$G_{max} = \frac{20V}{Rad} \times \frac{120 \text{ cps}}{Volt} \times 110.5 = 1.66 \times \frac{10^6}{sec} \tag{2}$$

At -144 dbm, the gain is:

$$G = G_{max} \times \alpha = \frac{1.66}{5.75} \times 10^6 = 2.9 \times \frac{10^5}{sec} \; ; \; \alpha \text{ is the loop suppression as plotted in Figure 5-8 of VB233FD102} \tag{3}$$

The one-sided noise bandwidth is given by:

$$B_L = B_{LO} \left(\frac{1}{3} + \frac{2\alpha}{3\alpha_o} \right)$$

and at -144 dbm, is:

$$B_L = 9 \left(\frac{1}{3} + \frac{2 \times \frac{1}{5.75}}{3 \times \frac{1}{16}} \right) = 19.7 \text{ cps}$$

The maximum rate of change of Doppler is 70 cps^2.

Then:

$$\sigma \sim \frac{101f}{B_L^{\,2}} = \frac{10^2 \times 70 \text{ cps}^2}{390} = 18 \text{ degrees.} \tag{4}$$

Where σ is the phase error required to track a frequency rate error.

$$f = \text{Doppler (at Mars Intercept)} = 40 \text{ cps}^2 \times 365 \text{ sec} = 14.4 \text{ kcps} \tag{5}$$

φ = phase error required to track Doppler offset:

$$\varphi = \frac{f}{G} = \frac{14.4 \times 10^{3} \text{ cycles/sec}}{2.9 \times 10^{5}/\text{sec}} = 5 \times 10^{-2} \text{ cycles} = 18 \text{ degrees} \qquad (6)$$

These calculations show that the planned loop has adequate tracking capability for deceleration at Mars intercept. If the 100 kw transmitter is employed, the phase errors are reduced to 2.4 degrees and 6.7 degrees respectively.

If the loop bandwidth is reduced the following disadvantages result.

a. Tracking errors are higher during acceleration thus increasing probability of losing lock.

b. Acquisition is more difficult.

c. Loop filter time constants become long and more difficult to implement.

d. More dynamic range is required in the i-f amplifiers to linearly handle the high N/S ratios encountered at receiver threshold.

e. The receiver gain margin is reduced. From this point of view, a low noise preamplifier offers a better solution.

f. It is unlikely that all of the calculated improvement can be realized. Some increase in phase error due to oscillator instability would undoubtedly occur.

If the loop bandwidth is increased, the rate error decreases but the lower frequency components of the command signal spectrum are likely to be "tracked out" by the carrier loop during high signal conditions. Thus, the loop threshold bandwidth is bracketed by two conflicting considerations; sensitivity for error tracking, and command modulation tracking. The Mariner C threshold bandwidth ($2B_{LO}$ = 18 cps) is a reasonable compromise, which when coupled with the ground rule concerning exploitation of Mariner experience, resolves the trade-off in favor of the loop threshold bandwidth of $2B_{LO}$ = 18 cps.

6.2.3 NOISE FIGURE VS RELIABILITY

Link calculations show that the telecommunications functions are supportable with a spacecraft receiver noise figure only slightly lower than than of Mariner C. Consistent with this, the receiver "front end" is of conventional design. Studies are being performed to attempt to obtain a high reliability, lower noise figure mixer diode. But, ultimately, only a high reliability device will be used. Differences from Mariner C are only in the order of 3 db.

A backup study needs to be performed on transistor preamplifiers. These devices are improving rapidly, since recent technology advances show the way to develop microwave transistor amplifiers. Within one year, an amplifier noise figure

of 5 db or less can be obtainable. Major emphasis in this backup program is development of reliability assurance. Although the over-all reliability of a transistor preamplifier followed by a conventional receiver may off-hand "calculate" to be less than that of a conventional mixer-receiver system, the exact arrangement needs to be analyzed carefully; for a pre-amplifier can reduce the critical nature of the local oscillator and first mixer operation, thereby improving the over-all reliability. These total system effects need to be studied.

A tunnel diode amplifier can be used, assuring a noise figure of 5 db. But, this is purchased at a cost of approximately 1 pound per amplifier and at a potential loss of reliability; a loss not due to calculated reliability of components but due to potential human error (errors of design that are found only after extensive system testing). Negative resistance amplifiers are more susceptible to this type of design failure. This is why the transistor amplifier investigation is recommended while the tunnel diode is not. A tunnel diode down-converter, a parametric amplifier, or other RF front ends can be considered, but are not recommended because of the reliability consideration. The present Mariner-C generic type rf circuitry is shown to work nominally for the Voyager mission. Additional complexity is not warranted.

6.2.4 PREDETECTION BANDWIDTH CONSIDERATIONS

A decrease of predetection bandwidth results in a smaller limiter suppression factor at the threshold bandwidth, but predetection bandwidth is also bounded by consideration of the command signal spectrum. That is, reduction of the predetection filter bandwidth is not tolerable because of rejection and distortion of the uplink command signals. Bandwidth increase is not desirable because it reduces the near threshold tracking gain suppression factor. The present Mariner C bandwidth is again taken as the best compromise.

6.3 EXCITER TRADE-OFFS

6.3.1 ALTERNATE CONFIGURATION

An alternate transmitter configuration considered is a locked S-band transistor oscillator. New semiconductor device technology now promises a silicon transistor oscillator capable of 0.5 watt output at 2.3 gc, with a collector efficiency of 20 per cent. This oscillator can be servo controlled to track a low power reference signal by means of a phase-lock loop employing a varactor control element across the transistor oscillator circuit. The additional circuitry required reduces the over-all system reliability and considerably complicates the operational requirements of the transmitter in order to assure lock-up of this loop. This approach does not appear attractive for this mission, but may be considered for future equipment.

6.3.2 TRANSPONDER SELF-LOCK CONSIDERATIONS

Appendix I of VB233FD101 describes the varactor multiplier conditions leading to nonharmonic spurious outputs. When any one of these spurious output signals lie within the passband of the ranging channel, a beat frequency is detected at the ranging channel demodulator. If the ranging channel is in use, the beat signal modulates all transmitter output spectral components, and can result in a coherent signal into the receiver. The receiver can lock to this signal, resulting in a coherent "self-lock".

Diplexer or preselector filter characteristics may be specified to eliminate the effect of certain spurious outputs, if they are constant, and known. But this is not good engineering practice, because the spurious frequency is subject to change as a function of temperature and time. An alternate, and more conservative, solution is to design following the guidelines of Appendix I - and verify the design margin by testing over wide temperature and voltage variation ranges. This later procedure needs to be followed in designing the Voyager exciter.

6.3.3 AUXILIARY OSCILLATOR STABILITY

Two types of oscillator noise are of concern; quiescent and vibration induced noises.

Quiescent auxiliary oscillator noise can be reduced by several methods. It is proposed to investigate potential improvements for application to the Voyager exciters. These potential improvements are: (1) Overtone crystals operating at a very high frequency, and (2) Low noise oscillator devices (new field effect devices offer potential circuit improvement).

Vibration susceptibility can be reduced by using small mass, high resonant frequency crystals, such as the Bell Laboratory crystals mounted on ribbon leads in a TO-5 transistor case. This component needs also be investigated.

6.4 RANGING CHANNEL TRADE-OFFS

6.4.1 GENERAL

Under the constraint that the spacecraft ranging mechanization be compatible with the Deep Space Instrumentation Facility, as it presently exists and as it is planned to exist, per EPD-283, there are two known methods for implementing the spacecraft. One method is called "Planetary Ranging". The other is called "Turnaround Ranging".

Briefly, the "Turnaround" scheme operates as follows. A pseudo-random (PR) code of known structure is generated at the ground tracking station and is transmitted to the spacecraft, using bi-phase modulation on a carrier which is phase coherent with the code. At the spacecraft the carrier is demodulated and the code recovered. The code plus channel noise is then remodulated on the downlink carrier. The downlink carrier is phase-coherently derived from the uplink carrier. At the ground the "turned-around"

range code is compared with the transmitted code by a process involving cross-correlation. A comparison in time delay, between the transmitted and received range codes, supplies ranging information concerning the spacecraft.

The "Planetary" scheme operates similarly to the "Turnaround" system except that the spacecraft contains a PR code generator. The code from this generator is synchronized with the code received from the ground and is then transmitted to the ground.

Prior to release of the JPL Mission Specification for Voyager, both the Planetary and Turnaround ranging schemes were examined theoretically.

Both schemes appear applicable to Voyager. The Planetary scheme appears more efficient from the standpoint of spacecraft transmitted power, since the downlink ranging signal is not contaminated by the uplink noise. However, additional spacecraft complexity is indicated, since a PR code generator and an acquisition device for the uplink code are required. Additional mission operation complexity is indicated since code acquisition by the spacecraft receiver is initiated at the ground.

After receipt of the Voyager Mission Specification which stipulates "Turnaround Ranging", no further examination was made of "Planetary Ranging".

6.4.2 TURNAROUND RANGING

Once "Turnaround Ranging" is specified, the trade-off problem evolves to the question of what specific type of spacecraft turnaround channel to implement. Two general types are used in space vehicles. These types differ mainly in the mechanization of turnaround signal limiting.

It is obvious that some kind of turnaround signal limiting is required to protect the downlink from over-modulation. In fact, the modulation indices for the downlink channels must be rigidly controlled to preserve the power apportionments in the data channels and residual carrier channel.

The Apollo spacecraft uses predetection limiting, that is, limiting at the intermediate frequency prior to range code detection in the spacecraft receiver *. Mariner spacecraft use post-detection limiting, that is limiting at the video frequencies, subsequent to range code detection in the spacecraft receiver**.

---

* "Unified S-band Telecommunications Techniques for Apollo, Vol. I" by John H. Painter and George Hondros. Technical Note D-2208, National Aeronautics and Space Administration, Washington, D.C., March, 1965.

** "Functional Specification, Mariner C Flight Equipment, Spacecraft Radio Subsystem", MC-4-320, Jet Propulsion Laboratory, 8 February 1963.

Empirically, from laboratory testing, either scheme seems to give equivalent results, so far as the ground ranging equipment is concerned.* Theoretically, there exists an approximate treatment of the predetection limiting scheme,** and an exact treatment of the post-detection limiting scheme.

The theoretical treatment of the predetection limiting scheme shows that the turned-around up-link noise affects not only the down-link ranging signal, but also the other downlink channels, notably the carrier.*** The theoretical treatment of the post-detection limiting scheme shows that the turned-around uplink noise affects only the downlink ranging signal and not the other channels.****

Based on the above observations and on Ground Rule of paragraph 3.2.4, concerning utilization of Mariner knowledge and experiences, post-detection limiting for the spacecraft ranging channel is selected.

6.5 ANTENNA TRADE-OFFS

A wide variety of antenna techniques is examined to establish the optimum approach for satisfying the antenna requirements of the Voyager telecommunications system. This section summarizes the advantages and disadvantages of the alternate approaches considered and documents the arguments leading to the recommended antenna approach.

Telecommunications requirements for the Voyager mission establish the need for two basic types of antenna performance. First, an antenna having substantial gain with associated narrow beamwidth is required for the transmission of large amounts of data at interplanetary distances. Second, pattern coverage approaching omni-directional is needed for early mission phases such as launch, injection, and acquisition, for communications to Earth during the various maneuver phases, and for emergency backup situations. To distinguish between these two different antenna requirements, the terminology of high-gain and low-gain is employed. In addition to the basic functional antenna requirements, an added requirement is placed for a fixed medium-gain antenna to provide a back-up capability to the steerable high-gain antenna.

6.5.1 HIGH-GAIN ANTENNA

The major trade-offs considered in determining the design approach for the high-gain antenna are discussed in the following paragraphs.

---

* Final Report, Apollo Unified S-band System Test, Phase I, Vol. I, Contract NAS 9-2563, Motorola Inc., Military Electronics Div., Western Center, Scottsdale, Arizona, 7 August 1964.

** "Unified S-band Telecommunications Techniques for Apollo - Vol. II", by John H. Painter and George Hondros. To be published in 1965 as a NASA Technical Note.

*** Op. Cit. Footnote 6.

**** Op. Cit. Footnote 7.

6.5.1.1 STOWAGE AND DEPLOYMENT

From a communications point of view, it is desirable to implement the largest antenna possible, consistent with the philosophy of simple and conservative design. Because of the physical constraints of the spacecraft and launch vehicle, antennas having dimensions greater than about nine feet must be collapsed in some manner for stowage within the shroud envelope. For this reason, various techniques for unfurling large, high-gain antennas are investigated. These include simple mechanical folding or re-arrangement of the antenna volume into more convenient shapes, mechanical erection where an assembly of rigid parts is stowed in a reduced volume, and inflation of thin skinned containers. An example of mechanical folding is the division of a parabolic reflector or array into two or more sections which could be hinged and folded for stowage. One mechanical erection technique developed for parabolic reflectors utilizes flexible metal ribs to support a reflector surface of gold-plated fiberglass fabric. The assembly is collapsed by wrapping the flexible ribs about a small central hub. Inflatable antenna structures commonly use aluminized mylar film which is formed to the desired shape. For deployment, the container is inflated by an external gas source or by a self-contained sublimating powder. Chemical rigidizing techniques are then employed to maintain the desired shape in the absence of internal pressure.

The use of any unfurling technique affects antenna reliability and performance in two ways. The first is simply due to the increased complexity of the antenna deployment mechanism. Secondly, the unfurling process makes it difficult to maintain the optimum antenna shape in the deployed configuration. For these reasons, it is decided that antenna unfurling should not be employed if adequate subsystem performance can be obtained with the largest rigid antennas that can be stowed. If the antenna must be collapsed for stowage, simple folding techniques are preferred over mechanical erection or inflation.

6.5.1.2 RF ANGLE TRACKING

Because of its narrow beamwidth, the high gain antenna must be pointed accurately in the direction of Earth. Consideration of spacecraft attitude control capabilities and sources of pointing errors indicates that antennas having half-power beamwidths greater than about 3 degrees (i.e., dimensions less than about 10 feet) can be pointed with sufficient accuracy by open-loop, programmed, or commanded control. However, larger antennas require more accurate alignment to avoid excessive losses in gain. A study of rf angle tracking techniques is undertaken to examine the trade-offs involved with their use in this application.

Three basic techniques are available for maintaining an antenna beam aligned in the direction of an rf source. These employ retrodirective antennas, sequential lobing, and simultaneous lobing. Retrodirective antennas use an active array of elements connected to appropriate circuitry such that the reradiated field from each element is in phase conjugation with the incident field. In this way, the energy reradiated from this array is focused back in the direction of the transmitting source. The number of active elements and receiver channels is at least as great as for a simultaneous lobing system, and the receiver complexity is considerably greater in a retrodirective system.

Sequential lobing employs either cyclic feed motion, as in conical or sector scan, or switching between discrete beams that are squinted with respect to each other. Only one IF receiver channel is required for sequential lobing, as compared with 2 or 3 channels for simultaneous lobing. However, this is offset by the additional switching circuitry or feed drive mechanisms required with sequential lobing. The boresight antenna gain of a sequential lobing system is reduced by the time average crossover level. This reduction can be on the order of 3 db and is not present in a simultaneous lobing system. It is decided that simultaneous lobing offers the most suitable approach for precision alignment of the high-gain antenna.

There are a number of disadvantages associated with the use of rf angle tracking techniques. Additional circuitry is needed, and subsystem power requirements and weight are increased. The antenna design is more complex and provision must be made for routing at least two additional rf lines across the antenna rotational axes, one for each of the orthogonal error signals. In accordance with the philosophy of simple, conservative design, it is concluded that rf angle tracking techniques should be used only if antenna dimensions greater than 10 feet are needed to obtain adequate radio subsystem performance.

6.5.1.3 SIZE OPTIMIZATION

Several studies were made to determine the optimum size for the Voyager high-gain antenna. Such a determination is very difficult to make because of the many different factors involved such as desired data rates, power amplifier capabilities, vehicle physical constraints, power consumption, and weight. In addition, because the high-gain antenna must be articulated and pointed accurately at Earth, true size optimization studies must include pointing error analyses for various antenna control methods. Most past investigations are based mainly on weight minimization within the telecommunications subsystem, and these establish optimum sizes for the high-gain antenna between 7 and 12 feet.

Studies of antenna unfurling and rf angle tracking, which are summarized above, involve the capabilities of other spacecraft subsystems. Both recommend antenna sizes under 10 feet based mainly on reliability considerations. Radio link calculations indicate that reasonable data rates can be maintained with antenna dimensions of 7 feet or more. Depending on the vehicle configuration, rigid antennas up to about 9 feet in diameter can be accommodated within the available dynamic envelope without unfurling. Thus, acceptable sizes for the high-gain antenna lie between 7 and 9 feet in diameter. A 7.5-foot diameter antenna is being utilized.

6.5.1.4 BEAM STEERING

Analysis of typical mission trajectories shows that a pencil beam 3 or 4 degrees wide must be steered about two axes to maintain Earth orientation during the appropriate mission phases. Antenna articulation mechanisms can have a significant effect on reliability and, for this reason, a number of alternate beam steering techniques are investigated.

One approach which can simplify beam steering requirements is the use of a fan-shaped beam such as that employed for the Mariner C high-gain antenna. Because the Voyager mission requires higher gain and the use of this antenna over longer periods, antenna steerage cannot be completely eliminated. However, it is possible that a fan-shaped beam can reduce steering requirements to only one axis. By proper orientation of the single axis of freedom, a beamwidth of about 12-16 degrees can provide satisfactory Earth coverage during late cruise and all of the orbital operation phase. To provide the same gain as a 4-degree pencil beam, the beamwidth in the orthogonal plane must be correspondingly narrowed (i.e., to about 1 degree). An aperture approaching 30 feet in length is required to generate the narrow beamwidth, and closed-loop antenna pointing is a necessity. In addition, the useable range of Earth-spacecraft geometrical relationships is limited, and versatility in missions and trajectories is sacrificed.

Beam switching techniques can eliminate one axis of antenna motion without an increase in aperture size or pointing accuracy requirements. For example, a 7.5-foot diameter parabolic reflector can be provided with multiple feeds which are selected by switching and fed one at a time to provide beam scanning in discrete steps. This approach can provide ± 20 degrees of scan in one plane with scan in the orthogonal plane achieved by mechanical rotation of the antenna. Thus, performance is nearly equivalent to two-axis mechanical scan. However, the elimination of one antenna gimbal axis is offset by the requirement for switches in the antenna feed, and antenna reliability is not really improved.

The use of electronically scanned arrays is also considered as a means of eliminating motion of the high-gain antenna. Such an approach requires a large number of rf variable phase shifters or switches together with the associated circuitry needed to select and control these components in a programmed manner. The reliability of an electronically scanned array is certainly far below that of a mechanically steered antenna, and the approach is considered to be inconsistent with the philosophy of simple, conservative design.

It is concluded that mechanical rotation offers the most acceptable means of beam steering for the Voyager high-gain antenna. Maximum reliability is achieved by using a rotary joint at the gimbal axis where the greatest rotation is required, and by using flexible cables at the second gimbal axis and at a separate deployment axis, if needed. Where feasible, antenna stowage configurations which enable one of the pointing axes to serve also as the deployment axis are preferred from reliability and performance points of view.

6.5.1.5 ARRAY ANTENNAS

The use of multielement arrays offers two principal advantages for the Voyager system. The high aperture efficiency of the two-dimensional array in comparison to that of the paraboloidal reflector makes it possible to obtain slightly higher gain (1.0 to 1.5 db) for the same aperture area. Alternately, for the same performance, the array aperture can be made smaller than that of the reflector. The reduced aperture size together with generally smaller structural depth greatly simplifies antenna stowage and deployment.

One of the main disadvantages of the array approach is its unproven reliability. A 6-foot square array requires at least 100 individual elements even if endfire radiators are used. The distribution assembly used to feed the array elements requires numerous rf connectors and transmission line components. Wave-guide slot arrays such as that being developed for Surveyor are highly reliable. However, this technique does not provide sufficient bandwidth for operation at both 2295 and 2113 mc. Performance over this frequency range generally requires a corporate type feed network which is inherently more complex.

The parabolic reflector is recommended for the Voyager high-gain antenna because it has no major shortcomings. All of its characteristics are within tolerable limits, considering both spacecraft and communications subsystem requirements. It offers uncompromised electrical performance in a configuration that is mechanically compatible with the spacecraft and its environment. The paraboloidal reflector is simple in construction, light weight, and straightforward in design. Hence, it is considered the most simple and conservative high-gain antenna approach for this application.

6.5.2 LOW-GAIN ANTENNAS

Low-gain antenna requirements are conveniently subdivided by mission phase. One set of requirements is defined for the early mission phases of prelaunch, launch, and injection when the spacecraft is in a stowed condition. Other low-gain antenna requirements are defined for the remainder of the mission when the spacecraft is in a deployed configuration. This paragraph describes alternate approaches considered for the latter period which constitutes the majority of the mission. Trade-offs covering low-gain requirements for the stowed vehicle are discussed separately under the launch antenna.

Upon separation from the launch vehicle the acquisition phase is initiated. Particularly important during this period is pattern coverage at cone angles greater than 90 degrees from the -z axis for any clock angle. After external references are acquired and the normal cruise attitude is established, pattern coverage in the hemisphere centered on the -z axis generally suffices. For communications during maneuvers (both for back-up to the high-gain antenna in the maneuver attitude and for low rate communication during the transition between cruise and maneuver attitudes), pattern coverage over cone angles from 0 to 180 degrees is required at least at one clock angle.

A number of different approaches are considered for meeting the low-gain antenna requirements. Adequate pattern coverage for the acquisition and cruise phases is provided by a hemispherical type pattern centered on the -z axis. A second hemispherical pattern with its axis normal to the thrust axis satisfies coverage requirements for the maneuver period. The preferred approach utilizes two antennas. The primary low-gain antenna gives the hemispherical pattern centered on the -z axis. The secondary low-gain antenna provides a toroidal shaped pattern which is essentially omnidirectional in the x-z plane (toroid axis of symmetry parallel to y-axis). This approach provides the same performance as the first with two additional advantages: (1) The secondary pattern also has good coverage for the cruise phase and, thus,

offers increased redundancy and reliability, and (2) the secondary antenna serves as a nearly omnidirectional emergency back-up antenna if vehicle stabilization should fail.

Another low-gain antenna approach which is considered, utilizes two hemispherical radiators diametrically opposed in the x-z plane. The axis of one is at a cone angle of 45 degrees (approximate direction of Earth at encounter), and the axis of the other is at a cone angle of 135 degrees. With these antennas mounted on the solar panels, pattern interference by the vehicle structure is minimized, and a good approximation to omnidirectional coverage is obtained. A major disadvantage of this approach is that either antenna can be optimum at a particular time, and a relatively large number of decisions is needed in selecting antennas throughout the mission. Furthermore, although omnidirectional coverage is good, two antennas are required to achieve it, and the implementation of combining methods presents a problem.

Also considered, are approaches using only one antenna and approaches using more than two antennas. For example, the secondary antenna (toroidal pattern) of the preferred approach very nearly satisfies all requirements alone except that pattern coverage during the acquisition period is less than optimum. It is decided that the use of two low gain antennas optimizes pattern coverage and provides maximum radio subsystem reliability. With a three-transponder system, the use of either a greater or a smaller number of antennas requires more complex rf switching circuitry.

6.5.3 LAUNCH ANTENNA

A low-gain antenna capability must be provided for transmission of telemetry during prelaunch, launch, and injection phases. It is possible that either the primary or secondary low-gain antenna can provide this function in their stowed positions. However, because it is undesirable to energize the power amplifiers during launch, a switch is needed to utilize either of these antennas. The use of a separate antenna fed through a directional coupler at an exciter output does not require a switch, and the basic subsystem reliability is not degraded. In addition, since the separate launch antenna is used only during these early mission phases, more optimum pattern coverage can be provided. It is decided that the addition of a small, lightweight antenna is well worth the improved reliability and performance offered by this approach.

6.5.4 MEDIUM-GAIN ANTENNA

The inclusion of a fixed medium-gain antenna eliminates the complete dependence of the spacecraft and capsule missions on the steerable high-gain antenna. Although the low-gain antennas can be utilized to provide minimal two-way communication and tracking to encounter range, their ability to satisfy all the requirements for successful capsule separation and orbit insertion is doubtful. Even after a successful orbit insertion neither could provide adequate data to make the orbiter mission meaningful. To provide adequate back-up capability for these functions the fixed medium-gain antenna should provide pattern coverage having substantial gain in the direction of

Earth for a period of several weeks both before and after planetary orbit insertion. The pattern coverage requirement can be met using antennas which generate a fan-shaped beam. The Mariner C high-gain antenna is selected as the preferred approach for this application. Alternate designs may be considered which provide increased gain at the expense of more restricted pattern coverage. It is decided that the performance of the Mariner C elliptical paraboloid, however, is adequate for the function; and, since this antenna has already been designed and qualified, no other approaches are seriously considered. Typical performance of the Mariner antenna is given in Appendix I for both 1971 and 1973.

6.6 POWER AMPLIFIER TRADE-OFFS

The telecommunication system power amplifier trade-offs and radio subsystem power amplifier trade-offs are affected by several overall spacecraft trade-offs. Where constraints result, reference is made to the overall trade-offs.

6.6.1 OVERALL SPACECRAFT SYSTEM CONSTRAINTS

The following constraints are imposed on the power amplifier trade-off study from other spacecraft system trade-offs.

6.6.1.1 SPACECRAFT PRIME POWER

There are several limitations on the available dc prime power for the power amplifier.

a. The prime power available for the Voyager spacecraft is limited by the amount of usable surface area for solar panel and the weight allocation for the power subsystem.

b. During the cruise phase and encounter prior to capsule separation the spacecraft dc prime power is limited because of the capsule power requirements.

c. During long sun occultations the dc prime power is supplied by batteries since the spacecraft solar panels may not be oriented towards the sun. Power requirements are minimized during these periods to prevent excessive drain on the batteries.

6.6.1.2 THERMAL CONTROL

The heat energy to be dissipated away from the power amplifier must be consistent with the thermal control characteristics of the outer thermal control plate of the bay containing the power amplifier.

6.6.1.3 HIGH-GAIN ANTENNA

The maximum diameter of a rigid reflector for the high-gain parabolic antenna is 7-1/2 feet.

6.6.2 RADIO SUBSYSTEM CONSTRAINTS

The design of the radio subsystem configuration affects the power amplifier trade-off study. As a result of the radio subsystem reliability analysis it is decided that the proposed Voyager radio subsystem will contain three power amplifiers.

The output of each amplifier is connected directly to a diplexer. The output from each diplexer is connected to the antenna system via two transfer switches.

The telemetry channel must support a maximum of 8533 bps during planet encounter and orbital operation and a maximum of 3 1/3 bps during spacecraft maneuvers. These are the worst case limits for the transmission of telemetry.

6.6.3 OUTPUT POWER

The selection of the output power level of the power amplifier is based on what is now available in space qualified devices.

Presently available devices have a power output of 20 watts. For the proposed antenna configuration a 20-watt power output supports the maneuver telemetry link to approximately 3×10^8 km.

For an efficiency of 35 percent the 20-watt power amplifier requires 57 watts. This is within the prime power allocations for battery operation.

During orbital operations the 20-watt power amplifier supports the 8533 bps telemetry link to approximately 1.9×10^8 km, which exceeds the worst expected encounter distance (June 25, 1971 Launch). However, the 20-watt level does not support 8533 bps for the entire mission. Therefore, a higher power output is needed for orbital operations.

Keeping in mind the constraints and development problems to be encountered: to space qualify a higher power device, the power allocation for the power amplifier, and the required communication range; a 50-watt power amplifier is chosen. Fifty watts supports 8533 bps to approximately 3×10^8 km, and 4266 bps to 4×10^8 km, which exceeds the worst case mission after 6 months in Mars orbit (June 25, 1971 launch).

Assuming an efficiency of 35 percent for the 50-watt device, the power amplifier requires 145 watts, which is within the maximum power allocation.

6.6.4 POWER AMPLIFIER CONFIGURATION

In the preceeding section it is found that the power amplifiers for the radio subsystem comprise a combination of two, containing at least one 50-watt device for orbital operations and at least one 20-watt device for cruise and maneuver operations prior to encounter. The choice of power level for a third device is a function of the system reliability. In order to provide a redundant mode at each power level, a 20-watt device programmable by command to 50 watts is chosen for the third power amplifier.

6.7 DIPLEXING FUNCTION TRADE-OFFS

The system trade-off concerning diplexing is simply whether or not to use a discrete diplexer. The requirement exists to transmit and receive, simultaneously, at different frequencies. This may be performed using separate transmitting and receiving antennas. However, for late mission phases, both the transmission and reception channels require high-gain, directional, antennas to support the channel data. The trade-off, then, is between supplying two antennas or a discrete diplexer. In terms of weight, reliability, and mission operation flexibility, the trade-off is resolved in favor of the discrete diplexer.

A second system trade-off concerns the number of diplexers to be implemented. That is, given multiple receivers and transmitters, should a single diplexer be used with input and output switching, or should multiple diplexers be implemented? This trade-off is resolved in favor of multiple diplexers, since the reliability of a diplexer is, in general, greater than that of an rf switch.

Given a requirement for multiple discrete diplexers, the only remaining question is that of the exact type of diplexer to implement. This trade-off is treated in Section 7.0 of VB233AA101.

6.8 SIGNAL DESIGN TRADE-OFFS

6.8.1 GENERAL

It is stated in the JPL Mission Specification that the spacecraft equipment must be compatible with the Deep Space Instrumentation Facility as it presently exists, and as it is planned to exist, per EPD-283. With this constraint, the signal design problem devolves to that of selecting the types of data waveforms to be phase modulated onto the up and down-link carriers and selecting the various carrier phase deviations.

6.8.2 RANGE CODE WAVEFORM

To maintain DSIF compatibility, the range code waveform on the up-link carrier is, ideally, square in shape, having values of plus and minus $\Delta\varphi_{ru}$, where $\Delta\varphi_{ru}$ is the

up-link carrier phase deviation. The transitions between plus and minus states occur at times which are integral multiples of the range code baud period, nominally one microsecond. The exact transition sequence is determined by the structure of the pseudo-random code used for ranging.

The range code waveform on the down-link carrier, due to the choice of post-detection code limiting, is ideally, square in shape, having values of plus and minus $\Delta\varphi_{rd}$, where $\Delta\varphi_{rd}$ is the down-link carrier phase deviation. The transition between states does not, in general, occur at integral multiples of the up-link range code baud period, due to effects of turned around noise and Doppler effects.

6.8.3 SUBCARRIER WAVEFORMS

Two subcarrier waveforms are considered: square waves and sine waves. No rate-limited waveforms are considered, since all carrier demodulation methods employ carrier tracking phase-locked loops to generate phase-stable references for coherent phase demodulation of the carriers. Good design practice ensures negligible modulation components falling within the carrier loop tracking bandwidths.

Square wave subcarriers are easily generated digitally for channels employing digital data waveforms. Sine wave subcarriers can be obtained from filtered square wave subcarriers or can be generated in an analog fashion, directly.

Appendix III shows that, compared on the basis of equal suppression of the residual carrier, the available subcarrier powers for the sinusoidal subcarrier or for the sinusoidal component of the square wave subcarrier are roughly equal. The available subcarrier power for the complete square wave is roughly one decibel greater than for the sine wave or fundamental component of the square wave. However, recovering the entire square wave requires roughly three times the noise bandwidth as that for the fundamental component of the sine wave. Hence, in terms of recovered signal to noise ratio, the square wave gives less performance than either the fundamental square wave component or the pure sine wave subcarrier. Also shown is the fact that for equal suppression of the residual carrier a square wave subcarrier causes the residual carrier component to be much more sensitive to changes, or tolerances, in phase deviation than is caused by a sinusoidal subcarrier.

6.8.4 SUBCARRIER FREQUENCIES

Constraints are generally placed on subcarrier frequencies so that predetection filtering of the received signal, prior to carrier demodulation, does not destroy subcarrier information. Also, subcarrier frequencies must be sufficiently high so that information is not destroyed by the carrier tracking phase-locked loop.

For channels containing more than one subcarrier or containing subcarriers and pseudo-random code waveforms, care must be exercised in selection of subcarrier

frequencies to insure negligible co-channel interference. That is, a subcarrier should not have a frequency equal to harmonics or cross-products of other subcarrier frequencies, or equal to the frequencies of dominant spectral lines in the spectra of the pseudo-random waveforms.

6.8.5 CARRIER PHASE DEVIATIONS

It is possible, for every signal channel in the system, to set minimum requirements for the ratios of signal power to noise power, or signal power to noise spectral density, which insure proper operation of the channels for stated operational criteria. That is, for a coherent phase-shift-keyed subcarrier, it is possible to set a minimum ratio of subcarrier power to noise spectral density which insures some minimum probability of error per bit.

The basic philosophy of selection of carrier phase deviations is to simultaneously satisfy the minimum requirements of all channels, with the possible exception of the residual carrier channel, under conditions of decreasing signal power. Stated another way, the philosophy is for all channels to reach "threshold" simultaneously. The exception to this philosophy occurs when the minimum requirement for a data channel far exceeds the minimum requirement for the residual carrier channel. Trying to meet such requirements, simultaneously, requires great suppression of the residual carrier power below the total signal power. It is shown in Appendix III that, when greatly suppressed, the residual carrier becomes very sensitive to changes, or tolerances, in phase deviation. Also, for sinusoidal subcarriers having phase deviations above about 1.4 radians, increasing deviation and, hence, increasing carrier suppression results in very little increase in subcarrier power.

For the reasons cited above, it is recommended that "Martin's rule"* apply to Voyager signal design. That is

$$\sum_{rms} \Delta\Phi \leq 1.0 \text{ radian} \tag{11}$$

where $\sum_{rms} \Delta\Phi$ is the root-mean-squared sum of all carrier phase deviations.

The exact method used to determine carrier phase deviations for Voyager will be that treated by Painter.**

---

* "The Pioneer IV Lunar Probe: A Mimimum-Power FM/PM System Design", by Benn D. Martin, Technical Note 32-215, Jet Propulsion Laboratory, March 15, 1962.

** "Synthesis Techniques for a Class of Phase-Modulated Signals", by John H. Painter, Proceedings of the 1965 IEEE Conference on Aerospace, June 20-24, 1965.

6.9 LAUNCH COMMUNICATION TRADE-OFFS

During the launch phase the requirement exists that signals from spacecraft antennas be reradiated through a parasitic antenna on the overall vehicle nose fairing.

Consideration was given to a separate telemetry generator and exciter to be used during the launch phase only. However, from the standpoint of equipment simplicity it is desired to have the launch telemetry compatible with the mission cruise phase telemetry and at the same time it is desirable to utilize a part of the existing radio subsystem. Since it is desirable to transmit as much real time data as possible, the normal cruise telemetry bit rate of 100 bps is chosen. Also taken into consideration is a trade-off of required transmit power versus bit rate. Since a power amplifier cannot be used during the launch phase, link calculations are made using an S-band power output level of 100 mw. Adequate circuit margins exist when employing a low-gain antenna, and a coupler, and parasitic antenna on the shroud.

A 3 db power splitter is inserted between the exciter power monitor and hybrid coupler of exciter number one in order to obtain more than 100 mw (actually about 200 mw) for the launch antenna. The exciter output power is nominally 400 mw, and the input to the power amplifier is 100 mw. Therefore, there is a 6 db drop between exciter output and the power amplifier input of which the hybrid coupler accounts for 3 db. Thus, if the power splitter is not inserted, a 3 db attenuator is. This coupling to exciter number one is chosen over number two because number two has two hybrid couplers between the exciter and PA input which already account for 6 db. Exciter one is chosen over three since number one is used during the early phases of the mission and number three is intended to be back-up exciter.

Either the primary or secondary low-gain antenna can be employed. However, a switch is needed to utilize them as the power amplifiers are not energized during launch. Since there is no basic reliability degradation a 3 db coupler is used in preference to a switch. The addition of a small, light-weight antenna is worth the improved reliability and performance. Also, a more optimum pattern coverage can be obtained during launch.

An isolated switch is inserted between the coupler and antenna so that upon command the rf power may be dumped into a matched load instead of being radiated.

7.0 SYSTEM BLOCK REDUNDANCY TRADE-OFFS

7.1 INTRODUCTION

An integral part of the design of the overall telecommunication system is ensuring the probability of successful transmission of data from the spacecraft and reception of commands from the DSIF. Also required is assurance of the probability of successful performance of turn-around ranging and Doppler tracking. For a given system configuration these probabilities are easily determined. However, there is no guarantee that the given system is optimum on the basis of overall system reliability, weight, and power. It is the purpose of this section to discuss the trade-offs made in optimizing the preferred telecommunication system design in turns of reliability, weight, and power.

7.1.1 SCOPE

The trade-offs made in optimizing the overall telecommunication system design are categorized by mission phase and system components used during each phase for telemetry, command, Doppler tracking, and turn-around ranging.

As a starting point in the trade-off analysis, a minimum system is derived which performs the functions of telemetry, command, Doppler tracking and turn-around ranging. However, the reliability of this system does not meet the apportionment goal for the Voyager mission and does not utilize the weight and power allocations set aside for the telecommunication system. System components are then added to provide various levels of redundancy within each subsystem and the overall system. An incremental cost analysis of the value of the added system components in terms of overall system weight and power consumption is also conducted. Thus, as each component is added to the system it is assessed in terms of its contribution to the system reliability, weight, and power consumption.

Since the solution to such a trade-off study is not unique, a certain amount of engineering judgment is used. In other words, engineering judgment is used to eliminate the trivial solutions. An additional aid in the system redundancy trade-off analysis is a reliability apportionment per subsystem function per mission phase. This apportionment is based on the required probabilities of success for each phase of the Voyager mission and the priority of each of the system functions such as telemetry, command, etc.

7.1.2 RELIABILITY APPORTIONMENT

The reliability apportionment for the Voyager mission is shown in Table 7-1. The mission is divided into four different phases.

Phase I - Launch
Phase II - Cruise
Phase III - Encounter
Phase IV - Orbit

Table 7-1. Reliability Apportionment

Phase	I Launch	II Cruise	III Encounter	IV Orbit	Overall Mission
Time	2 hrs	4272 hrs	48 hrs	720 hrs	5024 hrs
Radio	0.99978	0.9816	0.99978	0.9969	0.9781
Command	0.99957	0.9653	0.99957	0.9942	0.9590
TLM	0.99978	0.9814	0.99978	0.9969	0.9779
Telecomm.	0.99913	0.9298	0.99913	0.9911	0.9171

A typical time for each phase is assigned for the purposes of this study, which approximates the actual time intervals encountered in nominal missions. The probability of success required for each of the mission phases and the total mission is determined using these times together with the specified mission reliability and priority requirements from the JPL Mission Specification.

7.1.3 TELECOMMUNICATION SUBSYSTEMS

The subsystems used in this trade-off consist of a command subsystem, a telemetry subsystem, and a radio subsystem. Each subsystem performs a specific function which contributes to the overall system functions of obtaining and transmitting data, receiving and processing commands, and providing Doppler tracking and ranging.

7.1.3.1 COMMAND SUBSYSTEM

The command subsystem is defined to include the necessary detectors, program controllers, access logic and decoders to detect the received commands via the radio subsystem and decode the detected commands for distribution to the various spacecraft users.

7.1.3.2 TELEMETRY SUBSYSTEM

The telemetry subsystem is defined to include the data processing equipment, such as the engineering data accumulator, science data storage and capsule data storage, and the data format selector and a telemetry data subcarrier modulator.

7.1.3.3 RADIO SUBSYSTEM

The radio subsystem is defined to include the transponders, power amplifiers, antennas, and all associated switches and hardware necessary to perform the functions of transmitting telemetry, receiving command signals, Doppler tracking and ranging.

7.1.4 DEFINITION OF FAILURE MODES

As in any reliability analysis certain failure modes are considered. The exact nature of these modes is defined to clarify the analysis. The failure modes used in this analysis are concerned with failures at the subsystem level. A single component failure consists of a complete loss of the component to subsystem operations. No degraded or standby modes are considered. Loss of a power amplifier or a command decoder are examples of this type of failure.

A multiple component failure is defined to be two or more single component failures. Loss of an antenna and a tape recorder is considered to be a multiple component failure.

A conditional component failure is defined as a multiple component failure in series such as a command detector and decoder failure or a transponder and power amplifier failure.

7.2 SYSTEM DEVELOPMENT

A step-by-step system development is performed in order to determine the most reliable systems configuration within the weight and power allocations for the telecommunications system. The system is divided into four functions and analyzed for a mission time of 6320 hours which includes a worst case mission of 220 days plus 1000 hours prelaunch operation.

Each function employs basic subsystem components. The analysis of each function consists of adding redundant components as needed to make a particular system function meet the desired reliability. For example, the basic components of a function such as command or telemetry are evaluated. The component that proves to be the most unreliable is made redundant and the function re-evaluated. This process is continued until either the reliability, weight, and/or power allocations are met.

The advantage of taking this approach is that the cost in weight and/or power versus reliability is assessed in a logical step-by-step fashion.

7.2.1 RADIO FUNCTION

The radio function employs the receiver, exciter, power amplifier, diplexer, and associated hardware of the radio subsystem. The basic configuration analyzed is shown in Figure 7-1. This is the Basic Mariner C radio system with additional antennas and switching. Since several different operational modes are possible for the radio subsystem one is chosen to illustrate the reliability trade-off analysis performed. The following discussion is a summary of the trade-off analysis for the radio function of transmit and receive via a low gain antenna. Other antennas are pictured in the accompanying figures for completeness. However, only the primary low gain antenna is used in the illustration.

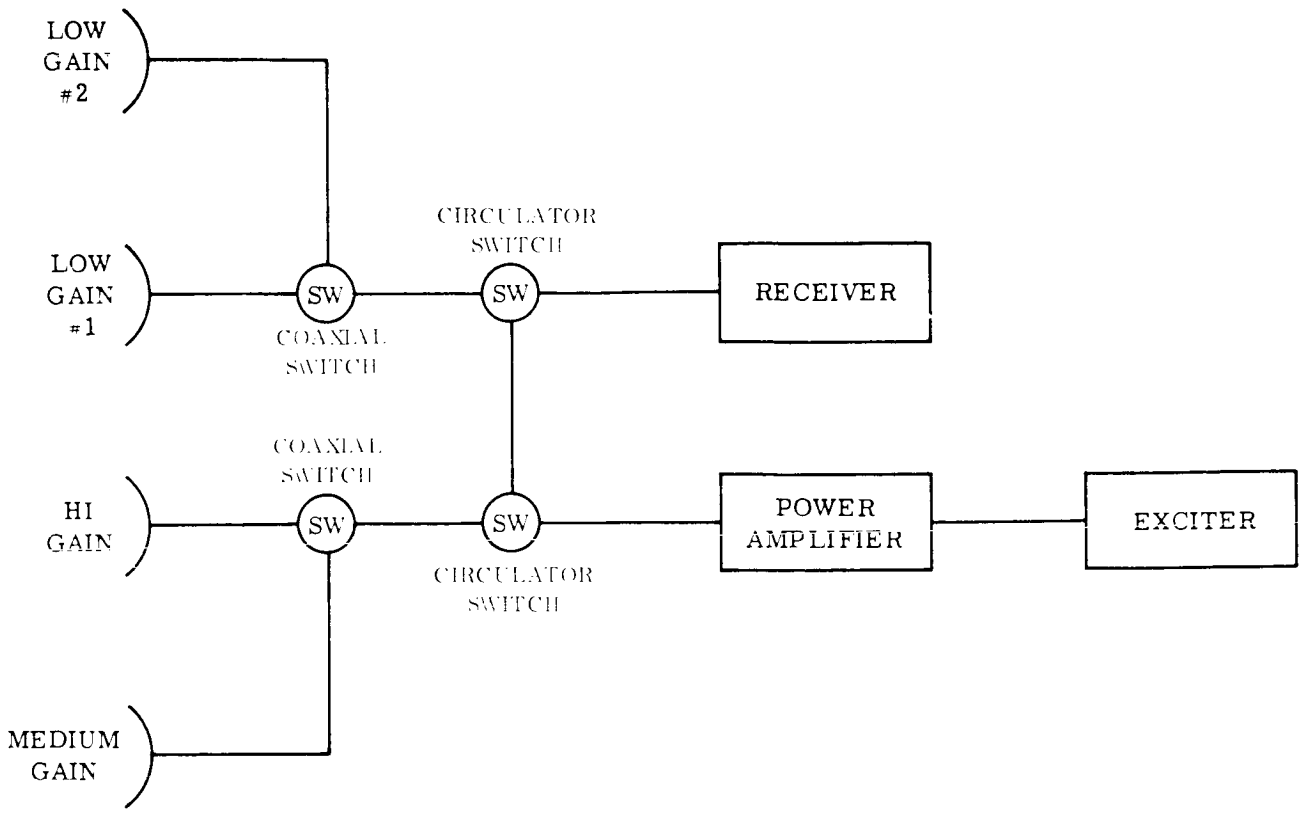

Figure 7-1. Basic Radio Configuration

7.2.1.1 ANALYSIS

The probability of success for the specified radio function as shown in Figure 7-1 is 0.777550. The weight for this system is 34.1 pounds. With all equipments ON the system consumes 217.2 watts of prime power.

A second receiver, exciter, power amplifier and diplexer in parallel redundancy is added to the basic configuration. This redundant system is shown in Figure 7-2. For this redundancy the reliability increases to 0.957677 for a weight increase of 36.5 pounds. The prime power required increases by the amount needed by the receiver, i.e., 7.14 watts, since all receivers are considered ON. Only one exciter and power amplifier are considered ON at any one time.

By modifying the interface between the exciters and the power amplifiers to include a hybrid coupler as shown in Figure 7-3 the radio function reliability increases to 0.971551. The hybrid is passive and consumes no prime power. The added weight due to the hybrid is negligible.

A third receiver, exciter, power amplifier and diplexer are added in parallel as shown in Figure 7-4. The reliability of the radio function increases to 0.991490 for an increase in weight of 35 pounds and an increase in power of 7.14 watts.

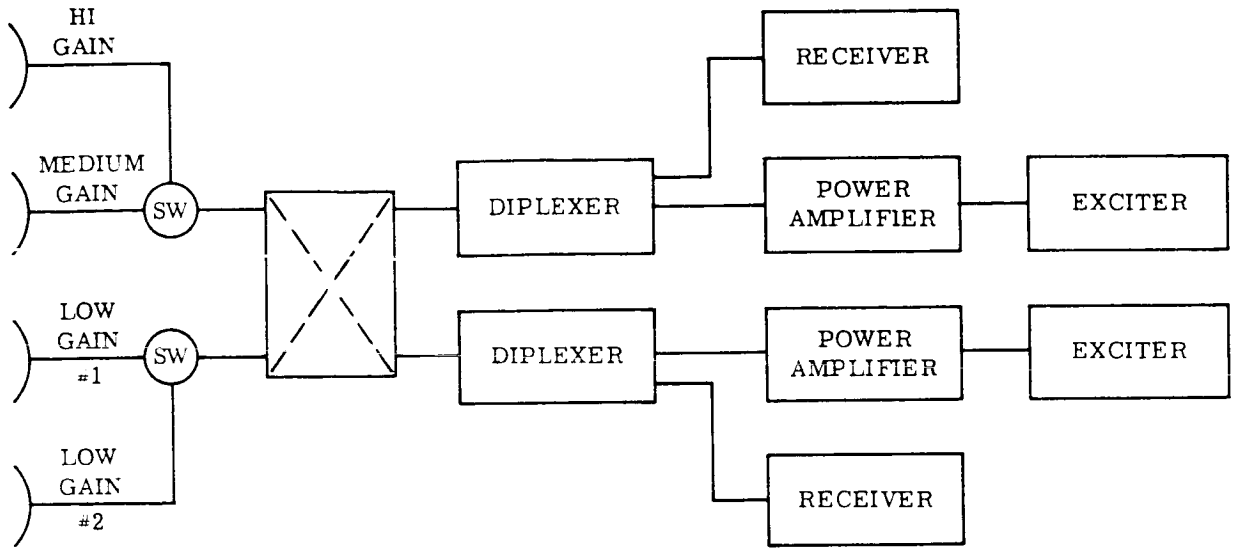

Figure 7-2. Configuration Number 2

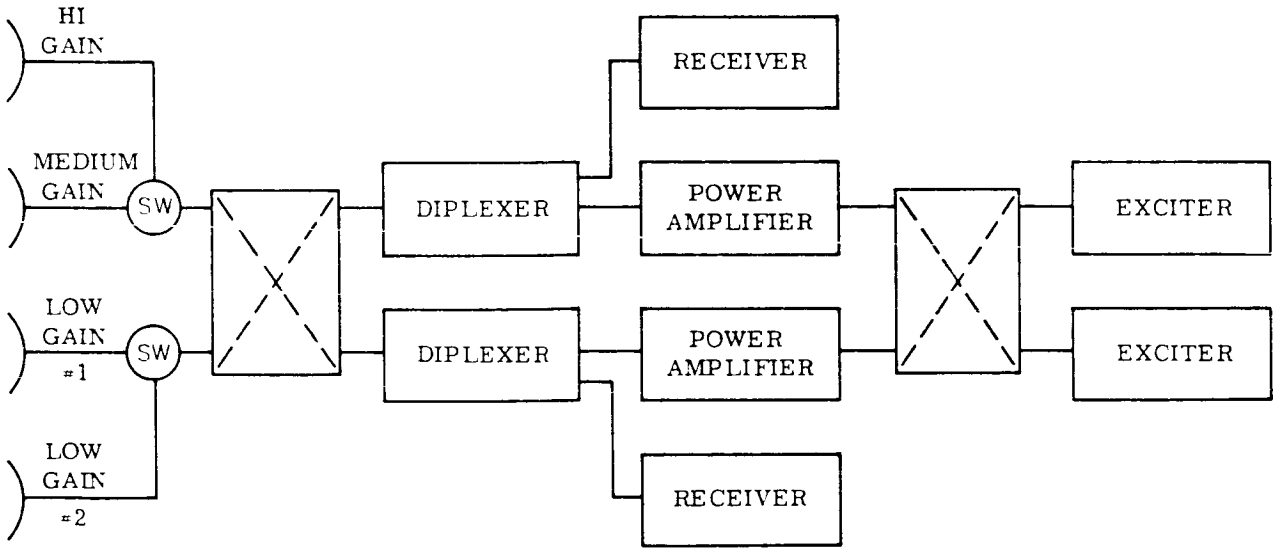

Figure 7-3. Configuration Number 3

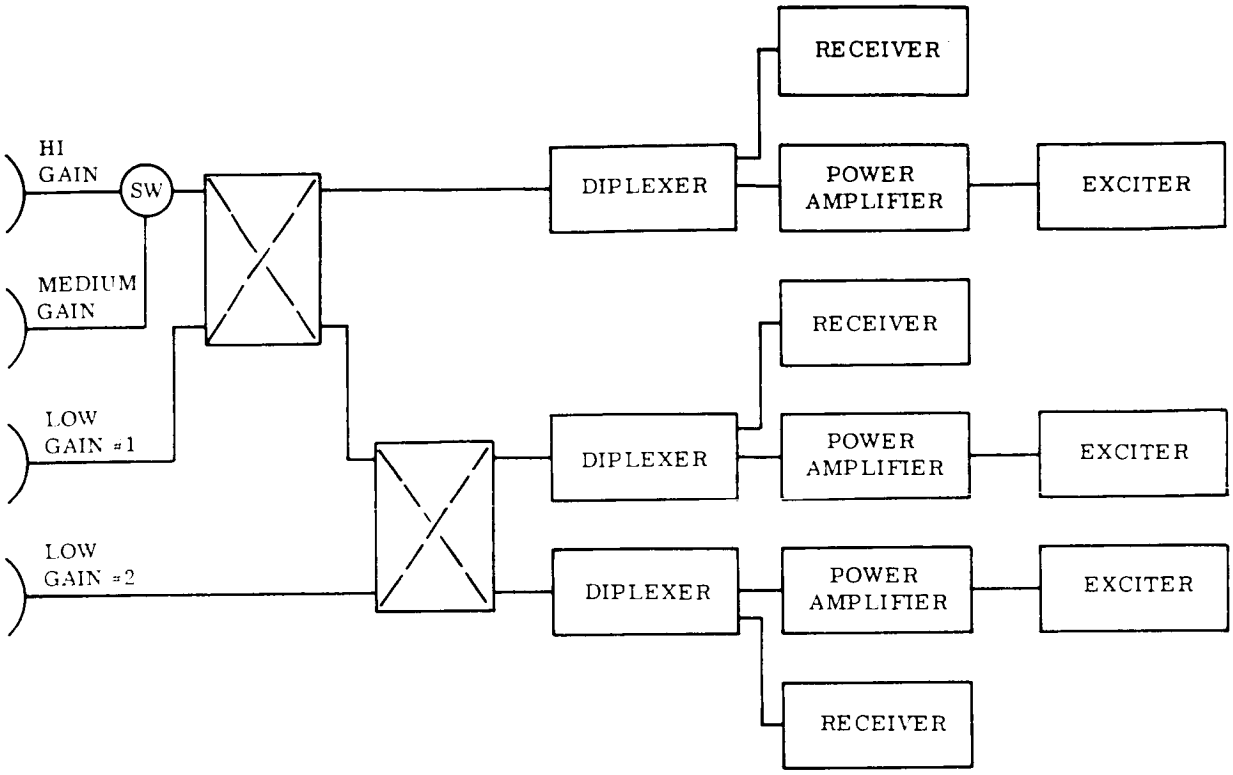

Figure 7-4. Configuration Number 4

Again, through the use of hybrid couplers connected as shown in Figure 7-5, the reliability of the radio function of transmit and receive via a low-gain antenna increases to 0.996335. As before the increase in weight due to the addition of the couplers is negligible.

Any further additions to the block diagram contribute very little to the reliability of the radio function but cause both the weight and power to exceed their respective allocations. A summary of the analysis is given in Table 7-2.

7.2.2 COMMAND FUNCTION

The reliability of the command function is analyzed as the probability of all commands given a modulated subcarrier at the command detector input. The basic configuration for the command function consists of a command detector, program control unit, decoder access logic, decoder and one power supply. A block diagram of this basic configuration is shown in Figure 7-6. The reliability of this basic configuration is 0.753291.

To increase the reliability of the command function a second decoder and power supply are added to the basic configuration as shown in Figure 7-7. The probability of command is increased to 0.951246 for an attendant increase in subsystem weight of eight pounds and an increase in consumed prime power of 14.2 watts.

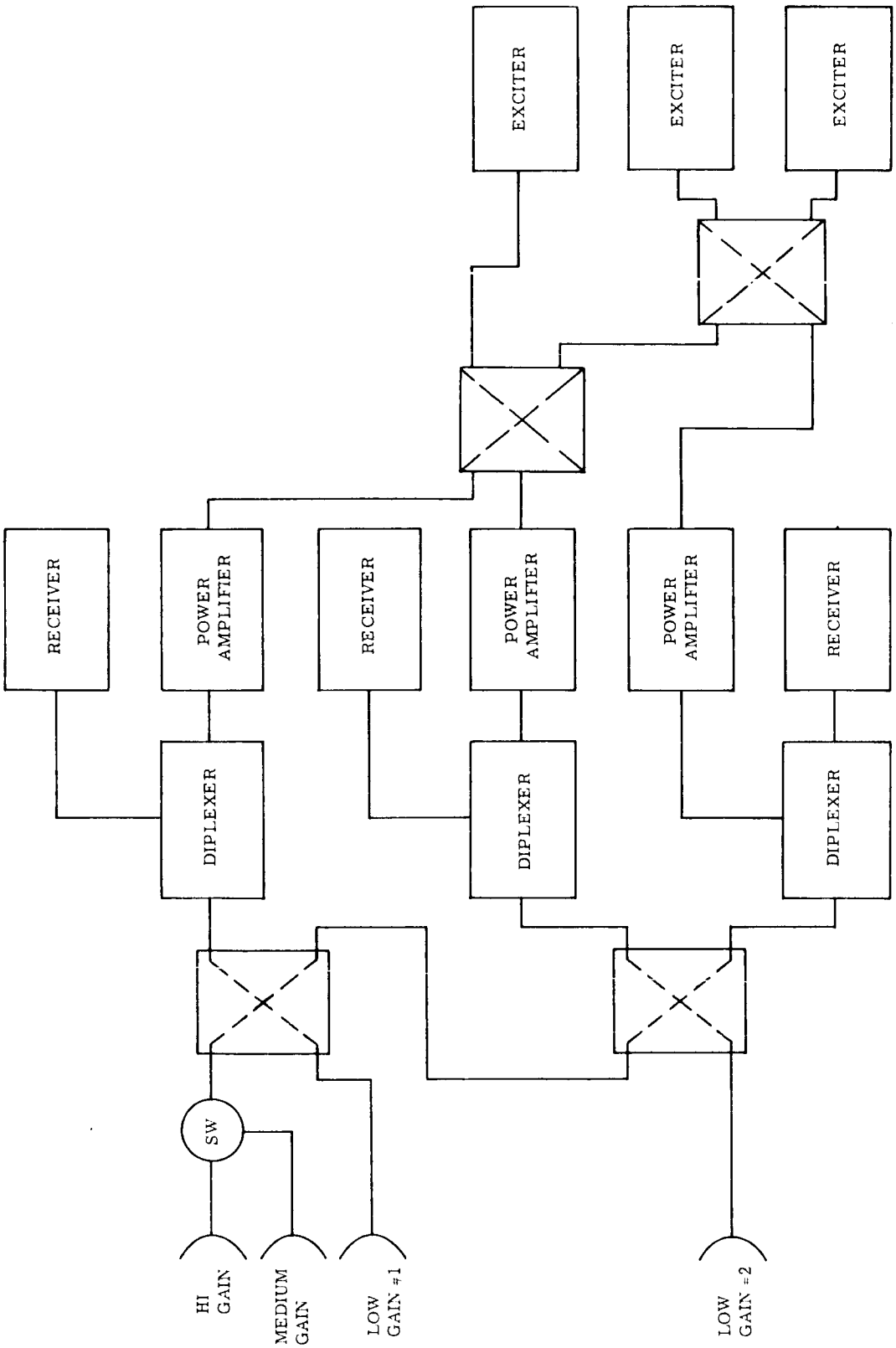

Figure 7-5. Configuration Number 5

Table 7-2. Radio Function, Mission Time - 6320 Hours

Configuration	Reliability	Decrease in Probability of Failures (%)	Weight (lbs)		Power	
			Added	Total	Added	Total
Basic radio subsystem with one receiver, one exciter, and power amplifier. See Figure 7-1.	0.777550	--	--	34.1	--	217.2
Add a receiver, exciter and power amplifier in parallel. See Figure 7-2.	0.957667	81	36.5	70.6	7.2	224.4
At the interface of the exciters and the power amplifiers a hybrid coupler is inserted. See Figure 7-3.	0.971551	32.8	0.1	70.7	--	224.4
Add a third receiver, exciter, and power amplifier in parallel. No hybrid coupler. See Figure 7-4.	0.991331	69.5	34.9	105.6	7.2	231.6
Add a second hybrid coupler at the exciter and power amplifier interface. See Figure 7-5.	0.996335	57.7	0.2	105.8	--	231.6

A redundant command detector and program control unit are added to the configuration as shown in Figure 7-8. With this added redundancy the reliability increases to 0.981815. The subsystem weight increases 2.5 pounds and the consumed prime power increases three watts.

A third redundant program control unit and command detector are added as shown in Figure 7-9. This addition required only a slight increase in the decoder access logic and increases the reliability of command to 0.985206. The subsystem weight increases 2.5 pounds and the consumed prime power increases three watts.

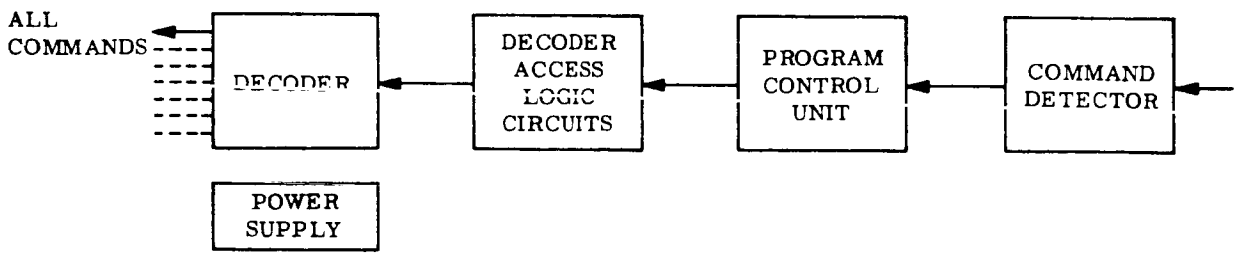

Figure 7-6. Basic Command Subsystem

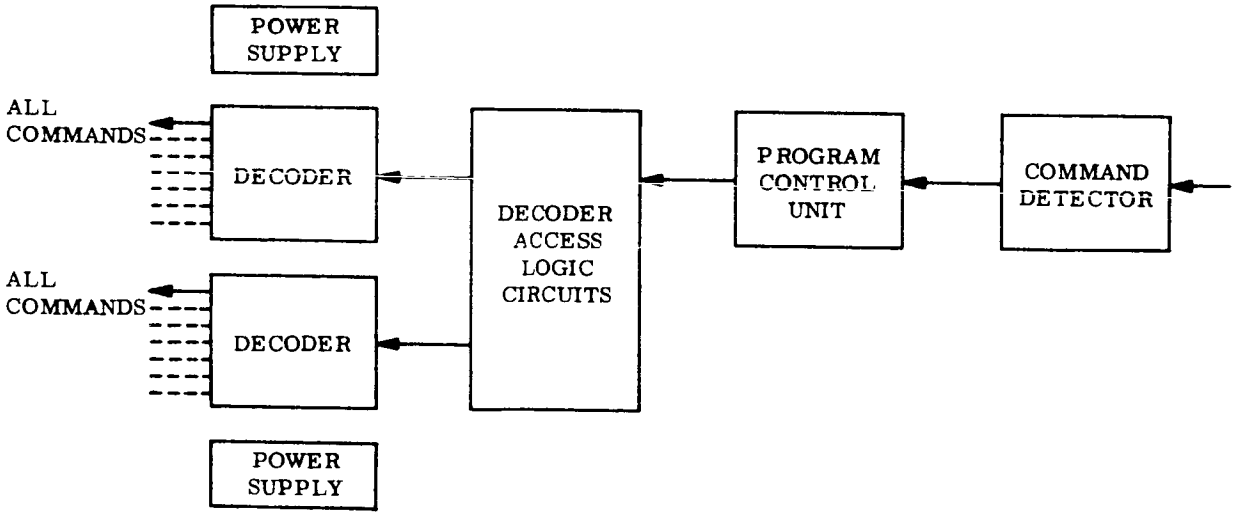

Figure 7-7. Basic Subsystem with Redundant Decoder and Power Supply

Any further redundancy can not be justified because of the command subsystem weight and power allocations. A summary of the analysis for the command function is given in Table 7-3.

Table 7-3. Command Subsystem, Mission Time - 6320 Hours

Configuration	Reliability	Decrease In Probability of Failure (%)	Weight (Lb)		Power (Watts)	
			Added	Total	Added	Total
Basic command subsystem with one detector, one program control unit, one decoder access, one decoder and one power supply See Figure 7-6.	0.753291	----	---	11.5	---	18.7
Add a redundant decoder and power supply. See Figure 7-7.	0.951246	80.5	8.0	19.5	14.2	32.7
Add a redundant program control and command detector. See Figure 7-8.	0.981815	90.8	2.5	22.0	3.0	35.7
Add a third redundant program and command detector. See Figure 7-9.	0.985206	18.6	2.5	24.5	3.0	38.7

7.2.3 TELEMETRY FUNCTION

The telemetry function employs the transmitting portion of the radio subsystem, the telemetry subsystem, and the command subsystem. The trade-off analysis consists of a step-by-step evaluation of the telemetry function as different subsystems components are added to the system. This analysis is performed for two modes to ensure all components of the telemetry subsystem are considered. The two modes are:

a. Mode 1 - Engineering and Capsule Data

b. Mode 2 - Tape Recorded science data with engineering data

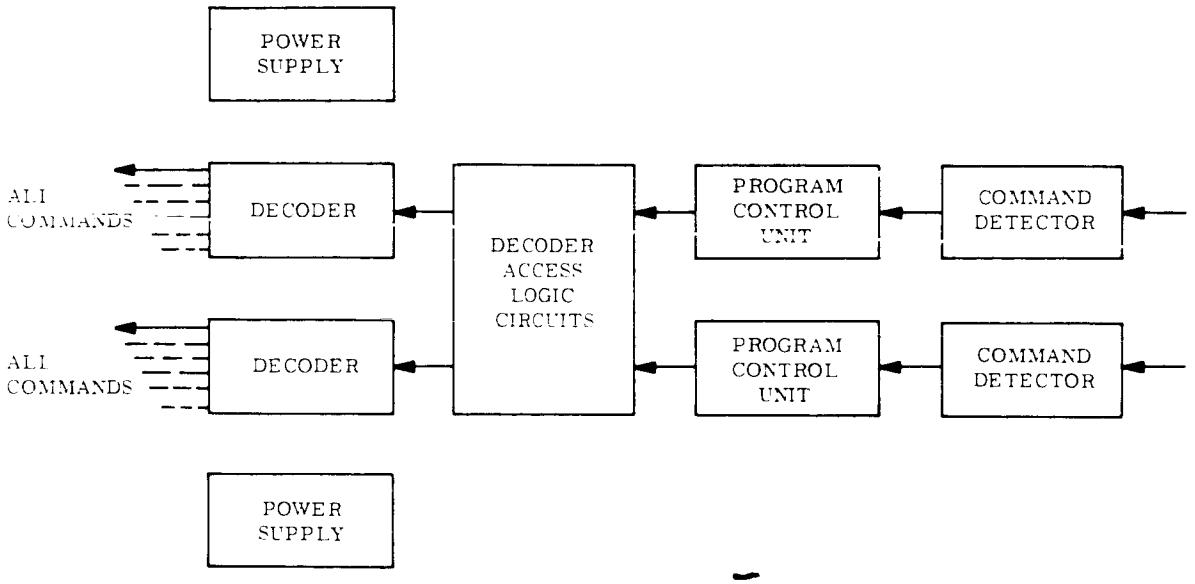

Figure 7-8. Redundant Command Subsystem

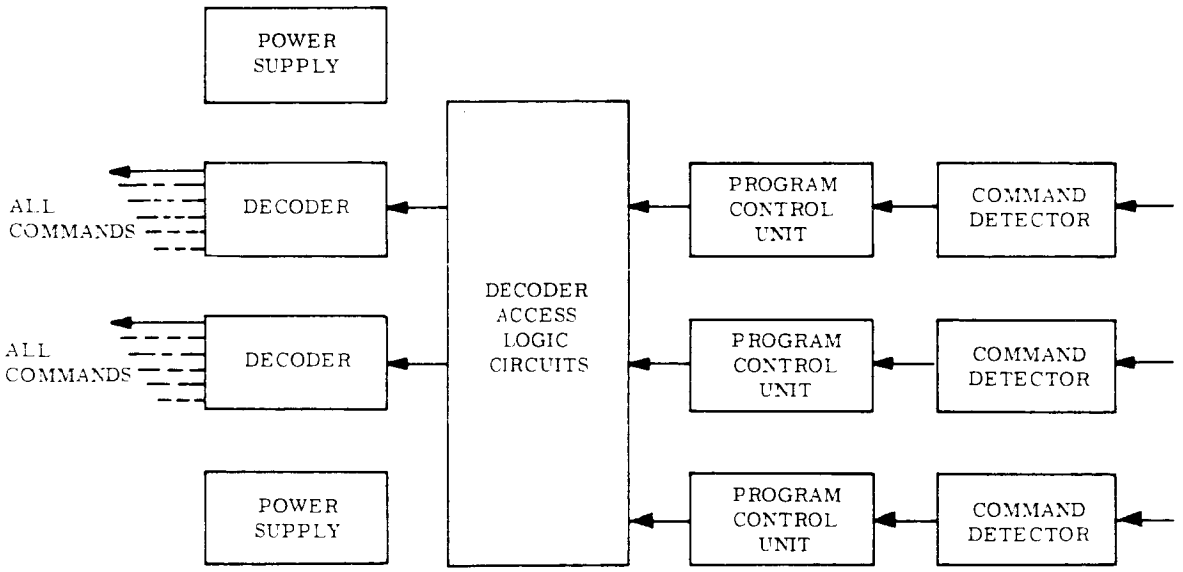

Figure 7-9. Redundant Subsystem with Additional Detector and Program Control Unit

7.2.3.1 MODE 1

The analysis for Mode 1 is concerned with the probability of successfully transmitting engineering and capsule data via the high gain antenna.

The basic or single configuration for this function is shown in Figure 7-10. This system reflects the equipment associated with engineering data operating for the entire mission of 6320 hours. The capsule data equipment is assumed to operate for a mission time of 5600 hours which corresponds to the cruise phase and part of the encounter phase.

Various subsystem components are added to this basic system to increase the reliability of the Mode 1 telemetry function in the same manner as is done for the radio and command functions. Instead of repeating all the block diagrams, a summary of the trade-offs made in the analysis of Mode 1 is listed in Table 7-4. Each system change is described in terms of the previous diagrams and the telemetry subsystem diagram shown in Figure 7-11.

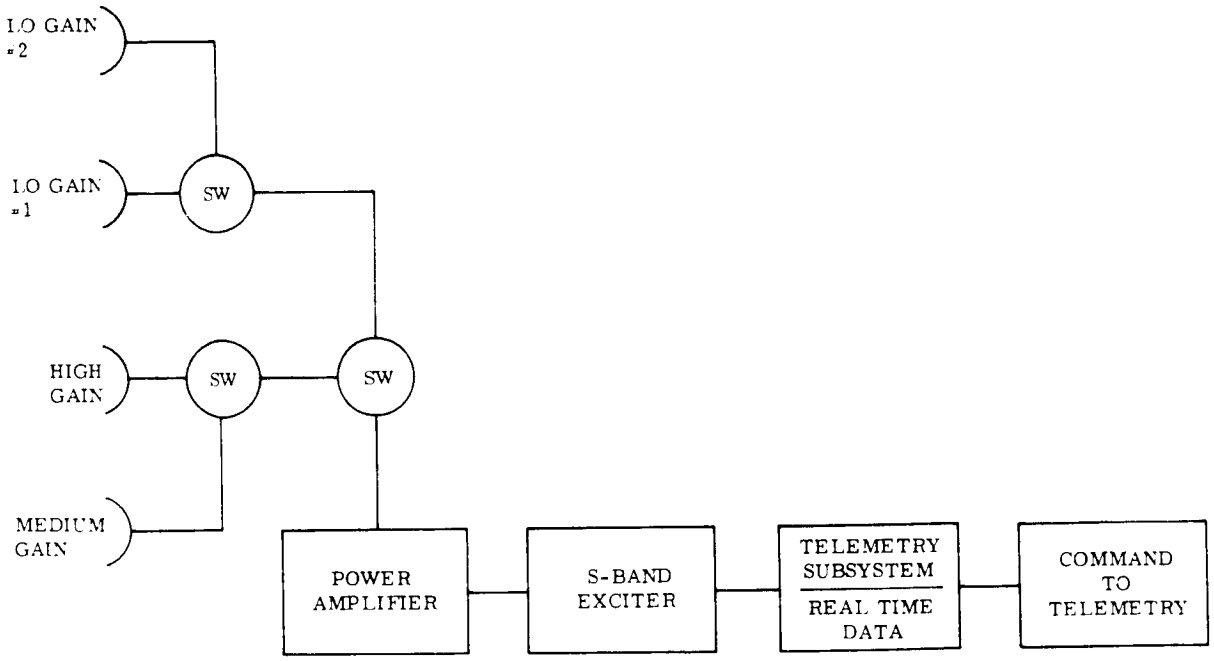

Figure 7-10. Real-Time Telemetry Function

Table 7-4. Telemetry Function - Mode 1

Configuration	Reliability	Decrease In Probability of Failure (%)	Weight (lb)		Power (watts)	
			Added	Total	Added	Total
Basic System. See Figures 7-10 and 7-11.	0.613961			66.6		235.9
Addition of redundant format program control to basic system.	0.649115	9.0	2.0	68.6	1.0	236.9
Addition of redundant power supply to previous system above.	0.681355	9.2	3.0	71.6	1.4	238.3
Addition of redundant commutator to system above.	0.713056	10	15.0	86.6	0.2	238.5
Addition of redundant Power Amplifier and Exciter.	0.786159	25.5	20.0	106.6	0	238.5
With redundant Decoder and Power supply in the command subsystem.	0.844060	27	8.0	114.6	14.2	252.7
With three capsule registers in parallel in the telemetry subsystem.	0.898767	35	1.0	115.6	0.10	252.8
Addition of redundant address Decoding Matrix in the telemetry subsystem.	0.925398	26.4	0.5	116.1	0.5	253.3
Addition of a second command detector, program control, and power supply to the command subsystem.	0.933020	10	4.5	120.6	10.7	264.0
Addition of one more redundant power amplifier and exciter to the radio subsystem.	0.943466	12.6	18.5	139.1		264.0

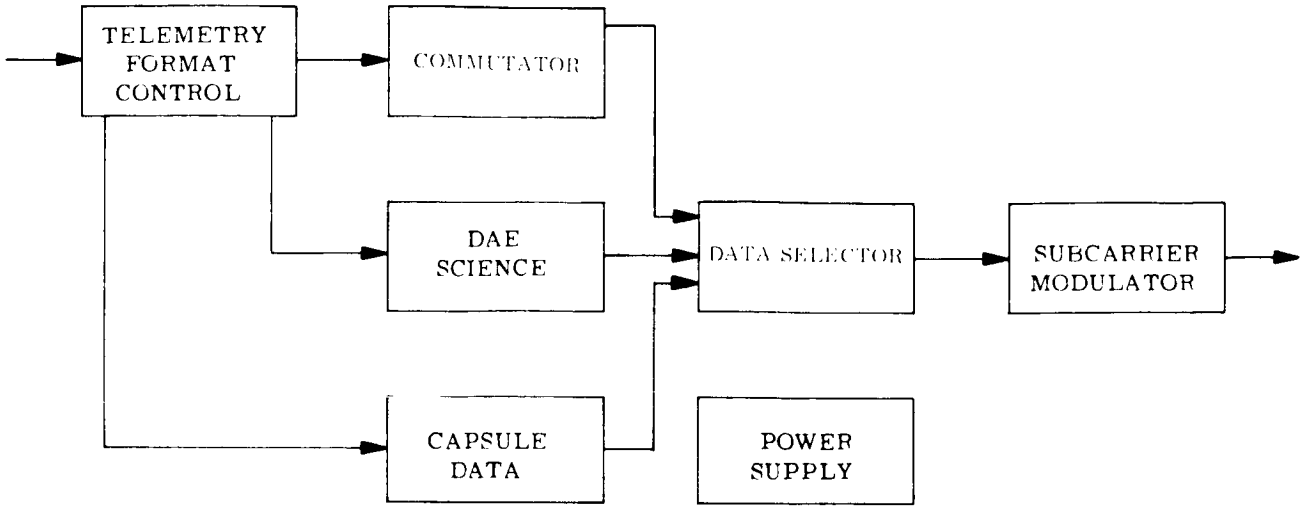

Figure 7-11. Real-Time Telemetry System

7.2.3.2 MODE 2

The analysis for Mode 2 is concerned with the equipment associated with the transmission of engineering data and tape recorded science data. The basic, or single, system for this mode is the same as shown in Figure 7-10 for Mode 1. However, the telemetry subsystem diagram for Mode 2 includes, in addition to the engineering data system, the tape recorders and associated components needed for the analysis of the tape recorded science data function. A telemetry subsystem diagram for Mode 2 is shown in Figure 7-12.

The recorded science data is present during orbiting of Mars only. Therefore, the mission time used in the evaluation of this equipment is analyzed for 720 hours. The engineering data is used throughout the complete mission and was evaluated for 6320 hours in the analysis.

The reliability of the single system is 0.662251. Various subsystem components are added to the single system to increase the reliability of the Mode 2 telemetry function in the same manner as is done for the radio and command functions.

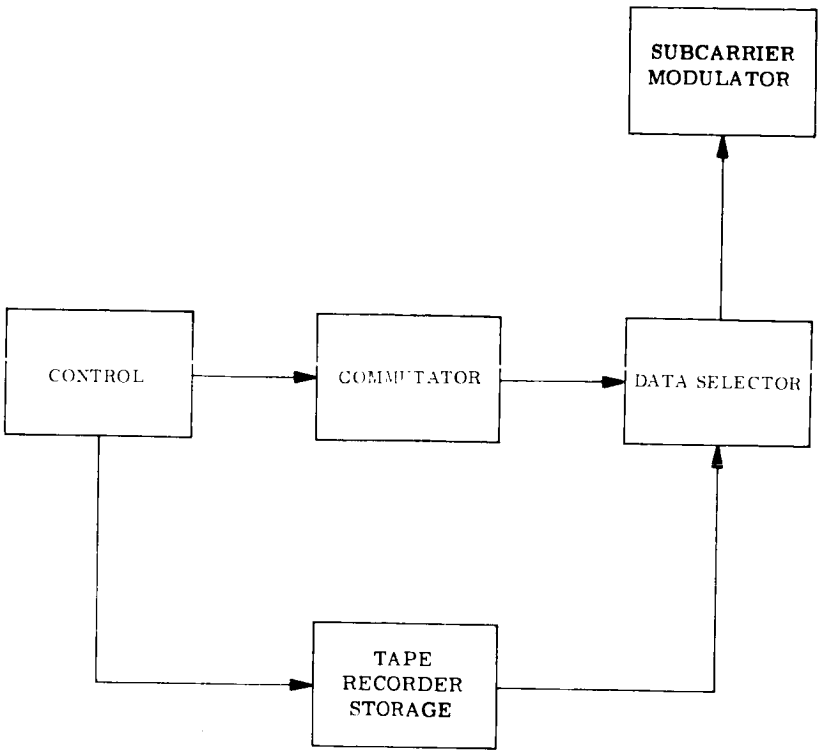

Figure 7-12. Tape Recorded and Real-Time Telemetry

7.3 ANALYSIS OF RESULTS

The preceding discussion is illustrative of the trade-off analysis performed in arriving at the preferred telecommunication system.

7.3.1 RADIO SUBSYSTEM

On the basis of the radio subsystem analysis the optimum configuration is three receivers, exciters, and power amplifiers in parallel redundancy as shown in Figure 7-5. All receivers are ON with only one exciter and power amplifier ON.

7.3.2 COMMAND SUBSYSTEM

The command subsystem trade-off analysis indicates that the optimum configuration is two detectors, two program control units, one decoder access unit, two decoders, and two power supplies in parallel redundancy as shown in Figure 7-8. The third command detector, however, is justified as a result of other trade-off analyses performed on the up link communication channel and the command subsystem. The third detector is a 30 bps command detector in contrast to the two nominal 1-bps detectors proposed. Thus, the command subsystem consists of two 1-bps detector, one 30-bps detector, three program control units, one decoder access, two decoders, and two power supplies. A block diagram of the proposed system is shown in Figure 7-13.

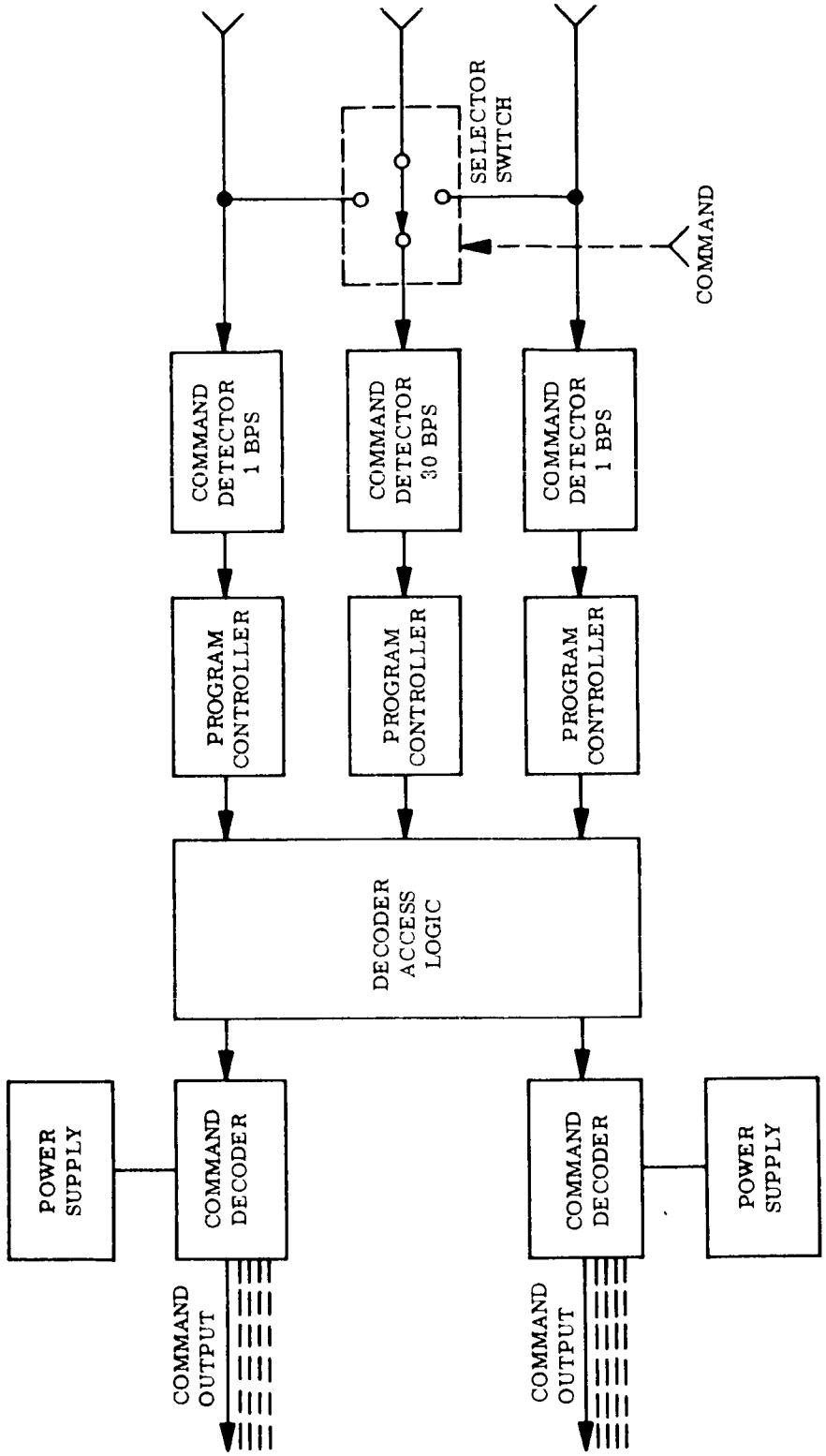

Figure 7-13. Preferred Command Subsystem Configuration

7.3.3 TELEMETRY SUBSYSTEM

The telemetry function analysis indicates that for the radio subsystem and command subsystem (1-bps mode) proposed, a certain amount of redundancy in the telemetry is required. Without this added redundancy one cannot justify the use of the redundant configuration proposed for the radio subsystem.

The final redundant configuration for the telemetry subsystem is analyzed in VB233AA105.

8.0 TELECOMMUNICATIONS EQUIPMENT TRADE-OFFS

8.1 EQUIPMENT PACKAGING TRADE-OFFS

The telecommunications equipment is generally divided into low frequency digital type electronics as typified by the Command Subsystem and radio frequency electronics as typified by the Radio and Relay Subsystems. Digital assemblies consist of many repetitive arrangements of components which require many in-out wires and connections. The rf assemblies use few repetitive circuits and many less in-out wires.

Because of the many repetitive higher level circuits, packaging of the digital assemblies is somewhat flexible, with the problems of handling the multitude of in-out wires causing the major constraint.

The design of rf circuitry has several difficulties which are not usually encountered in digital type equipment. These problems are generally due to the fact that linear rf circuits usually operate at low levels and are therefore many times more susceptible to interference, intermodulation, and crosstalk effects. Most successful radio frequency designs are characterized by the following:

a. Direct ground accessibility

b. Good component and power line decoupling

c. Controlled ground loops

d. Good shielding

e. Planned and controlled inter-connections

f. Controlled thermal paths

g. Good mechanical integrity.

The basic design philosophy for the Telecommunications system packaging is one which will afford the greatest flexibility in over-all spacecraft design without restricting system performance and will satisfy the above mentioned system characteristics. As defined in Section G "Spacecraft Design Criteria and Constraints" of the Preliminary Voyager 1971 Mission Specification, May 1, 1965, the system should contribute to the structural integrity of the spacecraft. The present design philosophy follows this to the extent that the individual subsystem module housings are used as stiffening members in the over-all spacecraft structure. To carry this approach further and attempt to utilize the actual component circuit boards, T-frames, etc., sacrifices the reliability of the system by stressing solder joints and component leads. It is intended in this design to isolate these from as many of the imposed spacecraft loads as possible.

Packaging techniques are used which permit standardization of connectors, system tiedown points, and certain of the housing dimensions where possible. This permits interchange of the subsystems or their subassemblies without the necessity of a major repackaging effort. A problem does exist in this area since the Radio Subsystem is designed so that the majority of the coax leads are held at a minimum length. Therefore standardization is traded-off in favor of lower coax power losses.

The allocations of bays for particular subsystems is coordinated with spacecraft design requirements. This bay allocation and the aforementioned standardization approach, in some instances, increases the volume requirements for a particular subsystem. As an example, the command subsystem requires approximately 964 cubic inches of volume. However, to be consistant with the standardized approach it occupies 1050 cubic inches.

8.2 EQUIPMENT ENVIRONMENT

The system is designed to take advantage of passive environmental control methods. The only environmental control system which can be termed active is required for temperature control of the system. However, it is actually a portion of the spacecraft and not the telecommunications system. This is defined more clearly in paragraph 8.2.3.

8.2.1 RFI PROTECTION

It is possible to shield the various portions of the system with extremely thin and lightweight housings. However, since it is desirable to assist in the structural make-up of the various subsystem bays where possible, the housing is adequately sized to do so. Not only does this ensure RFI protection but also ensures a relatively high resonant frequency for the housing which is compatible with the anticipated vibration inputs. Conduction heat transfer of the dissipated power also benefits.

8.2.2 VIBRATION AND SHOCK

The system is designed so that the subassembly forms a rigid tie from the thermal control/shear plate to the spacecraft structure and has the required strength and stiffness to withstand the rigorous shock and vibration inputs. With this design the shock and lower frequency vibration pulses are transmitted to the electronic housing at approximately one to one. The housing moves as a rigid unit for these inputs with no detrimental movement between individual components. The high frequency vibration pulses are attenuated by the vehicle structure. However, there is some input of these high frequencies which excites housing resonances. Degradation of circuit performance as a result of relative movement of components is reduced because the amplitude of this movement is small at high frequencies. The use of potted cordwood and integrated circuit modules in the Command subsystem completely eliminates the possibility of relative component movement.

This approach of using a relatively stiff housing rather than shock and vibration isolators reduces required volume and reduces the need for additional bay structure. It also serves the purpose of furnishing a good thermal conduction path.

8.2.3 TEMPERATURE AND PRESSURE

The system is designed so that it meets all of the three temperature-pressure environments encountered during a mission. The environments take place during: (1) prelaunch checkout, (2) launch, and (3) trajectory through mission end.

8.2.3.1 PRELAUNCH CHECKOUT ENVIRONMENT

During this phase, the equipment must be capable of operating with part temperatures well below their maximum rated limits. The equipment is designed to provide an optimum thermal path from the electrical components to their mounting plate, the "thermal integration plate". Analysis of the equipment mounted on this plate shows that during the prelaunch, some type of cooling must be provided for the thermal integration mounting plate. Further, the analysis shows that a simple mounting plate cooling system, incorporating a low velocity air flow over the plate, provides adequate cooling.

Two forced air cooling techniques are readily available. One incorporates a blower mounted to, and correctly oriented with, the thermal integration mounting plate. This design is somewhat prohibitive since the blower is a fixed part of the total equipment weight.

A more reasonable cooling approach is to use a cooling system which, during the prelaunch, circulates cool (60°F) air around the equipment. Air at this temperature and a nominal velocity of 4 ft/sec. provides adequate equipment part temperatures. It should be noted that this cooling system can be implemented with a removable shroud covering over the equipment, thus making the shroud a temporary fixture in terms of the mission phases, and an enclosure to conserve the system cooling air.

8.2.3.2 LAUNCH

During this phase of the mission, there is less than normal equipment power dissipation. The major source of heat is the aerodynamic heat input from the outer spacecraft shroud. However, due to the short time period ($\approx$ 100 sec) and the intervening spacecraft members, very little of this heat is transmitted to the equipment. The preliminary study shows that no special control systems are necessary for this environment.

8.2.3.3 TRAJECTORY THROUGH MISSION END

This temperature-pressure environment is the basis of the thermal design. As previously mentioned, thermal control is the only system which may be termed an active system. In actuality, the active portion is a set of controlled louvres attached to the spacecraft structure and is not a part of the telecommunications system. Heat transfer in general, in the compact nonisolated telecommunications system, takes the form of conduction from the components to the subsystem housings to the outer heat transfer plate. The outer plate is allowed to radiate to space through the open louvres or, depending on the temperature level, the louvers may be closed to conserve heat. It is necessary to selectively coat the outer plate with a pattern of varied emissivity finishes so that the entire subsystem is controlled uniformly in temperature. In this type system, the need for any integral active cooling system is eliminated and a saving in weight and complexity is made.

8.2.4 RADIATION

8.2.4.1 PROBLEM AREAS

A review of the Corpuscular Radiation for Preliminary Voyager, 1971, Mission Specification dated May 1, 1965, shows the following potential problem areas.

8.2.4.1.1 ON-BOARD ISOTOPE SOURCES

Assume 1 meter distance and 1 year.

Dose rate (both neutrons and gamma) $= 17.9 \times 10^{-3} \times 10^{2}$ ergs/hr

Number hours per year $= 8760$

Ergs/year $= \dfrac{8760 \times 17.9}{10} = 1.6 \times 10^{4}$ ergs/g(c) in 1 year.

This is approximately equivalent to a fatal dose for a human but its effect on electronic equipment would be negligible.

8.2.4.1.2 TRAPPED RADIATION BELTS (EARTH AND MARS)

Specified time-integrated flux;

Protons : 30 Mev = $10^7/cm^2$

Electrons: 500 Kev = $4 \times 10^{10}/cm^2$

Assume that in fly-by and orbit the worst case of 10^4 x the above time-integrated flux is received (as specified). Calculations show that under this assumption the total dose to an object outside the skin of the craft is extreme [about 10^{12} ergs/gm(c)]. However, the electrons are stopped by the spacecraft skin and intervening hardware. Assuming 0.01 percent of the electron radiation is converted to bremsstrahlung radiation (gamma), the dose is within a range tolerable to electronic equipment, namely, up to 2×10^8 ergs/gm(c). Normally, 1 millimeter of aluminum is assumed to reduce electron radiation to 1 per cent effectiveness. Lacking exact knowledge about the shielding provided in this spacecraft, it is observed that additional shielding may be required.

8.2.4.1.3 GALACTIC RADIATION

6 to 20 rads/year = 600 to 2,000 ergs/yr (negligible for electronic equipment).

8.2.4.1.4 SOLAR FLARES

Using the time-integrated proton flux specified, the yearly dose is calculated to be about 4×10^4 ergs/gm(c), which is of the same order of effectiveness as the on-board isotope source.

8.2.4.2 SUMMARY

In general, radiation problems are not anticipated, since the basic equipment packaging concepts are similar to Mariner C and "Venus Fly-by" equipments. These equipments have been successfully operated through typical radiation environment in interplanetary space.

Table 8-1, Summary of Permanent Radiation Effects upon Electronic Parts and Materials, shows that Teflon insulated materials are eliminated as an insulation material. For instance, where needed, B_eO standoff or feedthrough terminals are used.

Table 8-1. Summary of Permanent Radiation Effects Upon Electronic Parts and Materials

EFFECT OF GAMMA FLUX*

	General Effects	25% Permanent Damage Threshold
10^{12}	Resistors, capacitors, and ferrites seriously affected.	
		– Polystyrene
10^{11}		– High temp. epoxy (w/aromatic type catalysts) Glass-silicone laminates
	Transistors and diodes destroyed; Resistors, capacitors, and ferrites affected.	– Tubes (less if glass contains boron.)
10^{10}		– Melamine, Polyethylene, Mylar, Epoxy (w/dicyaniamide catalysts)
	Transistors and diodes seriously affected; only polyethylene-insulated wire and cable withstands.	
10^{9}		– Natural rubber, Neoprene, Phenolics (unfilled), Polyvinyl chloride (liberates hydrogen chloride)
	Transistors and diodes and plastic-insulated wire and cable affected	– Silicone rubber
10^{8}		– Nylon
10^{7}	Photocells affected	
	Equivalent Gamma Dose inside Spacecraft for 1 year in Inner Van Allen Belt	Teflon**
		Equivalent Gamma Dose Inside Spacecraft for 1 year in OUTER Van Allen Belt
10^{6}		
10^{5}		
	←Estimated fatal dose	
10^{4}		

*Note that temporary ionizing effects during irradation can disturb electrical functions.

**DuPont data shows Teflon in vacuum is better than shown by factor of 10.

Table 8-1. Summary of Permanent Radiation Effects Upon Electronic Parts and Materials (Continued)

EFFECT OF FAST NEUTRON FLUX

General Effects	Application Limits
10^{18}	
(Wirewound) (Film) Ferrites seriously affected; Resistors affected	
10^{17}	Silicon-iron, aluminum-iron, and 2v Permendur magnetic materials
(Composition) Ferrites affected	
10^{16}	
Capacitors affected	Glass, mica, ceramic capacitors Tubes (less if glass contains boron) Thermistors Nickel-iron magnetic materials
10^{15}	
10^{14} Transistors and diodes destroyed	Nylon and silicone rubbers
10^{13}	Plastic capacitors
Transistors and diodes seriously affected	Germanium semiconductors Magnetrons
Equivalent Neutron Dose Inside Spacecraft for 1 year in INNER Van Allen Belt*	Teflon** and most fluorinated compounds Oil-impregnated paper capacitors. Tantalum cap(tantalum is activated by neutron bombardment)
10^{12}	
Transistor and diode damage begins Photocells seriously affected	Silicon semiconductors
10^{11}	
10^{10} Estimated fatal dose	

*Based on assumption that protons with E > mev have some destructiveness as 1 mev neutrons. Also 1/10 of energy penetrates spacecraft.

**DuPont data shows Teflon in vacuum is better than shown by factor of 10.

The following items are used as guidance to achieve the expected radiation resistant operation of the equipment.

a. Eliminate Teflon and other fluorinated compounds

b. Avoid oil-filled paper capacitors and tantalum capacitors; use glass, mica, ceramic, and, if necessary, Mylar or polystyrene capacitors

c. Recognize wire insulation as a problem area, use polyethylene-insulated wire and cable.

d. Avoid elastomers; natural rubber is best if elastomers can't be eliminated.

e. If temperature permits, choose germanium transistors and diodes rather than silicon; also choose the narrow basewidth, high-frequency types as they are more radiation resistant than those with heavy bases. P-n-p types are preferred over n-p-n types.

f. Recognize that transistors fail by loss of current gain (β) and rise in leakage current (I_{CBO}); germanium diodes fail in the reverse direction, and silicon diodes fail by deterioration of forward characteristics (increase in forward voltage drop).

g. Structural metals should cause no concern.

Otherwise suitable additional shielding materials are utilized in the packaging design.

9.0 BIBLIOGRAPHY

9.1 JET PROPULSION LABORATORY DOCUMENTS

Request for Proposal 3601	Voyager Spacecraft System, January 19, 1965
V-MA-004-001-14-03	Preliminary Voyager 1971 Mission Specification May 1, 1965
V-MA-004-002-14-03	Voyager 1971 Mission Guidelines, May 1, 1965
Technical Memorandum 33-83 (Revision 1)	System Capabilities and Development Schedule of the Deep Space Instrumentation Facility, 1964-68, April 24, 1964
EPD-232	Mariner Mars 1966 Initial Design Concept, July 17, 1964

EPD-139, Vol. III	Study of Mars and Venus Orbiter Missions Launched by the Three-Stage Saturn C1B Vehicle, Dec. 31, 1963
EPD-158	Mariner Mars 1966 Study Report, July 29, 1963
EPD-250	Mariner Mars 1969 Orbiter Technical Feasibility Study, November 16, 1964
EPD-277	Mariner Spacecraft Functional Description, 5 May 1965
339-101	Typical Mechanization, Advanced Mariner Spacecraft Telemetry Subsystem
339-102	Typical Mechanization, Advanced Mariner Spacecraft Data Storage Subsystem
339-103	Typical Mechanization, Advanced Mariner Spacecraft Antenna Subsystem
339-104	Typical Mechanization Advanced Mariner, Spacecraft Radio Subsystem
339-105	Typical Mechanization, Advanced Mariner, Spacecraft Command Subsystem

APPENDIX I

MARINER C ANTENNA PERFORMANCE

Figure I-1 and I-2 indicate the performance of the Mariner C high-gain antenna in the region of planetary encounter for the 1971 and 1973 missions. Performance versus time is given and referenced to maximum antenna gain and a transmission range of 1.0 A. U. It is obtained from the relationship.

$$\text{System Performance} = -20 \log R_{AU} - (G_{max} - G)$$

where:

R_{AU} is range in AU

G_{max} is antenna gain on axis in db (23.5 db at 2295 mc)

G is antenna gain in the direction of earth in db

In Figure I-1, pre-encounter range versus time is based on the trajectory for a May 3, 1971 launch and November 1, 1971 encounter. After encounter, the Mars - Earth relationship is used. An August 15, 1973 launch and a January 26, 1974 encounter are assumed in Figure I-2.

$(G_{max} - G)$, the antenna pointing loss, is determined as follows:

a. The clock and cone angle to the earth from a sun-Canopus stabilized spacecraft are plotted for the late-cruise and in-orbit mission phases (May 3, 1971 plot shown in Figure I-3; August 15, 1973 plot shown in Figure I-4).

b. A transparent overlay is placed on the previously described plot. Inscribed on the overlay are scaled concentric ellipses representing the cross-section of the antenna beam. Each ellipse is for constant loss off axis.

c. Each curve of Figures I-1 and I-2 is constructed by placing the overlay in a particular position on the plot representing a fixed antenna position on the spacecraft. From the overlay the pointing loss is then determined for different positions of the earth on the focus as a function of time, assuming a one-degree additional pointing error due to alignment and spacecraft pointing errors.

d. To obtain the three curves for the May 3, 1971 launch, the overlay was placed such that the 0 db, 3 db, and 6 db points of the pattern's major axis fell on the point, J.D. 244,1286.5.

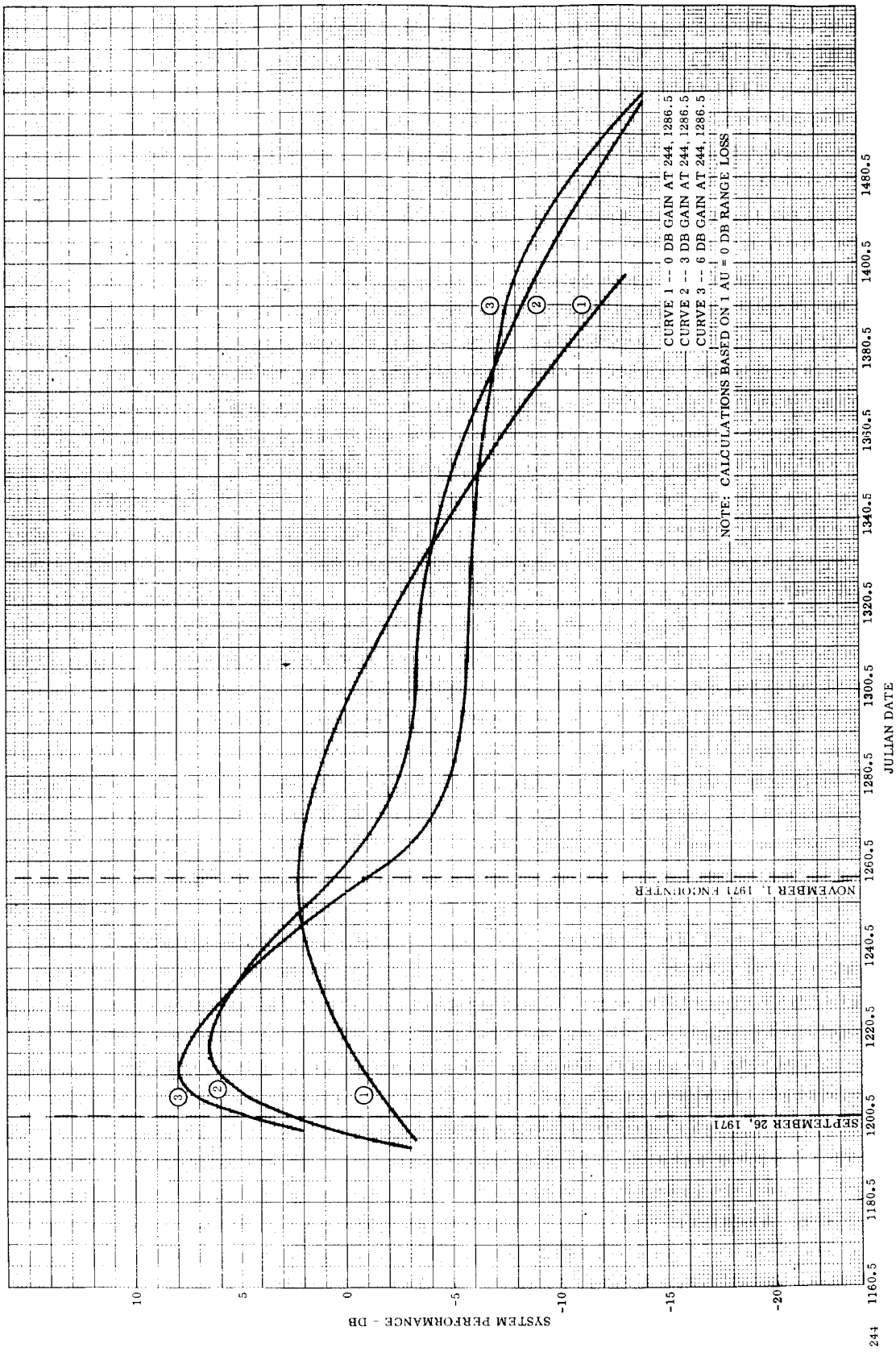

Figure I-1. System Performance Vs. Julian Date for May 3, 1971 Mission

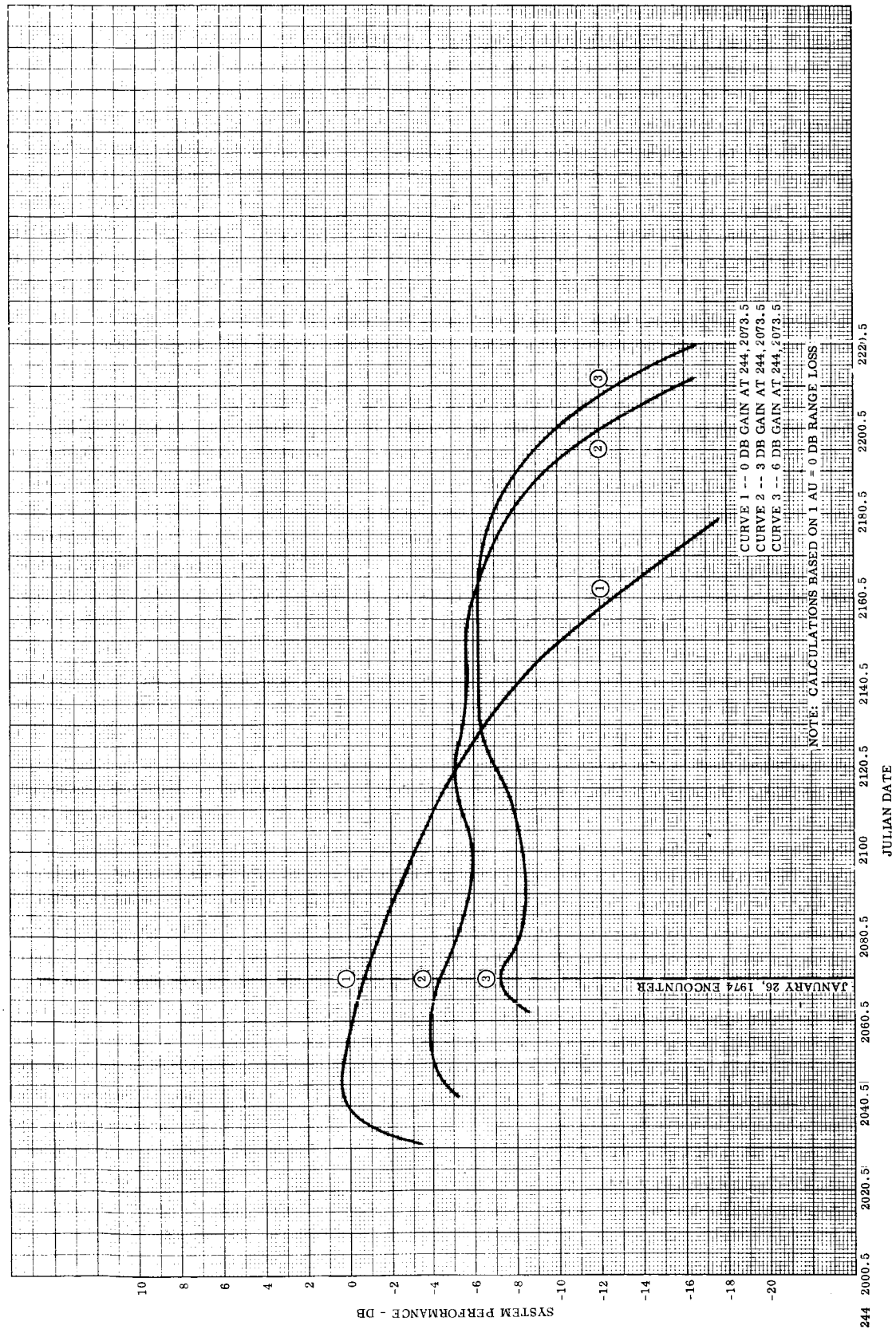

Figure I-2. System Performance Vs. Julian Date for August 15, 1973 Mission

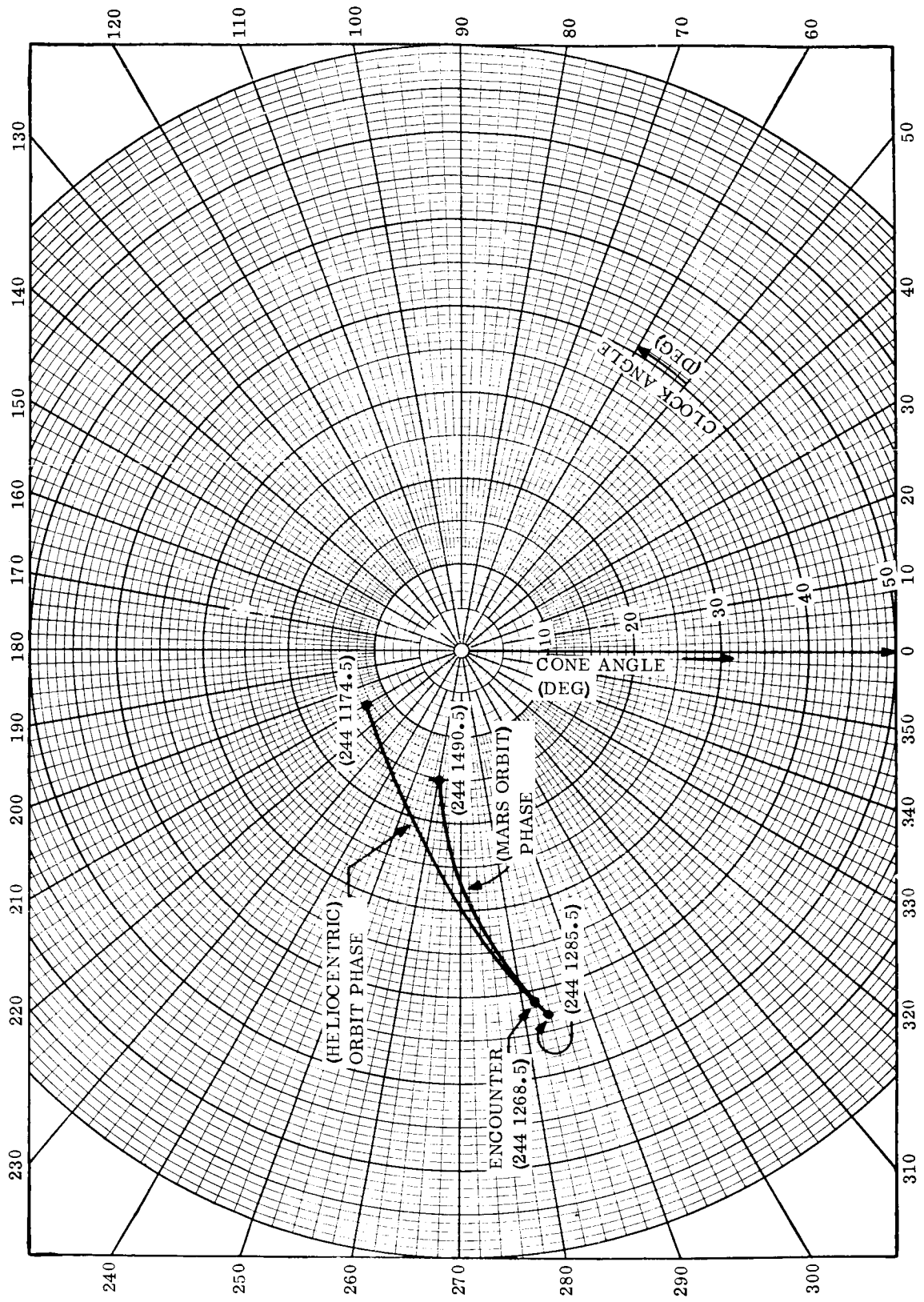

Figure I-3. Cone and Clock Angles to Earth Sun - Canopus Reference May 3, 1971
Launch November 1, 1971 Encounter

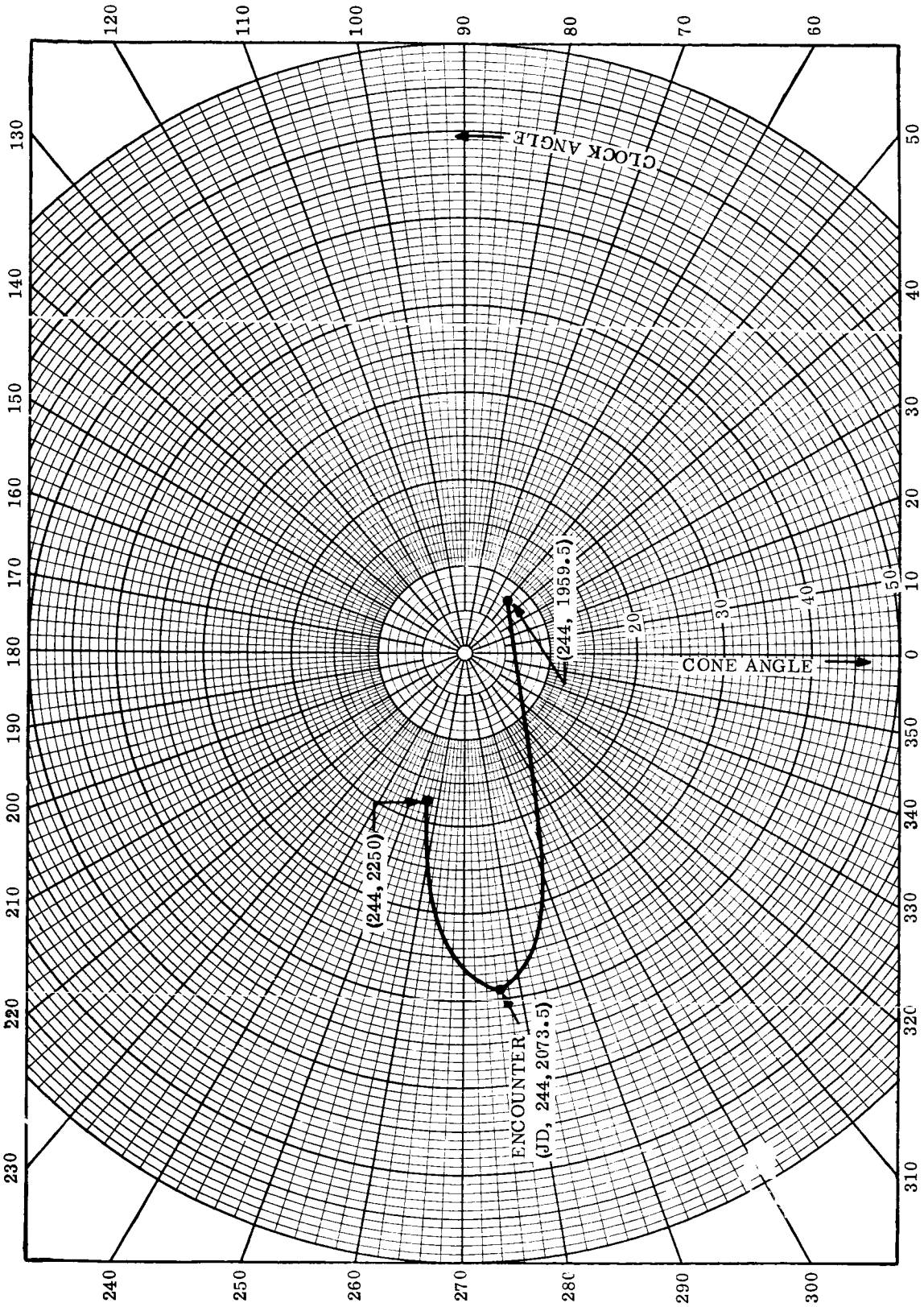

Figure I-4. Cone and Clock Angles to Earth Sun - Canopus Reference August 15, 1973
Launch January 26, 1974 Encounter

e. For the August 15, 1973 launch these points of the pattern were placed at J.D. 244, 2073.5.

f. In each case, the minor axis of the pattern was placed so as to give maximum coverage for the longest period of time.

The following conclusions were reached using the results of this investigation to determine transmission capability:

a. Several hundred bits per second can be transmitted through the fixed Mariner C antenna (fifty watts transmitter power) for several weeks, both before and after encounter.

b. Although the results are shown here for a single trajectory for each year, investigations using other trajectories indicated that the above conclusion is valid for all trajectories being considered.

APPENDIX II

RANGING

II.1 GENERAL

From the JPL Mission Specification, a constraint is placed on the Voyager Telecommunication System that the spacecraft equipment be compatible with the Deep Space Instrumentation Facility as it presently exists, and is planned to exist, per JPL document EPD-283. An additional constraint is that "turnaround" ranging shall be used.

II.2 SPACECRAFT TO GROUND RANGING SIGNAL

From the constraints, a working assumption is made that the ground ranging subsystem is of the Mod II type, and operates similarly to the Mark I. The theoretical performance of the Mark I ranging subsystem has been analyzed in Reference 1.*

If range code acquisition time is not a governing factor, the threshold of the ground ranging system is essentially the threshold of the range clock tracking phase-locked loop in the range clock receiver. A block diagram of the range clock receiver is reproduced below as Figure II-1 from JPL Specification DOR-1076-DSN, Figure 24.

From equation F.1.3 (6), Reference 1, the signal to noise ratio (SNR) at the input to the range loop may be written as

$$\left.\frac{S_c}{N_c}\right]_{B_L} = L_D L_K \sin^2(\Delta\varphi_r) \prod_{i=1}^{K} J_o^2(\Delta\varphi_i) \left[\frac{S_i}{N_i}\right]_{B_L} \qquad \text{(A2-1)}$$

where:

B_L is the closed-loop noise bandwidth of the clock-loop,

L_D is a detection loss factor between zero and unity,

L_K is a correlation loss factor between zero and unity,

$\Delta\varphi_r$ is the carrier phase deviation of the range code,

$\Delta\varphi_i$ are the carrier phase deviations of an arbitrary number, K, of sinusoidal subcarriers, and $\left.\frac{S_i}{N_i}\right]_{B_L}$ is the ratio of total signal-to-noise at the input to the range clock receiver, with noise computed in the bandwidth of the range clock loop.

*Reference numbers refer to corresponding references listed on page II-10 at the end of this appendix.

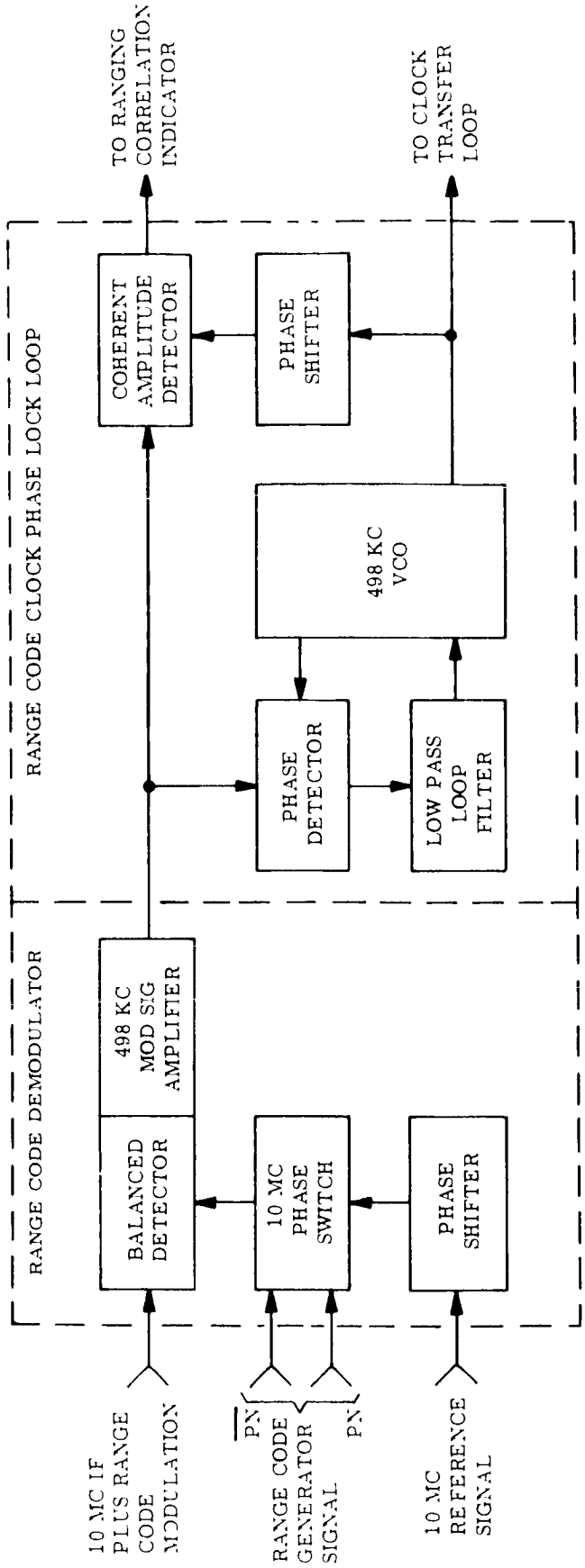

Figure II-1. Range Code Demodulator and Clock Detector

Since the Voyager Spacecraft employs a square wave telemetry subcarrier, equation (A2-1) must be modified somewhat. There are two cases. The range code may be transmitted separately or with the square wave telemetry subcarrier.

$$\left.\frac{S_c}{N_c}\right]_{B_L} = L_D L_K \sin^2(\Delta\varphi_r) \left[\frac{S_i}{N_i}\right]_{B_L} ; \text{ Range code only} \qquad \text{(A2-2)}$$

$$\left.\frac{S_c}{N_c}\right]_{B_L} = L_D L_K \sin^2(\Delta\varphi_r) \cos^2(\Delta\varphi_t) \left[\frac{S_i}{N_i}\right]_{B_L} ; \text{ Range Code and Telemetry} \qquad \text{(A2-3)}$$

where $\Delta\varphi_t$ is the carrier phase deviation by the telemetry square wave.

Equations (A2-2) and A2-3) employ the idealizing assumptions that the carrier modulating signals are perfectly square; that is, they have only the values plus or minus $\Delta\varphi_r$ and $\Delta\varphi_t$. Also, the correlation loss, L_K, includes losses due to partial acquisition of the range code by the range clock receiver and losses due to the range code "turnaround" in the spacecraft channel. Losses due to interference between the ranging and telemetry signals are neglected under the assumption that if the signals are transmitted simultaneously, proper selection of the telemetry subcarrier frequency may be made to minimize interference.

From equation F.1.5(10), Reference 1, the ratio of correlation signal-to-noise spectral density at the output of the range code correlator is given as

$$\frac{S_o}{|\Phi_o|} = L_D L_O \sin^2(\Delta\varphi_r) \prod_{i=1}^{K} J_o^2(\Delta\varphi_i) \frac{S_i}{|\Phi_i|} \qquad \text{(A2-4)}$$

where $|\Phi_i|$ is the value of spectral density at the input of the range clock receiver, L_O is a correlation loss factor, between zero and unity, due to sequential acquisition of the sub-codes of the ranging code, and spacecraft turnaround correlation loss.

As in equations (A2-2) and (A2-3), equation (A2-4) may be modified for Voyager as

$$\frac{S_o}{|\Phi_o|} = L_D L_O \sin^2(\Delta\varphi_r) \frac{S_i}{|\Phi_i|} ; \text{ Range Code only} \qquad \text{(A2-5)}$$

$$\frac{S_o}{|\Phi_o|} = L_D L_O \sin^2(\Delta\varphi_r) \cos^2(\Delta\varphi_t) \frac{S_i}{|\Phi_i|} ; \text{ Range Code and Telemetry} \qquad \text{(A2-6)}$$

From equation F.1.5 (13), Reference 1, an expression for range code acquisition time may be written as

$$T_a = \left[\Sigma P_i\right] \left[T_1 N_1 + T_m\right] \qquad \text{(A2-7)}$$

where

T_a is acquisition time,

ΣP_i is the sum of the bauds in the subcodes,

T_1 is the integration time in the digital ranging equipment required for the sub-code having the greatest information content.

N_1 is the number of information bits in the longest sub-code.

T_m is the machine delay time between trial correlations.

The approximation in equation (A2-7) is valid for the sum of bauds in the sub-codes much greater than unity.

The required integration time in the digital ranging equipment is a function of the available $S_o / |\Phi_o|$ and the information content of the longest sub-code. Required integration time may be obtained from Easterling's Figure, Reference 2.

From Reference 1 the worst case value of the various losses are taken as

$$\left.\begin{aligned} L_D &= -0.8 \text{ db} \\ L_K &= -12 \text{ db} \\ L_o &= -16 \text{ db} \end{aligned}\right\} \quad \text{not including spacecraft turnaround losses} \qquad \text{(A2-8)}$$

II.3 GROUND TO SPACECRAFT SIGNAL

The square wave channel of the spacecraft receiver may be taken to be the turnaround ranging channel, containing a video limiter which feeds the phase modulator of the spacecraft transmitter. This channel is shown, explicitly, in Figure II-2.

For the Voyager the SNR at the limiter input are taken as in equations (A3-15), (A3-16), and (A3-17) of Appendix III.

$$\left.\frac{S_m}{N_m}\right] B_L = \sin^2 (\Delta\varphi_r) \left[\frac{S_i}{N_i}\right] B_L \quad ; \quad \text{Range code only} \qquad \text{(A2-9)}$$

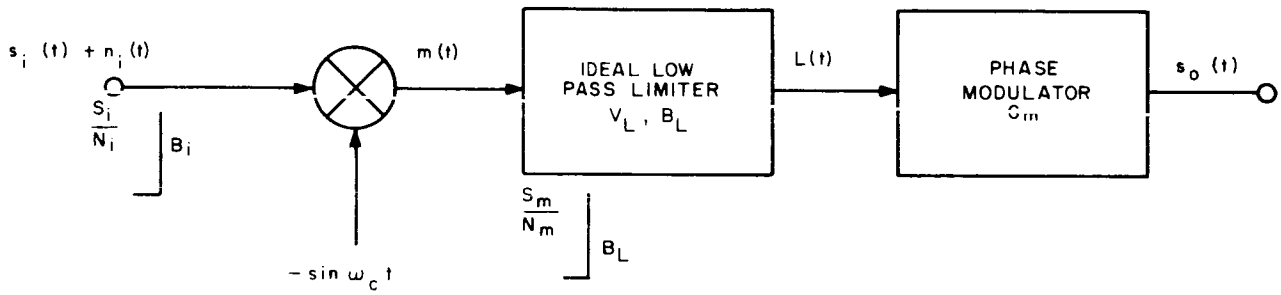

Figure II-2. Turnaround Channel with Post-Detection Limiting

$$\left.\frac{S_m}{N_m}\right]_{B_L} = \sin^2(\Delta\varphi_r)\cos^2(\Delta\varphi_{cs})\,J_o^2(\Delta\varphi_{cd})\left[\frac{S_i}{N_i}\right]_{B_L};$$

Range Code and command (A2-10)

where $\Delta\varphi_{cs}$ is the carrier phase deviation by the command synchronizing signal, and $\Delta\varphi_{cd}$ is the carrier phase deviation by the command data signal. The equations employ the idealizing assumption that the input bandwidth is at least twice the limiter bandwidth.

The terms which are functions of the carrier phase deviations may be defined as "modulation losses", L_m, so that in general,

$$\left.\frac{S_m}{N_m}\right]_{B_L} = L_m \left.\frac{S_i}{N_i}\right]_{B_L} \qquad \text{(A2-11)}$$

The input noise is taken as a sample function of a white Gaussian band-limited process as

$$n_i(t) = x(t) \cos \omega_c t - y(t) \sin \omega_c t \tag{A2-12}$$

where x (t) and y (t) are sample functions of independent lowpass Gaussian processes.

The variance of the noise process, y (t), is defined

$$\text{Var } y(t) \overset{\Delta}{=} \sigma_y^2 \tag{A2-13}$$

σ_y^2 is related to the variance of the input noise process, $n_i(t)$, by

$$\sigma_y^2 = \sigma_{n_i}^2 \tag{A2-14}$$

It is assumed that the limiter has an ideal square transmission bandwidth, B_L, which is equal to or narrower than half the ideal square input bandwidth, B_i. That is,

$$B_L \leq \frac{B_i}{2} \tag{A2-15}$$

The signal to noise ratio (SNR) into the limiter is then dependent on a white Gaussian, band-limited noise process, $y_L(t)$, whose variance is related to that of y (t) by

$$\sigma_{y_L}^2 = 2 \frac{B_L}{B_i} \sigma_y^2 \tag{A2-16}$$

It is seen that the limiter SNR is a function not only of the bandwidth ratio, but also of the modulation loss, L_m.

Assuming for simplification that the signal has range code modulation only, the limiter output L (t), is a waveform having only the values $\pm V_L$, where V_L is the voltage limiting level. Under no-noise conditions the limiter output is identically

$$L(t) = V_L C_r(t) \text{ ; no-noise; } C_r(t) = \pm 1 \text{ only.} \tag{A2-17}$$

With increasing channel noise, the limiter output contains increasing false transitions and decreasingly resembles the code $C_r(t)$.

In general, the limiter output may be defined as

$$L(t) \triangleq V_L C_L(t) \; ; \; C_L(t) = \pm 1 . \tag{A2-18}$$

$C_L(t)$ is identically equal to $C_r(t)$ only in the no-noise case.

In Reference 3, Easterling has derived a normalized correlation factor, C, which is the relative correlation between $C_r(t)$ and $C_L(t)$. C is given in Reference 3 as

$$C = P(A) - P(D) \tag{A2-19}$$

where P(A) is the probability of agreement of $C_r(t)$ and $C_L(t)$ and P(D) is the probability of disagreement between $C_r(t)$ and $C_L(t)$. Since $C_L(t)$ must either agree or disagree with $C_r(t)$,

$$P(A) + P(D) = 1 \tag{A2-20}$$

and

$$C = 2P(A) - 1 \tag{A2-21}$$

It is seen that the limiter output will agree with $C_r(t)$ if the following two conditions are met:

1. $y_L(t) > -A\sqrt{L_m}$ when $C_r(t) = +1$

and

2. $y_L(t) < A\sqrt{L_m}$ when $C_r(t) = -1$

where A is carrier amplitude.

Conditions 1 and 2 are expressible in probabilistic notation as

$$P(A) = P\left\{\left[y_L(t) > -A\sqrt{L_m}\right] \cdot \left[C_T(t) = +1\right]\right\} \vee P\left\{\left[y_L(t) < A\sqrt{L_m}\right]\left[C_T(t) = -1\right]\right\} \tag{A2-22}$$

where

$\cdot$ is the logical "and"

$\vee$ is the logical "or"

Since $C_T(t) = +1$ and $C_r(t) = -1$ are mutually exclusive events and since the code variable C_r is statistically independent of the noise variable, y_L, equation (A2-22) simplifies to

$$P(A) = P\left\{\left[y_L(t) > -A\sqrt{L_m}\right] P\left[C_r(t) = +1\right] + P\left[y_L(t) < A\sqrt{L_m}\right] P\left[C_r(t) = -1\right]\right\} \quad \text{(A2-23)}$$

Now, $Y_L(t)$ is Gaussian, with zero mean and variance $\sigma_{y_L}^2$, so that

$$P\left[y_L(t) > -A\sqrt{L_m}\right] = 1 - \Phi\mu\left(\frac{-A\sqrt{L_m}}{\sigma_{y_L}}\right) \quad \text{(A2-24)}$$

and

$$P\left[y_L(t) < A\sqrt{L_m}\right] = \Phi\mu\left(\frac{A\sqrt{L_m}}{\sigma y_L}\right) \quad \text{(A2-25)}$$

where $\Phi\mu$ is the normal distribution function. Assuming for simplicity that the range code is balanced so that

$$P\left[C_r(t) = +1\right] = P\left[C_r(t) = -1\right] = 1/2 \quad \text{(A2-26)}$$

we have

$$P(A) = 1/2\left[1 - \Phi_u\left(\frac{-A\sqrt{L_m}}{\sigma y_L}\right)\right] + 1/2\left[\Phi_u\left(\frac{A\sqrt{L_m}}{\sigma y_L}\right)\right] \quad \text{(A2-27)}$$

and

$$C = \Phi_u\left(\frac{A\sqrt{L_m}}{\sigma y_L}\right) - \Phi_u\left(\frac{-A\sqrt{L_m}}{\sigma y_L}\right) \quad \text{(A2-28)}$$

Also,

$$\frac{A\sqrt{L_m}}{\sigma y_L} = \sqrt{L_m \frac{B_i}{B_L} \frac{S_i}{N_i}}\,B_i \quad \text{(A-29)}$$

Since, also,

$$\Phi_u (X) = 1/2 \left[1 + \text{erf} \left(\frac{X}{\sqrt{2}} \right) \right] \tag{A2-30}$$

and

$$\text{erf} (-X) = - \text{erf} (x) \tag{A2-31}$$

We have, finally

$$C = \text{erf} \left[\sqrt{\frac{L_M}{2} \frac{B_i}{B_L} \frac{S_i}{N_i}} \; B_i \right] \tag{A2-32}$$

The factor C represents a loss in correlation of the turned-around ranging code with a noiseless replica code. As such, C may be applied to computations involving the ground system range clock receiver and code correlator.

For purposes of uniformity of symbolism we will redefine C as

$$C \triangleq \sqrt{L_c} \triangleq \text{erf} \left[\sqrt{\frac{L_m}{2} \frac{B_i}{B_L} \frac{S_i}{N_i}} \; B_i \right] \tag{A2-33}$$

The output signal from the phase modulator may now be defined as

$$s_o (t) = A_o \cos [\omega_c t + G_m V_L C_L (t)] \tag{A2-34}$$

A code phase deviation, $\Delta\varphi_{ro}$, for the down-link may be defined as

$$\Delta\varphi_{ro} \triangleq G_m V_L \tag{A2-35}$$

so that

$$s_o (t) = Ao \cos [\omega_c t + \Delta\varphi_{ro} C_L (t)] \tag{A2-36}$$

Several important observations to be made about the post-detection limiting scheme are that although the retransmitted code may suffer a loss in correlation with the original range code, the retransmitted carrier is "clean", being unperturbed by turned-around noise, and the modulation level of the retransmitted code is exactly adjustable.

REFERENCES

1. Painter, John H., and Hondros, George, "Unified S-band Telecommunication Techniques for Apollo, Vol. II", to be published as a Technical Note in 1965 by the National Aeronautics and Space Administration, Washington, D. C.

2. Easterling, M., and Schootler, P. H., "Maximum Likelihood Acquisition of a Ranging Code", Research Summary 36-12, Vol. I, Jet Propulsion Laboratory, Pasadena, California, Jan. 2, 1962, page 81.

3. Easterling, M., "Analysis of the Effect of a Limiter on a Square Wave Signal Plus Additive Gaussian Noise", Research Summary No. 36-14, Jet Propulsion Laboratory, Pasendena, California, May 1, 1962, pp. 59-61.

APPENDIX III

SIGNAL DESIGN

III.1 GENERAL

In the JPL Mission Specification, the radio frequency signals and modulation techniques are constrained to be compatible with the Deep Space Instrumentation Facility (DSIF) equipment as it presently exists and as it is planned to exist according to JPL document EPD-283. The implications of the constraint are that the rf carriers are phase modulated using relatively small phase deviations. The modulating waveforms are sinusoids and square waves, which may, themselves, be angle modulated.

An integral part of the design of a telecommunication system employing such signals is the design of the signals themselves. This appendix presents the design equations necessary for signal design.

These types of signals are treated in detail in Reference 1*. Although, at the time of writing of this appendix, Reference 1 was not published in final form, it had been reviewed in rough draft form by JPL on January 19, 1965.

Reference 1 forms the basis for much of the following appendix. Material from the reference is so noted.

III.2 SIGNAL MODEL

A signal which is phase modulated by one square wave and an arbitrary number, K, of sinusoids is modeled as

$$s(t) = A \cos \left[\omega_c t + \Delta\varphi_r C_r(t) + \sum_{i=1}^{K} \Delta\varphi_i \sin \left(\omega_i t + \varphi_i(t) \right) \right] \qquad \text{(A3-1}$$

where

A is the carrier peak amplitude,

ω_c is the carrier radian frequency,

$\Delta\varphi_r$ is the peak radian deviation of the carrier by the square wave

$C_r(t)$ is a square wave having only values of plus and minus unity,

$\Delta\varphi_i$ is the peak radian deviation of the carrier by the ith sinusoid,

*Reference numbers refer to correspondingly numbered reference listed on a separate page at the rear of this Appendix.

ωi is the radian frequency of the ith sinusoid, and

$\varphi_i(t)$ is the angle modulation function on the ith sinusoid.

With the aid of the Giacolleto expansion (Reference 2) the signal is written as

$$s(t) = \Bigg[A \cos \Delta\varphi_r \sum_{n_1=-\infty}^{\infty} \cdots \sum_{n_k=-\infty}^{\infty} \prod_{i=1}^{K} J_{n_i}(\Delta\varphi_i) \cos \Bigg[\Big(\omega_c t + \sum_{i=1}^{K} n_i (\omega_i t + \varphi_i(t)) \Big] - C_r(t) \sin \Delta\varphi_r \sum_{n_1=-\infty}^{\infty} \cdots \sum_{n_k=-\infty}^{\infty} \prod_{i=1}^{K} J_{n_i}(\Delta\varphi_i) \sin \Bigg[\omega_c t + \sum_{i=1}^{K} n_i \Big(\omega_i t + \varphi_i(t)\Big) \Bigg\} \tag{A3-2}$$

III.3 NOISE MODEL

It is assumed that to the signal channel is added a noise process which is characterized by Gaussian statistics. Furthermore, the frequency spectrum of the noise is idealized as being "white," "band-limited" over the frequency region of interest. A sample function of the process is modeled as

$$n(t) = x(t) \cos \omega_c t - y(t) \sin \omega_c t \tag{A3-3}$$

where ω_c is the center radian frequency of the noise spectrum, and $x(t)$ and $y(t)$ are sample functions of independent Gaussian processes. The expected values of the processes are zero. The variances are related as

$$\sigma_x^2 = \sigma_y^2 = \sigma_n^2 \tag{A3-4}$$

The spectral desnity of the band-limited process is idealized as being constant within a bandpass of width, Δ_ω, and zero elsewhere. Then the spectral densities are related as

$$\Phi_x(\omega) = \Phi_y(\omega) = 2 \left| \Phi_N(\omega) \right| ; \left| \omega \right| \leq \frac{\Delta\omega}{2} = 0 \text{ ; all other } \omega . \tag{A3-5}$$

It should be noted that since spectral densities of time functions are either Fourier transforms of autocorrelation functions or products of Fourier transforms with their conjugates, and since the noise process is modeled as a real function of time, then the spectral densities are two-sided; that is, the spectral densities exist for positive and negative real frequencies.

If the noise spectral density is characterized in terms of an equivalent noise temperature, we have

$$|\Phi_N| = \frac{KT_n}{2} \qquad \text{(A3-6)}$$

where K is Boltzmann's constant and T_n is the equivalent noise temperature in degrees Kelvin.

III.4 SIGNAL DEMODULATION

The signal channel demodulator is idealized as a perfect, balanced, product detector. The demodulating reference signal is generated by a modulation restrictive phase-locked loop. The bandpass limiter preceding the modulation restrictive loop is of sufficient bandwidth to pass the residual carrier component of the modulated signal, but is sufficiently narrow to reject most of the modulation products.

The signal-to-noise ratio at the input to the bandpass limiter for the residual carrier component, computed in a bandwidth equal to the threshold loop noise bandwidth of the modulation restrictive loop, is taken from equation 2.1. (3) of Reference 1 as

$$\left.\frac{S_c}{N_c}\right]_{B_{L_o}} = \cos^2(\Delta\varphi_r) \prod_{i=1}^{K} J_o^2(\Delta\varphi_i) \left[\frac{S_i}{N_i}\right]_{B_{L_o}} \qquad \text{(A3-7)}$$

where $\left.\frac{S_i}{N_i}\right]_{B_{L_o}}$ is the ratio of total channel signal power to noise in the loop noise bandwidth, B_{L_o}. It should be noted that the modulated signal occupies a bandwidth greater than B_{L_o}. However, it is only the noise computation which involves B_{L_o}. The total signal power is taken regardless of its modulated bandwidth.

Equation (A3-7) is modified specifically for Voyager which has signals containing one sine wave, or one square wave, or one sine wave and square wave, or one sine wave and two square waves. The latter case is not directly derivable from equation (A3-7) but is easily derived in a like manner.

$$\left.\frac{S_c}{N_c}\right]_{B_{L_o}} = J_o^2(\Delta\varphi) \left.\frac{S_i}{N_i}\right]_{B_{L_o}} \quad ; \text{ one sine wave} \qquad \text{(A3-8)}$$

$$\left.\frac{S_c}{N_c}\right] B_{L_o} = \cos^2 (\Delta\varphi) \left.\frac{S_i}{N_i}\right] \cdot B_{L_o} \quad ; \text{ one square wave} \qquad \text{(A3-9)}$$

$$\frac{S_c}{N_c} B_{L_o} = \cos^2 (\Delta\varphi_{sq}) J_o^2 (\Delta\varphi_{sin}) \left.\frac{S_i}{N_i}\right] B_{L_o} \quad ; \text{ one sine wave and one square wave} \qquad \text{(A3-10)}$$

$$\left.\frac{S_c}{N_c}\right] B_{L_o} = \cos^2 (\Delta\varphi_{sq_1}) \cos^2 (\Delta\varphi_{sq_2}) \quad ; \text{ one sine wave and two square waves} \qquad \text{(A3-11}$$

$$J_o^2 (\Delta\varphi_{sin}) \left.\frac{S_i}{N_i}\right] B_{L_o}$$

Assuming that the reference signal is sufficiently "clean" that no additional loss is incurred, signal-to-noise ratios (SNR) are derived at the inputs of the various sinusoidal and square wave detection channels in the appropriate input bandwidths. The square wave channels generally have low-pass input filters, while the sine wave channels have bandpass input filters.

From equation D.1.4.1.(6) of Reference 1, equations for the cases analagous to those of equations (A3-8), (A3-10), and (A3-11) are derived for the SNR at the input to the sine wave channel in its bandwidth, B_{sin}.

$$\left.\frac{S_{sin}}{N_{sin}}\right] B_{sin} = 2J_1^2 (\Delta\varphi_{sin}) \left[\frac{S_i}{N_i}\right] B_{sin} \quad ; \text{ one sine wave} \qquad \text{(A3-12)}$$

$$\left.\frac{S_{sin}}{N_{sin}}\right] B_{sin} = 2J_1^2 (\Delta\varphi_{sin}) \cos^2 \quad ; \text{ one sine and one square wave} \qquad \text{(A3-13)}$$

$$(\Delta\varphi_{sq}) \left[\frac{S_i}{N_i}\right] B_{sin}$$

$$\left.\frac{S_{sin}}{N_{sin}}\right] B_{sin} = 2J_1^2 (\Delta\varphi_{sin}) \cos^2 \qquad \text{; one sine and two square waves} \qquad \text{(A3-14)}$$

$$(\Delta\varphi_{sq_1}) \cos^2 (\Delta\varphi_{sq_2}) \left[\frac{S_i}{N_i}\right] B_{sin}$$

Likewise, from equation F.1.3.(6) of Reference (1), equations for the cases analagous to those of equations (A3-9), (A3-10), and (A3-11) are derived for the SNR at the input to one square wave channel in its bandwidth, B_{sq}.

$$\left.\frac{S_{sq_1}}{N_{sq_1}}\right] B_{sq_1} = \sin^2 (\Delta\varphi_{sq_1}) \left[\frac{S_i}{N_i}\right] B_{sq_1} \qquad \text{; one square wave} \qquad \text{(A3-15)}$$

$$\left.\frac{S_{sq_1}}{N_{sq_1}}\right] B_{sq_1} = \sin^2 (\Delta\varphi_{sq_1}) J_o^2 \qquad \text{; one sine and one square wave} \qquad \text{(A3-16)}$$

$$(\Delta\varphi_{sin}) \left[\frac{S_i}{N_i}\right] B_{sq_1}$$

$$\left.\frac{S_{sq_1}}{N_{sq_1}}\right] B_{sq_1} = \sin^2 (\Delta\varphi_{sq_1}) \cos^2 \qquad = \text{one sine and two square waves} \qquad \text{(A3-17)}$$

$$(\Delta\varphi_{sq_2}) J_o^2 (\Delta\varphi_{sin}) \left[\frac{S_i}{N_i}\right] B_{sq_1}$$

The functions of phase deviations in equations (A3-8) through (A3-11) are defined as carrier suppressions, L_c . The functions of phase deviations in equations (A3-12) through (A3-17) are defined as modulation losses, L_m .

Equations (A3-8) through (A3-17) are valid if the channel transmission bandwidths are sufficient to pass the modulation products. For the sinusoidal signals, it is sufficient to pass the first order modulation products, since these are the only products detected. For the square wave channels, the required bandwidth is theoretically infinite. Practically, a bandwidth which passes the third order products is sufficient, since less than 10% of the square wave power resides in products higher than third order.

III.5 SIGNAL DESIGN

Signal design is essentially choosing the various carrier phase deviations according to some rule. Subcarrier frequencies and square wave repetition rates are generally constrained by the individual channels, themselves. Care should be exercised so that higher order modulation products and cross-modulation products do not fall in any of the data channels.

For Voyager, design of the signals is performed as given in Reference 3. The rule is to pick phase deviations so that all data channel SNR reach minimum allowable values simultaneously under conditions of decreasing total signal power. Care is exercised so that the residual carrier component is not overly sensitive to changes or tolerances in phase deviation. Martin's rule is applied to keep the rms carrier phase deviation at approximately one radian (Reference 4).

III.6 SENSITIVITY OF RESIDUAL CARRIER TO SINE WAVE AND SQUARE WAVE NARROW-PHASE MODULATION

This section examines the sensitivity of the residual carrier component of a signal, which is narrow-phase modulated by either sine waves or square waves, to small changes in modulation index.

The signal model is

$$s(t) = A \cos \left[\omega_c t + \Delta\varphi_s \sin \left(\omega_s t + \varphi_s(t)\right)\right] \tag{A3-18}$$

for the sine wave modulation, or

$$s(t) = A \cos \left[\omega_c t + \Delta\varphi_c C(t)\right] \tag{A3-19}$$

for the square wave modulation. The power remaining in the residual carrier component may be described by a carrier suppression factor, L_c, which is the ratio of residual carrier component power to total signal power. L_c is given (Reference 1) for the two models above as

$$L_c = J_o^2(\Delta\varphi_s) \; ; \; 0 < L_c < 1 \tag{A3-20}$$

and

$$L_c = \cos^2(\Delta\varphi_c) \; ; \; 0 < L_c < 1 \tag{A3-21}$$

respectively.

In decibel notation,

$$L_c \triangleq 20 \log_{10} \left[\frac{1}{J_o(\Delta\varphi_s)} \right] \text{ db} ; \quad 0 < L_c < \infty \tag{A3-22}$$

$$L_c \triangleq 20 \log_{10} \left[\csc(\Delta\varphi_c) \right] \text{ db}; \quad 0 < L_c < \infty \tag{A3-23}$$

Now the rate of change of L_c with respect to modulation index, in db per radian is given by the derivatives as

$$\frac{d(L_c)}{d(\Delta\varphi_s)} = 20 \log_{10} e \left[\frac{J_1}{J_0} (\Delta\varphi_s) \right] \text{ db/rad} \tag{A3-24}$$

$$\frac{d(L_c)}{d(\Delta\varphi_c)} = 20 \log_{10} e \left[\tan(\Delta\varphi_c) \right] \text{ db/rad} \tag{A3-25}$$

or approximately as

$$\frac{d(L_c)}{d(\Delta\varphi_s)} = 8.67 \frac{J_1}{J_0} (\Delta\varphi_s) \text{ db/rad} \tag{A3-26}$$

$$\frac{d(L_c)}{d(\Delta\varphi_c)} = 8.67 \tan(\Delta\varphi_c) \text{ db/rad} \tag{A3-27}$$

Equations (A3-26) and (A3-27) are graphed in Figure III-1 over the range of zero to 2.0 radians.

Figure III-2 plots carrier suppression and modulation loss versus carrier phase deviation for modulation by square waves and sinusoids.

Observation of Figure III-2 shows several interesting facts. In the region of one radian rms phase deviation, the sine wave and square wave give approximately equal carrier suppression. The pure square wave has less modulation loss than the sinusoid by about 0.75 db. The fundamental sinusoidal component of the square wave has modulation loss almost equal to the sine wave.

It is assumed that about equal noise bandwidths are required to cover either the sine wave or sinusoidal component of the square wave. However, to recover the entire square wave requires at least three times the noise bandwidth of the other two. This reduces the net SNR of the square wave some 4 db below either the pure sine wave or the sinusoidal component of the square wave.

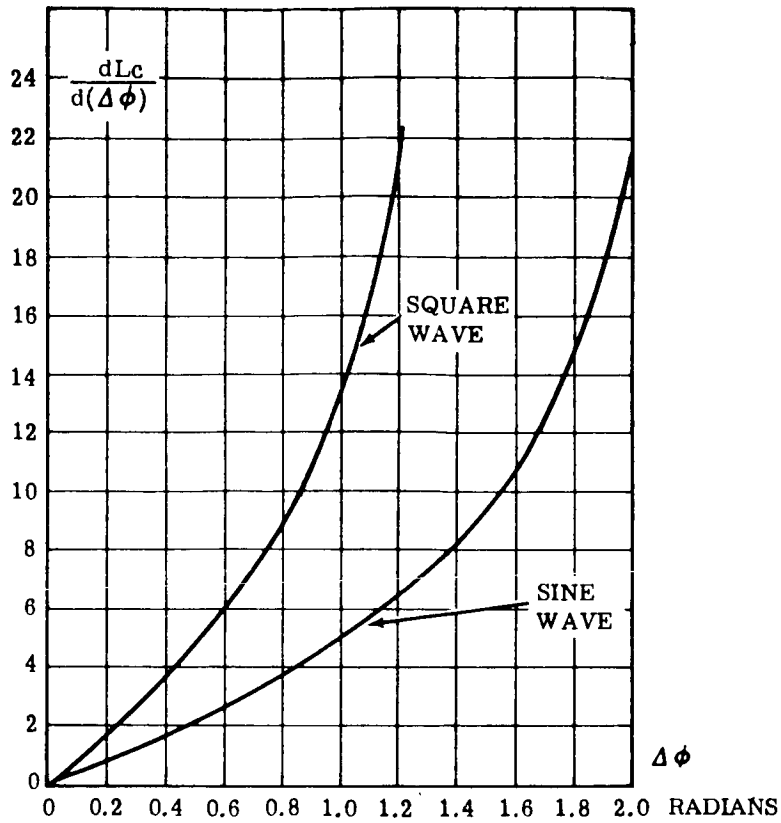

Figure III-1. Rate of Change of Carrier Suppression Versus Modulation Index in Decibels per Radian

Observation of Figure III-1 shows that for the region of one radian rms deviation, the carrier is three times more sensitive to tolerances in deviation for the square wave than for the sine wave.

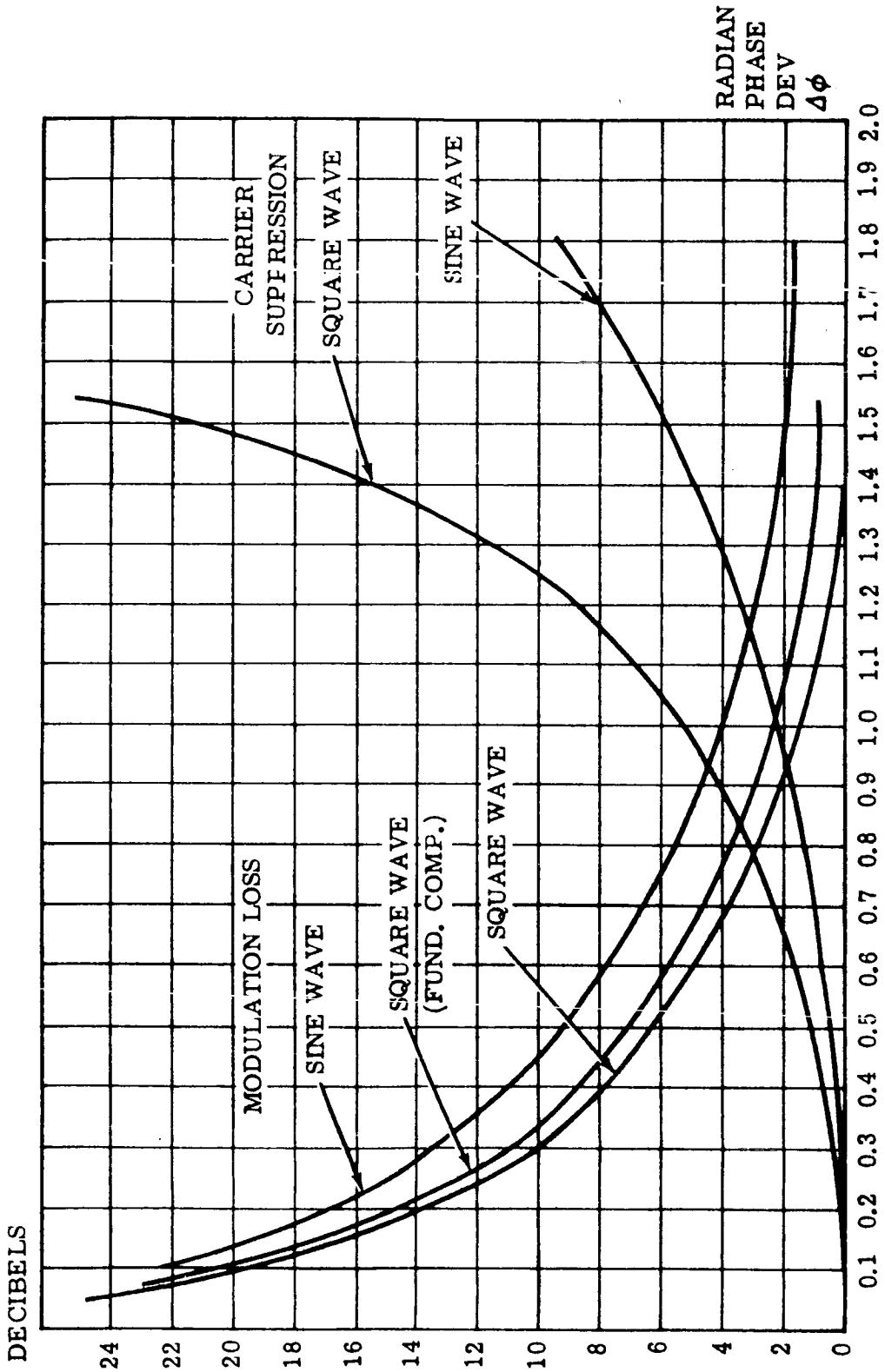

Figure III-2. Modulation Loss and Carrier Suppression Versus Modulation Index for Sine Wave and Square Wave

REFERENCES

1. Painter, John H., and Hondros, George, "Unified S-band Telecommunication Techniques for Apollo -- Volume II," to be published as a Technical Note in 1965, by National Aeronautics and Space Administration, Washington, D. C.

2. Giacolleto, L. J., "Generalized Theory of Multitone Amplitude and Frequency Modulation," Proc. IRE, Vol. 35, pp. 680-693, July 1947.

3. Painter, John H., "Synthesis Techniques for a Class of Phase-Modulated Signals," Proceedings of the 1965 IEEE Conference on Aerospace, Vol. AS-3, Number 2, Supplement, June 1965, pp. 264-269.

4. Martin, Benn D., "The Pioneer IV Lunar Probe: A Minimum-Power FM/PM System Design," Technical Note 32-215, Jet Propulsion Laboratory, Pasadena, California, March 15, 1962, page 22.

APPENDIX IV

SAMPLE RELIABILITY CALCULATION

IV.1 INTRODUCTION

As an example of the trade-off analysis made on the telecommunication system of the Voyager, the radio subsystem operational mode of transmit and receive via a low-gain antenna was selected. This is the only case in the telecommunication system analysis where a function does not include portions of more than one subsystem. The mission time of 6320 hours plus an environmental use factor of 8 to adjust for the effect of vibration and shock during a one-hour launch is used in the analysis.

IV.1.1 SCOPE

The analysis is made starting with a basic configuration consisting of a receiver, exciter, power amplifier, and associated switching as shown in Figure IV-1. The basic configuration is then modified by adding redundant components for the least reliable component until the system constraints are met. The receiver and exciter are considered a transponder pair, i.e., when a redundant receiver is added a corresponding exciter must also be added. Each time redundant components are added the reliability is re-evaluated. This process is continued until either the reliability, weight, and/or power allocations are met.

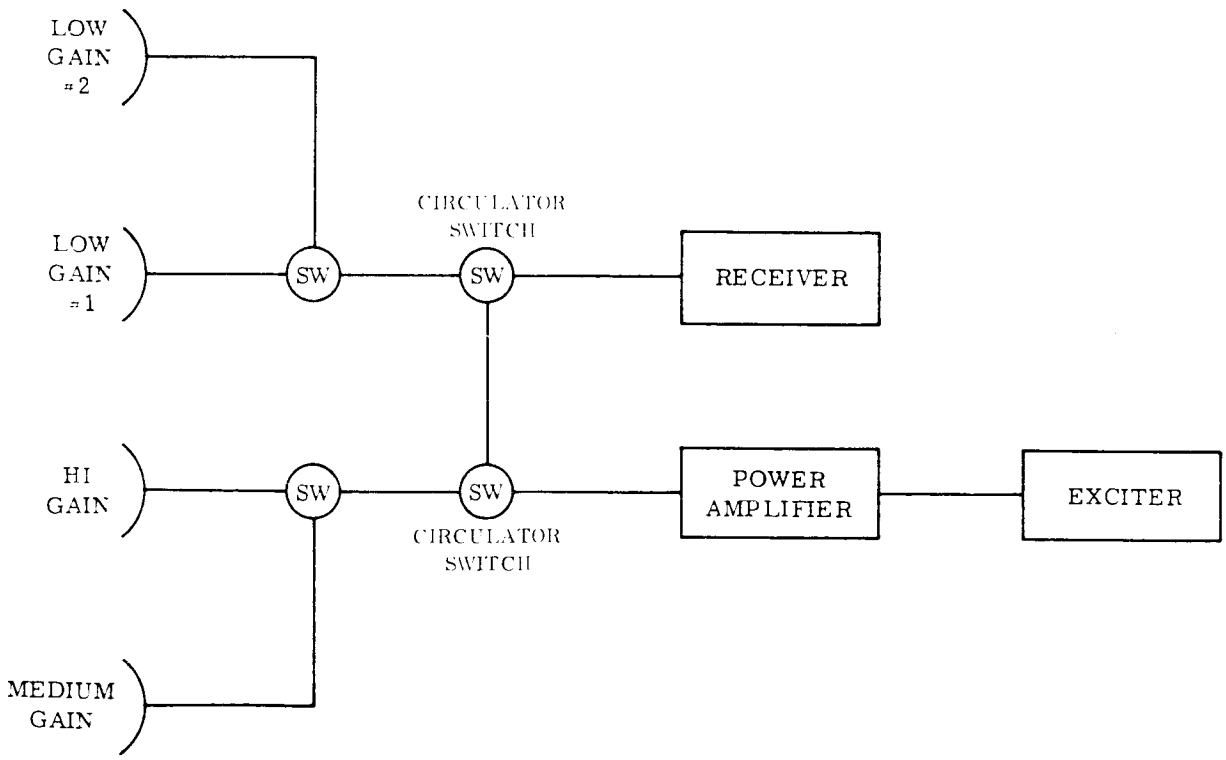

Figure IV-1. Basic Radio Configuration

IV.2 RELIABILITY ANALYSIS

IV.2.1 BASIC CONFIGURATION

The failure rate for the basic configuration shown in Figure IV-1 was evaluated by adding the failure rates for the equipment.

Receiver	1.7169	$\times 10^{-5}$
Power Amplifier	0.7826	$\times 10^{-5}$
Exciter	0.9266	$\times 10^{-5}$
Coaxial Switch (Normal)	0.025	$\times 10^{-5}$
Coaxial Switch (Normal)	0.025	$\times 10^{-5}$
Circulator Switch	0.250	$\times 10^{-5}$
Circulator Switch	0.250	$\times 10^{-5}$
FR_1 =	3.9761	$\times 10^{-5}$

The failure rates for the switches reflect the failure rate for one switch needed in both switching conditions to complete the radio function.

The reliability of this configuration is calculated from the expression

$$SR_1 = \exp(-FR_1 \times t) \qquad (1)$$

or

$$SR_1 = \exp(-3.9761 \times 10^{-5} \times 6328) = 0.777551.$$

IV.2.2 CONFIGURATION TWO

A second receiver, exciter, power amplifier, and diplexer in parallel redundancy is added to the basic configuration. A block diagram of this system is shown in Figure IV-2.

The reliability analysis considers the two sets of equipments operating in parallel with a transfer switch.

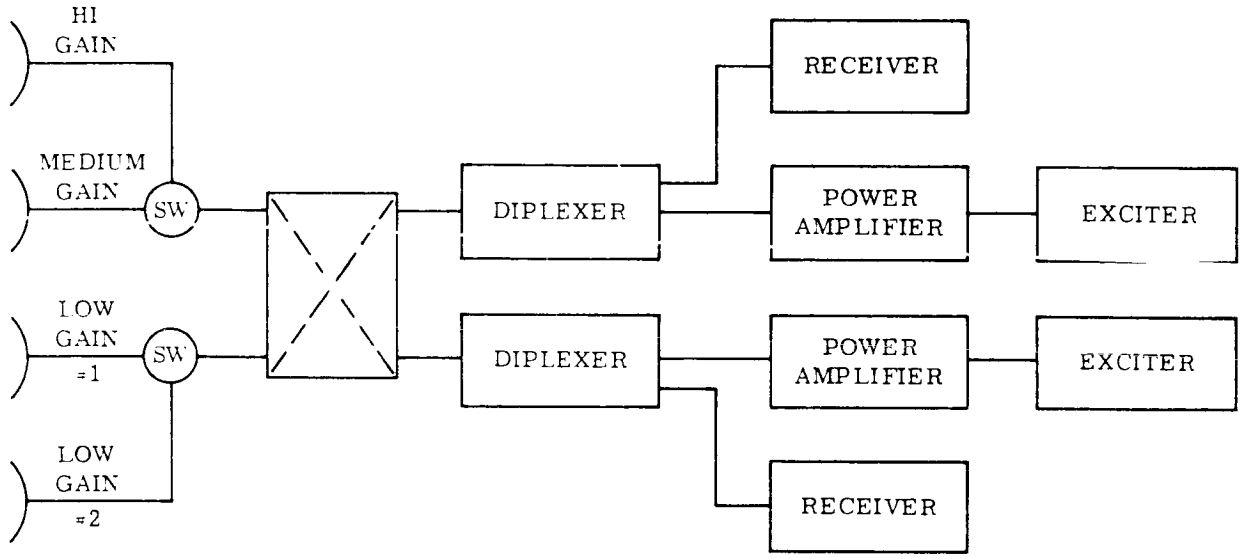

Figure IV-2. Configuration Number Two

IV.2.2.1 TRANSFER SWITCH

The reliability for the coaxial switch is determined by applying its failure rate, $FR_2 = 0.025 \times 10^{-5}$ to the expression

$$R_2 = \exp(-FR_2 \times t) \qquad (2)$$

or

$$R_2 = \exp(-0.025 \times 10^{-5} \times 6328) = 0.998418.$$

IV.2.2.2 RECEIVER/TRANSMIT SETS

Each redundant set of equipments is analyzed separately.

The failure rate for the set using the normal switch mode of the transfer switch is:

Receiver	1.7169	$\times 10^{-5}$
Exciter	0.9266	$\times 10^{-5}$

Power Amplifier	0.7826	$\times 10^{-5}$
Diplexer (3 Conn.)	0.0300	$\times 10^{-5}$
Transfer Switch (Normal)	0.0200	$\times 10^{-5}$
FR_3 =	3.4761	$\times 10^{-5}$

The reliability of this set is calculated using the expression

$$R_3 = \exp(-FR_3 \times t) \tag{3}$$

or

$$R_3 = \exp(-3.4761 \times 10^{-5} \times 6328) = 0.80251.$$

The failure rate for each set using the activated transfer switch is:

Receiver	1.7169	$\times 10^{-5}$
Exciter	0.9266	$\times 10^{-5}$
Power Amplifier	0.7826	$\times 10^{-5}$
Diplexer (3 Conn)	0.0300	$\times 10^{-5}$
Transfer Switch (Activated)	0.2000	$\times 10^{-5}$
FR_4 =	3.6561	$\times 10^{-5}$

The reliability for this set is found using

$$R_4 = \exp(-FR_4 \times t)$$

or

$$R_4 = \exp(-3.6561 \times 10^{-5} \times 6328) = 0.79342. \tag{4}$$

IV.2.2.3 OVER-ALL RELIABILITY

The reliability for the second configuration is given by the expression

$$SR_2 = R_2 \left[R_3 + (1 - R_3) R_4\right] \tag{5}$$

or

$$SR_2 = 0.998418 \left[0.80251 + (1-0.80251)(0.79342)\right] = 0.957682.$$

IV.2.3. CONFIGURATION THREE

The third configuration shown in Figure IV-3 is identical to the second configuration, except with a hybrid connecting the exciters and power amplifiers to allow either exciter to drive either power amplifier.

IV.2.3.1 RECEIVER/POWER AMPLIFIER COMBINATION

The failure rate for the series string items is the sum of the failure rates for each component in the string. The failure rate of the series string with the transfer switch in its normal position is:

Receiver	1.7169	$\times 10^{-5}$
Diplexer	0.0300	$\times 10^{-5}$
Transfer Switch (Normal)	0.0200	$\times 10^{-5}$
Power Amplifier	0.7826	$\times 10^{-5}$
Hybrid (1 Conn.)	0.005	$\times 10^{-5}$
FR_5 =	2.5545	$\times 10^{-5}$

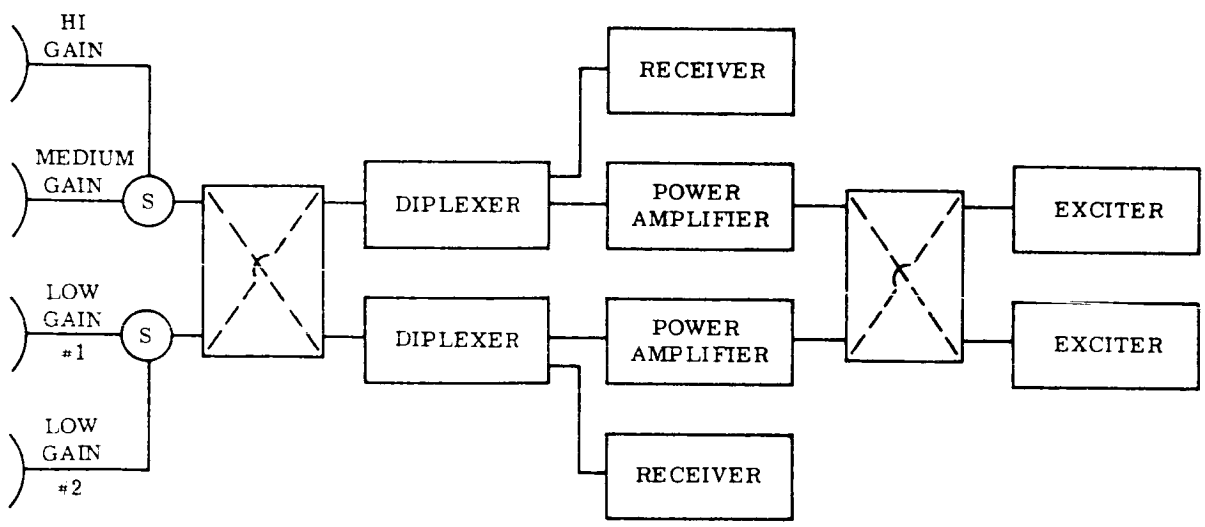

Figure IV-3. Configuration Number Three

The reliability of this string is calculated using

$$R_5 = \exp(-FR_5 \times t) \qquad (6)$$

or

$$R_5 = \exp(-2.5545 \times 10^{-5} \times 6328) = 0.85078.$$

The failure rate of the series string with the transfer switch activated is:

Receiver	1.7169	$\times 10^{-5}$
Diplexer	0.0300	$\times 10^{-5}$
Transfer Switch (Active)	0.2000	$\times 10^{-5}$
Power Amplifier	0.7826	$\times 10^{-5}$
Hybrid (1 Conn)	0.005	$\times 10^{-5}$
$FR_6 =$	2.7345	$\times 10^{-5}$

The reliability of this string is calculated using (7)

$$R_6 = \exp(-FR_6 \times t)$$

or $$R_6 = \exp(-2.7345 \times 10^{-5} \times 6328) = 0.84113.$$

The reliability of the receiver/power amplifier string is calculated using

$$R_7 = R_5 + (1-R_5)\ R_6 \qquad (8)$$

or

$$R_7 = 0.85078 + (0.14922)(0.84113) = 0.97629.$$

IV.2.3.2 REDUNDANT EXCITERS

The failure rate for an exciter and coupler is:

Exciter	0.9266	$\times 10^{-5}$
Hybrid (1 Conn)	0.0050	$\times 10^{-5}$
$FR_8 =$	0.9316	$\times 10^{-5}$

The reliability of this set is calculated using

$$R_8 = \exp(-FR_8 \times t) \tag{9}$$

or

$$R_8 = (0.9316 \times 10^{-5} \times 6328) = 0.94275.$$

The reliability of the two exciter-coupler sets redundant is calculated using

$$R_9 = R_8 [1 + (1-R_8)] \tag{10}$$

or

$$R_9 = (0.94275)(1.05725) = 0.99672.$$

IV.2.3.3 OVER-ALL RELIABILITY

The reliability for the third configuration is given by the expression

$$SR_3 = R_2 \times R_7 \times R_9 \tag{11}$$

or

$$SR_3 = (0.998418)(0.97629)(0.99672) = 0.97155.$$

IV.2.4 CONFIGURATION FOUR

A third receiver, exciter, power amplifier and diplexer set was added in parallel redundancy as shown in Figure IV-4.

IV.2.4.1 REDUNDANT SETS

The failure rate for this redundant set using the normal mode transfer switch is:

Transfer Switch (Normal)	0.0200
Receiver	1.7169
Power Amplifier	0.7826
Exciter	0.9266
Diplexer (3 Conn)	0.0300

$$FR_{10} = 3.4761 \times 10^{-5}$$

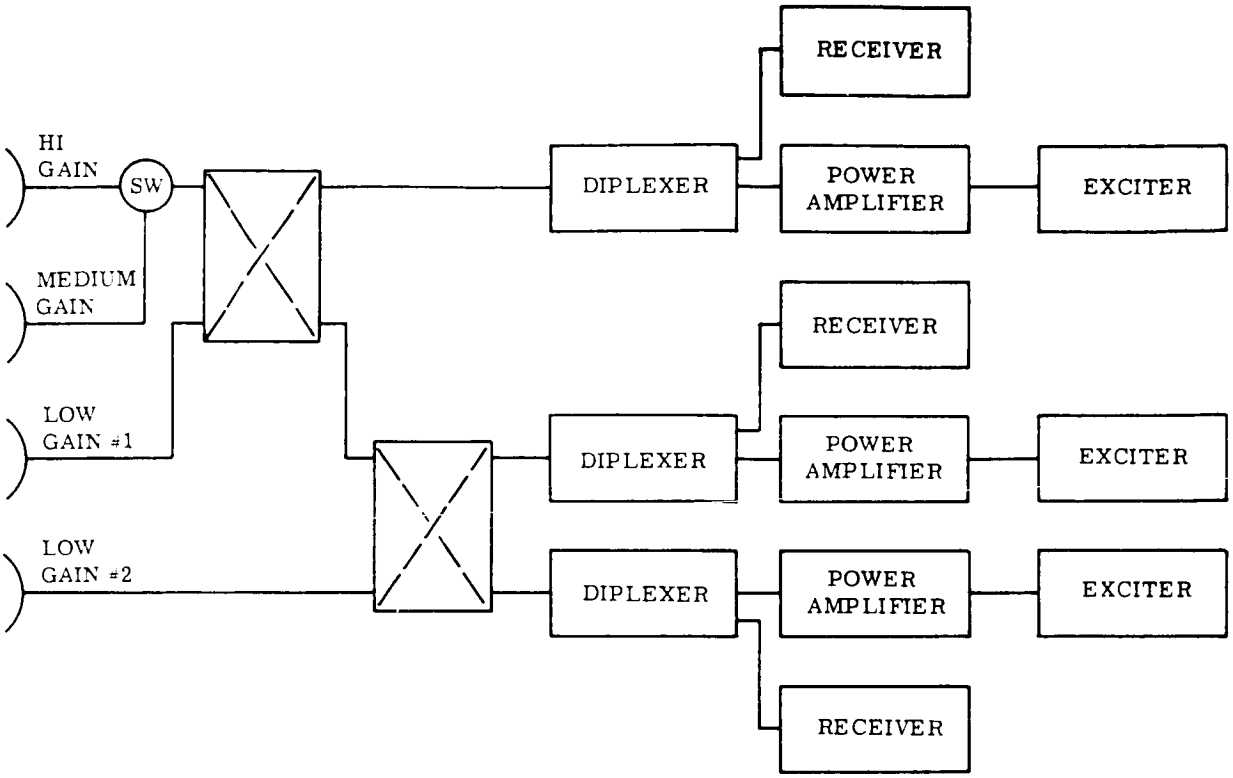

Figure IV-4. Configuration Number Four

The reliability of this set is calculated using

$$R_{10} = \exp\ (-FR_{10} \times t) \tag{12}$$

or

$$R_{10} = \exp\ (-3.4761 \times 10^{-5} \times 6328) = 0.80267.$$

Two of the redundant sets are connected by a transfer switch in its activated mode. The failure rate of these sets is

Receiver	1.7169	$\times 10^{-5}$
Power Amplifier	0.7826	$\times 10^{-5}$
Exciter	0.9266	$\times 10^{-5}$
Diplexer (3 Conn)	0.0300	$\times 10^{-5}$
Transfer Switch (Active)	0.200	$\times 10^{-5}$
FR_{11} =	3.6561	$\times 10^{-5}$

The reliability of each of these sets is calculated using

$$R_{11} = \exp\ (-FR_{11} \times t) \tag{13}$$

or

$$R_{11} = \exp\ (-3.6561 \times 10^{-5} \times 6328) = 0.79342.$$

IV.2.4.2 TRANSFER SWITCH

The reliability of the transfer switch in its normal position (nonactivated) is calculated using

$$R_{12} = \exp\ (-0.02 \times 10^{-5} \times 6328) \tag{14}$$

or

$$R_{12} = 0.998734.$$

IV.2.4.3 OVER-ALL RELIABILITY

The reliability of configuration four is given by the expression

$$SR_4 = R_{12}\ [R_{10} + (1-R_{10})\ R_{11}] + \left\{1 - R_{12}\ [R_{10} + (1-R_{10})\ R_{11}]\right\} R_{11} \tag{15}$$

or

$$SR_4 = 0.99133.$$

IV.2.5 CONFIGURATION FIVE

The fifth configuration is the same as number four, except there are two hybrid couplers connected as shown in Figure IV-5. The addition of these couplers allows more than one exciter to be used with a power amplifier. The analysis for this configuration is divided into three phases of redundant operation

IV.2.5.1 PHASE I

This phase considers the probability of at least one exciter providing drive for power amplifier number one and receiver one operating. From previous calculations the reliability of each exciter is 0.94275.

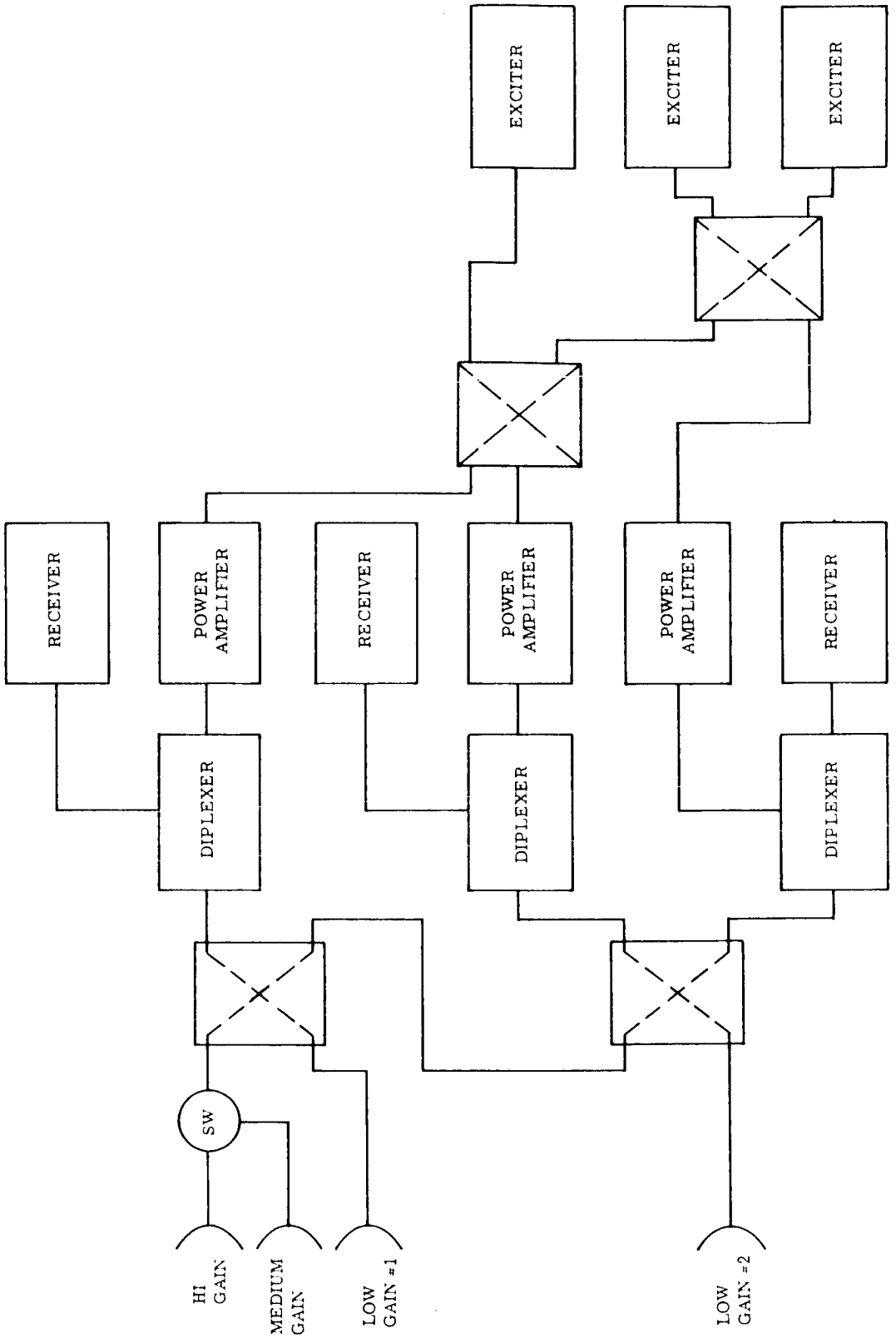

Figure IV-5. Configuration Number Five

IV.2.5.1.1 HYBRID COUPLER

The rf output from exciters two and three must travel through two common connections of the hybrid coupler to reach the input of the power amplifier.

The probability of success for these two connections is calculated using

$$R_{13} = \exp\ (-FR_{13} \times t) \tag{16}$$

where FR_{13} is the failure rate of the two connections. The reliability, R_{13}, is

$$R_{13} = \exp\ (0.01 \times 10^{-5} \times 6328) = 0.999367.$$

IV.2.5.1.2 POWER AMPLIFIER #1/RECEIVER #1 COMBINATION

The failure rate for the entire power amplifier number one through receiver number one series string is:

Power Amplifier	0.7826	$\times 10^{-5}$
Diplexer	0.0300	$\times 10^{-5}$
Receiver	1.7169	$\times 10^{-5}$
Transfer Switch (Active)	0.2000	$\times 10^{-5}$
Hybrid (1 Conn)	0.005	$\times 10^{-5}$
FR_{14} =	2.7345	$\times 10^{-5}$

The reliability of this string is calculated using

$$R_{14} = \exp\ (-FR_{14} \times t) \tag{17}$$

or

$$R_{14} = \exp\ (-2.7345 \times 6328) = 0.84109.$$

IV.2.5.1.3 REDUNDANT EXCITERS

The reliability of exciter two and exciter three in parallel redundancy via the hybrid coupler is calculated using the expression

$$R_{15} = [R_{Exciter} + R_{Exciter}\ (1-R_{Exciter})]\ R_{13} \tag{18}$$

Evaluating equation (18) the probability of success, R_{15}, is

$$R_{15} = [0.94275 + (0.94275)(0.05725)]\ 0.999367$$

or

$$R_{15} = 0.99609.$$

IV.2.5.1.4 OVER-ALL RELIABILITY

The reliability for Phase I is calculated using the preceding reliabilities in the expression

$$R_{16} = [R_{15} + (1-R_{15})\ R_{14}]\ R_{14} \qquad (19)$$

or

$$R_{16} = [0.99609 + (0.00391)(0.94275)]\ 0.84109 = 0.84090.$$

IV.2.5.2 PHASE II

This phase considers the reliability of set number two together with the three exciters and two hybrid couplers.

IV.2.5.2.1 POWER AMPLIFIER #2/RECEIVER #2 COMBINATION

The failure rate for one coupler, power amplifier, receiver, diplexer and transfer switch is:

Power Amplifier	0.7826	$\times\ 10^{-5}$
Receiver	1.7169	$\times\ 10^{-5}$
Diplexer (3 Conn)	0.0300	$\times\ 10^{-5}$
Hybrid (1 Conn)	0.005	$\times\ 10^{-5}$
Transfer Switch (Normal)	0.0200	$\times\ 10^{-5}$
FR_{17} =	2.5545	$\times\ 10^{-5}$

The reliability of this string of equipments is calculated using the expression

$$R_{17} = \exp\ (-FR_{17} \times t) \qquad (20)$$

or

$$R_{17} = \exp\ (-2.5545 \times 10^{-5} \times 6328) = 0.85078.$$

IV.2.5.2.2 OVER-ALL RELIABILITY

Using the transfer switch in its normal unswitched condition, the expression for the reliability of Phase II is

$$R_{18} = [R_{15} + (1-R_{15})\ R_{Exciter}]\ R_{Switch}\ R_{17} \tag{21}$$

or

$$R_{18} = (0.99978)\ (0.85078)\ (0.99873).$$

Therefore, the reliability for Phase II is 0.84951.

IV.2.5.3 PHASE III

Phase III considers the reliability of set number three with exciters two and three and one hybrid coupler. Because of identical components the reliability of this phase can be expressed using previously calculated quantities as

$$R_{19} = [R_{Exciter} + R_{Exciter}\ (1-R_{Exciter})]\ R_{14}\ R_{Switch} \tag{22}$$

or

$$R_{19} = [0.94275 + (0.005725)\ (0.94275)]\ (0.85078)\ (0.998734).$$

Therefore, the reliability of Phase III is 0.84691.

IV.2.5.4 OVER-ALL EVALUATION

For the three sets in parallel as shown in Figure IV-5, the reliability of configuration five is given by the expression

$$SR_5 = [1 - (1-R_{16})\ (1-R_{18})\ (1-R_{19})]$$

or

$$SR_5 = 1 - (0.15910)\ (0.15049)\ (0.15309) = 0.996335.$$

CII - VB233AA102

ALTERNATE SUBSYSTEM MECHANIZATIONS CONSIDERED

RADIO SUBSYSTEM

Index

1	Scope
2	Applicable Documents
3	Receiver
4	Transponder
5	Ranging Channel
6	Power Amplifier Trade-offs
7	Diplexer Trade-off
8	Antenna Implementation Trade-off
9	Control Circuitry Trade-off
10	Power Supplies
11	Radio Subsystem Redundancy Trade-offs
12	Equipment Environment
13	Packaging

1.0 SCOPE

This study treats trade-offs which are internal to the radio subsystem. That is, only trade-offs between parameters or techniques which are confined to the radio subsystem are considered here. In so far as practicable, trade-offs between the radio subsystem and other subsystems or systems are treated in the Telecommunication System Trade-off Study, VB233AA101.

2.0 APPLICABLE DOCUMENTS

Documents applicable to this trade-off study are essentially those listed in Section II, VB233AA101.

3.0 RECEIVER

3.1 GENERAL

3.1.1 TELECOMMUNICATION TRADE-OFFS

Certain radio receiver trade-offs are made on a system basis in Section 6.2, VB233AA101 Trade-off Studies, Telecommunication System. These are summarized here.

a. The carrier tracking loop is optimized to have a two-sided threshold noise bandwidth of 18 cps ($2\beta_{Lo}$ = 18 cps) at a unity SNR computed in $2\beta_{Lo}$ (SNR = 0 db in $2\beta_{Lo}$).

b. The receiver rf input stage is a diode mixer of the Mariner C generic type.

c. The carrier loop predetection bandwidth is the same as in Mariner C.

3.1.2 PREFERRED CONVERSION TECHNIQUE

A dual conversion receiver is proposed which has coherent intermediate frequencies. Dual conversion is required for practical implementation of the high receiver gain required. Coherent IF's are proposed as the simplest, least susceptible dual conversion technique. This technique has been built and demonstrated. Other systems employing a fixed offset second IF, have the advantage of no frequency shift through the narrowband filters as a function of Doppler frequency. But these also have the potential problem of additional frequencies of susceptibility due to the introduction of the noncoherent signal frequency and its harmonics.

3.2 RF "FRONT END" DESIGN TRADE-OFFS

The following designs are considered for the Voyager radio subsystem:

a. Conventional microwave balanced mixer, point contact or "Hot Carrier" diodes.

b. Transistor preamplifier into conventional mixer.

c. Three-stage transistor preamplifier into conventional mixers.

d. Tunnel diode preamplifiers into conventional mixers.

e. Tunnel diode down-converters.

These are shown in block diagram form in Figures 3-1 through 3-5.

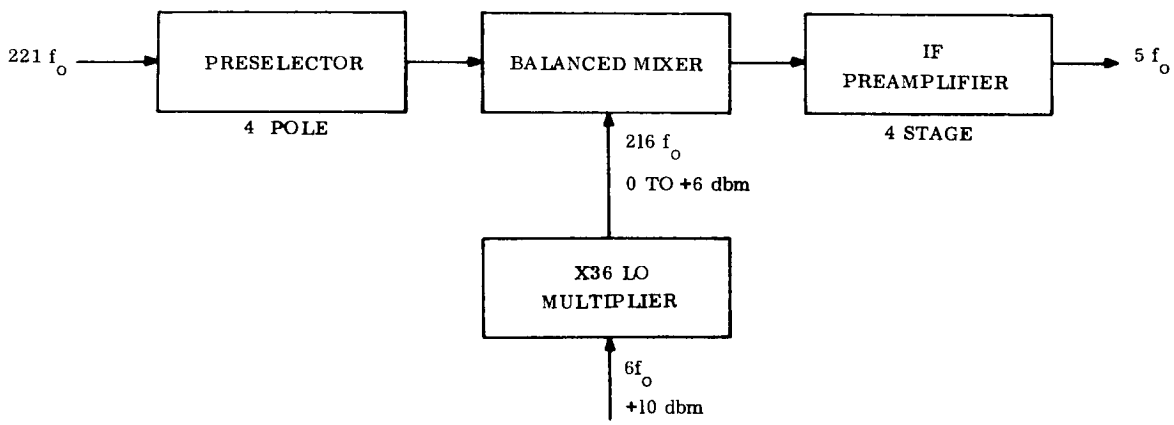

Figure 3-1. Conventional Mixer, RF Converter

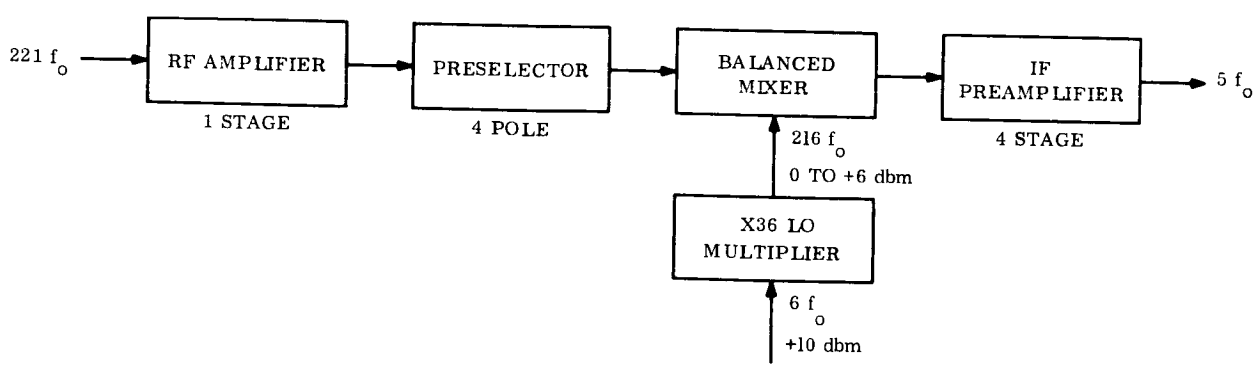

Figure 3-2. RF Amplifier Plus Mixer, RF Converter 2

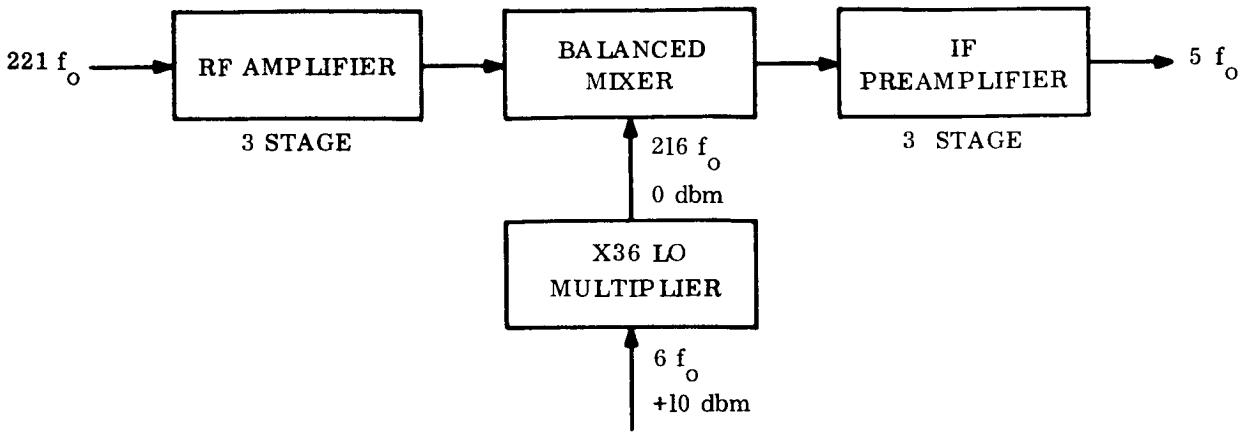

Figure 3-3. RF Amplifier Plus Mixer, RF Converter 3

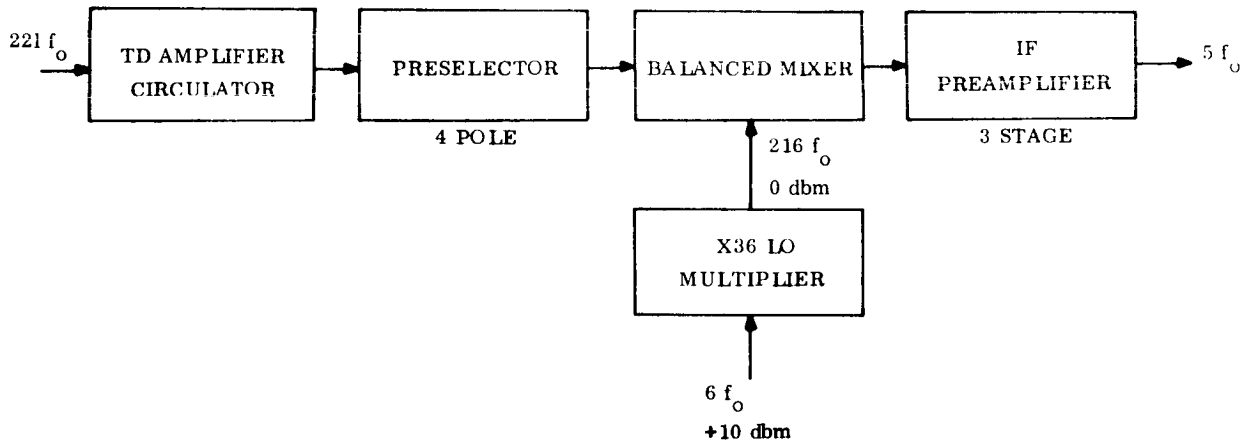

Figure 3-4. Tunnel Diode Amplifier Plus Mixer, RF Converter 4

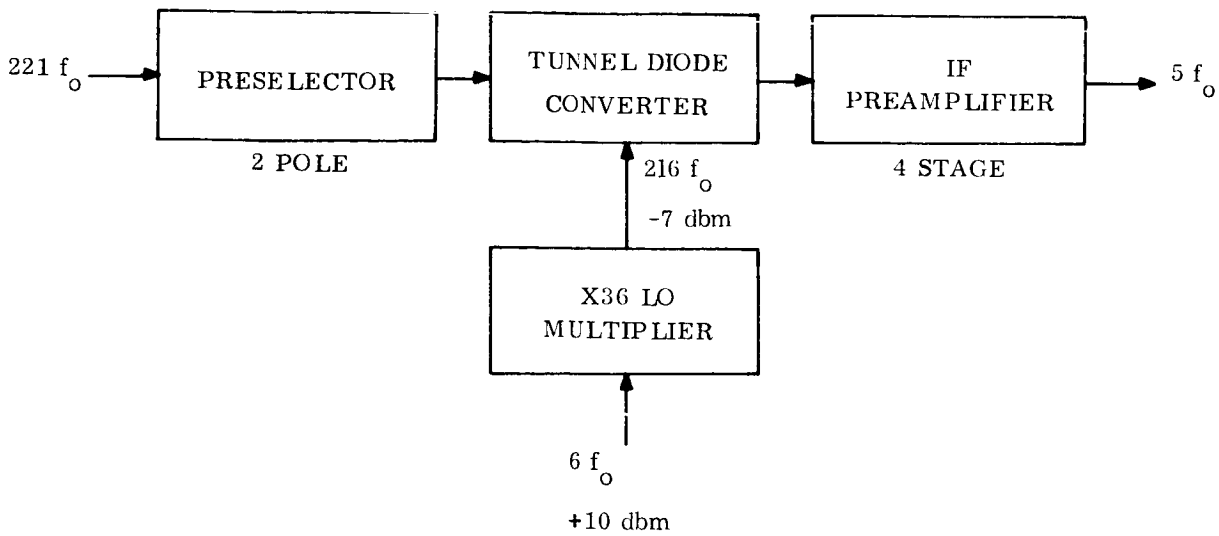

Figure 3-5. Tunnel Diode Converter, RF Converter 5

3.2.1 CONVENTIONAL MIXER "FRONT END"

The conventional microwave balanced mixer uses a preselector coaxial cavity design which has been found experimentally to be the best compromise for size, weight, and loss when compared against interdigital or comb-line filters of the same bandwidth. The size chosen (7.6 cubic inches) reduces the loss to 0.3 db. Reducing the size to 1.9 cubic inches increases the loss 0.5 db. This loss directly adds to the system noise figure.

The balanced mixer has the advantages of inherent local oscillator noise cancellation, minimal local oscillator power requirements and diode redundancy when compared to a single-ended mixer. The hot carrier diodes, compared to point contact types, have a lower noise figure because their noise temperature ratio is unity or less. The hot carrier diodes have potentially higher reliability because they are junction devices with higher vibration resistance. However, point contact diodes are chosen for the present application because of their known reliability. Hot carrier diodes will be considered further when better reliability data is available.

The 4-mw local oscillator power is required to achieve minimum noise figure and minimum rf and LO port vswr. Lower local oscillator drive power may be used at a slight degradation of noise figure.

The if preamplifier consists of cascode pairs because of the superior isolation and stability obtained compared to cascaded common emitter amplifiers. Noise figure is not compromised with the cascode circuit if high gain, low noise transistors are used in the common emitter input stage of the cascode pair.

The prime factors involved in multiplying X36 are $2^2 \times 3^2$. Selection of the optimum multiplication factors and sequence is governed by the efficiency to be obtained, the output spectral purity required, the frequency, and the multiplication device used

(transistor, varactor, or step recovery diode). To obtain adequate spectral purity, at least two discrete multiplication steps are required; i.e. X2X18, X3X12, or X4X9. Using a step recovery diode multiplier to S-band to maximize efficiency and eliminate varactor idler circuits, X9 is a conservative, easily filtered choice. Since a nominal 100 mw of drive at 24 f_0 is required, the X4 is transistorized. The limiter is added to stabilize the X4 output signal for temperature and X6 input level variations. Investigation of existing transistors applicable to multiplication at the frequencies and power levels involved reveals that efficiency is increased by cascading two doublers. The coaxial cavity filter on the X9 output is used to provide adequate suppression of the other local oscillator varactor multiplier harmonics.

3.2.2 RF TRANSISTOR AMPLIFIER CONVERTERS

The addition of a single stage rf amplifier ahead of the balanced mixer reduces the noise figure significantly but degrades reliability because of the additional series function. An overall receiver noise figure of better than 5.5 db is possible in the time scale available for Voyager. The transistor considered for this application is the Texas Instruments germanium L78B. The high reliability version of this device has a 4 db maximum noise figure and 6 db minimum power gain at 2.1 gc. This device is presently available in small quantities and is structurally similar (but superior in performance) to the Texas Instruments TIX3024 germanium transistor. At present, Texas Instruments is evaluating reliability of this device with a maximum junction temperature of +125° C.

The addition of two or three rf stages using the L78B transistor sufficiently defines an improved converter noise figure to permit use of existing mixer-preamplifiers. Thus, the three-stage rf converter (rf converter c) has several distinct advantages over the conventional mixer. An 11 db noise figure mixer-amplifier is adequate for this application. The allowable increased mixer noise figure is used advantageously to simplify the X36 multiplier and mixer design. The use of a three-stage tuned rf amplifier also makes it possible to eliminate the preselector. The amplifier is designed with frequency response characteristics similar enough to the four-pole preselector to obtain sufficient LO, transmitter and image rejection. This significantly reduces converter weight and volume.

The Voyager Radio Subsystem diplexer maintains 100 db minimum transmitter signal (240 f_0) rejection. Thus the maximum level of this signal seen at the rf input is -53 dbm, which is not considered harmful to the transistor rf amplifier.

3.2.3 TUNNEL DIODE CIRCUITS

A tunnel diode amplifier requires a five-pole circulator to assure stable operation with varying vswr's. A post filter is required (in addition to a preselector) to prevent noise figure degradation through the mixer image channel and to prevent the LO from overdriving the tunnel diode amplifier (TDA).

The TDA implies an increase in weight of about 1 pound per amplifier, additional power, and some reduction in reliability.

The tunnel diode down-converter has been theoretically analysed and laboratory models have been built, but S-band units are not known to be in field service yet. Analysis shows that the down-conversion gain varies sharply as a function of local oscillator signal and d-c bias variations. These considerations result in a questionable reliability factor for the tunnel diode down-converter.

3.2.4 SUMMARY

Tables 3-1 through 3-3 summarize the relative performance of the rf converter designs considered for the Voyager Radio Subsystem receiver. Comparison of these data shows the conventional mixer converter (rf converter a) to be the simplest, most reliable, highest confidence design which meets the noise figure requirements of the receiver.

It is additionally proposed, however, that the three-stage rf amplifier converter (rf converter c) be simultaneously developed as a backup and increased sensitivity program to supplement the conventional mixer approach. The decrease in noise figure potentially obtainable with this system, if realizable, improves the signal-to-noise ratio in the receiver detection circuits while adding a safety margin of 3 db. Significant weight, size, and d-c power reductions are other potential advantages. Reliability must be studied carefully. If the new transistor proves reliable, adjustments may be made to improve the overall subsystem reliability.

3.3 TRACKING LOOP IMPLEMENTATION CONSIDERATIONS

It is recommended that the phase-tracking loop be implemented as in Mariner C. The following discussion describes alternate implementations and their associated problems.

3.3.1 D-C OPERATIONAL AMPLIFIERS

Use of d-c operational amplifiers allows an increase of loop gain or alternatively the same loop gain with a reduced integrating capacitor. The problem in this implementation is a slight reduction of reliability because of the additional circuitry. Actual d-c drift contributions of present day transistorized d-c amplifiers are far below the d-c imbalance variations of the loop phase detectors. Therefore, the amplifier is not recommended because it degrades reliability; although it does permit use of a smaller loop filter capacitor for the same loop gain.

Table 3-1. RF Converter Performance Summary

RF Converter System	Nominal System NF	RF Gain	Mixer Loss	IF Gain	IF Linearity (dbm) (Note 1)	LO Interference (Note 2)	Prime Power mw	Approx. Size (in^3.)	Approx. Weight (oz.)	Relative Failure Rate
a	8.0 db	0 db	5.5 db	51.5 db	-30 dbm	-46 dbm	775	34	35	1.00
b	6.5 db	6 db	5.5 db	45.5 db	-27 dbm	-46 dbm	795	35	37	1.15
	See Table 3-2 for Variations									
c	5.5 db	18 db	6.0 db	34.0 db	-27 dbm	-62 dbm	140	26	25	1.22
d	5.3 db	16 db	6.0 db	36.0 db	-40 dbm	-100 dbm	130	48	47	1.26
e	5.7 db	0 db	0 db	46.0 db	-40 dbm	-46 dbm	145	32	30	17.5

NOTE 1 – For 1 db Gain Compression

NOTE 2 – At R-F Input

Table 3-2. Transistor Amplifier Converter Variations

Number RF Stages	Over-all Converter NF	Number RF Stages	RF Gain (db)	* IF Gain
0	8.0 db	0	0	51.5
1	6.2 db 7.5 db	1	6	45.5
2	5.4 db 5.9 db 6.7 db	2	12	39.5
3	5.2 db 5.3 db 5.5 db	3	18	33.5

*5.5 db Mixer Loss

Table 3-3. Comparison of R-F Converter Systems

R-F Converter System	Advantages	Disadvantages
a	Uses existing and reproducible circuit techniques. Reliability maximum, components minimum.	NF not minimum capability.
b	NF reduced significantly.	Utilizes recently developed germanium transistor with tentative specification. RF transistor circuit techniques in developmental stage and unproven in production quantities. Reliability unknown.
c	Preselector function supplied by r-f amplifier bandwidth. Low NF Obtainable. NF relatively independent of mixer-preamp.	Utilizes recently developed germanium transistor with tentative specification. RF transistor circuit techniques in developmental stage and unproven. Reliability unknown.
d	Lowest proven S-Band NF. NF relatively independent of mixer-preamp.	Heavy and bulky 5-port circulator required for amplifier stability. Greater than -50dbm transmitter power input will cause serious intermodulation products. Reliability of TD's uncertain. TD amplifier output subject to overload from LO interference or signal. D-C overvoltage could burn out TD, extra protection required.
e	5-port circulator not required.	Conversion gain sensitive to LO and bias variation. Field-proven TD converter not known to exist. NF based on theoretical capability. D-C overvoltage could burn out TD. Reliability of TD's uncertain. Theory shows very NB tendency for TD converter.

3.3.2 REDUCED LOOP GAIN

By reducing the strong signal loop gain, the integrating loop filter time constant is reduced, thus reducing the loop filter capacitor size for a constant impedance level. This appears attractive but results in lower tracking capability than that required at Mars intercept.

Effects of loop bandwidth variations are discussed in Section 6.2 of VB233AA101.

3.4 VCO STABILITY

VCO stability is considered to be of two types; long term and short term. Here, long term includes temperature effects and aging, while short term includes those variations that occur within the order of seconds. Long term drifts are considered to be tracked out by adjusting the ground transmitter frequency for transponder "rest" frequency, or zero static phase error. Long term drifts are of the order of ±10 or 15 ppm. Temperature variations give about ±8 ppm for 25° C operation. Crystal aging produces about 1 ppm/year for the first 1 – 2 years. Oscillator voltage sensitivity produces 1 to 2 ppm variation over the temperature range. The d-c unbalance of phase detector produces approximately 1 – 2 ppm frequency offset, resulting in the total long term instability of 10 to 15 ppm.

Short term stability is principally determined by the design of the oscillator circuit. The coherence time of the oscillator defines this noise, except for the low frequency noise observed in narrow bandwidth systems. This short term noise limits the reduction of carrier tracking loop noise bandwidths. A VCO coherence time greater than 7 seconds is anticipated. Design work will be done on the basic oscillator circuit in an attempt to further increase coherence time and eliminate low frequency noise.

3.5 AGC

The agc loop bandwidth is chosen to be narrow compared to the narrowest tracking loop bandwidth. This is to maintain a high S/N ratio in the agc channel at all levels suitable for carrier tracking. This minimizes remodulation of the incoming signal by the AM noise through the agc detector. The phase tracking channel is operated nominally in 10 db of limiting. This allows considerable variation of antenna gain, due to spacecraft maneuvers, without appreciable effect on the tracking or command channel. A narrower agc can probably be tolerated. This is a trade-off of antenna variation rate vs agc rate, but there is no advantage to narrower agc, and it can potentially result in inadequate loop gain during a spacecraft maneuver. A slightly wider agc loop can be used with little degradation but good engineering practice requires that a margin be allowed for loop tolerances. The present Mariner C design will be used.

3.6 COMMAND DEMODULATOR

The command signal can be obtained from either the wideband demodulator or the narrowband phase tracking detector. The predetection bandwidth of the narrowband channel is adjusted to a value corresponding to that desired for the command signal.

If the command signal is derived from the wideband demodulator, a low-pass video filter of approximately 2 to 2.5 kc must be added, as well as a video amplifier with a gain of approximately 40 to 60 db. This permits reducing the narrow channel predetection bandwidth, thus reducing the gain suppression factor. This is advantageous for some missions, but is not required for the Voyager. Therefore, the present compromise design is adequate and eliminates the requirement for a post-detection video amplifier and filter.

4.0 TRANSPONDER EXCITER

4.1 BASIC EXCITER CONFIGURATION

The basic multiplication ratio of the exciter derives from the coherent frequency relationship between received and transmitted frequency, and the receiver implementation. That is, the transmitter must multiply the receiver basic oscillator by 120 to provide a proper output signal. The selection of an output X5X3 is made to minimize transmitter harmonic interference with the receiver. An output multiplication of X3X4 in any sequence, generates a more significant spurious signal at 110 f_o, just 0.5 f_o from the desired received frequency. The present multiplier sequence minimizes this problem. The balance of the configuration determination is simply, "where is the auxiliary oscillator introduced and where does phase modulation occur?"

The auxiliary oscillator is built essentially identical to the receiver vco. This choice is made in order to minimize development time and numbers of component types.

Phase modulation is performed at +76 mc, a frequency low enough to permit a high multiplication after modulation, and good phase linearity. The frequency is high enough to permit adequate modulation bandwidth from the modulation point to the output of the transmitter and to minimize high order carrier harmonic sidebands at the output. This design is a compromise between requirements, and is considered a good compromise.

4.2 EXCITER OUTPUT POWER

In VB233AA101, Section 6.3, an alternate transmitter configuration using a locked oscillator is discussed. This section considers alternatives of implementation involving direct transistor power amplification and varactor frequency multiplication.

The power output required is 400 milliwatts at 2295 mc. Transistors are not currently available that are capable of amplification at that frequency and power level. The output multiplier ratio is determined to be X15. So transistor operation at 1/3, 1/5, and 1/15 of the output frequency must be examined. At 1/3 the output frequency, a new RCA transistor exists which is capable of 1-watt output and some gain. But the device has no operational background information available for reliability analysis. The power, 1 watt, is marginal for this application and allows no derating margin for reliability. This assumes a loss of 60 percent through the output varactor multiplier, load isolator, and transmitter filter.

At 1/5 frequency, only the above mentioned transistor is available and its power capability is inadequate for driving a varactor multiplier to the required output power at S-band.

At 1/15 of the output frequency, the 2N3375 family of transistors provide good efficient operation, with power capabilities well in excess of those required to generate the 400 mw of S-band power through a X5 and X3 varactor multiplier. Operation at a lower frequency requires additional multiplication, resulting in higher varactor losses. Collector efficiencies of 60 percent are realized at 155 mc, 1/15 of the output frequency. Operation at lower frequencies does not improve collector efficiency appreciably and so results in lower over-all efficiency (d-c to output r-f). The most efficient, present-day transmitter chain, with proper component derating for reliable operation, uses a transistor power amplifier at 155 mc, followed by a X15 varactor multiplier.

The X15 varactor multiplier can be a single-step multiplier but this requires a combination high Q, very high voltage, high dissipation varactor diode with several idler circuits. The output spectrum has higher levels of nearby multiplier harmonics than an X5-X3 arrangement with intermediate filtering. Therefore, the latter arrangement is selected. The multiplier sequence may be X5 - X3 or X3 - X5. The former is chosen in order to provide 1/3 the output frequency as a transition region from lumped to distributed circuits, and also because the higher Q diodes required for the output multiplier are generally lower $_C$, lower voltage, lower dissipation units. Operating the output multiplier as an X5 rather than an X3 results in selection of a different diode for reliability considerations. The X5 output multiplier diode then has higher loss. Therefore, the better sequence appears to be X5 - X3. Overall efficiency is then approximately 60 percent for the transistor. A 3 db loss through the X5, 0.6 db loss through the filter, 3 db loss through the X3, and circulator and filter results in an overall power output efficiency of 10 percent, not including the modulator or low level power amplifiers.

The transmitter power amplifier, multiplier chain trade-off results in a clear conclusion of the best, present day approach in terms of reliability, and performance. The efficiency is reasonable, and size and weight are less than that of the companion receiver; therefore, they are judged reasonable, also. Details of design to prevent "self-lock" problems are discussed in Section 3.4.2 of VB233AA101.

5.0 RANGING CHANNEL

The ranging channel is defined to utilize video limiting[1]. The following discussion describes trade-offs in implementing the video channel.

In order to assure nearly linear operation of the ranging channel phase detector, a dynamic range of 64 db is required. To provide this dynamic range, the detector is operated at a voltage level corresponding to approximately -76 dbm across 50 ohms. Reverse isolation is required such that the IF reference signal fed back through the input shall be 40 db below the received signal at the common point within the receiver channel. This requires a reverse attenuation of approximately 140 db through the if and detector portion of the ranging channel. No compromise may be made here.

The output of the wideband detector must be raised to a level suitable for remodulation, say 1 volt pk-pk, with 1 radian input modulation, at strong signals. This requires a voltage gain of approximately 80 db to assure 10 db video clipping. As the received signal strength is reduced, the agc increases the noise to 54 db greater than the signal, with peak to 64 db. Therefore, the video amplifiers ahead of the video limiter must accommodate this dynamic range or permit sequential amplifier limiting without appreciable time delay variation. The latter method appears most practical, for the limiter must operate at a level of nearly one volt. A dynamic range of 64 db above one volt is not practical in transistor video circuitry.

The circuitry is implemented in the same manner as in Mariner C.

6.0 POWER AMPLIFIER TRADE-OFF

Because of the extensive development of traveling wave tube (TWT) amplifiers for space use in the 10 to 20 watt class, a 20 watt TWT can be recommended for the Voyager radio subsystem with high confidence that an efficient, reliable amplifier of well-defined characteristics can be obtained. In order to increase the potential scientific data pay-off of the mission, a higher power amplifier is desired. In this section, the studies made to determine the feasibility of obtaining a higher power amplifier are discussed.

Tube manufacturers have indicated that it is reasonable to achieve an output power of 100 watts or more. However, as discussed in VB233FD102, a goal of 50 watts was established for the tube. Three tube types were considered in detail for the 50 watt amplifier. These were the TWT, electrostatically focused klystron (ESFK) and the Amplitron. They are the principal candidates because:

a. Models of these tubes have already been built and operated at power levels in the 50 to 100 watt range.

---

[1] "Turnaround Ranging", Section 6.4.2., VB223AA101

b. The gain of these devices is nominally 26-30 db, which is desirable from the point of view of the exciter output required to drive the power amplifier.

c. The efficiencies of these devices are near or exceed 35%. It is reasonable to assume that this goal can be met by July, 1966.

In the following sections, each of these devices is briefly described, and their advantages and disadvantages discussed.

6.1 TRAVELING WAVE TUBE

6.1.1 DESCRIPTION

The basic traveling-wave tube amplifier consists of an electron gun which projects a focused electron beam through a helically-wound coil to a collector electrode, shown in Figure 6-1. The focused electrons are held in a pin-like beam through the center of the helix by a powerful magnetic field around the full length of the tube.

A cw signal coupled into the gun-end of the helix travels around the turns of the helix and thus has its lineal velocity reduced by an amount equal to the ratio of the length of wire in the helix to the length of the helix itself. The electron beam velocity, determined by the potential difference between the cathode and the helix, is adjusted so that the electron beam travels a little faster than the cw signal. The electric field of the cw signal on the helix interacts with the electric field created by the electron beam and increases the amplitude of the signal on the helix, thus producing the desired amplification.

6.1.2 ADVANTAGES OF THE TWT

a. The most significant argument in favor of the twt is the fact that it is presently being used in nearly all the major space programs and has been flight proven. It shows a MTBF in excess of 50,000 hours which enhances the reliability of the telecommunication system.

b. The twt has a nominal gain of 30 db which eliminates the requirement for high output powers from the exciter.

c. The efficiency of a twt is greater than 30% at the present and is being continually improved. Efficiencies as high as 42% now appear feasible.

d. The twt is essentially a wideband device, i.e., at S-band frequencies bandwidths in excess of 10 mc are possible. This provides good phase linearity over the bandwidth needed for turnaround ranging.

e. The physical size and weight of the twt lend the device to high density packaging. The sizes of present devices are being reduced to the extent that the dimensions of an overall power amplifier package are determined by the size of the power supply and not the device.

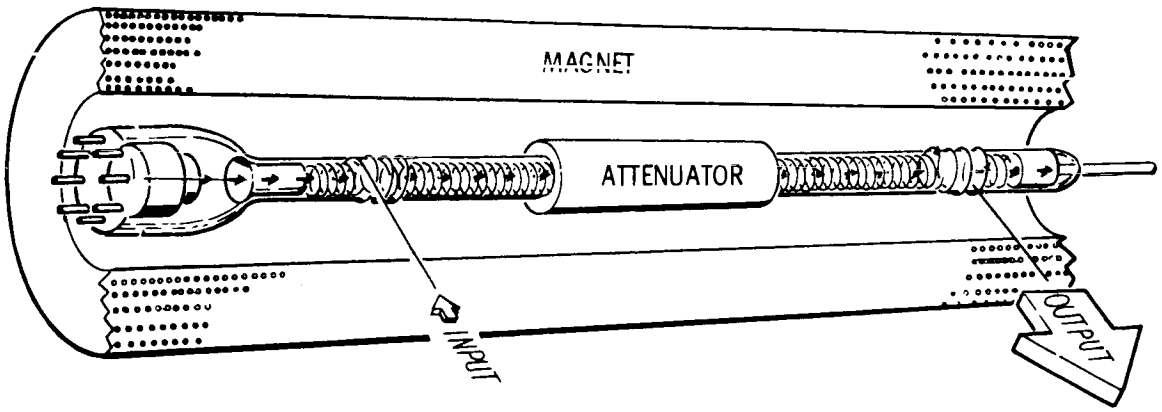

Figure 6-1. Cutaway View, Showing Important Elements Of A Traveling - Wave Tube Amplifier

f. The twt is capable of stable operation at elevated temperatures which might occur in the absence of rf drive. Without rf drive all the prime power is dissipated through the collector.

6.1.3 DISADVANTAGES OF THE TWT

a. Of most concern to the radio subsystem is the noise generated by the tube. Although the noise figure is less than 30 db in a 10-mc bandwidth, the tube, over a wide frequency range behaves as a noise source. This is troublesome in diplexed configurations as the noise from the twt degrades the equivalent noise figure of the receiver connected to the diplexer. Therefore, to use the twt in diplexed configurations the diplexer must reject this noise in the receiver bandwidth spectrum, i.e., the noise at the receiver port of the diplexer must be at least 100 db down from the noise at the power amplifier port.

b. Even though the twt is capable of operating at extremely high temperatures it is recognized that the reliability of the device at these temperatures is questionable. Therefore, for reliable performance, the twt must be mounted to a dissipative heat sink. The temperature of this heat sink must be held to a nominal 80° C.

c. It is desired that the external magnetic fields within the spacecraft be minimized. To minimize the external magnetic field of the twt, complicated field balancing techniques are required to cancel the effects of the beam-forming magnetic field around the full length of the tube.

6.2 ESFK

6.2.1 DESCRIPTION

The basic electrostatically focused klystron consists of a cathode or electron gun which projects an electron beam through a series of tuned cavity structures to a collector electrode as shown in Figure 6-2. The electrons are focused by the application of periodic focusing electrodes at each space charge region. Focusing with these electrodes between cavities is known as Einzel lens focusing. This type of focusing permits a narrower and longer beam that can be used with r-f structures comparable to those used in magnetically focused klystrons.

The klystron uses the principle of velocity modulation for amplifying a cw signal. A cw signal is coupled into the beam-forming cavity or drift region which imparts a small velocity variation on the electrons in the beam. As the electrons drift through the first cavity they tend to bunch at intervals proportional to the input velocity. The region at which the electrons bunch is known as the space charge region.

The amplification of the input signal is accomplished by the space charge mechanism, i.e., the electron current density is increased as the electrons drift from the input cavity to the space charge region. This phenomenon continues through each stage of space charge. As the high density electron beam passes through the output cavity, the beam current variations are coupled to the output load, thus providing a high power output.

The tuned cavity is used to fix the gain-bandwidth product of the device. The dimensions of the cavity, however, are limited by the length of the drift space which in turn is a function of the input frequency.

The focusing electrodes are located in each space charge region to eliminate beam dispersion. Beam transmission efficiencies as high as 99% are easily achieved in well designed systems.

6.2.2 ADVANTAGES OF THE ESFK

a. The esfk is capable of greater than 28 db gain for a given bandwidth.

b. The esfk is capable of operating at efficiencies greater than 35%. This is desirable because it improves the spacecraft prime power requirements and the thermal control problem.

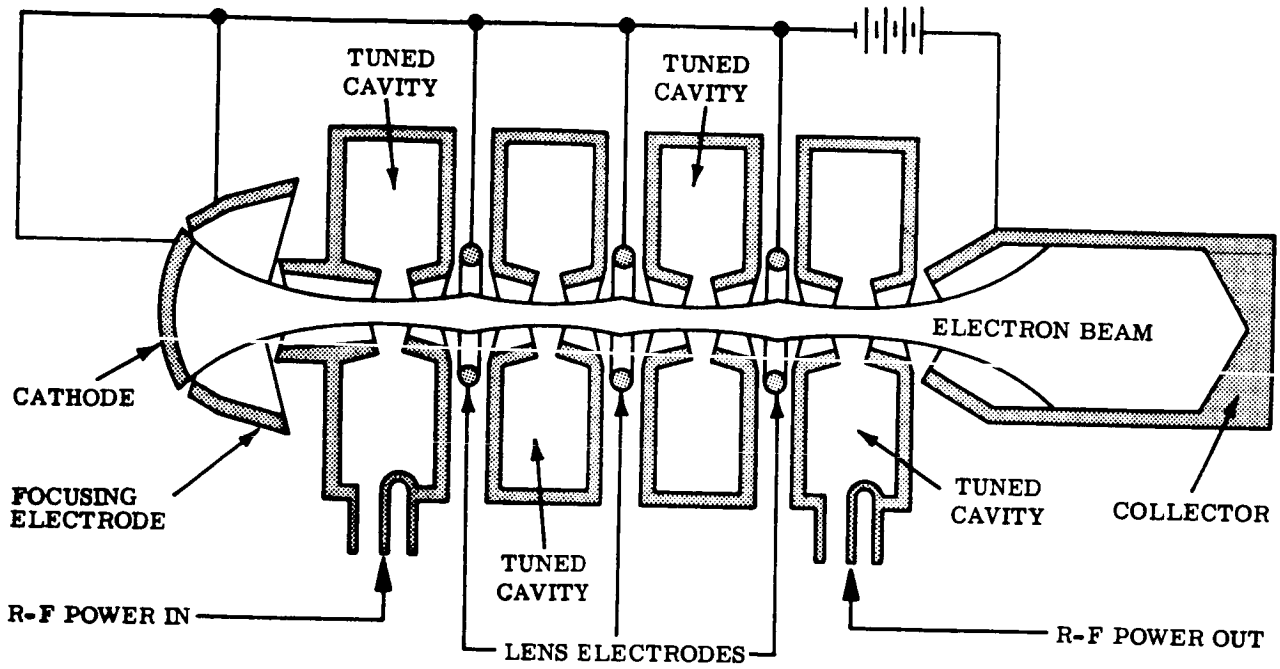

Figure 6-2. Klystron Power Amplifier Electrostatically Focused

c. In diplexed applications it is desirable to have the noise figure of the power amplifier reasonably low. The esfk noise figure of less than 28 db is considered reasonably low.

d. The esfk has no external magnetic fields which makes it attractive for applications where a magnetically clean system is desired.

e. In the event of an exciter failure, the drive signal is not present at the power amplifier input. The esfk is well suited to this situation. Its output is a direct function of the input; i.e., with no drive signal there are no signals present at the output.

f. The structure of the esfk, both internal and external, is rugged and suffers little from thermal deformations.

6.2.3 DISADVANTAGES OF THE ESFK

a. Since the gain-bandwidth product is determined by the length of the drift space the esfk is considered a narrow-band device. Therefore, in the design of the esfk a trade-off must be made between realizable gain and bandwidth.

b. Little is known at this time on the effect of phase jitter and phase non-linearity of the esfk when placed in a DSIF system. Preliminary estimates indicate no incompatibilities but tests need to be performed.

c. Since the esfk is a relatively new addition to the devices suitable for space applications, it has never undergone actual flight tests as have the twt power amplifiers. In addition, life test data is not complete.

d. The collector structure of the esfk is capable of dissipating the entire beam power (this would occur in the absence of drive), if a suitable thermal interface is established with the spacecraft. This requires a heat sink on which to fasten the collector.

6.3 AMPLITRON

6.3.1 DESCRIPTION OF THE AMPLITRON

The Amplitron uses a basic crossed-field interaction process which is similar to the magnetron, i.e., a traveling rf wave interacts with electrons rotating about and drifting radially from a cylindrical cathode. When the electron angular velocity is in synchronism with that of the rf wave, the electrons lose energy to the rf fields at nearly the same rate at which they accept energy from the d-c field. The potential of the d-c field is thereby converted to rf energy without the electrons ever having achieved a velocity corresponding to the full d-c potential.

The electrons are collected on an anode structure which consists of a number of individual resonant cavities or slots radially positioned about the cathode. An external high density magnetic field is supplied by a permanent magnet positioned such that its flux lines are parallel to the axis of the cathode. Under proper conditions of magnetic field, anode voltage, etc, as much as 90 percent of the d-c power supplied to the anode structure can theoretically be converted to rf energy. The remaining 10 percent is absorbed by electrons that are emitted from the cathode in an unfavorable rf phase and are returned to the cathode producing back bombardment of the cathode and secondary emission. In practice, however, due to power dissipated in cavity losses, the power actually delivered to an external load is typically 55-60 percent of the d-c anode power.

The Amplitron has a non re-entrant, periodic rf structure matched to its input and output connectors. There is no added attenuation in the circuit as there is in a twt so that when no voltages are applied the device behaves as a short section of transmission line in its operating range of frequencies. Reflected energy also passes through the Amplitron.

The possible condition of a high vswr at the output of the amplifier requires isolation between the exciter and the Amplitron and the Amplitron and diplexer. See Figure 6-3.

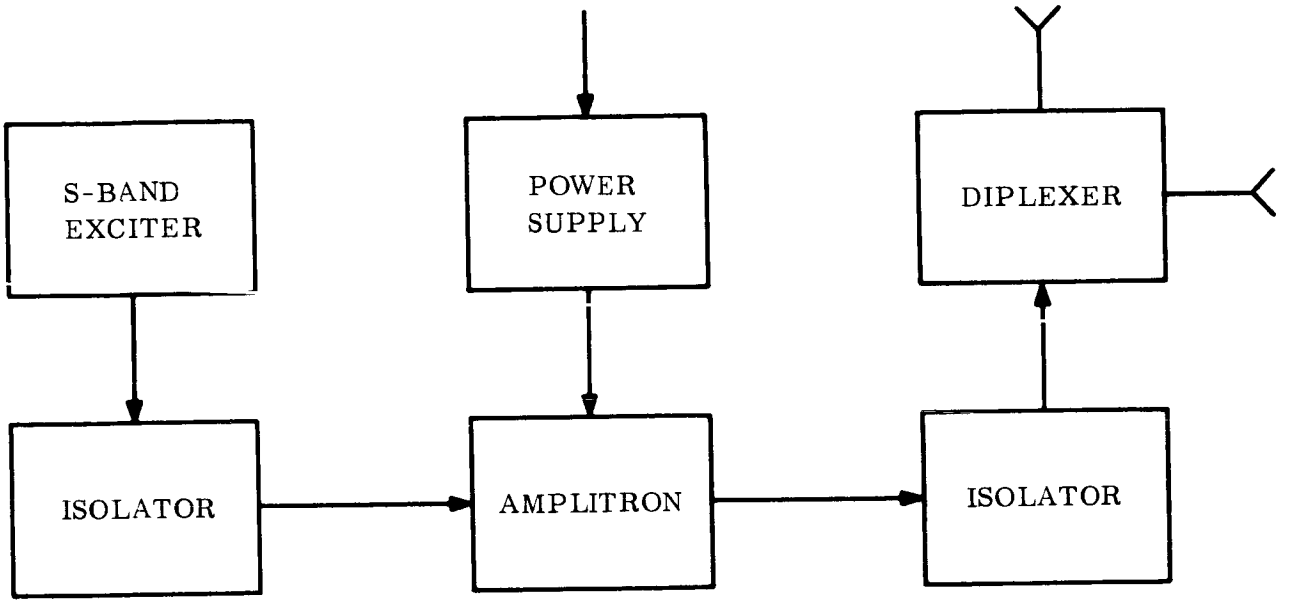

Figure 6-3. Typical Amplitron Configuration

6.3.2 ADVANTAGES OF THE AMPLITRON

a. Much time and effort have been expended in developing a 20-watt version for use in the Apollo spacecraft. The Lunar Excursion Module uses the Amplitron.

b. Another advantage is the feed-through feature in which the device acts as a short section of transmission line approximately 2 λ long. This is very useful in designing redundant systems.

c. The Amplitron has greater than 18 db gain with a bandwidth of greater than 10 Mc.

d. The efficiency of the device is at least 35 percent, which is desirable from prime power and thermal dissipation requirements for the spacecraft.

e. The structure of the Amplitron is very rigid and has a high resistance to modulation or damage from severe shock and vibration

6.3.3 DISADVANTAGES OF THE AMPLITRON

a. In the absence of the drive the Amplitron becomes unstable. The anode voltage rises above its nominal value corresponding to the frequency of

operation. As the voltage goes up so does the frequency until a threshold circuit interrupts the input d-c line. As the power supply again recycles the anode voltage starts to increase. During these recycling periods the tube generates a multitude of frequencies at high power levels. This is very undesirable in diplexed applications..

b. Since the operational frequency range of the Amplitron is a function of the anode voltage, the power supply must provide excellent regulation and must be able to track the input voltage variations to less than 1 percent. This requires a very complicated power supply.

c. Although the over-all weight of a typical package is approximately 9 pounds, the reliability of such a package is questionable because of all the components required. (See Figure 6-3.)

d. The output power and anode voltage are affected by temperature variations. The output power varies as much as two or three watts over the specified temperature range -25° C to +75° C.

e. Because of the isolators and the permanent magnet in the device itself, a heavy case for shielding is required to meet the criteria for a magnetically clean spacecraft.

f. The gain of the Amplitron is limited by the level of the drive signal. If the input is insufficient the inherent feedback of the device, which results from an interaction of the electron stream at the input and output ports, causes the Amplitron to oscillate.

6.4 RESULTS OF COMPARISON

The results of the preceding discussion are tabulated in Table 6-1. Of the three devices considered, the twt and the esfk appear to be best suited for the Voyager radio subsystem. The Amplitron is not considered for the Voyager radio subsystem because:

a. The automatic recycling and switching of its power supply reduces the reliability of the device.

b. In the absence of drive it generates a broad spectrum of frequencies at near peak power levels as the power supply recycles. This interferes with the receiving channels and may even damage the receivers.

In order to obtain high confidence that a 50-watt amplifier could be developed in the Voyager time scale, definitive proposals were requested of tube manufacturers for TWT and ESFK power amplifiers. Each of the manufacturers solicited responded with extensive technical proposals, and outlined programs to produce a qualified 50-watt amplifier by July 1966.

Table 6-1. Comparison of Results of Power Amplifier Trade-off Study

Characteristic	TWT	ESFK	Amplitron
Gain (db)	30	28	18
Efficiency (min) (%)	35	35	35
Bandwidth	Wide	Narrow	Moderately Narrow
Noise Figure (db)	30	28	60
Magnetic Shielding	Yes	None	Yes
Size (with power supply in.)	4x6x2 1/2 in.	4 x 6 x 6 in.	6 x 7 x 5 in.
Weight (with power supply, lb.)	6	8	8.7
Operation in Space Environments			
Temperature	Good	Good	Fair
Vibration & Shock	Fair	Good	Good
Affected by Absence of Drive	No	No	Yes
Stability of Output Power	Good	Good	Fair
Reliability	Good	Good	Questionable
Heat Dissipation	Fair	Good	Good
Capability of Unattended Operation	Yes	Yes	Questionable

The following manufacturers submitted proposals in response to the request:

TWT	Eimac Hughes Aircraft Watkins - Johnson
ESFK	Eimac Litton Industries

Table 6-2 is a summary of the three proposals submitted to Motorola on the characteristics of a 50-watt twt power amplifier. Table 6-3 summarizes the two proposals submitted to Motorola on the characteristics of a 50-watt esfk power amplifier.

Table 6-2. Summary - Proposed Characteristics for 50-Watt TWT

Motorola Specification of Characteristics For a 50-watt TWT	Hughes Microwave Tube Div. Proposed Characteristics	Watkins-Johnson Proposed Characteristics	Eitel-McCullough Proposed Characteristics
Operating Frequency: 2.1-2.4GC Duty Cycle: CW	Operating Frequency: 2.1-2.4GC Duty Cycle: CW	Operating Frequency: 2.1-2.4 GC Duty Cycle: CW	Operating Frequency: 2.1-2.4 GC Duty Cycle: CW
Output Power: 50 watts min Input Drive: 50 mw max.	Output Power: 50 watts CW Input Drive: 50 mw max.	Output Power: 50 watts CW min. Input Drive: 50 mw max ±2.5 db variation for 50 watts ±1 db out.	Output Power: 50 watts Input Drive: 50 mw For 20 watt mode the drive must be increased to 125 mw.
Gain ≥ 30 db (saturated) The gain variation over the specified bandwidth <0.5 db	Saturated gain: 30 db min Gain variation will be less than 0.5 db over the specified bandwidth.	Saturated gain = 30 db Gain variation less than 0.1 db.	Saturated gain = 30 db Variation < 1 db over specified bandwidth. At 20 watt mode gain drops 8 db.
Efficiency: TWT-45% min Power Supply-90% min Overall - 40% min	For 46% depression or 96% transmission TWT - 45% Power Supply - 90% Overall - 40%	For 78% collector-helix depression TWT - 40% Power Supply - 85% Overall - 34%	For 50% helix voltage depression TWT - 42% firm, 45% goal Power Supply - 88% firm, 90% goal Overall - 37% firm, 40% goal
Bandwidth: 0.5 db bandwidth of 10 MC (min.)	Bandwidth: 0.1 db, 10 MC	No Comment	Bandwidth: 0.5 db, 10 MC
Noise Figure ≤ 30 db	Noise Figure = 30 db nominal	Noise Figure = 30 db (max)	Noise Figure = 33 db firm 30 db must be goal
Phase: Linear within ±2.5° over 10 MC 0.5 db bandwidth. Phase noise ≤ 2° rms in $2\beta_L = 20$ CPS.	Less than ±2.5° over 10 MC, 0.5 db bandwidth. No comment on phase noise	No Comment	±2.5° per 10 MC acceptable. No knowledge of phase lock receiver response with tube.
Time Delay: Absolute time delay< 10nsec Time delay variation < 0.5 nsec	Time Delay = 7 n sec Negligible variation with temperature	No Comment	No Comment

Table 6-2. Summary - Proposed Characteristics for 50-Watt TWT (Continued)

Motorola Specification of Characteristics For a 50-watt TWT	Hughes Microwave Tube Div. Proposed Characteristics	Watkins-Johnson Proposed Characteristics	Eitel-McCullough Proposed Characteristics
VSWR: Input VSWR < 1.4:1 Output VSWR < 1.4:1 Stable operation for VSWR < 3:1	VSWR: Input, Output-1.4:1 Tube will be stable under no drive conditions when terminated into a short of any phase	Input VSWR: Operating - 1.5:1 max non-operating-1.25:1 max Output load VSWR 3:1 max	No Comment
Reliability: TWT Operational Lifetime > 50,000 hours Power Supply - not specified Overall MTBF > 136,000 hours	TWT MTBF = 600,000 hours Power Supply MTBF = 278,000 hours Overall MTBF = 136,000 hours	Design Life = 50,000 hours Power Supply MTBF = 467,000 hours Failure rate requirement meaningless in light of expected tube life.	TWT Wearout Time > 150,000 hours Power Supply MTBF >200,000 hours
Temperature: Operating: -10 C to +75 C	Operating Temperature: -10 C to + 75 C	Operational Temperature: -25 C to +75 C Storage Temperature without tube damage: -55 C to +100 C	All environmental conditions acceptable.
Size: Minimum	TWT (Length) = 11 in. Power Supply = 2.5 in. x 6 in. x 4 in. Overall = 12 in. x 5 in. x 4 in.	Overall package volume less than 110 cu in. TWT (length) = 8 in.	TWT = 1 in. x 1 in. x 9 in. Volume < 120 cu in.
Weight: minimum	TWT - 36 oz. Power Supply - 3.5 lb Overall - 6.75 lb	TWT-12.1 oz encapsulated Power Supply 2.2 lb (Excluding RFI enclosure) Overall <5 lb	TWT - 12 oz Power Supply <3.5 lb Overall ≤ 7.0 lb
Induced Ripple: Minimize to introduce negligible AM and PM at the amplifier output.	PM=2° /volt of cathode-helix voltage PM=0.5° /volt of anode voltage PM=0.2° /volt of collector voltage	PM < 3° /volt of helix-cathode voltage Power supply relatively insensitive to ripple.	AM and PM noise level on r-f output shall be -70db below carrier.

Table 6-2. Summary - Proposed Characteristics for 50-Watt TWT (Continued)

Motorola Specification of Characteristics For a 50-Watt TWT	Hughes Microwave Tube Div. Proposed Characteristics	Watkins-Johnson Proposed Characteristics	Eitel-McCullough Proposed Characteristics
Telemetry: Telemetry outputs to assess the condition of the tube shall be provided.	1. Helix Current 2. Helix Voltage 3. Collector Current 4. Collector Temperature 5. RF Power Output	No Comment	1. Collector Temperature 2. Helix Voltage 3. Helix Current 4. Heater Voltage & Current 5. Cathode Current (0-3 volt level into a 1 Megohm load)
Cooling: Conduction Mounting plate temp ≤ 80 C Amount of power dissipated not specified	Conduction cooling Mounting plate temp ≤ 80 C 65 watts must be dissipated with drive. Temperature rise of collector above package base temp is 0.4 C per watt.	Conduction Cooling Mounting plate temp ≤ 80 C 97 watts must be dissipated with drive. [illegible] watts without drive.	Conduction Cooling Mounting plate temp ≤ 75 C [illegible] watts must be dissipated without drive
Switching: Power supply "ON" and "OFF"	Entire power supply floats on d-c bus and can be turned "on" or "off" by a low level signal.	No Comment	"ON" or "OFF" by presence or absence of high impedance 25 volt potential.
Power Supply: Heater warm-up time - not specified Power Output stabilization time - not specified	Heater warm-up time=80 sec No comment on stabilization time	Heater warm-up time=90 sec Stabilization time = 10 millisec.	Heater warm-up time=80 sec No comment on stabilization time
Power Level change from 50 watts to 20 watts, programmable by Command	Add second anode as a [illegible] intercepting control grid. The efficiency will be reduced 10% for same drive level.	Lower both beam voltage and current. Gain and efficiency can be preserved for the same drive level.	Output level changed by changing anode voltage. Gain drops and drive must be increased.

Table 6-3. Summary - Proposed Characteristics for 50 Watt ESFK

Motorola Specification of Characteristics for a 50 Watt ESFK	Litton Industries Proposed Characteristics	Eitel-McCullough Proposed Characteristics
Operating Frequency: 2.1-2.4 GC Duty Cycle: CW	Operating Freq. 2.1 to 2.4 GC Duty Cycle: CW	Operating Frequency: 2.1-2.4 GC Factory tuned. The tubes will operate CW.
Output Power: 50 watts min. Input Drive: 150 mw. max	RF Output power = 50 watts min Input Drive: 150 mw max Output power stable within No. 0.05 db	Power Output = 50 watts Input Drive = 150 mw
Gain ≥ 25 db (saturated) The gain variation over the specified bandwidth < 0.5 db	Gain = 25 db No comment on gain variation	Gain ≥ 25 db min. Amplitude variation ≥ 1 db
Efficiency: ESFK 45% min Power Supply 90% min Overall 40% min	ESFK - 50% (depressed collector) Power Supply-88%-goal of 90% Overall-43.8% (At 20 watt level) ESFK 45% Power Supply 80% Overall 36%	ESFK - 38.5% (At 20 watt level) Power Supply - 85% ESFK - 30% Overall - 33%
Bandwidth: 0.2 db bandwidth of 5 MC minimum	Instantaneous bandwidth: 3 db min - 5 MC 1 db min - 3.5MC 0.2 db, 5 MC bandwidth theoretically possible	1 db bandwidth - 5 MC
Noise Figure < 30 db	Noise Figure = 26 db max.	Noise Figure = 25 db
Phase: Linear ±2.5° min over 5MC 0.2 db bandwidth Phase Noise ≤ 2° rms $2\beta L$=20 cps	Phase characteristics not available - results of computer program will be submitted as soon as they are available	Linear within ±8° max., ±2.5° is goal. No comment on phase noise.
Time Delay: Absolute time delay < 10 ns Time Delay variation < 0.5 ns.	Absolute time delay < 1 ns Absolute time delay variation < 0.5 ns	Absolute time delay = 2 ns No variation with temperature

Table 6-3. Summary - Proposed Characteristics for 50 Watt ESFK (Continued)

Motorola Specification of Characteristics for a 50 Watt ESFK	Litton Industries Proposed Characteristics	Eitel-McCullough Proposed Characteristics
VSWR: Input VSWR ≤ 1.4:1 Output VSWR ≤ 1.4:1 Stable operation for VSWR ≤ 3:1	Input VSWR - 1.2:1 Output VSWR - 1.2:1 Nonfailing max - 2:1 Stable for VSWR of 3:1 in all phases	No comment on Input & Output VSWR VSWR of 3:1 will reduce output power but will not lead to unstable operation.
Reliability: ESFK Operation life > 50,000 hours Power Supply - not specified Overall MTBF ≥ 136,000 hours	ESFK MTBF = 500,000 hours Power Supply = 300,000 hours Overall MTBF = 142,000 hours Operational life > 80,000 hours	Lifetime > 50,000 hours Power Supply ≦ 136,000 hours Entire unit will be pressurized to 15 psia.
Temperature: Operating -10 C to +75 C	Operating Temp: - 10 C to + 75 C	For -10 C to +75 C resonant frequency of cavity changes 0.1 MC
Size: Minimum	Overall: 6 in. x 6 in. x 4 in. ESFK: 6 in. x 3.4 in. diam. Max clearance diam = 5.6 in.	ESFK: 5 in. x 4 in. diam. Max clearance diam = 5 5/8 in. Power Supply 8 in. x 4 in. x 4 in. max Overall: 5 in. x 10 in. x 8 in.
Weight: Minimum	Overall: 8 lb	ESFK: 3 lb Power Supply: 5 lb Overall Package: no comment
Induced Ripple: Minimize to introduce negligible AM and PM at the amplifier output. Discuss	Phase ripple at power supply frequency (10kc) = 0.025° PM = 0.25° /volt	No comment
Telemetry: Telemetry outputs shall be provided	1. Cathode current 2. Collector hot-spot temperature Dependent on specific redundancy design concept.	1. Filament Current 2.. Collector Current 3. Collector Temperature 4. Regulated current 1 Megohm load minimum

Table 6-3. Summary - Proposed Characteristics for 50 Watt ESFK (Continued)

Motorola Specification of Characteristics for a 50 Watt ESFK	Litton Industries Proposed Characteristics	Eitel-McCullough Proposed Characteristics
Cooling: Conduction Mounting plate temperature < 80 C Amount of power dissipated - not specified Discuss requirements	Heatsink Temp: -25 C to +75 C operating -50 C to +100 C nonoperating Conduction Cooling	Conduction Cooling: No comment on mounting plate temperature or power dissipation.
Switching: Power supply "on & "off"	No comment	No comment
Power Supply: Heater warmup time - not specified Power output stabilization time (not specified)	No comment	Heater warmup time - 120 sec. Unit will be pressurized and held at 15 psia.
Power level change from 50 watts to 20 watts, programmable by Command	Relay is added to power supply to switch level. Power is lowered by lowering cathode voltage. If depressed collector is used collector voltage must be changed also.	Beam voltage is reduced from 2000 volts to 1550 volts for 20 watt operation. No degradation in reliability. Efficiency is reduced.

In order to minimize the risk of a developmental problem which might delay the delivery of the power amplifiers, it is recommended that the development of both a 50-watt TWT and ESFK be initiated.

7.0 DIPLEXER TRADE-OFF

7.1 BASIC ELECTRICAL TRADE-OFFS

The fundamental determining parameters of a microwave filter element are the required isolation to an adjacent frequency and the allowable passband insertion loss. It can be shown that, for a specified rejection, there is an optimum number of resonators to be used in a conventional direct-coupled resonator filter which will develop the required rejection with a minimum passband loss. The number of resonators to be used is indicated by the formula

$$N = (6 + R) / 8.68 \qquad (1)$$

when R is the required rejection in decibels. The number N must be an integer and literally should be taken as the next integer greater than the value given by (1). If the value of R is fairly large (say greater than 40) so that N is greater than 5, it will be found that the over-all loss will vary by only a few hundredths of a decibel, if N is taken to be 1 or 2 less than the value given by (1).

It can also be shown that, if the above optimum filter is constructed of resonators having unloaded Q's equal to Q_u, the loss will be

$$L = 1.36 (6 + R) / Q_u F_R \text{ decibels} \qquad (2)$$

where F_R is the fractional rejection bandwidth.

Strictly speaking, equations (1) and (2) apply only to "equal-element" filters, but it has been found that they give results which are approached by filters having a conventional Tchebyscheff or Butterworth response to a greater precision than the actual unloaded Q can be predicted.

Equation (2) shows that the passband loss in db is inversely proportional to the resonator unloaded Q, if the passband shape is specified. The unloaded Q for a coaxial resonator having copper conductors, an electrical length of $\lambda/4$, and an inside diameter of "b" inches is given by

$$Q_u = \frac{106 \, b\sqrt{f}}{1 + \frac{b\,f}{10{,}600}} \qquad (3)$$

where f is the resonant frequency in megacycles per second and the ratio of the inner and outer conductor sizes is 3.59 which gives a line having a characteristic impedance of 76.7 ohms and a maximum Q_u for a given b. This is an idealized Q and it is found

that the inevitable result of imperfections in surface roughness, sliding contacts for tuning, and other factors reduce the practical resultant Q_u to about 0.7 of the value given by (3).

Equations (1) and (2) along with (3) indicate that there is a relationship between loss and physical size which can be calculated. An expression for the passband loss for values of "N" other than that given by equation (1) enables the making of more general calculations. Such relationships along with tabular or graphical data on the relationship between the passband and reject-bandwidths are available in the published literature on filters. As an example of the use of such information, Table 7-1 has been prepared. It shows the approximate relationship between physical volume and the number of resonators for a filter having fixed rejection loss and bandwidth and a fixed passband loss. The example is for a case where the rejection bandwidth is 360 Mc, the rejection is 100 db and the passband loss is 0.5 db. Design data is based on a prototype having 1.2:1 maximum passband vswr or an amplitude ripple of 0.036 db. The last column is the product of b^2 and N and, as the length is fixed by frequency considerations, it should be proportional to filter volume. Apparently a minimum volume will result if a filter having 8 resonators which is substantially less than the value of N for a minimum loss filter - which from equation (1) would be 12 or 13. If a different value of passband ripple is chosen, the effect would be a slight change in the figures but the trends would be the same. If a different value of passband loss is chosen, the figures will change by appreciable amounts. However, the trends will be

Table 7-1. Optimum Physical Size For A Bandpass Filter

100 db Rejection ± 180 Mc

1.2/1 VSWR 0.036 db Ripple

0.5 db Loss

					0.7 Q Ideal		
N	BW_r	BW_3	Q/Q	Q_f	Q_u	b	Nb^2
3	5.54	8.7	0.027	264.	9780		
4	18.7	24.5	0.019	93.7	4930	1.96	15.35
5	38.7	46.3	0.015	49.6	3310	1.12	6.28
6	62.7	71.2	0.012	32.3	2690	0.89	4.75
7	88.0	96.8	0.010	23.7	2370	0.78	4.26
8	113.2	121.6	0.0087	18.9	2170	0.70	3.92
9	136.8	144.8	0.0076	15.9	2090	0.67	4.04

in the same directions and it is unlikely that the optimum number of resonators would change. There would, however, be a significant change in the required volume and, if the critical diameter is exceeded, cases other than that of the 3 resonator solution in Table 7-1 would become impossible.

Thus it may be seen that the trade-offs in the design of the filter portion of a diplexer involve the electrical requirements in such a way that requirements for high rejection and low passband loss combine to require a large unit. In particular it should be realized that over-designing or specifying on rejection results in an increase in size and/or weight with no compensating advantages.

About the same statement can be made in connection with designing to withstand a mechanical environment more rigorous than will actually be encountered. The result is a unit larger and heavier (or both) than it actually needs to be and there will be no compensating advantages.

7.2 DIPLEXING

The action of diplexing can be accomplished in several ways. The simplest is probably that of using two bandpass filters and connecting them in series or parallel at the common connection. This technique accomplishes the result with little or no addition of size or volume over that which would be required to accomplish the equivalent filtering without diplexing.

Additionally, it is possible to combine the signals by means of a circulator as indicated in Figure 7-1. Signals from the transmitter are passed on to the antenna and signals from the antenna (at the receiver frequency) are passed on to the receiver. Junction problems are eliminated and there is no restriction on the length of the lines between the circulator and the bandpass filters. There is a penalty in the form of the added loss and weight of the circulator.

Another form of diplexer (which can be extended to provide multiplexing of more than 2 units) is shown in Figure 7-2. As shown here it can be used to diplex a receiver and a transmitter but it does not provide preselecting action for the receiver. If this is required a second unit must be added, tuned to the receiver frequency, to form a complete diplexer. It may be possible, under these conditions, to add only a bandpass filter to provide preselecting action but there may be undesired action between the diplexer and the preselector. This can be determined by a computer study.

8.0 ANTENNA IMPLEMENTATION TRADE-OFFS

8.1 TELECOMMUNICATION TRADE-OFF

Certain antenna trade-offs are made on a system basis in section 6.5, VB233AA101. These are summarized here.

a. The high-gain antenna is a parabolic reflector of 7.5-foot diameter, rather than an array or unfurlable antenna.

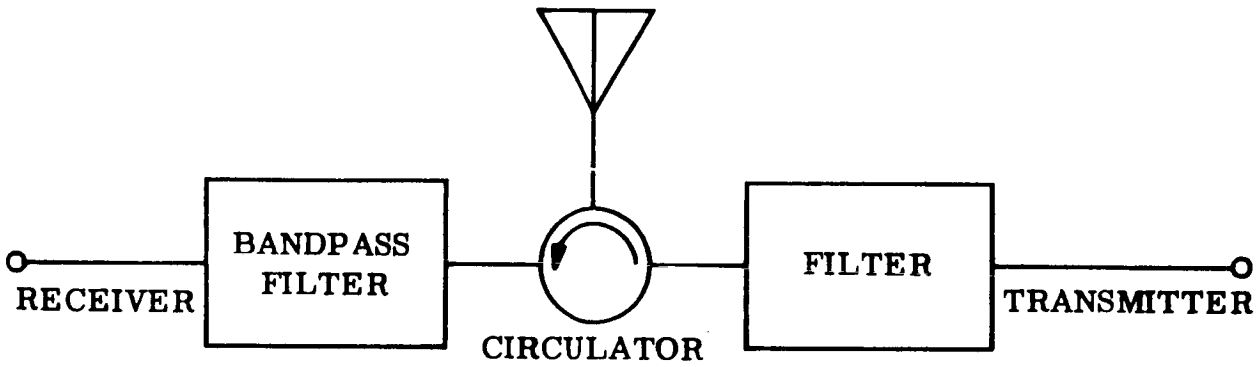

Figure 7-1. Diplexing with Circulator

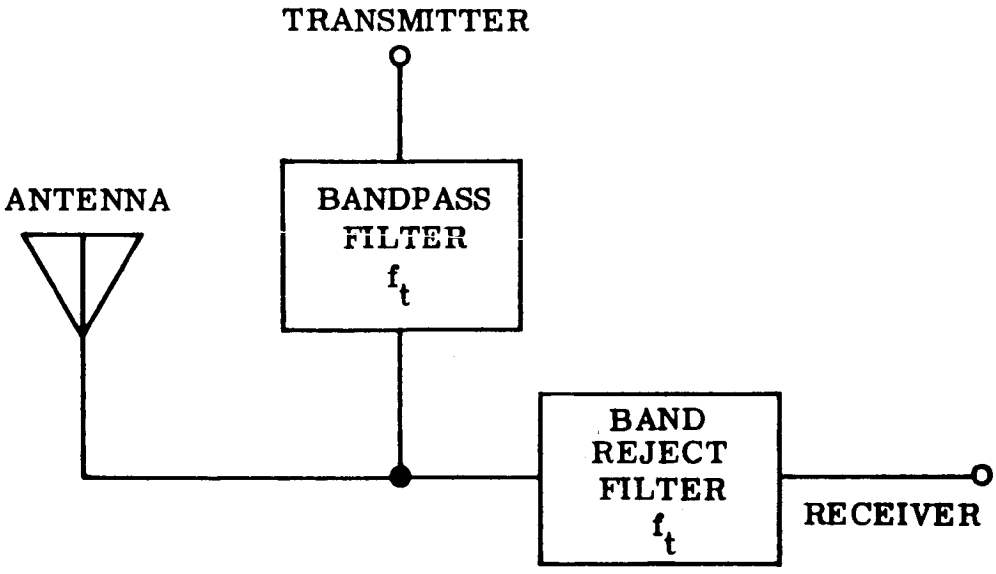

Figure 7-2. Diplexer

b. R-F angle tracking is not recommended.

c. Beam steering for the high-gain antenna is obtained by mechanical pointing of the parabolic dish.

d. Two low-gain antennas are recommended; one having essentially hemispheric coverage centered on the spacecraft -Z axis, the other having a toroidal pattern, omnidirectional in the X - Z plane.

e. Use of a separate low-gain antenna for launch coverage is recommended.

8.2 HIGH-GAIN ANTENNA

The preferred high-gain antenna approach is a rigid 7.5-foot diameter paraboloidal reflector of aluminum mesh construction. It is fed at its focal point by a turnstile radiating element.

8.2.1 ALTERNATE ELECTRICAL DESIGNS CONSIDERED

8.2.1.1 CASSEGRAIN VERSUS FOCAL-POINT FEEDING

A Cassegrain geometry offers several advantages in reflector antenna design, particularly when there is a requirement for angletracking capability. In such a configuration, a large magnification factor is available which increases the effective focal length of the paraboloid. With the choice of magnification factors available, a paraboloid with a smaller f/D ratio can be used, thus reducing the antenna volume. A Cassegrain geometry also allows the feed to be placed at or near the vertex of the parabola which minimizes transmission line length and insertion loss.

The disadvantages of using the Cassegrain geometry for the high-gain antenna are: (1) The weight of the antenna is greater, since a hyperbolic sub-dish and a larger feed are required, and (2) The complexity of the antenna increases with the addition of a sub-dish.

For the preferred approach, where no tracking is required, a focal-point fed antenna is more desirable. A small feed of about one-half wavelength in size can be placed at the focal point of the paraboloid, and a reasonable f/D ratio (about 0.32) can be used.

8.2.1.2 FEED DESIGN

Various types of radiating elements are considered for feeding the parabola. These are crossed dipoles, the equiangular spiral, and a waveguide pyramidal horn. The major considerations for the feed choice are simplicity of design and the adequacy of the feed to perform its function.

Of the choices listed above, the crossed dipole feed is the simplest in design. The crossed dipole feed uses the impedance properties of the dipoles to obtain the

quadrature phasing required for circular polarization. This is accomplished by establishing different lengths for the orthogonal dipoles. A ground plane is used that acts as a parasitic radiator to equalize the E-and H-plane primary patterns for each of the orthogonal dipoles. The ground plane acts as a shorted square waveguide whose pattern is super-imposed on the dipole pattern. Such a technique is employed in the Mariner C high-gain antenna.

The equiangular spiral provides pattern and polarization performance which is superior to that of the crossed dipole. However, the mechanical design of this device is more complex, and thus it may be considered to be less reliable.

The waveguide pyramidal horn is simple to construct, but in addition to the radiating aperture, a quarter-wave phase shifting section is needed to obtain quadrature phasing of orthogonal field components. A waveguide-to-coax transition is also required and some compensation structure must be placed in the horn aperture to equalize its pattern. A pyramidal horn assembly is thus more complex than a pair of crossed dipoles, and this approach offers no performance advantages.

8.2.2 MECHANICAL DESIGN CONSIDERATIONS

Three different structural design approaches are considered for the high-gain antenna:

a. Opaque honeycomb sandwich reflector bonded to an integral box-section support ring and a three-member feed support truss.

b. Conventional open mesh reflector supported on a structure of six radial beams, one main structural ring, and two auxiliary rings. Three-member feed support truss.

c. Tensioned open mesh reflector forming an integral structure with three compression-loaded rings, one axial compression strut, and filament tension members.

Approaches (a) and (b) have been subjected to preliminary structural analysis and approach (c) has not. Based on the analysis, several comparisons are apparent and are summarized in the following table:

Hi-Gain Antenna Structural Design Evaluation

	Structural Approach	Solar Opacity	Weight	Electrical Performance	Reliability	Cost	Totals
(a)	Sandwich	3	1	1	1	2	8
(b)	Conventional Mesh	2	3	2	2	1	10
(c)	Tensioned Mesh	1	2	3	3	3	12

1 = Best 3 = Worst

No attempt is made in the table ratings to weight each factor in relative importance to the spacecraft system. The factors considered in arriving at the relative ratings of the table are briefly discussed below.

a. Solar opacity - The fuel penalty due to the high solar drag of an opaque reflector is prohibitive. This eliminates the sandwich approach from serious consideration even though it is lightest in weight and highest in reliability. The tensioned mesh is judged best on the basis that supporting members will present the smallest area due to the structural contribution of the mesh.

b. Weight - The tensioned mesh approach is estimated to weigh about 35 pounds. This compares with 26 pounds for the sandwich and 45 pounds for the conventional mesh. The structural contribution of the tensioned mesh accounts for its reduced weight.

   Electrical Performance - The tensioned mesh approach appears least desirable due to the shadowing effect of the compression-loaded axial tube which reacts the mesh and filament tension loads and supports the dipole feed. The structural sandwich gives superior electrical performance because of its dimensional stability.

c. Reliability - The tensioned mesh approach will probably require many detail fasteners and fittings in order to properly position and stress the reflector surface. The dimensional stability of the antenna is thus least predictable. The simplicity and rigidity of the sandwich makes it the most reliable approach.

d. Cost - The conventional mesh approach design and fabrication involves well known techniques. Its overall cost is therefore lowest.

In summary, the conventional mesh approach is judged most nearly optimum at this time. Additional analysis and weighting factors could alter this conclusion. If forces on the antenna due to solar pressure could be suitably compensated, the honeycomb sandwich would be the preferred structural design.

8.3 PRIMARY LOW-GAIN ANTENNA

The primary low-gain antenna must provide approximately hemispherical pattern coverage centered on the spacecraft roll axis (-z axis). In addition, for use during the initial acquisition phase, pattern coverage is needed out to cone angles of 110 degrees with roll axis symmetry. The preferred design selected for this antenna is the waveguide-fed crossed slot radiator used for the Mariner C low gain antenna.

Several other design approaches are considered for the primary low-gain antenna. A turnstile radiating element mounted over a conical ground plane provides good pattern coverage over a hemisphere. By properly adjusting the antenna dimensions, nearly uniform + 2 db gain is obtained over the sector ± 45 degrees from the axis of symmetry.

This type of pattern ensures the availability of + 2 db gain in the cruise mode at encounter as well as over most of the mission lifetime. This antenna can be made extremely lightweight and highly reliable.

Another antenna configuration considered for this application is the conical equiangular spiral. The off-axis polarization characteristics of this device are generally superior to both the turnstile and crossed slot radiators. Pattern characteristics are readily controllable by adjustment of spiral parameters. The bandwidth of the conical spiral can be made extremely wide, and the requirements of this application can be easily accommodated.

In comparison, the Mariner C type low-gain antenna provides +5 db gain on axis, but the gain at encounter may fall to 0 db or less. Good pattern coverage is available at large cone angles for use during acquisition. The weight of this antenna is greater, but it requires no separate supporting mast and cable run. In addition, the insertion loss of the circular waveguide is very small in comparison to an equivalent length of coaxial cable. It is concluded that there are no significant performance advantages offered by other antennas over the Mariner C crossed slot. Furthermore, because this type of antenna is developed and qualified, it offers proven reliability at minimum cost.

8.4 SECONDARY LOW-GAIN ANTENNA

The secondary low-gain antenna must provide a toroidal pattern with circular polarization. In addition to the quad-dipole arrangement that is chosen as the preferred approach for this application, the circularly polarized biconical horn, the "electric-magnetic" dipole, and a ring array are considered for this application.

The biconical horn gives a toroidal pattern and can be made circularly polarized by exciting the biconical horn with slots canted at 45 degrees to the horn axis. The electric vector perpendicular to the constraining walls of the horn is not affected while the electric vector parallel to the walls is retarded. By adjusting the length of this region, the quadrature phasing necessary for circular polarization is obtained. A major disadvantage of this configuration is the narrow pattern that exists in the plane perpendicular to the toroid because of the aperture size inherently required. Another disadvantage is that the horn is relatively narrow band, since the phasing of orthogonal field components is a function of length in the feed region of the horn.

The "electric-magnetic" dipole consists of a vertical monopole around which a loop radiator is placed. Circular polarization is obtained by adjusting the amplitude and phases into each of the orthogonal radiators. It is difficult, in practice, to make the monopole and loop patterns coincide, and, as a result, the polarization circularity is not as good as that of the quad-dipoles.

A ring array consists of radiating elements placed symmetrically about the circumference of a circle. To obtain a smooth pattern, many elements are required and the feed structure for the elements becomes relatively complex for operation over the required bandwidth. The axial ratio obtainable from this type of structure is also not as good as that of the quad-dipoles at angles off the principal plane.

The quad-dipole configuration, on the other hand, exhibits good axial ratios and is not as frequency selective as the other configurations discussed. Theoretically, the axial ratio from 2110 mc to 2300 mc is less than 1 db, both in the principal plane and ± 45 degrees from this plane.

8.5 LAUNCH ANTENNA

The launch antenna is used during the comparatively short period of launch and injection. It should provide approximately hemispherical pattern coverage centered about an axis normal to the vehicle thrust axis at a clock angle which will permit Earth coverage from the time of shroud separation to the initial acquisition phase. The antenna type recommended for this function is a turnstile element over a conical ground plane. This device will reliably satisfy all requirements with the smallest and lightest configuration.

The Mariner C type crossed slot antenna is also considered for the launch antenna function. However, pattern coverage over a ±75-degree cone (required for Earth coverage in parking orbit) is not as uniform as that provided by the turnstile. Furthermore, since a long support mast is not required, the advantages of the circular waveguide feed cannot be realized, and the weight of this configuration becomes a disadvantage. Conical equiangular spirals are also considered for this application, but they are ruled out because of their relative complexity in comparison to the turnstile.

9.0 CONTROL CIRCUITRY TRADE-OFFS

Alternate approaches considered in the development of the preferred control circuitry are discussed and summarized in this section.

9.1 BASIC GROUND RULES

9.1.1 GENERAL DESCRIPTION

The control circuitry considered performs the following two basic functions:

1. Provide rf paths for three transponder exciters to drive three power amplifiers, where each exciter must be capable of driving each of several power amplifiers.

2. Provide rf paths from the power amplifiers to the spacecraft antennas. Each antenna must be capable of being excited by each of several power amplifiers.

9.1.2 GENERAL REQUIREMENTS

The control device must present a reliable, low attenuation rf path for a phase modulated S-band carrier at a frequency of 2295 mc (nominal). In addition, multiple rf paths must be isolated and input and output impedances must match 50 ohms (nominal). Size, weight, reliability, and power consumption are the other prime considerations and are discussed with regard to the alternate approaches.

9.2 POWER AMPLIFIER DRIVE

9.2.1 PREFERRED DESIGN

The preferred control device is a hybrid coupler. The unit functions as a power splitter in the forward direction and provides isolation between the two input terminals and the two output terminals. Figure 9-1 is a functional block diagram of this configuration and Table 9-1 lists the path losses for the hybrid coupler.

Table 9-1.

R-F Path	Path Loss (db)
1:3	3
1:4	3
2:4	3
2:5	3
1:2	20
3:4	20

The hybrid coupler permits the output of one exciter to be applied simultaneously to several power amplifiers exclusive of any rf switching. The exciter to be selected for operation is simply activated by a "command on" pulse.

9.2.2 ALTERNATE DESIGN CONSIDERATIONS

9.2.2.1 TRANSFER SWITCH

Transfer switches fulfill the required switching function when substituted for the hybrid coupler and have the advantage of offering minimum insertion losses. However, the added reduction in reliability due to the mechanical switching is not warranted and is prohibitive in this case.

9.2.2.2 POWER DIVIDERS

Figure 9-2 is a block diagram showing a configuration employing power splitting. The advantages of this approach are that it enables each exciter to drive all the power amplifiers and that the power dividers provide reliability approximately equal to that when using hybrid couplers. This technique, however, introduces insertion losses that are prohibitive when using the presently proposed transponder and power amplifier.

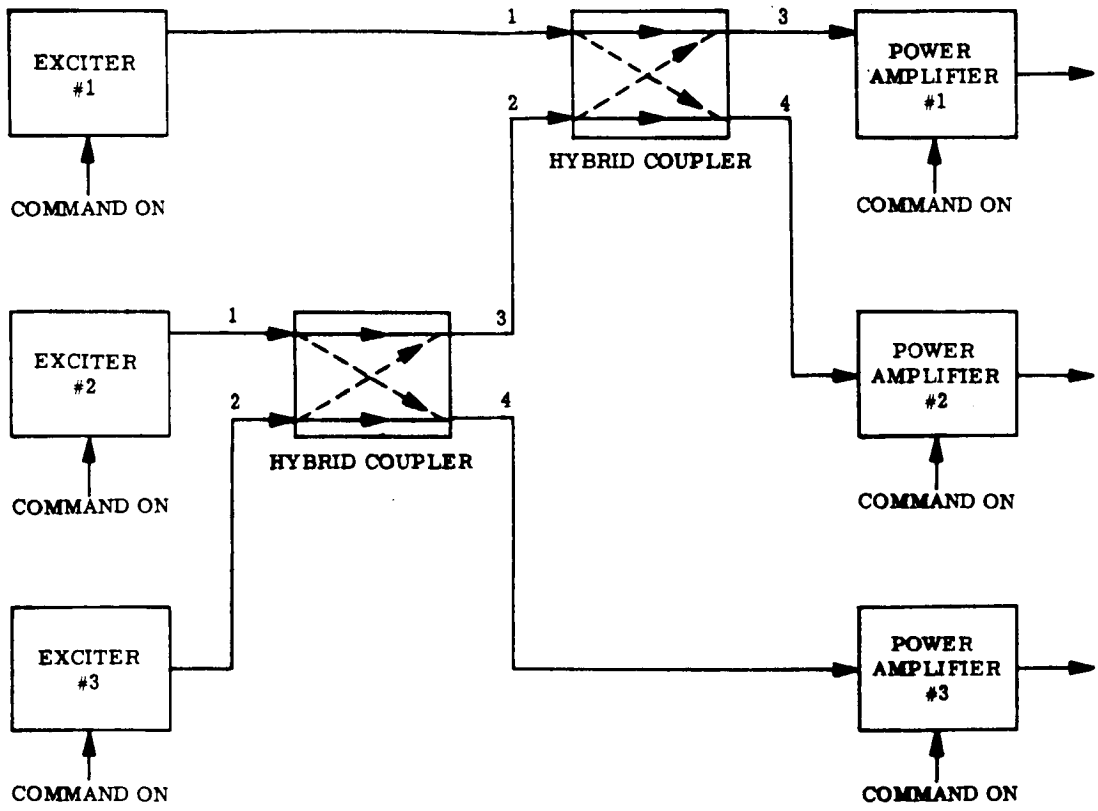

Figure 9-1. Preferred Approach, Hybrid Couplers

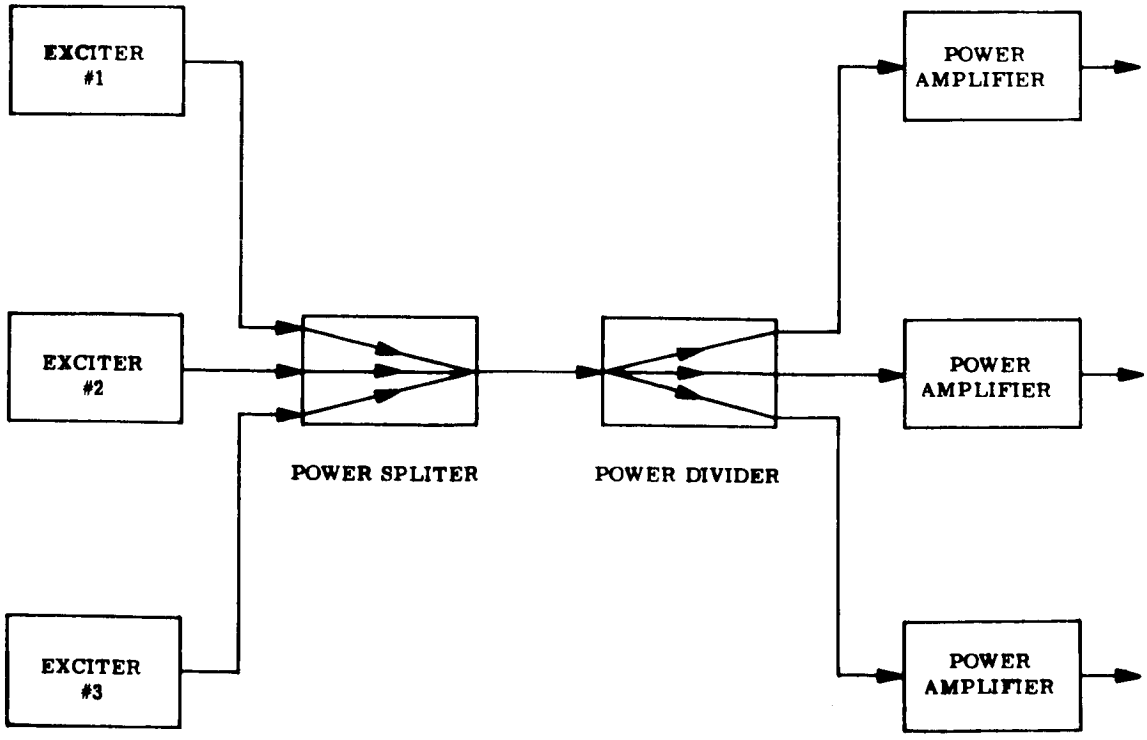

Figure 9-2. Alternate Approach, Power Splitter and Divider

9.3 ANTENNA SWITCHING

9.3.1 PREFERRED DESIGN

The preferred antenna switching scheme is illustrated in Figure 9-3. Transfer switches provide minimum insertion losses and have maximum isolation between alternate rf paths. The switches permit the power amplifier outputs to be applied to several antennas. The amplifier to be used is simply commanded on.

Weight and size of the transfer switches are suitable for spacecraft applications and efforts are being directed toward further reduction in these areas. The transfer switch proposed is of the latching type and does not require constant power to maintain switching. It is operated only once in a normal mission. It is being developed for the Apollo program and it is expected that it will have demonstrated reliable performance in space operation during the development of Voyager.

9.3.2 ALTERNATE DESIGNS

9.3.2.1 FERRITE SWITCH

An alternate approach to the antenna switching problem is through the use of ferrite or voltage operated circulator switches. These switches offer matched input and output impedances and a means of changing the rf path. Application of a positive or negative drive voltage causes the rf signal to circulate in a clockwise or counterclockwise direction from the input to the next terminal which then becomes the output terminal. This switch has the disadvantage of requiring holding power. However, through the use of permanent magnet biasing, a switch can be built which would operate with negligible holding power and include only slight increases in size and weight.

Weight and size of the transfer and ferrite switches are comparable. The ferrite switches have drawbacks, however, in that magnets are not desirable from the standpoint of a magnetically "clean" spacecraft and are subject to space radiation effects. The insertion loss of the circulator switches is significantly higher than the transfer switch.

10.0 POWER SUPPLIES

10.1 RECEIVER POWER SUPPLY

The receiver requires a voltage regulator to reduce power line audio frequency voltage susceptibility. L-C filtering can be used but high attenuation, broadband, low frequency filtering requires large, heavy components. The voltage regulator is used in place of this low frequency filtering, as a practical compromise of efficiency vs. weight. The efficiency reduction is approximately 10 per cent for the series regulator while a low loss, L-C filter weighs several pounds.

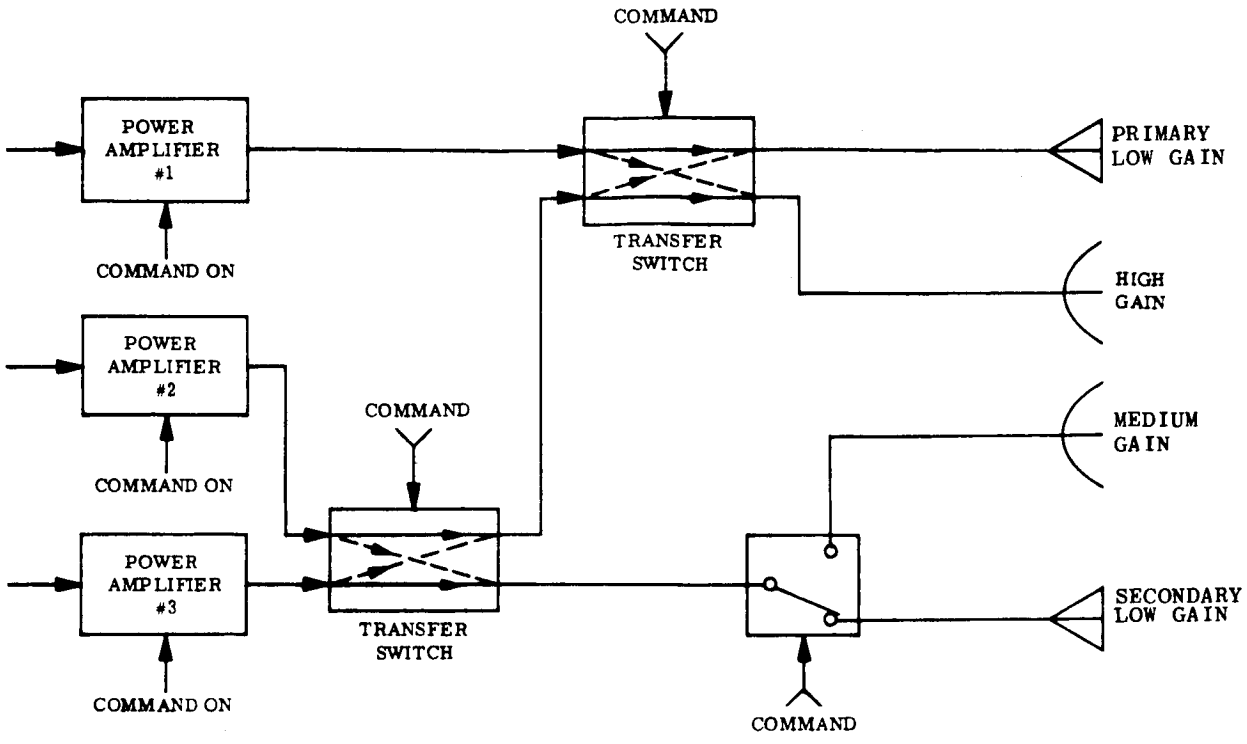

Figure 9-3. Preferred Approach Antenna Transfer Switches

Regulation is required because of the power supply audio voltage susceptibility of the vco and the video amplifier. These areas may be regulated independently but simple zener regulation is inadequate and multiple regulators reduce system reliability.

The ranging circuitry supply voltage is turned on and off through a latching relay as a means of gating the ranging channel. This is considered to be very reliable and much less susceptible to audio modulation or rfi than a transistor gating system, as well as resulting in a low energizing energy gate.

10.2 TRANSMITTER POWER SUPPLY

The transmitter requires a voltage regulator to reduce powerline audio frequency voltage susceptibility. The trade-offs of the transmitter supply are identical to those of the receiver in paragraph 10.1.

In the transmitter, the auxiliary oscillator is the most susceptible circuit, but the transistor amplifiers and multipliers also require regulation to adequately reduce susceptibility. For these circuits, a series regulator is more efficient than a zener regulator so the best choice again appears to be a series regulator.

Transmitter power on-off gating is performed through a latching relay in the primary circuit of the power supply.

11.0 RADIO SUBSYSTEM REDUNDANCY TRADE-OFFS

11.1 INTRODUCTION

To supplement the overall telecommunication system redundancy trade-offs, a trade-off analysis is conducted for the radio subsystem. The purpose of the radio subsystem redundancy trade-offs is to optimize the design of the radio subsystem based on the the mission phases of the Voyager and the functions to be performed by the radio subsystem in each phase.

11.1.1 SCOPE

Since the radio subsystem is to operate as an integral part of the telecommunication system, the results of the redundancy trade-offs affect the whole system. To provide a traceable path through the trade-off analysis so that each step may be reconsidered at any time a step-by-step procedure is used.

A basic system is first configured which satisfies all the required mission functions but fails to provide any redundancy for any mission function. Next, one level of redundancy is added.

With the added level of redundancy various methods of implementing the system are analyzed. Each time a component is added, the increase in weight and power is noted in addition to the decrease in probability of failure for the function. Thus, by manipulating the components, a parametric solution involving reliability, weight, and power for a particular function is found.

A second level of redundancy is added to the radio subsystem configuration. For each particular mission function, i.e., transmitting telemetry, receiving commands, and etc, the decrease in failure, weight, and power is evaluated.

This procedure is continued through a redundancy of level four. It is found that level three redundancy is optimum for the Voyager mission.

11.1.2 DEFINITION OF BOUNDARIES

For the purposes of this study the radio subsystem includes:

a. Transponders

b. Power Amplifiers

c. Antennas

d. RF Switches

e. Diplexers

f. Other rf hardware

The input interface to the radio subsystem is the input to the transponder exciter. The interface at the output of the radio subsystem is the output of the transponder receiver.

The transponder is divided into three subassemblies for the purposes of this study.

a. S-Band Exciter

b. S-Band Receiver

c. Turnaround Ranging Channel

Each of these three subassemblies is assigned a particular failure rate which includes the corresponding power supplies.

The power amplifier is considered a complete subassembly which includes the power amplifier, its power supply, and an output power monitor.

The antennas are considered to have a reliability of one, with the exception of articulated types. For articulated antennas the reliabilities are less than one. This is adequate information for a trade-off to be made in the subsystem design of articulated versus fixed antennas so far as reliability is concerned.

The antenna contributes to a great extent to this trade-off analysis in evaluating the subsystem configuration versus mission phase.

All other equipments are treated as components within the radio subsystem with fixed failure rates.

11.1.3 DEFINITION OF FAILURE MODES

There are two basic types of failure modes considered in the reliability trade-off analysis of the radio subsystem, i.e., component failures and function failures.

11.1.3.1 COMPONENT FAILURES

Component failures are considered failures in the operation of a particular component.

The components and their associated failure modes are stated in Table 11-1.

Table 11-1.

Component	Failure Mode
Transponder	
Exciter	Complete Failure No Signal Output
Receiver	Complete Failure - Nonoperational
Ranging Channel	Channel Unuseable
Power Amplifier	Given an input signal, no output signal present
Antennas	None assumed.
RF Switch	Given an input signal, no output signal present.
RF Couplers	Same as above
RF Diplexer	Given an input signal at transmit or antenna port, no signal present at the antenna or receive port.

11.1.3.2 FUNCTION FAILURES

Each component of the radio subsystem performs some basic function which contributes to the over-all successful operation of the subsystem. In analyzing the system for this trade-off study, failures in a particular component function are also considered. A tabulated list of the components and their failure modes as to subsystem functions is shown in Table 11-2. In the trade-off analysis to find the preferred subsystem, the component failures listed in Table 11-1 are used. Once the subsystem is optimized it is evaluated further using the function failures listed in Table 11-2.

Table 11-2.

Component Function	Failure Mode
Exciter	
Provide rf drive to Power Amplifier	No output or high noise and spurious present.
Non-coherent drive to Power Amplifier	Auxiliary Oscillator Failure
Receiver	
Detect command subcarriers	No output
Coherent Drive to Exciter	VCO Failure
Power Amplifier	
Amplify rf signal to 50 watts	No output
Change output level to 20 watts	Output still at 50 watts
Antennas	
Receive and transmit rf signals	Antenna no longer in view of Earth
Antenna Pointing	Articulation not possible
Rotary Joints	No signal path through joint
RF Switches	
Switch rf paths	Switch will not operate
Switch in normally closed position	Contacts open (environmental causes).
Latching Switch	Switch will not latch
RF Couplers	
Provide 3 db coupling between a source and two loads	No output
Provide directional coupling	No output
Isolator	
Prevent rf signal interference	No output
Diplexer	None assumed

11.2 SUBSYSTEM DEVELOPMENT

The trade-off analysis for the radio subsystem consists of the same step-by-step development used in the system trade-off analysis. The results of the radio subsystem trade-off analysis are discussed in Section 7.3, Appendix IV, Sample Reliability Calculation VB233AA101.

12.0 EQUIPMENT ENVIRONMENT

Environmental protection of the Radio Subsystem is entirely passive. A particular design approach required to insure protection from a specific environment is investigated in an effort to determine whether it is detrimental or helpful in the solution to other protection systems. This philosophy is followed to its fullest extent where possible. As an example, the transponder housing may serve many useful mechanical functions. Properly designed, it serves as a structural member for the subsystem bay, as a thermal path for the power dissipated by the components and as an RFI shield, along with its primary function of providing containment of the components.

12.1 VACUUM

Due to the rapid decay in pressure during the launch phase, it is necessary to insure venting of the subsystem housings. Since the majority of the system need be rf tight, a large vent is not desirable. In most instances, there is sufficient venting at cable entries to the housings.

In most instances, voltages during this launch are low and arc-over is not a problem. However, should the need arise, local high voltage areas can be protected by foaming rather than sacrificing subsystem weight with a pressurized design.

12.2 TEMPERATURE

The choice must be made as to the method of heat removal from the components. Any full active temperature control system adds weight and size to the subsystem. Therefore, it is desirable to utilize the natural means of heat transfer. The majority of the mission results in a vacuum environment. Heat transfer within the subsystem can only take place by means of conduction and radiation. Because of the relatively low temperatures involved and the natural heat flow paths provided in a design which stresses a mechanical strength and rigidity, conduction will prevail. The dissipated power must then be removed from the subsystem. This transfer is by radiation, if it is assumed that the spacecraft structure may not be used as a conduction sink. Due to the orientation of the spacecraft, the outer plate to which the subsystem is fastened is normally looking at space as a low temperature heat sink. It is not feasible to allow the subsystem to continuously radiate to space or to be thermally shielded from space. Therefore, the use of adjustable louvers on the spacecraft is necessary. The control unit for these louvers need not be a part of the subsystem, but rather a part of the outer mounting plate. Since there are concentrated heat

loads within the subsystem, such as the power amplifiers, a method for maintaining low thermal gradients within the system is desirable. This may be done easily by locating these heat sources near the outer plate and then coating the outer plate in a selective fashion with varied emissivity finishes.

12.3 AGING - MATERIALS

Materials used within the system are selected so that their useful life is not shortened by any of the environments. Should a material be suspect, adequate protection is provided even at the expense of a slight increase in weight.

12.4 RFI PROTECTION

It is possible to shield the various portions of the radio subsystem with extremely thin and lightweight housings. However, since it is desirable to assist in the structural makeup of the equipment bay where possible, the housing is adequately sized to do so. Not only does this insure RFI protection but it insures a relatively high resonant frequency for the housing, which is compatible with the anticipated vibration inputs. Heat transfer of the dissipated power also benefits by the increased cross sections available for conduction.

12.5 SHOCK AND VIBRATION

The Voyager packaging concept requires the electronic housing to enclose the electronics and to add to the structural integrity of the vehicle. The overall weight of the vehicle is thereby reduced. The "T-frame" module packaging scheme, is ideally suited in this respect.

The use of T-frames not only provides a cross section necessary to conduct heat but is also a very good structural member. This permits the design of housings with primary natural frequencies of 500 cps and above. The high frequency resonances avoid "stacking" of housing resonances on the vehicle resonances. This minimizes both housing and component vibration loads. It also results in small relative displacements between circuit components. By utilizing the same material for both heat transfer and structural purposes of the module and spacecraft; overall weight is held to a minimum.

13.0 PACKAGING

Radio Subsystem packaging reflects trade-offs between such items as weight, mechanical strength, and environmental protection. In order to satisfy these various requirements in an optimum design, an equipment housing which is compartmented or modular in configuration is desirable. Because of RFI, it is necessary to isolate many of the basic functional blocks within their own enclosures. This also allows many of the high heat dissipating components to be mounted to good thermal conductors and results in relatively low component temperatures. These same enclosures also furnish a basic structure within the confines of an equipment bay which aids in stabilization of the bay structure. The T-frame concept which is used in the transponder

section of the subsystem satisfies all of the above requirements. It also allows the use of a proven transponder design with very little re-packaging effort [1].

The remaining portions of the Radio Subsystem do not lend themselves to this T-frame configuration. Therefore, it is desirable to package these separately from the transponders. On a weight basis only, since the remaining portions are generally large piece parts (excluding the power amplifier power supply), merely fastening them to the thermal control/shear panel would appear to be a practical approach. However, this structure depends on the equipment for stabilization. Also the concept of standardized connector and tie-down locations for all the bays is desirable. Therefore, the packaging of the power amplifiers, diplexers, transfer switches, etc. in rigid housings is desired.

The power amplifiers and their supplies are mounted such that the high dissipated power is easily transferred to the outer plate of the bay. Otherwise there is no practical method of temperature control without the use of an active cooling system. Final design of the outer plate (specific thickness) will determine the overall weight and volume of the power amplifiers. If the decision is to use a thin outer plate, the power amplifier package will have a relatively thick plate so that the power will be distributed over a large area and may be dissipated without a large temperature rise. This is also the best approach from a bay standardization standpoint.

There is a trade-off in the desired packaging of the diplexers and transfer switches. It is essential that the coax leads be of minimum length between the power amplifiers and the diplexers and the diplexers and the transfer switches so that power losses may be minimized. The number and type of connectors must also be minimized. In order that this may be accomplished, it is necessary to deviate from a standard connector pattern and location. It is also necessary that all diplexers and transfer switches be packaged with the same subassembly.

With the design incorporating three twt power amplifiers, it is possible to package the radio subsystem within a total volume slightly less than one and one-half bays. Since it is desirable, under certain circumstances, to use two twt's and one Klystron type power amplifier, sufficient space is allotted for this configuration. Because of the larger sized Klystron and the cable length considerations mentioned previously, the volume used for this design is slightly larger. A detailed packaging study is necessary during the design phase to ensure efficient volume usage with an optimum radio subsystem design.

Dimensionally the design approach taken allows the radio subsystem to be packaged within the total volume of one and one-half bays. Physically it allows limited standardization of connectors and mounting locations and permits the spacecraft structure weight to be a minimum.

---

[1] Motorola Final Report, S-Band Transponder Mark I, 20 Cycle Bandwidth, JPL Contract No. 950413.

CII - VB233AA103

ALTERNATE SUBSYSTEM MECHANIZATIONS CONSIDERED

COMMAND SUBSYSTEM

Index

1 Scope
2 Applicable Documents
3 Design Criteria and Constraints
4 The Two-Channel Command Detector Tradeoff
5 Coding
6 Decoder Mechanism
7 Circuits Design
8 Environmental and Packaging Considerations
9 References

Appendix I Manchester Coded Transmissions

1.0 SCOPE

This tradeoff study covers all tradeoffs internal to the command subsystem. That is, only tradeoffs between characteristics and parameters confined to the command subsystem are considered herein. Tradeoffs between the command subsystem and other system parameters are treated in the Telecommunications System Tradeoff Study, VB233AA101. This study directly supports VB233FD103.

2.0 APPLICABLE DOCUMENTS

Reference to the following documents is required for completeness in this description.

JPL Documents

MC4322A	Functional Specification - Mariner C Flight Command Subsystem, 3 June 1963
Doc. No. 339105	Typical Mechanization - Advanced Mariner Spacecraft Command Subsystem
GMG50109DSNA	Design Specification - Telecommunications Development - GSDS Command System - Ground Subsystem, 20 Oct 1964 (Command Verification Equipment)

GE/Motorola Documents

VB220SR101	Design Characteristics
VB220SR102	Design Restraints
VB220FD107	DSN Interface
VB220FD112	Flight Sequence
VB233FD101	Functional Description - Telecommunication System
VB233AA101	Tradeoff Study - Telecommunication System

3.0 DESIGN CRITERIA AND CONSTRAINTS

3.1 CONSTRAINTS

a. The bit error probability for the command link at threshold shall be less than 1×10^{-5}.

b. The command equipment shall be compatible with Command Verification Equipment (See Specification GMG-50109-DSN-A).

c. The command equipment shall employ pseudo-noise synchronization techniques.

3.2 DESIGN CRITERIA

The Mariner R, Mariner B, and the present successful Mariner C command systems have a proven reliability, unsurpassed to date. These techniques are the basis for the recommended Voyager approach and accordingly some of the detection and coding tradeoffs which were considered during the evolution of these designs, have not been duplicated here.

3.3 TELECOMMUNICATION TRADEOFFS

Certain command tradeoffs are made on a system basis in Section IV, VB233AA101 Tradeoff Studies, Telecommunication System. These are summarized here.

1. The low command transmission rate is one sub-bit per second.

2. The high transmission rate is thirty sub-bits per second.

3. Synchronization is achieved using a "two-channel PN code" implementation.

4.0 THE TWO-CHANNEL COMMAND DETECTOR TRADEOFF

4.1 GENERAL

Previous implementations of the proposed two-channel command detector on the Mariner R and C spacecraft systems require a normalized SNR of 19.5 db to achieve a bit error probability, P_e, of less than 1×10^{-5}. The degradation from the ideal threshold of 14.3 db ($P_{sync} = 2\ P_{command}$) is due to excessive phase jitter of the $2f_s$ reference signal which is used to demodulate the bi-phase modulated $2f_s$ $\angle 90°$ command tone. The phase jitter may be reduced by narrow-banding the phase-locked loop from which the reference is derived. On Mariner R the detector PLL threshold loop bandwidth, $2\beta_{Lo}$, is set at 2.0 cps because of the necessity for the PLL to acquire the maximum frequency offset without slipping a cycle, i.e., the PLL must acquire within the time of PN code correlation. The frequency offset is due to vco stability and acquisition time. In Mariner R the long term vco stability at the locking frequency f_s is approximately ±0.25 cps and the intentional acquisition offset at f_s for a PN code search time of approximately 5.5 minutes is 0.75 cps, resulting in a maximum offset of 1.0 cps. The requirement for the loop to lock without slipping a cycle is $\dot{\Theta} \leq \beta_L$, which results in a minimum bandwidth, $2\beta_{Lo}$, of 2.0 cps if the above constraints are to be satisfied.

4.2 OPERATION AT REDUCED SNR

Laboratory measurements made with the Mariner R and B command detectors indicate that a probability of bit error, P_e, of 1×10^{-5} is achieved with a normalized SNR of 16 db (instead of 19.5 db) if the bandwidth, $2\beta_{Lo}$, is 0.5 cps.

4.3 ACQUISITION PERFORMANCE

The impact of this lower threshold on acquisition performance must also be considered.

The measured (100 independent samples) probability of acquiring lock on the breadboard Mariner C command detector with a normalized input SNR of 19.5 db, $2\beta_{Lo} = 2.0$ cps (SNR in $2\beta_{LO} = 13.9$ db) and an offset at the locking frequency f_s of $\dot{\theta} = 0.75$ cps was 0.3. The tests also indicated that the PLL locking limit for the above breadboard with $\dot{\theta} = 0.75$ cps was very nearly reached with a normalized composite input SNR of 14 db, which corresponds to PLL parameters of $2\beta_L = 1.0$ cps, SNR in $2\beta_L = 11.4$ db and a damping ratio of 0.4.

Much of the previously noted degradation in the acquisition performance might be attributed to an excessive search rate relative to β_L ($\dot{\theta} > \beta_L$), to an underdamped loop and to excessive signal suppression in the limiter when the PN codes are not correlated. The two former conditions can be eliminated by optimizing the loop at the lower threshold and the latter condition could be alleviated by narrowing the bandwidth of the filter which precedes the limiter.

In previous command detectors, the limiter input noise bandwidth was 67 cps, resulting in a limiter suppression factor of $\alpha_o = 0.60$ for an input SNR of 19.5 db and full PN code correlation. If the PN codes are 50% correlated (±1/2 bit) the suppression factor is 0.35. Likewise, for the previously noted measurement with an input SNR of 14 db, the corresponding suppression factors are 0.37 and 0.2. Narrowing the limiter input bandwidth would allow the PLL to acquire under near optimum conditions over a larger portion of the time period when the PN codes are partially correlated. For example, if the normalized threshold composite input SNR is 16 db, with equal power for sync and data, and the limiter input noise bandwidth is 10 cps, the suppression factor 50 percent correlation would be 0.5, and 0.74 at full correlation.

The SNR in a PLL optimized at $2\beta_{Lo} = 2.0$ cps with a normalized composite input SNR of 16 db ($P_C = P_S$) is 9.1 db in $2\beta_{Lo}$ which is satisfactory for maintaining lock. On the basis of the above, although subject to further study, it appears that the acquisition performance of the command detector optimized for a normalized composite input SNR of 16 db can very nearly approach the performance achieved on previous higher threshold detectors.

4.4 IMPLEMENTATION OF THE NARROW-BAND COMMAND DETECTOR

Two approaches to narrow banding the PLL are considered:

1. A narrow band PLL using an automatic acquisition method such as squaring the $f_s \angle 90°$ command tone and recovering ambiguous $2 f_s$ PN clock or;

2. A PLL with an adaptive feature so that after lock-up the bandwidth narrows.

The former method has the advantage that the PN code search is in discrete steps and the probability of acquiring at threshold SNR is much higher. On the other hand, it requires an additional PLL and lock indicator which is estimated to be a 30% increase in circuitry over the Mariner C command detector. This hardware requirement is considered to be excessive.

The adaptive loop approach consists of using the detector lock signal to adapt the PLL from 2.0 cps to 0.5 cps at the expense of 5% additional circuitry over the Mariner C detector.

4.4.1 THE ADAPTIVE LOOP COMMAND DETECTOR

Figure 4-1 presents a block diagram of the recommended one sub-bit per second double channel detector.

In the Mariner R and Mariner C command detectors the phase-locked loop velocity gain constant, K_V, is approximately 100 sec^{-1} at threshold (composite SNR of 19.5 db in 1 cps). Considering only the detector oscillator uncertainty of ±0.25 cps at f_s, the static phase error at this frequency is held to ±1 degree and to ±2 degrees at 2 f_s. The SNR in the loop at threshold ($2\beta_{LO}$ = 2.0 cps) is 14 db, which results in an rms phase jitter at f_s of 8 degrees and 16 degrees at 2 f_s. Correspondingly, if the loop is adapted to

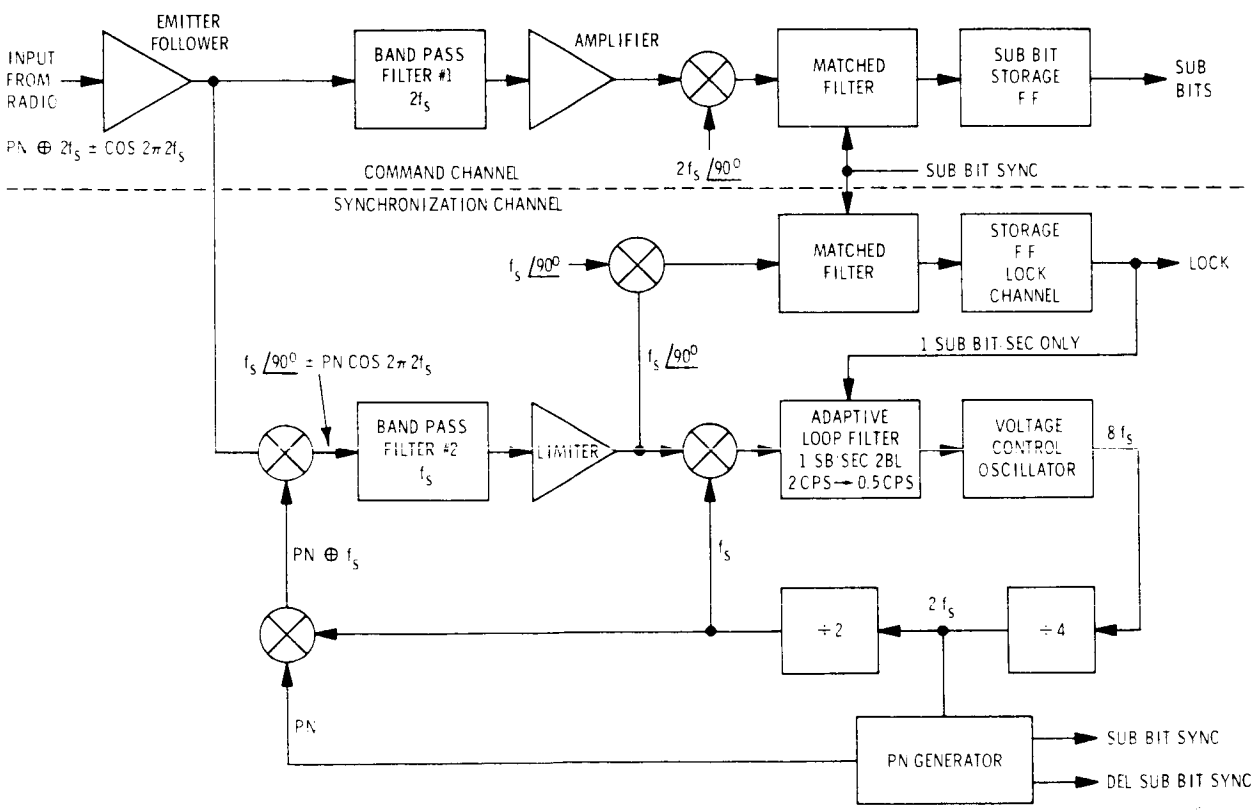

Figure 4-1. Command Detector, Block Diagram

$2\beta_{Lo} = 0.5$ cps, the rms phase jitter is 4 degrees and 8 degrees, respectively. However, the lag time constant in the compensation filter for $K_V - 100\ sec^{-1}$ and $2\beta_{Lo} = 0.5$ cps is 450 seconds, which is extremely difficult to implement.

In the implementation of the proposed lower threshold command detector and its associated adaptive loop, a tradeoff of these two phase errors to equalize their impact is considered. For instance, for $2\beta_{Lo} = 0.5$ cps at the 16 db threshold, the rms phase jitter at f_s is 6.4 degrees and at $2f_s$ it is 12.8 degrees. Also, for a static phase error of 6.4 degrees at f_s and the uncertainty of ±0.25 cps, the required velocity gain constant, K_V, is 14 sec^{-1} and the corresponding compensation filter time constant is 63 seconds. A time constant of approximately 100 seconds is achievable with passive components and allows a K_V of 22 sec^{-1} at threshold. For time constants in excess of 100 seconds, capacity multiplier methods may be utilized. The loop is adapted by switching out, with the lock indication, resistive components which determine the lead and lag time constants in the loop compensation filter. Rate limiting is utilized to prevent step transitions from upsetting loop quiescence.

4.4.2 ACQUISITION TIME PROPERTIES

The acquisition time required by the adaptive loop method is longer than that required by the automatic acquisition method. The acquisition time of the adaptive system will be longer than the present Mariner C detector. It is desirable to determine the mean time to lock the PLL as a function of the input SNR for the adaptive system shown in Figure 4-1. There are two basic difficulties.

First, no exact analytical method exists for determining locking characteristics of Type II Phase Locked Loops with a fixed amplitude input (this loop is actually a Type I second order with a long time constant and approximates the dynamics of a Type II). The Type I PLL is solved by Viterbi using the Fokker-Planck equations. Some asymptotic approximations are made for higher order loops. These are usable provided the amplitude is constant. Sanneman & Rowbatham (Reference 4-2) also obtain these results by digital simulation using constant amplitude. They show, by statistical experimental estimation, that the mean time to lock does not change appreciably with noise injected in the system. This conjecture based on digital simulation is useful.

Secondly, in the case treated here, the amplitude of the input to the PLL is varying because of the correlation characteristic at the input to the bandpass filter. See Figure 4-2.

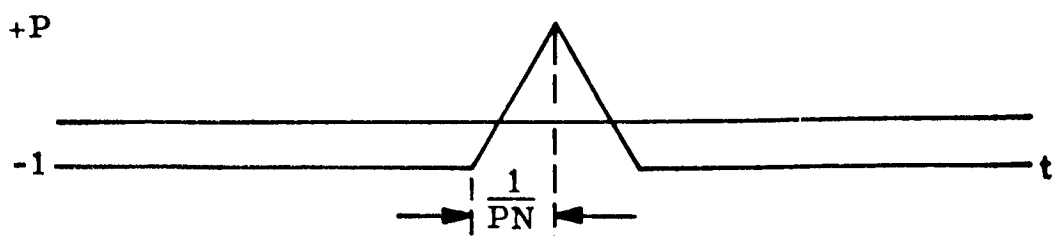

Figure 4-2. PN Correlation Function

The time variation of the amplitude depends upon this correlation function as well as the limiter suppression factor, which is also a time function. This time variation is comparable to the bandwidth of the system and hence cannot be neglected. It, therefore, seems doubtful that analytical results of Viterbi or simulation results of Sanneman & Rowbotham are applicable, However, there is some possibility of extending Viterbi approximations to this time varying case. Work on this extension is in progress and will continue during Phase 1B. The sure way of arriving at a reasonable solution is to simulate the loops digitally and make a deterministic plot of error versus error rate and hence find the mean time to lock. Noise may then be injected to determine its effects.

4.5 SYNCHRONIZATION SUBCARRIER CONSIDERATIONS

In the Mariner R and Mariner C command detectors, the sync subcarrier is transmitted as a square wave, with a resultant loss of approximately 0.9 db in the f_s bandpass filter. By transmitting the sync subcarrier as a sine wave, i.e.,

$$PN \oplus f_s \times f_s < 90°, \tag{4-1}$$

it appears that the above loss may partially be recovered. Further investigation in phase 1B is indicated.

4.6 ALTERNATE IMPLEMENTATION OF THE COMMAND CHANNEL.

One of the sources of departure from theoretical performance of the double channel 1 BPS system is the placement of data at $2f_s$. An advantage of placing the data at f_s can be seen by observing the phase variance at the demodulating $2f_s$ frequency. The phase variance at the f_s frequency from the phase-locked loop of Figure 4-1 is σ_1^2. σ_2^2 is the variance at $2f_s$. Then the relationship of σ_1 to σ_2 is given by the following equation.

$$\sigma_2 = 2\sigma_1$$

$$\sigma_2^2 = 4\sigma_1^2 \tag{4-2}$$

The mean-squared phase jitter is approximated by (Reference 4-3):

$$\sigma^2 = \frac{1}{2}\frac{N}{S} \tag{4-3}$$

$$\left(\text{if } \frac{S}{N} > 10 \text{ db}\right)$$

Thus, an improvement of 6 db in the reference is obtainable if the data is placed at f_s instead of $2f_s$. A block diagram of such a system is presented in Figure 4-3. Further investigation is required during phase 1B to see if this implementation is realizable.

Both the sync and command channel bandpass filters are now at f_s. There is some power at f_s in the PN x f_s $\angle 90°$ spectrum; however, it is down from the total power by approximately 58 db. However, f_s crosstalk or coupling at the demodulator (PN $\oplus$ f_s $\angle 90° \oplus$ PN) is possibly severe enough to cause a false lock.

4.7 AN ALTERNATE COMMAND DETECTOR (SPLIT PHASE)

4.7.1 DETECTOR MODEL

A command detector is formulated to detect one bit per second data with the following objectives:

a. Performance equal to or better than single channel.

b. Complexity not greater and preferably less than single channel.

c. Acquisition time of less than 5 minutes.

d. Not sensitive to transponder receiver bandwidth changes due to signal-to-noise ratio varying over complete dynamic range.

e. Probability of acquiring lock greater than 0.9 at threshold.

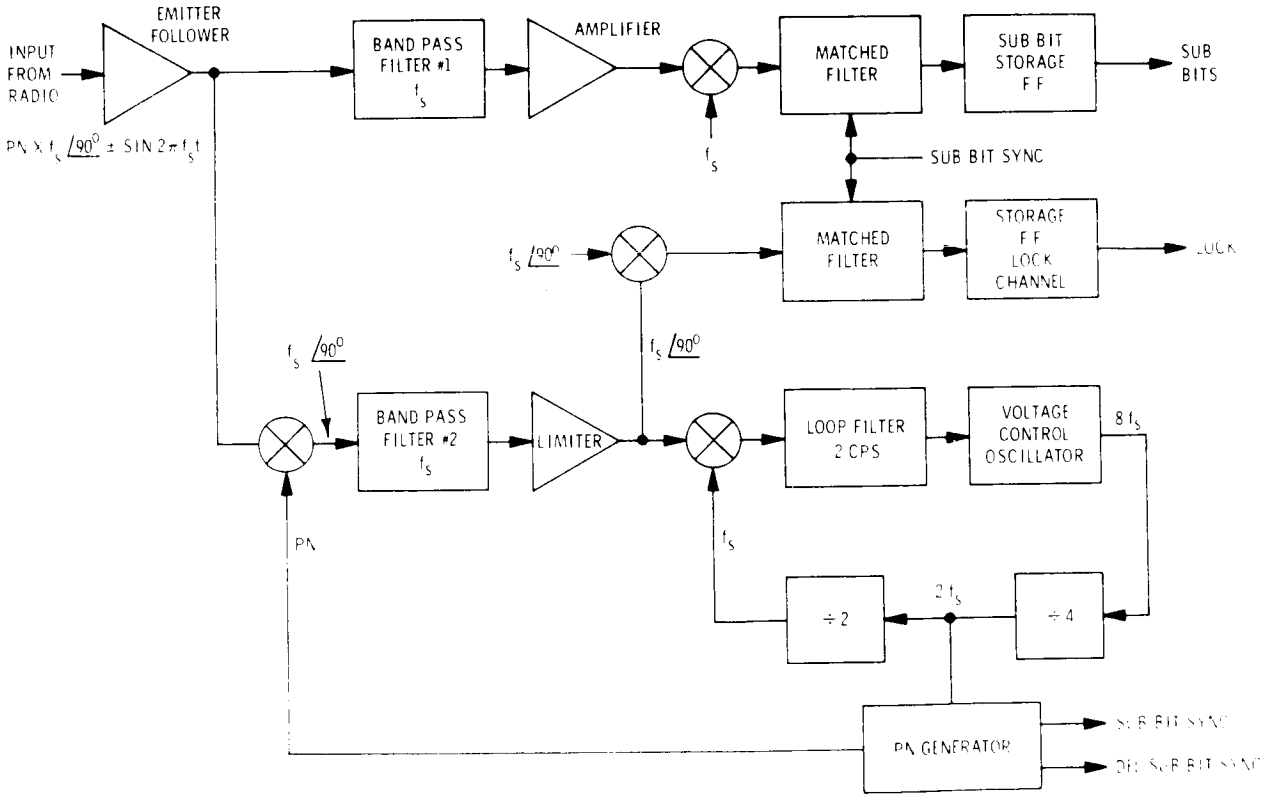

Figure 4-3. Command Detector, Block Diagram

The use of PN coding serves primarily to provide bit sync to an extremely high accuracy (better than 1/5000 of a data bit). Although it is desirable to have accurate bit sync, it is not necessary to have bit sync as accurately as the PN system provides. As an example, if bit sync is off by 5 percent of a bit, and the data is alternate ones and zeros, the effect of the bit sync error is approximately a loss of one db in signal-to-noise ratio. In the single channel case, there is hardly any loss in signal-to-noise ratio, but there is a loss of about 3 db due to the noisy reference signal which results because of not being able to sufficiently reduce the bandwidth of the coherent reference loop. A primary reason for not being able to reduce the loop bandwidth is that of acquisition. Certainly there are some tradeoffs to be effected in this area.

Because the use of PN does not provide any advantages except for bit sync accuracy and because PN causes an acquisition problem, the system formulated does not utilize PN coding.

A system is formulated which uses direct bi-phase modulation of a subcarrier. The subcarrier is low in frequency so that narrow band filtering is easier to obtain. The bi-phase modulated subcarrier is filtered by a bandpass filter with a noise bandwidth of 10 cps. Assuming that the signal-to-noise ratio of the command data is 13 db in a 1 cps noise bandwidth, the SNR at the output of the filter becomes 3 db. The filtered output is then frequency doubled by a very simple full wave rectifier. The SNR at the output of the full wave rectifier is degraded by 3 db resulting in a zero db SNR at the phase-lock loop input in a 10 cps bandwidth. The phase-lock loop has a $2\beta_L$ of 0.2 cps with a resulting rms phase jitter of 5.8 degrees at twice the frequency of the subcarrier and 2.9 degrees at the subcarrier frequency. This phase jitter has a net effect equal to less than 1/4 db reduction in SNR.

In order to obtain bit sync, the method of sensing crossovers is chosen. In order to guarantee crossovers, split bit coding of the information bits is selected. The low pass filter (#1) has a $2\beta_L$ of 4 cps in order to minimize sync error caused by variations in the time constant. A time constant variation of ±20 percent then is a variation of approximately ± 1/80 bit. The threshold levels for sensing crossovers is assumed to be at zero volts. The jitter on the crossovers is that of a 7 db SNR or ±25 degrees (±0.07 bit). The bit sync error caused by the threshold circuit switching from + 20 mv (out of one volt swing from a one to a zero at the LPF output) is about ±0.005 bit. The threshold circuit operates a monostable multivibrator which has a pulse width of 250 ms plus or minus 5 ms which results in a worst case bit sync error of 0.0025 bit. Adding up the individual contributions to bit sync error,

0.0125	from time constant variations
0.005	from threshold variations
0.0025	from monostable
0.0200	total

a peak error of ±0.02 bit results.

It is desirable to hold the error due to white noise to the same magnitude or less. Assuming the bit sync jitter due to noise to have an rms value of 0.01 bit, the bandwidth of the bit sync loop is calculated. The SNR in the LPF 4 cps noise bandwidth is 7 db. Conservatively, a loss of 3 db is assumed through the threshold circuit-monostable combination. A jitter of 0.01 bit requires a SNR of $(50/\sqrt{2}\,\pi)^2$ of $(16)^2/2$. This is equivalent to 21 db. A bandwidth reduction from 4 cps to 0.08 cps provides the 21 db SNR for bit sync. Bit sync then has a worst case offset of ±.02 bits due to implementation tolerances and an rms jitter of 0.01 bits. The peak bit sync error is then ±.05 bits for the 3σ noise jitter case. This results in a loss of signal-to-noise ratio of about 1 db and is adequate.

The phase-lock loop uses a separate oscillator for bit sync. The oscillator stability may be as bad as one percent and not cause an offset frequency large enough to prevent proper loop acquisition. The loop must be designed to minimize lag caused by frequency offset. The loop gain is calculated using a 1/4 percent stability oscillator.

$$K_v = \frac{\Delta F}{\theta_\epsilon} = \frac{0.9 \text{ deg/sec}}{3.6 \text{ deg}} = 1/4 \text{ per sec} \tag{4-4}$$

With a K_v of 1/4 per sec, the lag is a maximum of 1% of a bit. The loop bandwidth is 0.08 cps in order to obtain a 21 db SNR. The loop transfer function is

$$H(s) = \frac{K_v/T_2\,(T_1 S + 1)}{S^2 + \frac{K_v T + 1}{T_2} S + \frac{K_v}{T_2}} = \frac{\frac{32}{9}\beta_1^2\,(\frac{3}{4\beta_L} S + 1)}{S^2 + \frac{8}{3}\beta_1 S + \frac{32}{9}\beta_1^2} \tag{4-5}$$

$$T_2 = \frac{0.25}{\frac{8}{9}(2\beta_1)^2 - 8(0.08)^2} = \frac{0.25}{0.57 \times 10^{-2}} = 44 \text{ sec} \tag{4-6}$$

$$T_1 = 3/4\,\beta_1 = \frac{3}{2\,(.08)} = \frac{3}{0.16} = 18.8 \text{ sec} \tag{4-7}$$

The resulting open loop transfer function is then,

$$G_{(s)} = \frac{K_v\,(T_1 S + 1)}{(T_s S + 1)\,S} = \frac{0.25\,(18.8\,S + 1)}{S\,(44\,S + 1)} \tag{4-8}$$

The output of the bit sync loop supplies sample pulses to the word sync detector integrate and dump filter at a rate of 2 per second. The word sync detector then generates a pulse which resets a flip-flop at the word sync time for proper phasing of the split phase reference, and resets a second flip-flop to provide phasing of the reference

to the data detector. The reference for the data detector is then split-phase modulated by the proper reference phase signal to provide detection of split phase one bit per second data without a loss of 3 db due to the split-phase coding. Each data bit is integrated for a full second.

The resulting system as shown in Figure 4-4 has the following attributes:

1. Performance equal to or better than single channel.
2. Complexity not greater than single channel and probably less.
3. Acquisition time of about 1 minute.
4. Insensitive to transponder receiver bandwidth changes over input signal dynamic range.
5. Probability of lock in 1 minute greater than 0.95 at threshold and 3 db lower than threshold.

It appears that the system described has potential and should be further considered.

The system described above requires that the data bits be manchester coded at a symbol rate of two symbols per second. Therefore, the unique symbol pattern of 111000 and 000111 may be utilized to obtain word sync and bit sync, simultaneously.

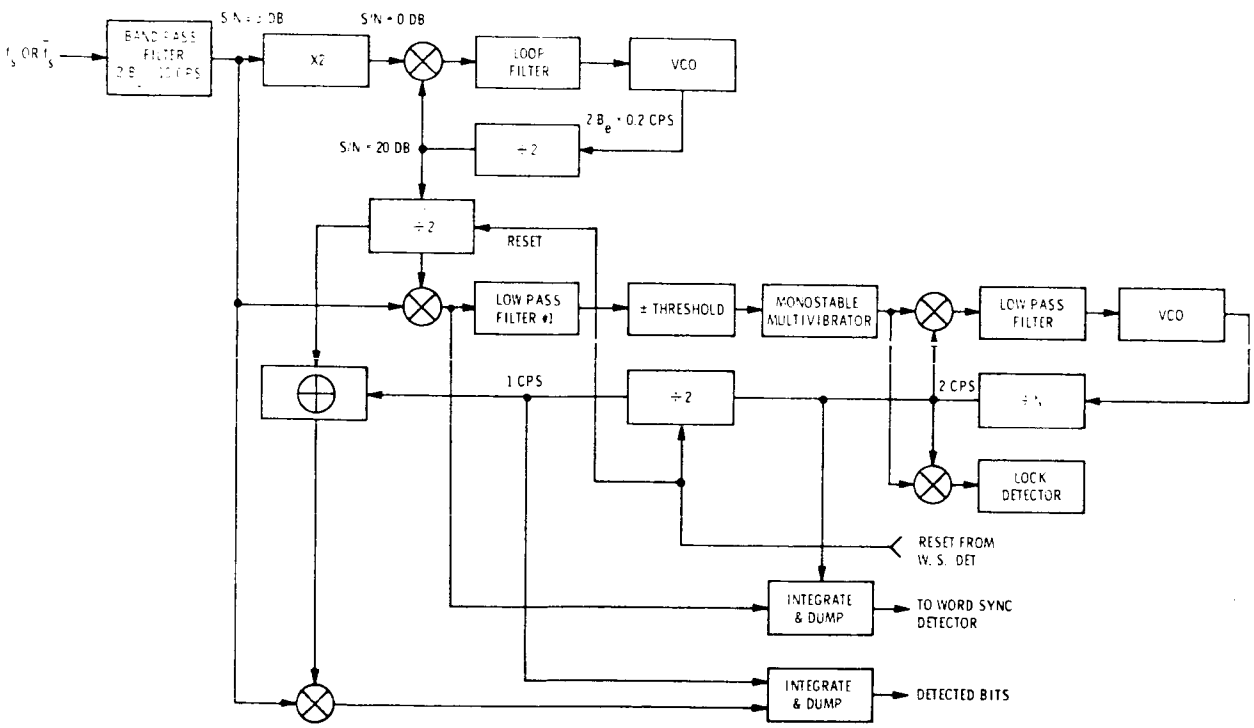

Figure 4-4. Split Phase Bit Decoder

The probability of obtaining word sync and bit sync on the first sync pattern is 0.994 and on the second word sync pattern 0.99998. By transmitting the above six symbol code (3 sec transmission time) unambiguous word synchronization is obtained at every word transmission. Therefore, at encounter and beyond, the loss of data due to a detector out of lock indication is reduced to one word. The probability of rejecting more than one word after an "in lock" indication is less than 1.2×10^{-6}.

4.7.2 EFFECT OF TRANSPONDER PHASE JITTER ON THE COMMAND SUB-CARRIER

Assuming that the linear transfer function of the transponder is:

$$G(s) = \frac{K_v}{S}\left(\frac{\tau_1 S + 1}{\tau_2 S + 1}\right) \tag{4-9}$$

Then

$$\frac{\theta_o}{\theta_i}(s) = \frac{K_v/\tau_2\ (\tau_1 S + 1)}{S^2 + \left(\frac{K_v \tau_1 + 1}{\tau_2}\right) S + \frac{K_v}{\tau_2}} = \frac{\omega_n^2\ (\tau_1 S + 1)}{S^2 + 2\delta\omega_n S + \omega_n^2} \tag{4-10}$$

and

$$\frac{\theta_e}{\theta_i}(s) = \frac{\theta_e}{\theta_i}(s)\frac{1}{G(s)} = \frac{1/\tau_2\ (\tau_2 S + 1)\ S}{S^2 + 2\delta\omega_n S + \omega_n^2} \tag{4-11}$$

The present transponder gain K_v' at strong signal is equal to $17 \times K_v$ at threshold.

$$\omega_n^2\ (\text{Threshold}) = 8/9\ (2\beta_L)^2 = 8/9\ (400) = 356\ \text{cps}^2/\text{sec}^2 \tag{4-12}$$

where

$$2\beta_L = 20\ \text{cps}$$

$$\delta\ (\text{threshold}) = 0.707 \tag{4-13}$$

Then ω_n' (strong sig) $= \sqrt{17}\ \omega_n$

Therefore

$$\frac{\theta_e}{\theta_i}(s)_{ss} = \frac{S}{\tau_2}\ \frac{(\tau_2 S + 1)}{S^2 + \sqrt{2} \times 17 \times 18.85\ s + 356\ (17)} = \frac{S(S + \frac{1}{\tau_2})}{S^2 + 453.0\ s + 6050} \tag{4-14}$$

and

$$S = -14, -439, \frac{1}{\tau_2} = 0.00362\ \sec^{-1} \tag{4-15}$$

$$\frac{\theta_e}{\theta_i}(s)_{ss} = \frac{S\ (S + 0.00362)}{(S + 14)\ (S + 439)} \tag{4-16}$$

$$\frac{\theta_e}{\theta_i}(s) \simeq A_e^{j\theta} \text{ where } \theta = \frac{\pi}{2} - \tan^{-1}\frac{\omega}{\omega_o} \tag{4-17}$$

$$\omega >> 14,\ \omega_o = 439$$

$$\frac{\partial \theta}{\partial \omega} = \frac{\frac{1}{\omega_o}}{1 + \frac{\omega^2}{\omega_o^2}} = \frac{\omega_o}{\omega_o^2 + \omega^2} \tag{4-18}$$

$$\frac{\partial \theta}{\partial \omega}\ \omega = \omega_o = \frac{\omega_o}{2\omega_o^2} = \frac{1}{2\omega_o}\ \text{rad}/_{\text{rad/sec}} \tag{4-19}$$

Assuming that the command subcarrier is placed at $\omega = 439\ \sec^{-1} = 70$ cps and bi-phase modulated at a 2 bit/sec rate the maximum phase error due to the transponder is as follows:

From Equation (4-19)

$$\frac{\partial \theta}{\partial \omega}_{\omega = 439} = \frac{1}{878}\text{rad}/_{\text{rad/sec}}$$

$$= \frac{57.2}{874/2\pi} \text{ deg/cps}$$

$$= 0.41 \text{ deg/cps} \qquad (4\text{-}20)$$

Therefore, the worst case phase error is less than 1 degree at strong signal and the maximum signal input to the command detector is suppressed by 3 db thus reducing the dynamic range requirements of the detector. The desirability of reducing the command subcarrier to the lowest value possible without affecting the transponder has the distinct advantage of reducing the requirements on the detector bandpass filters.

5.0 CODING

In order to evaluate the relative merits of coding the command transmissions, a review of the Mariner "B" and Mariner "C" command subsystems is presented.

5.1 MARINER C COMMAND DECODER

The command decoder accepts serial binary words, bit sync, and lock information from the command detector. Figure 5-1 is a block diagram of the command decoder. The command decoder processes words of fixed length only (word length - 26 bits). The

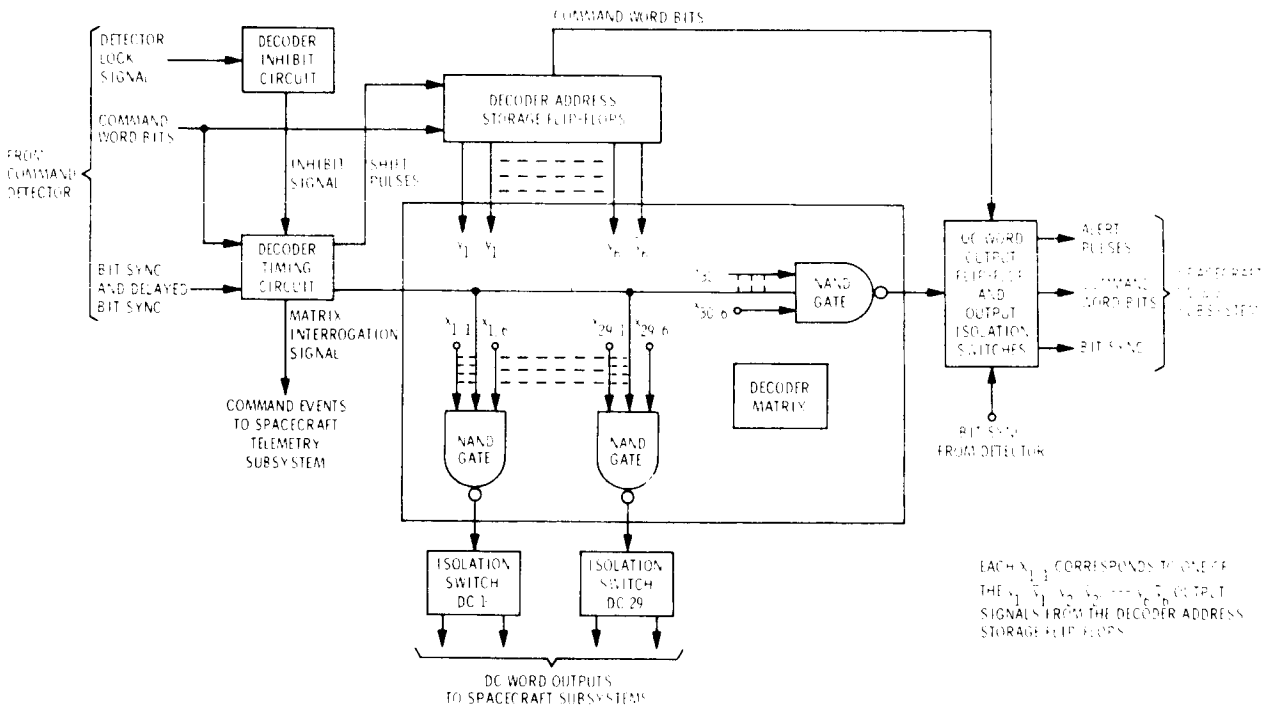

Figure 5-1. Command Decoder, Simplified Block Diagram

word format is a three-bit word start pattern, an eight-bit address, and fifteen bits of quantitative information. Word synchronization is obtained by presenting 26 consecutive zeros to the command decoder after the detector indicates a locked condition. Upon recognition of the word-start bits and the correct bit sync pulse, the decoder matrix is interrogated. The address bits stored in the decoder address storage flip-flops enable one of the NAND gates in the matrix and closes an output isolation switch (or switches) in the case of a direct command (DC). For a quantitative command (QC), serial QC bits are directed to the spacecraft central computer and sequencer (CC and S) along with bit sync through isolated switches. When QC information is absent, CC and S receives alert pulses through a separate isolated switch to clear the QC command storage registers.

5.2 MARINER B COMMAND SUBSYSTEM

The Mariner B Flight Command Subsystem accepts command information from the transponder, and demodulates and decodes these signals into commands for the various flight subsystems. There are two general types of commands, discrete commands (DC) and quantitative commands (QC). The DC commands are utilized for ON-OFF control. The QC commands contain quantitative information and are transferred in serial binary form to the spacecraft user.

The message format for the Mariner B Flight Command subsystem is different from the Mariner R and C formats. A command message is comprised of 8 command bits for DC commands, and either 23 or 40 command bits for QC commands. Each command bit is encoded into two sub-bits (Manchester code), such that a "1" command bit is transmitted as the sub-bit pair 01, a "0" command bit is transmitted as the sub-bit pair 10, and the remaining sub-bit pairs 11 and 00 are prohibited and provide a basis for sub-bit error detection and command bit rejection. This coding allows the use of a unique six sub-bit frame sync (111000) which cannot occur in a command transmission sequence unless two particular sub-bit errors occur. A typical command sequence is presented in Table 5-1 to illustrate the message format. The sub-bit rate is 1 sub-bit per second. Command bits are at 1/2 BPS.

Table 5-1. Typical Command Sequence

			Command Address Bits								
Transmitted Bits	0	Word Sync	0	0	1	0	1	1	1	1	0
Transmitted Sub-bits	10	111000	10	10	01	10	01	01	01	01	10

Quantitative Command Bits (23)																								
1	0	0	1	1	0	1	0	0	0	1	1	0	0	0	1	0	1	1	1	0	1	0	1	Word Sync
01	10	10	01	01	10	01	10	10	10	01	01	10	10	10	01	10	01	01	01	10	01	10	01	111 000

The command subsystem is comprised of five major functional units as follows:

1. Command detector
2. Program control
3. Command decoder
4. Telemetry
5. Power Supply

Redundancy at the functional element level is provided to improve the probability of command operation throughout the Mariner B mission by supplying two command detectors and two program control units. The functional block diagram for the command subsystem is presented in Figure 5-2.

Briefly, the operation of the command subsystem is as follows. The detector and program control pair are selected by means of a unique coding of the subcarrier and the selected detector coherently demodulates the sub-bits and provides timing pulses. These signals are presented to the program control where logic circuits recognize the frame sync pattern, start the master clock, and decode the sub-bit patterns into information or command bits. The unit also contains the logic circuits for controlling the detector selection switch, which routes the command bits and timing pulses from the proper detector - program control units to the decoder. The decoder transforms the serial command bits into ground isolated solid state switch closures which transfer the commands to the other flight subsystems. The telemetry unit contains the conditioning circuits and data storage required to transform certain command subsystem parameters into the proper form for transmission to the ground.

5.3 MANCHESTER CODING REVIEW

The utilization of the Manchester code provides a convenient method for implementing error rejection, unambiguous word synchronization, and variable length command words. The problem of word synchronization without coding necessitates the transmission of a word sync pattern at least as long as the command word. The round trip time for command verification at Mars is between 18 and 24 minutes at encounter and approximately 40 minutes at maximum range. Therefore, the establishment of word sync at every command word transmission is desirable in order to insure that command data is not lost due to spurious detector out-of-lock indications, transponder and detector degradations, etc.

The Mariner C command subsystem utilizes a fixed word length for command transmissions. This restricts the transmission time for discrete commands to be equal to that of a quantitative command. By utilizing the properties of the Manchester code, a command transmission may be variable in length. Command decoding can be inhibited by deliberate insertion of a sub-bit error. In order to implement error

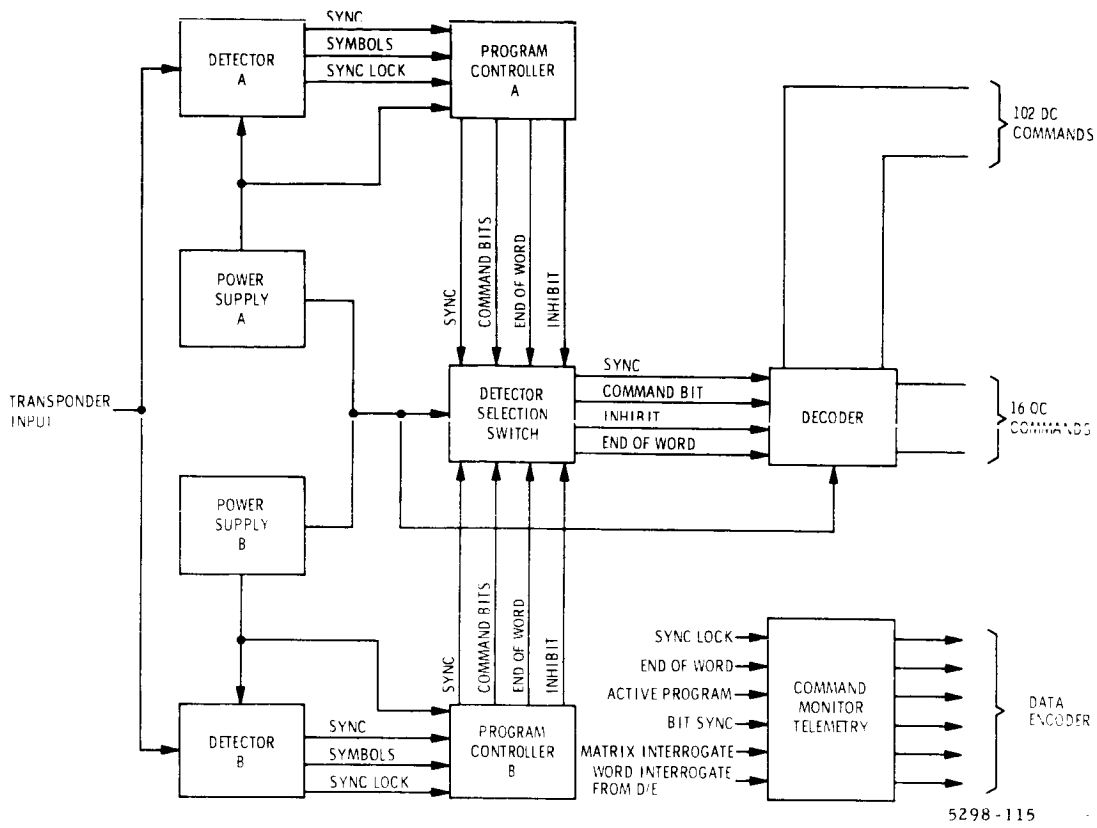

Figure 5-2. Flight Command Subsystem - Mariner B

rejection within the Mariner C system, the out-of-lock threshold is set to be greater than the probability of a bit error. (Probability of Out of Lock, $P_{OL} = 2 \times 10^{-5}$.) This probability of out-of-lock is the first factor to render the system inoperative, since an out-of-lock indication requires a new word sync pattern of 26 consecutive zeros before the decoding process can continue. Using the properties of the Manchester code, the out-of-lock threshold of the sub-bit detector may be set well below the probability of a sub-bit error, and the command subsystem is still operational well below threshold as long as the sub-bit detector does in fact remain in lock and reacquisition is not required.

5.3.1 WORD ERROR PROBABILITIES USING MANCHESTER CODE

For the purpose of comparison, the following word error probabilities are derived utilizing the Manchester code (See Appendix I for derivation of equations for word error probabilities using Manchester Code.)

a. Manchester code, sub-bit error rejection.

b. Manchester code, sub-bit error rejection, and rejection of all odd bit errors (bit parity).

Each command bit is independent and defined by two sub-bits.

Binary Bit "1" = 01

Binary Bit "0" = 10 (5-1)

The probabilities associated with an information bit are then calculated using the binomial distribution.

$$b(k; n, q) = \binom{n}{k} p^k q^{n-k} \tag{5-2}$$

where

k = number of successful sub-bits.

n = number of sub-bits/bit.

p = probability of a sub-bit success.

q = probability of a sub-bit error.

and

$p = 1 - q.$

A bit of information has three separate probabilities; it is correct, undefined, or incorrect. The undefined state will be rejected as incorrect.

If $\theta_1 = P_{cb}$ - Probability of a bit being correct

$$= b(2; 2, p) = p^2 \tag{5-3}$$

$\theta_2 = P_{eb}$ = Probability of a bit being in error

$$= b(0; 2, p) = q^2 \tag{5-4}$$

$\theta_3 = P_{rb}$ = Probability of a bit being rejected

$$= b(1; 2, p) = 2(1-q)\, q \tag{5-5}$$

A word transmission is multinomially distributed:

$$f(x_1, x_2, x_3) = \binom{m}{x_1}\binom{m-x_1}{x_2} \theta_1^{x_1} \theta_2^{x_2} \theta_3^{x_3} \tag{5-6}$$

where

x_1 = number of correct bits

x_2 = number of bits in error

$x_3 = m - x_1 - x_2$ = number of bits rejected

m = number of bits/word

$$\theta_1 + \theta_2 + \theta_3 = 1 \tag{5-7}$$

By definition:

P_{cw} = Probability of a correct word (accepted and correctly executed)

P_{rw} = Probability of a rejected word (rejected by command subsystem before execution)

P_{ew} = Probability of a word being in error (incorrect execution of a command)

5.3.1.1 COMMAND WORD PROBABILITIES

The following command word probabilities are summarized for sub-bit error rejection only. From Equation (5-6) it follows that:

$$P_{cw} \cong 1-2\ mq \tag{5-8}$$

$$P_{rw} \cong 2\ mq \tag{5-9}$$

$$P_{ew} \cong mq^2 \tag{5-10}$$

where

q = probability of a sub-bit error

m = number of bits/word.

The following command word probabilities are summarized for sub-bit error rejection and all odd bit errors. (Command word parity). From Equation (5-6) it follows that:

$$P_{cw} \cong 1-2\ mq \tag{5-11}$$

$$P_{rw} \cong 2\ mq \tag{5-12}$$

$$P_{ew} \cong \frac{m}{2}\ (m-1)\ q^4 \tag{5-13}$$

m = number of information bits/word

5.3.1.2 MAXIMUM COMMAND WORD LENGTH

The maximum length command word is assumed to be approximately 100 sub-bits; therefore the probability of correctly executing a command is 0.999. The probability of incorrectly executing a command is: (where $q = 1 \times 10^{-5}$)

$$P_{ew} \cong 50 \times 10^{-10} \text{ (From Equation 5-10) no word parity bit} \tag{5-14}$$

and

$$P_{ew} \cong 1.2 \times 10^{-17} \text{ (From Equation 5-13) with word parity bit} \tag{5-15}$$

5.3.2 RECOMMENDED MANCHESTER CODING

From paragraph 5.3.1.2, it is seen that the probability of executing an incorrect command using Manchester coding and command word parity is approximately 1.2×10^{-17} when the probability of a sub-bit error is $P_e^{SB} = 1 \times 10^{-5}$. Utilizing the properties of the Manchester code for rejection, the out-of-lock threshold may be set well below the probability of a sub-bit error. Even if the sub-bit error rate degrades to say $P_e^{SB} = 10^{-2}$, the probability of executing an incorrect command is approximately 1.2×10^{-5}.

The error detection capability, the simplified word sync pattern, and the ease of implementing variable length command words, are advantages of the Manchester code. Even though the command information bit transmission rate is halved by Manchester coding, the command word transmission rate is the same as Mariner C, since each command word was preceded by a 26-bit preface. For these reasons, the Manchester code with command bit parity is recommended for Voyager.

6.0 DECODER MECHANIZATION

The problem of decoding a unique address in a serial bit stream is fairly simple whenever word synchronization is given and the address is stored in a buffer register. Two methods of address recognition may be considered:

a. Gating of address register, i.e., using a digital logic gate with n inputs where n is the storage register length.

b. Magnetic Core selection, i.e., using activated sense windings for core selection.

The problem with magnetic detection is that output pulse widths are limited unless storage after sensing is utilized.

Under the assumption that discrete and quantitative outputs from the command decoder are required, which have a capability of pulse and d-c levels, the Mariner C type

decoding logic is recommended. Variable command data rates may be employed, since the decoder output is then limited only by the speed of the digital family used and the response time of the output switches.

Although 185 discrete and six quantitative commands have been identified (VB220FD112) for the 1971 Voyager mission, any decoder mechanization considered should have sufficient flexibility to accommodate more or less commands depending on the mission objectives for other Voyager flights. The recommended decoder mechanization has the capability to provide up to 246 total commands.

A discrete command results in a single switch closure of a duration from 2 ms to greater than 100 ms. A quantitative command results in the transfer of digital information at the designated bit rate to the command user. A quantitative command requires four separate outputs, alert pulses, command bit levels (at bit rate duration), bit synchronization pulses, and a sub-bit error pulse.

An estimate of the size, weight and power required for the command decoder can be established by considering a typical command decoder (Table 6-1).

Table 6-1. Command Decoder Module Count

250 Command Decoder	No. Required
Flip-Flops	50
Dual 3 Input and Gates	50
Isolated Step Switches	100
Isolated Pulse Switches	200
9 Input and Invert Gates	250
Dual Drivers	12
	662 modules

With conventional circuits, modular construction, the above decoder requires approximately 1,270 cubic inches, weighs approximately 33 lbs and requires 4 watts of power. This estimate is based on the present size, weight, and average power dissipated for a Mariner C type module. By utilizing microelectronics (integrated circuits), the above decoder may be packaged in a volume of approximately 207 cubic inches and weight less than 5.4 pounds. The power requirements of integrated circuits and conventional discrete modules are essentially the same. The weight savings of the integrated approach over that of the conventional module is approximately 28 lb/decoder. Table 6-2 shows a comparison of the present Mariner C failure rates/discrete module as compared with the estimated failure rates for the integrated circuit approach.

Table 6-2. Command Decoder Failure Rate

Module	Failure Rate/ 1000 Hr		No./Sys	Total Failure Rate 1000 Hr	
	Discrete	I. C.		Discrete	Integrated
Flip Flop	0.0045	0.002	50	0.2250	0.100
Dual and	0.00496	0.0020	50	0.2480	0.100
I. S. Switch*	0.03306	0.0100	100	3.3060	1.000
I. P. Switch*	0.03168	0.0100	200	6.3360	2.000
9 Input and	0.00398	0.00200	250	0.9950	0.500
Dual and Dr.	0.00500	0.00200	12	0.0600	0.024
			TOTALS	11.1700	3.724

*These failure rates have been revised to reflect the new estimated failure rates for double screened pulse transformers.

From Table 6-2, it is seen the use of integrated circuits for all digital logic within the command subsystem produces a much more reliable unit. This fact together with the savings in weight and volume by a factor of 6 is sufficient to justify the use of integrated circuits within the command subsystem.

7.0 CIRCUITS DESIGN

7.1 GENERAL

Selection of a family of integrated circuits will be carried out following the Phase 1A effort (VB220AA050). Mariner "C" analog circuits will be used in implementing the command detectors, since they have demonstrated their reliability in the present Mariner program. All circuits will be designed consistent with the design restraints imposed in VB220SR102.

7.2 ISOLATION SWITCHES

In order to reduce the size and weight of the command subsystem, and in order to achieve a degree of standardization between the isolated pulse (I.P.) and the isolated

step (I. S.) switches, a study of alternative circuit approaches will be initiated following the Phase IA effort. This study will involve the following activities:

a. A review of all command users to establish the switch characteristics required.

b. A tradeoff analysis of the possible circuit alternatives

A preliminary consideration of the second activity suggested two possibilities.

a. Repackaging the electronics portion of the switches in an integrated circuit form and using the Mariner C transformer.

b. Redesigning the switches with the objective of utilizing one circuit for both applications.

The first approach allows a packaging density of 3 I.S. or I.P. switches per Mariner "C" module (0.56 in. x 0.630 in. x 1.5 in.). This is approximately the maximum packaging density obtainable due to the size of the present pulse transformers (0.31 in. x 0.34 in. x .475 in.).

In the second approach, the redesign of the I.P. switch is ruled out because of the need for a long duration pulse. Therefore, the I.S. switch is considered to be the basis for redesign into an integrated circuit package and a packaging density of greater than 6:1 over that of Mariner "C".

7.2.1 I.S. SWITCH CONSIDERATIONS

One possible way to reduce the size of the drive transformer within the I.S. switch would be to increase the drive frequency. For good response, when used as an I.P. switch, the drive frequency should be greater than 1 megacycle. The use of a central high frequency drive oscillator for all I.S. switches is not considered to be good practice because of anticipated radiation problems due to interconnecting wires acting like antennas. Figure 7-1 presents one proposed approach for implementing a universal isolation switch and utilizes a self-contained 10-megacycle oscillator which is input controlled. A circuit similar to that of Figure 7-1 has been successfully implemented in I/C form by Motorola and no major problems are anticipated at this time.

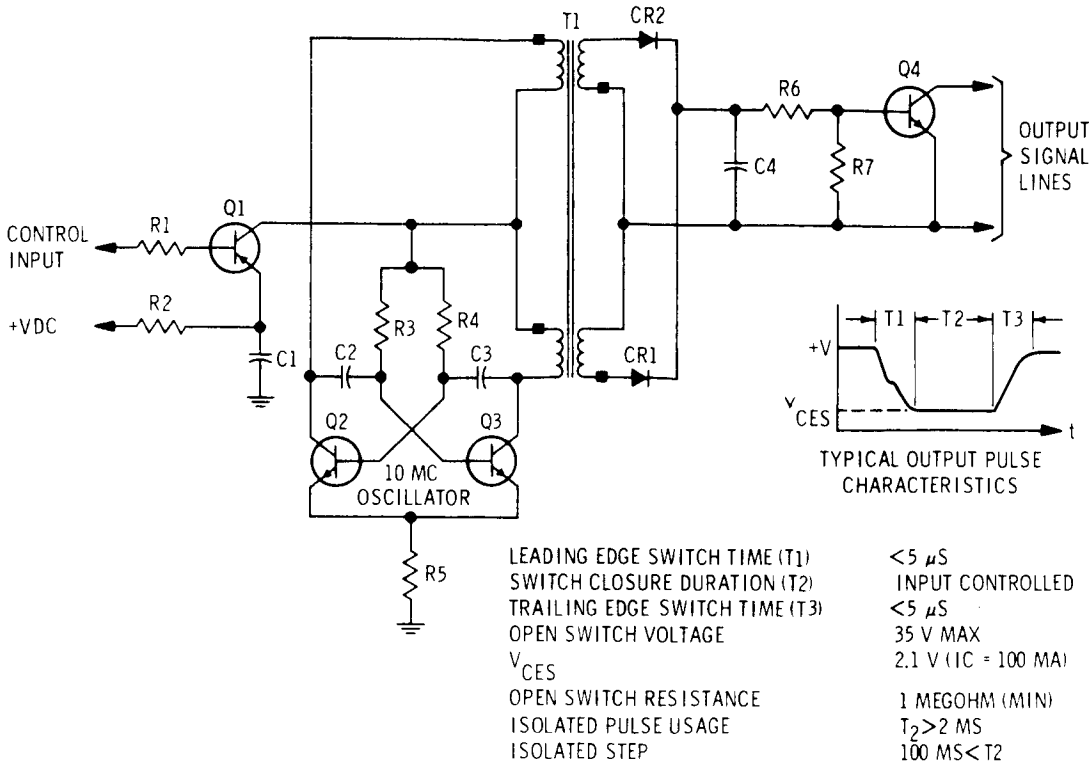

Figure 7-1. Universal Isolation Switch

8.0 ENVIRONMENTAL AND PACKAGING CONSIDERATIONS

The Environmental and Packaging Considerations are discussed in the overall telecommunications equipment tradeoffs, Section 8 of VB233AA101.

9.0 REFERENCES

3-1. Preliminary Voyager Mission Specification, Section II, G, May 1, 1965 - JPL Project Document No. 45, V-MA-004-001-14-03.

4-1. JPL Technical Report 32-495, "Telemetry and Command Techniques for Planetary Spacecraft," J. C. Springett, 15 January 1965.

4-2. Sanneman and Rowbatham, "Unlock Characteristics of the Optimum Type I Phase-Locked Loop," IEEE Transactions on Aerospace and Navigational Electronics, Volume ANE-11, Number 1, March 1964.

4-3. Martin, Benn D., "The Pioneer IV Lunar Probe: A Minimum Power FM/PM System Design," JPL Technical Report 32-215, 15 March 1962.

APPENDIX I

MANCHESTER CODED TRANSMISSIONS

I.1 WORD DEFINITION

Binary "1" = 01 (2 sub-bits)

Binary "0" = 10 (2 sub-bits)

Word length = m bits

I.2 BIT PROBABILITIES

Within the decoding of a Manchester coded bit the only defined states are "01" and "10". The states "11" and "00" are undefined and represent the case where a sub-bit error has occurred and the bit is rejected as being incorrect. Therefore, within the decoding process, there are three probabilities associated with an information bit. They are:

θ_1 = the probability that a bit is decoded correctly, i.e., both sub-bits are correct.

θ_2 = the probability that the bit is decoded incorrectly, i.e., both sub-bits are in error.

θ_3 = probability that the bit is rejected as being in error, i.e., the undefined state was detected, one sub-bit error/bit.

Since each bit may be assumed independent of all preceding bits, the binomial distribution may be used to calculate the above probabilities:

$$b\ (k;\ n,\ p) = \binom{n}{k}\ p^k q^{n-k} \qquad \text{(I-1)}$$

(binomial distribution)

where

k = number of correct sub-bits/bit.

n = number of sub-bits/info bit.

p = probability of success (sub-bit).

q = probability of error (sub-bit).

$$q = 1 - p. \tag{I-2}$$

It follows that:

$$\theta_1 = b\,(2;\,2,\,p) = p^2 \tag{I-3}$$

$$\theta_2 = b\,(0;\,2,\,p) = q^2 \tag{I-4}$$

$$\theta_3 = b\,(1;\,2,\,p) = 2\,(1 - q)\,q \tag{I-5}$$

I.3 WORD PROBABILITIES

There are three separate probabilities associated with a command word. They are as follows:

P_{cw} = Probability that a word is correctly received and executed, i.e., all sub-bits are correct.

P_{ew} = Probability that a word is in error, i.e., a required number of bit errors occur - this implies a command word may or may not contain a parity bit.

P_{rw} = Probability that the word is rejected by the command subsystem prior to execution, i.e., one sub-bit error per bit.

If

X_1 = number of correct bits received,

X_2 = number of bits in error, and

X_3 = the number of bits rejectable as indeterminant,

then the joint distribution of the random variables X_1, X_2, X_3 is given by

$$f\,(X_1,\,X_2,\,X_3) = \frac{M!}{X_1!\;X_2!\;X_3!}\;\theta_1^{X_1}\;\theta_2^{X_2}\;\theta_3^{X_3} \tag{I-6}$$

for $X_i = 0, 1, 2 \ldots\ldots m$ for each i, subject to the restriction that

$$\sum_{i=1}^{k} X_i = m = \text{number of information bits/word.}$$

This joint distribution is called the multinomial distribution and may be rewritten as

$$f(X_1, X_2, X_3) = \binom{m}{X_1}\binom{m-X_1}{X_2} \theta_1^{X_1} \theta_2^{X_2} (1 - \theta_1 - \theta_2)^{m-X_1-X_2} \qquad \text{(I-7)}$$

since

$$\theta_1 + \theta_2 + \theta_3 = 1$$

I.4 MANCHESTER CODED TRANSMISSION WITHOUT A WORD PARITY BIT

$$P_{cw} = f(m, 0, 0) = \theta_1^m; \text{ all sub-bits correct.}$$

$$= (1 - q)^{2m}$$

$$= 1 - 2mq + m(2m-1)q^2 - \frac{2m(2m-1)(2m-2)}{3!}q^3 + \ldots\ldots \qquad \text{(I-8)}$$

$$P_{ew} = \sum_{X_1=0}^{m-1} \sum_{X_2}^{m-X_1} \binom{m}{X_1}\binom{m-X_1}{X_2} \theta_1^{X_1} \theta_2^{X_2} \theta_3^{m-X_1-X_2} \qquad \text{(I-9)}$$

where

$X_1 + X_2 = m$, i.e., no rejectable bits.

$$P_{ew} = m\theta_1^{(m-1)}\theta_2 + \frac{m(m-1)}{2!}\theta_1^{(m-2)}\theta_2 2 + \ldots\ldots$$

$$= m(1-q)^{2(m-1)}q^2 + \frac{m(m-1)}{2}(1-q)^{2(m-2)}q^4 + \ldots\ldots$$

$$= mq^2\left[1-(2m-2)q + \frac{(2m-2)(2m-3)}{2}q^2 - \ldots\ldots\right]$$

$$+ \frac{m(m-1)}{2}q^4\left[1 - (2m-4)q + \frac{(2m-4)(2m-5)}{2}q^2 - \ldots\ldots\right]$$

$$+ \ldots\ldots\ldots$$

$$= mq^2 - m(2m-2)q^3 + \frac{m(2m-2)(2m-3)q^4}{2} - \ldots\ldots$$

$$+ \frac{m(m-1)}{2}q^4 - \ldots\ldots\ldots \qquad \text{(I-10)}$$

$$P_{ew} = mq^2 - m\,(2m-2)\,q^3 + \ldots\ldots \tag{I-11}$$

$$P_{rw} = 1 - P_{cw} - P_{ew}$$

$$= 1 - 1 + 2\,mq\frac{2m(2m-1)}{2}\,q^2 + \frac{2m(2m-1)\,(2m-2)}{3!}\,q^3 - \ldots\ldots$$

$$- m\,q^2 \qquad + m\,(2m-2)\,q^3 - \ldots\ldots$$

$$+ 2mq - 2\,m^2q^2 + \ldots\ldots\ldots \tag{I-12}$$

In summary,

$$P_{cw} = 1-2\,mq + m(2m-1)\,q^2 - \frac{m(2m-1)\,(2m-2)\,q^3}{3} + \ldots\ldots \tag{I-13}$$

$$P_{ew} = mq^2 - 2m\,(m-1)\,q^3 + \ldots\ldots \tag{I-14}$$

$$P_{rw} = 2\,mq - 2\,m^2\,q^2 + \ldots\ldots \tag{I-15}$$

where q = probability of a sub-bit error

m = number of bits/word.

I.5 MANCHESTER CODED TRANSMISSION WITH A WORD PARITY BIT

P_{cw} = P (all bits are correct); see Equation (I-9) (I-16)

$$= 1-2\,mq + m(2m-1)\,q^2 - \frac{m}{3}\,(2m-1)\,(2m-2)\,q^3 1 \ldots.$$

P_{ew} = P (< m-1 bits are correct/no rejections due to sub-bit or word parity) (I-17)

$$P_{ew} = \sum_{\substack{X_1 = 1,3,5 \ldots\ m \text{ is odd} \\ X_1 = 2,4,6 \ldots\ m \text{ is even}}}^{m-2} \sum_{X_2}^{m-X_1} \binom{m}{X_1}\binom{m-1}{X_2}\,\theta_1^{X_1}\,\theta_2^{X_2}\,\theta_3^{m-X_1-X_2} \tag{I-18}$$

$$= \frac{m(m-1)}{2}\,\theta_1^{\,m-2}\,\theta_2^{\,2} + \ldots\ldots$$

$$= \frac{m(m-1)}{2}\,[1-q]^{2(m-2)}\,q^4 + \ldots.$$

$$= \frac{m}{2}(m-1)\,q^4\,[1 - 2\,(m-2)\,q + \frac{(2m-4)\,(2m-5)\,q^2}{2} - \ldots.] + \ldots.$$

$$P_{ew} = \frac{m}{2}(m-1)\,q^4 - m\,(m-1)\,(m-2)\,q^5 + \ldots\ldots \tag{I-19}$$

$$P_{rw} = 1 - P_{cw} - P_{ew} \tag{I-20}$$

$$P_{rw} = 1 - 1 + 2\,mq - m(2m-1)\,q^2 + \frac{m}{3}(2m-1)\,(2m-2)\,q^3 - \ldots. \tag{I-21}$$

$$-\frac{m}{2}(m-1)\,q^4 + m(m-1)\,(m-2)\,q^5 - \ldots..$$

$$P_{rw} = 2\,mq - m(2m-1)\,q^2 + \frac{m}{3}(2m-1)\,(2m-2)\,q^3 - \ldots.. \tag{I-22}$$

In summary,

$$P_{cw} = 1-2\,mq + m(2m-1)\,q^2 - \frac{m}{3}(2m-1)\,(2m-2)\,q^3 + \ldots.. \tag{I-23}$$

$$P_{ew} = \frac{m}{2}(m-1)\,q^4 - m(m-1)\,(m-2)\,q^5 + \ldots.. \tag{I-24}$$

$$P_{rw} = 2mq - m(2m-1)\,q^2 + \frac{m}{3}(2m-1)\,(2m-2)\,q^3 - \ldots.. \tag{I-25}$$

where

q = probability of a sub-bit error

m = number of bits/word

CII - VB233AA104

ALTERNATE SUBSYSTEM MECHANIZATIONS CONSIDERED

RELAY RADIO SUBSYSTEM

Index

1 Scope
2 Applicable Documents
3 Subsystem Boundary Considerations
4 Communication Trade-offs
5 Receiver and Detector Trade-offs
6 Relay Antenna Trade-offs
7 Control and Sensing Circuitry
8 Power Supply
9 Internal Redundancy

1.0 SCOPE

This study considers trade-offs between the spacecraft relay radio subsystem and other system parameters. Also considered are trade-offs between characteristics and parameters internal to the spacecraft relay radio subsystem. This study directly supports VB233FD104.

2.0 APPLICABLE DOCUMENTS

The following documents are used as references for this trade-off study:

VB220SR101	Design Characteristics
VB220SR102	Design Restraints
VB220FD109	Telemetry Criteria
VB220FD110	Telemetry Channel Assignment
VB220FD112	Flight Sequence
VB220FD113	Layout and Configuration
VB233FD101	Telecommunication Subsystem
VB233FD104	Relay Radio Subsystem

3.0 SUBSYSTEM BOUNDARY CONSIDERATIONS

This section is divided into three areas - Mission Operation, Capsule, and Spacecraft Considerations.

3.1 MISSION OPERATION CONSIDERATIONS

3.1.1 MISSION DYNAMICS

The following flight dynamics are used for the evaluation of the various trade-offs:

a. Maximum Communicating Distance: 8000 km

b. Maximum Range Rate: 3.0 km/second

c. Maximum Range Acceleration: 0.5 km/second^2.

3.1.2 ADDITIONAL CONSTRAINTS

a. Interfering Noise Spectral Density: The surrounding spacecraft equipment may contribute a maximum noise spectral density of -150 dbm/cps which is assumed to be white.

b. Acquisition Time: The receiver will have a 90 percent probability of locking on to the desired signal within 10 seconds.

c. Data Rate: The assumed PCM data is transmitted at a 10-bit per second rate.

d. Bit Error Rate: The overall telemetry channel will have a maximum bit error rate of 5×10^{-3}; therefore, the relay link is assigned a bit error rate no worse than 5×10^{-4}, so as not to degrade overall channel performance.

3.1.3 RELAY RELIABILITY

The reliability for the relay radio subsystem is considered for an operating time of 48 hours. Since the relay is in series with the Orbiter-to-Earth telemetry channel, the relay must have a higher probability of success than the Orbiter-to-Earth telemetry.

3.2 CAPSULE CONSIDERATIONS

3.2.1 TRANSMITTER CHARACTERISTICS

It is assumed that the capsule transmitter shall be capable of operating in a 20-watt mode for the entire mission after capsule separation. The possibility exists that the transmitter may be programmed to transmit a lower power during the early phases after separation. The range of transmit frequencies is between 100 and 200 Mc.

3.2.2 ANTENNA CHARACTERISTICS

It is assumed that the capsule antenna provides 0 db gain at maximum range. Also for circular polarization on the spacecraft the assumed maximum polarization mismatch loss is 3 db.

3.2.3 MODULATION TECHNIQUES

Various methods of modulating the capsule transmitter are considered. These trade-offs are discussed in sections which follow.

3.3 SPACECRAFT CHARACTERISTICS

3.3.1 SIZE, WEIGHT, AND POWER

The size, weight, and power apportionment for the relay radio subsystem is included in that of the radio and telecommunications equipment. The major consideration is the spacecraft antenna size and weight plus the manner in which the vhf antenna is attached to the spacecraft.

4.0 COMMUNICATION TRADE-OFFS

The following subsections consider transmit frequency, coding, and modulation technique.

4.1 TRANSMIT FREQUENCY

It is desirable to make the transmit frequency as high as possible, to reduce antenna size and weight and for ease of antenna deployment. However, as the frequency decreases, the path loss decreases and the receiver loop bandwidth can be narrowed due to a decrease in sweep range, both of which are desirable.

The weight of the relay system is shown in Figure 4-1 as a function of frequency. Items such as receiver and battery weight on the spacecraft, and transmitter weight on the capsule are not included since they do not vary significantly with frequency. The maximum operating time during entry is about 20 hours and will probably be much lower, thus the choice of 200 mc/s as the center frequency is optimum in regard to weight. The antenna volume at 200 mc/s is not prohibitive and the battery volume is directly related to battery weight. Since the operating frequency does not affect the reliability of the relay link, the only basis for optimization is the total weight of the system.

4.2 CODING

Configurations for modulating and demodulating Manchester coded capsule relay data are presented in Figures 4-2 and 4-3 along with a chart of system waveforms, Figure 4-4. Manchester coded data is generated by the modulo two addition of data and bit sync and is utilized to maximize transitions in the data stream. The transitions are detected in a phase-locked loop in the data demodulator from which symbol sync is recovered. Symbol sync has the clock rate of the Manchester symbols and has twice the bit sync rate. The symbols are then detected in a matched filter. The SNR required for a symbol error rate of 5×10^{-4} is approximately 10 db in a 20-cps bandwidth. Bit sync is recovered by dividing symbol sync by two and the bits are recovered by the modulo two addition of bit sync and the recovered symbols. However, as indicated in the chart, the recovered bit sync and thus the recovered bits may be ambiguous. The ambiguity is resolvable. A configuration which is utilized for this purpose is presented in the data demodulator diagram. If no ambiguity exists, the backward forward counter goes forward (say for a three count which requires three bit transitions and a probability of false correction of P_e^3) and sets the correction store flip-flop which enables the lock gate.

Likewise, if an ambiguity exists, the counter goes backward for three counts to reset the divide-by-two bit sync flip-flop, whereupon the ambiguity is resolved and the counter goes forward to enable the lock gate. An alternate technique, if Manchester coding is used, is to store 20 bps symbols or ambiguous 10 bps data. This data modulation method is not used because it requires data bit transitions to resolve the ambiguity in the bit stream, whereas the proposed system operates independently of the data format.

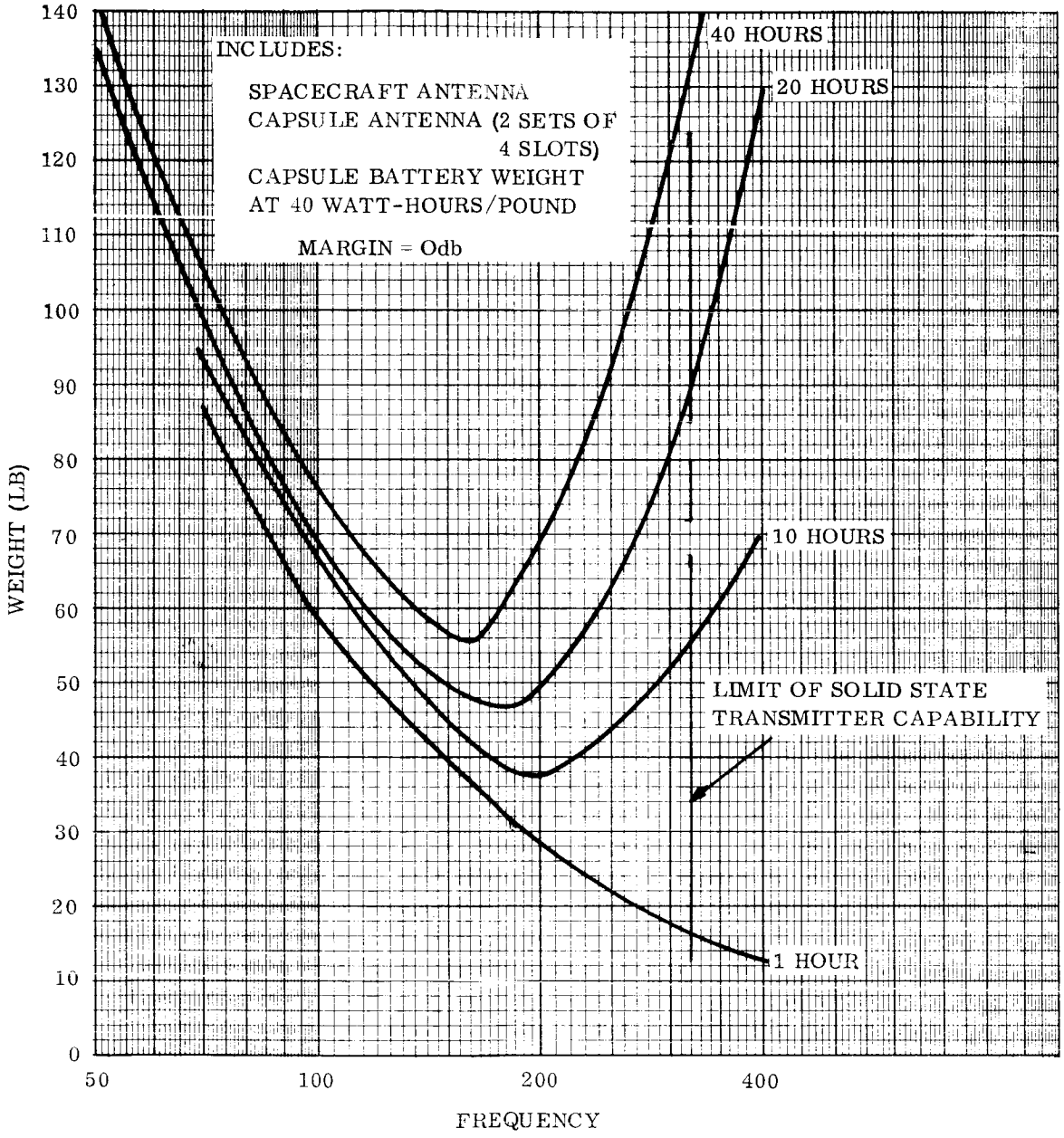

Figure 4-1. Relay System Weight versus Frequency

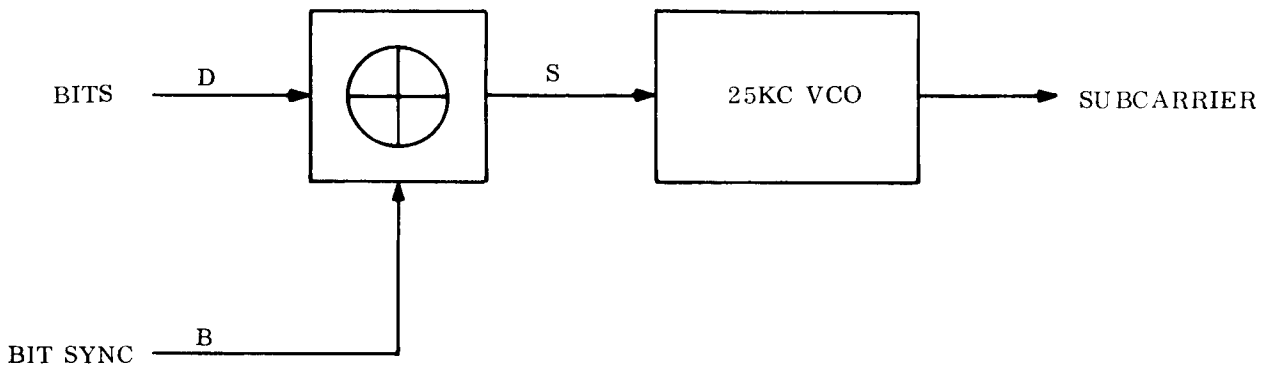

Figure 4-2. Data Modulator (Manchester Code)

4.3 MODULATION TECHNIQUE

The following subsections discuss the various modulation techniques considered for the relay radio subsystem.

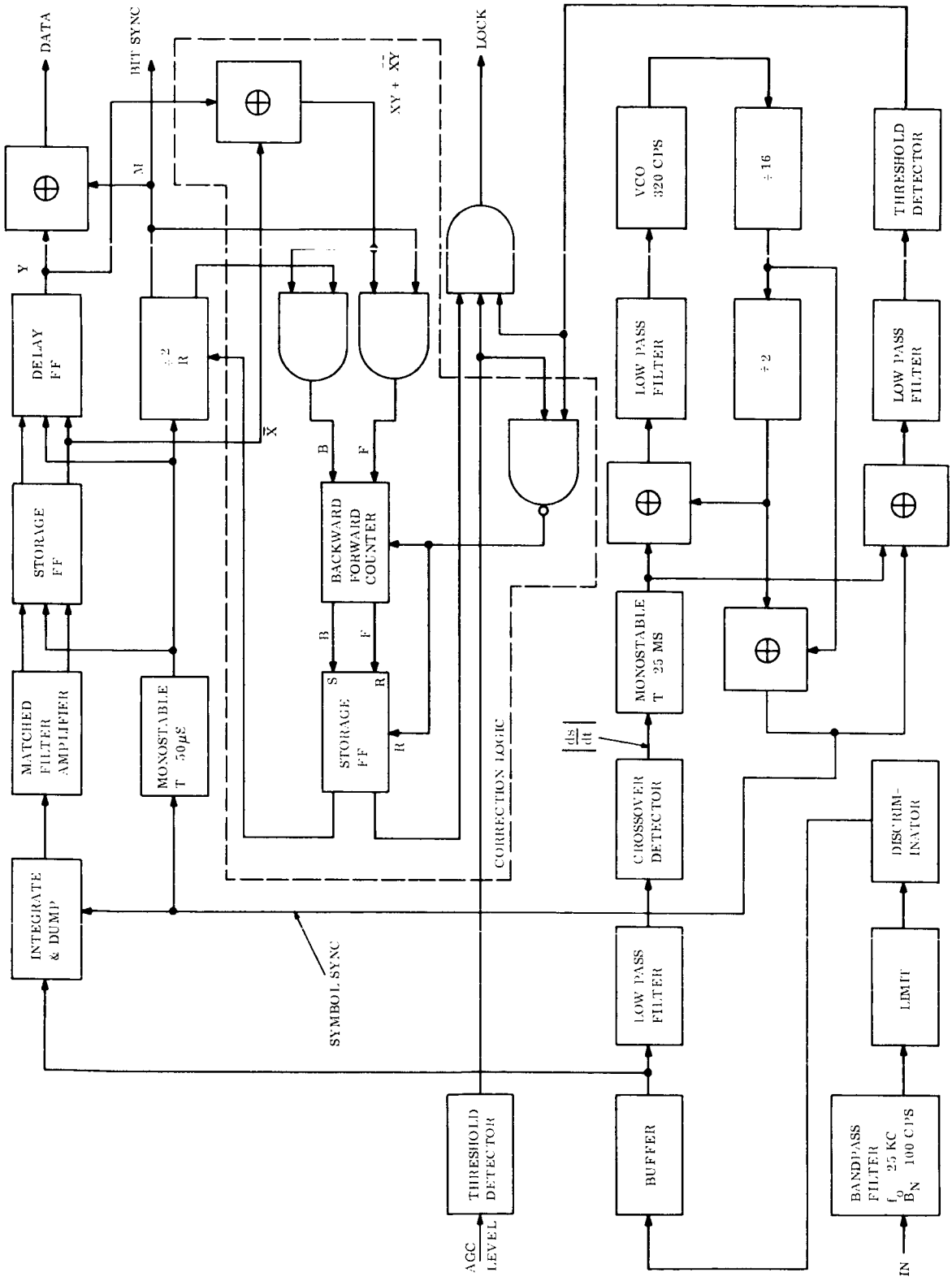

Figure 4-3. Data Detector (Manchester Code)

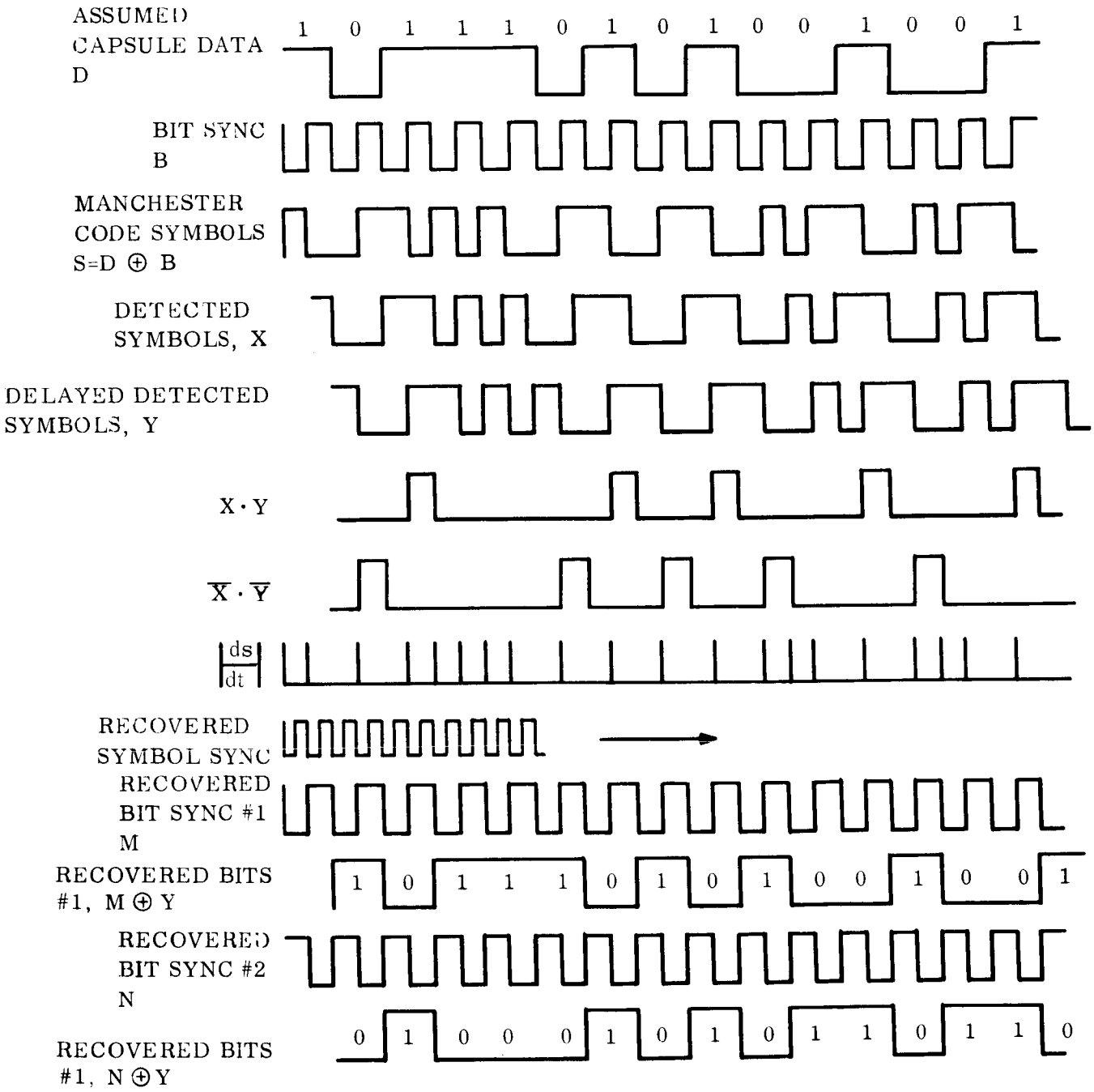

Figure 4-4. Detector Waveforms

4.3.1 PSK/FM/PM

This is the proposed modulation technique in which bi-phase modulated data and bit sync are frequency modulated onto a 25-kc subcarrier and the subcarrier is phase modulated onto the carrier. Block diagrams of the subsystem, receiver and detector configurations are shown in Figures 4-5, 4-6, and 4-7, respectively. A carrier tracking, type 1 phase-lock receiver is employed to demodulate the carrier. The subcarrier is then demodulated by a discriminator having a narrowband predetection filter with linear phase characteristics over the 3-db bandwidth. A worst case 9.5 db SNR in the predetection bandwidth is near the discriminator threshold. A bit error rate of 5×10^{-4} has been attained for this SNR. Matched filter detection using an integrate and dump technique is employed to detect the data bits and a phase-lock loop is locked to the bit sync. Some of the advantages of this system are:

a. The restrictions on the subcarrier oscillator stability are not severe.

b. No restrictions are placed on the coding technique to insure transitions.

c. The bit rates can be used by changing the detector only; the receiver remains the same.

d. Voltages from the receiver agc and the quadrature detector logic in the detector provide an indication that both receiver and detector are working properly and that the received data is good.

4.3.2 PSK/PM/PM

This technique phase-modulates the data and bit sync onto the subcarrier and then phase-modulates the subcarrier onto the carrier. The receiver remains the same as previously mentioned, and the change in the detector replaces the subcarrier discriminator with a narrow-band modulation restrictive loop. However, to insure lock to the subcarrier and not to the bit sync or data, which can be 5 and 10 cps away from the 25 kc subcarrier, stringent stability requirements are placed on the subcarrier oscillator and the vco stabilities in the subcarrier demodulator. Thus, even for high SNR into the subcarrier demodulator, the possibility of locking to the data or bit sync still exists and increases as $2\beta_L$ increases. For a higher data rate, this problem does not exist. Thus this method might be preferred, since the modulation restrictive loop would have a lower threshold, and bit error rate degradation due to discriminator impulse noise would not be present.

4.3.3 PCM-FM (FSK)

For this type of modulation, a modulation-tracking, type 1 phase-lock receiver is considered. However, due to the loop noise bandwidth required for acquisition and the amount of peak modulation error introduced into the loop, the deviation (Δf) must be kept small on the order of 20 to 30 cps. Thus the Doppler rate of 333 cps/second for a 200-Mc carrier masks the received data. This technique could possibly be used

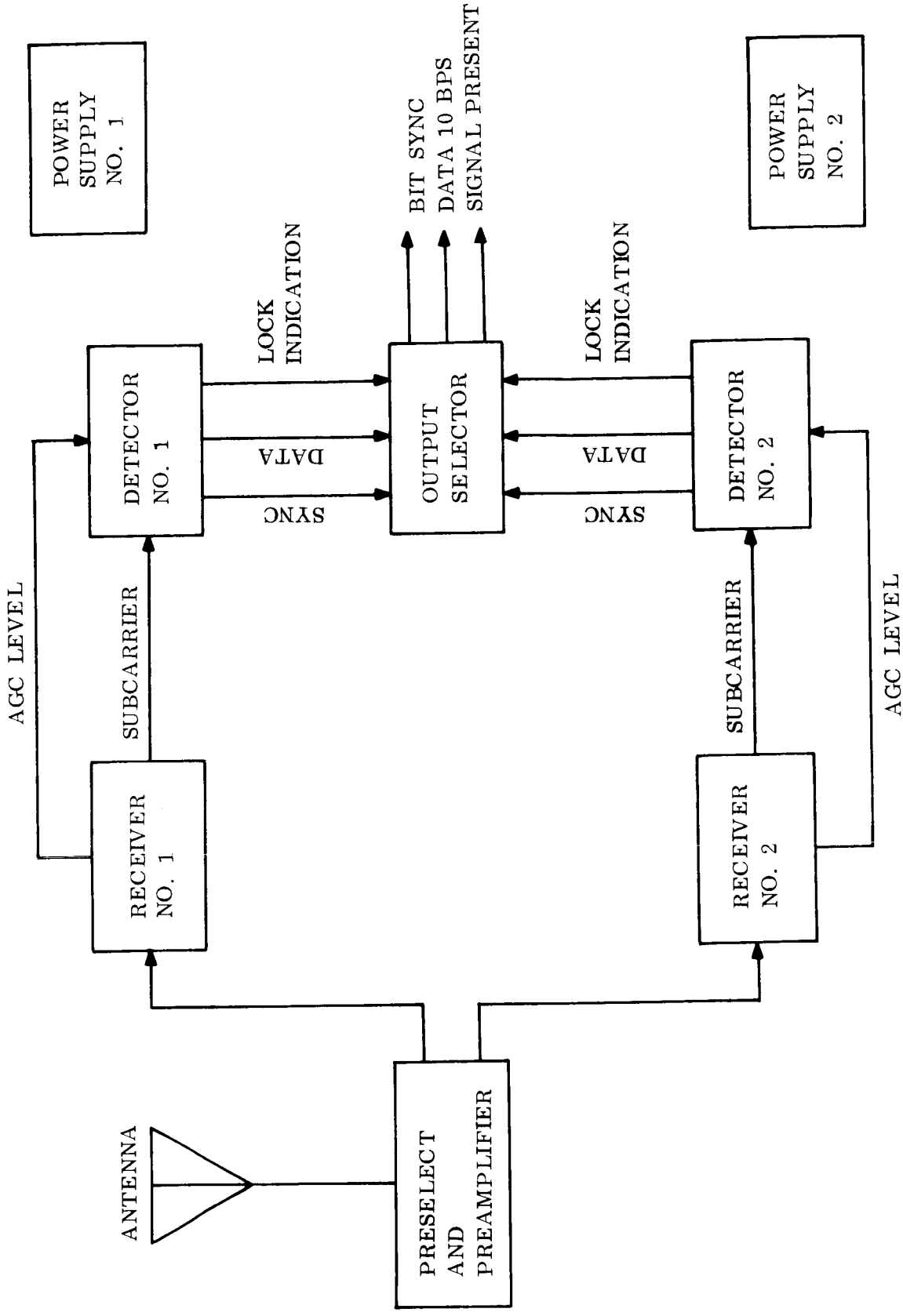

Figure 4-5. Relay Radio Subsystem Configuration

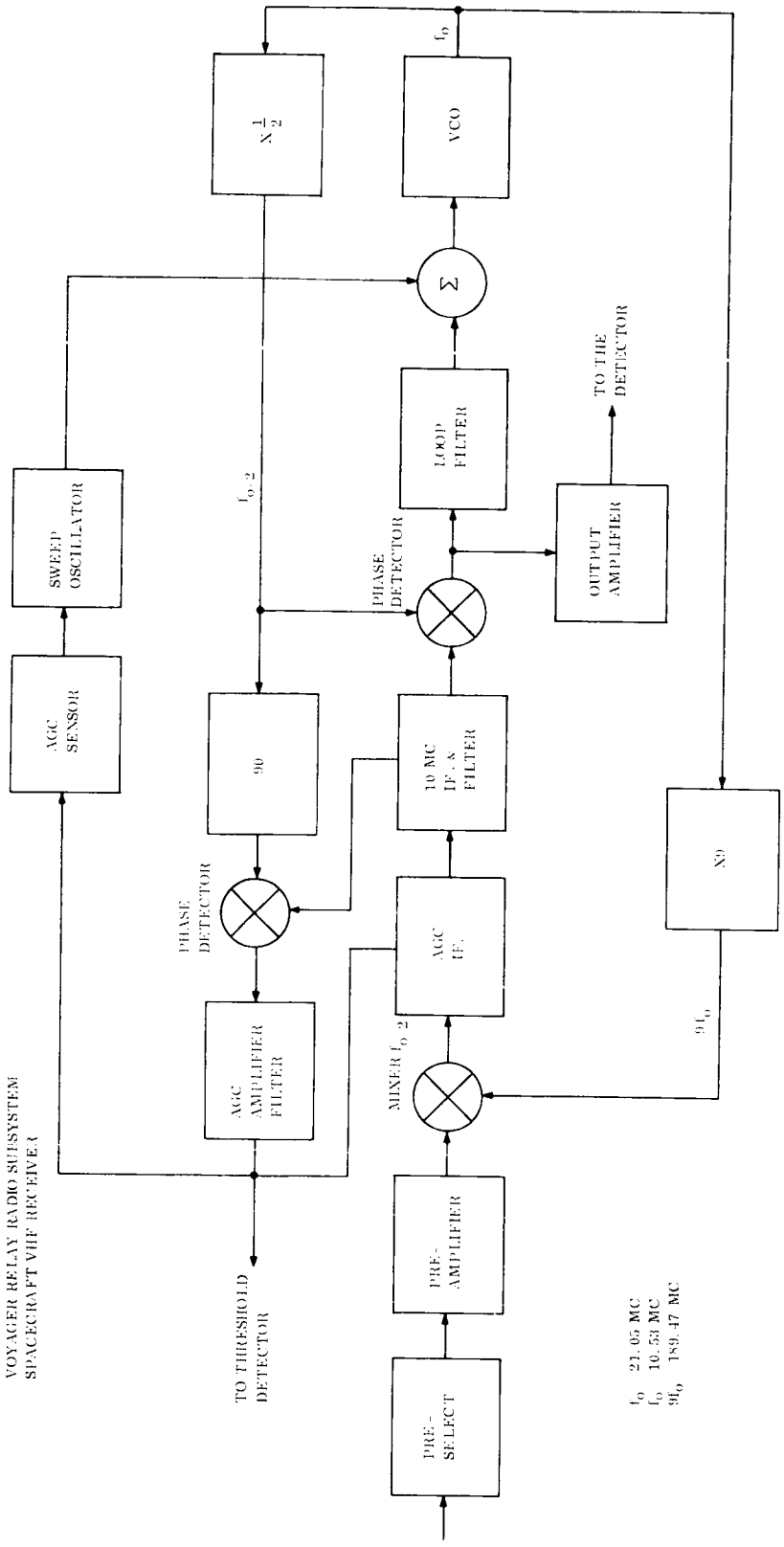

Figure 4-6. Modulation Restrictive Phase-Lock Loop

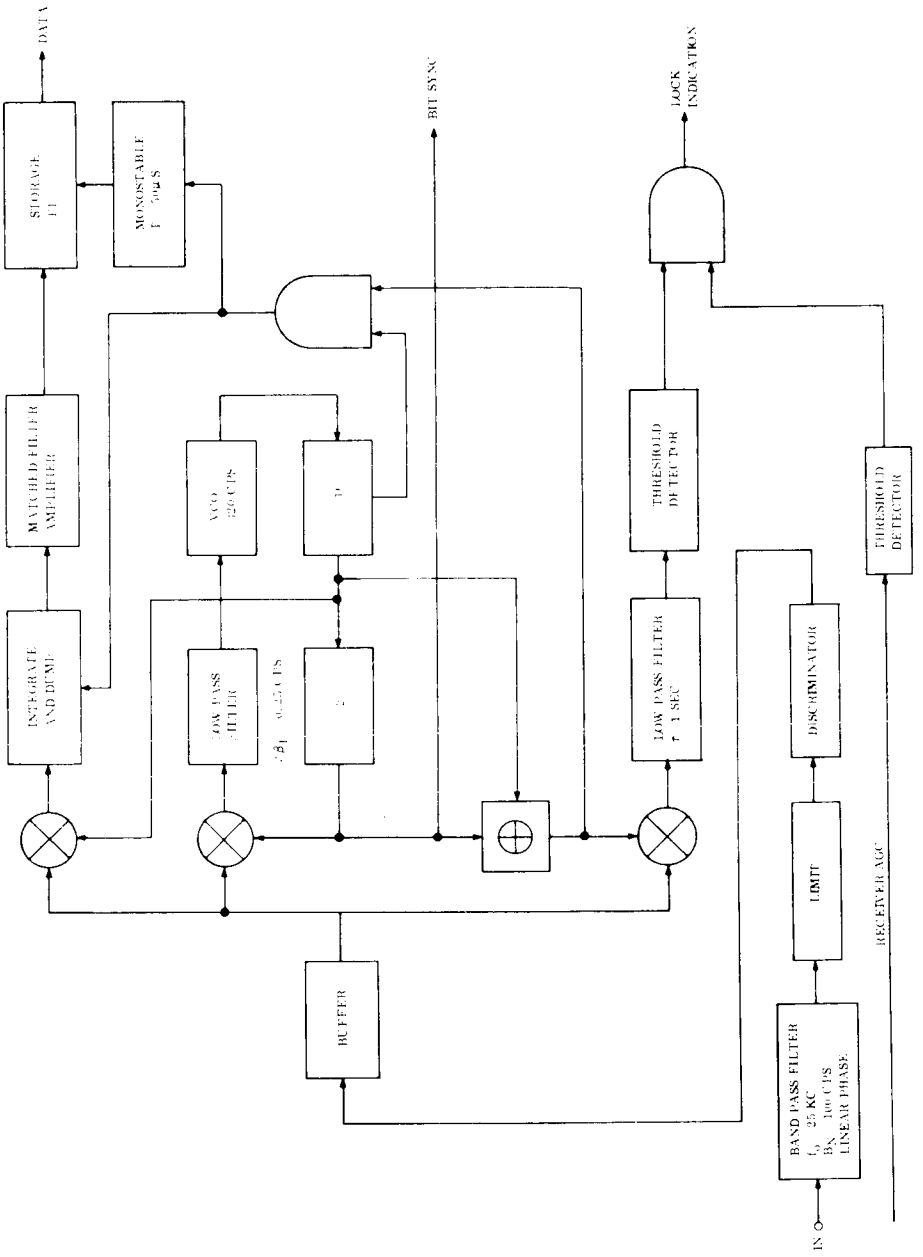

Figure 4-7. Data Detector

after capsule impact when the doppler is not as great. Link calculations show a 0-db link margin for 10-db SNR in a $2\beta_L$ of 200 cps with a transmit frequency of 200 Mc, 20 watts of capsule power, and 0-db transmit and receive antenna gains, under maximum noise interference conditions. Again the problem of obtaining bit sync requires transitions, thus placing a restriction on code format.

A noncoherent FSK system was also analyzed. This involves mixing down the received carrier to an intermediate frequency; then employing two bandpass filters and envelope detectors for the mark and space frequencies. This system is not degraded by the expected Doppler rate because of the high deviation (on the order of 5 kc) which insures that signal power does not spill over into the opposite channel. However, because of the expected oscillator instabilities and Doppler offset, the predetection filters are on the order of 10 to 20 kc. With this bandwidth and the maximum noise spectral density of -150 dbm/cps, the SNR into the envelope detectors is less than unity at maximum range. Since the detector is a square law device, a low input SNR results in further degradation in output signal-to-noise ratio. Again, in order to obtain bit sync a restriction is placed on the code format to insure transitions. Amplitude variations in the channel produce a phase variation in the bit sync. A limiter could be used in the IF or prior to the envelope detector to keep the signal power constant for high input SNR. However, as the SNR decreases, the output SNR is degraded by an additional 1 db and the noise tends to suppress the received signal.

5.0 RECEIVER AND DETECTOR TRADE-OFFS

This section treats the trade-offs in implementation and design of the receiver and detector.

5.1 BASIC RECEIVER CONFIGURATION

A single conversion phase-lock receiver is employed. A frequency multiplication of nine is chosen from the vco output to the LO injection into the mixer. This multiplication allows for a reduction in the frequency uncertainty and Doppler offset bandwidth requirements by a factor of nineteen.

5.2 INPUT STAGE

A preselector bandwidth of 4 Mc is chosen as it can be realized from lumped constant components. It is wide enough to pass all uncertainties, due to Doppler and frequency instabilities, and wide enough to pass the J_1 sidebands from the subcarrier modulation. At the same time it does not place undue requirements on the amount of noise power the mixer must handle. A noise figure of 4 db is provided; the signal-to-noise improvement can be as great as 20 db if the -150 dbm/cps interference level is not present.

5.3 LOOP AND MODULATION INDEX OPTIMIZATION

In order to acquire the transmitted carrier from the capsule with a 90 percent probability of lock within 10 seconds, a loop noise bandwidth of at least 200 cps is needed

for the 20-kc sweep range anticipated. In order to acquire under these conditions, a minimum of 6 db carrier-to-noise ratio must be maintained in the loop bandwidth and the damping ratio should be between 0.85 and 0.50. Thus the following parameters are chosen:

$$2\beta_L = 200 \text{ cps}$$

$$\beta = 0.707$$

$$\text{Minimum CNR in } 2\beta_L = 6 \text{ db.}$$

Under worst case signal conditions, a minimum CNR of 6 db must be maintained in $2\beta_L$. The modulation index which maximizes the power in the subcarrier and meets this requirement is 1.2 radians. This results in a 3.5 db carrier suppression which gives a 6-db CNR in $2\beta_L$ under worst case signal conditions. The corresponding subcarrier modulation loss is 3.0 db.

The predetection filter is narrow to reduce the amount of noise power the phase detector must handle. At the same time it is wide enough to pass the information and accomodate the Doppler and oscillator instability. A 3-pole crystal filter with a 3-db bandwidth of 70 kc is chosen. At weak signal the N/S ratio into the loop phase detector can be as high as 17 db.

5.4 OSCILLATOR STABILITY

The transmit and receiver oscillators have a stability requirement of ±15 ppm over a 7-month period and a temperature environment of -10°C to +75°C.

5.5 AGC

Coherent AGC is used to keep the carrier component at a constant level into the loop phase detector and thus keep the loop gain and bandwidth constant. AGC is chosen instead of i-f limiting because AGC is desirable for telemetry and no appreciable advantage exists in having an adaptive loop, since the minimum $2\beta_L$ must be 200 cps. At strong signal with the limiter, the loop bandwidth increases, thereby increasing the probability of lock. However, the strong signal loop gain is unreasonably large. At the same time the sweep rate remains constant, due to the requirement of being able to acquire at weak signal. A reasonable dynamic range for the AGC is 80 db. The r-f limiter in the pre-amplifier takes care of the strong signal conditions after capsule separation.

6.0 RELAY ANTENNA TRADE-OFFS

The radiation pattern of the relay antenna must be sufficiently broad to permit communications between spacecraft and capsule during the descent period from shortly after separation to landing. During this time, the spacecraft attitude changes, as well

as the relative positions of the two vehicles. Adequate coverage is provided by a hemispherical-type pattern which is properly oriented with respect to the spacecraft.

Antenna size is one of the major considerations in selecting the optimum approach for the relay antenna. For example, at 200 Mc, a dipole must be almost three feet long. Stowage and erection of the relay antenna then presents a difficult problem.

The relay antenna design for the spacecraft must also consider the impact of its performance on the capsule antenna requirements, since the design of the capsule antenna is severely constrained by other system requirements. An electrically small transmission line radiator is briefly considered for the spacecraft relay antenna to simplify stowage problems. However, it is difficult to obtain circular polarization from such a device, and the use of linear polarization makes the capsule antenna design more difficult.

The use of a toroidal type pattern for the relay function was also considered, but the hemispherical pattern can be obtained with simpler antenna configurations.

It was decided that the optimum approach for the relay antenna is to provide a circularly polarized hemispherical pattern using the smallest and most reliable conventional antenna available. Deployment of the antenna is necessary, but the actual erection of the antenna structure is avoided, if possible.

The recommended design for this antenna is a turnstile element over a conical ground plane. A number of other configurations were considered for the relay antenna, such as the conical equiangular spiral and conical helix. The turnstile device provides adequate performance with minimum size and is the most simple, reliable, and lightweight approach for this application.

An r-f test probe is used for prelaunch checkout of the radio relay subsystem. A conventional stub type probe is about 15 inches long, and if adequately supported for the launch environment, it can become relatively heavy. Equivalent performance is obtained from an electrically small transmission line type antenna which is less than three inches in overall dimensions. This device is comparatively narrow-band and slightly less efficient, but adequately performs the probe function. Accordingly, an electrically small probe is recommended to minimize size and weight without affecting reliability.

7.0 CONTROL AND SENSING CIRCUITRY

The data handling and storage equipment requires data, bit sync, and signal present from one channel only. The relay link utilizes redundant receivers and demodulators. Thus, a decision must be made relative to which receiver/detector combination to use. Threshold detectors are used for each receiver AGC and detector IN LOCK indications. The detector lock and AGC lock indications are compared in logical AND circuits. A provision must be made for exclusive selection of one channel when both subsystems

are locked and provide good data. The bit sync and data must be inhibited in a way such that only data and sync from the same channel are transmitted. This is accomplished by the negated lock output. The channels are combined in an OR function by connecting the isolated switch outputs in parallel. The switches provide the desired isolation between the relay and the data handling and storage equipments.

A signal from the command subsystem is provided to turn on the power supplies for the relay radio subsystem. Since it may be desirable to turn off the relay after the two-day encounter phase of the mission in order to conserve power, the same command signal can be used to turn off the power supplies. Thus, if the power supplies are on and a command is received, the supplies can be turned off, and vice versa.

8.0 POWER SUPPLY

Two power supplies are included for the relay radio subsystem. Each power supply operates off the spacecraft 50 v rms, 2400/cps square wave and is capable of providing power for a receiver/detector combination and an output selector. During the mission, the output selector receives its power from one supply; however, if a failure occurs, the other supply is switched on to the output selector.

Since the relay is not operating during the first seven months of the mission, the command input is used to turn on and off the transformer rectifier instead of the power to the actual circuitry. In order to prevent low-frequency signals from the detector circuitry appearing in the receiver circuitry, especially the vco, the receiver and detector each have their own regulators. Sufficient filtering is included on the detector regulator to prevent low-frequency components from appearing on the receiver power lines. The overall efficiency of the power supplies is at least 75 percent.

9.0 INTERNAL REDUNDANCY

Since the relay radio subsystem is in series with the telemetry subsystem, the relay must have a higher probability of success than the telemetry for the 48-hour encounter phase when it is the prime link for capsule data. The TLM design goal for probability-of-success during the encounter phase is 0.99978. This apportionment is based on the primary objective for the Voyager 1971 mission as outlined in the Preliminary Voyager 1971 Mission Specification.

Three configurations were analyzed:

a. A single subsystem consisting of a single antenna, preselector, preamplifier, receiver, detector, and power supply.

b. A redundant subsystem consisting of a single antenna, preselector, preamplifier and output selector, and two receivers, detectors, and power suppliers. In this configuration the output to data handling and storage is based on receiver AGC only.

c. A redundant subsystem similar to that in b., except that the output selector bases its decision on receiver AGC and on the in-lock indication from the detector phase-lock loop which provides bit sync.

The failure rates for the evaluation of probability of success for each configuration are:

	Failure Rate in % Per 1000 Hours
Preselector and Preamplifier	0.220
Receiver	1.838
Detector	0.5398
Power Supply	0.1244
Output Selector	0.044

Table 9-1 summarizes the probability of success for the three configurations for a mission time of 48 hours.

The selected redundant configuration, where both receivers and detectors are monitored, comfortably exceeds the apportioned probability of success by a good margin.

Table 9-1. Probability of Success Summary (Mission Time - 48 hours)

Configuration	Reliability
Relay Radio Single Subsystem	0.9987
Redundant Subsystem Receiver AGC Monitored	0.999708
Redundant Subsystem Receiver AGC and Detector Monitored	0.9999666
Telemetry Apportionment	0.99978

CII - VB233AA105

ALTERNATE SUBSYSTEM MECHANISMS CONSIDERED

DATA HANDLING AND STORAGE SUBSYSTEM

Index

1 Scope
2 Applicable Documents
3 Justification of the Preferred Approach to Voyager '71 Data Handling and Storage

1.0 SCOPE

This document justifies the preferred approach to Data Handling and Storage (DH&S) for the 1971 Voyager mission. It is primarily concerned with the DH&S requirements and design concepts as influenced by the mission sequence. The alternate requirements and associated implementation trade-offs which were considered are described.

2.0 APPLICABLE DOCUMENTS

VB220SR101	Design Characteristics
VB220SR102	Design Restraints
VB220FD106	Capsule Interface
VB220FD108	Science Interface
VB220FD109	Telemetry Criteria
VB220FD112	Flight Sequence
VB233FD105	Data Handling and Storage
VB233TA106	Data Encoder Subsystem
VB233TA107	Data Storage Subsystem

3.0 JUSTIFICATION OF THE PREFERRED APPROACH TO VOYAGER '71 DATA HANDLING AND STORAGE

3.1 GENERAL

The simplified block diagram of the preferred DH&S subsystem is shown in Figure 3-1. The mission sequence of DH&S operations for the preferred design as presented in VB-233-FD-105 is shown in Table 3-1.

In the following sections, the preferred approach to data handling and storage will be justified by considering the following topics:

a. Apportionment of total data collection rate among the various data sources (3.2)

b. Engineering data handling (3.3)

c. Capsule data handling (3.4)

d. DAE data handling (3.5)

e. Multiplexing of stored and real time data (3.6).

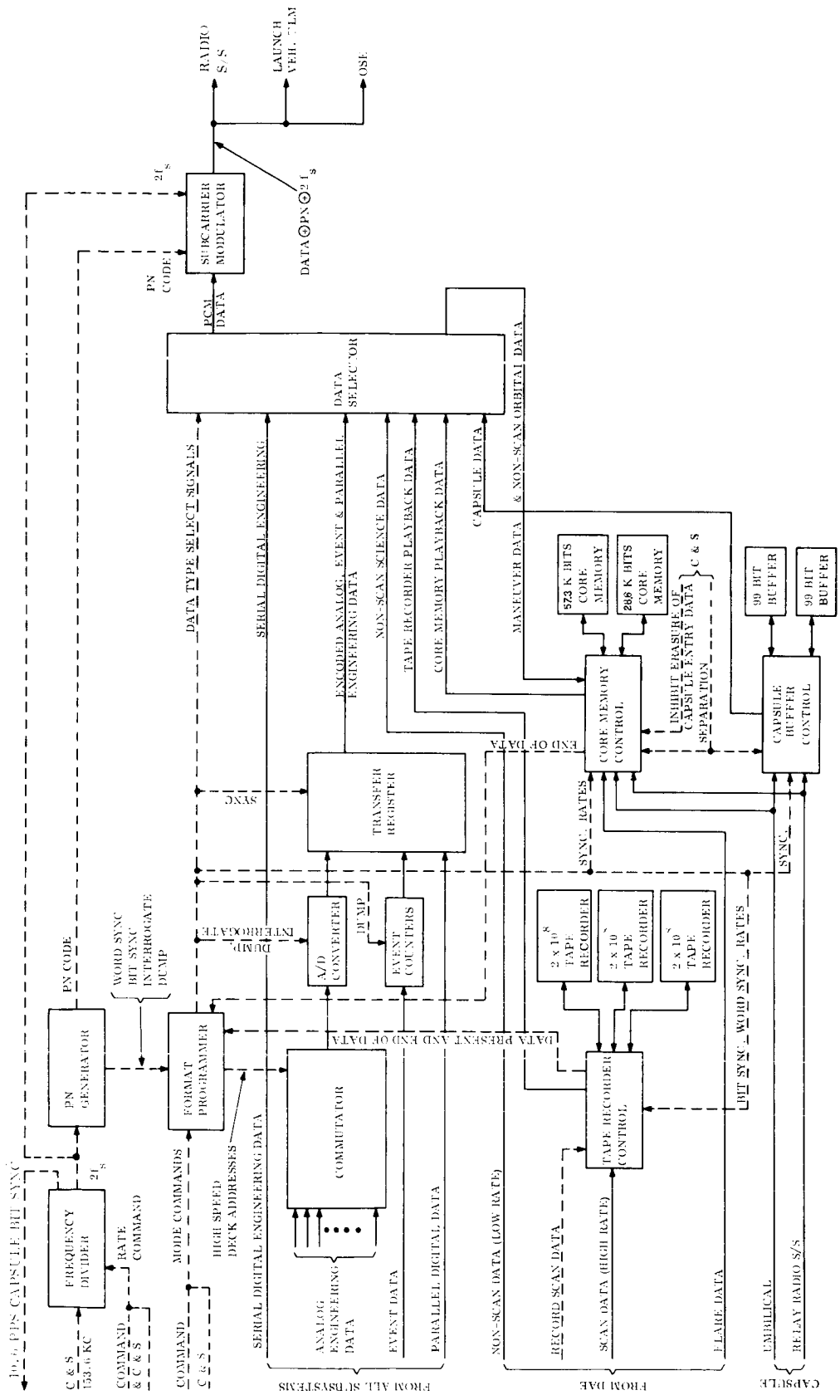

Figure 3-1. Simplified Block Diagram of DH&S Subsystem

Table 3-1. DH&S Subsystem Operation

Mission Phase	Time	Collection	Storage	Transmission
1.0 Pre-launch	T<60 days	(all modes, formats and rates as per the LCE Test Requirements)		
2.0 Launch and injection	21 min. ≤ T ≤ 41 min.	71.1 bps of cruise engineering 25.4 bps of cruise science 10.1 bps of capsule umbillical data via 70 bit buffer registers	No data stored	All collected data formatted into 105 word cruise mode minor frames. Transmitted through Launch Vehicle Telemeter at 106.66 bps.
3.0 Acquisition		71.1 bps of cruise engineering 25.4 bps of cruise science 10.1 bps of capsule umbilical data via 70 bit buffer registers	No data stored	All collected data formatted into 105 word cruise mode minor frames. Transmitted by S/C radio subsystem through low gain antenna at 106.66 bps.
4.0 First Interplanetary Cruise Period				
4.1 Normal	1 day ≤ T T≤10 days	71.1 bps of cruise engineering 25.4 bps of cruise science 10.1 bps of capsule umbilical data via 70 bit buffer registers	No data stored	All collected data is formatted into 105 word cruise mode minor frames; transmitted by S/C radio subsystem through the primary omni antenna at 106.66 bps.
4.2 Flare		In addition, DAE flare data can be collected at any rate less than 100 Kbps and stored. upon command from the DAE.	If collected, DAE flare data stored in core memories, max storage of 85,995 bits; engineering data signals ground control that flare data has been stored.	Upon ground command, stored flare data is transmitted three times at 2133 bps through high gain antenna.
5.0 First Interplanetary Trajectory Correction				
5.1 During pre-burn orientation	68 min	3.33 bps of maneuver engineering 10.1 bps of capsule umbilical data	Maneuver engineering data is stored in a core memory as a back up to the simultaneous transmission. Capsule data is stored in a core memory for later transmission.	Only the maneuver engineering data is transmitted at 3.33 bps through the omni antenna. The data is formatted into a 46 word maneuver mode minor frames.
5.2 Orientation Completed	2 min	No data collected	No data stored	The C&S commands the playback of the core memories. The stored maneuver engineering data and stored capsule data is transmitted three times at 2133 bps through the high gain antenna.

Table 3-1. DH&S Subsystem Operation (Continued)

Mission Phase	Time	Collection	Storage	Transmission
5.3 Pre-engine burn		71.1 bps of cruise engineering 25.4 bps of cruise science 10.1 bps of capsule umbilical data via 70 bit buffer registers	No data stored	All collected data is formatted into 105 word cruise mode minor frames: transmitted by S/C radio subsystem through high gain antenna at 106.66 bps.
5.4 Engine burn		106.6 bps of maneuver engineering data	Capsule data is stored in a core memory for post maneuver transmission.	Only the maneuver engineering data is transmitted at 106.6 bps through the omni antenna. The data is formatted into a 46 word maneuver mode minor frames.
5.5 During post burn orientation	90-102 min	3.33 bps of maneuver engineering data 10.1 bps of capsule umbilical data	Maneuver engineering data is stored in a core memory as a back up to the simultaneous transmission. Capsule data is stored in a core memory for post maneuver transmission.	Only the maneuver engineering data is transmitted at 3.33 bps through the omni antenna. The data is formatted into a 46 word maneuver mode minor frames.
5.6 Reacquisition Completed	2 min	No data collected	No data stored	The C&S commands the playback of the core memories. The stored maneuver engineering data and stored capsule data is transmitted three times at 2133 bps.
6.0 Second Interplanetary Cruise Phase	as required	71.1 bps of cruise engineering 25.4 bps of cruise science 10.1 bps of capsule umbilical data via 70 bit buffer registers	No data stored	All collected data is formatted into 105 word cruise mode minor frames: transmitted by S/C radio subsystem through high gain antenna at 106.66 bps.
7.0 Second Trajectory Correction Phase	same as first correction	Same as first correction phase (5.0)	Same as first correction phase (5.0)	Same as first correction phase (5.0)
8.0 Third Interplanetary Cruise Phase				
8.1 During initial period	as required	71.1 bps of cruise engineering 25.4 bps of cruise science 10.1 bps of capsule umbilical data via 70 bit buffer registers	No data stored	All collected data is formatted into 105 word cruise mode minor frames: transmitted by S/C radio subsystem through high gain antenna at 106.66 bps.

Table 3-1. DH&S Subsystem Operation (Continued)

Mission Phase	Time	Collection	Storage	Transmission
8.2 Approach guidance	T < 76 hours	50.8 bps of cruise engineering 27.6 bps of approach guidance engineering 18.1 bps of cruise science 10.1 bps of capsule umbilical via 90 bit buffer registers	No data stored	All collected data is formatted into 147 work, approach guidance mode, minor frames. Transmitted by S/C radio subsystem through high gain antenna at 106.66 bps.
9.0 Spacecraft-Capsule Separation and Third Trajectory Correction				
9.1 During S/C-Capsule separation orientation	36 min	3.33 bps of maneuver engineering 10.1 bps of capsule umbilical data	Maneuver engineering data is stored in a core memory as a back up to the simultaneous transmission. Capsule data is stored in a core memory for post maneuver transmission.	Only the maneuver engineering data is transmitted at 3.33 bps through the omni antenna. The data is formatted into a 46 word maneuver word minor frames.
9.2 Orientation Completed	2 min	No data collected	No data stored	The C&S commands the playback of the core memories. The stored maneuver engineering data and stored capsule data is transmitted three times at 2133 bps through the high gain antenna.
9.3 During pre-separation, separation, post-separation		71.1 bps of cruise engineering 25.4 bps of cruise science 10.1 bps of capsule umbilical data via 70 bit buffer registers	No data stored	All collected data is formatted into 105 work cruise mode minor frames; transmitted by S/C radio subsystem through high gain antenna at 106.66 bps.
9.4 During S/C pre-burn orientation	35 min	3.33 bps of maneuver engineering 10.1 bps of capsule relay data	Maneuver engineering data is stored in a core memory as a back up to the simultaneous transmission. Capsule data is stored in a core memory for later transmission.	Only the maneuver engineering data is transmitted at 3.33 bps through the omni antenna. The data is formatted into a 46 word maneuver mode minor frames.
9.5 Orientation Completed	2 min	No data collected	No data stored	The C&S commands the playback of the core memories. The stored maneuver engineering data and stored capsule data is transmitted three times at 2133 bps through the high gain antenna.

Table 3-1. DH&S Subsystem Operation (Continued)

Mission Phase	Time	Collection	Storage	Transmission
9.6 During remaining pre-burn		71.1 bps of cruise engineering 25.4 bps of cruise science 10.1 bps of capsule relay data via 70 bit buffer registers	No data stored	All collected data is formatted into 105 word cruise mode minor frames; transmitted by S/C radio subsystem through high gain antenna at 106.66 bps.
9.7 Engine burn		106.6 bps of maneuver engineering data	Capsule data is stored in a core memory for post maneuver transmission.	Only the maneuver engineering data is transmitted at 106.6 bps through the omni. The data is formatted into a 46 word maneuver mode minor frame.
9.8 During post-burn orientation	102 min	3.33 bps of maneuver-engineering 10.1 bps of capsule relay data	Maneuver engineering data is stored in a core memory as a back up to the simultaneous transmission. Capsule data is stored in a core memory for later transmission.	Only the maneuver engineering data is transmitted at 3.33 bps through the omni antenna. The data is formatted into a 46 word maneuver mode minor frames.
9.9 Reacquisition Completed	2 min	No data collected	No data stored	The C&S commands the playback of the core memories. The stored maneuver engineering data and stored capsule data is transmitted three times at 2133 bps through the high gain antenna.
10.0 Fourth Interplanetary Cruise	T <76 hours	50.8 bps of cruise engineering 27.6 bps of approach guidance engineering 18.1 bps of cruise science 10.1 bps of capsule umbilical via 90 bit buffer registers	No data stored	All collected data is formatted into 147 word, approach guidance mode, minor frames. Transmitted by S/C radio subsystem through high gain antenna at 106.66 bps.
11.0 Orbit Injection				
11.1 During S/C retrofire orientation	36 min	3.33 bps of maneuver engineering 10.1 bps of capsule relay data	Maneuver engineering data is stored in a core memory as a back up to the simultaneous transmission. Capsule data is stored in a core memory for later transmission.	Only the maneuver engineering data is transmitted at 3.33 bps through the omni antenna. The data is formatted into a 46 word maneuver mode minor frames.

Table 3-1. DH&S Subsystem Operation (Continued)

Mission Phase	Time	Collection	Storage	Transmission
11.2 Orientation Completed	2 min	No data collected	No data stored	The C&S commands the playback of the core memories. The stored maneuver engineering data and stored capsule data is transmitted three times at 2133 bps through the high gain antenna.
11.3 During capsule entry to capsule impact	58 min (max)	71.1 bps of cruise engineering 25.4 bps of cruise science 10.1 bps of capsule relay data via 70 bit buffer registers	Capsule entry data is stored in a core memory as a back up to the simultaneous transmission.	All collected data is formatted into 105 word cruise mode minor frames; transmitted by S/C radio subsystem through high gain antenna at 106.66 bps.
11.4 During retrofire		106.6 bps of maneuver engineering	No data stored	Only the maneuver engineering data is transmitted at 106.6 bps through the omni antenna. The data is formatted into a 46 word maneuver mode minor frames.
11.5 During S/C post burn orientation	102 min	3.33 bps of maneuver engineering	Maneuver engineering data is stored in a core memory (separate from previously stored capsule entry data) as a back up to the simultaneous transmission.	Only the maneuver engineering data is transmitted at 3.33 bps through the omni antenna. The data is formatted into a 46 word maneuver mode minor frames.
11.6 Reacquistion Completed	2 min	No data collected	No data stored	The C&S commands the playback of the core memories, containing maneuver engineering data, and capsule entry data three times at 2133 bps.
12.0 Orbital Operations				
12.1 During second orbit	< 20 hours	4267 bps of orbital engineering; 4267 bps of orbital non-scan DAE; frames of DAE planet scan data at 50,000 bps	Planet scan DAE data stored on cascaded tape recorders, in 10^6 bit frames, separated by a minimum of 1 second. Maximum storage of 6×10^8 bits (600 frames) per orbit.	Orbital engineering data and non-scanned orbital DAE data formatted into 180 word orbit mode minor frames, and transmitted through high gain antenna at 8533 bps.

Table 3-1. DH&S Subsystem Operation (Continued)

Mission Phase	Time	Collection	Storage	Transmission
12.2 During continuing orbits until sun occultation	120 days (minimum)	213.33 bps orbital engineering; 213.33 bps orbital non-scan DAE data; frames of DAE planet scan data at 50,000 bps	7020 words of engineering and non-scan DAE data are stored in the core memories during the playback and transmission of each scan data frame. Planet scan DAE data stored in cascaded tape recorders in 10^6 bit frames, separated by a minimum of 1 second. Maximum storage of 6×10^8 bits per orbit (600 frames).	10^6 bit scan data frames, alternated with 49,252 bit blocks (39 minor frames) of non-scan engineering and DAE data are played back at 8533 bps through the high gain antenna. Engineering and non-scan DAE data is formatted into 180 word, orbit mode, minor frames. The core memories, containing the non-scan data, are played back during the passing over the tape recorder play back head of each data free gap between scan data frames.
12.3 During sun occultation	180 min (maximum)	53.3 bps orbital engineering 53.3 bps orbital non-scan science frames of DAE planet scan data at 50,000 bps	7020 words of engineering and non-scan DAE data are stored in the core memories during the playback and transmission of each scan data frame. Planet scan DAE data stored in cascaded tape recorders in 10^6 bit frames, separated by a minimum of 1 second. Maximum storage of 6×10^8 bits per orbit (600 frames).	10^6 bit scan data frames, alternated with 49,252 bit blocks (39 minor frames) of non-scan engineering and DAE data are played back at 2133 bps through the high gain antenna. Engineering and non-scan DAE data is formatted into 180 word, orbit mode, minor frames. The core memories, containing the non-scan data, are played back during the passing over the tape recorder play back head of each data free gap between scan data frames.
12.4 During earth occultation	61 min (maximum)	3.33 bps of maneuver engineering	Maneuver engineering data is stored in a core memory as a back up to the simultaneous transmission.	The maneuver engineering data is transmitted at 3.33 bps through the omni antenna. The data is formatted into a 46 word maneuver mode minor frames.
12.5 Earth Occultation Period Completed	2 min	No data collected	No data stored	The C&S commands the playback of the core memories, containing maneuver engineering data, three times at 2133 bps.
12.6 During use of medium gains S/C antenna (Science Back up)	T < 45 days	13.33 bps orbital engineering 13.33 bps orbital non-scan DAE data frames of DAE planet scan data at 50,000 bps;	7020 words of engineering and non-scan DAE data are stored in the core memories during the playback and transmission of each scan data frame. Planet scan DAE data stored in cascaded tape recorders in 10^6 bit frames, separated by a minimum of 1 second. Maximum storage of 7.3×10^7 bits (73 frames) per orbit.	10^6 bit scan data frames, alternated with 49,252 bit blocks (39 minor frames) of non-scan engineering and DAE data are played back at 533 bps through medium gain antenna. Engineering and non-scan DAE data is formatted into 180 words, orbit mode, minor frames. The core memories, containing the non-scan data, are played back during the passing over the tape recorder playback head of each data free gap between scan data frames.

In each case the discussion will summarize the preferred approach (usually by mission phase), present the reasons for selection of this approach and, when appropriate, present a description and comparison of especially important alternates.

3.2 APPORTIONMENT OF TOTAL DATA COLLECTION RATE AMONG THE VARIOUS DATA SOURCES

3.2.1 GENERAL

In this section the total data collection rate and the fraction of this rate allotted to each of the principal data sources during each mission phase is justified. In the DH&S block diagram (Figure 3-1) the principal Voyager data sources are shown. These correspond to the four principal data types which are:

a. Engineering data

b. Capsule data

c. Non-scan DAE data

d. Planet scan DAE data.

3.2.2 APPORTIONMENT USED IN THE PREFERRED APPROACH

The total data collection rate and the source apportionment of it, as implemented in the preferred design, is summarized in Table 3-2 by mission phase. Table 3-2 is a summary of the data collection portion of the complete mission sequence of DH&S operations defined in Table 3-1.

3.2.3 JUSTIFICATION OF DATA COLLECTION RATES FROM LAUNCH TO ORBITAL OPERATIONS

The total rate and apportionment for these mission phases was based on a study of cruise and maneuver requirements. It was assumed that the launch and acquisition requirements were not radically different from those of cruise and, consequently, no special provision for these short, early mission phases was made.

3.2.3.1 DURING NORMAL CRUISE

The normal cruise rate of 106.6 bps was determined by assessing the respective source requirements, summing them, and then selecting the nearest conveniently implemented rate. A firm requirement of 10 bits per second for capsule data was assumed. The nearest conveniently implemented capsule rate was 10.1 bps and this rate was selected. Study of the typical cruise science instrumentation as described in VB-220-FD-108 (Science Interface) showed the non-scan science data rate to be bounded by 15 bps minimum and 45 bps maximum. 25 bps was arbitrarily chosen as being representative of the requirement. The engineering data requirement was estimated by two methods.

Table 3-2. Data Collection Rate and Apportionment

Mission Phase	Total Collection Rate (bps)	Apportionment (bps)			
		Engineering Data	Capsule Data	Non-Scan DAE Data	Planet Scan DAE Data
Launch to Orbital Operations					
Normal Cruise	106.6	71.1	10.1	25.4	0
Maneuvers	13.4	3.3	10.1	0	0
Motor Burn	106.6	106.6	0	0	0
Approach Guidance	106.6	77.4	10.1	18.1	0
Orbital Operations					
Normal Orbits	50,426.6	213.3	0	213.3	50,000 (max of 3 1/3 hours/20 hour orbit)
First Orbit - until recorder full	8,533	4267	0	4267	0
Sun Occultation (Normal Orbit Operations)					
Earth Occultation	3.3	3.3	0	0	0
Science Back-up (med. gain antenna)	50,053.3	26.67	0	26.67	50,000 (max of 0.21 hours/20 hour orbit)

The early cruise rate of Mariner C (11 bps or 1/3 of 33 1/3 bps) was scaled up by the ratio of Voyager engineering channels to Mariner C engineering channels (factor of 3) and then doubled to allow for the increased diagnostic complexity of Voyager. This resulted in an estimate of 66 bps. A second estimate was obtained as follows. In the late phases of the Phase 1A study, Voyager subsystem preliminary design engineers were asked to generate a preliminary telemetry list with sampling requirements for their respective subsystems. This list is given in VB-220-FD-110 (Telemetry Channel Assignment). This resulted in an estimate of approximately 15 bps. However, to allow for abnormal operation, the sampling rates were increased. 70 bps was thus selected as the closest, conveniently implemented rate.

3.2.3.2 DURING MANEUVERS

During maneuvers, the maximum transmission rate that can be supported, using the omni-directional antenna is 3 1/3 bits per second. A minimum of 10 bps of capsule data are, however, still assumed to be a firm requirement. Our study of the bus engineering data requirements during maneuvers showed 3 1/3 bps to be marginal. Rather than further reduce this rate by including some fraction of the capsule data, we elected to store the 10.1 bps of capsule data during maneuvers and thus, also, provide the maximum bus engineering data to the ground. Since the maneuver interval is less than 4 hours long, it was furthermore assumed that no significant degradation in scientific mission objectives would be incurred by inhibiting the collection of cruise science data during maneuvers. The alternative of storing the cruise science data, in a manner similar to that of the capsule data, was considered but rejected because of the nearly threefold increase in temporary storage capacity it would have required.

3.2.3.3 DURING MOTOR BURN

During the motor burn interval, there is a requirement for high sampling of a small number of motor burn data channels. These channels are included in the set of maneuver channels, which when sampled at a total rate of 106.6 bps provides 23.2 bps of motor burn data. Capsule data is collected at the same 10.1 bps rate, but stored in order not to further reduce the collection rate of the motor burn channels. The cruise science collection is inhibited for the same reason, and is justified on the basis of the short duration of these intervals.

3.2.3.4 DURING APPROACH GUIDANCE

During the two approach guidance intervals of the cruise portion of the mission (see Table 3-1) there is a requirement for high rate readout of a buffer memory in the G&C subsystem. This data was included in the normal cruise mode format by effectively adding channels on the high deck of the commutator. This results in a slightly reduced sampling rate. The differences relative to the normal cruise apportionment were felt to be negligible because they were well within the margins for error on our estimates of the cruise sampling requirements.

3.2.4 JUSTIFICATION OF DATA COLLECTION RATES DURING ORBITAL OPERATIONS

During normal orbital operations, the engineering and non-scan science data is time multiplexed with the playback of stored DAE scan data. The approach selected for transmission multiplexing, discussed and justified below in sections 3.5 and 3.6, provides for engineering and non-scan science orbital data to be transmitted between 10^6 bit blocks of stored scan data. The resultant fraction of the transmission capacity allotted to non-scan data is determined by the start/stop time of the magnetic tape recorder or the time between scan data blocks. A nominal allottment of five percent is made in the preferred design assuming a 1 sec recorder start/stop time which at the normal transmission rate of 8533 bps, provides an average non-scan collection rate of 26.6 bps which is apportioned equally between non-scan DAE and orbital engineering data. During orbital operations, no capsule relay data is collected in the preferred design. An alternate to this is considered below in Section 3.4.

The orbital non-scan DAE data collection requirement was estimated based on VB-220-FD-108. A nominal estimate of 100 bits per second is assumed. The estimated orbital engineering data requirement, while slightly greater than during cruise, was still less than 100 bps. Consequently, the total 426 bps engineering and non-scan science allotment at the 8533 bps transmission rate exceeds the estimated requirement by slightly more than a factor of 2. However, at the alternate orbital transmission rate of 4267 bps the 5% allotment is 213.3 bps, which essentially meets the requirement. The increased complexity required of the magnetic tape recorder in order to vary the allotment with the transmission rate and thus provide a uniform 200 bps average real time collection rate, was assumed to be too great to justify its implementation. Furthermore the resultant inefficiency in the utilization of the link capacity amounts to less than 3%.

The decision to apportion the 426.6 bps equally between the engineering data and non-scan DAE data was made in order that when transmitting data at 4267 bps, 100 bps of non-scan DAE data could still be collected.

The planet scan DAE collection requirement, of 50,000 bps, was based on the expected science payload. The maximum orbital transmission rate of 8533 bps allows for a maximum of 6.14×10^8 bits to be transmitted per 20 hour orbit, or equivalently, planet scan DAE data to be collected at 50,000 bps for a maximum of 3 1/3 hours per 20 hour orbit. A study of a typical planet scan sequence for the nominal 20 hour target orbit shows a requirement for a maximum collection interval of approximately 2 1/2 hours (terminator to terminator plus 10 degrees). The resultant margin of about 50 minutes was felt to be adequate for potential planet scan experiments on the dark side of the planet as well as non-scan data which might be included in the format of the scan data by the DAE.

3.2.4.1 DURING THE FIRST ORBIT

During the first orbit, when no planet scan DAE data is yet available for playback, the total collection rate is equal to the orbital transmission rate (normally 8533 bps). The same equal apportionment between engineering and non-scan DAE data is made as during normal orbit operations, resulting in 4267 bps for each source. The high engineering data rate permits a high resolution status check of the system following the orbit insertion maneuver. The alternate of providing a special transmission rate of 200 bps for the first orbit was rejected on the basis of the increased system complexity required in return for little more than an aesthetic gain in system performance.

3.2.4.2 DURING SUN OCCULTATION

Normal orbital operations are possible, therefore no alternatives need be considered.

3.2.4.3 DURING EARTH OCCULTATION

During an earth occultation (maximum of 61 minutes) when no data is received by the DSN, the collection rate is reduced to 3.3 bps of maneuver engineering data which is stored in the magnetic core memories as during cruise maneuvers. It is played back after the occultation period. Planet scan data is stored in the recorders as in normal orbit operations. The three alternates which were considered and rejected were:

a. Maintaining non-scan DAE and orbital engineering data collection at some rate near the nominal 200 bps normal requirement and storing the data as above.

b. Allowing the data collection to be interrupted.

c. Storing selected non-scan science data in the memories used for capsule data storage in the cruise mode.

The first alternate has the obvious advantage of providing a full record of events during the transmission interruption. However, the storage requirement is of the order of 10^6 bits. Providing this storage capacity, either by special memories or time sharing the tape recorder between scan data and non-scan data, was felt to be too complex and was the basis for the rejection of the alternative.

The second alternative has the advantage of being the simplest to implement, since it is achieved by merely maintaining normal operations and accepting the data loss on the ground. However, a minimal record during occultation was felt to be a requirement, and employing the existing cruise maneuver DH&S capability to achieve it required only the added C&S complexity needed to command it into use. Consequently the second alternative was also rejected.

The third alternative was rejected mainly out of lack of definition of possible selected non-scan science channels.

3.2.4.4 DURING USE OF MEDIUM GAIN ANTENNA

In the event of the failure of the high gain antenna during the first 30 to 45 days of orbital operations, a medium gain, fixed antenna capable of supporting a transmission rate of 533 bps is used. This is a backup provided to allow a degraded science mission objective to be achieved. Since it is a backup mode, no additional data formatter complexity has been introduced in the preferred design to allow alteration of the apportionment of five percent of the transmission rate (in this case, equal to 26.67 bps for orbital engineering data and 26.67 bps for non-scan DAE data).

3.3 ENGINEERING DATA HANDLING

3.3.1 GENERAL

This section discusses and justifies the preferred approach to engineering data handling. In particular, the following aspects of the preferred approach are justified:

a. The preferred collection and handling approach by mission phase

b. The degree of sampling flexibility and efficiency provided by the preferred encoding approach

c. The use of multiple minor frame lengths

d. The use of one fixed word length of 7 bits

e. The specific characteristics of the 3 formats defined

f. The types of engineering input signals.

3.3.2 JUSTIFICATION OF ENGINEERING DATA HANDLING IN THE PREFERRED APPROACH

Table 3-3 summarizes the preferred approach to engineering data handling by mission phase and is based on the full subsystem sequence shown in Table 3-1. Requirements for launch and acquisition were not studied in detail but assumed to be nominally the same as during normal cruise.

3.3.2.1 JUSTIFICATION OF PREFERRED APPROACH

The requirements for storage of engineering data are justified in this section, while the rates and format characteristics of the preferred approach are justified in Sections 3.3.3 through 3.3.6.

Table 3-3. Preferred Approach for Engineering Data Handling

Mission Phase	Engineering Data Handling
LAUNCH TO ORBITAL OPERATIONS	
Normal Cruise	70.1 bps of data collected from a set of cruise channels (nominally 264) formatted into 70 word minor frames and transmitted in real time at 106.66 bps.
Maneuvers	3.33 bps of data collected from a high priority set of maneuver channels (nominally 109) formatted into 46 word minor frames; data is transmitted and simultaneously stored at 3.33 bps.
Engine Burn	106.66 bps of data collected from the maneuver set of channels and again formatted into 46 word minor frames; data is transmitted in real time at 106.66 bps.
Approach Guidance	50.8 bps of data collected from the cruise set of channels plus 16.7 bps of approach guidance data is collected from G&C; data is formatted into 93 word minor frames and transmitted in real time at 106.66 bps.
ORBITAL OPERATIONS	
Normal Orbits	213.33 bps of data collected from a set of orbital channels (nominally 284) formatted into 90 word minor frames and temporarily stored for transmission in block of 39 frames at 8533 bps.
First Orbit	4267 bps of data collected from the orbital set of engineering channels and formatted into 90 word minor frames; data is transmitted at 8533 bps.
Sun Occultation	Normal orbit operation, but at 2133 bps.
Earth Occultation	3.33 bps of data collected from the maneuver set of channels and formatted into 46 word minor frames for storage (and simultaneous transmission); transmitted following the 61 min. (maximum) occultation at 8533 bps.

During maneuvers, when the 3.33 bps transmission through the omni antenna is subject to interruption because of the changing orientation of the spacecraft, the maneuver engineering data is also stored as a backup to the transmission. The storage capacity required is nominally 20,380 bits (102 minutes during cruise re-acquisition).

During normal orbital operations, the 213.33 bps of engineering data is temporarily stored during the transmission of a frame of DAE scan data. At the 8533 bps rate approximately 117 sec is required to playback one scan data block. Between frames of scan data, the engineering data is transmitted at 8533 bps along with the non-scan science data. For the 213.33 bps collection rate 39 frames plus the 56 bit data type preamble must be stored (24,626 bits). The alternative of inhibiting collection during the scan frame transmission is available for backup but was rejected for prime use in order to permit engineering data channels to be uniformly sampled. The alternate approach constrains the sampling to be done in bursts, every 120 seconds (nominally), implying a minimum sampling interval of essentially 120 seconds.

During earth occultation, the 3.33 bps of engineering data is stored, since ground reception is interrupted. The maximum occultation period is 61 minutes requiring a storage capacity of 12,200 bits.

3.3.3 ENGINEERING DATA ENCODING APPROACH

3.3.3.1 SUMMARY OF PREFERRED ENCODING APPROACH

The preferred design uses three fixed minor frame engineering data formats. They are:

a. A normal cruise format

b. A normal orbit format

c. A maneuver format.

Each of the formats provides 3 sampling rates - high, medium, and low. The medium rate is always 1/10 of the high rate and the low rate is 1/200 of the high rate. Groups of channels are added or deleted from a basic set of channels in each format.

3.3.3.2 ALTERNATE APPROACHES TO ENGINEERING DATA ENCODING CONSIDERED

The selection of the preferred approach was based on a study of mission requirements and the following four basic approaches:

a. Single Format Approach (Mariner C Approach) - In this case a single engineering data frame format is defined early in the system design. Specification of the format fixes the number of sampling rates, the number of channels sampled at each rate, the ratios of the sampling rates to the frame rates, and ultimately the specific channel assignment. It is the most simple and the least flexible of the four approaches considered.

b. Multiple Fixed Format (Preferred 1971 Voyager Approach) - In this case, the encoder design allows one of N fixed formats (of the type described above) to be selected. Each format is defined to meet the maximum a priori requirement of a particular phase or circumstance of the mission.

c. Programmable Format - In this case, an encoder design is made where the format depends on a set of binary words stored in an on-board memory. Adequate logic is provided to interpret and implement a fixed format. The contents of this memory are capable of being loaded before or after launch and with such data that any of a very large number of fixed formats may be generated.

d. Adaptive Sampling Encoding - In this case, fixed sampling rates are not defined. Instead, some prediction algorithm, in conjunction with a channel priority scheme, is employed by the encoder to effectively vary the sampling rate on each channel in accordance with some measure of its current information concept. Such schemes are commonly termed data compression schemes.

3.3.3.3 COMPARISON OF ALTERNATES AND REASONS FOR PREFERRED SELECTION

Of the four approaches considered, the single format approach has the advantage of being the most simple and consequently provides the highest reliability per pound. Preliminary estimates of the number of engineering data channels showed that about 300 would be required. Furthermore, their individual sampling requirements could be established sufficiently well to allow limiting the number of sampling rates to 3. While the relative importance of the channel information varies over the mission, a single fixed format can be defined for the entire mission which meets or exceeds the estimated sampling rate requirements for each channel. Such a fixed format is likely to result in a high proportion of redundant samples at any given time in the mission. The cost to the overall system performance of this redundancy was given careful consideration and the tradeoffs involved in reducing it were examined. In general, the cost of this redundancy is small. Because of the fixed transmission rate character of deep space links, no very effective means of realizing a positive system gain can be made by collecting data at variable rates. Thus, in the case of Voyager, the minimum sampling rate requirements could be satisfied with one format. In this event the principal cost of the redundancy to the system is that of an increased ground-data handling burden. However, ground-data reduction routines which eliminate redundant samples can be used to effectively solve this problem without incurring any increase in spacecraft design complexity.

The use of a single format was not, however, selected as the preferred approach for the 1971 Voyager mission. Instead the use of the multiple format approach was selected. This was chosen principally because during spacecraft maneuver turns the high gain antenna is not available for transmission. Instead, an omni-directional antenna is used which lowers the maximum transmission rate to 3.33 bits per second.

Also, a study of the engineering data requirements during maneuvers revealed that approximately 2/3 of the channels are of low priority or little interest at this time. In order to meet the minimum sampling rate requirements of the remaining high priority channels and transmit the data during the maneuver a new format was required which would sample only a selected set of high priority channels. Thus there was a minimum mission requirement for at least two engineering formats.

One of the features of the preferred implementation of the data encoder is that it is capable of implementing additional formats at a very low cost in complexity and weight per additional format (nominally four gates/format). This low cost, coupled with the fact that some gain in efficiency would be made by defining an additional format led to the decision to include a third format.

The full set of engineering data channels was factored into three channel subsets:

a. A basic high priority set required throughout the mission (approximately 35%)

b. A set required during normal cruise only (approximately 30%)

c. A set required during normal orbital operations only (approximately 35%).

The definition of the three formats was then made in essentially the following manner:

a. Maneuver Format = A

b. Cruise Format = A + B

c. Orbit Format = A + C

The small, but significant, advantage gained in ground data handling by virtue of the elimination of definitely meaningless data justified the small increase in spacecraft cost incurred by using 3 instead of 2 formats.

Approaches a and b suffer the disadvantage that formats must be specified exactly early in the encoder design and require wiring changes in order to make format changes once the encoder has been fabricated. Clearly, the information upon which a format definition is based should ideally be the signal's behavior as they are actually experienced.

The shortcoming of increased risk of either inefficient or inadequate sampling rate definitions are lessened by the third approach of a programmable format. In this case, the memory contents may be changed at any time, including after launch, using a radio command. Several specific implementation approaches for a programmable encoder are described in varying degrees of detail in VB-233-TA-106 (Data Encoder) differing in their cost and format flexibility. In all but the simplest case, these were rejected as being too complex to warrant the reliability risks and the weight penalty they incurred in view of the small overall system performance improvement they would be expected to provide.

In the simplest case, a memory is added to supplement the hard wired logic of the preferred design. The memory requirement is very small (less than 200 bits) and allows simple alterations to be made in the format by command. While this approach is viewed as a prime alternate to the preferred approach, it is our opinion that a more firm mission requirement for increased format flexibility is required before even it could be justified as the preferred design.

Many of the inefficiencies resulting from the use of fixed formats (all of the above approaches) can be reduced, in principle, by using the adaptive sampling approach. Several specific designs for this approach have been defined in the literature. However, this approach always requires substantially more complex logic than do the fixed format approaches, as well as an increase in the complexity of the synchronization and data reconstruction problem on the ground. Furthermore, their net gain in practice is absolutely dependent on the particular characteristics of the fixed format chosen as a base line reference and is consequently difficult to evaluate. Based on studies reported in the literature [1, 2, 3] the potential improvement is estimated to be a factor of 2 to 3 in average encoding efficiency (relative to the preferred approach). For these reasons, the adaptive sampling approach was rejected for the 1971 Voyager.

3.3.4 ONE VS. SEVERAL MINOR FRAME LENGTHS

In the preferred design, three different minor frame lengths are used. The alternative of constraining all frame lengths to be equal was considered and rejected. The principal factor in this decision was the result of the analysis of alternative decommutation approaches. The use of a general purpose computer to perform the decommutation was examined. The maximum decommutation capacity was estimated and found to be compatible with our preferred commutation approach. By using the general purpose computer, the relative decommutation cost of several versus one frame length becomes negligible in that it involves only changes in the software. Furthermore, allowing different frame lengths permits both a closer approximation to the signal sampling requirements and less complex spacecraft hardware to be recommended than that which results if a single frame length is imposed.

3.3.5 ONE VS. MULTIPLE WORD LENGTHS

The preferred design is a bit and word synchronous design. The detailed justification for this decision is given in VB-233-AA-106 (Data Encoder). The principal factors in this decision were twofold. First, decommutator synchronization (especially frame

1. Medlin, J.E. - "The Comparative Effectiveness of Several Telemetry Data Compression Techniques". Int. TLM Conference Vol. 1, Sept. 1963
2. Swartz, J.W. - "Data Processing in Scientific Space Probes" NASA-NSG-138-61 Tech. Note 5, Yale Univ.
3. Jewell, T., and Bourke, D.G. - "Some Considerations in Establishing the Feasibility of Data Compression in Unmanned Spacecraft". Symposium on Unmanned Exploration of Solar System, Feb. 1965, AAS Preprint 65-25

sync) can be obtained more quickly and reliably in a word synchronous system that in one employing only bit and frame sync. Second, the cost of word sync is made very small by the use of the PN bit synchronization technique, since it involves little more than lengthening the PN code. These two implementation considerations together with the fact that accuracy requirements for engineering analog signals are all approximately equal resulted in the decision to constrain the word lengths to be equal. While techniques for word synchronous designs compatible with multiple word lengths are known, they are not compatible with the PN sync technique and are substantially more complex in both spacecraft and ground equipment design.

A standard seven bit word length is specified for the preferred design. The use of 8 bits or 9 bits was considered to meet the accuracy requirements of the Voyager engineering data. However, upon examination of the preliminary subsystem telemetry list and in discussing accuracy requirements with subsystem engineers, it was determined that a 3% total error on high level analog signals and a 5% total error on low level signals would be adequate. The apportionment of this total error between quantization error and linearity margins of the analog signal handling portions of the encoder could be reliably implemented with a seven bit ADC (approximately 1% quantization error). Since the complexity of the analog to digital converter design is strongly dependent upon the accuracy requirements, it was decided that the potential performance improvement provided by increasing the word length could not be justified for the preferred design.

3.3.6 SPECIFIC SAMPLING CHARACTERISTICS OF THE THREE ENGINEERING DATA FORMATS

The three formats implemented in the preferred design are defined in detail in VB-233-FD-106 (Data Encoder). The number of sampling rates, the absolute sampling rates and the format channel assignment selected were based on the telemetry list of VB-220-FD-110 (Telemetry Channel Assignment) and the design details of the data encoder formatter. Since the telemetry list is a preliminary estimate, the formats defined must also be viewed as preliminary. The factors considered in their definition were:

a. Minimization of commutator and programmer complexity

b. Estimated minimum sampling requirements.

Additional study in Phase 1B should be made of the requirements and the results used to revise the details of these formats and the implied sampling rates.

3.3.7 TYPES OF ENGINEERING INPUT SIGNALS

Six standard types of engineering input signals are accepted by the data encoder. They are:

a. High level analog

b. Low level analog

c. Bi-polar analog

d. Parallel digital

e. Serial digital

f. Pulse digital

The waveform descriptions of these signal types are given in VB-233-FD-106 (Data Encoder).

In establishing the types and number of types of inputs to be encoded, the prime requirement was that of minimizing the overall spacecraft system complexity. The signal conditioning required in the respective source subsystems to convert sensor outputs to one of these six standard forms is, in general, unique to each sensor. However, the signal conditioning required to convert these six standard forms to a single form compatible with the A/D converter or digital telemetry signal can, in general, be shared among several sensors. Thus, this set of input types permits overall system minimization of signal conditioning equipment complexity.

3.4 CAPSULE DATA HANDLING

3.4.1 GENERAL

This section discusses and justifies the preferred approach to capsule data handling for the 1971 Voyager. A requirement for at least 10 bps of capsule data from launch through impact was considered firm and is not justified here. Post impact data at 10 bits per second and higher rates is discussed briefly.

3.4.2 CAPSULE DATA HANDLING IN THE PREFERRED APPROACH

Table 3-4 summarizes the preferred approach to capsule data handling by mission phase and is based on the full subsystem sequence shown in table 3-1. Requirements for launch and acquisition were not studied in detail but merely assumed to be nominally the same as during normal cruise.

Table 3-4. Preferred Capsule Data Handling by Mission Phase

Mission Phase	Capsule Data Handling
Interplanetary Cruise	
Normal	70 bit blocks (10 words) formatted with buffer registers and inserted into cruise format at about 7 sec intervals (ave. rate of 10.16 bps).
Maneuver	10.16 bps continuously stored in core memories; readout upon completion of maneuver; no real time transmission.
Spacecraft - Capsule Separation to Entry	
Cruise	10.16 bps via relay is formatted with buffers into 70 bits blocks and inserted into cruise format as during pre-separation cruise.
Maneuver	10.16 bps via relay is stored in core memories; readout upon completion of maneuver; no real time transmission.
Capsule Entry to Impact	10.16 bps via relay is formatted with buffers into 70 bits blocks and inserted into cruise format, simultaneously, received data is stored in two core memories to backup this transmission.
Post Impact	No post impact capsule data is relayed through the bus.

3.4.3 JUSTIFICATION OF PREFERRED CAPSULE DATA HANDLING APPROACH

3.4.3.1 NORMAL PRE-SEPARATION CRUISE

During this phase, capsule data is shifted serially into the bus using capsule bit sync and inserted into the bus cruise format. The data is formatted into 70 bit blocks with two buffer registers which are dumped approximately every 7 seconds (Results in an average rate of 10.16 bps.). The alternative of using bus bit sync to transfer the data from the capsule was considered because of the potential loss of capsule data due to slight differences in the bus and clock frequencies. However, assuming a 0.01%

clock stability, the nominal data loss that may be expected over the pre-separation time of typically 6 months is only 3×10^4 bits. This is equivalent to a bit error rate of 2×10^{-4}. This alternative was rejected because of this negligible total loss and furthermore, the potentially awkward capsule interface that results. However, using some form of clock synchronization is a desirable alternate, in order to guarantee a negligible data loss.

3.4.3.2 PRE-SEPARATION MANEUVERS

During this phase the transmission rate is 3.33 bits per second. To meet the firm requirement of a continuous 10 bit per second capsule collection rate, this data is stored in the magnetic core memories in the storage subsystem resulting in a storage requirement of 62,180 bits (102 min. x 10.16 bps). The data is readout upon completion of each maneuver interval. No capsule data is transmitted in real time during maneuvers. The alternative approach of reducing the collection rate from 10 bits per second to some small fraction of 3.33 bits per second in order to allow capsule data to be inserted into the real time format during maneuvers was considered and rejected. This decision was based primarily on our belief that a continuous 10 bit per second requirement was firm.

3.4.3.3 POST CAPSULE SEPARATION CRUISE

Following separation, capsule data is received via a radio relay subsystem at 10.16 bits per second. In order to allow insertion into the cruise format, this data is again formatted into 70 bit blocks using the capsule relay buffers in the storage subsystem. An alternative approach of using the magnetic core memories to perform this buffering operation was considered and rejected.

This decision was based on the fact that if capsule data were formatted into blocks equal to the capacity of one core memory an initial delay of 2866 seconds would be incurred. Furthermore, the reliability of the magnetic core memories was estimated to be less than that of the capsule relay buffers and consequently the preferred approach promises higher reliability. The cost in size and weight of these buffers together with the potential reliability and operational advantages was felt to justify this approach.

3.4.3.4 POST SEPARATION MANEUVERS

During maneuver turns, as in "Pre-Separation Maneuvers", the real time transmission rate is 3.33 bits per second. For the reasons given above in section 3.4.3.2 capsule data is again stored in the magnetic core memories during this time with the same storage requirement of 62,180 bits.

3.4.3.5 CAPSULE ENTRY TO IMPACT

The data received from the capsule during its Martian atmospheric entry phase was believed to be of highest priority. Consequently the preferred approach is to transmit

the received data in real time in the same manner as during capsule cruise and simultaneously store the received 10.16 bits per second in magnetic core memories. Two magnetic core memories are used in series in order to provide the required storage and a highly reliable backup in the event of RF loss during this critical mission phase. The entry data stored in the magnetic core memories is read out automatically after the orbit injection maneuver. If the data still is not received, a ground command can prevent further use of the memory until the data is recovered.

3.4.3.6 POST IMPACT

In the preferred design no provision is made for post impact capsule relay data.

3.4.4 ALTERNATES CONSIDERED FOR POST IMPACT RELAY DATA HANDLING

The preferred approach to capsule data handling may be summarized as one where capsule data is handled as real time data. It is stored only as a backup to the real time transmission except during the relatively short maneuver periods. This approach is adequate, basically, because of the continuous and uniform nature of the capsule data from launch to impact. In the event that post impact capsule data was required to be relayed by the bus (bus in orbit), this real time approach becomes very awkward and inefficient. This is true, basically, because the capsule is in view of the bus for only relative short intervals during each orbit. The particulars of the view time profile are determined by the specific capsule impact location and the specific orbit obtained by the bus. Furthermore, even in the case of a circular orbit, any orbital inclination to the Martian equator would result in an essentially non-periodic view time sequence. Finally, if the orbit has a significant degree of ellipticity, the capsule-bus range will also vary with the view time, with the consequence that a high performance relay link could be expected to be implemented with several transmission rates depending upon the range.

Because of these factors, employing a real time post impact capsule data handling approach would lead to a design where a fixed apportionment of the bus transmission capacity would be made, based on the maximum capsule data rate during the orbit, or alternatively, to a design where the apportionment between bus data and capsule data would be varied throughout the orbit. In the first case, which is simple to implement, a substantial degree of inefficiency would result since the total view time per orbit is small (a 4,000 km, 55 degree inclination orbit averages less than 20%). In the second case, the complexity of the control logic and the resultant awkward constraint on bus experiment programming combine to make it unattractive.

As alternates to employing a real time approach to post impact capsule data handling, two stored data approaches were considered. In the first, the bulk storage capacity of the storage subsystem would be increased to accommodate twice the total amount of capsule data expected to be transmitted in one orbit. During each orbit the capsule data collected in the previous orbit would be multiplexed on to the bus transmission link at a uniform rate while the capsule data received in real time would be stored. This approach required the addition of two storage devices, each with a storage capacity

of typically 4×10^5 bits (100 bps capsule rate, 4000 km circular orbit, 55 degree inclination, equatorial capsule site).

The second alternative considered was that of multiplexing the data with the DAE scan data and storing the combined data on the already required magnetic tape recorders. A simple multiplexing approach would be to make a fixed tape apportionment for capsule data during planet scan during non-scan intervals to start and stop the tape recorder upon command from the capsule.

While the second alternative is less efficient in its use of bus transmission capacity, it requires a minimal amount of increased tape on the magnetic tape recorders. Consequently, unless a long life time for the capsule was anticipated, this second approach would be preferred to the more efficient approach using separate storage devices.

3.5 DAE DATA HANDLING APPROACH

3.5.1 GENERAL

This section discusses and justifies the preferred approach to DAE data handling. In particular, the following four aspects of the preferred approach are justified:

a. DAE Data Rates, collection intervals and amounts

b. DAE/DH&S interface definitions

c. Preferred approach during cruise

d. Preferred approach during orbit.

The typical science interface and payload described in Volume VB-220-FD-108 is the basis for the preferred approach to the DAE data handling.

3.5.2 SCIENTIFIC DATA TYPES, RATES, AND AMOUNTS

A study of the expected scientific instrumentation disclosed that three basic types of data, having the following characteristics, were expected to be generated by the bus science payload. No justification for these characteristics or requirements will be made in this document.

a. Non-scan, Planetary and Interplanetary Instruments Data. This data is continuously collected. During cruise the rate is expected to be between 15 and 45 bps with a typical rate of 25 bps. During orbit, the typical rate is 100 bps.

b. Solar Flare Instrumentation Data. These instruments are sampled at a high rate (less than 100 Kbps) during solar flare intervals.

c. Scan Instruments. These instruments are sampled at a nominal 50 Kbps rate during planet scan cycles. Scan cycles are unequally spaced over the orbit. Assuming that a 20 hour orbit is established, the total amount of scan data per orbit will be less than or equal to the transmission capability per orbit as follows:

a. At 8533 bps, 600 frames (6×10^8 bits) may be collected

b. At 4267 bps, 300 frames (3×10^8 bits) may be collected

c. At 2133 bps, 150 frames may be collected

d. At 533 bps, 37.5 frames may be collected

3.5.3 DAE/DH&S INTERFACE DEFINITION

3.5.3.1 PREFERRED INTERFACE

The preferred design defines a DAE/DH&S interface having three parallel DAE data channels. These are:

a. Real time data channel; data rate synchronous with the D/E clock, data inserted into bus real time data format.

b. Solar flare instrument data channel; DAE clock used, data stored in magnetic core memory in blocks of less than 85,935 bits.

c. Planet scan instrument data channel; DAE clock used, single rate of 50 kbps, data stored on magnetic tape recorder in blocks of 10^6 bits upon command from DAE.

This definition was based on a study of the above data types and on the relative merits of the following alternative interface definitions.

3.5.3.2 ALTERNATES CONSIDERED

For the first alternate a single data channel for transfer of all types of data from the DAE to the DH&S subsystem was defined. Data transfer is made using a DAE clock. During cruise phases of the mission, DAE data would be temporarily stored in magnetic core memories and then multiplexed onto the transmission link in blocks equal to the memory capacity. During orbital mission phases, the data would be stored on the magnetic recorder. Both scan and non-scan data would be time multiplexed and formatted into uniform blocks by the DAE.

For the Second Alternate two channels were defined. The first would be a real time channel over which data would be transferred using a D/E clock. The instruments whose data would be transferred over this channel would be selected by the DAE. All

data transferred over this channel would be inserted into the bus real time data format. The second channel would be a stored data channel. Data would be transferred over this channel using a DAE clock having a single rate. Again, the instruments whose data would be transferred over this channel would be selected by the DAE. All data transferred over this channel would be stored on the magnetic tape recorder in blocks of less than or equal to 10^6 bits.

Note: Flare data if sampled at rates higher than the real time transmission rate would necessarily be transferred over the stored data channel.

3.5.3.3 COMPARISON OF ALTERNATES

The single channel interface was rejected for the following reasons:

a. Throughout the mission, a storage element is always required to be operational. Consequently, the probability of successful science data transmission is lower than that of the preferred design.

b. The DAE is constrained to prempt normal data collection in order to transfer flare data or else provide special storage for non-flare data during solar flares.

The double channel was rejected because flare data is expected to be collected during cruise at rates in excess of the cruise transmission rate. Consequently, flare data would be stored on the magnetic tape recorder during cruise. This would necessitate cruise operation of the magnetic tape recorders. It is believed this would shorten the expected tape recorder lifetime. The preferred three channel interface was selected as that one which could be most reliable and simply implemented and yet provide the greatest flexibility in DAE data handling.

3.5.4 PREFERRED APPROACH TO DAE DATA HANDLING FROM LAUNCH TO ORBIT OPERATIONS

Table 3-5 describes the preferred DAE data handling approach for each mission phase. It is based on the total mission sequence Table 3-5.

3.5.4.1 NORMAL CRUISE

No further justification beyond that given in Section 3.2 (Rate Apportionment) will be made here. It should be noted however that the approach for normal cruise is based on the assumption that instrument calibration sequences will generate no more than 25 bits per second during launch and acquisition. Additional studies should be made to verify this assumption.

Table 3-5. Preferred DAE Data Handling by Mission Phase

Mission Phase	DAE Data Handling
Launch through orbital injection	
Normal Cruise	25 bps transmitted in real time; collected in 24 word blocks approximately every 7 seconds using D/E bit sync
Flare During Cruise	Flare data collected and stored in magnetic core memory simultaneous with real time cruise science transmission; max storage of 85,939 bits; transmitted upon command; any input rate < 100 kbps
Maneuvers	No data collected
Approach Guidance	18.1 bps transmitted in real time; collected in 24 word blocks approximately every 9.3 seconds using D/E bit sync
Orbital Operations	
Normal Orbits	213.33 bps of non-scan data collected for insertion into real time format; collected in blocks of 90 words approximately every 2.9 sec using D/E bit sync Scan data simultaneously stored on MTR; 10^6 bit blocks input at 50 kbps; MTR records upon DAE command; Maximum storage of 6×10^8 bits
First Orbit	4267 bps of non-scan data transmitted in real time; collected in 90 word blocks every 0.15 second using D/E bit sync
Sun Occultation	Normal orbit operation
Earth Occultation	No data collected

3.5.4.2 FLARES DURING CRUISE

Flare data is collected and stored in the magnetic core memories simultaneous with the collection and transmission of the non-scanned cruise science data. The maximum storage capacity of 85,939 bits was based mainly on the storage capacity which has been provided to meet other mission requirements.

3.5.4.3 MANEUVER

During maneuvers no DAE data is collected. The justification for this is principally that the transmission rate is reduced to 3.33 bps. Further discussion of the justification for this approach during maneuvers was given in Section 3.2.

3.5.4.4 APPROACH GUIDANCE

During the two approach guidance periods of cruise, the apportionment is nominally reduced to 18.1 bps.

3.5.5 PREFERRED APPROACH TO DAE DATA HANDLING DURING ORBITAL OPERATIONS

3.5.5.1 NORMAL ORBITS

Non scan orbital science data is collected at a rate of 1/20 of the orbital transmission rate. It is collected in blocks of 90 words spaced at 90 word intervals. The intervening 90 words are bus engineering data. This data is temporarily stored in the magnetic core memories during the transmission interval of a block of scan data from the tape recorder. The storage required is 24,626 bits.

An alternative to this approach was considered. In this case the data collected was not temporarily stored in magnetic core buffers. Instead no data was collected during the transmission interval of the scan block. All data was collected in the interval between transmitted scan data blocks. While this approach has the advantage of not requiring an operational magnetic core memory, it causes the non-scanned data to be collected in bursts, which at the maximum transmission rate of 8533 bps, are spaced at 120 second intervals. It was believed this would necessitate providing special buffer storage in the DAE. This alternative was rejected in favor of the preferred approach principally because the temporary storage, in this case, is available not only for DAE data but for bus engineering data as well, allowing uniform collection rates for both.

Scan data during normal orbital operations is stored on the magnetic tape recorders. It is constrained to be transferred in blocks of 10^6 bits in order that the resultant apportionment of the orbital transmission rate for non-scanned data may be maintained at 5%. Increasing the block size will reduce this apportionment and conversely decreasing the block size increases it. The data input rate is constrained to a single rate, nominally specified at 50 kbps. This data is recorded on the tape recorder upon

command from the DAE. Between data blocks, the tape recorder is stopped or a 1 sec period of no data is recorded. Three tape recorders are provided, which in series provide a maximum storage capacity of 6×10^6 bits. The actual amount of data to be stored per orbit will be determined by the amount of data that can be transmitted per orbit as discussed earlier (section 3.5.2).

In VB 233 TA 107, an alternate storage subsystem configuration is considered which allows the DAE scan data to be transferred to the data handling and storage subsystem at variable rates, and in arbitrary block lengths. The detailed justification for the selection of the preferred approach to handling scan data in orbit is given in that document. The principal reason that the preferred approach was selected is that it required a minimum of operational storage elements and consequently has the highest reliability. While it imposes a more severe constraint on the DAE than the more complex alternative considered, this was believed justifiable, principally because it is expected that several planetary scan instruments will be involved in the planetary scan experiment. This will require the DAE to already possess substantial format buffering capacity.

3.5.5.2 FIRST ORBIT

As was discussed earlier (section 3.2), the apportionment available to non-scan orbit science during the first orbit is 4267 bps, due mainly to the lack of scan data at this time. No special provision was felt to be justifiable for the first orbit because of its single occurrence.

3.5.5.3 SUN OCCULATION

Normal orbital operations are carried out by the DH&S during sun occultations.

3.5.5.4 EARTH OCCULTATION

During earth occultation periods, the ground reception of data is interrupted for a maximum of 61 minutes. Consequently, DAE non-scan data collection is inhibited. Normally, scan data would not be expected to be collected during the majority of these periods since the spacecraft is mainly on the dark side of the planet. If required, however, it may be collected in the normal manner.

3.6 TRANSMISSION MULTIPLEXING OF STORED AND REAL TIME DATA

3.6.1 GENERAL

In the following section the approach to multiplexing stored and real time data is justified.

3.6.2 PREFERRED APPROACH

3.6.2.1 CRUISE APPROACH

During cruise, data which has been stored in the magnetic core memories is readout in data blocks. It is done in block lengths of 3 times the capacity of the magnetic core memories at a rate of 2133 bps. (i.e. played back three times). During the transmission of stored data, collection of real time data is inhibited. This is justified by the infrequent requirement to transmit stored data during cruise.

3.6.2.2 ORBITAL APPROACH

In the orbital phases of the mission, stored and real time data is again time multiplexed. In order to provide a uniform collection rate of real time data, the magnetic core memories are used to temporarily store the non-scan data during the transmission of a block of tape recorder scan data. Alternative approaches to implementing the time multiplexing of stored and real time data are considered in detail in VB 233 TA 107.

3.6.2.3 GROUND SYNCHRONIZATION

A 56 bit synchronization preamble is inserted at the start of blocks of core memory data, and real time data. 49 bits of this preamble are a "preamble sync" word which signals the decommutator of a data type change. Seven bits are used to specify the type of data as follows:

a. Maneuver engineering

b. Stored capsule

c. Cruise

d. Flare

e. DAE scan data

f. Orbital engineering and non-scan science data

g. Approach guidance engineering

The preamble word length was derived as follows:

Define:

L_{fa} = average loss per frame due to false sync acquisition.

L_{fd} = average loss per frame due to false dismissal of preamble sync.

E = the number of errors allowable in the ground preamble sync detection circuitry

P = the preamble word length in bits (multiple of 7)

P_e = maximum transmission bit error probability of 5×10^{-3}.

F = number of bits/frame = 10^6

If E errors are allowed in a P bit preamble, the number of preamble codes which will be accepted is:

$$N = \sum_{E=O}^{E=E} \frac{P!}{(P-E)!\,E!} \leq P^E$$

The probability of the random occurrence of any one P bit pattern in a frame with word sync is:

$$P_r = 2^{-P} \frac{F}{7}$$

The probability of false lock is then:

$$P_{fa} = N \cdot P_r$$

and the average bit loss per frame may be shown to be for random, uniformly distributed errors

$$L_{av} = F/2 \text{ (bits)}$$

Therefore, the average false alarm loss per frame is

$$L_{av} = \frac{(P)^E}{2^P} \quad \frac{F^2}{14} \text{ (bits/frame)}$$

The probability of false dismissal of a frame preamble depends on more than E errors occurring. If the errors are random and independent, the probability of false dismissal is given by:

$$P_{fd} = 1 - \sum_{i=o}^{E} \frac{P!\,(P_e)^i\,(1-P_e)^{P-i}}{i!\cdot(p-i)!} \doteq \frac{(P\,P_e)^{E+1}}{E!}$$

The approximation neglects the contributions due to more than E+1 errors on the basis that $P_e \ll 1$ and $E \ll P$.

The average loss per frame due to false dismissal is the entire frame of F bits.

Therefore:

$$L_{fd} = \frac{(P\,P_e)^{E+1}\,F}{E!} \quad \text{(bits/frame)}$$

Substituting in the system values gives:

$$L_{fa} \doteq \frac{P^E\,10^{12}}{2^P\,14} \quad \text{(bits/frame)}$$

and

$$L_{fd} \doteq \frac{(P \cdot 5 \times 10^{-3})^{E+1}}{E!}\,10^6 \quad \text{(bits/frame)}$$

It is desired to limit the losses due to these causes to one tenth those due to link errors:

$$L_{fd},\ L_{fa} \leq (.1)\ P_e F = 5 \times 10^2$$

Trial solutions show that the combinations P=49, E=3 are the minimum values of P and E that satisfy this criteria. These values were therefore chosen for preamble length and allowable preamble errors respectively.

3.6.3 ALTERNATE APPROACH

In addition to the alternate approaches to time multiplexing stored and real time data considered in VB 233 TA 107, the alternate approach of frequency multiplexing the stored and real time data during the orbital phase of the mission was considered.

The principal advantage of this alternative from an operational point of view is that it makes the apportionment of the orbital transmission capacity given to real time or non scan data independent of the manner in which data is stored on the magnetic tape recorder. Recall that in the preferred design, the fraction of the tape footage not used for storage of scan data is equal to the fraction of the transmission capacity allotted to real time or buffered non scan data (Nominally 5%).

The alternative of frequency multiplexing stored and real time data was rejected for the following reasons:

a. Additional weight, volume, power and design complexity are required in order to implement two subcarrier modulators.

b. The overall transmission efficiency is reduced when more than one subcarrier is used.

c. While the frequency multiplexing alternative eliminates the requirement for temporary storage of the non scan real time data in the orbital phase, additional requirements for this storage have already been established by consideration of maneuver backup data, flare data and capsule data storage. Consequently, the magnetic core memories could not be eliminated from the preferred design even if frequency multiplexing were chosen.

d. The complexity of the demodulator and decommutator is increased if two frequency multiplexed subcarriers are used rather than a single subcarrier onto which stored and real time data are time multiplexed.

CII - VB233AA106

ALTERNATE SUBSYSTEM MECHANISMS CONSIDERED

DATA ENCODER

Index

1	Scope
2	Applicable Documents
3	General
4	Distributed vs Centralized Commutation and Conversion
5	Commutator Arrangement and Control
6	Commutator Switches
7	Analog to Digital Converter
8	Signal Conditioning
9	Format Programmer
10	Power Supplies
11	Subcarrier Modulation Detection and Synchronization
12	Error Control Coding

Appendizes

I	Subcarrier Interference in RF Loop
II	Sine Wave vs. Square Wave Signalling
III	SNR Performance of Subcarrier Acquisition Multiplier
IV	PN Code Acquisition Decision Analysis
V	Estimate of the Probability, P_1
IV	Probability Density Function for Correlator Output
VII	Analysis of Acquisition of Word and Frame Sync
VIII	Efficiency Comparison of Single and Double Channel Systems
IX	Error Control Coding - (15.7) Bose Chadhuri Encoder/Decoder
X	Error Control Coding - (73.45) Bose Chadhuri Encoder/Decoder
XI	Error Control Coding - (15, 5) BI - TRANSORTHOGONAL Encoder/Decoder

1.0 SCOPE

This document justifies the preferred design of the 1971 Voyager data encoder, and presents the alternates considered and tradeoff analysis performed.

2.0 APPLICABLE DOCUMENTS

VB220SR101	Design Characteristics
VB220SR102	Design Restraints
VB220FD110	Telemetry Channel Assignment
VB233FD105	Data Handling and Storage Volume A
VB233AA105	Data Handling and Storage Volume B
VB233FD106	Data Encoder Subsystem

3.0 GENERAL

The function of the Voyager data encoder is the sampling of spacecraft engineering data and conversion of this data to 7-bit NRZ binary form. The NRZ data is then combined with subcarrier and synchronization signals forming the telemetry signal which modulates the RF carrier. A functional block diagram of the data encoder is shown in Figure 3-1. The major functional elements of the data encoder are the commutator, signal conditioning, analog to digital converter, control unit, power supply and subcarrier modulation and synchronization. Alternate implementation methods for each major element are analyzed in the following sections. In particular, the following topics are considered:

Distributed vs. Centralized Commutation and Conversion

Commutator Arrangement and Control

Commutator Switch

Signal Conditioning

Analog-to-Digital Converter

Format Programmer (Control Unit)

Power Supplies

Subcarrier Modulation and Synchronization

Error Control Coding.

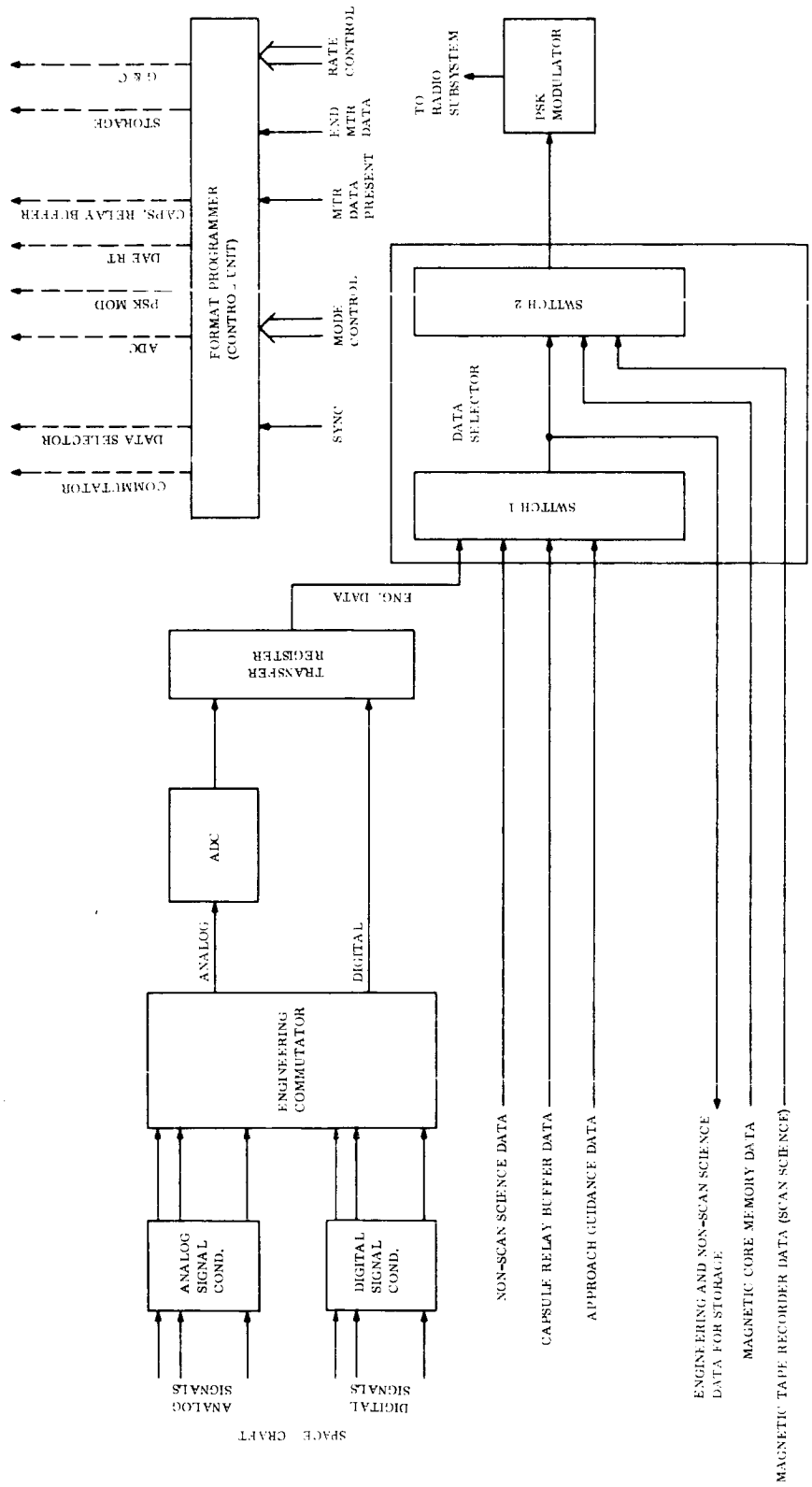

Figure 3-1. Data Encoder Simplified Block Diagram

4.0 DISTRIBUTED VS CENTRALIZED COMMUTATION AND CONVERSION

4.1 SCOPE

This section discusses the effort expanded in the investigation of the feasibility of distributing the engineering commutator among various subsystems. An arrangement in which the commutator multiplexer switches, signal conditioning, and analog to digital conversion circuits would be distributed among various spacecraft subsystems is followed by an arrangement, in which the low level signal conditioning would be distributed. The preferred design, a centralized system is discussed.

4.2 APPROACHES

4.2.1 DISTRIBUTED BY SPACECRAFT LOCATION, SIGNAL CONDITIONING AND CONVERSION

Figure 4-1 is a block diagram of the circuitry which would be located in a particular subsystem for signal conditioning, commutation and data conversion. In this scheme only digital data would be transferred from the various subsystems to the data encoder multiplexer. Control of the analog switches would be by the data encoder programmer or a ring counter sequencer arrangement located in the subsystem.

4.2.2 DISTRIBUTED BY SPACECRAFT LOCATION, LOW LEVEL, SIGNAL CONDITIONING ONLY

Figure 4-2 is a block diagram showing the circuitry located in a particular subsystem for commutation and conditioning of the low level signals only. Control of the switches would be by the data encoder programmer, or a sequencer arrangement located in the subsystem.

4.2.3 CENTRALIZED SYSTEM

In a centralized system all commutation, signal conditioning, and conversion would be located in the data encoder subsystem. Control of the commutator would be by the data encoder programmer.

4.3 INITIAL SELECTION CRITERIA

Distributed commutator arrangements have the potential advantage of lower noise sensitivity since the number of analog signals that would be transferred over long lines to the data encoder subsystem is reduced or eliminated. In the case of the distributed technique shown in Figure 4-1, only digital data would be transferred to the data encoder multiplexer. Since digital data should be much less noise sensitive, this type of system is potentially more accurate than a centralized system. On the other hand, a distributed system has several apparent disadvantages. More signal conditioning circuitry is required in the distributed systems. The problem in commutator control is

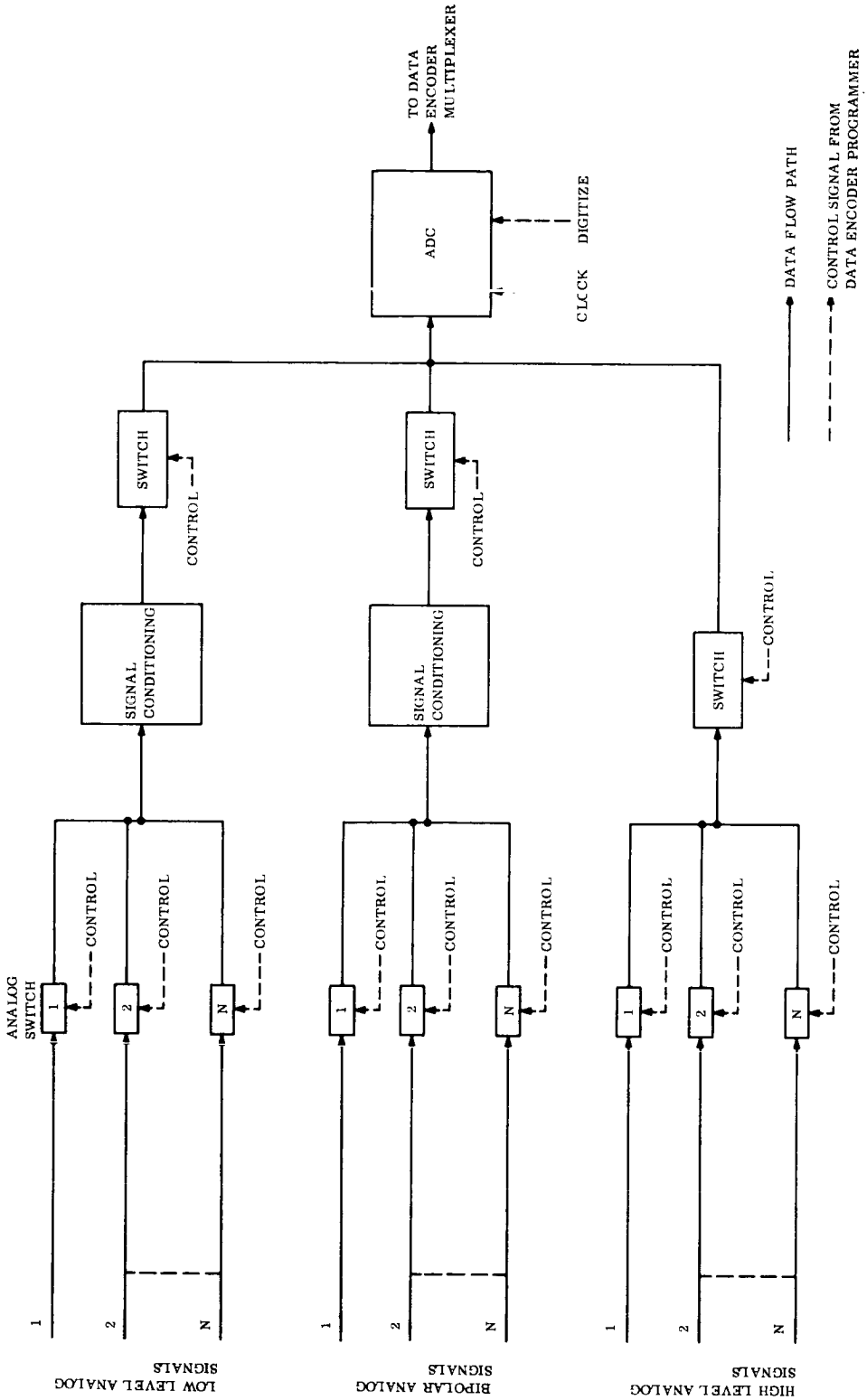

Figure 4-1. Distributed Commutator and Data Conversion

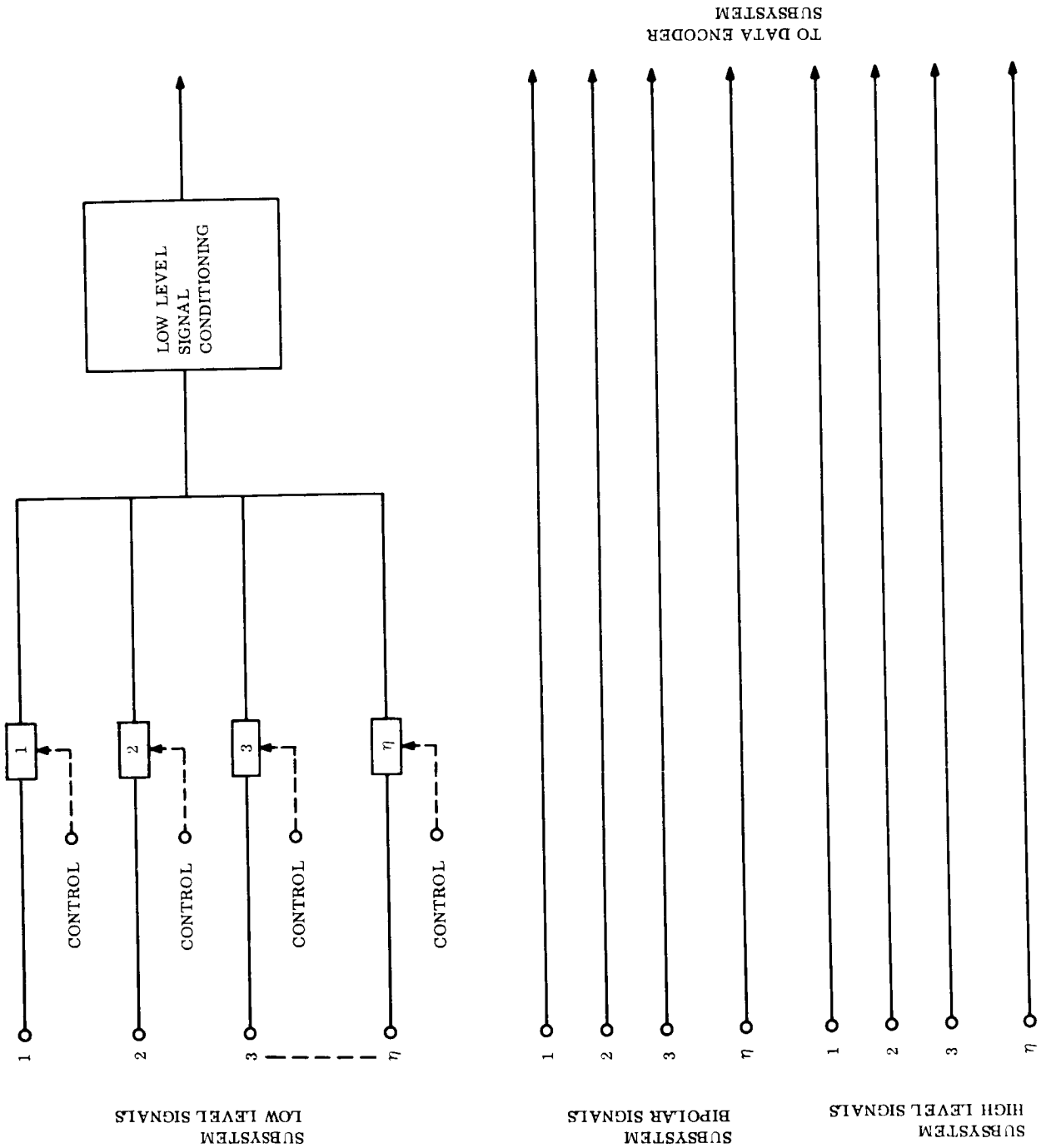

Figure 4-2. Low Level Signal Conditioning and Commutation Distributed

much greater in the distributed systems than in a centralized system. No reliability advantage is apparent with a distributed system since the added parts and weight of the distributed conditioning circuitry could be added as redundancy for the centralized scheme.

4.4 SELECTION OF PREFERRED DESIGN

Since the commutator arrangement of the preferred design is very similar to the Mariner C commutator arrangement, and that experience with Mariner has indicated no particular problems with signal noise sensitivity, the added circuit complexity in signal conditioning, commutation, and control in the distributed system is not justified at this time. The preferred design is therefore a centralized data encoder system.

5.0 COMMUTATOR ARRANGEMENT AND CONTROL

5.1 SCOPE

This section covers the alternate commutator arrangement approaches and the criteria from which the preferred design was selected. A commutator with no sub-commutation is followed by a commutator with one level of sub-commutation, and finally, the preferred design, a commutator with two levels of sub-commutation is discussed. Since the main criteria which determines the commutator arrangement is the control complexity required for maximum reliability, several control methods are presented with each commutator arrangement. These control circuits would be physically located in the programmer (see Section 9.0).

5.2 FUNCTIONAL OBJECTIVE

The objective of this section is to determine the optimum commutator arrangement for the Voyager Data Encoder. It will be necessary for the engineering commutator to time division multiplex approximately 250 to 300 channels of information. The analog data channels will be conditioned by the various subsystems to three standard levels, 0 to 100 mv, 0 to 3.2 V, and ±1.6 V. The sampling rates required will vary between a high of 7 samples per second and a low of 5 samples per 10,000 seconds. Flexibility will be required to the extent that different engineering data formats can be selected for various mission phases, refer to Data Handling and Storage Volume B (VB233AA105) for a discussion on data encoder flexibility required.

5.3 APPROACHES

5.3.1 COMMUTATOR WITH NO SUBCOMMUTATION

Figure 5-1 is a block diagram of a 256 channel commutator with the switches arranged in 16 groups of 16 switches per group. No sub-commutation is provided.

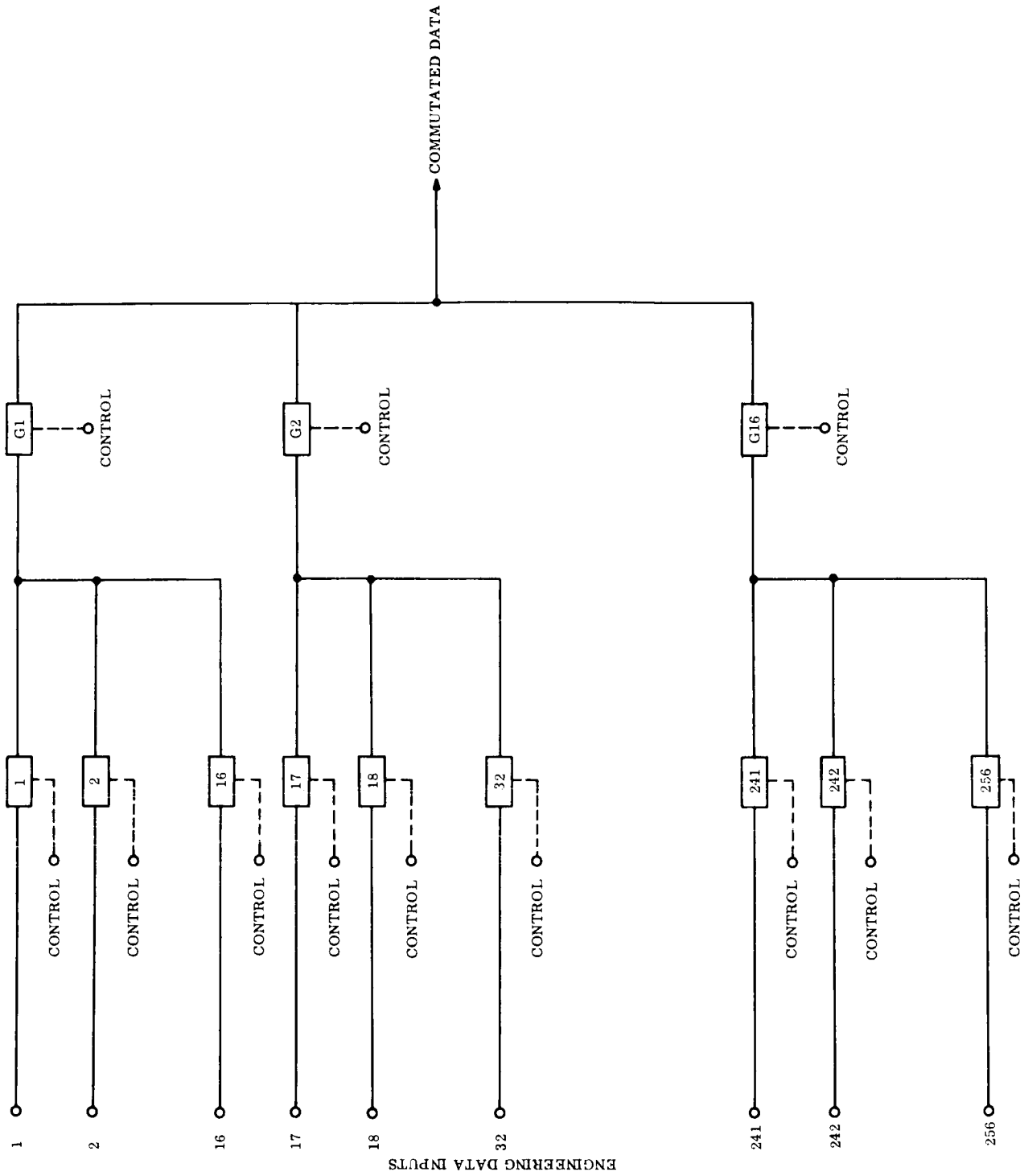

Figure 5-1. Commutator Arrangement with No Sub-Commutation

Sequencer Selection: The commutator switches can be selected by a sequencer type counter which drives one switch in each group and selects the correct switch by selection of one of the group switches. This type of a control arrangement is shown in Figure 5-2. With this type of control, a short in any deck switch could result in loss of 16 channels of information. A failure by shorting of any group switch could result in loss of all channels. An advantage of this arrangement is that it requires only two sync pulses from the programmer.

Sequential Selection: A second type of control would be to select the 256 switches sequentially and leave the group switches on for all of the 16 switches per group. A short in any deck switch could still result in loss of 16 channels as in the previous scheme, but with this selection method a short in a group switch would have no effect. An example of this type of control is shown in Figure 5-3.

Completely Programmable Arrangement: The type addressing scheme which would result in the most flexible system would be to generate the eight bit address with a completely programmable memory. The address words would be stored in the memory in a pattern which would result in the desired sampling rate for each channel. The number of words stored in the memory would be equal to the number of words in a major frame (one complete sampling cycle of all channels). For example, in order to span the range of 7 samples per second to 5 samples per 10, 000 seconds approximately 50, 000 words of storage would be required. Change of the program would require transmission of 400, 000 bits of information.

Burst Addressing Method: Figure 5-4 is a block diagram of a second addressing scheme using a programmable 768 bit memory to control the rate at which each channel is sampled. The memory contains a 3 bit rate selection word for each commutator channel. At the beginning of each word a channel address is generated by the binary counter and the rate at which that channel is to be sampled is generated by the memory. The channel is sampled only on the coincidence of the channel address and the rate pulses. For example, if a channel is to be sampled once each pass of the commutator (WORD/256) the memory generates the code word for selection of rate r (gate G_1) coincident with the generation by the binary counter of the channel address. The address and the output of G_1 are decoded in the decoding network and the switch is sampled. If the channel is to be sampled only once each 128 passes of the commutator, the memory generates the word for selection of r/128. The address for this channel and the output of gate G^8 would be true coincidentally only once each 32, 768 words or once each 128 passes of the 256 channel commutator. It is apparent that in a address programmer of this type the data from the commutator switches would not be outputted at a constant rate. However, the data pattern would be periodic with a period equal to that of the lowest sampling rate. Therefore, it would be necessary to interpose a pair of high capacity buffer memories between the encoder commutator and the RF transmitter. One of the buffers would be storing the data while the other is being read out at a

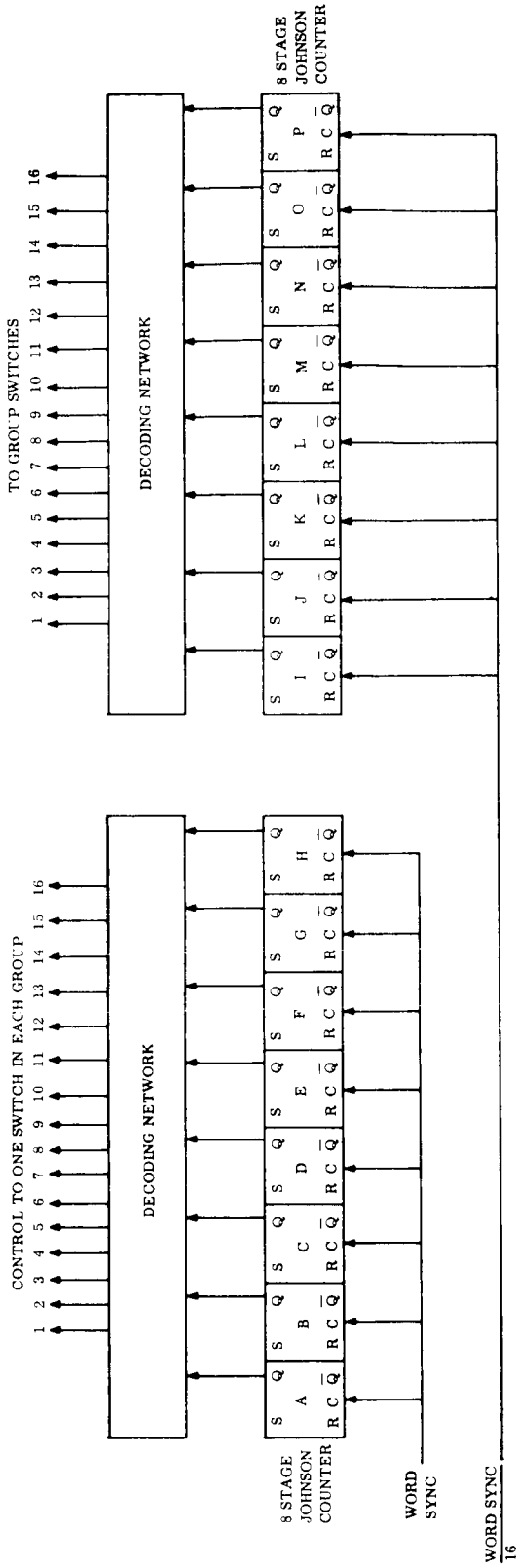

Figure 5-2. Sequencer Control for Commutator with no Sub-Commutation

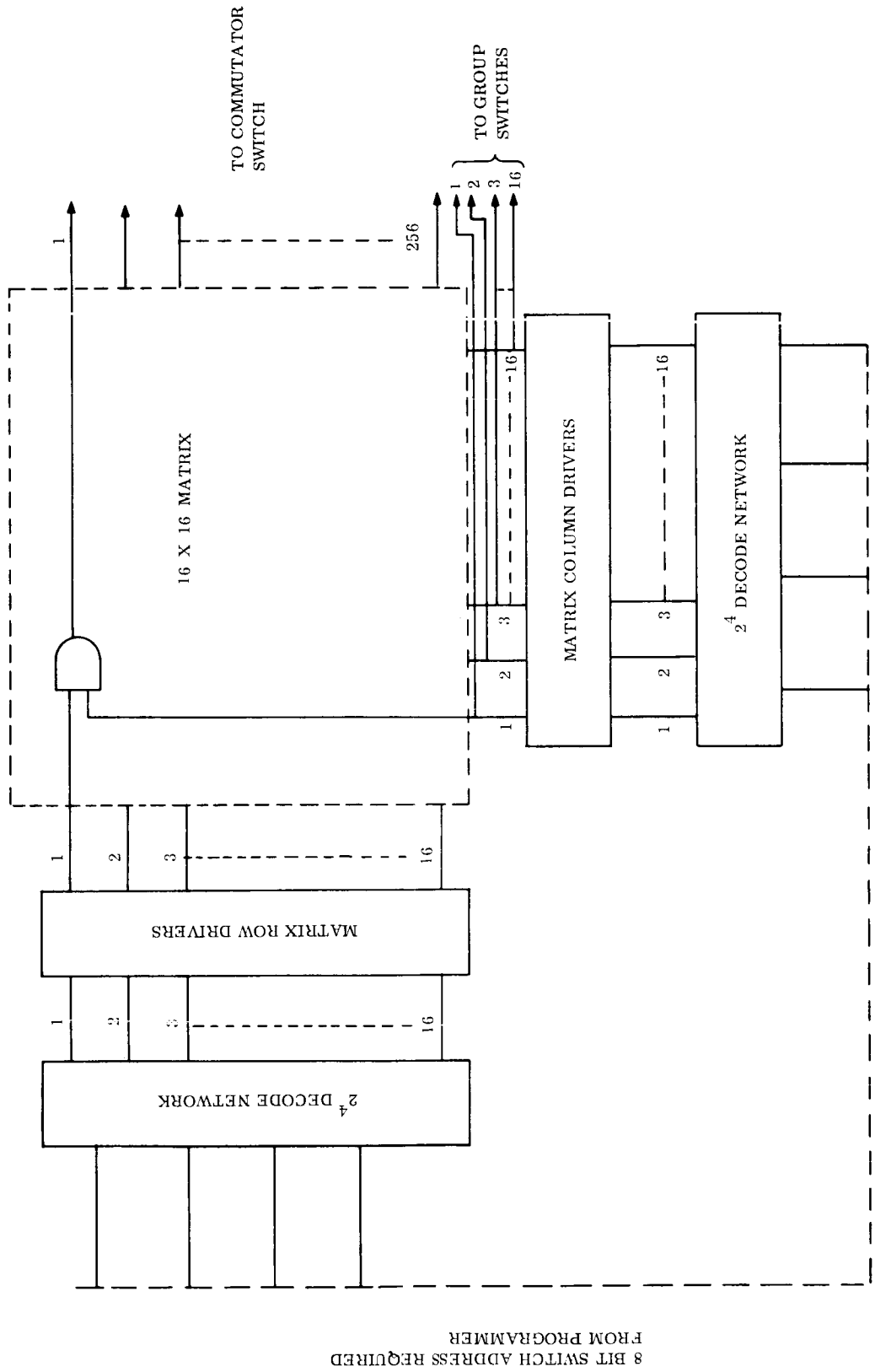

Figure 5-3. Sequential Selection Network

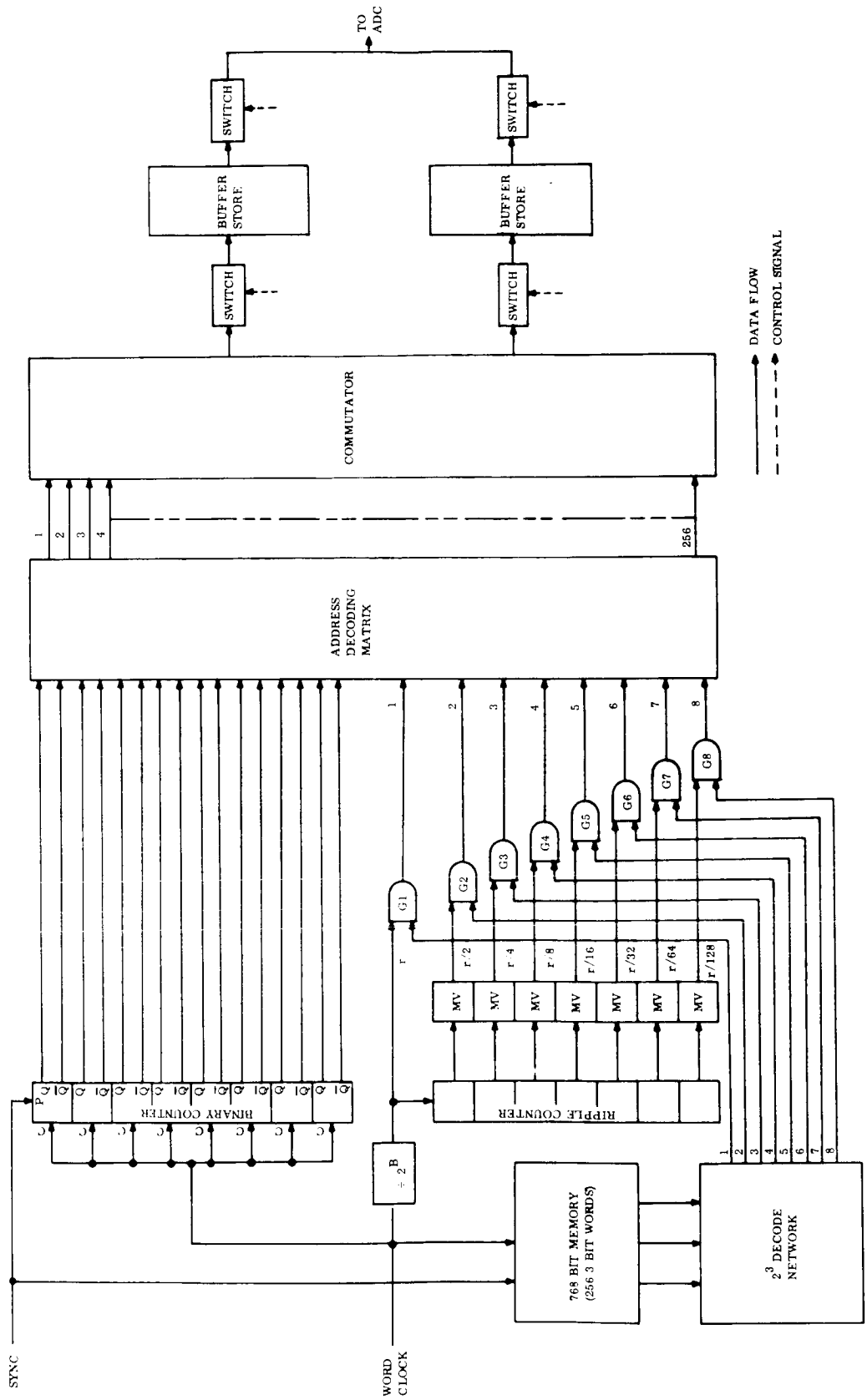

Figure 5-4. Burst Address Scheme

constant bit rate. If it is assumed that a channel is being sampled at the lowest rate of once each 32,768 words the storage capacity of each buffer would be:

$$\frac{(32{,}768 \text{ words}) \quad (7 \text{ bits/word})}{2} = 114{,}688 \text{ bits}$$

This system requires less memory capacity than the previous system, and the command requirements to change programs are less strenuous.

5.3.2 COMMUTATOR WITH ONE LEVEL OF SUBCOMMUTATION

Figure 5-5 is a diagram of a commutator with one level of subcommutation. The switches are arranged in a fast deck of length 128 and 8 medium decks each of length 16. This arrangement gives a ratio of medium deck sampling to high deck sampling of 16 to 1. The length of the medium deck is directly proportional to the sampling ratio desired.

Sequencer Selection: Figure 5-6 is a logic diagram for a possible control network for the commutator shown in Figure 5-5. Stages A through H are connected as a Johnson Counter driven from the programmer supplied word clock. The output of the counter is decoded and drives one high deck switch in each group. After turn off of the switch 16 in the high deck, Johnson Counter 2 is stepped to the next group and the high deck cycle is repeated. After completion of the last group (group 8) Johnson Counter 3 steps the medium deck one position and the cycle is repeated.

Sequencial Selection: Figure 5-7 illustrates a better but more complex method of sequencing the high deck of the commutator. With this control technique the high deck is sampled sequentially with the group switch being on for the complete group. A short in one of the group switches would have no effect in this scheme. Stages A through G are connected as a synchronous binary counter with 128 States. These states are decoded and provide the addresses of the switches on the high deck. The outputs of the column drivers are also used to drive the group switches. The medium deck switches are driven by a Johnson Counter which is stepped once each pass of the high deck.

5.3.3 COMMUTATOR WITH TWO LEVELS OF SUBCOMMUTATION

Figure 5-8 is a diagram of a commutator arrangement with two levels of subcommutation. In this arrangement the medium deck is sampled at 1/10 the high deck rate and the low deck is sampled at 1/200 the high deck rate.

Sequencer Selection: The switches in this arrangement can be selected with a sequencer network similar to that discussed for the previous section (Figure 5-6). The failure mode of a shorted group switch causing loss of all data would still exist with this scheme.

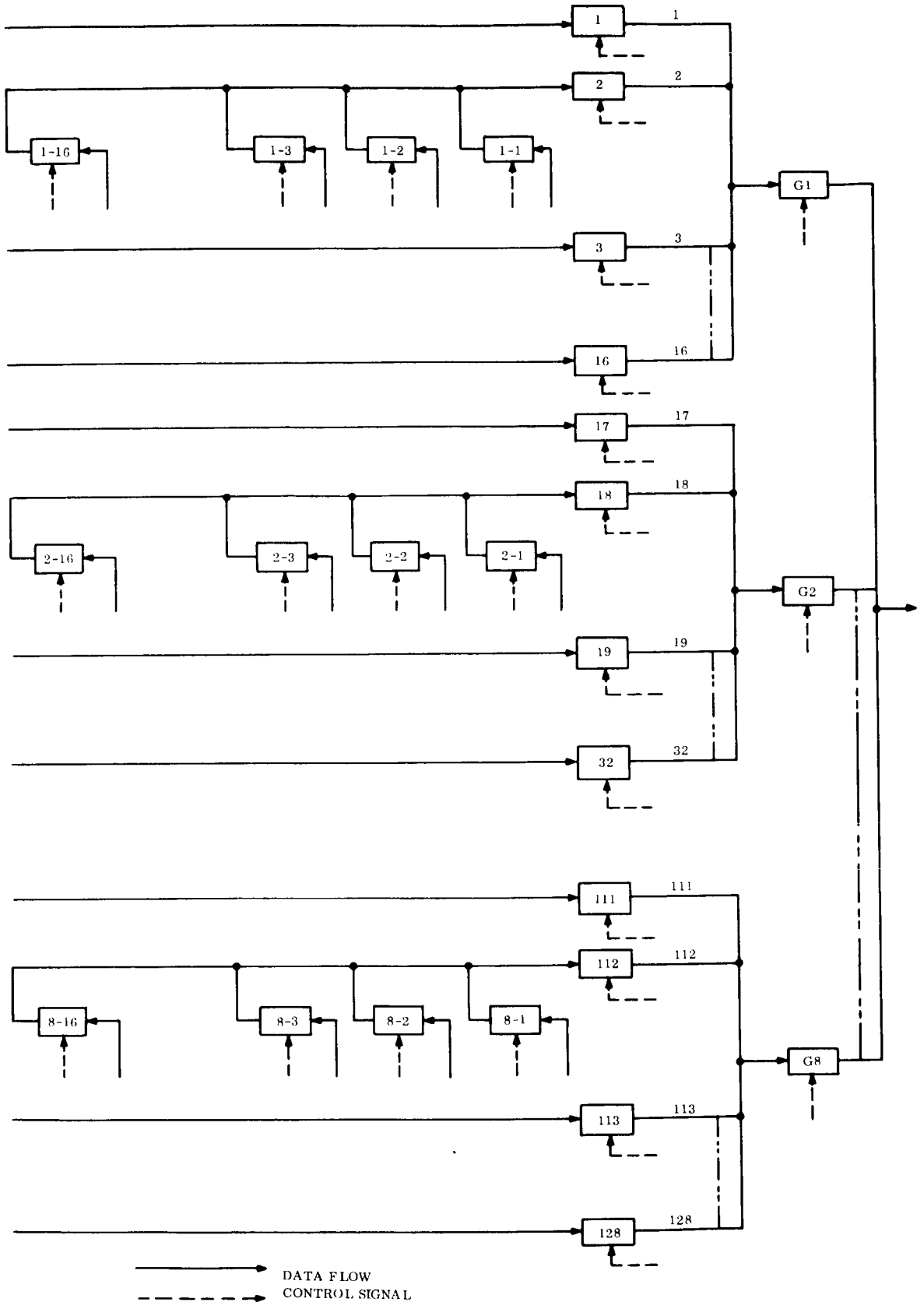

Figure 5-5. Commutator with One Level of Subcommutation

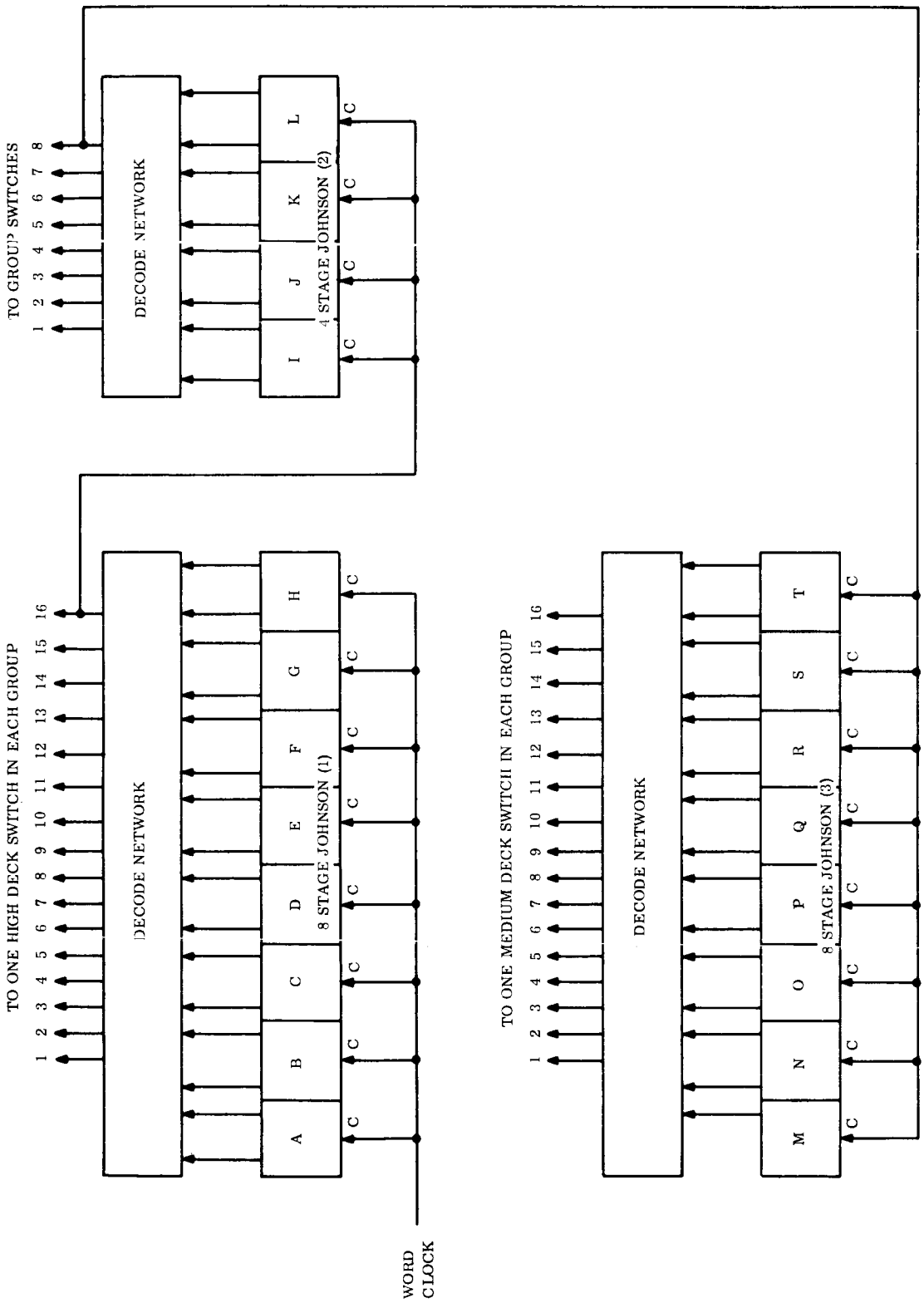

Figure 5-6. Sequencer Control for Commutator with One Level of Sub-commutation

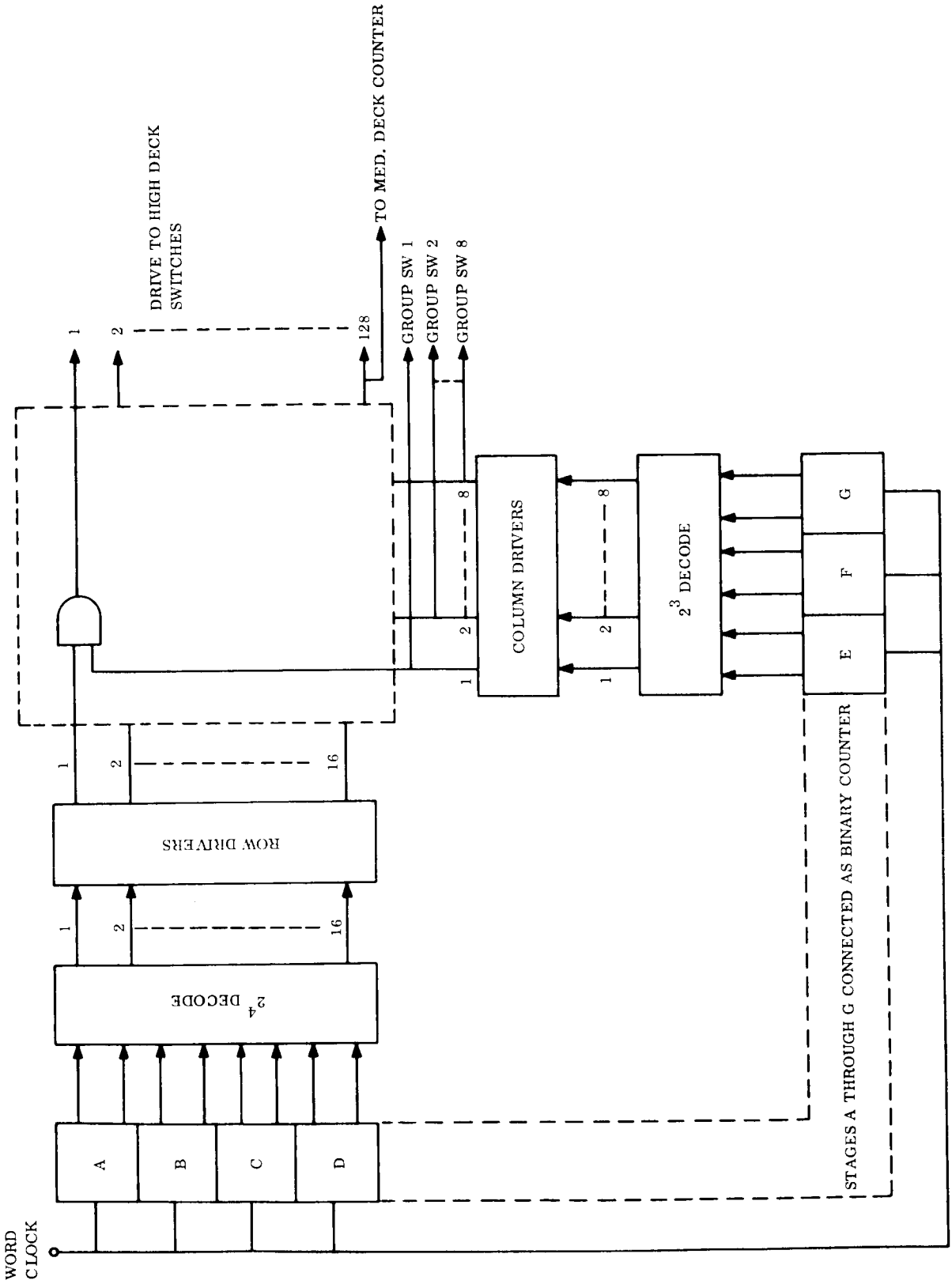

Figure 5-7. Sequencer Control for Commutator with One Level of Subcommutation

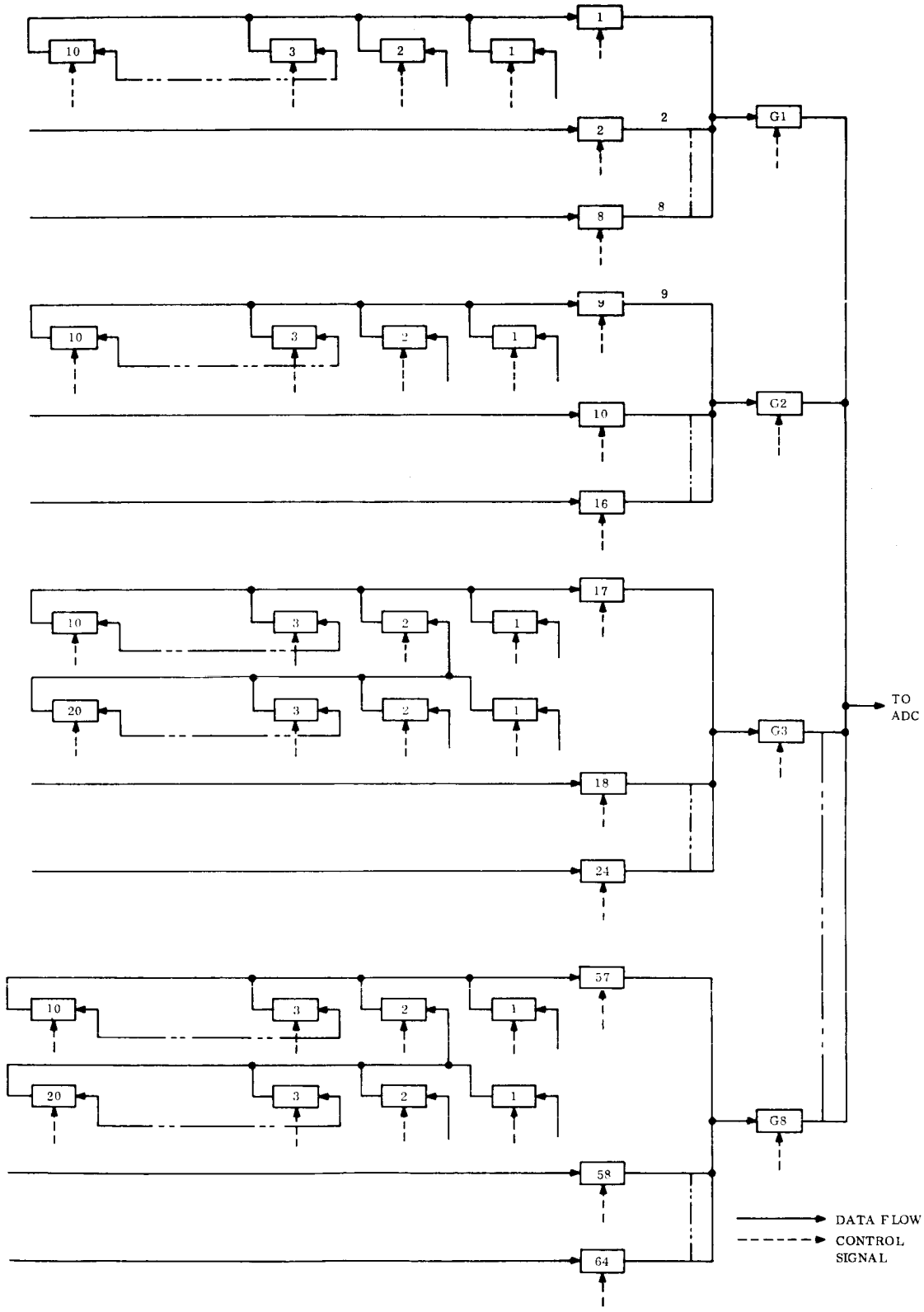

Figure 5-8. Commutator with Two Levels of Subcommutator

Sequential Selection: Figure 5-9 is a logic diagram of a network to sequentially select the high deck switches. Stages A through F are connected as a synchronous binary counter with each of the 64 states representing a high deck switch address. The medium and low decks will be stepped one position per pass of the high deck and the low deck counter will be stepped one position per pass of the medium deck.

Flexibility by Programmable Memory: Figure 5-10 is a logic diagram of the sequential selection network described in the previous section with the last three stages of the binary counter replaced with a programmable memory. The memory allows the high deck groups to be sequenced in any given order. This type of selection will give a high degree of flexibility with low memory capacity requirement. For example, if the me nory contained 24 3 bit words the 8 commutator groups could be sequenced in any of 2^{72} possible combinations, and would require only 72 bits from the command system to change the sampling format. The switches on the high deck in each group are sequenced by the ABC counter. After the last switch in the group is addressed, the next group to be sampled is read from the memory. To better illustrate the flexibility, two example formats are shown in Table 5-1. In example A, the 24, 3 bit words are stored in a sequence which results in group 1 being sampled 8 times per frame, group 2 sampled 4 times per frame, and groups 3 through 8 sampled twice per frame. In example B, the storage sequence results in groups 1 and 2 sampled 8 times per frame, groups 3 and 4 twice per frame, and groups 5 through 8 once per frame. Since each group has 3 basic sampling rates (high, medium, and low decks), and the groups are sampled at 3 different rates, 9 channel sampling rates are obtained in each of the examples given. Another interesting storage combination would result by storing the same word in the 24 word memory. This combination would allow selection of any one group and effectively increase the sampling rate by a factor of 8. The memory could also be reduced to 8, 3 bit words which would allow 2^{24} possible group sampling combinations. However, if it were desired to sample all groups in any one frame they would have to be sampled at the same rate.

Flexibility by Fixed Format Memories: In Figure 5-11 the programmable memory has been replaced by a series of permanent memories each containing a specified format. The fixed format memories required here are very simple flip-flop registers located in the format programmer (see Section 9.0).

5.4 INITIAL SELECTION CRITERIA

Two of the commutator arrangements are further evaluated for use in the Voyager spacecraft; these are the commutator with two levels of subcommutation with programmable memory flexibility and the commutator with two levels of subcommutation with fixed format flexibility. These arrangements are discussed further in the following section.

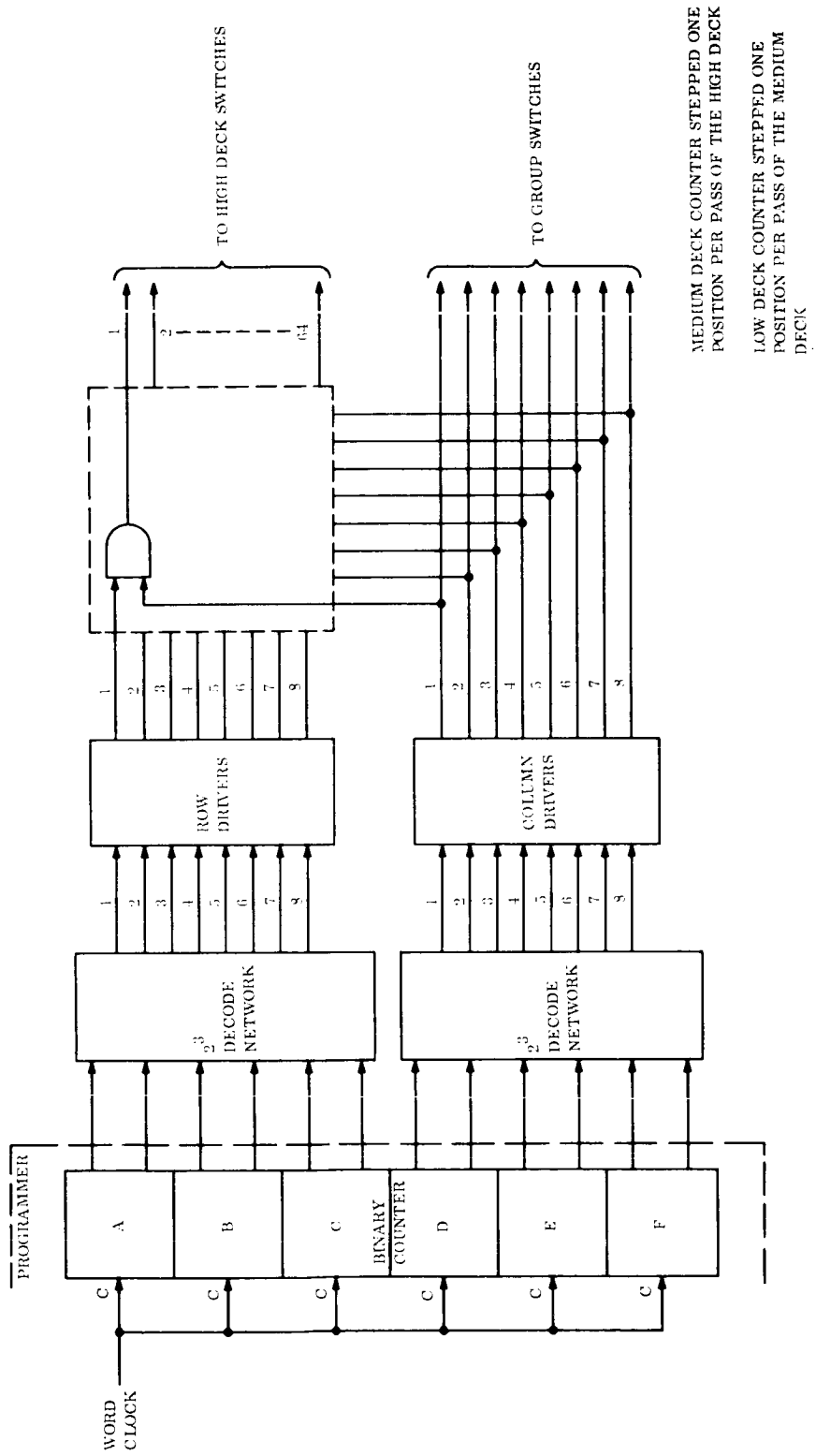

Figure 5-9. Sequential Selection Network for Commutator with Two Levels of Subcommutation

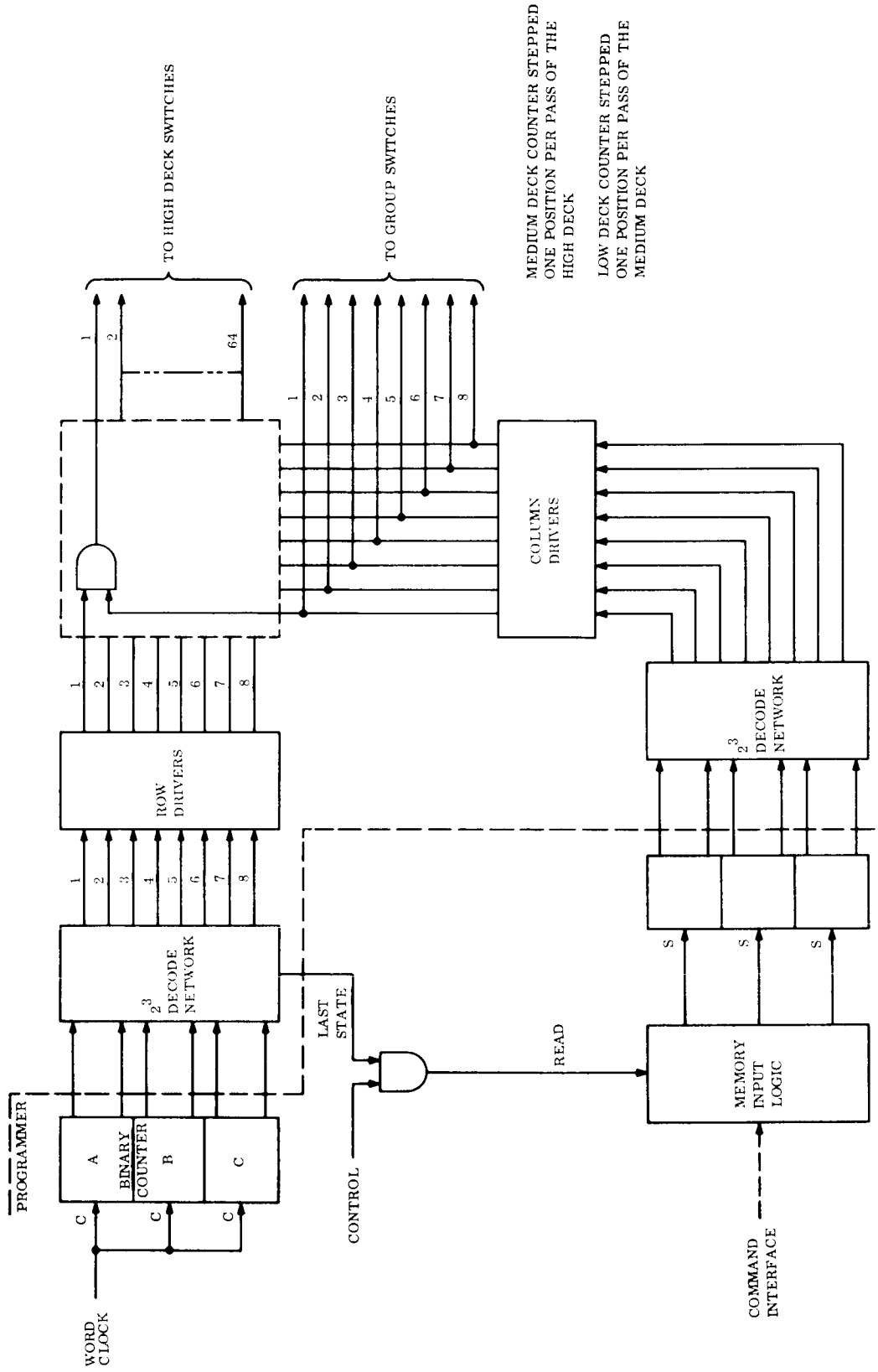

Figure 5-10. Sequential Selection Network with Programmable Memory

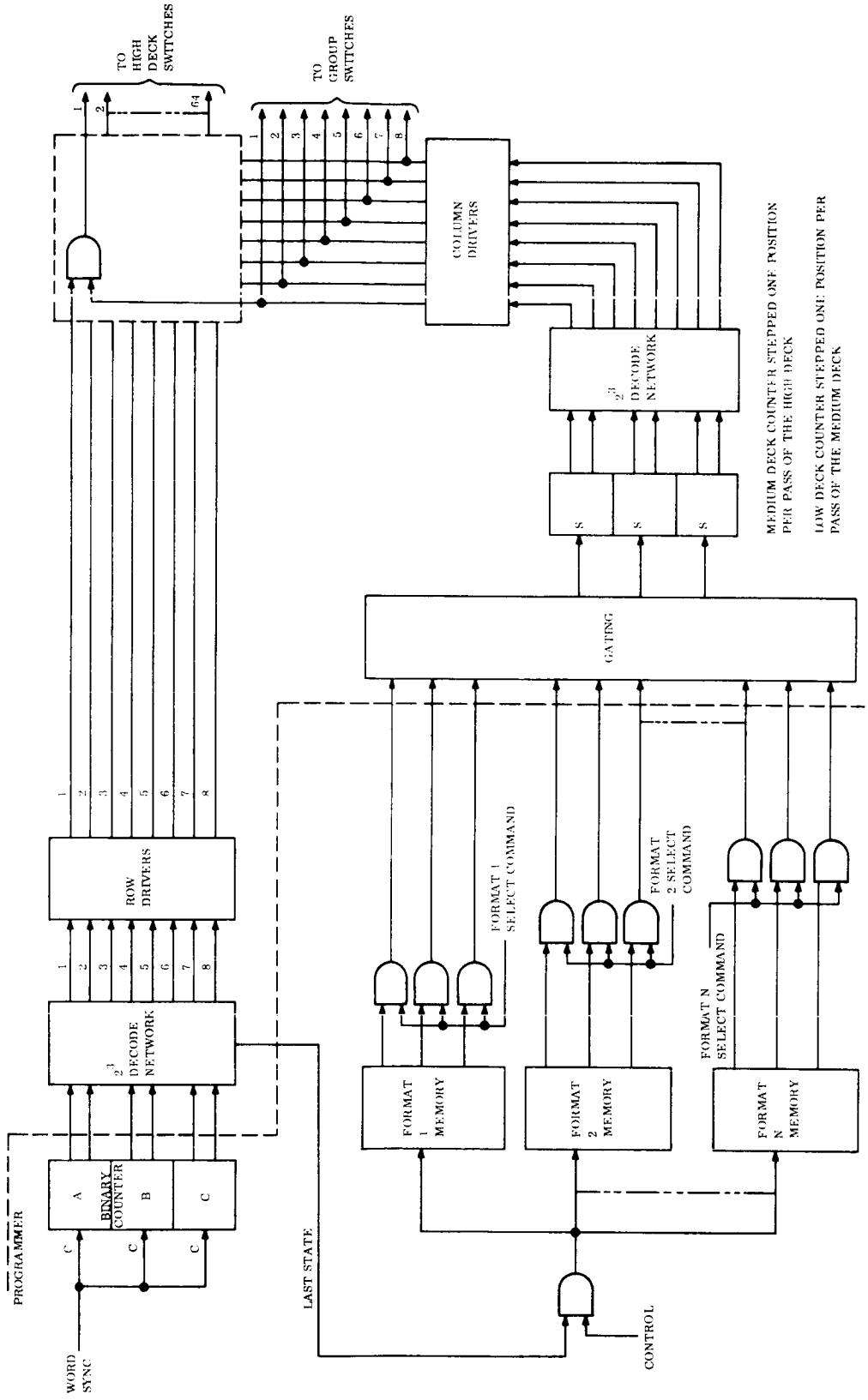

Figure 5-11. Sequential Network with Fixed Format Memories

Table 5-1 Programmable Memory

Example A				Example B			
	Storage Word	Group Selected	Group Sampling Rate (Samples/Frame)		Storage Word	Group Selected	Group Sampling Rate (Samples/Frame)
1	000	1	8	1	000	1	8
2	001	2	4	2	001	2	8
3	010	3	2	3	010	3	2
4	000	1	8	4	000	1	8
5	011	4	2	5	001	2	8
6	100	5	2	6	011	4	2
7	000	1	8	7	000	1	8
8	001	2	4	8	001	2	8
9	101	6	2	9	100	5	1
10	000	1	8	10	000	1	8
11	110	7	2	11	001	2	8
12	111	8	2	12	101	6	1
13	000	1	8	13	000	1	8
14	001	2	4	14	001	2	8
15	010	3	2	15	010	3	2
16	000	1	8	16	000	1	8
17	011	4	2	17	001	2	8
18	100	5	2	18	011	4	2
19	000	1	8	19	000	1	8
20	001	2	4	20	001	2	8
21	101	6	2	21	110	7	1
22	000	1	8	22	000	1	8
23	110	7	2	23	001	2	8
24	111	8	2	24	111	8	1

The configurations which were eliminated and the reasons for their elimination are summarized below.

Commutator with no Subcommutation

Sequencer Selection	Configuration has no flexibility. Has failure mode which could cause loss of all data. All channels are sampled at the same rate.
Sequential Selection	Failure modes are less critical but still has no flexibility. All channels are sampled at the same rate.
Completely Programmable	Has highest degree of flexibility but command requirements are too strenuous.
Burst Method	Has high degree of flexibility but requires a high capacity storage series element.

Commutator with One Level of Subcommutation

Sequencer Selection	Critical failure mode and no flexibility.
Sequential Selection	No flexibility.

Commutator with Two Levels of Subcommutation - this is the preferred approach, however the following control configurations were eliminated.

Sequencer Selection	Critical failure modes. No flexibility.
Sequential Selection	Failure modes are less critical and a ratio of high deck sampling to low deck sampling is 1/200, but does not allow for format flexibility.

5.5 APPROACHES ANALYZED

The factors used in evaluating the fixed format and programmable arrangements are reliability, flexibility required, and command requirements.

5.6 ANALYSIS DESCRIPTION

The programmable system is clearly the more flexible of the two approaches, and has many very desirable characteristics. The data formats would not need to be finally defined as early in the design phase and could be changed in flight. However, this arrangement does require the command capability of changing the program. For reliability consideration a minimum of two memories would be required.

The fixed format memory configuration has a degree of flexibility in that one of several predetermined formats can be selected by a single command. The format storage required would consist of only a few flip-flops. A failure in any flip-flop would result

in maximum loss of one format. Loss of one format could not result in loss of the most important channels, since these channels are contained in all formats.

The flexibility presently required of the engineering data commutator can be obtained by use of the commutator with two levels of subcommutation with fixed format flexibility. The added size, weight, and power (see Table 9-2) required in the programmable system can not be justified at this time. Therefore, the fixed format arrangement represents the best engineering choice for the preferred design.

6.0 COMMUTATOR SWITCHES

6.1 SCOPE

To discuss the various commutator switches available and recommend a type for use on the Voyager spacecraft. A more detailed evaluation should be performed in Phase 1B.

6.2 FUNCTIONAL OBJECTIVE

The switches used in the commutators will be required to meet certain systems constraints. The switches must pass analog signals of the following magnitude:

High Level	0-3.2v
Low Level	0-100 mv
Bi-polar	±1.6v

The value of 3.2v was selected, mainly because of test and checkout considerations. It leads to an easier fundamental delta voltage to deal with. In the particular case of the Voyager ADC with a seven bit word this increment would be 3.2v divided by 2^7 which is 25 mv. The bipolar value of ±1.6v is related to the basic ADC working voltage levels by unity gain with a level shift. This means that the signal conditioning required to force the bipolar signal to the 3.2v level is kept to a minimum.

The low level signal value of 0 to 100 mv is a recommended level based on past experience with the Mariner R and C data encoders. The final value for low level signal levels is actually a compromise between the amount of signal conditioning required in the encoder and the signal level that the various users of the low level channels can generate, i.e., temperature measurements, attitude control, and so on. The value of 0 to 100 mv is a standardized level which is high enough to allow use of a single, as opposed to differential, input low level amplifier and minimizes the effects of switch impedance, switch offset voltages, output impedance of the sensor, and input impedance of the low level amplifier.

The switches are also required to operate over the commutation rates specified in Table 6-1.

Table 6-1. Commutation Rates

Mode	Transmission Rate	Collection Rate	Switch On Time (word duration)
(I) Maneuver	3.33 bps 106.66 bps	3.33 bps 106.66 bps	2.102 sec 65.62 ms
(II) Cruise	106.66 bps	106.66 bps	65.62 ms
(III) Normal Orbit	8.533 Kbps	426.66 bps	16.4 ms
(IV) MCM Dump	2.133 Kbps	0	--
(V) Non Scan Orbit	8.533 Kbps	8.533 Kbps	0.82 ms
(VI) Approach Guidance	106.66 bps	106.66 bps	65.62 ms

A third system constraint which will effect the switch selection is the overall system accuracy. This is 3 percent for high level and bipolar signals and 5 percent for low level signals. This is a minimum worst case requirement for the Voyager data encoder. A complete error analysis will be performed in Phase 1B after the design of the ADC, low level amplifier, and constant current source. The switches effect these parameters by virtue of their series resistance and their offset voltages. These parameters are particularly important for the low level signals.

6.3 APPROACHES

There are at least five switches available today which should be considered for use on the Voyager spacecraft. These switches are listed below with a brief description. The analysis and selection criteria follow.

6.3.1 MARINER C TYPE

The Mariner C type switch is a discrete component switch capable of switching rates from DC to several hundred cps used in the Mariner C Mars probe.

6.3.2 GENERAL ELECTRIC TYPE

This is a hybrid monolithic silicon device packed two per flat pack. Each switch driver is located on a single silicon chip. The actual switching transistor is a second pellet transistor wired into the circuit within the flat pack.

6.3.3 MINUTEMAN INTEGRATED

This is a TI Solid Circuit Network (SN 354A) switch designed for and used in the Minuteman program. The switch requires an external capacitor to set the minimum repetition rate and has offset voltage in the millivolt range.

6.3.4 JUNCTION FET

The junction field effect transistor switch is a silicon planar device. The device can be switched at rates from dc to several kc and has no offset voltage.

6.3.5 METAL OXIDE FET SWITCH

The MOS FET switch is a silicon planar device suitable for use as a normally off switch. This FET is capable of rates from dc to several Kcps and has no offset voltage.

6.4 INITIAL SELECTION CRITERIA

It should be emphasized that the selection is based on a preliminary study and that a more detailed study should be carried out in Phase IB. Based on our preliminary study two of the five switches are considered as possible for use in the Voyager spacecraft. These are the Mariner C switch and the junction FET switch. These switches are discussed further in the sections to follow.

The other three switches were eliminated and the reasons for elimination are itemized by switch below:

6.4.1 GENERAL ELECTRIC TYPE

Little information was able to be obtained on this switch. The series transistor is a single NPN transistor GE, SPP, 10J, Pellet. Since a series pair is not used the high offset voltage across the switch will affect the accuracy of the low level signals. When additional information is obtained on this switch, it should be further evaluated for possible use in the high level channels.

6.4.2 MINUTEMAN INTEGRATED

This is a pulse type switch and will not operate at the low rates necessary for all commutation decks at the slow bit rates.

6.4.3 METAL OXIDE FET SWITCH

The state-of-the-art industry wide today does not justify the selection of the MOS FET. Generally, problems exist in building the device so that the parameters are not repeatable. Reliability is not yet established for the devices. Handling of the devices is

evidently a critical function. If static charges are allowed to build up the isolation layer is highly subject to punching through because of its thinness.

6.5 APPROACHES ANALYZED

Several factors can be used as guidelines to determine that the switches are compatible with the Voyager spacecraft and which would be the best to use based on present information. These criteria are listed below:

a. Reliability

b. Offset Voltage

c. Series Impedance

d. Power Dissipation

e. Size and Weight

f. Operating Speed

A relative comparison will be made of the expected failure rates of the switches from two aspects. These are the individual switch failure rate and the probability of a switch failing short and thus causing an entire commutator deck failure. A deck is defined as a series of switches whose outputs are tied in parallel.

6.6 ANALYSIS DESCRIPTION

6.6.1 FACTORS EVALUATED

The following factors are those which are important switch considerations and are defined in this paragraph. They are summarized in paragraph 6.7 for the two switches considered.

a. Complete Reliability - For the purpose of this section this will be defined as the expected failure rate for a single switch and for a switch failing shorted.

b. Leakage - This is the current flowing from the input to the output of the switch when the switch is off. It is a measure of the effectiveness of the circuit in operating as a switch. Ideally this measurement would be zero.

c. Off set voltage - This is the voltage measured across the switch when the switch is on and there is no signal current flowing. This is the series voltage generator of a transistor and will add to any signal voltage being switched causing an error to be generated.

d. Size, Weight, Power - Self explanatory

e. Saturation Resistance - This is the resistance between the input and output of the switch when gated on.

f. Switching time - The time required for the switch to be turned on and off. This is a good indication of the maximum allowable operating frequency.

6.6.2 ANALYSIS OF MARINER C SWITCH

Figure 6-1 is a schematic diagram of the Mariner C switch. The circuit consists of a gated colpits oscillator, a rectifier, and a switch transistor. When the oscillator is gated on,energy is coupled across the transformer and is rectified to generate a dc voltage. This dc voltage bias is applied to the back to back transistors which are operated inverted to give lower offset voltage, switching them on allowing a low impedance path for the signal.

When the gate is removed the oscillator is switched off removing the bias voltage and turning off the switch. The capacitor from the switch input to ground is necessary to remove transients coupled through the distributed capacitance of the transformer to the secondary.

The switch offset voltage is the difference between the V_{ce} drops of the back to back transistors when they are switched on but have no current flowing through them. The best silicon transistors available today have a Vce on the order of 1 to 2 millivolts with optimum base current and can be matched to give a total offset voltage of 50 microvolts.

The turn on and turn off times of the switch are mainly controlled by the time it takes for the oscillator to turn on and off. The rectifier time constant is small in comparison with this build up.

The switch saturation resistance is simply the sum of the saturation resistances of the two series transistors.

6.6.3 ANALYSIS OF JUNCTION FET SWITCH

Figure 6-2 is a schematic of a P channel FET switch with a redundant inverter drive. When the inverters are switched off by a low gate voltage, +V is applied to the gate (g) of the FET causing the switch to be turned off.

When it is desired to turn the switch on the gate voltage input is made high saturating the two transistors, removing the +V from the gate (G) of the FET allowing it to conduct. The conduction path is the simple ohmic path of the p channel with off-set voltage equal to 0 volts.

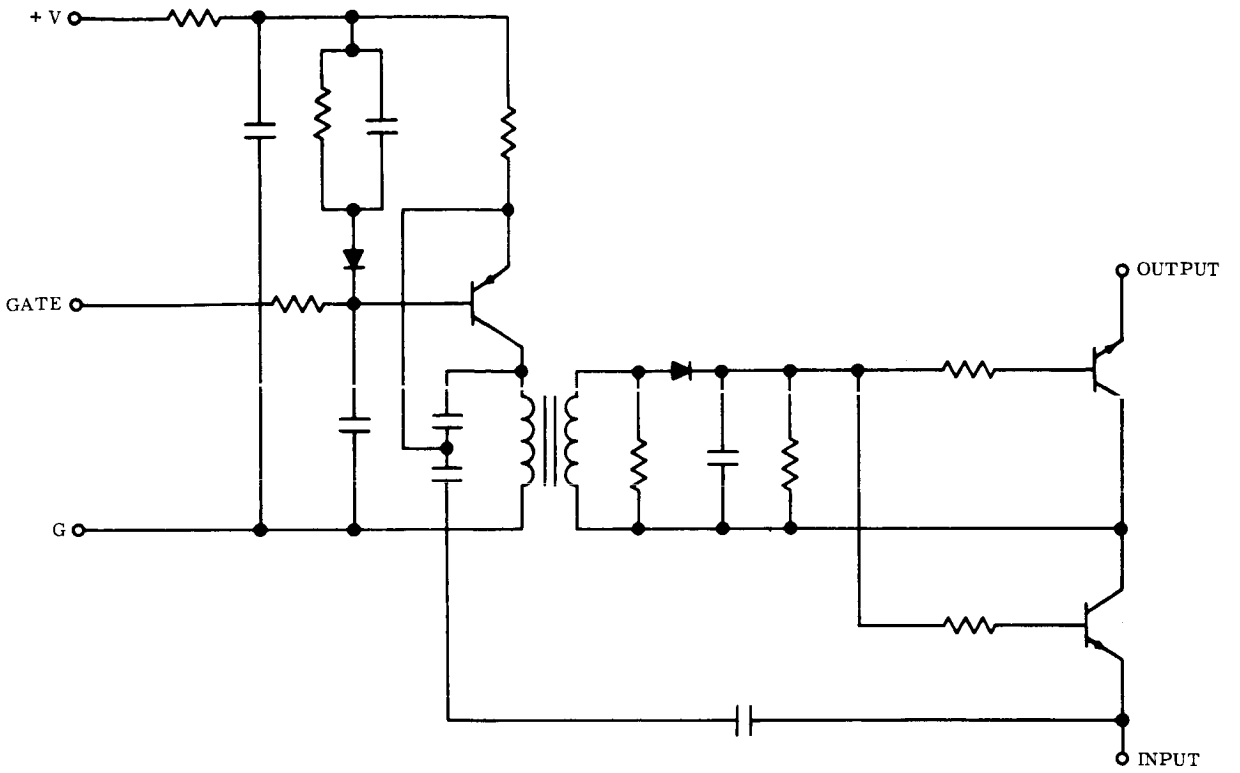

Figure 6-1. Mariner C Switch

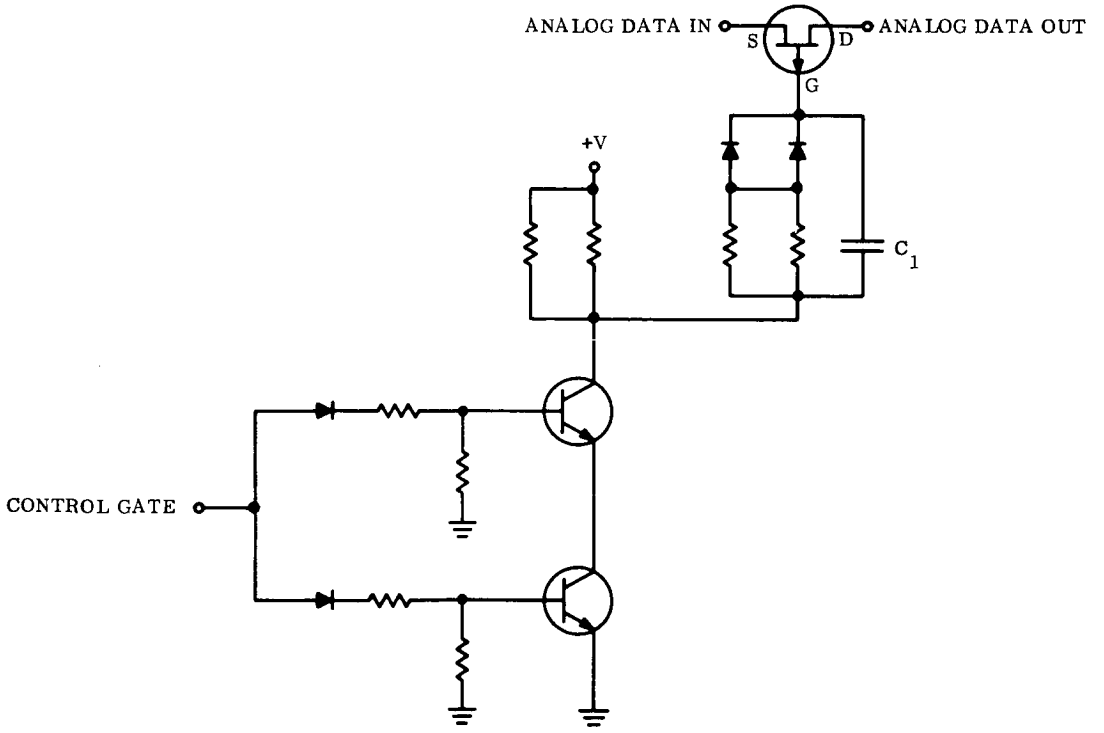

Figure 6-2. Redundant Driver FET Switch

The inverter drive for the FET is made redundant to reduce the probability of failure of this circuitry such that the +V could be removed from the FET when it should be off. Failure of the switch in a shorted mode would cause failure of all measurements in parallel with the failed switch.

6.7 TRADE OFFS AND COMPARISON OF DESIGN

6.7.1 ANALYSIS RESULTS

The operating and reliability characteristics of the Mariner C and the junction FET switches are shown in Table 6-2.

Table 6-2. Analysis Results

Function		Switch
	Mariner C	Junction FET
Probability of Failure switch * failed short *	 0.008 0.0005	 0.005 0.000007
Leakage	≤ 10 na	≤ 10 na
Offset Voltage	< 100 microvolts	0
Isolation		
Size	0.50 in.^{3}	0.40 v in.^{3} (estimated)
Weight	15 grams	10 grams
Power	≤ 30 mw	≤ 10 mw
Saturation Resistance	< 200 ohms	< 200 ohms
Turn on Time	≥ 100 microseconds ≤ 400 microseconds	≥ 10 microseconds
Turn off Time	≤ 70 microseconds	≤ 10 microseconds

*Probabilities are based on part history for the Mariner C switch. Probabilities are based on limited data and projected failure rates for the FET. The device is manufactured using established techniques so it is felt that the numbers are realistic.

6.7.2 TRADE OFF FACTORS

The trade-off factor are reliability, size, weight, and power consumption. In all cases the junction FET switch appears slightly better. The two most significant factors are power consumption (on power in both cases) and probability of failing short.

The switching time for the Mariner C switch maintains an advantage over the FET switch. As commutation through a deck occurs all switches are definitely off before another switch can be turned on. This is by virtue of the long turn-on time with respect to the turn-off time. In the case of the FET switch where both turn-on and turn-off are specified as 10 microseconds, some cross talk could occur between switches within one deck. It is not felt that this will be harmful because of the short time duration of the cross talk and the long time delay before digitizing occurs.

6.8 SELECTION OF PREFERRED DESIGN

Based on present information it is proposed that the junction FET switch be used as the commutation switch in the Voyager system. This recommendation is based on the smaller size, lower power consumption, and projected higher reliability shown for the unit. Use of the FET switch allows built in redundancy with a lower parts count per switch and the elimination of an oscillator and transformer. This last consideration should be helpful on any RFI or magnetic specifications to be met.

6.9 HIGH AND LOW LEVEL SWITCH CONSIDERATION

The switch consideration discussed above has placed a lot of emphasis on utilization of the same switch for low and high level applications. Either of the two switches analyzed can be used in both cases. This presents several advantages; channel assignments need not be firm as early in the design phase since the same switch would be used in all channels; the overall accuracy of the system would be improved since a high level switch implies higher offset voltage, and this results in switch standardiaztion and thus facilitates testing. However, in the more detailed evaluation performed in Phase 1B, a good high level switch (possibly an integrated circuit analog switch) may be found which if used, would result in considerable savings in size, weight, and power.

7.0 ANALOG TO DIGITAL CONVERTER

7.1 SCOPE

To present the various ADC's considered and recommend a type for use in the Voyager data encoder.

7.2 FUNCTIONAL OBJECTIVE

The ADC will be required to convert a 0 to 3.2 V analog voltage to a 7 bit digital word. The ADC will have parallel readout on the arrival of the programmer dump pulse. The frequency available to drive the ADC is 153.6 kc.

7.3 APPROACHES

Little is known at the present time about the characteristics of the analog signals to be converted by the ADC. One important characteristic of these signals which influences the type of ADC to be chosen is their time rate of change.

If conversion were done either at a low rate such as at the bit sync rate (variable from 4 bps to 8K bits/sec) or some rate derived from bit sync, error could be introduced into the digitized word due to the time variance of the input signal. The difficulty of prediction of the error would be compounded by the fact that it would be different for each bit rate from which the digitizing clock would be derived.

The error anticipated from the time variance of the input signal can be minimized by making the actual digitizing time as short as possible. The prediction of the error can be simplified by using a constant digitizing time for all bit rates.

The various methods of analog to digital conversion considered are listed with a brief discussion below. Figure 7-1 is a block diagram of the ADC's considered.

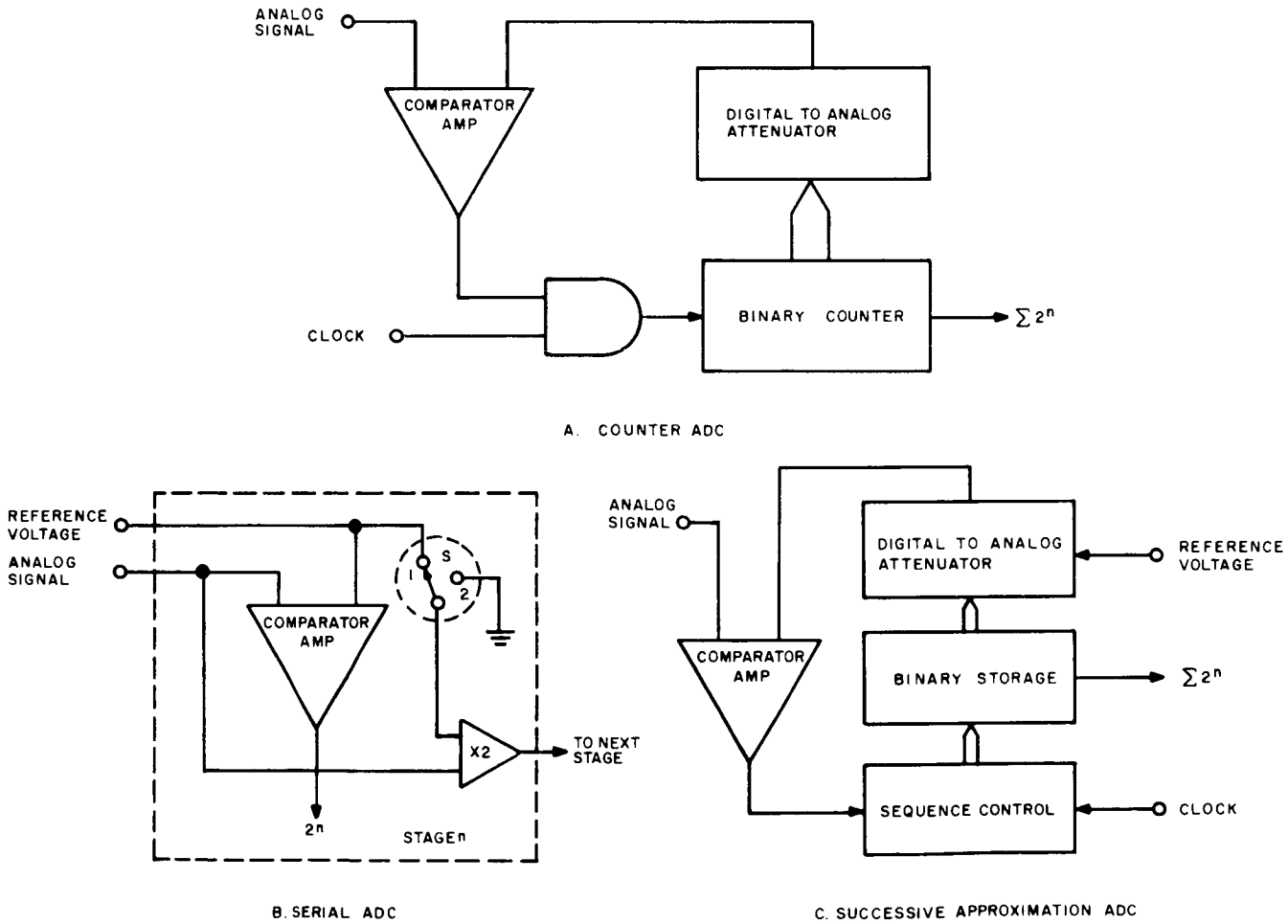

Figure 7-1. ADC Block Diagram

7.3.1 COUNTER ADC

The attenuator ratios are selected to give an ever increasing voltage output from the D to A attenuator by the binary counter. When the comparator senses that the attenuator output voltage is greater than the analog input the binary counter clock input is stopped and the counter contains the digitized analog input. This scheme requires as much as 2^n-1 counts to complete digitizing of a word.

7.3.2 SERIAL ADC

The analog input to any stage is compared to the reference voltage. If the analog input if greater than the reference voltage the comparator output goes to a one level and causes switch S to go to position 1. The difference between the reference voltage and the analog voltage is then multiplied x 2 and applied to the next stage. If the analog voltage is less than the reference voltage the switch is in position 2 and the analog voltage is multiplied by 2 directly. Binary weighting is obtained through the use of the times 2 amplifier and the switch S. Digitizing time is dependent on the bandwidth of the amplifiers and would run less than 20 microseconds.

7.3.3 SUCCESSIVE APPROXIMATION ADC

The analog voltage and the D to A attenuator output voltage are applied to a comparator. The comparator output is used by the sequence control circuitry to determine if any particular stage of the binary storage register is to be reset. The sequence control circuitry presets the binary storage register to all zeros at the beginning of a digitizing cycle and then sequentially sets the stage from the N bit to the 0 bit, switching the D to A attenuator stages from 0 volts to the reference voltage. If when a particular stage is switched to the one level the D to A voltage is less than the analog input the particular stage is not reset by the sequence control circuits. If the D to A voltage is greater than the analog input it is known that the digital weighting of the particular bit is too great and the stages is reset to 0. The scheme requires n counts of the clock source to complete digitizing of one word. A serial logarithmic ADC was also considered but was disregarded because of the high power consumption and additional circuit complexity inherent in the device.

7.4 SELECTION OF THE PREFERRED DESIGN

The counter and the serial ADC's were eliminated for the reasons given below.

a. Counter ADC - If a counter type ADC is used the digitizing time becomes dependent upon the level of the input analog signal. The maximum digitizing time 2^n-1 counts of the digitizing clock (153.6 kc) extends the digitizing time allowed for the ADC beyond that available at the maximum bit rate of 8.533 kc.

b. Serial ADC - Power consumption is too great and initial set up is extremely tedious.

c. Successive Approximation - The complexity of a successive approximation ADC is only slightly greater than that of a counter type. The added complexity comes in the sequence control circuitry. It is felt that the added complexity will be more than outweighed by the speed and constant digitizing advantages of this ADC.

The successive approximation ADC is recommended for use. This ADC has moderate circuit complexity, low power consumption when compared to the serial ADC, good accuracy, and has sufficiently high speed and accuracy to meet the requirements of the Voyager system. Error prediction is a simpler function when using this type of ADC. The successive approximation ADC will use the 153.6 KC clock as a digitizing clock source and will take approximately 50 microseconds to complete a digitizing cycle. Reference voltage for the ladder attenuator will be + 3.200 volts for a 25 millivolt per bit resolution.

8.0 SIGNAL CONDITIONING

8.1 SCOPE

This section will discuss different techniques of analog signal conditioning and recommend an approach for the Voyager data encoder.

8.2 FUNCTIONAL OBJECTIVE

Three types of analog signals will be accepted by the data encoder; 0 to 3.2 volts, ±1.6 volts, and 0 to 100 millivolts. In addition temperature measurements must be converted into voltages for transmission as data. All analog signals must be conditioned to a standard 0 to 3.2 volts for digitizing in the ADC. The 0 to 3.2 volt signals need no conditioning and these are taken directly from the commutator to the ADC.

The 0 to 100 millivolt signals are amplified by a gain of 32 amplifier.

The ± 1.6 volt signals are bucked by a series 1.6 volt bucking supply.

The basic consideration for the selection of the signal conditioning circuits is the accuracy that is required from the system. This is ± 3 percent for high level signals and ± 5 percent for low level temperature and voltage measurements. This is the minimum worst case specification that the Voyager equipment will be required to meet. Figure 8-1 shows the circuits in the signal flow path which will contribute to the accuracy of the system. The constant current source, low level amplifier, bucking supplies, and ADC circuits will be designed in Phase 1B. Completion of this design will allow a complete error analysis to be performed. Circuit improvements as a result of Mariner experience will insure that accuracy specifications can be met.

The following sections will discuss the methods considered to date for temperature measurement mechanization.

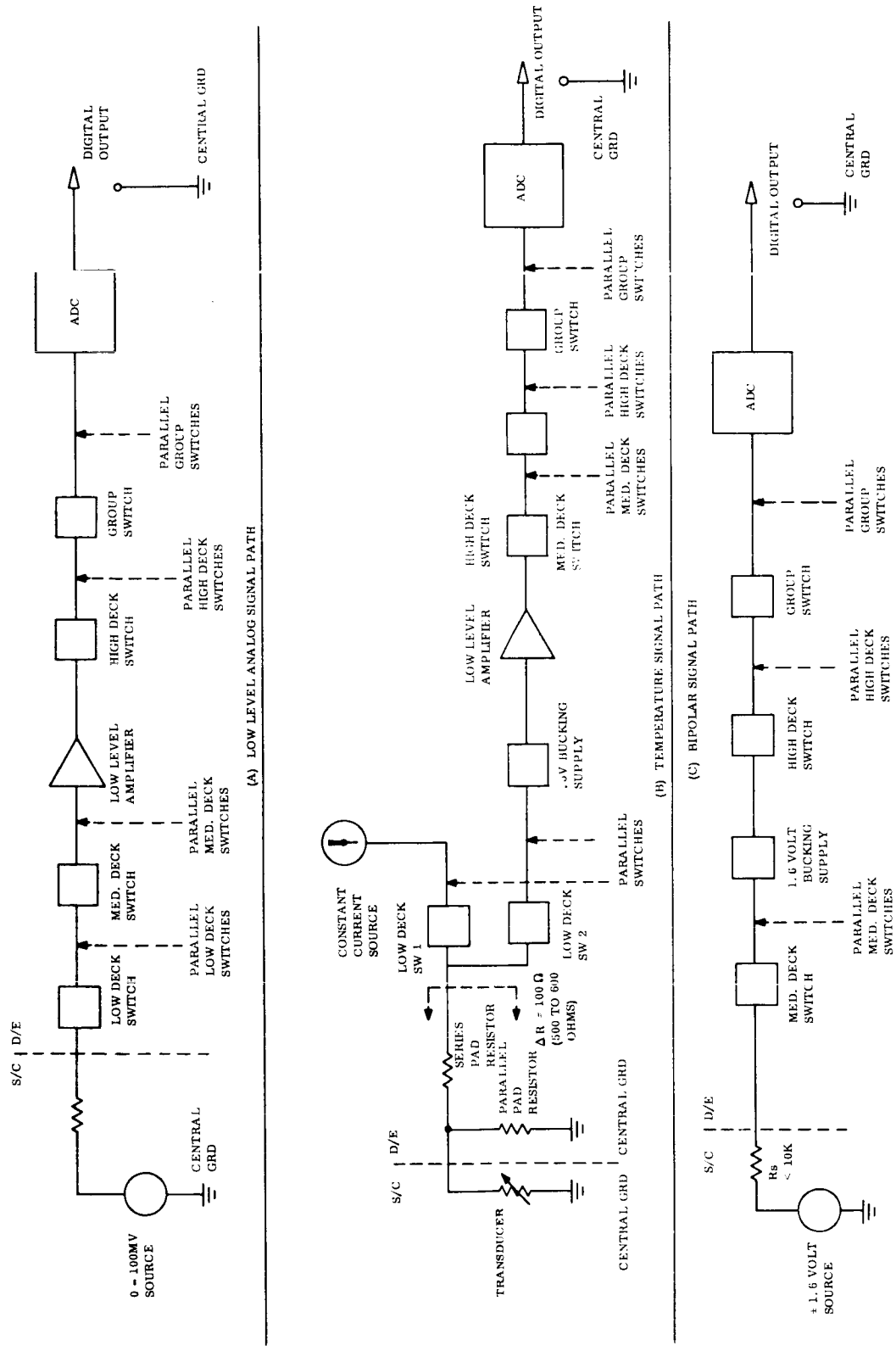

Figure 8-1. Signal Path

8.3 APPROACHES

8.3.1 VOLTAGE DIVIDER METHOD

Figure 8-2 is a diagram of the circuitry required for the voltage divider technique. Rt represents the temperature transducer resistance which varies with temperature. Several variations of the basic voltage divider method are available but are all the same basic circuit.

8.3.2 CONSTANT CURRENT METHOD

The constant current method is shown in Figure 8-3. The temperature transducers are excited one at a time by a constant current generator and the voltage dropped across the transducer resistance is sampled by a second switch, amplified and transmitted to the ADC.

8.4 SELECTION OF PREFERRED DESIGN

The voltage divider method requires less components than the constant current method, but the power drain by this type of circuit is fairly high. Approximately 125 temperature transducers will be required on the Voyager spacecraft, and with the voltage divider method, current would be flowing through the transducers at all times.

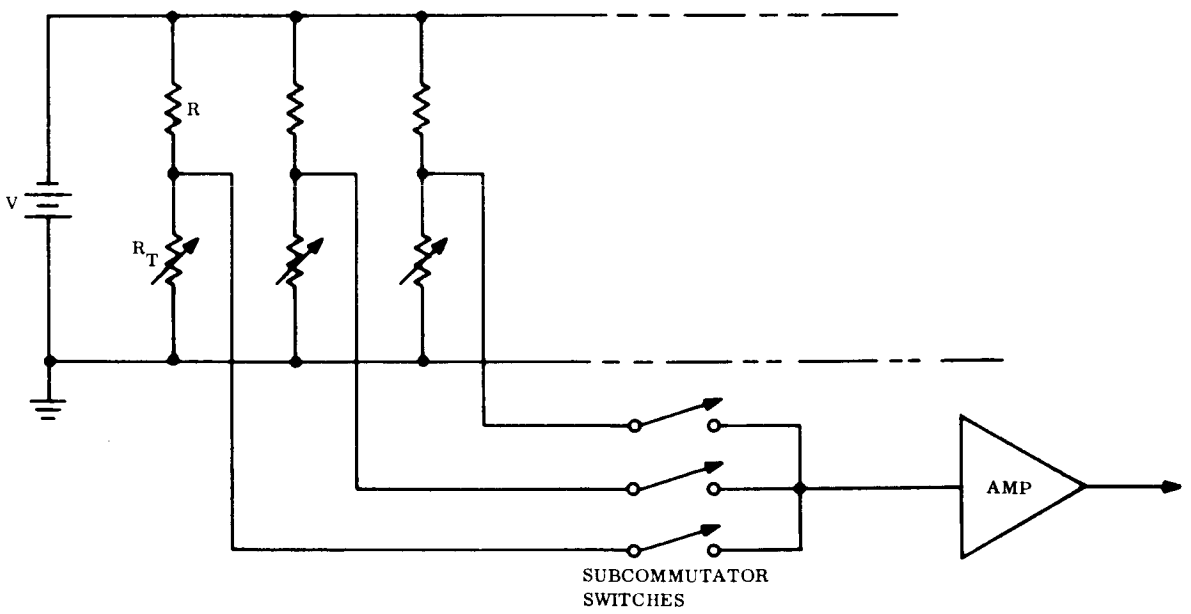

Figure 8-2. Voltage Divider Circuitry

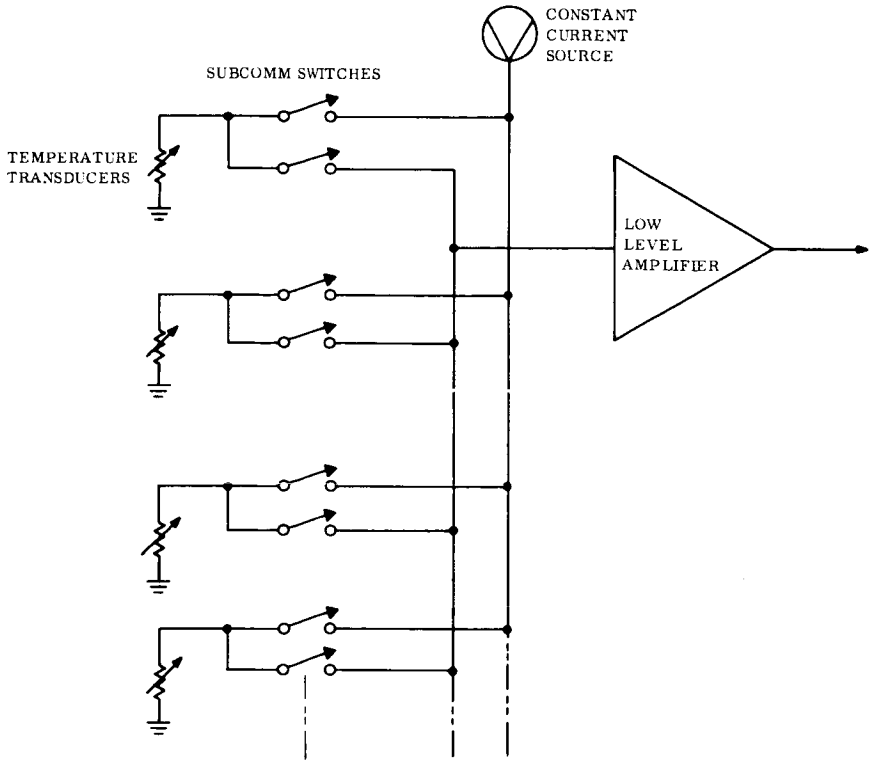

Figure 8-3. Constant Current Method

The preferred design is the constant current method of converting temperature measurement into voltage.

The constant current method is the most accurate method considered. No nonlinearity is introduced in the circuit since the current through the transducer is constant and the power drain is small since only one transducer is excited at a time.

9.0 FORMAT PROGRAMMER

9.1 SCOPE

This section covers the format programmer. Several techniques are discussed and one is recommended for the Voyager data encoder.

9.2 FUNCTIONAL OBJECTIVE

The format programmer generates the timing signals required to obtain the real time data minor frame format with a commutator arrangement such as selected in section 2.0. The real time data format consist of multiplexing engineering data, non-scan science data, approach guidance data, and capsule data (umbilical and relay).

9.3 APPROACHES

9.3.1 SINGLE FIXED FORMAT PROGRAMMER

Figure 9-1 is a logic diagram of a single fixed format real time data programmer. This programmer controls the formatting of all real time data. Flip-flops D through H are connected as a length 32 synchronous counter which counts the word clock input starting with the preset condition and counting to the all zero condition. This counter controls the number of words to be read into the format from the selected real time data source and generates the fast deck address for the engineering commutator. Flip-flops A, B, and C are storage flip-flops and contain the address of the data source. This circuit assumes eight data sources; these sources and the decoding of ABC are shown below:

STATE	DATA SOURCE
ABC	
000	Eng. Comm. Groups 1 & 2 (A)
100	Eng. Comm. Groups 3 & 4 (B)
010	Eng. Comm. Groups 5 & 6 (C)
110	Eng. Comm. Groups 7 & 8 (D)
001	Non-Scan Science
101	Capsule Relay Buffer
011	Approach Guidance
111	Approach Guidance

For this initial analysis the eight groups of the engineering commutator have been reduced to four groups by combining groups 1 and 2, 3 and 4, 5 and 6 and 7 and 8.

The control register contains the data source sequencing instructions. The register outputs, when decoded, indicate which of stages A through H are to be reset. The length of the register is determined by the number of data sources and the number of words to be read into the format from each data source. To aid in the operational discussion, the example format shown in Table 9-1 is presented. The seven bit register has eight states. Each advance in state occurs on receipt of an advance clock pulse $\overline{D} \cdot \overline{E} \cdot \overline{F} \cdot \overline{G} \cdot \overline{H}$)(Dump) i.e., when the count in the D to H stages reaches all zeroes. For the example format, stages A through H are reset to the 0 0 0 0 1 1 1 1 condition. This selects group A of the engineering commutator and starts the synchronous counter at count 15. Each clock pulse then decreases the count by one giving a total of 16 words from group A of the commutator. When the all zero state and the dump pulse are true, the synchronous counter is set to the all ones condition and the storage register is advanced to state 2. Stages A through H are advanced to the 1 0 0 0 1 1 1 1 state which selects group B of the engineering commutator and starts the counter at

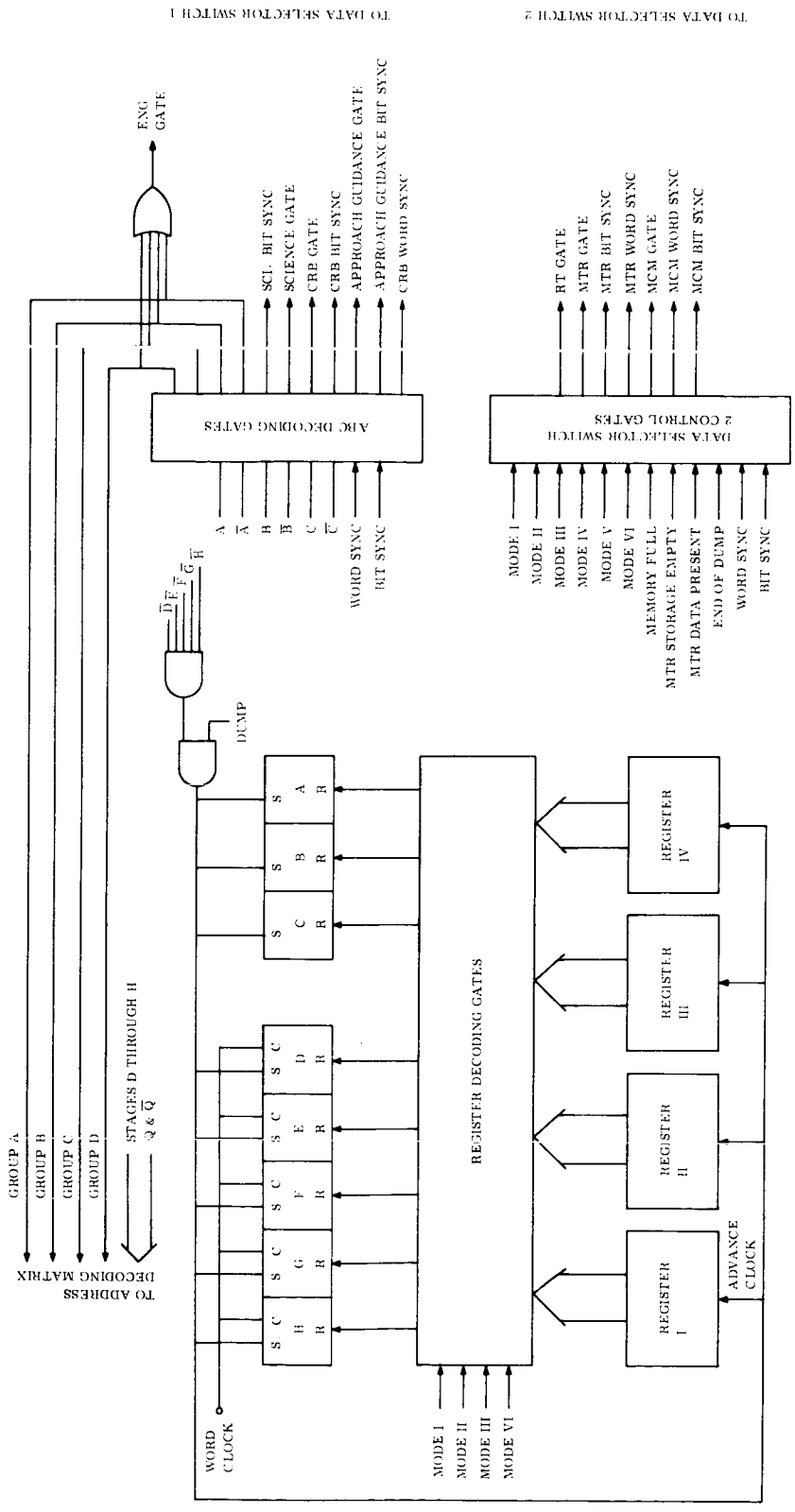

Figure 9-1. Single Fixed Format Programmer

Table 9-1 Single Fixed Format

	Register State								Data Source	Number of Words
	Source			No. of Channels						
	A	B	C	D	E	F	G	H		
1	0	0	0	0	1	1	1	1	Eng. Comm. Groups 1 & 2 (A)	16
2	1	0	0	0	1	1	1	1	Eng. Comm. Groups 3 & 4 (B)	16
3	0	1	0	0	1	1	1	1	Eng. Comm. Groups 5 & 6 (C)	16
4	1	1	0	0	1	1	1	1	Eng. Comm. Groups 7 & 8 (D)	16
5	0	0	1	1	1	1	1	1	Non-Scan Science	32
6	1	0	1	0	1	1	0	1	Capsule Relay Buffer	14
7	0	1	1	1	0	1	1	0	Approach Guidance	23
8	1	1	1	0	1	1	1	0	Approach Guidance	15
										148 words/frame

count 15 giving a total of 16 words of group B. This process continues until the format is complete.

9.3.2 MULTIPLE FIXED FORMAT PROGRAMMER

The addition of one control register per format desired to the fixed format programmer of Figure 9-1 and the command capability to select any one of the stored formats would result in a programmer with multiple format capability. This would allow selection of the real time data format most pertinent to any particular mission phase. The engineering commutator groups could be selected in any predetermined order (with the groups not pertinent to the particular phase left out) and multiplexed with any of the other data sources. The maximum number of register stages added per additional format would be one stage per data source, assuming a maximum of 32 words per source per minor frame. However, since the advantage gained with multiple formats is the capability of addressing selected data sources the addition of 4 flip-flops per additional format will be used as an average.

9.3.3 PROGRAMMABLE FORMAT CONTROL

Figure 9-2 is a simplified logic diagram of the format programmer with the control registers replaced with a programmable 64 bit memory. The memory contains one 8 bit word per data source. The program illustrated is the fixed format program discussed in paragraph 9.3.1. The memory would contain the necessary logic to short count the memory such that its effective word length equals the number of data sources

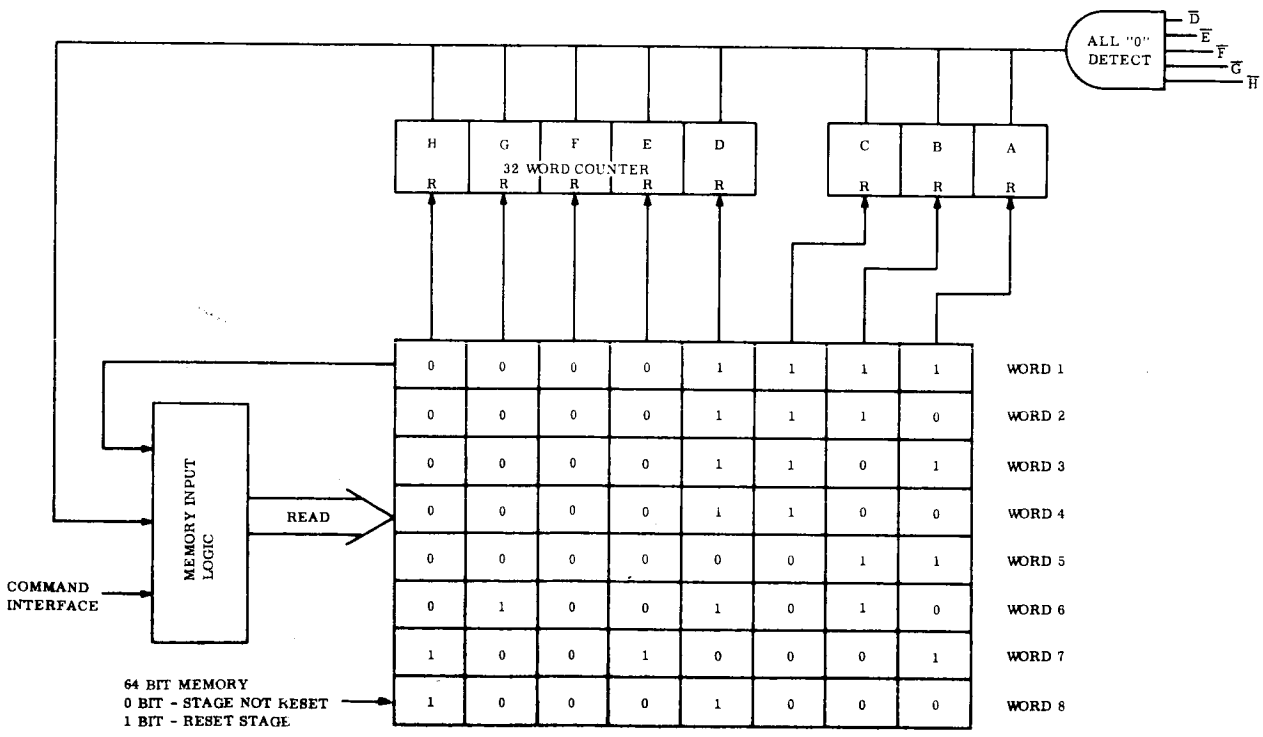

Figure 9-2. Programmable Format Control

in the format. This approach has many very desirable characteristics. 64 bits of memory stores the information necessary to sequence the groups of the engineering commutator in any order and controls all real time data formatting. Refer to paragraph 5.3.3 under Flexibility by Programmable Memory. This scheme provides for many possible sampling rates and the selection or deletion of many data sources, as desired.

The most reliable system using the programmable memory would result if this approach were used in conjunction with the multiple fixed format approach. The known formats for each mission phase would be stored as in paragraph 9.3.2 and the memory used for in flight changes.

9.4 SELECTION CRITERIA

Each of the three approaches are further analyzed and the following factors evaluated:

a. Reliability

b. Size

c. Weight

d. Power

e. Flexibility

In all cases the only difference in the approaches is the format storage logic. Therefore, only the format storage logic will be considered in the following section. An integrated circuit failure rate of .005 percent per thousand hours will be used for the reliability comparison. The size and weight estimates assume an integrated circuit weight density of 300 networks per pound and a volume density of 10 networks per cubic inch.

9.5 ANALYSIS DESCRIPTION

9.5.1 SINGLE FIXED FORMAT PROGRAMMER

This is the least flexible of the approaches. Only one real time data format would be available. Size, weight, power, and reliability, and flexibility for this approach are given in Table 9-2.

9.5.2 MULTIPLE FIXED FORMAT PROGRAMMER

This approach has medium flexibility. Calculation results for size, weight, power, and reliability for this approach are given in Table 9-2 with 2, 3, 4, and 5 formats. Only the storage logic was considered in the calculation.

Table 9-2. Results of Size, Weight, Power and Reliability Calculations

Approach	Size in^3	Weight lbs	Power mw	Flexibility	Mission Failure Rate (9 months)
Fixed Format Programmer	0.7	0.02	14	None	0.0023
Multiple Format Programmer					
(2)	1.1	0.035	22		0.0036
(3)	1.5	0.05	30	Medium	0.0049
(4)	1.9	0.065	38		0.0062
(5)	2.3	0.08	46		0.0074
Programmable Programmer	14	0.5	425	High	0.045

9.5.3 PROGRAMMABLE FORMAT CONTROL

Figure 9-3 shows the memory used for calculation of size, weight, power, and reliability. The results of these calculations are shown in Table 9-2. This is the most flexible of the methods considered.

9.6 SELECTION OF PREFERRED DESIGN

The programmable approach allows the highest degree of flexibility but the mission required flexibility, as it is presently understood, does not warrant the added size, weight, and power. As can be seen in Table 9-2 the cost in terms of size, weight, power and reliability for multiple fixed formats is very nominal. The degraded reliability would be higher for multiple formats since a failure would result in maximum loss of one format. The loss of one format however does not imply loss of the most important channels since these channels would be contained in all formats. The preferred design is therefore the multiple fixed format approach.

10.0 POWER SUPPLIES

10.1 SCOPE

To recommend a type of power supply to be used for the Voyager data encoder.

10.2 FUNCTIONAL OBJECTIVE

To convert the regulated primary power bus 100 v pp, 2400 cps square wave to a form usable by the data encoder. The data encoder requires the voltages listed below. All supplies will be ground isolated from the primary bus.

+3.5v	5 percent, for use by logic circuits
+3.2v	0.1 percent, for use as the ADC reference
±20v	5 percent, for use by analog circuitry.

The presently projected power level required is 7.5 watts usable. This will require no more than 11 watts of primary bus power.

10.3 APPROACHES

To gain the voltage required for system operation it will require an ac to dc converter. The input voltage will be stepped down through a transformer. The several voltages required will be obtained from secondary windings where the ac will be rectified and regulated as necessary to obtain the required voltage supplies. The rectifiers used will be either bridge or full wave. The choice of which to use will be made during the design phase and will be determined by two factors: which is most efficient and which

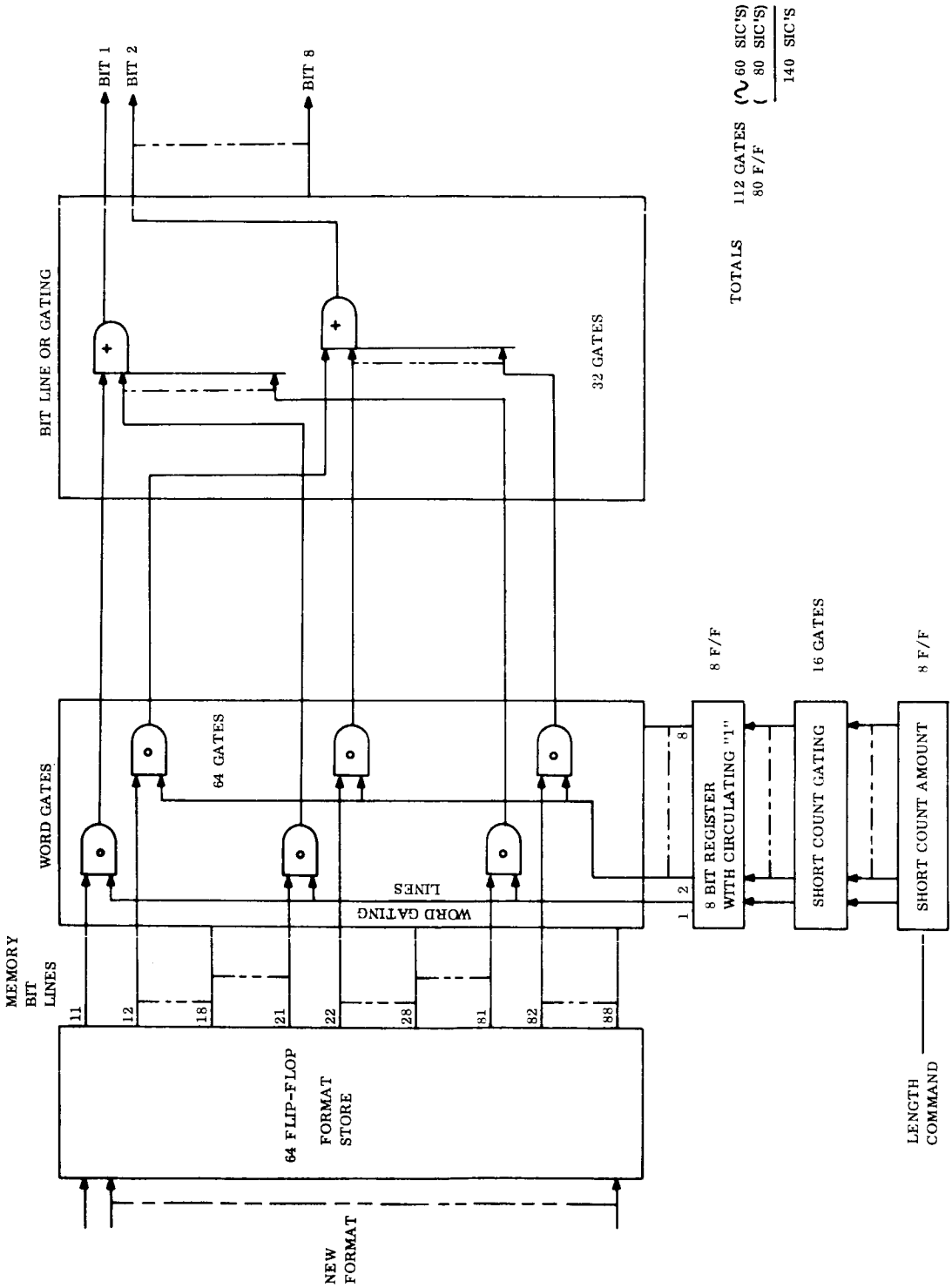

Figure 9-3. Semiconductor Format Store with Short Count Control

gives the best utilization of the transformer. There are three types of regulators which will be considered. They are listed with a brief description below. See Figure 10-1.

10.3.1 SERIES REGULATION

A variable impedance element is placed in series with the supply voltage and is varied to maintain a constant supply output voltage.

10.3.2 PARALLEL REGULATION

A fixed impedance is placed in series with the supply voltage and a parallel variable impedance is placed across the supply output. As the input or output voltage varies, the parallel impedance varies in magnitude to change the voltage divider action and maintain a fixed voltage.

10.3.3 SWITCHING MODE REGULATION

This is a type of regulator from which high efficiency can be obtained if the output voltage is equal to 1/2 the input voltage. It consists of a series switch and inductor. The switch on time is controlled by the output voltage. The lower the output voltage the longer the switch is on and vice versa. This is done by using a sensing element to control the period of an astable multivibrator which controls the series switch. The series switch is run in a saturated mode so the power loss is reduced from that of either a series or parallel. During the off period time, energy stored in the series inductor is supplied to the output to maintain the power output voltage.

10.4 SELECTION OF PREFERRED DESIGN

The ±20 volt supplies will be used to power the ADC comparator, the low level amplifiers, and the constant current generators. Circuits can be designed for these applications which will allow ±5 percent variations in the supply voltages and stay within the accuracy requirements of the system. The ±5 percent variation in the ±20 volt supplies can be met with no additional regulation other than the specified ±2 percent primary power input regulation. The 3.5 volt logic supply will also require no additional regulation. The 3.2 volt ADC reference supply will definitely require regulation to minimize ADC error. In the detailed evaluation performed in Phase 1B, it may be concluded that regulators should be used on all D/E voltages. An unregulated supply would have no protection against shorts in the output, a common mode of failure during subsystem testing. Using regulators short circuit protection could easily be built in. The power dissipation of the 3.2v supply is small in comparison with that required for the +3.5v supply. This is indicative that the power dissipation in these regulators will be small in comparison with total power and thus the type regulator selected should have only a small effect on the total power supply efficiency. For this reason the switching mode regulator will not be considered. The added circuit complexity is not warranted. The parallel regulator has several disadvantages when compared directly with the series regulator for the same application. First the supply is less efficient

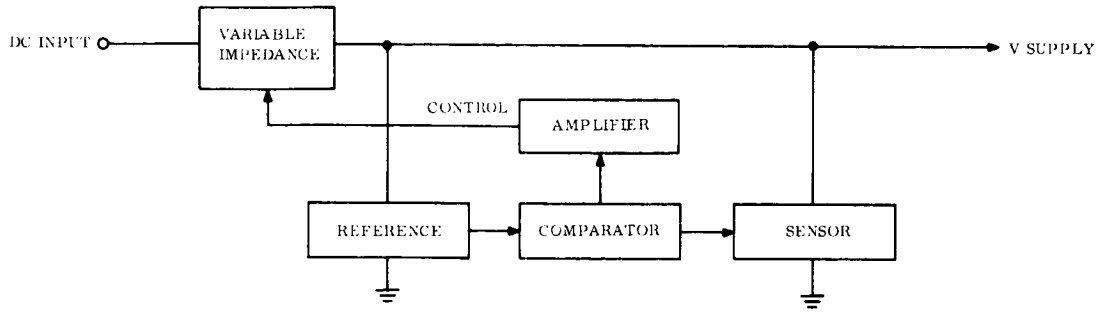

SERIES REGULATOR

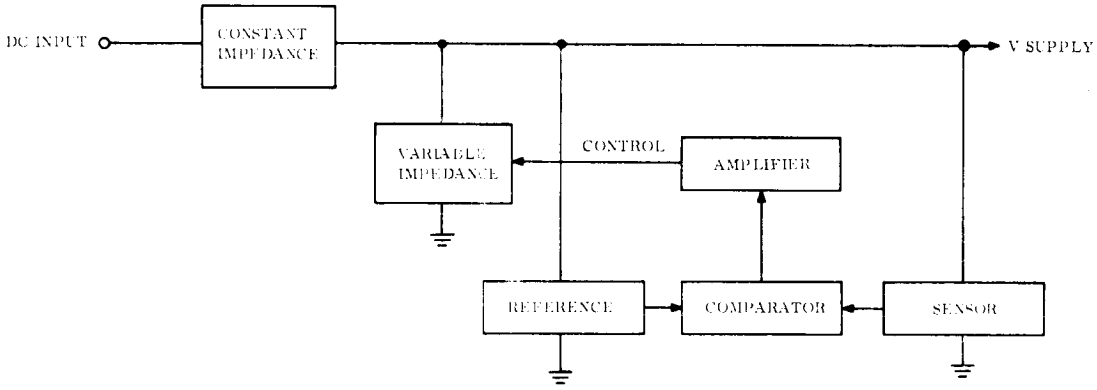

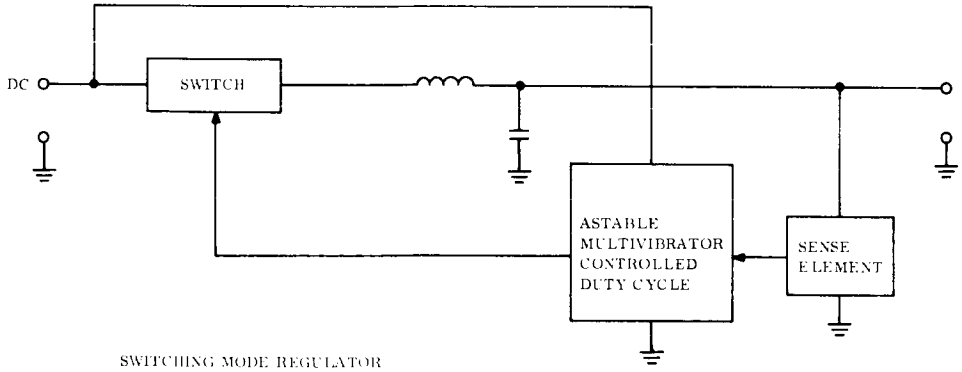

SWITCHING MODE REGULATOR

Figure 10-1. D.C. Regulators

because of the power dissipation required in the parallel element. The power transistor is required to meet more stringent requirements because it has the full supply voltage across it. If through some systems failure, such as a loose connector, the parallel regulator is required to operate under no load conditions the full load power must be dissipated in the parallel transistor to maintain the regulated output voltage. This could damage the regulator. In the series regulator power dissipation decreases under the same conditions. For over current conditions current limiting can be applied to both regulators.

It is recommended that the power supply for the Voyager data encoder contain a series regulator for the ADC reference supply.

11.0 SUBCARRIER MODULATION DETECTION AND SYNCHRONIZATION

11.1 SCOPE

The purpose of this section is to explain the selection process for the recommended PSK subcarrier modulation, detection and synchronization system and define its performance parameters.

11.2 FUNCTIONAL OBJECTIVES AND DESIGN CONSTRAINTS

11.2.1 SYSTEM OBJECTIVES

The main objective of the subcarrier modulation is to PSK modulate data onto the subcarrier so that data detection can be implemented at the demodulator with an average probability of bit error, $P_B = 5 \times 10^{-3}$. The system selected should operate in the most efficient manner possible while being constrained by the mission and physical implementation problems.

The type of system implementation must provide high spacecraft reliability, and at the same time be able to adapt to varying data rates (from 3 1/3 bps up to 8533 1/3 bps). It must use state-of-the-art technology that can provide unique bit, word (7 bits), and frame (multiple frame lengths with a minimum of 322 bits each) synchronization with minimum reduction in available data power.

11.2.2 FUNCTION DESCRIPTION

With the selection of PCM-PSK as the data modulation technique, a more compact list of system functions can be defined since coherent matched filter detection imposes synchronization requirements different from those imposed by other data modulation techniques. System functions are things that must be done to attain the desired objectives of the mission. The physical implementation of these functions defines the system.

The modulation and synchronization functions can be factored into 6 basic functions:

a. Signalling techniques

b. Subcarrier acquisition

c. Bit sync

d. Word sync

e. Frame sync

f. Sync multiplexing

A brief description of each of these functions will now be given.

a. Signalling – This function indicates the type of waveform which will be used for the subcarrier; either sine wave or square wave.

b. Subcarrier Acquisition – This function stems from the requirements imposed by the coherent demodulation in that the incoming subcarrier must be acquired before data detection can occur.

c. Bit Sync – In PCM communications, unique bit timing is required in order not to degrade the detection process.

d. Word Sync – After bit synchronization is obtained, the sectionaling of the incoming data bits into words is a necessary requirement.

e. Frame Sync – When numerous sources of information are to be transmitted, frame sync must be provided to identify the source from which the data word originated.

f. Sync Multiplexing – The synchronization information for bit, word, and frame sync must be inserted into the transmitted signal. This insertion will be defined as the Sync Multiplexing function.

11.2.3 IMPLEMENTATION OF FUNCTIONS

For each function necessary to perform a given task, there are usually numerous ways in which the function can be physically implemented into a system. Given below is a list of the functions and some of the most likely ways they could be implemented to comply with the subcarrier objectives and constraints:

Signalling:	(1) Sine wave (2) Square wave
Subcarrier acquisition:	(1) From data channel (2) From a separate channel
Bit sync:	(1) Zero crossings (2) A count down from subcarrier (3) PN code
Word sync:	(1) From a known bit sequence (2) PN code (3) Count down from acquired frame sync
Frame sync:	(1) PN code (2) Known data word (3) Parity check with PN code generator (Reference 1)

Sync multiplexing: (1) Double channel
(2) Single channel

If the selection of the implementation of the functions could be selected independently, there would be for these listed implementations 216 possible system configurations. Fortunately, the selections can not be made independently and the number of possible combinations is somewhat less than 216.

The dependency between implementation selection is considered in the next section where the number of possible configurations is greatly reduced. Further reduction is obtained by eliminating the obvious impractical implementations that would violate constraints imposed on the data encoder.

11.3 ALTERNATE SYSTEMS

11.3.1 POSSIBLE CONFIGURATIONS

The synthesis of the candidates for the optimum system is accomplished considering the possible implementation, and the dependency between the implementation of the previously defined functions. When a certain functional implementation is selected, its selection will sometime generate new functional needs which must be implemented. For this reason, the synthesis of the alternate systems lends itself quite well to a flow chart analysis which will allow the dependency between the functional implementation and the generation of new functional needs to be resolved.

A flow chart showing the synthesis of different system configurations is given in Figure 11-1. The circles represent the functions to be implemented and the lines flowing from the circle represent the possible implementation. (Single Channel as used in this section implies that PN code and data are represented by a two level signal modulated on to the same subcarrier. This definition does not restrict the use of an auxiliary subcarrier for clock or subcarrier acquisition purposes.)

Note that some of the functions shown in the list of legend have not been previously mentioned. These are functional needs that are generated by a previous selection of a functional implementation. For instance, if subcarrier is to be acquired from the data channel, and if bit sync is to be obtained from this subcarrier, some means must be provided to eliminate the bit timing ambiguity caused by acquiring the subcarrier from the data channel. Another example is when PN code is selected as the means by which bit sync will be acquired. This PN code selection requires that some means be provided to align the incoming and local PN codes; this alignment is called the code acquisition function.

In the flow chart, such implementation as acquiring frame sync from a PN code are ruled out due to the flexibility requirement in the data format. Furthermore, such implementation as only acquiring word sync with PN codes is also ruled out as not being a very practical use of the PN code equipment.

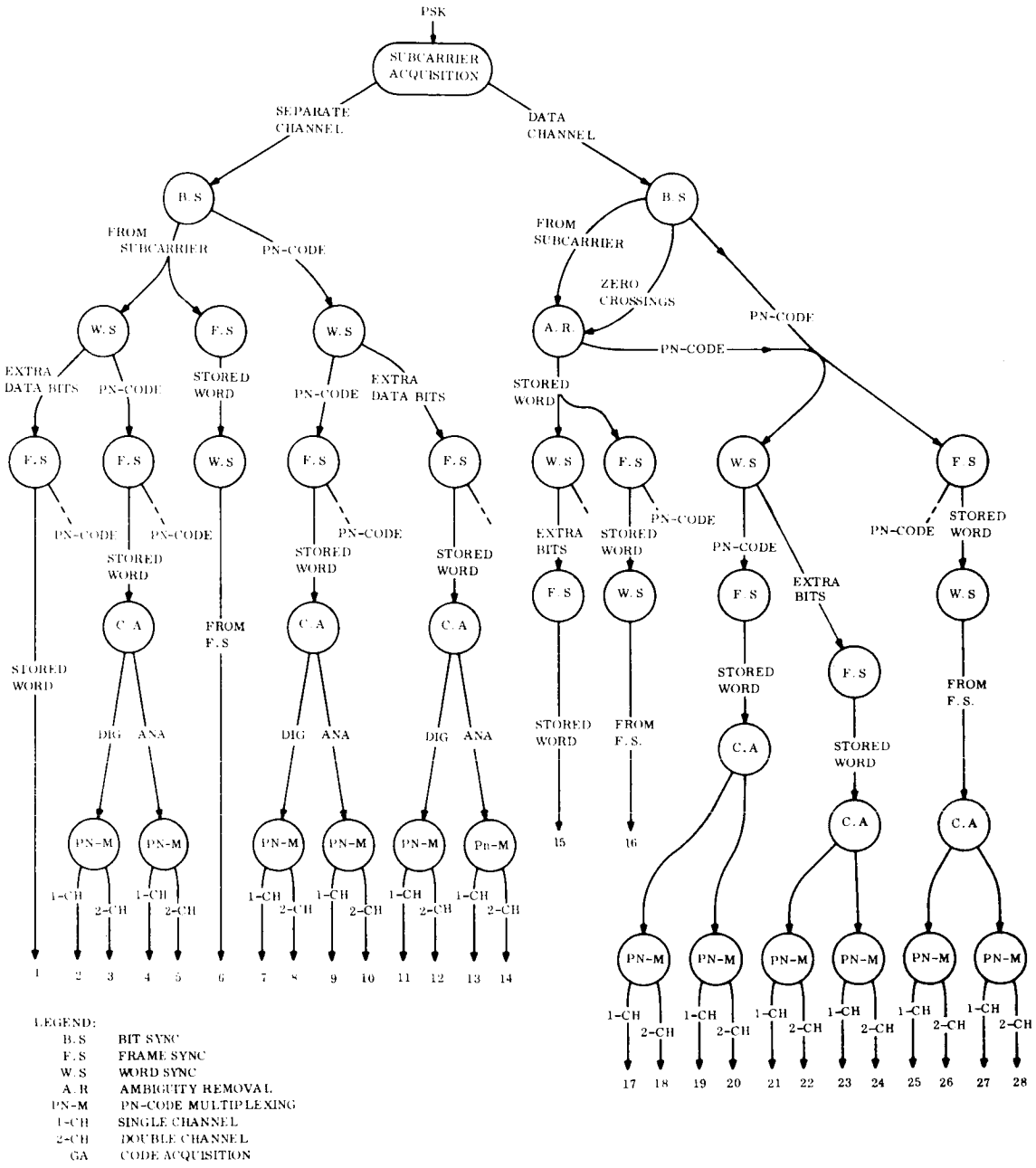

Figure 11-1. Flow Chart Showing System Synthesis

Table 11-1. Classification of Alternative Configurations

Classification	Configuration #	Reference to Typical Block Diagram
Single Channel No PN Code	15, 16	Figure 11-2, No PN Code
Single Channel with PN Code	17, 21, 25 *2, 7, 11	Figure 11-3, PN, 1-Channel Digital Code Acquisition
	19, 23, 27 3, 8, 12	EPD-139 pp 4-213, Fig. 4-106 (Reference 2) PN, 1-Channel, Analog Acq. of Code
Double Channel with PN Code	18, 22, 26 4, 9, 13	Figure 11-4, PN, 2-Channel Digital Code Acquisition (Mariner C)
	20, 24, 28 5, 10, 14	Springett pp. 110, Fig. 20 Reference 3) 2-Channel, PN, Analog Code Acquisition
Double Channel No PN Code	1, 6	Similar to EPD-139 pp. 4-232, Fig. 4-115 (Reference 2) (Relay Link)

*A circle around the configuration number means that the subcarrier is not acquired from the data channel as shown in reference typical block diagram, but is acquired instead from a separate sync channel.

11.3.2 CLASSIFICATION OF CONFIGURATIONS

The flow chart produces 28 possible configurations that are considered candidates for the optimum subcarrier modulation system. These 28 possibilities can be classified into four sets:

(1) Single Channel - Without PN Code

(2) Single Channel - With PN Code

(3) Double Channel - With PN Code

(4) Double Channel - Without PN Code

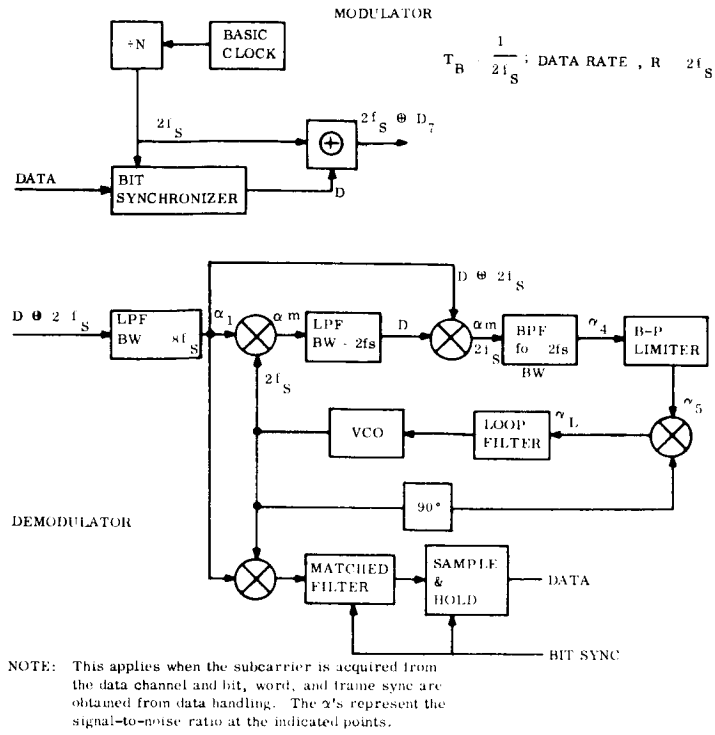

Figure 11-2. Block Diagram for Typical Subcarrier Modem

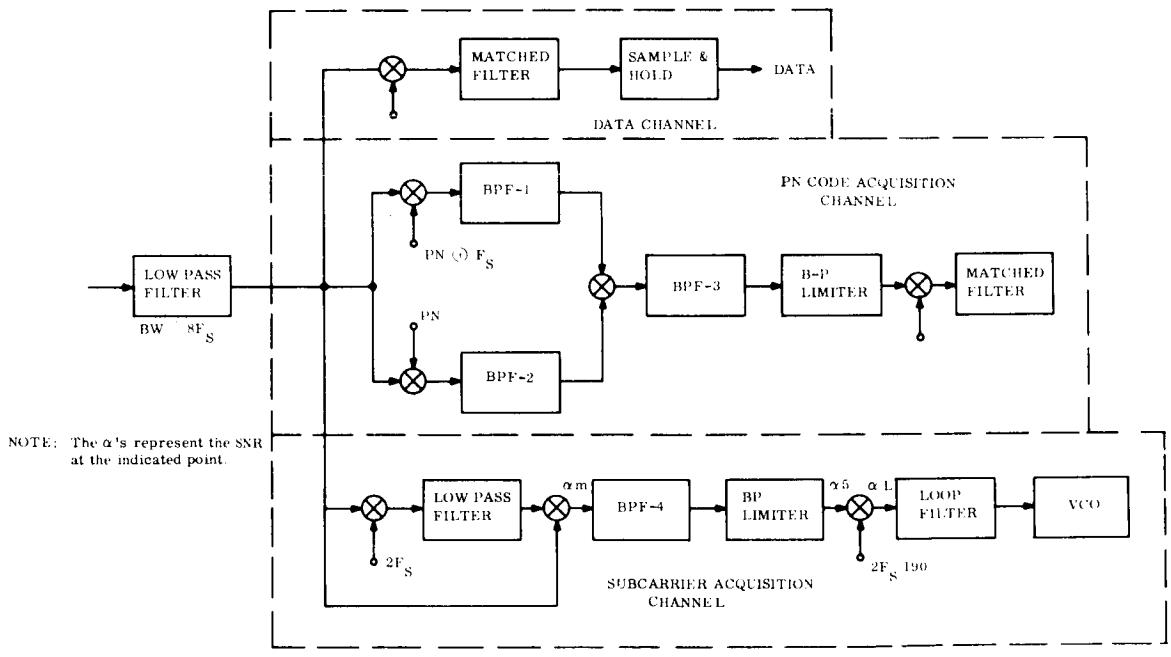

Figure 11-3. Block Diagram of Typical Single Channel Telemetry Demodulator

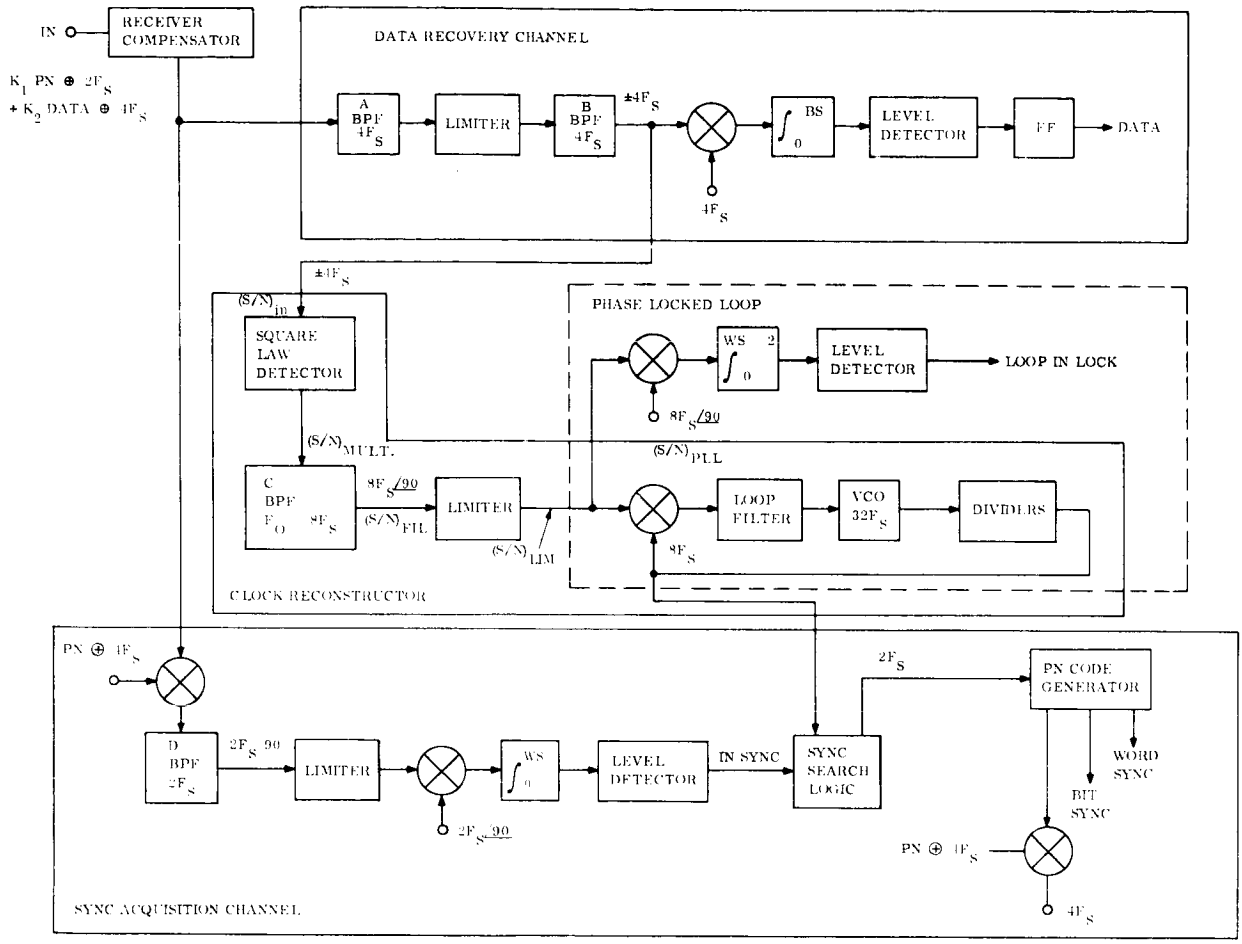

Figure 11-4. Typical Block Diagram for Two-Channel Demodulator with Digital Code Acquisition

Configurations falling under each classification are shown in Table 11-1 where reference to a typical block diagram is also given. The typical block diagrams will not show the technique employed in obtaining word, and frame sync unless the PN codes are employed since these functions are usually implemented in the data handling area.

11.4 SYSTEMS SELECTION

The approach that was employed to select the optimum system for the subcarrier modulation is shown by a flow diagram in Figure 11-5 where the names in the ovals represent the function and the lines flowing from the ovals represent the methods available for implementing the function. The primary reasons for selecting a particular implementation of a function is given in Table 11-2. A more detailed rationalization for the implementation selection is given in the following paragraphs.

11.4.1 RATIONALIZATION FOR SELECTIONS

11.4.1.1 Subcarrier – The choice in the subcarrier selection is based on the requirements of the single channel sync multiplexing method. The subcarrier frequency is $2f_s = 9R$ where R is the data rate. In Appendix I, it is shown that at 106 2/3 bps the reduction in the carrier PLL signal-to-noise ratio caused by the subcarrier interference is less than 0.0035 decibels. At the low data rate of 3 1/3 bps and using $2f_s$ as the subcarrier, the reduction in carrier PLL signal-to-noise ratio caused by subcarrier interference is approximately 0.1 decibels. ($2B_L = 12$ cps). For the low data rate system this 0.1 decibel loss in the signal-to-noise ratio of the carrier phase locked loop might be critical; and it may be necessary to increase the subcarrier to $4f_s$. Increasing the subcarrier causes an increase in the PN code acquisition time (about twice as long), but the cost in acquisition time could be worth reducing the carrier PLL interference. The potential use of $4f_s$ as the subcarrier frequency for the 3 1/3 bps system will have to be resolved in the development phase of the study.

11.4.1.2 Signalling – In Appendix II, it is shown that for the single channel approach to data modulation the square wave signalling has a small power advantage over the sine wave signalling for both the low and the high data rate systems. Furthermore, using square wave signalling in the spacecraft permits higher spacecraft reliability for the multiple data rate system since sine wave restoring filters are not necessary for each data rate. Therefore, square wave signalling is the implementation selection for the signalling function.

11.4.1.3 Subcarrier Acquisition – Adequate signal-to-noise ratio could be maintained in the channel which contains the data modulation so that a PLL could be used in this channel to acquire the subcarrier without having to supply power to a separate subcarrier channel. The increase in sync efficiency outweighed the bit timing ambiguity incurred by using the data channel acquisition instead of a separate subcarrier sync channel.

11.4.1.4 Bit Sync – When the subcarrier is acquired from the data channel, a bit timing ambiguity exists when bit sync is obtained from a count-down version of the subcarrier. Searching for known data bits was ruled out as being too time consuming

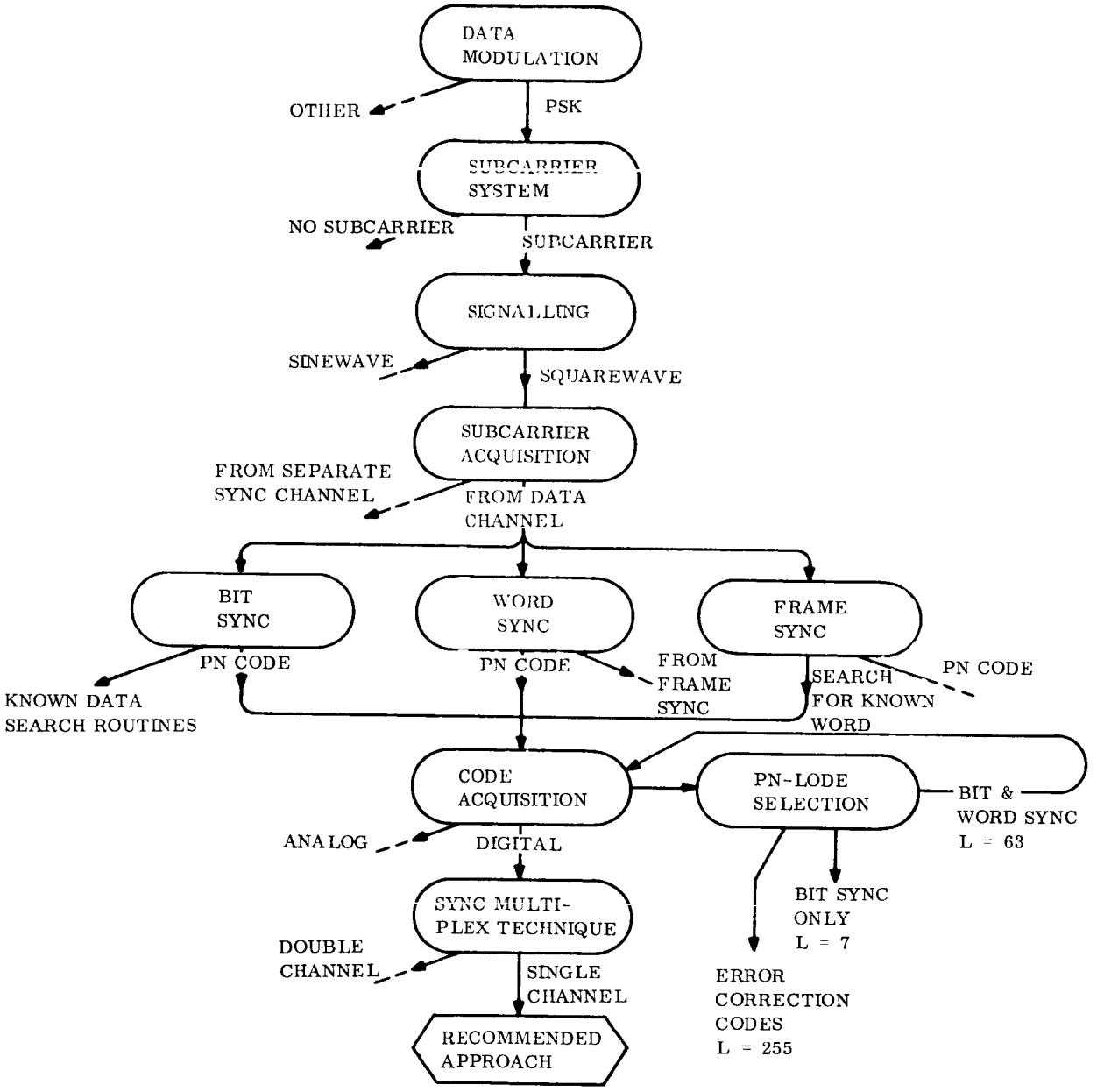

Figure 11-5. Flow Diagram of Approach Used to Select Optimum System

Table 11-2. Functions, Implementations, and Reasons for Selections

Function	Configuration Selection	Reasons
Data Modulation	PCM-PSK	1. Reliability* 2. Transmission Efficiency
Subcarrier	Subcarrier at $2f_s = 9$ R	1. Permits RF Carrier Tracking
Signalling	Square Wave	1. Modulation Efficiency 2. Reliability 3. Size and Weight
Subcarrier Acquisition	From Data Channel	1. Sync Efficiency
Bit Sync	PN Code	1. Sync Efficiency 2. Better Detection 3. Word Sync Requirement
Word Sync	PN Code	1. Enhance Frame Sync Detection
Frame Sync	Search for Known Data Word	1. Flexibility
PN Code	L = 63, 9 PN Bits/Data Bit	1. Best Fit to Data Format
Code Acquisition	Digital Search	1. Maximum Likelihood Detection 2. Simpler
Sync Multiplexing	Single Channel	1. Sync Efficiency

*Reliability Indicates Spacecraft Reliability

as well as increasing the possibilities of acquiring erroneous bit sync. The PN code technique of eliminating the bit timing ambiguity decreases this probability of acquiring an erroneous bit sync.

11.4.1.5 Word Sync – Acquiring word sync after acquiring frame sync was eliminated because errors involved in acquiring frame sync without first knowing word sync were too great. Since the word length was to remain constant at 7 bits the use of the 63-bit PN code to acquire word sync as well as bit sync was a natural selection. Correlation techniques could be used together with maximum likelihood detection to align the codes thereby decreasing the chance of erroneous word sync.

11.4.1.6 Frame Sync – PN codes could have been used to acquire frame sync, but due to varying frame length PN code techniques would not give the needed flexibility. It was found that acquiring frame sync by searching for a known data word (with word sync known) gave a probability of a false alarm error on the first pass of 0.034. (See Appendix VII). The probability of accepting erroneous data from frame sync error was reduced by first knowing word sync. Searching for a known data word is the the recommended approach to obtaining frame sync.

11.4.1.7 PN Code Acquisition – The digital search routine was selected as the best way to acquire the PN code since we had previously acquired the subcarrier from the data channel. Stepping the code along allows us to use correlation techniques with maximum likelihood detection to obtain word and bit sync.

Given below is a list of the advantages and disadvantages in using the PN code:

a. Advantages:

1. Permits easier implementation of the demodulator for the low data rate system.

2. Provides word and bit sync from maximum likelihood detection thereby reducing the probability of accepting erroneous data format.

3. No additional power is required to transmit the PN code.

4. Spacecraft reliability is not appreciably affected with the addition of the PN sequence generator, since some type of bit and word counter is needed even if PN codes are not used.

b. Disadvantages:

1. Use of the PN codes will require a larger transmitter bandwidth.

2. Use of the PN codes will cause an increase in the complexity of the subcarrier demodulator equipment, but will reduce some of the complexity of the data handling and storage requirements at the demodulator.

3. The use of the PN codes will require, under certain situations, an increase in synchronization time in that the codes must be aligned before data decoding can start.

When we are not bandwidth limited, benefits gained from using the PN code as the means to acquire bit and word sync appear to outweigh the slight disadvantages that their use incurs. For the highest data rate, R = 8533 1/3 bps, the bandwidth of the PN spectrum is 18R or 153,600 cps. In the selection of the optimum system, it is assumed that this is not a limiting bandwidth, and therefore, the PN code technique is the selection for obtaining bit and word sync.

At this point in the selection process, we have selected the following:

Function	Implementation
Subcarrier	From channel that contains the data
Bit sync	PN code
Word sync	PN code
Frame sync	Stored data word
PN Code Acquisition	Digital Search

These selections for implementating the functions have eliminated all of the competing configurations of Figure 11-1 except configurations numbers 17 and 19. These are:

Configuration #17	Single channel-PN Code-Digital Acquisition
Configuration #19	Double channel-PN Code-Digital Code Acquisition

Of these two competing systems, the single channel system (configuration number 17) was selected as the preferred design from the standpoint of efficiency and spacecraft reliability. The efficiency and reliability are given for both the high and low data rates in Table 11-3.

Modulation efficiency is defined as the percent of the total transmitter power that can be supplied to the data channel, and the sync efficiency is defined as the percent of the subcarrier power supplied to the data channel. The reliability refers to the spacecraft reliability where the "+" indicates that the single channel spacecraft implementation will be more reliable than that of the double channel configuration.

The reliability, however, is not appreciably different for either scheme: the difference being that in the double channel system a linear summer is used to combine the data and the PN signals. For the single channel system, this linear sumer is replaced with a mod 2 adder which is slightly more reliable than the linear sumer that must maintain a constant division of power between the sync and the data channel.

For the low data rate system, the single channel is the more efficient system to use, but as the data rates increase, the difference in efficiency becomes less and less.

Table 11-3. Comparison of Single and Double Channel Efficiency and Reliability

System	Modulation Efficiency %	Sync Efficiency %	Reliability
Low Data Rate			
(1) Single Channel	30	100	+
(2) Double Channel	22.2	74	-
High Data Rate			
(1) Single Channel	70	100	+
(2) Double Channel	57	81.5	-

At the higher data rates, the efficiency will be about the same when the code correlation period is many code lengths. However, the single channel system will always exhibit a better efficiency than the double channel system regardless of the data rate, since some power must always be delegated to the sync channel.

The calculations for the efficiency metrices is shown in Appendix VIII. The comparison between the double and single channel efficiency was based on equal code alignment decision errors by the following method: In the single channel system, the required E/N_0 in the data channel to maintain BEP of 5×10^{-3} is directly related to the decision errors in the code acquisition network. When the false alarm and false dismissal errors are assumed equal, the E/N_0 in the data channel will produce a certain decision error (called error probability) in the code acquisition channel. The procedure used in the efficiency comparison was to determine the required SNR in the double channel sync channel to maintain the same decision error that was obtained in the single channel system directly from the available E/N_0.

11.5 PERFORMANCE OF PREFERRED SYSTEM

In this section, the anticipated performance of the single channel preferred system will be given. The performance has been divided into a) the SNR performance, and b) the code acquisition performance. A review of the analysis leading to the performance parameters will be given in the next section. Listed below are brief definitions of the performance parameters:

a. SNR Performance

1. E/N_0 required – This is the E/N_0 required at the data detector to maintain BEP of 5×10^{-3}. It consists of the theoretical value in addition to the estimated loss terms.

2. Threshold SNR – This is the signal-to-noise ratio per 1 cps of noise bandwidth required at each data rate in order to maintain the BEP of 5×10^{-3}.

3. Sync Tracking PLL Threshold SNR – This is the input signal-to-noise ratio into the $2B_L$ bandwidth that is necessary to maintain BEP of 5×10^{-3}.

b. Sync Acquisition Performance

1. Average Time Required to Sync – This is the mean time required to align the PN codes. Two values will be given, (1) the average time to sync when no errors can be made in the decision, and (2) the average time required to sync when decision errors are present.

2. Probability of Loss of Sync – This is the probability that the PN codes will become unaligned. It will be stated for a one second time period.

Tabulation for these performance parameters are given in the following paragraphs.

11.5.1 Required E/N_0

The E/N_0 required at the data detector in order to maintain BEP of 5×10^{-3} is shown below for the two data rates:

High Data Rate System ($R \geq 106\ 2/3$ bps)

Theoretical Value	5.2 db
RMS Subcarrier Phase Jitter Loss	0.15
Predetection Filter Loss	0.32
Integrate and dump, Carrier Phase Jitter and other losses	0.23
Required E/N_0	5.9 db

Low Data Rate System ($R = 3\ 1/3$ bps)

Theoretical Value	5.2 db
RMS Subcarrier Phase Jitter Loss	0.5
Predetection Filter Loss	0.32
Integrate and dump, Carrier Phase Jitter and other losses	1.98
Required E/N_0	8.0 db

11.5.2 THRESHOLD SNR

The threshold signal-to-noise ratio in a 1 cps noise bandwidth that must be present at the demodulator data detector is given below for the different data rates

Bit Rate	$(S/N_O) = (E/N_O)\ R$
8533 1/3	45.2 db
4267 2/3	42.2
2133 1/3	39.2
533 1/3	33.2
106 2/3	26.2
3 1/3	13.2 db

11.5.3 SYNC TRACKING PLL THRESHOLD SNR

The sync tracking phase locked loop threshold signal-to-noise ratio (αL) in the threshold noise bandwidth will be

At Detector Input: α_L (R = 3 1/3 bps) = 17 db into $2B_{LO}$ = 1/4 cps

Actual In Loop: $\alpha_L \approx 15$ db

At Detector Input: α_L (R $\geq$ 106 2/3) $\geq$ 24 db into 2 B_{LO} = 1 cps

Actual In Loop: $\alpha_L \geq 21$ db

11.5.4 AVERAGE TIME REQUIRED TO SYNC

The mean time to acquire bit sync for the threshold SNR for the different data rates is

Data Rate	Average Time to Sync No Decision Errors	Average Time to Sync With Decision Errors
8533 1/3	0.258 sec	0.2582 sec
4267 2/3	0.516	0.5164
2133 1/3	1.034	1.036
533 1/3	4.13	4.134
106 2/3	20.64	20.66
3 1/3	132.30 sec	138.92 sec

The expression for the average time to sync in terms of the decision errors is given in Appendix IV.

11.5.5 PROBABILITY OF LOSS OF SYNC

The probability of loss of bit, word and frame sync for threshold SNR will be:

a. Low Data Rate, (R = 3 1/3 bps)

The probability of loss of sync during a one second interval is

$$P_1 = 3.8 \times 10^{-11} \text{ (15 db in PLL)}$$

b. High Data Rate (R $\geq$ 106 2/3 bps)

The probability of loss of sync during a one second interval is

$$P_1 < 10^{-16} \text{ (21 db in PLL)}$$

In both estimates of P_1, the random phase excursion of the clock PLL that would cause the PLL to slip a cycle was assumed to be 45°. The equations for P_1 are derived in Appendix V.

11.6 REVIEW OF PERFORMANCE ANALYSIS

This section gives a review of the analysis that was performed to a) compare the performance of the competing systems, and b) to calculate the performance of the preferred system. The review is divided into two sections; the SNR performance and the Code Acquisition. Most of the detailed analysis is carried out in the Appendices and this review is concerned mostly with summarizing the results.

11.6.1 SNR PERFORMANCE

11.6.1.2 Input Signal-to-Noise Ratio: The input SNR at the matched filter is defined as

$$(S/N)_{IN} = (E/N_o) \frac{1}{TB_1} = (E/N_o) \frac{R}{B_1}$$

where

B_1 = noise bandwidth of the input channel

T = 1/R, the bit period

R = the data rate

E/N_o = bit energy per noise density

For negligible loss between the subcarrier demodulator input and the data detector, this $(S/N)_{in}$ represents the input signal-to-noise ratio.

For the single channel system of Figure 11-3, the input noise bandwidth, B_1, is defined as $8f_s$ where the subcarrier $2f_s = 9R$; the number 9 represents the number of PN bits per data bit. Thus, $B_1 = 8f_s = 36R$, and the input signal-to-noise ratio becomes:

$$(S/N)_{in} = (E/N_o) \frac{R}{36R} = 1/36 \ (E/N_o)$$

11.6.1.2 Required (E/N_o): For PSK modulation, the probability of bit error, P_B, is given by

$$P_B = 1/2 \left[1 - \text{erf} \sqrt{(E/N_o)}\right]$$

where erf(.) is the error function. This expression for P_B represents the theoretical value which assumes an ideal matched filter and precise (exact) synchronization between the transmitter and the receiver – inferring infinite SNR in the phase locked loop. Since the telemetry must operate in a noisy environment, a finite SNR will exist in the loop, therefore, P_B, will be greater than that given by the theoretical value. For $P_B = 5 \times 10^{-3}$, this theoretical value of $E/N_o = 5.208$ db.

The increase in the probability of bit error over the theoretical value is caused by (1) the phase jitter of the acquired carrier and subcarrier, (2) the non-ideal integrate and dump circuit used as the matched filter, and (3) the predetection filter loss. When bit sync is obtained from the subcarrier, this rms phase jitter will cause errors in bit timing which will increase P_B. However, when many cycles of the subcarrier are contained within one bit period, the rms phase error in the bit timing is reduced to a point where it can generally be neglected.

Lindsey (Reference 4) has developed curves relating this probability of bit error P_B to the required E/N_o for different values of the phase locked loop signal-to-noise ratio. In his derivation, he neglected the degradation of P_B caused by the error in bit timing and only considered the effect of an rms phase error in the acquired subcarrier. In Figure 11-6, a curve is plotted using Lindsey's results that shows the relationship between the required signal-to-noise ratio, α_L, present in the phase locked loop to maintain a probability of bit error of $P_B = 5 \times 10^{-3}$, as a function of the E/N_o. Notice that to maintain $P_B = 5 \times 10^{-3}$ as E/N_o approaches the theoretical value of $E/N_o = 5.2$ db, the signal-to-noise ratio in the phase locked loop must approach infinity. However, the specified P_B can be achieved when the signal-to-noise ratio in the loop is 10 db if 6 db of E/N_o is supplied to the data detector.

Further increase in E/N_o above 10 db will not allow appreciable reduction in the required signal-to-noise ratio, α_L, of the loop. It appears that a value does exist for α_L below which the required E/N_o must increase appreciably to permit a slight decrease in α_L and still maintain $P_B = 5 \times 10^{-3}$.

Therefore, to determine the E/N_o required at the data detector to maintain a BEP of 5×10^{-3}, the E/N_o value is located on the curve of Figure 11-6 that corresponds to the signal-to-noise ratio in the phase locked loop. The curve of the required α_L versus E/N_o to maintain BEP of 5×10^{-3} has been superimposed on the set of curves that represent the calculated α_L for a given E/N_o, Figure 11-7. From this curve we see that the required E/N_o corresponding to the signal-to-noise ratio in the PLL to maintain BEP of 5×10^{-3} is, for the high data rate system

$$E/N_o = 5.2 + 0.15 = 5.35 \text{ db}$$

and for the low data rate system

$$E/N_o = 5.2 + 0.5 = 5.7 \text{ db}$$

There are other losses which must be considered when estimating the required E/N_o needed to maintain BEP of 5×10^{-3}; the integrate and dump circuit will have losses as well as the losses occurring in the predetection filter. In the preferred design the predetection filter has been selected as $8f_s$. This prefiltering of the spectrum will result in .32 db loss in the matched filter detection regardless of the data rate. In the low data rate system, it will be difficult to design as efficient filters and integrate and dump network as can be accomplished in the high data system more loss will have to be tolerated in the E/N_o estimation. These losses for both of the high and the low data rate systems have been estimated as

0.23 db for the high data rate system

and

1.98 db for the low data rate system

Therefore, the total required E/N_o for both systems are estimated as

$$E/N_o = 5.9 \text{ db (high data rate)}$$

$$E/N_o = 8.0 \text{ db (low data rate)}$$

11.6.1.3 <u>SNR Performance Equations</u>: The system equations used to calculate SNR performance for the single channel system of Figure 11-3 are given in Table 11-4.

These equations were used to calculate the set of curves (Figure 11-7) showing the relationship between the input E/N_o to the SNR in the phase locked loop, α_L, for the different data rates, and the values for the loop noise bandwidths shown in Table 11-5.

11.6.1.4 <u>Estimate of the Loop Noise Bandwidth</u>: For a first order loop, operating under noisy conditions, to have a high probability of acquiring lock at the first locked-point encountered, the loop noise bandwidth at threshold, $2B_{Lo}$, must be greater than

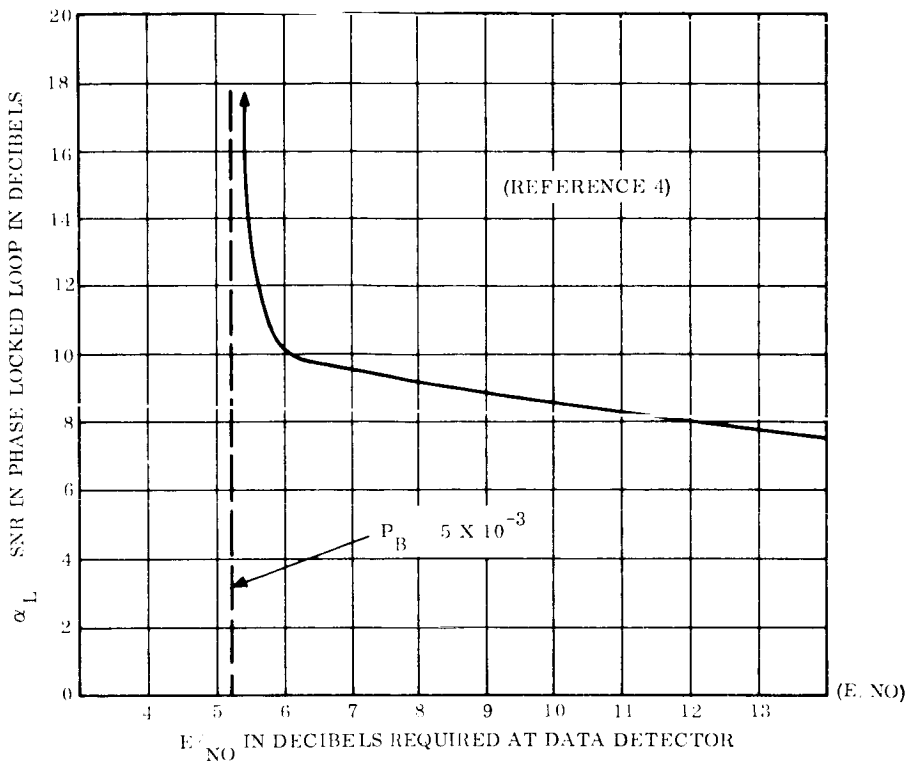

Figure 11-6. Phase-Locked Loop SNR as a Function of the Required E/N_o at Data Detector to Maintain Probability of Bit Error, $P_B = 5 \times 10^{-3}$

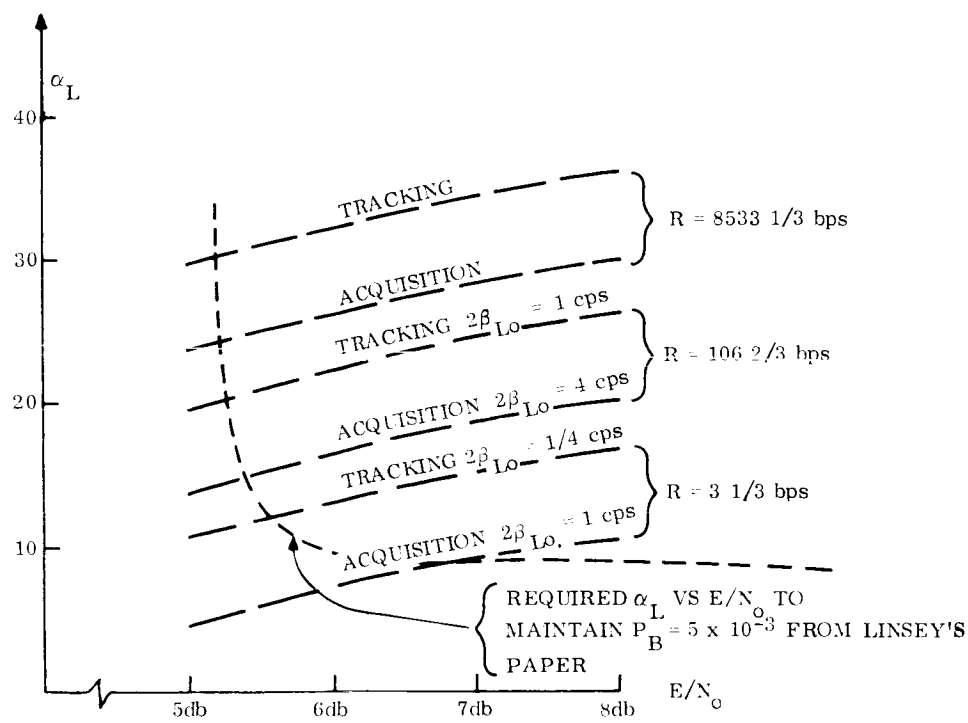

Figure 11-7. Phase-Locked Loop SNR as a Function of the Input E/N_o for the Different Data Rates

Table 11-4. SNR Performance Equations for Subcarrier Acquisition Channel of Figures 11-2 and 11-3

Definition	Equation	Comments
1. Input signal-to-noise ratio, α_1	$\alpha_1 = \frac{1}{4n}\left(\frac{E}{N_o}\right)$	n = number of PN bits per data bit (E/N_o) = bit energy per noise spectral density
2. Multiplier's output SNR, α_m	$\alpha_m = \frac{4\alpha_1^2}{5\alpha_1 + 1}$	Derivation is in Appendix III
3. Multiplier's output (S/N_o), β_m	$\beta_m = 8f_s\left(\frac{5\alpha_1 + 1}{6\alpha_1 + 1}\right)\alpha_m$	Derivation is in Appendix III
4. Output SNR of BPF-4, α_4	$\alpha_4 = \left(\frac{1}{BW_4}\right)\frac{\beta_m}{F_L}$	BW_4 = Bandwidth of BPF-4 F_L = loss in filter
5. Output SNR of BP-limiter, α_5	$\alpha_5 = \lambda\left(\alpha_4\right) \cdot \alpha_4$	$\lambda(\alpha_4)$ = Multiplier factor for BP-limiter from Davenport (Reference 5)
6. Phase locked loop SNR, α_L	$\alpha_L = \left(\frac{BW_4}{2B_L}\right)\alpha_5$	$2B_L$ = Loop noise bandwidth

the two-sided maximum frequency deviation, Δf. The maximum frequency difference between the VCO and the incoming $2f_s$ is defined as Δf. Therefore,

$$2B_{Lo} > 2\,\Delta f$$

Since this frequency difference will depend mainly on the stability of the spacecraft clock, Δf can be related to the subcarrier $2f_s$. Let σ_f be the short term stability of the spacecraft oscillator, then Δf will be

$$\Delta f = 2f_s\,\sigma_f = nR\sigma_f$$

where n is the number of PN bits per data bit. Therefore, the loop noise bandwidth must satisfy the inequality

$$2B_{Lo} > 2nR\sigma_f$$

for a clock stability of $\pm 10^{-4} = \sigma_f$, and $n = 9$

$$2B_{Lo} > (18 \times 10^{-4}) \cdot R = R/555$$

to insure rapid acquisition.

Usually, a PLL is designed to have its optimum performance at threshold, and thus the threshold loop noise bandwidth, $2B_{Lo}$ is defined for a specific threshold SNR. As the SNR into the PLL varies, so does the loop noise bandwidth.

To be able to acquire an incoming subcarrier that can be located within a range of frequencies, the loop bandwidth will have to be widened. However, once the frequency is acquired the loop bandwidth can be made smaller effectively increasing the SNR performance of the loop. This is the approach that was taken on Mariner C, i.e., utilization of two loop filters, one for acquisition and the other for tracking. This approach is also recommended for Voyager.

In Table 11-5, the loop bandwidths for the acquisition and tracking loops are shown for the different bit rates. These bandwidths are within the constraints imposed by the clock stability yet are easy to implement in the loop filters.

11.6.2 CODE ACQUISITION ANALYSIS

In acquisition of the PN codes, the time required to obtain the subcarrier clock used to step the code in time is rather insignificant when compared to the time required to achieve alignment between the codes. Therefore, t_1 is defined as the time to achieve code alignment between the codes.

Table 11-5. Bandwidths for the Phase Locked Loop

Data Rate	Acquisition	Tracking
3-1/3	1 bps	1/4 cps
106-1/3	4	1
533-1/3	8	2
2133-1/3	16	4
4266-2/3	$16\sqrt{2}$	$4\sqrt{2}$
8533-1/3	32	8

In aligning the code by a correlation process, a threshold must be established at the output of the integrate and dump so when the output exceeds this threshold the codes are assumed to be aligned. On the other hand, if this threshold is not exceeded after an integration period the codes are assumed not to be aligned and the search is continued. In making this automatic decision there is a possibility of making an error in the decision; the probabilities associated with these errors are classified as the, probability of a false alarm error, α, and the false dismissal error probability, β. Both of these errors will cause an increase in the average time required to sync the codes. Thus, they need be considered in the acquisition analysis.

In Appendix IV a signal flow graph technique is used to analyze the search routine to obtain an expression for the average time required to align the codes, t_1, as a function of the α and β error probabilities, the length of the integration period, T_o, and the length of the PN code, L.

The α and β error probabilities are defined from the probability density functions of the output of the correlator for the in-sync and out-of-sync alignment of the PN codes. These density functions are derived in Appendix V for both the single channel and the double channel correlator. Both the in-sync and out-of-sync density functions were derived for the double channel; however, only the in-sync density function was obtained for the more complex single channel code correlator.

To compare the single and the double channel code correlation techniques, we selected a decision circuit threshold setting so that $\alpha = \beta$. Since only the in-sync probability density was derived for the single channel code correlator, only the β error probability could be defined for this code correlation technique. To define this β error probability, we selected the same threshold setting for the single channel correlator that was needed in the double channel code alignment correlator to make $\alpha = \beta$. These error probabilities are functions of the correlator integration time, T_o, the threshold

setting, the correlator's input signal-to-noise ratios, and the length of the code, L. For the double channel code correlator, the error probabilities are

$$\alpha = \beta = 1/2 \left\{ 1 - \mathrm{erf} \left[1/2 \ \frac{A}{\sigma_N} \sqrt{\frac{k_L}{2}} \right] \right\}$$

where

A/σ_N = the input voltage signal-to-noise ratio of the correlator

L = the length of the PN code = 63 bits

k = 1, 2. . . . . , the number of code lengths the correlation period lasts.

$$\mathrm{erf}(x) = \frac{2}{\sqrt{\pi}} \int_0^X e^{-u^2} du \quad ; \text{ the error function}$$

for the single channel code correlator, the error probabilities are

$$\alpha = \beta = 1/2 \left\{ 1 - \mathrm{erf} \left[\frac{\mu_o}{2\sqrt{2\sigma_o}} \right] \right\}$$

where

$$\frac{\mu_o}{2\sqrt{2\sigma_o}} = \frac{\sqrt{k7}}{2} \left\{ \frac{(S/N)_{in}}{\sqrt{1 + 2\ (S/N)in}} \right\}$$

$(S/N)_{in}$ = the input signal-to-noise ratio to the multiplier preceding the single channel code correlator,

The expression for t_1 obtained in Appendix IV is

$$t_1 = \frac{T_o L}{2} \left\{ \frac{(1+\alpha) \left[1 - \beta + \beta^2 \right]}{(1-\beta)\ (1-\alpha)} \right\}$$

When no errors are made in the decision process, i.e., $\alpha = \beta = 0$, the error free average time required to sync is:

$$t_1 = \frac{T_o L}{2}$$

For the actual single channel system implementation this value for t_1 will have to be increased by a factor of 2 since the ambiguity in the acquired $2f_s$ clock requires that the code alignment be tested at one-half a PN bit per correlation test.

11.7 REFERENCES

1. Goode, George E, "A New Method of Frame Synchronization Using Linear Sequential Feedback Generators," 1963 National Telemetering Conference.

2. "Study of Mars and Venus Orbiter Missions Launched by the Three-Stage Saturn C1B Vehicle," JPL-EPD-139, Vol. III, 31 December 1963.

3. Springett, J. C., "Telemetry and Command Techniques for Planetary Spacecraft," Advances in Communications System, Vol. 1, Academic Press, New York, 1965

4. Lindsey, W. C., "The Detection of PSK Signals with Noisy Reference," 1965 National Telemetry Conference, pp. 50-52 of Proceedings.

5. Davenport, W. B., "Signal-to-Noise Ratio in Band-Pass Limiter," Journal of Applied Physics, Vol. 24, Number 6, pp. 720-727, June 1953.

12.0 ERROR CONTROL CODING

12.1 SCOPE

This section considers the question of the applicability of error control coding to the Voyager bus-to-earth telemetry link. The functional objectives and design constraints are stated followed by a discussion of four types of error control coding of increasing complexity considered initially in the earlier approaches to the problem. An initial selection process narrowed the field to two types of codes for further analysis, viz., Bose-Chaudhuri and bi-orthogonal/transorthogonal types. A detailed discussion is given with regard to code evaluation criteria, after which results of the code evaluation, trade-offs and comparisons are presented. Finally, a preferred approach is stated along with an ordering of alternatives. Presented last are: the basis for the selection; assumptions made; a strong alternate (and conditions for preference); and additional study recommended in support of the selected code.

12.2 FUNCTIONAL OBJECTIVES AND DESIGN CONSTRAINTS

The primary objective in considering error control coding for use in the Voyager mission is to achieve a degree of increased efficiency in the bus-to-earth telemetray link. Increased efficiency may be expressed in terms of signal-to-noise ratio or it may be translated into several other parameters of potential importance to the Voyager mission. In particular:

a. For a fixed transmitter power and a given tolerable bit error rate, the data rate may be increased using the increased signal-to-noise ratio available and thereby reduce the time required to transmit back to the earth important scientific data (such as TV mapping data); consequently, the required life time on the Voyager bus may be reduced accordingly, or, alternately, the total amount of collected data from the mission during whatever its lifetime could be increased; or

b. for a fixed transmitter power and a fixed data rate, the increased signal-to-noise improvement implies that all or selected data may be received with a decreased bit error rate.

In certain marginal operational circumstances it is possible that the improved efficiency due to error control coding may provide the critical additional gain required to change an unsatisfactory operation into a satisfactory one.

The primary design constraints are: (1) the added complexity (and, hence size, weight, power and unreliability) of the error control encoder and synchronizer aboard the spacecraft, and (2) implications of the increased bandwidth. If error control coding were used at some data rates, but not all, or only under certain circumstances, then the additional unreliability of switching, from uncoded to coded and vice-versa, could be a design constraint.

From the standpoint of the several DSIF, any additional requirement for mission dependent equipment would be a design constraint, especially if such equipment had to be developed. Forward-acting error correcting coding places most of the equipment burden and complexity at the receiving terminal which is the only alternative when considering deep space missions; nevertheless, cost and technical risk of developing a mission dependent error control decoder of adequate efficiency must be considered.

12.3 APPROACHES TO ERROR CONTROL CODING

Error correcting codes may be categorized in several different ways. One very important distinction is whether decoding is done bit-by-bit digitally or is accomplished by analog cross correlation over the entire code interval.[5] In the latter case no elementary symbol (bit) decision need be made while the code word is being received - the only decision is made at the end of each word based on the locally generated or stored code word replica having the highest cross correlation with the received code word. In practice, the analog cross correlation is often approximated using an analog-to-digital converter and associated digital scaler and integration circuitry.[1]

Codes utilizing both methods of decoding were studied and are listed below in an increasing order of decoder complexity:

a. Wagner (n, n-1) single error correction codes;[6]

b. Bose-Chaudhuri (n, k) multiple independent error correction codes;[7]

c. Transorthogonal (2^{k-1} -1, k), and bi-orthogonal (2^{k-1}, k) codes[2, 8], and

d. Convolutional codes.[9]

The first two types represent the class of cyclic error correcting codes and were included because of their inherent decoding simplicity. A cyclic (n, k) code has an encoder consisting of k or n-k stages (depending upon which is smaller) and utilizes a decoder (for digital bit-by-bit decoding) consisting of generally a shift register arrangement wherein the same decoding logic is time shared to decode serially all information bits of the received word.[3]

The minimum redundancy Wagner code represents a special sub-class and was considered due to its unique simplicity and inherent advantages resulting from its requirement for only one parity bit per word. The single parity bit of the Wagner code may be easily utilized as a "carrier" to encode frame sync information as reported in the literature.[10] However, since the signal-to-noise improvement for this code was less than 1 db at the desired bit error rate it was not seriously evaluated any further. On the other hand, Bose-Chaudhuri codes are representative of the most efficient algebraic codes and thus were given strong consideration. Transorthogonal and bi-orthogonal codes are typical of a class of codes which trade bandwidth for signal-to-noise ratio and are optimum for cross-correlation word decoding; hence, they, too, were given strong consideration.

Convolutional codes represent an efficient class of "sliding parity check" codes which utilize bit-by-bit digital decoding usually accomplished with a general or special purpose computer. A sizable buffer or queue memory is required which occasionally over-flows and causes loss of data.[4, 11] Therefore a feedback channel is required in order to request retransmission and resynchronization as needed.[12] The command channel could be used for requesting retransmission and resynchronization but the data encoder aboard the spacecraft would have to be redesigned to incorporate some type of temporary storage in order that data lost in an over-flow might be retransmitted. The inherent nature of a convolutional coded channel with its occasional over-flows implies that both the input and output data rates are non-uniform with concomitant complications for real-time, constant data rate systems. However, for non-real-time applications convolutional decoding can provide almost perfect decoding between buffer over-flow conditions. An increase in buffer memory size decreases the probability of over-flow; nevertheless, a "finite" memory implies a "finite" probability of over-flow.

Convolutional codes were dropped from further consideration due to their peculiar weakness of data loss and discontinuity and the special requirement for retransmission and resynchronization necessary in every instance when the decoder buffer memory overflows - a requirement which is not presently compatible with deep space telemetry operations. Thus, only Bose-Chaudhuri and transorthogonal/bi-orthogonal codes were evaluated in detail with regard to several criteria discussed in the following paragraphs.

12.4 INITIAL SELECTION CRITERIA

The central question in regard to initially selecting a code or codes is: How efficient is the code as opposed to how much it costs in terms of various parameters? To be discussed in more detail later are the four system parameters of: (1) code efficiency in terms of improved signal-to-noise ratio at a given bit (decoded) error rate; (2) size, weight, power penalty; (3) reliability (MTBF) penalty (both 2 and 3 with respect to the spacecraft encoder; and (4) cost of decoder implementation (if special equipment is required) or cost of decoding if a general purpose computer is used.

It is well recognized that as the length of the code, n, increases, the efficiency of the code also increases (fundamental coding theorem); yet, the complexity of decoding long codes is so great that in most applications they cannot even be considered. Also well known is the fact that as the signal-to-noise improves in the system, the efficiency of the code increases but the real need is for efficiency when the signal-to-noise ratio is at a nominal or degraded value.[13]

The above discussion on approaches to error control coding indicated that only two categories of codes need to be considered. If we ignore, for the moment, the desired minimum telemetry bit error rate of 5×10^{-3}, the selection of a particular Bose-Chaudhuri code from the many available (see Stenbit[14] for table of code generators) would be based largely on the maximum length, with reasonable redundancy, that could be realized without excessive complexity in the decoder implementation. A longer length code would tend to improve efficiency with a concomitant increase in complexity and cost of the decoder; hence, a practical upper limit on n is thereby implied. An n of less than 100 has, therefore, been selected as reasonable.

The same problem exists with transorthogonal/bi-orthogonal correlation decoders wherein for a k-information bit code word, 2^k correlations (or 2^{k-1} for bi-orthogonal) must be performed either in parallel or serially before a word decision is made. This rapidly becomes costly for even moderate values of k; therefore, the region of interest for k appears to be from about 4 to 6, with a corresponding improvement in decoding efficiency for larger values of k. In addition, bandwidth constraints necessarily restrict k to the range indicated. Each increment of k by 1 doubles the bandwidth.

From the standpoint of utilizing a general purpose computer for real-time decoding, such as one used in the Telemetry, Command and Data Handling (TCD) system, a shorter length Bose-Chaudhuri code is suggested in order to keep the code word length no greater than the computer word size to avoid excessive computer command execution times due to multiple-precision type operations.

The spacecraft error control encoder, in any case, does not appear initially to limit the selection of what codes (and code lengths) to analyze in detail, since its implementation is much simpler relative to the decoder even though it is located at the critical terminal.

12.5 CODES SELECTED FOR ANALYSIS

Based on the discussion above, three error correcting codes were selected for detailed analysis:

a) (15, 7) Bose-Chaudhuri double-error correcting code;

b) (73, 45) Bose-Chaudhuri quadruple-error correcting code; and

c) (15, 5) bi-transorthogonal, or "augmented m-sequence", code.

The (15, 7) code was selected because its shorter word size would be compatible with the 24 bit word size in the SDS 900 series computers and the 7 information bits corresponds to the telemetry word size; consequently, a detailed discussion of its encoder and decoder design and operation is presented in Appendix IX.

The (73, 45) code was selected because its decoder implementation is within reasonable bounds and is representative of the efficiency to be expected from codes of similar lengths and redundancy where bit-by-bit digital decoding is performed. A description of the (73, 45) encoder-decoder design and operation is given in Appendix X. The (15, 5) bi-transorthogonal code was selected as representative of the category of optimum correlation codes because its k = 5, is a reasonable and realizable value; in addition, the two sets of cyclic shifts of a pseudo-random maximal length sequence and its complement are readily decoded on a relatively simple hybrid correlator and the code compares closely in efficiency to a (16, 5) bi-orthogonal code. Appendix XI contains the details on this code, its encoder and decoder.

12.6 CODE EVALUATION CRITERIA

12.6.1 MEASURES OF CODE EFFICIENCY

Whenever two or more codes are compared and each has different values of n and/or k, an immediate measure problem is that of normalization. In simpler cases when an error correcting code is compared with no coding most analysts stipulate that both the coded word and uncoded word (with identical number of information bits) must be transmitted (or received) with an equal amount of energy; that is

$$kE_k = nE_n = \text{energy/word} \tag{1}$$

Where E_k = energy/bit for the k-bit uncoded word and E_n = energy/bit for the n-bit (n, k) code word. Hence, the ratio of bit energies is

$$E_k/E_n = k/n \tag{2}$$

and a simple comparison can be made in terms of one or more error probabilities. Another more general comparison measure for binary modulation and demodulation is that of

$$E/N_o = \frac{\text{received signal energy per bit}}{\text{noise power per unit bandwidth}} \tag{3}$$

used by Lawton and others.[15] When data is encoded with an error correcting (n, k) code then E is the average energy per information bit. Thus, assuming that two codes have an equal E/N_o, a measure of their performance can be derived from one or more types of error probability. Specifically, the three error rates of interest are:

a. Equivalent Bit Error Probability, p_e;

b. Code Character (or k bit uncoded word) Error Rate P_c and

c. Equivalent Data Word (w-bits per word) Error Rate P_w.

Each of these error rates have been considered and a detailed discussion of some of the relative merits and limitations of each will be given.

12.6.1.1 EQUIVALENT BIT ERROR PROBABILITY

The main limitation of the equivalent bit error probability, p_e, is in deriving it, which entails determining precisely the number of decoding errors resulting from a failure of the error correcting decoder to correct all errors that are received. As a simple example, consider a perfect E - error correcting code in which E or fewer errors will always be corrected. Then whenever E + 1 or more errors are received the decoder collapses and results in a certain distribution of errors in the decoded k information bits. With the exception of orthogonal type codes, there is no known simple way of determining the distribution of decoding errors. Therefore, until a better way is found, one must simulate the decoder's operation when E + i errors (for $i > 0$) are received and tabulate the resulting decoding errors. Then, and only then, would it be possible to derive precisely an equivalent bit error probability. The expressions which Mitchell has derived for use in evaluating the equivalent bit error probability will be given below, but they are only useful when one has actually tabulated all cases of decoding errors for a specific error correcting code.[16] He defines P_o as the ensemble average probability that an information bit delivered by the decoder to the data sink is in error (same as p_e defined above).

Thus,

$$P_o = \sum_{u=E+1}^{n} C(u) \binom{n}{u} p^u (1-p)^{n-u} \tag{4}$$

where p is the independent bit error probability and C (u) is the expected number of information bit errors out of u-errors in n (total number of information bits per code word).

$$C(u) = 1/k \sum_{j=1}^{k} j\, F(j|u), \tag{5}$$

$$\text{and } F(j/u) = \frac{N(j|u)}{\binom{n}{u}} \tag{6}$$

= fraction of u-digit errors in n bits for which the k decoded information bits have j errors,

and,

N (j/u) = number of u-digit errors in n bits for which the k decoded information bits have j errors.

Note that when $u \leq E$, where E is maximum number of correctable errors for the given code and decoder, then $C(u) = 0$.

12.6.1.2 CODE CHARACTER ERROR RATE

We consider next the character error rate P_c for a code in which k bits are information and n-k bits are check bits. This particular error probability is very simple to compute since one merely has to compute all cases in which the code collapses as given by the expression,

$$P_c = \sum_{u=E+1}^{n} \binom{n}{u} p^u (1-p)^{n-u} \tag{7}$$

for a perfect E-error correcting code and

$$P_c = \sum_{u=E+1}^{n} F(u) \binom{n}{u} p^u (1-p)^{n-u} \tag{8}$$

for a quasi-perfect or any other code having partial error-correcting capability for u-digit errors where $u > E$. The expression

$$F(u) = \frac{N(u)}{\binom{n}{u}} \tag{9}$$

is the fraction of all possible u-error patterns that are correctable by the decoder.

This would be a very satisfactory way to evaluate an error correcting code when $k = w =$ data word size. But a problem arises when using this measure to evaluate two different codes where the k's for each code are different and also when neither k is equal to w. To take one example, assume that k is considerably larger than w such that there are exactly j data words equal to k. Then any comparison of uncoded k bits to an error correcting (n, k) code will show considerable improvement for the error correcting code since the probability of at least one error in the uncoded k data bits is generally greater than P_c for an error correction code word for most bit error rates of interest and appears even more disadvantageous as k increases. The expression for the probability of at least one error (uncoded k-bit word) is

$$P_{uc} = 1 - (1 - p)^k \tag{10}$$

which results in what appears to be a 1 to 2 db improvement at nominal p_e for the error correcting code.

12.6.1.3 EQUIVALENT DATA WORD ERROR RATE

The more meaningful measure for the user of the data is not this character error rate but the error rate of the data words being received. In short, the question is: Given that the k (for $k >> w$) information bits of an error correcting code or k information bits of an uncoded word are received in error, what is the conditional probability that a given data word of length w bits (contained in the k bits) is in error?

The problem of using the character error rate as a measure of comparison, therefore, collapses when one considers codes of different size and where the number, k, of information bits in the code is considerably larger (generally the case) than the word size, w. If it is assumed that each data bit in the word is of equal weight (not usually the case, but nevertheless, this assumption simplifies the analysis) then the only concern of the user would be the data word error rate. Of course the data word error rate is identical to the character error rate whenever $k = w$.

When k is not equal to w then one has a difficult time computing the word error rate since one must tabulate the decoded errors and construct a conditional probability distribution of the cases where 1, 2, . . . , j words in the k bits are in error (here we assume that $k = jw$).

Summarizing, one may say that for a specific system in which the data word is fixed in length, a meaningful measure of evaluation would be based on the decoded data word error rate although there is no simple method of computing it. In systems where the data word length is not constant a better measure would be the equivalent bit error probability of the decoded bits, p_e. The least useful measure is that of the code character error rate, unless the data word length is equal to the number of information bits in the error correcting code.

In the following section, code efficiency comparisons were based on available data on equivalent bit error probabilities and code character error rates for several codes most of which required considerable numerical calculations on high-speed digital computers.

12.6.2 CODE EFFICIENCY COMPARISON

The results presented are taken from the work done by Viterbi,[2] Mitchell,[16] and Hackett.[17] Figure 12-1 is a graph of the equivalent bit error probability for bi-orthogonal codes for various values of k. It is taken from Viterbi and indicates approximately 2.3 db improvement at the bit error rate of 10^{-3}. From this graph it appears that at a bit error rate of 5×10^{-3} the improvement is approximately 1.76 db, or a factor of 1.5.

For the (73, 45) code, Figure 12-2, taken from Mitchell, shows the improvement over no coding at a bit error rate of 10^{-3} is approximately 1.3 db assuming that the decoder corrects all 5 bit error patterns that are correctable but none that have more than 5 errors. Notice that at a bit error rate of 5×10^{-3} the improvement of the (73, 45) code is less than 0.3 db.

Figure 12-3 indicates the performance of the (15, 7) code which, in general, is poor.[16] At a bit error rate of 5×10^{-3} it is worse than no coding. Even at very low bit error rates its improvement is barely 1 db better than no coding.

An important insight as to how some significant gains may be achieved with error correction coding is found in Hackett's work.[17] Although reported in terms of word error probability his ideal curves show dramatically the improvement to be expected when correlation decoding is used on an error correcting code. Referring to Figure 12-4 it can be seen that even in the poorest case shown where the word error rate is 10^{-2}, correlation decoding of the (23, 12) perfect Golay code provides an improvement over no coding of approximately 3.3 db. It should be emphasized, however, that this can be slightly misleading in view of the fact that the error probability of more interest to the user is the data word error rate. The information word size given in Hackett's graph is 12 bits, and if it were composed of two data words, then in many instances where the 12 uncoded bits contained an error or errors only one data word would be affected; therefore, the other data word would be correct, which would not appear to be as poor an error rate as that of the gross code character error rate. Furthermore, it should be noted that in order to actually perform correlation decoding on the (23, 12) code, $2^{12} = 4096$ correlations have to be made followed by a "greatest of" decision <u>for each received word</u>. It is thus clear why correlation decoding is practical at present only for relatively small values of k.

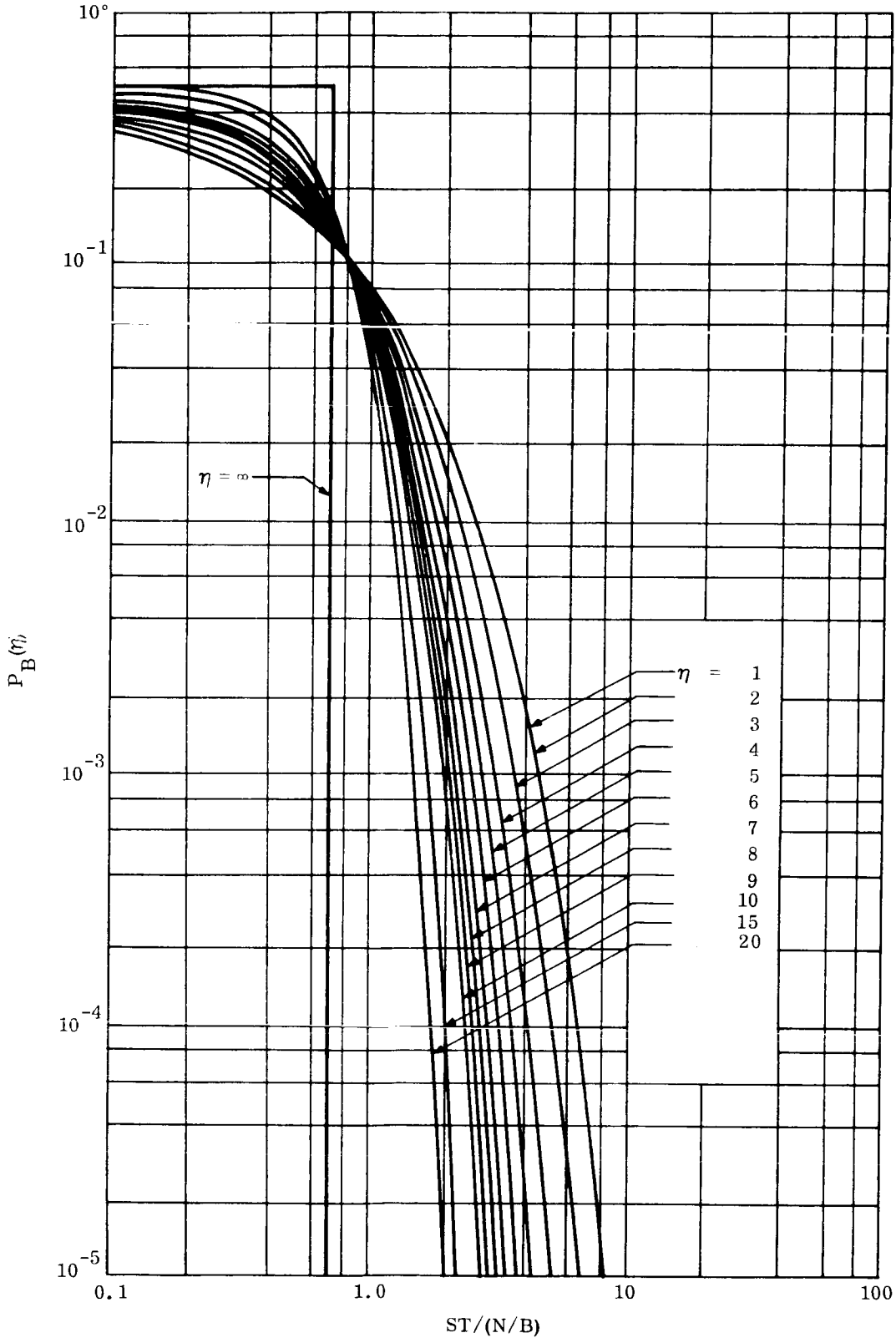

Figure 12-1. Equivalent Bit Error Probability - Bi-orthogonal Codes

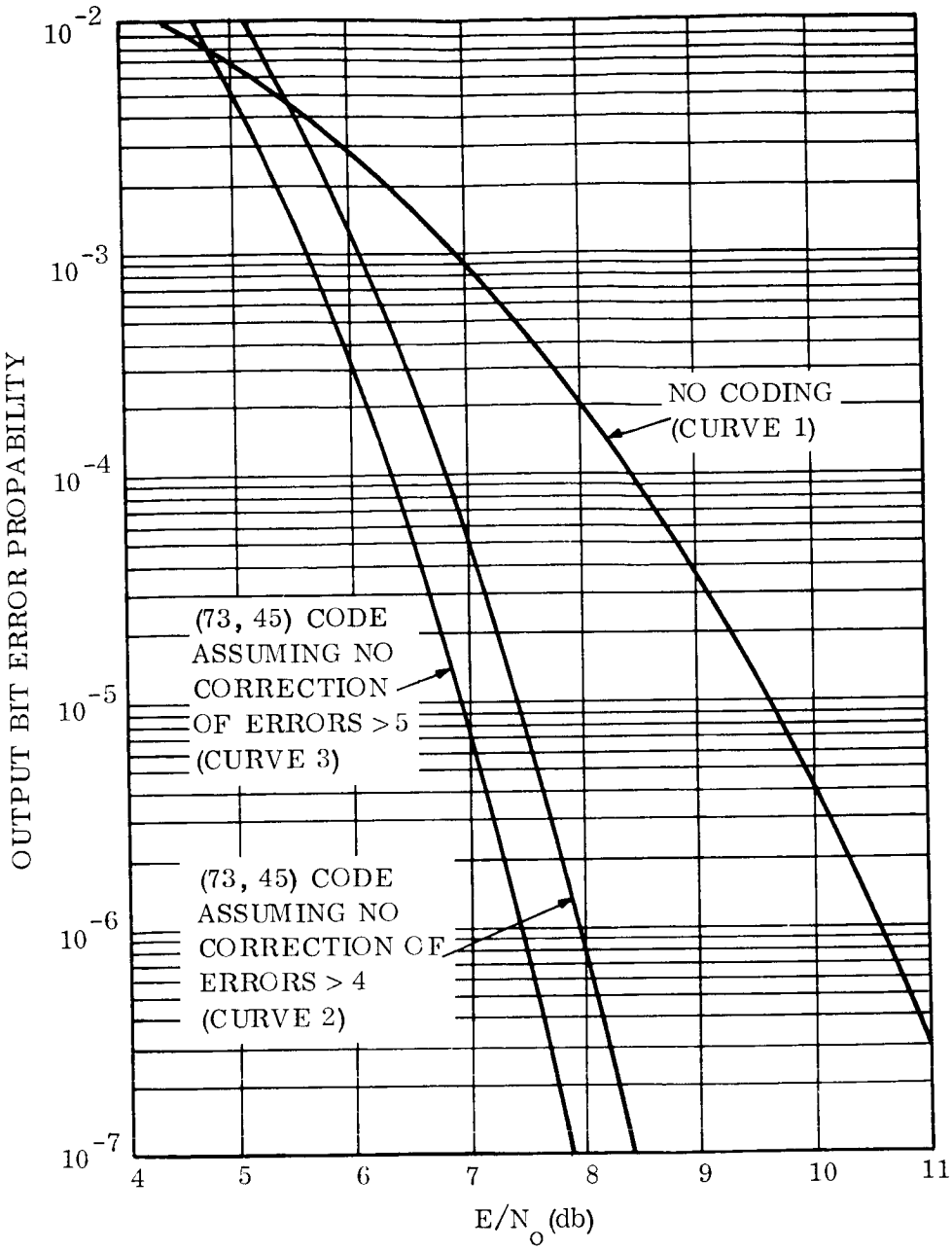

CURVE 3

j	N(j/5)	F(j/6)
0	7,526,282	0.5011
1	2,883,462	0.1920
2	1,660,381	0.1105
3	1,470,125	0.0979
4	1,114,685	0.0762
5	335,399	0.0223

$$\sum_{j=0}^{5} N(j/5) = \binom{73}{5}$$

$$0(5) = \frac{1}{45} \sum_{j=j}^{45} jF(j/5)$$

$$=0.0250$$

$N(j/5) = 0.\ j>5$

Figure 12-2. Equivalent Bit Error Probability, (73, 45) Code

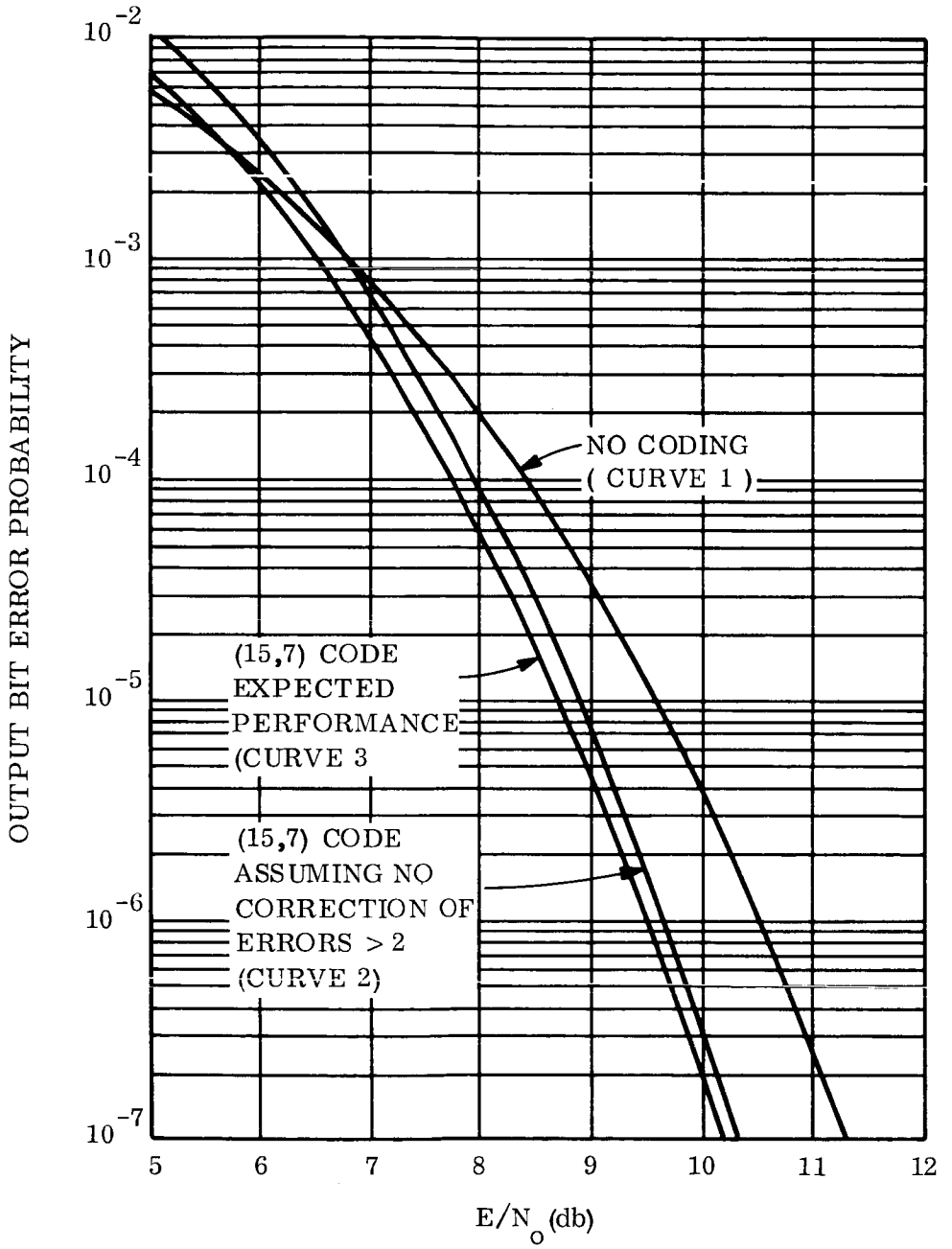

Figure 12-3. Equivalent Bit Error Probability, (15, 7) Code

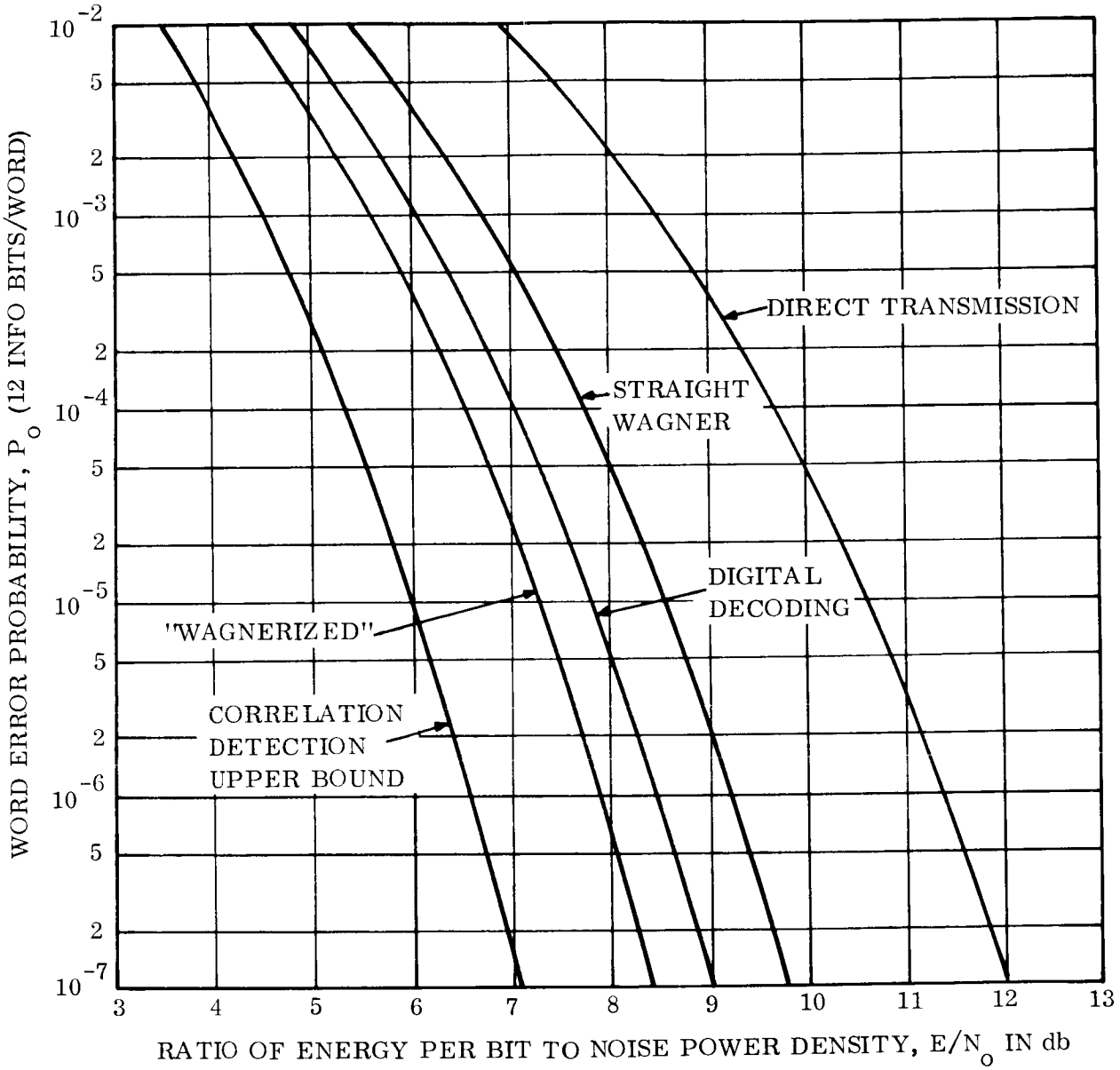

Figure 12-4. Code Character Error Probability, (23, 12) Code

12.6.3 HARDWARE CONSIDERATIONS

12.6.3.1 Spacecraft Encoder: Table 12-1 summarizes the requirements of the two principal error correcting codes with reference to the spacecraft encoder. In terms of the parts count it is clear that the (15, 5) transorthogonal encoder is simplier by a factor of approximately 4.

Table 12-1. Spacecraft Error-Correcting Encoder

Code	Encoder and Timer			Total Failure Rate %/Khrs (1)	Power RQD (mw) (2)	Weight (lb) (3)	Size (in.^{3}) (4)
	FF	Mod 2 Gates	Nand Gates				
(73, 45) Bose-Chaudhuri	35	11	9	0.275	429	0.18	4.2
(15, 5) Bi-Transorthogonal	9*	2	10**	0.075	113	0.05	1.1

*Includes buffer register, but not programmer

**Two-input diode transfer gates, considered equal to 4 NAND gates.

DATA ON SEMI-CONDUCTOR NETWORKS

Failure rate:	0.005%/Khrs
Power (milliwatts):	7 for FF and NAND gates, 11 for Mod 2 gates
Size:	13.1 networks/in.^{3}
Weight:	300 networks/lb

12.6.3.2 Decoder: In the hopes of avoiding the requirement for mission dependent equipment to handle decoding, a brief investigation was made to determine if it were possible for a high speed general purpose computer, such as the SDS 930, to decode the Bose-Chaudhuri or bi-transorthogonal codes in real time. In most cases where the general purpose computers have been used to decode error correcting codes, it has been at low data rates or, for higher data rates, non-real-time. Using the simpler (15, 7) Bose-Chaudhuri code as an example, a first-cut look at the flow diagram of a routine to decode a single data bit indicated that it would take at least

1 millisecond (rough approximation) to decode a 7-bit word. Thus the maximum word rate it could handle working full time would be somewhere in the neighborhood of 1000 words per second. The (15, 7) code was chosen because its word length was less than the 24-bit word length of the computer; therefore, if one attempted to decode the (73, 45) code on the same computer the problem would be more complex and time consuming due to the code word size being much larger than the computer word size. In the case of (15, 5) bi-transorthogonal correlation decoding it appears that computer would be equally saturated and unable to handle the maximum received word rate of 1219 words/sec.

12.7 TRADEOFFS AND COMPARISON OF APPROACHES

In view of the results shown in Section 12.6.2, if error control coding is considered for use in Voyager, the choice based on efficiency would be the bi-orthogonal or bi-transorthogonal code since it provides approximately 1.76 db of improvement at a 5×10^{-3} bit error rate which is the largest gain of the codes considered. However, such a relatively small improvement, approximately 50% in the telemetry channel, appears marginal when compared with the inherent simplicity of no coding together with all that this implies.

The advantages and disadvantages of the two main alternatives are shown in Table 12-2. The higher cost (including risk) of implementing error control coding in both the spacecraft and ground stations would buy either a shorter mission time or permit more data to be transmitted from the spacecraft during the same mission time. The former implies a higher probability or confidence factor of total mission success.

It is evident in either case that a special purpose decoder would be necessary in order to handle at all times the real time decoding essential to system operation. A measure of the complexities of the two decoders is given by the number of flip-flops that each requires for their shift registers and buffers. The (15, 5) transorthogonal correlator requires 45 k flip-flops whereas the (73, 28) code requires 125. If k (word size of the ADC) is five, the correlator is approximately twice as complex as the (73, 45) decoder. (See Appendices X and XI).

12.8 SELECTION OF PREFERRED APPROACH

12.8.1 SELECTION CRITERIA, RATIONALE, AND PREFERRED APPROACH

The marginal gain in efficiency, the higher development and production costs, and the greater overall system complexity implicit in the use of error control coding suggest that the preferred approach for the Voyager telemetry link is to use no coding. If the required bit error rate were lowered to the point where the code efficiency were approximately 3 db or better, or if there were a general purpose computer available at the DSIF that could handle the decoding in real-time for all data rates — error control coding should seriously be considered.

Table 12-2. Comparison of Coding and No Coding Alternatives

Alternative	Advantages	Disadvantages
Error Control Coding - (15, 5) Bi-Transorthogonal Code	• 50% improvement in telemetry channel efficiency at 5×10^{-3} bit error rate (approximately) - greater efficiency at lower bit error rates; this implies one or more of several practical consequences: - a reduction of transmitter power; - higher data rate and thus a lowering of required mission lifetime; - more data from spacecraft using same lifetime as with no coding; - greater accuracy in telemetry data. • would be compatible with the trend toward the requirement in the design of deep space mission systems for greater efficiency in the telemetry channel; eventually, error control coding may become standard and be handled by a programmable decoder at the DSIF.	• Increased complexity in spacecraft - thus implying - lower MTBF unless offset by redundancy - greater size, weight, and power requirements of encoder. • Mission-dependent-equipment required for decoding unless coding is used only for lower data rates wherein an available general purpose computer might be used to handle real-time decoding. • Increased complexity in word synchronizer very probable since both error control code word sync and data word sync are essential and one may not imply the other. • The cost and risk in the development of an MDE decoder.
No Coding	• Inherent simplicity in spacecraft of a proven technique which implies: - higher reliability without redundancy; - lower power, weight and size requirements with respect to encoder. • Simpler ground station requirements especially - no special decoder - simpler word sync circuitry	• Requirement for higher transmitter power, or equivalent, longer mission life - both of which are of prime importance.

12.8.2 STRONGLY COMPETING ALTERNATIVE

The use of error control coding may be considered a strong alternative, especially under the conditions mentioned above. In addition, at lower data rates, such as during critical maneuvers, error control coding could be used to provide increased efficiency but without the cost of developing an MDE decoder. This may be possible by using one of the DIS digital computers with a minimum of additional hardware and software, to handle decoding. It would seem that during the reception of the lower data rates the DIS computers would have more time available for other functions such as error control decoding.

12.8.3 ADDITIONAL STUDY OR DEVELOPMENT RECOMMENDED

Further study of the feasibility of using one of the TCD computers for decoding an error control code during the reception of the lower data rates is recommended. This should include the requirement for conversion and buffering prior to computer input. The problem of acquiring word sync for both the error control code words and the data words needs further study to determine the optimum method. The primary method of synchronization considered so far for use with the (15, 5) bi-transorthogonal code involves the use of a 255-bit PN sequence over the 15-bit code interval. Three decoded code words containing 3 x 5 = 15 bits would consist of two 7-bit data words plus a parity bit used for the dual purpose of monitoring errors and resolving the ambiguity in the data word sync. Furthermore, the parity bit could also be used as a carrier for frame sync information so that frame synchronization may be acquired at no additional cost in data rate or channels.[10]

12.9 REFERENCES

1. "Bi-orthogonal Coded Telemetry", JPL Space Programs Summary No. 37-18, Vol. III, Nov. 30, 1962, pp, 68-72.

2. Viterbi, A. J., "On Coded Phase-Coherent Communications", JPL Technical Report No. 32-25, August 15, 1960.

3. Perlman, M., "Implementation of Error Detection and Correction Using Binary Cyclic Codes," (Part 1), JPL Technical Report No. 32-324, Oct. 1, 1962.

4. Jacobs, I., "Performance Parameters for Sequential Decoding", JPL Space Programs Summary No. 37-32, Vol. IV, April 30, 1965, pp. 303-306.

5. Mitchell, M., Burton, C., Hackett, C., Schwartz, R., "Coding and Decoding Operations Research", Vols. II and III, General Electric Company, L.M.E.D., prepared for Air Force Cambridge Research Laboratories under contract AF 19(604)-6183, 14 January 1961 (AD 257420).

6. Silverman, R.A., and Balser, M., "Coding for Constant Data Rate Systems", Proceedings IRE, Vol. 42, No. 9, pp. 1428-1435, Sept. 1954.

7. Bose, R.C. and D.K. Ray-Chaudhuri, "On a Class of Error Correcting Binary Codes," Information and Control, Vol. 3, 1960, pp. 279-290.

8. Viterbi, Andrew J., "Phase-Coherent Communications over the Continuous Gaussian Channel," Chap. 7 in Digital Communications with Space Applications, edited by S. W. Golomb, Prentice-Hall Inc., Englewood Cliffs, N.J., 1964.

9. Wozencraft, J.M. and B. Reiffen, "Sequential Decoding," Technology Press (MIT) and John Wiley and Sons, Inc., New York, 1961.

10. Goode, G.E., "A New Method of Frame Synchronization Using Linear Sequential Feedback Generators," 1963 National Telemetering Conference, Proceedings, Albuquerque, New Mexico May 20-22.

11. Wadden, W.R., D.M. Jones, and J. Pennypacker, "An Investigation of Sequential Decoding," RCA Review, Vol. 22, Sept. 1961,

12. Lebow, Irwin, "Sequential Decoding for Efficient Channel Utilization," IEEE First Annual Communications Convention, Conference Record, pp. 47-53, June 7-9, 1965.

13. Palmer, James, E., "A Note on the Applicability of Error Correcting Codes," 1960 MIL-E-CON, 4th National Convention on Military Electronics June 27-29, 1960, Washington, D.C., pp. 190-193.

14. Stenbit, John P., "Table of Generators for Bose-Chaudhuri Codes," IEEE Transactions on Information Theory, Vol. I T-10, No. 4, pp. 390-391, October 1964.

15. W. Lawton, J.G., "Comparison of Binary Data Transmission Systems," Proceedings of the IRE Second National Convention on Military Electronics, June 1958, pp. 54-61.

16. Mitchell, M., "Performance of Error-Correcting Codes," General Electric Company, LMED, AF 19(604)-6183, Report No. R61ELC78, November 1961.

17. Hackett, C.M., Jr., "Word Error Rate in Group Codes Detected by Correlation and Other Means," General Electric Company, LMED Technical Information Series No. R62ELC5, February 1962.

APPENDIX I. 0

SUBCARRIER INTERFERENCE IN RF LOOP

The carrier tracking PLL signal-to-noise ratio, $(S/N)_c$, can be defined as follows:

$$(S/N)_c = \frac{P_c}{2B_L N_o + P'_{sc}} = \frac{1}{\frac{2B_L N_o}{P_c} + \frac{P'_{sc}}{P_c}}$$

where

$P_c/2B_L N_o$ = the RF carrier signal-to-noise ratio

P_c = signal power in the carrier

$2B_L N_o$ = noise power in $2B_L$

N_o = noise density

$2B_L$ = carrier loop noise bandwidth

P'_{sc} = $2\int_o^\infty |H(f)|^2 P_{sc}(f)df$

$H(f)$ = loop transfer function

$P'_{sc}(f)$ = power spectrum of subcarrier

If we define $|H(f)|^2$ is an ideal spectrum of one-sided bandwidth B_L, then the portion of the subcarrer power that enters the carrier loop, P'_{sc} can be approximated by

$$P'_{sc} = 2\int_o^{B_L} P_{sc}(f)\,df = K_1 P_{sc}$$

where K_1 is the portion of the total subcarrier power is the carrier $2B_L$ bandwidth.

For the low data rate system, the division of the transmitter power between the subcarrier and the carrier is as follows:

$$P_{sc}/P_c = 3/7 = 0.429$$

For the single channel system K_1 can be evaluated from the integral of the power spectrum of $(D + PN + 2f_s)$ where $f_s = 15$ cps for the low data rate system. The required SNR of the P_{LL} is 6db and the loop noise bandwidth of the carrier tracking loop for the low data rate is $2B_L = 12$ cps; therefore, K_1 is

$$K_1 = \int_0^{.4f_s} \frac{\sin^4 (\pi f/4f_s)}{f_s(\pi f/4f_s)^2} \, df \approx 1.7 \times 10^{-2}$$

Inserting these values into the expression for the signal-to-noise ratio of the carrier tracking PLL we have

$$(S/N)_c = \frac{1}{0.25 + (.429)\, 1.7 \times 10^{-2}} = 5.9 \text{ db}$$

or a loss of 0.1 db in the regular signal-to-noise ratio of the loop.

At the higher data rates, the loss will be less than this 0.1 db. As an axample, for R = 106 2/3 bps the $2B_L = 48$ cps and the subcarrier will be

$$2f_s = 9R = 960 \text{ cps}$$

$$f_s = 480 \text{ cps}$$

For these values the range on the integral is 0 to $0.05f_s$, and K_1 is less than 10^{-4}. The ratio of the subcarrier power to carrier is greater for the high data system, i.e., $P_{sc}/P_c = 7/3$, but the $(S/N)_c$ for the carrier loop becomes

$$(S/N)_c = 5.9965 \text{ db}$$

or a loss of less than 0.0035 db. The loss is much less for the higher bit rates.

Consequently, the low data rate (3 1/3 bps) is the only data rate that would cause us concern about the subcarrier interfering with the carrier loop. To eliminate this problem, $4f_s$ could be used as the subcarrier for the low data rate system which

should give us sufficient protection from subcarrier interference in the carrier loop. All that is needed in the spacecraft to implement this subcarrier change at the low data rate is one switch. At the demodulator, however, it will take twice as long to acquire the PN sync since now the bit timing ambiguity has doubled. Also, the detection range for the matched filter has been decreased which could also cause a greater length of time to acquire the codes. Nevertheless, the RF carrier must be tracked before the data can be detected, and this margin that we obtain in the carrier loop signal-to-noise ratio by using $4f_s$ as the subcarrier may be worth the increased complexity of the demodulator.

APPENDIX II. 0

SINEWAVE VERSUS SQUAREWAVE SIGNALLING

To determine which type of signalling is better to employ in the subcarrier modulation, the relationship for the total power division between the carrier and the subcarrier for squarewave and sinewave signalling at the different data rates is required. Curves in Figure II-1 give this relationship.

The top curve of Figure II-1 shows the division of power for squarewave signalling for different values of the PM modulation index. The bottom curve gives the same relationship for the sinewave signalling. Both of these curves are for the single channel modulation approach to data modulation, and no predection filter loss is considered for either.

From the curve, it is obvious that squarewave signalling has the power advantage over the sinewave signalling when the single channel approach to modulation is employed. There will be some filter losses in the subcarrier acquisition network when the squarewave signalling is employed, however, sufficient power is available at the data detector for a BEP of 5 x 10^{-3} so that the subcarrier channel can tolerate this loss (approximately 0.9 decibel). For the recommended approach of single channel modulation, squarewave signalling is therefore selected.

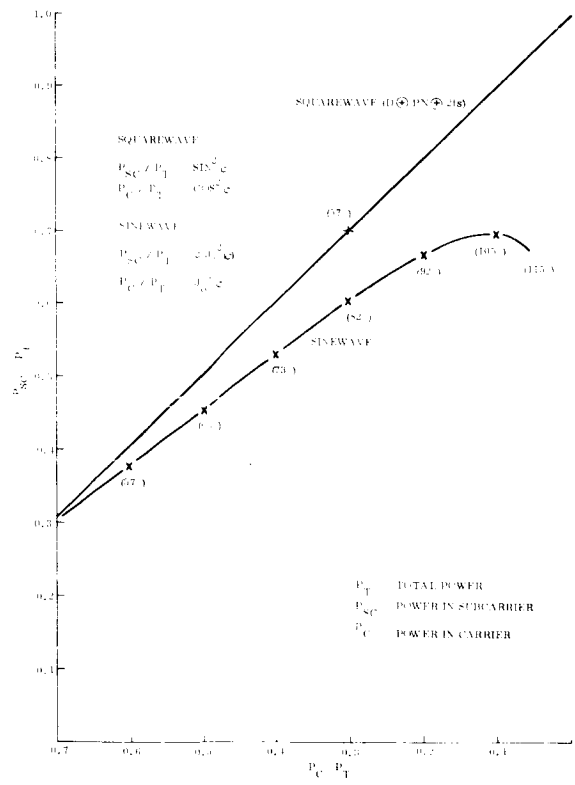

Figure II-1. Power Division Relationship

APPENDIX III. 0

SNR PERFORMANCE OF SUBCARRIER ACQUISITION MULTIPLIER

The purpose of this Appendix is to derive the output signal-to-noise ratio performance for the multiplier shown in Figure III-1.

The input signals to the multiplier are, from the low pass filter ($s_2 + n_2$) and from the demodulator input ($s_1 + n_1$). The output of the multiplier, Z, is given by

$$Z = s_1 s_2 + s_1 n_2 + s_2 n_1 + n_1 n_2$$

where

$$s_1 = D + PN + 2f_s \qquad s_1 s_2 = 2f_s = S_o(t) = \pm A^2$$

$$s_2 = D + PN$$

n_1 = input noise assumed normally distributed

n_2 = input noise that has been low passed filtered.

The power spectrum for the input signals are also given in Figure III-1. In the analysis we will assume that both the noise and random signal have zero mean value, and the product of the two signals $s_1 s_2$ will yield a squarewave which is a statistical constant $S_o(t)$ and is the desired output.

In the derivation of the SNR performance of the multiplier we will use the analysis of variance approach in order to resolve the dependency between the two noise signals, n_1 and n_2. The variance of the output, VAR(Z), will represent the output noise power and the output signal power will be the power in the squarewave $S_o(t)$. The variance of the input signals can be obtained by integrating over the spectra shown in Figure III-1. These are

$$VAR(s_1) = A^2$$

$$VAR(s_2) = A^2$$

$$VAR(n_1) = 16 f_s N_o$$

$$VAR(n_2) = 4 f_s N_o$$

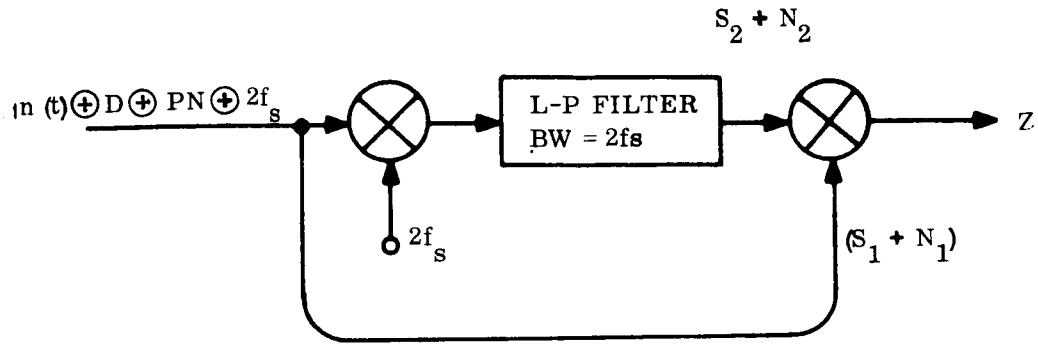

$$Z = (S_2 + N_2)(S_1 + N_1) = S_1S_2 + S_1N_2 + S_2N_1 + N2N1$$

where $S_2 = D \oplus PN$

$S_1 = D \oplus PN \oplus 2f_s$

$S_1S_2 = 2f_s = S_o(t)$ = A STATISTICAL CONSTANT

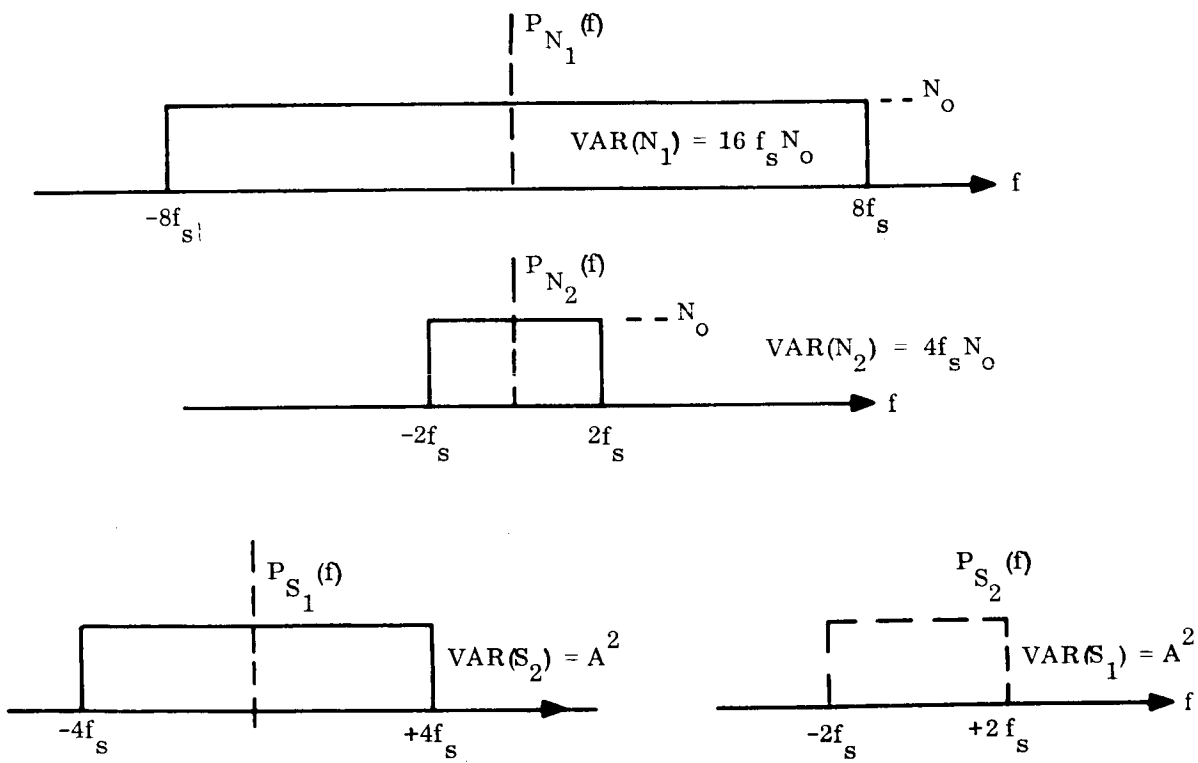

Figure III-1. Block Diagram of Multiplier, Output Equation and Input Power Spectrum

From the above relationship, it follows that the variance of the two noise terms are related:

$$VAR(n_2) = 1/4\ VAR(n_1)$$

The variance of the output signal VAR(Z) is given by

$$VAR\ (Z) = E(Z^2) - (E(Z))^2$$

Where E(Z) is the expected value of Z. From the expression for Z and the independency between the noise and the signal the following expressions can be derived:

$$E(Z) = S_o(t) + E(n_1 n_2)$$

$$E(Z^2) = S_o^2(t) + VAR(s_1)VAR(n_2) + VAR(s_2)VAR(n_1) +$$

$$E(n_1^2\ n_2^2) + 2S_o(t)E(n_1 n_2)$$

Substituting the values of the variances into the expression for VAR(Z) we have

$$VAR(Z) = 5/4\ A^2\ VAR(n_1) + VAR(n_1 n_2)$$

If we define the correlation coefficient, ρ, between the two noise terms as

$$\rho = \frac{E\{n_1 n_2\}}{\sqrt{VAR(n_1)VAR(n_2)}} = \frac{2E\{n_1 n_2\}}{VAR(n_1)}$$

and a relationship given by Deutsch (Reference 1) for the variance of the produce of two dependent gaussian distributed random varibales as

$$VAR(n_1 n_2) = (1 + \rho^2)VAR(n_1)VAR(n_2)$$

the output variance can be written as

$$VAR(Z) = \overline{A^2 5/4\ VAR(n_1) + \frac{(1+\rho^2)}{4}[VAR(n_1)]^2}$$

The input signal-to-noise ratio (S/N) will be defined as the power in the spectrum for s_1 to the power in the spectrum for n_1:

$$(S/N)_{in} = A^2/VAR(n_1) = A^2/16f_sN_o$$

For the squarewave, the output signal power will be defined as A^4 where the desired squarewave $S_o(t)$ is $\pm A^2$. Therefore, the output signal-to-nosie ratio of the multiplier is

$$(S/N)_{out} = \frac{4(SIN)_{in}^2}{5(S/N)_{in} + (1 + \rho^2)}$$

The correlation coefficient for the two noise signals can have any values between ±1. Therefore, the range of the output SNR can be stated as

$$(S/N)_{out}(max) = \frac{4(S/N)_{in}^2}{5(S/N)_{in} + 1}$$

$$(S/N)_{out}(min.) = \frac{4(S/N)_{in}^2}{5(S/N)_{in} + 2}$$

At high input signal-to-nosie ratios the output signal-to-noise ratio of the multiplier will approximately be the same for all values of ρ :

$$(S/N)_{out} = (4/5)\ (S/N)_{in} \quad ; \quad (S/N)_{in} >> 1$$

When the input signal-to-noise ratio is very small, the minimum SNR output of the multiplier is about three decibels lower than the maximum situation.

When ideal square filtering is assumed, the two noise terms, $n_1 n_2$, are independent random variables. This can be shown in the following manner: let the output term Z_1 be the product of the two noise terms

$$Z_1 = n_1 n_2$$

and consider the block diagram of Figure III-2. The input noise signal is low pass filtered to obtain n_2 and bandpass filtered to obtain another random variable n_3. These

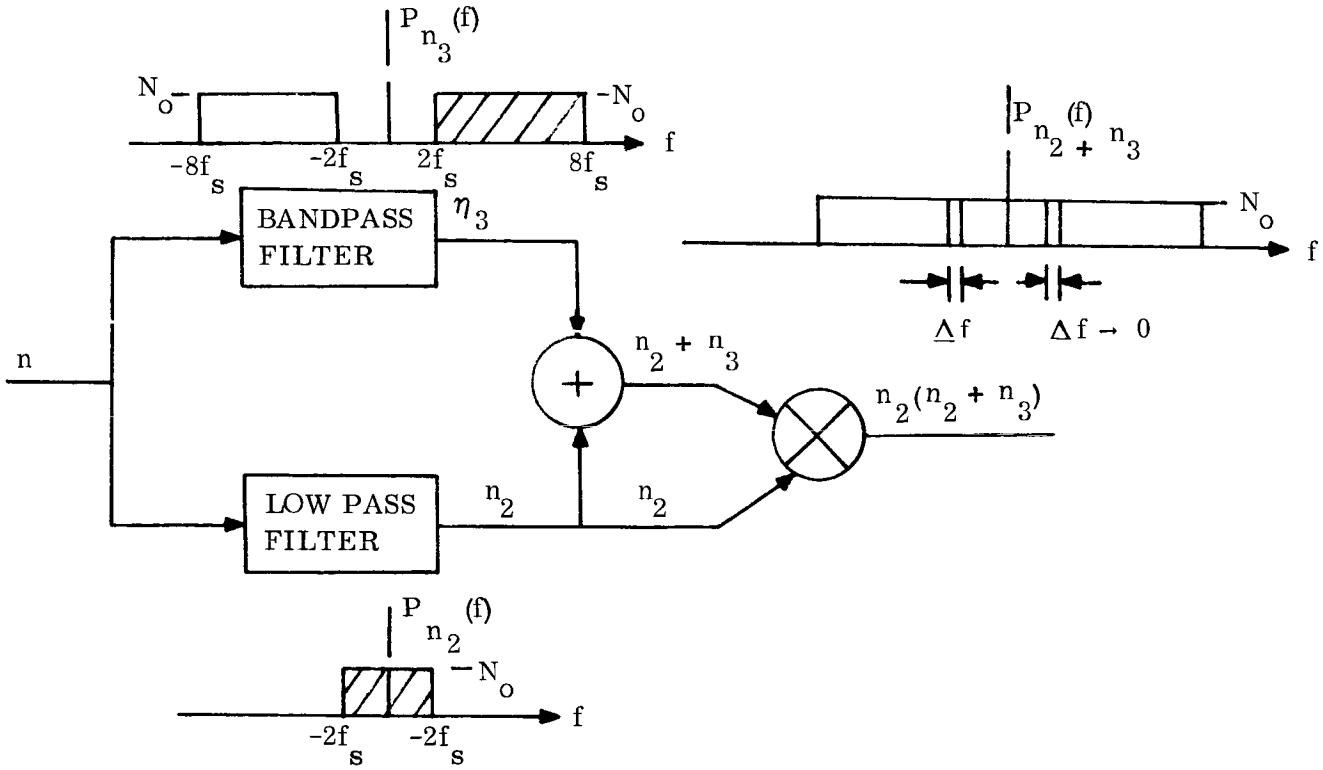

Figure III-2. Block Diagram and Noise Spectra Relationship

two random variables are added so that the desired noise term $n_1 = n_2 + n_3$ is obtained. The product $n_1 n_2 = n_2(n_2 + n_3)$ is then constructed.

The variance of n_1 is

$$VAR(n_1) = E(n_2 + n_3)^2 = E(n_2^2) + 2E(n_2 n_3) + E(n_3^2) = N_o 16 f_s$$

From the spectra shown in Figure III-2, the values of $E(n_2^2)$ and $E(n_3^2)$ are

$$E(n_2^2) = 4 f_s N_o$$

$$E(n_3^2) = 12 f_s N_o$$

Therefore, the only way in which $VAR(n_2) = N_o 16 f_s$, is for $E(n_2 n_3) = 0$. When this is true, the variance of Z_1

$$VAR(Z_1) = E(Z_1^2) - E(Z_1)^2 = VAR(n_1) VAR(n_2)$$

and the two noise terms n_1 and n_2 are independent.

The output power spectrum of the multiplier can be obtained by convolving the product terms in the expression for Z when the two noise terms are independent. Regardless of whether or not the two noise terms are independent, an expression for the output power spectrum can be obtained by first obtaining the correlation function for the output signal Z.

The power spectrum obtained from the correlation function for Z is

$$P_Z(f) = P_{so}(f)\,(1 + \rho^2)\,\sigma_{n_1}^2 \sigma_{n_2}^2\,\delta(f) + \overbrace{\int_{-\infty}^{\infty} Ps_1(f')Pn_2(f-f')\,df'}^{I_1} +$$

$$\overbrace{2\int_{-\infty}^{\infty} P_{s_1 x s_2}(f')P_{n_1 n_2}(f-f')df'}^{I_2} + \overbrace{\int_{-\infty}^{\infty} Pn_1(f')Ps_2(f-f')\,df'}^{I_3} +$$

$$\overbrace{\int_{-\infty}^{\infty} Pn_1(f')Pn_2(f-f')df}^{I_4} + \overbrace{\int_{-\infty}^{\infty} Pn_{1 x n_2}(f')\,P_{n_1 x n_2}(f-1')\,df'}^{I_5}$$

where the P(f) represent the power spectrum of the particular signal of interest, ρ is the correlation coefficient between the noise signals, and $P_{S_o}(f)$ is the power spectrum of the output squarewave

where

$$P_{s_1 \times s_2}(f) = \int_{-\infty}^{\infty} R_{s_1 \times s_2}(\tau)\, e^{j\omega\tau} d\tau$$

$$R_{s_1 \times s_2}(\tau) = E\left\{S_1(t) S_2(t+\tau)\right\}$$

$$P_{n_1 \times n_2}(f) = \int_{-\infty}^{\infty} R_{n_1 \times n_2}(\tau)\, e^{j\omega\tau} d\tau$$

$$R_{n_1 \times n_2}(\tau) = E\left\{n_1(t) n_2(t+\tau)\right\}$$

When the noise terms are independent, the I_2 and I_4 terms in the expression for P_Z (F) reduce to zero as well as $\rho = 0$.

We can estimate the noise bandwidth BWN of the multiplier by this equation:

$$BW_N = \frac{1}{P_Z(2fs)} \int_{o}^{\infty} P_Z(f) df$$

If we assume that we will always banpass filter the output of the multiplier, the D-C spectral spike can be ignored in the estimate of the effective noise bandwidth of the multiplier. For the ideal filter situation, the output spectrum can be obtained by convolving the proper input spectrum of Figure III-1 and the resulting effective noise bandwidth is

$$BW_N = 8fs \left\{ \frac{5\,(SIN)_{in} + 1}{6\,(SIN)_{in} + 1} \right\}$$

In the SNR calculations of Section 11, we will assume ideal square filtering, therefore, the output signal-to-noise ratio of the multiplier as well as the effective noise bandwidth for the independent noise signals will be used.

When the output squarewave is bandpass filtered to obtain the fundamental frequency of $2f_s$, a 0.9 db loss will have to be considered to account for the sideband power loss of the squarewave.

III.1 References

1. Deutsch, Ralph, "Nonlinear Transformations of Random Processes," p.43, Prentice-Hall, Inc., 1943.

APPENDIX IV. 0

PN CODE ACQUISITION DECISION ANALYSIS

IV. 1 SEARCH ANALYSIS

In analyzing the search routine, we will assume that we have "L" states or cells which we have to search. For searching a PN code, L represents the length of the code. As we search each cell four possible events pertaining to the decision process can occur:

a. the event that sync is present, and the detection circuit indicates sync

b. the event that sync is not present, and is so indicated

c. the event that sync is not actually present but the detection circuit indicates sync (False Alarm or α type error)

d. the event that sync is actually present but the detection circuit fails to indicate sync (False Dismissal, β type error)

These last two events are the errors associated with the signal detection process. The probabilities of occurrence of these errors are defined from the probability density function for the output of the correlator when the codes are in-sync and when the codes are out-of-sync.

Let $p_0(Z)$ be the probability density function for the output of the correlator when the codes are out-of-sync and let $p_1(Z)$ be the density function when the codes are in-sync where Z is the random variable that represents the output of the correlator. A sketch of these density functions is shown in Figure IV-1.

The probability of a false alarm, α, is defined as the area under $p_0(Z)$ to the right of the detection threshold level, Z_T:

$$\alpha = \int_{Z_T}^{\infty} p_0(Z)dZ$$

The probability of false dismissal, β, is defined as the area under $p_1(Z)$ to the left of the threshold setting:

$$\beta = p_1(Z)\, dZ$$

IV. 2 AVERAGE TIME REQUIRED TO SYNC, t_1

The sequential search routine for acquiring sync is a discrete Markov process that can be analyzed by signal flow graph techniques (Reference 1). The tactics used to find the average time required to sync are the same as those employed to find the average length of a game of chance by a Markov process. The use of the signal flow graphs allows us to approach the problem in a well known straight forward manner.

The method used in this type of analysis is to:

a. Develop the signal flow graph for the particular search routine of interest

b. Derive the transmittance of the flow graph between the start and the end-of-search

c. Obtain the average time or the length of the game differentiation of the transmittance with respect to the time delay variable, Z, and then setting Z = 1.

By a similar procedure, we can obtain the other moments of the distribution of the synchronization time.

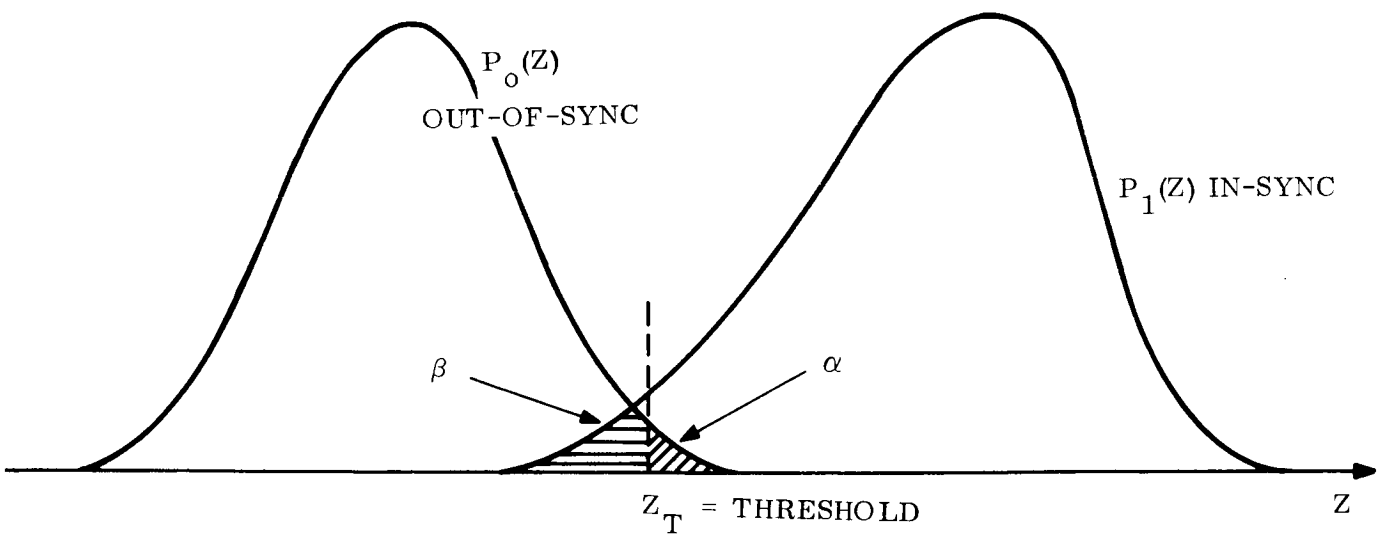

Figure IV-1. Representative Probability Density Functions for the Output of the Correlator

The graph used by McBride for the complete search routine is shown in Figure IV-2. In this graph, the time lost due to false alarm is assumed to be a constant "b". For his analysis to adapt to our problem, the time lost due to a false alarm will have to be a random variable that depends on the tactics used in the sync acquisition routine. Before we can define the false alarm signal flow graph, it will be necessary to establish a satisfactory search routine for sync acquisition.

In this analysis we will not try to define an optimum search routine for PN sync acquisition, but will only define a reasonable search routine that can be analyzed rather easily since the purpose of the analysis is to compare the efficiency of the competing systems for a particular search routine. The search routine will be the same for all PN systems. This is the search routine that we will use:

> "When a sync indication occurs regardless of its validity, data handling will start looking for frame sync. As we search for frame sync, the incoming and the local PN-codes will continuously be correlated. Should an out-of-sync indication occur during any of these searches, the control system will store the first and wait until the next occurs. On the second occurrence of the out-of-sync indication, the control will delay the local PN-code by one bit then continue with the search. After an in-sync indication and when frame sync occurs, the out-of-sync accumulator will be cleared and the search routine set up to handle out-of-lock indications,"

Since on an average many PN-code correlations will take place before frame sync is located, we can simplify the analysis without introducing too great an error by allowing this time to approach infinity. When we do this, we can obtain a close approximation to the actual process with the signal flow graph shown in Figure IV-3.

This graph of Figure IV-3 is a modification of McBride's graph for searching the first cell or state of the PN-codes. In our graph, going from node C_{11} to node C_{12} with probability $(1 - P_1)$ indicates that this particular alignment of the PN-codes does not match; now the network must make a decision. If the decision is true, the search will go to the next cell (node C_{21}) with probability $(1 - \alpha)$, and proceed to search that cell. On the other hand, if the decision is in error, we continue searching the same cell but now move to node C_{13} with probability α_Z .

When the search routine arrives at node C_{13}, the control network is erroneously informed that sync has occured and the search for frame sync is started. If at the next correlation of the same code alignment no in-sync indication is observed, the search moves to node C_{16}. If again on the next correlation of the same code alignment no in-sync indication is observed, the local PN-code will be delayed one bit and the search continued. This is the general procedure carried-out for all paths from node C_{11} to node C_{21}, i.e., two out-of-sync indications must occur before the search is continued.

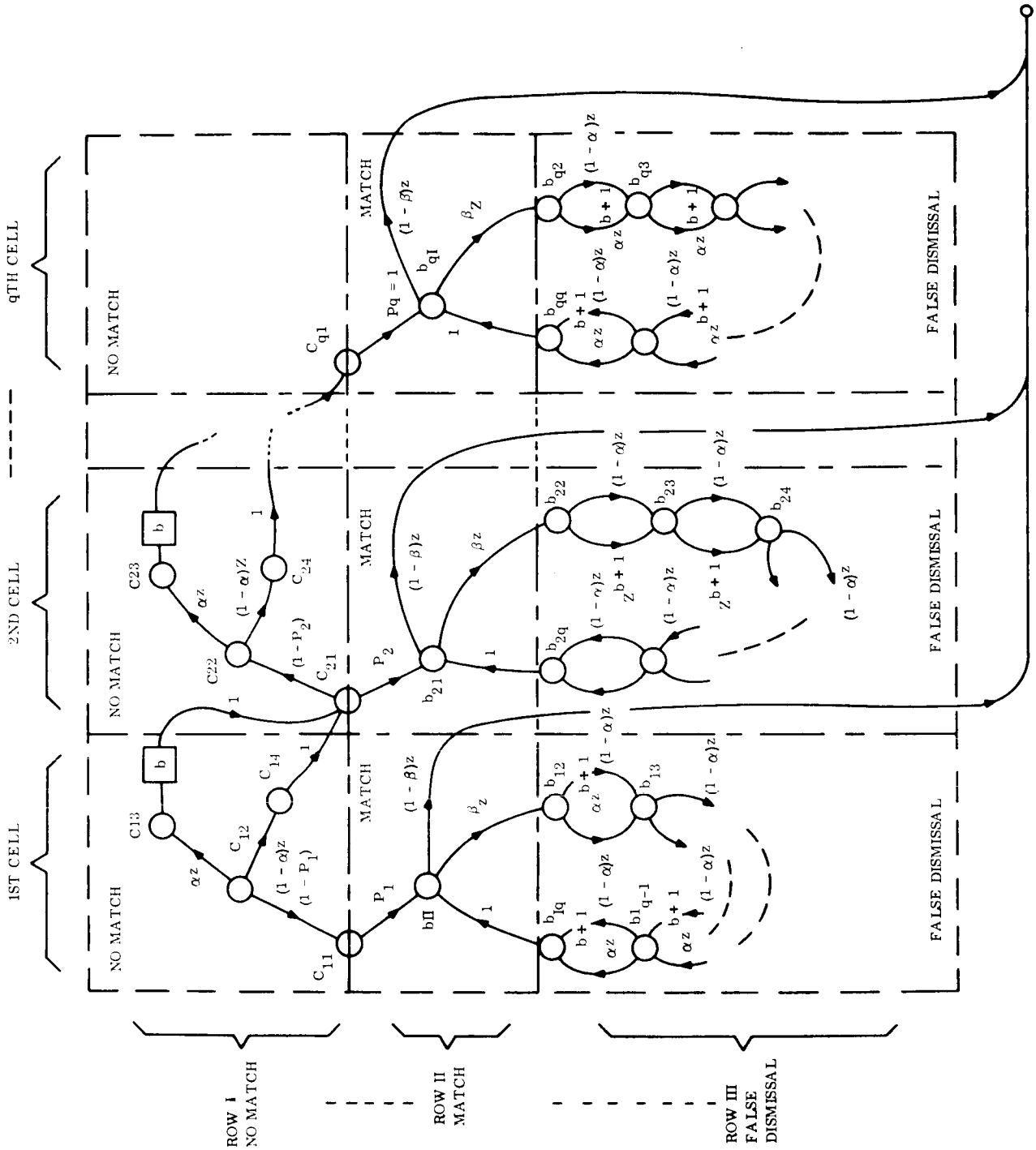

Figure IV-2. Complete Signal Flow Diagram for the Sequential Search Routing

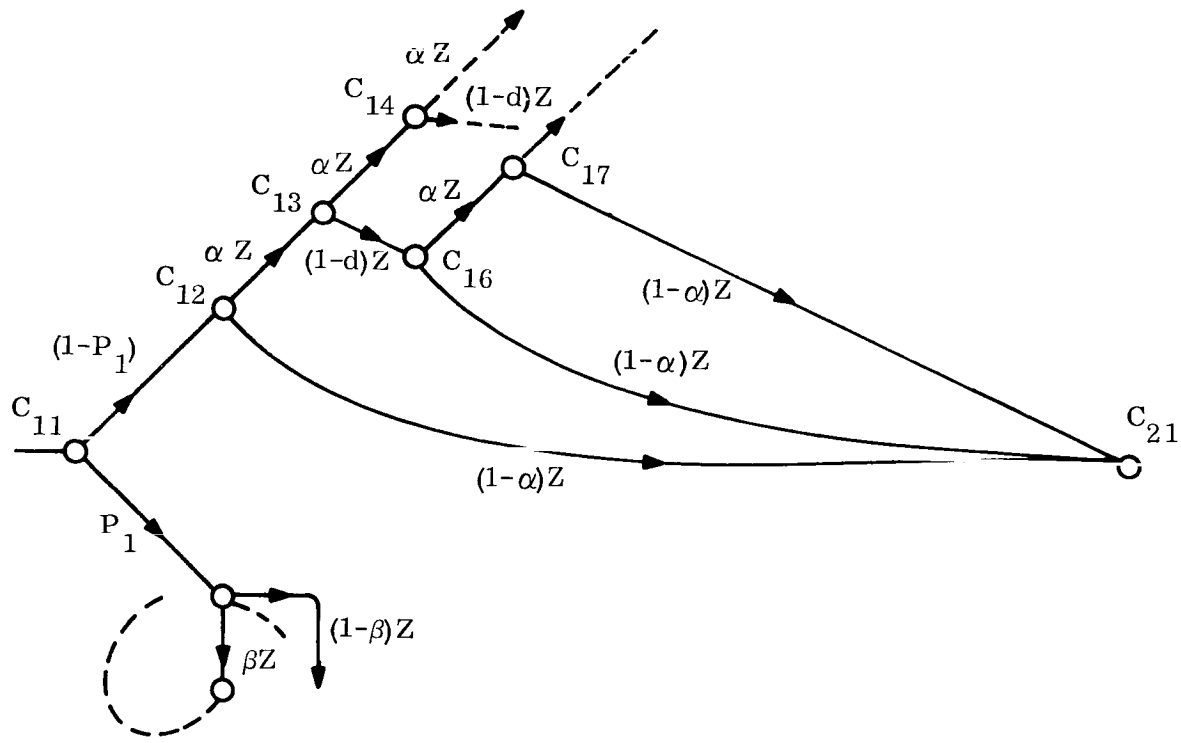

EQ 1 $$T_{C_{13}-C_{21}} = (1-\alpha)Z \quad (1-\alpha)Z + \alpha Z(1-\alpha)Z + \alpha^2 Z^2 (1-\alpha)Z + \ldots$$

EQ 2 $$F(Z) = T_{(C_{13}-C_{21})}(Z) = (1-\alpha)^2 \sum_{k=0}^{\infty} \alpha^k Z^{k+2}$$

EQ 3 $$T_{C_{11}-C_{21}}(Z) = (1-P_1) \quad (1-\alpha)Z + \alpha Z F(Z) + \alpha^2 Z^2 F(Z) + \ldots$$

$$= (1-P_1) \quad (1-\alpha)Z + F(Z) \sum_{n=1}^{\infty} \alpha^n Z^n$$

LET $B(Z) = \sum_{n=0}^{\infty} \alpha^n Z^n$

EQ 4 $$T_{C_{11}-C_{21}}(Z) = (1-P_1) \quad (1-\alpha)Z - F(Z) + F(Z)B(Z)$$

LET $H(Z) = (1-\alpha)Z - F(Z) + F(Z)B(Z)$

EQ 5 $$T_{C_{11}-C_{21}}(Z) = (1-P_1)\, H(Z)$$

Figure IV-3. Signal Flow Graph for Searching the 1st Call in the Search Routine and the Appropriate Transmittance Equations

Other search routines could be employed such as having two out of three out-of-sync indications occur before the search is continued or two successive out-of-sync indications and so on. Since this particular analysis is not to be used as an absolute measure of the average time to sync, but only used for efficiency comparison of competing sync systems the type of search routine is not too important. The only constraint is that it must be reasonable.

The transmittance equations are shown in Figure IV-3. The transmittance from node C_{11} to node C_{21} is given by Equation 5 and is

$$T_{C_{11} - C_{21}}(Z) = (1 - P_1)H(Z)$$

where P_1 is the probability that the correct alignment of the codes will occur in the first cell search, and H(Z) is the transmittance between nodes C_{12} and C_{21}. Except for the precise value of $H(Z)_1$ this is the same equation obtained by McBride for his search routine. Therefore, we may use the total graph transmittance T(Z) that he has derived:

$$T(Z) = \frac{(1 - \beta)Z}{L\left\{1 - \beta Z[H(Z)]^{L-1}\right\}} \sum_{n=0}^{L-1} \left[H(Z)\right]^n$$

where L = the length of the PN code.

The average time required to sync, t_1, is given by the following equation:

$$t_1 = T_o \left(dT(Z)/dZ\right)\Big|_{Z=1}$$

where T_o is the integration time of the correlator.

In performing the differential of T(Z), H(Z) and dH(Z)/dZ need to be evaluated for Z=1. By taking the derivative of the infinite series contained in H(Z) and making use of the identities:

$$\sum_{n=0}^{\infty} \alpha^n = \frac{1}{(1 - \alpha)}$$

$$\sum_{n=o}^{\infty} n\alpha^{n-1} = \frac{1}{(1 - \alpha)^2}$$

H(Z) and dH(Z)/dZ reduce to

$$H(Z)\Big|_{Z=1} = 1$$

$$dH(Z)/dZ\Big|_{Z=1} = \frac{(1+\alpha)}{(1-\alpha)}$$

For length of the code L >>1, the expression for the average time required to sync, t_1, reduces to

$$t_1 = \left(\frac{T_o L}{2}\right)\left\{\frac{(1+\alpha)\,[\,1-\beta+\beta^2\,]}{(1-\beta)\,(1-\alpha)}\right\}$$

where

T_o = the integration time of the correlator

L = the length of the PN code

β = the probability of a false dismissal

α = the probability of a false alarm

The average time required to sync in the error free situation can be obtained by setting α and β equal to zero. When this is done, the average time required to sync, for the error free search becomes:

$$t_1 = T_o L/2$$

In Figure IV-4, the increase in the error free average time required to sync is plotted for $\alpha = 0$, the curve on the right, and for $\beta = 0$, the curve to the left. For values of α and β greater than zero the true increase in the error free average time required to sync will lie to the left of the curve $\beta = 0$. This indicates that the α type of decision error will cost us the most in the time required to sync the PN-codes.

In Figure IV-5 the increase in error free average time required to sync is plotted for $\alpha = \beta$. This is probably not the best selection of the α and β relationship, but it does give us some idea of anticipated average time required to sync the PN-codes. When $\alpha = \beta = 0.05$, there is a 10 per cent increase in the average time required to sync above the error free situation. It will be shown later in the analysis $\alpha = \beta = 0.05$ is a reasonable constraint to impose on the system. Therefore, it would appear that a 10% increase in the error-free average time required to sync the

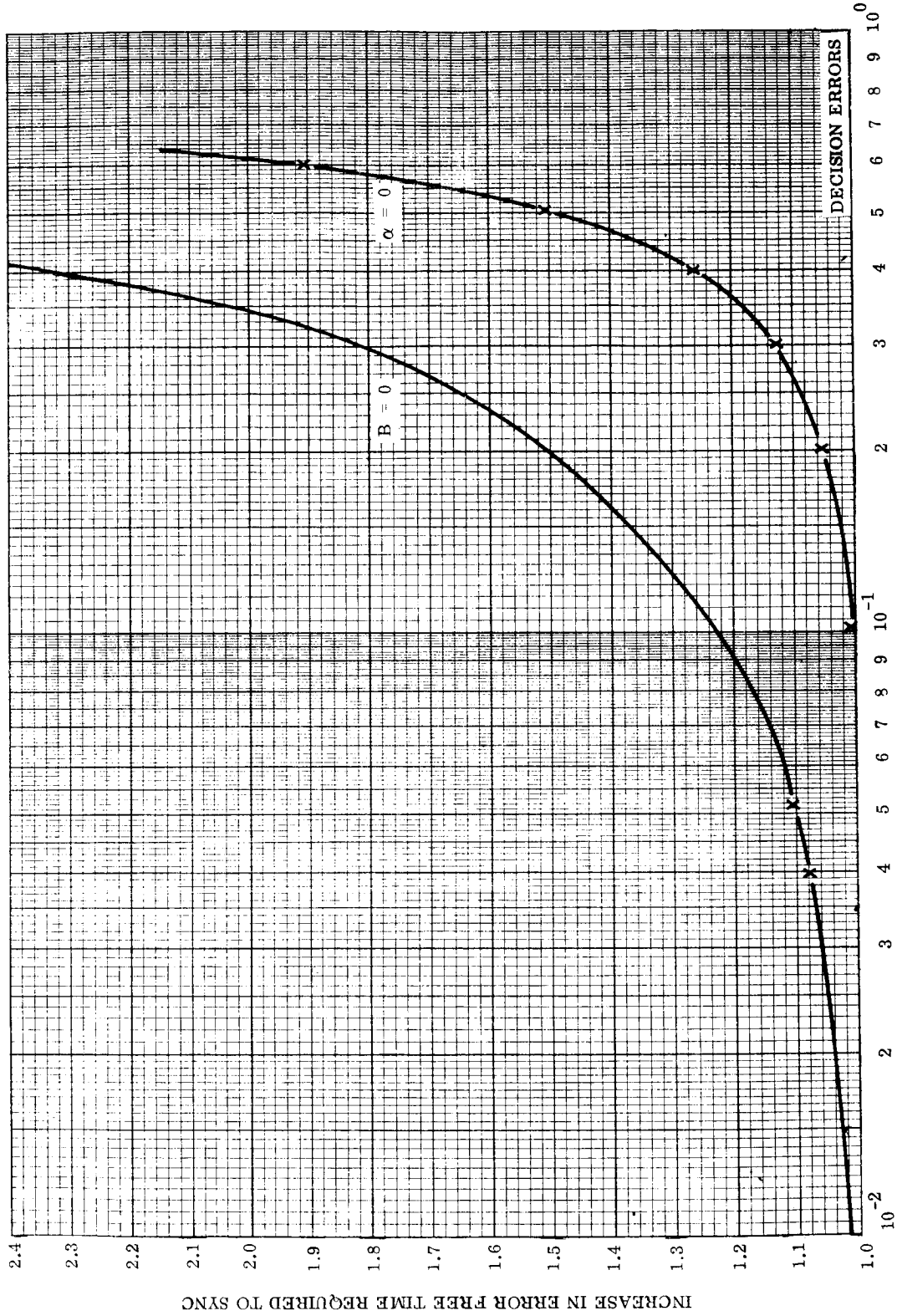

Figure IV-4. Increase in the Error-Free Average Time Required to Sync the PN Codes for (1) $\beta = 0$ and α Varies and (2) when $\alpha = 0$ and β Varies

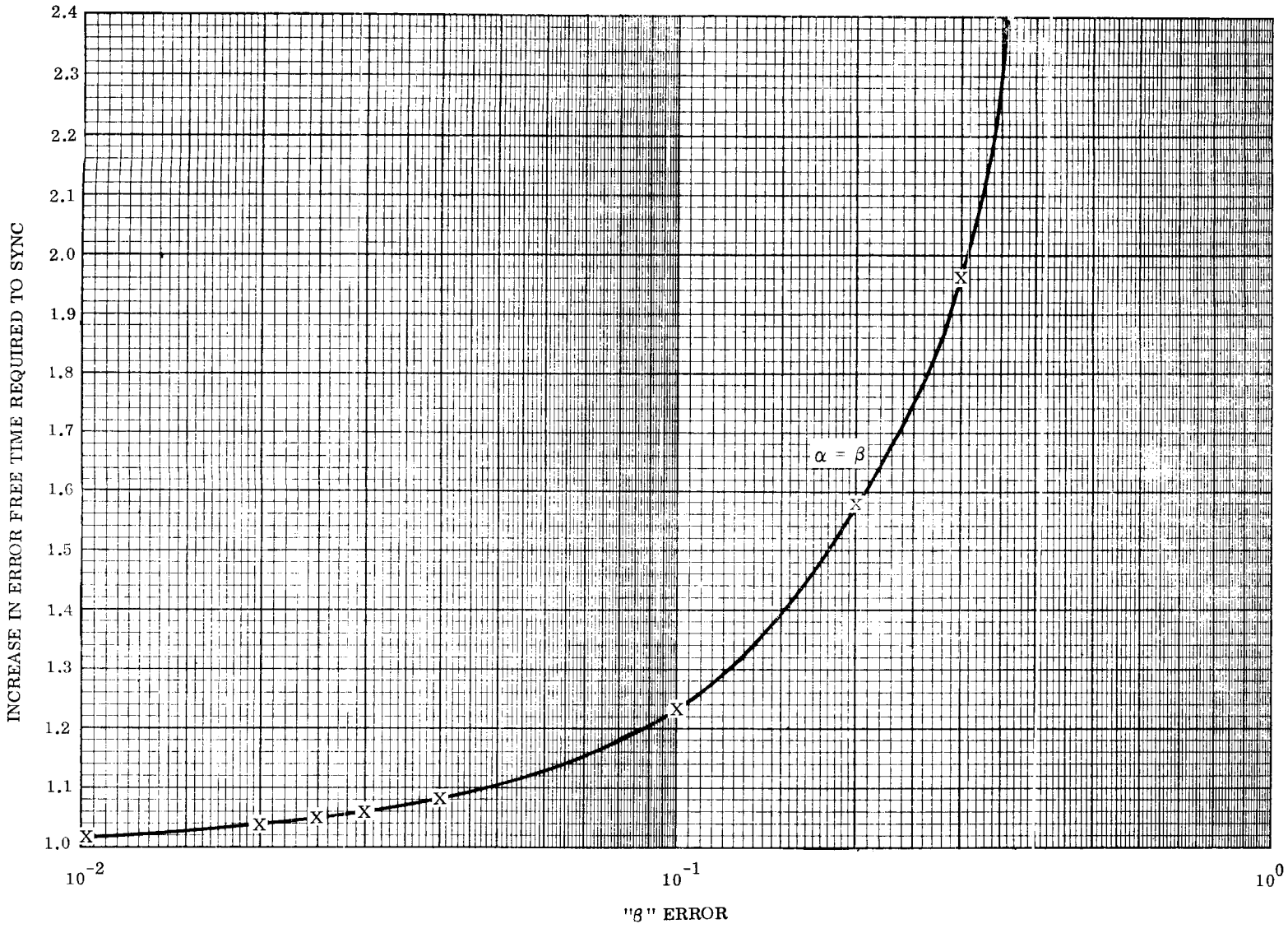

Figure IV-5. Increase in the Error-Free Average Time Required to Sync the PN Codes when the α and β Errors Have Equal Probability of Occurring, i.e., $\alpha = \beta$

PN-codes is so small compared to the length of transmission time that it could be ignored in the analysis. This would be the case if we had only to sync the system once during a transmission. Unfortunately, as we allow α and β to increase the system will lose sync quite often and must be re-synchronized again. Therefore, the average time required to sync must be complemented by the average time the system stays synchronized.

IV.3 REFERENCES

1. McBride, Alan L., " Synchronization Detection Analysis by Signal Flow Graph Techniques, " Ninth National Communication Symposium Record, p. 268, October 1963.

APPENDIX V.0

ESTIMATE OF THE PROBABILITY, P_1

The probability, P_o , that the clock acquisition PLL will slip a cycle of the sub-carrier is the probability that random phase jitter caused by the noise will exceed a certain value. For an ideal linear PLL, the frequency should not slip a cycle until the ramdom phase jitter, θ, exceeds $\pi/2$ radian. However, since we do not have an ideal PLL we will assume that $\theta \geqq \pi/4$ radians will cause the PLL to slip a cycle causing the codes to be out of alignment.

To determine this probability, we will assume gaussian noise in the PLL; therefore, the random phase jitter, θ, can be described by a normal distribution of zero mean and variance, σ_θ^2, where

$$\sigma_\theta^2 = (1/2)(N/S)$$

with S/N = the signal-to-noise ratio in the loop. Thus, P_o can be represented by an error function equation as

$$P_o = P_r(\theta \geq \pi/4) = (1/2)\left\{ 1 - \mathrm{erf}\left[(\pi/4)\sqrt{S/N}\right]\right\}$$

For S/N $\geq$ decibels (this must always be the case for proper data detection), P_o becomes

$$P_\theta \geq 2.3 \times 10^{-4}$$

For an arbitrary δ that will cause PLL to lose lock

$$P_o = P_r(\theta \geq \theta^1) = 1/2\left\{1 - \mathrm{erf}\left(\theta^1\sqrt{(S/N)_{PLL}}\right)\right\}$$

This probability, P_o, is the probability that one noise spike will force the PLL out of lock. The probability that is needed in the analysis of the average time till out of sync occurs in the probability that the PLL will lose sync during the total correlation period, T_o.

The number of noise spikes, m, that can enter the PLL during one second can be estimated by

$$M = 2B_L$$

where 2 B_L is the loop noise bandwidth. During the correlation time, T_o, the number of possibilities to lose lock that the PLL encounters is the number of noise spikes that will enter the loop. This number is

$$T_o m = T_o 2B_L$$

The probability, P_1, that the PLL will lose lock when $T_o 2B_L$ spikes enter the system is one minus the probability that lock will not be lost on any of the $T_o 2B_L$ spikes:

$$P_1 = 1 - (1 - P_o)^{T_o 2B_L}$$

APPENDIX VI.0

PROBABILITY DENSITY FUNCTION FOR CORRELATOR OUTPUT

To estimate the α and β probabilities of errors, we need to derive the probability density function for the output of the correlator. Since there are two approaches that can be used to align the incoming and local PN codes, the single channel and the double channel approach, two models of the correlation process need be analyzed. The double channel system will be analyzed first since of the two techniques, it is much the easiest to analyze. A block diagram of the double channel PN code acquisition detector is shown in Figure VI-1.

V1.1 CORRELATOR OUTPUT P.D.F. (DOUBLE CHANNEL SYSTEM)

The density function to be derived will be for the output of a correlator which can be expressed by $Z(\tau)$

$$Z(\tau) = \frac{1}{2f_s} \int_o^T X(t)\, Y(t+\tau)dt.$$

where X(t) is the incoming signal and Y(t) is the local signal. When X(t) and Y(t) are bandwidth limited functions between $-f_s$ and f_s, the integral can be approximated by

$$Z = \sum_{i=1}^{k} X_i Y_i$$

where X_i and Y_i are k samples at the Nyquist interval corresponding to T and W of the incoming and locally generated sync codes, respectively. If the incoming signal is perturbed by additive gaussian noise, Z can be expressed as

$$Z = \sum_{i=1}^{k} X_i Y_i = \sum_{i=1}^{k} \left(AS_{xi} + N_{xi}\right) S_{yi} = \sum_{i=1}^{k} AS_{xi} S_{yi} + \sum_{i=1}^{k} N_{xi} S_{yi}$$

where S_{xi} and S_{yi} are the signal samples and N_{xi} is a sample of gaussian noise.

Roe and White (Reference 1) have derived the probability density function for the output of a correlator when both the local and the reference signal were perturbed by additive gaussian noise. In their derivation, the signal components S_{xi} and S_{yi} were statistical constants, but for our present problem these signals will appear as random variables taking on assumed values of ±1 with probabilities defined by the sync code structure.

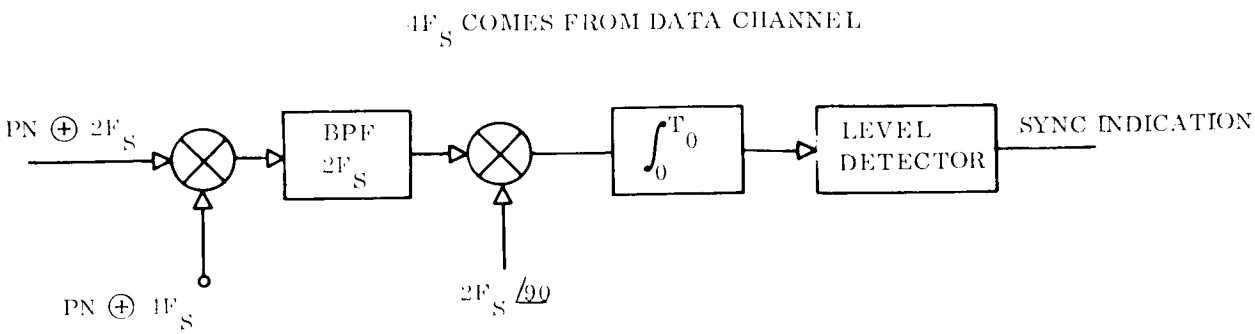

Figure VI-1. Block Diagram of the Double Channel PN Code Acquisition Detector

The derivation is simplified if we assume that we integrate over exactly one code length or multiples of one code length since the correlation function for the PN codes is a two value function when the integration period is over the code length. The output probability density function of the correlator has been derived (Reference 2) for very long codes and when the integration period is not over a multiple of the code length, and as would be expected, the distribution has a wider spread (larger variance) for this situation. The larger spread will necessarily increase the α and β probabilities. Therefore, we will confine this derivation to integration periods that are multiples of the code lengths, and k, the number of samples, will now be equal to the code length, . L = k.

We will begin our derivation by considering the ith sample Z_i from the output of the correlator where

$$Z_i = AS_{x_i} S_{y_i} + N_{x_i} S_{y_i}$$

The last term, $N_{x_i} S_{y_i}$, is the product of two independent random variables with probability density functions defined as

$$p(S_{y_i}) = 1/2\,\delta(S_{y_i} - 1) + 1/2\,\delta(S_{y_i} + 1)$$

$$p(N_{x_i}) = (1/\sqrt{2\pi\sigma_N})\,\mathrm{EXP}\,(-N_{x_i}^2/2\sigma_N^2)$$

where δ is the delta function and S_{y_i} can take values of ±1 with equal likely probability. What must be done now is to derive the probability density function for a new random variable, $\varphi_i = S_{y_i} N_{x_i}$. The transformation that we need to perform is to determine the probability density function $p(\varphi_i N_{x_i})$ then integrate over all N_{x_i}

where

$$p(\varphi_i, N_{x_i}) = p(N_{x_i}, S_{y_i}) \cdot |J| = P(N_{x_i})\, p(S_{y_i}) / |N_{x_i}|$$

In the above equation $|J|$ is the Jacobian of the transformation. In performing the integration we must take care not to integrate through the singularity at the origin. Performing the integration we see that the random variable φ_i is normally distributed with zero mean and variance, σ_N^2

$$p(\varphi_i) = (1/\sqrt{2\pi\sigma_N})\,\mathrm{EXP}\,(-1\,\varphi_i^2/2\sigma_N^2)$$

The sum of L of these random variables, $W_1 = \sum_i^L \varphi_i$, gives a new probability density function $p(W_1)$ of

$$p(W_1) = (1/\sqrt{2\pi L\sigma_N})\,\mathrm{EXP}\,(-W_1^2/2L\sigma_N^2)$$

The other term in Z_i which we must consider is

$$AS_{x_i} S_{y_i}$$

This term depends solely on the properties of the PN code, and when we integrate over multiple code lengths it can take on only two values defined for the in-sync and out-of-sync conditions of the code

$$\text{(in-sync)} \quad \sum_{L=1}^{L} AS_{x_i} S_{y_i} = LA$$

$$\text{(out-of-sync);} \quad \sum_{L=1}^{L} AS_{x_i} S_{y_i} = -A$$

Therefore, the output probability density function of the correlator is, for both cases, a normally distributed random variable plus a constant.

For the in-sync case, $Z = W_1 + LA$, which has a probability density function, $p_1(Z)$ of

$$p_1(Z) = (1/\sqrt{2\pi L}\,\sigma_N)\ \mathrm{EXP}\left\{-(Z - LA)^2/2L\sigma_N^2\right\} \quad \text{(in-sync)}$$

and for the out-of-sync codes, $Z = W_1 - A$ which has a probability density function, $p_o(Z)$, of

$$p_o(Z) = (1/\sqrt{2\pi L}\,\sigma_N)\ \mathrm{EXP}\left(-(Z + A)^2/2L\sigma_N^2\right) \quad \text{(out-of-sync)}$$

A sketch of these two density functions is given in Figure VI-2. The threshold that must be exceeded before the equipment assumes the codes are in-sync is defined as Z_T on the sketch of Figure VI-2.

VI.2 DEFINITION OF THE α AND β PROBABILITIES

The α and β error probabilities are defined from the area under the curve as given by the following two equations:

$$\alpha = \int_{Z_T}^{\infty} P_o(Z)dZ$$

$$\beta = \int_{-\infty}^{Z_T} P_1(Z)dz$$

By using the error function definition [erf(x)] derived from integrating the normal distribution, the α and β probabilities become

$$\alpha = 1/2\ (1 - \mathrm{erf}\left\{(Z_T + A)/\sqrt{2L}\,\sigma_N)\right\}$$

$$\beta = 1/2\ (1 - \mathrm{erf}\left\{(LA - Z_T)/\sqrt{2L}\,\sigma_N)\right\}$$

If we now let $\alpha = \beta$, we can solve for the threshold setting Z_T which must be pre-set. We find that the threshold is

$$Z_T = A(L - 1)/2$$

For $L >> 1$, Z_T reduces to

$$Z_T = AL/2$$

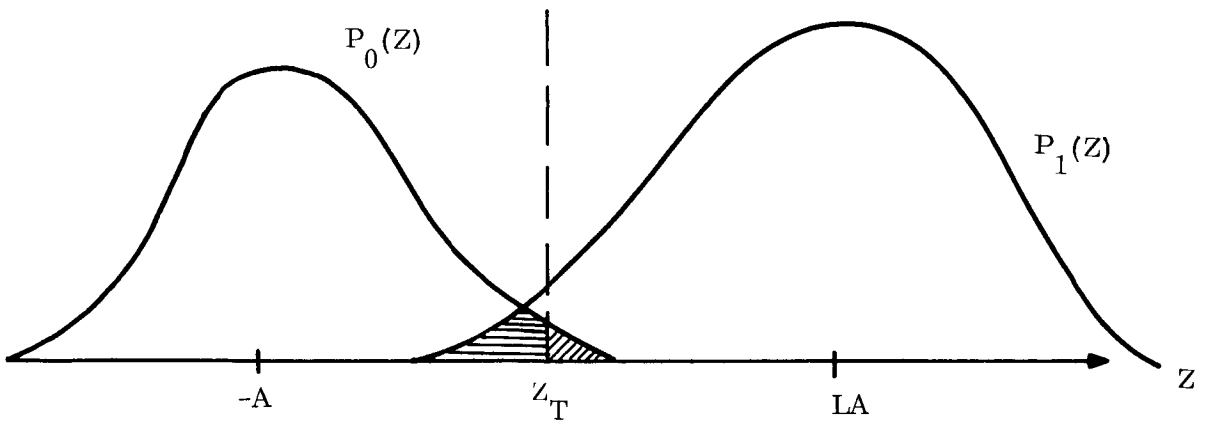

Figure VI-2. In-sync and Out-of-sync Probability Density Functions

The α and β probabilities then become

$$\alpha = \beta = 1/2 \left[1 - \text{erf} \left\{ \left(\frac{A}{\sigma_N} \right) \frac{\sqrt{L}}{2\sqrt{2}} \right\} \right]$$

The parameter A/σ_N, is the voltage signal-to-noise ratio at the input to the correlator. When we wish to integrate over more than one code length all that we need to do is let $L = kL'$ where $k = 2,3,\ldots$ and L' is one code length.

Figure VI-3 is a plot of the decision errors as a function of the input signal-to-noise ratio to the correlator for a code length, $L = 63$.

VI.3 CORRELATOR OUTPUT P.D.F. (SINGLE CHANNEL SYSTEM)

The derivation of the probability density function for the output of the PN-code alignment correlator for the double channel system was a rather straightforward derivation since the input signal did not undergo any nonlinear transformations. However, in the single channel approach, before the PN-codes can be correlated, the data must be removed from the signal since in this approach the PN-code and the data are both time multiplexed onto the subcarrier.

A block diagram of a typical single channel subcarrier demodulator for the single channel system is shown in Figure VI-4. For the code synchronization, the input signal $(PN \oplus 2f_s \oplus D)$ is brought into an in-phase and quadrature channel. The subcarrier clock is acquired from the data channel by phase locked loop techniques. Once the clock is acquired the local PN code can be stepped along a bit at a time until the incoming and local codes are in time alignment.

When the codes are aligned, the output of the top phase comparator is $f_s \underline{|90^\circ} \oplus D$, and the output of the bottom phase comparator of Figure VI-4 is $(2f_s \oplus D)$. These two signals are then passed through a bandpass filter which has sufficient bandwidth to

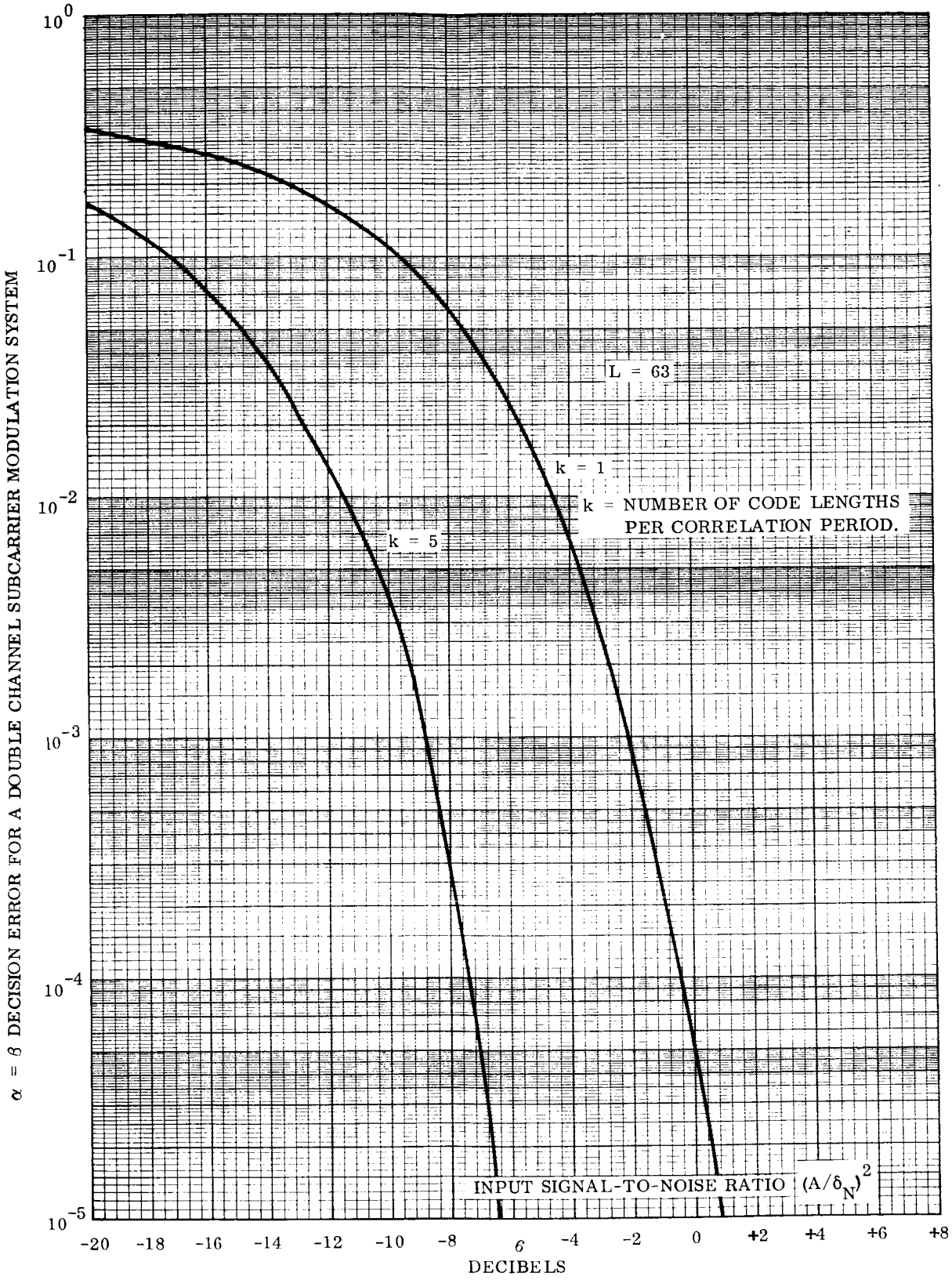

Figure VI-3. β Error Probability as a Function of Double Channel Correlator Input SNR

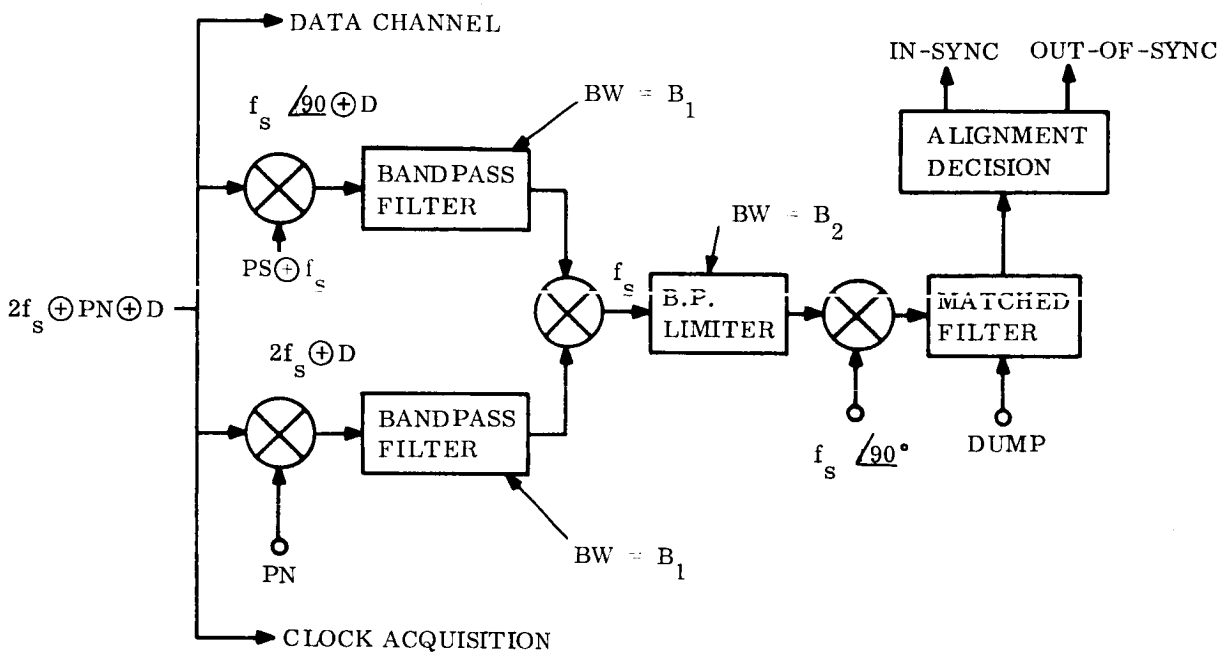

Figure VI-4. Block Diagram for a Typical Single Channel Subcarrier Demodulator Employing a Digital Search Routine to Align PN Codes

pass the data spectrum. If the data rate is denoted as "R" the bandwidth of these bandpass filters must at least be 2R to pass approximately 86 percent of the data spectrum. After passing through these filters, the in-phase and quadrature channels are multiplied together to eliminate the data. The output of the multiplier is again filtered and then passed to the sync code alignment matched filter (integrate and dump circuit).

Since the multiplication of the in-phase and quadrature channel introduces a nonlinearity into the signal processing, the derivation of the probability density function for the output of the code correlator will be very difficulty to derive--particularly for the out-of-sync condition of the codes. However, since we have based the analysis of the double channel system on $\alpha = \beta$ error probabilities, we can obtain an estimate of the performance of the single channel code correlator by obtaining only the β error probability. Fortunately, the β error probability is defined from the in-sync probability density function which can be estimated without too much difficulty.

When the codes are in-sync or aligned, the power spectrum of the noise at the output of the multiplier can be represented by the sketch shown in Figure VI-5 (Reference 3).

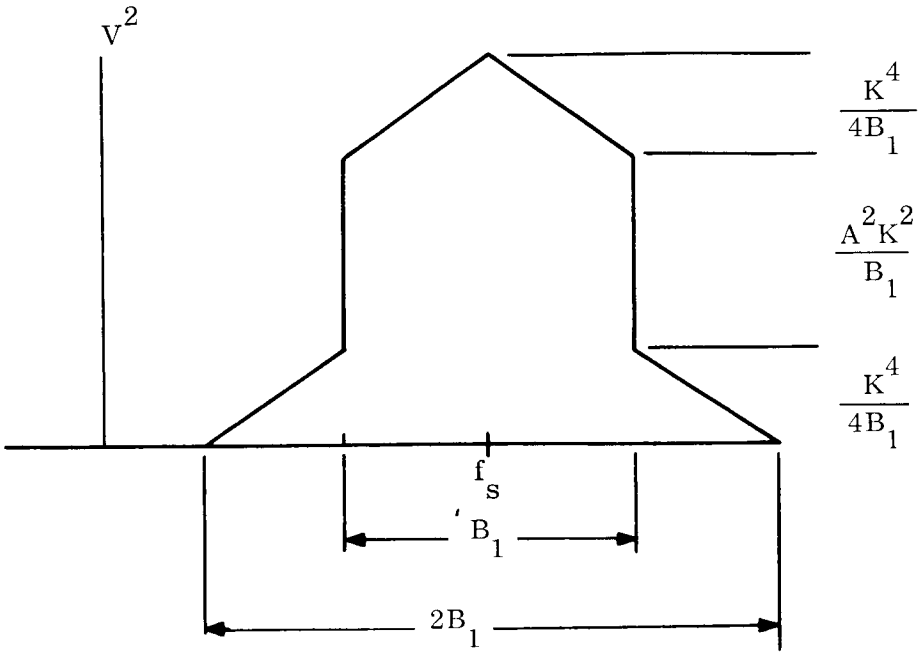

Figure VI-5. Noise Spectrum at the Output of the Multiplier of the Single Channel System

The average noise density N_o at the output of the multiplier can be obtained by dividing the noise power by the effective noise bandwidth of the spectrum, BW_N;

$$N_o = \frac{(3/8)\ K^4 + A^2K^2}{BW_N}$$

where the denominator of the expression for N is defined from the area under the curve of Figure VI-6. The effective noisebandwidth is defined as

$$BW_N = \frac{1}{P_N(f_s)} \int_o^\infty P_N(f)df$$

where $P_N(f)$ is the power spectrum of the noise. After performing the indicated integration over the curve of Figure VI-6, we find the effective bandwidth is

$$BW_N = 4B_1 \left\{ \frac{(3/8)\ K^4 + A^2K^2}{2K^4 + 4A^2K^2} \right\}$$

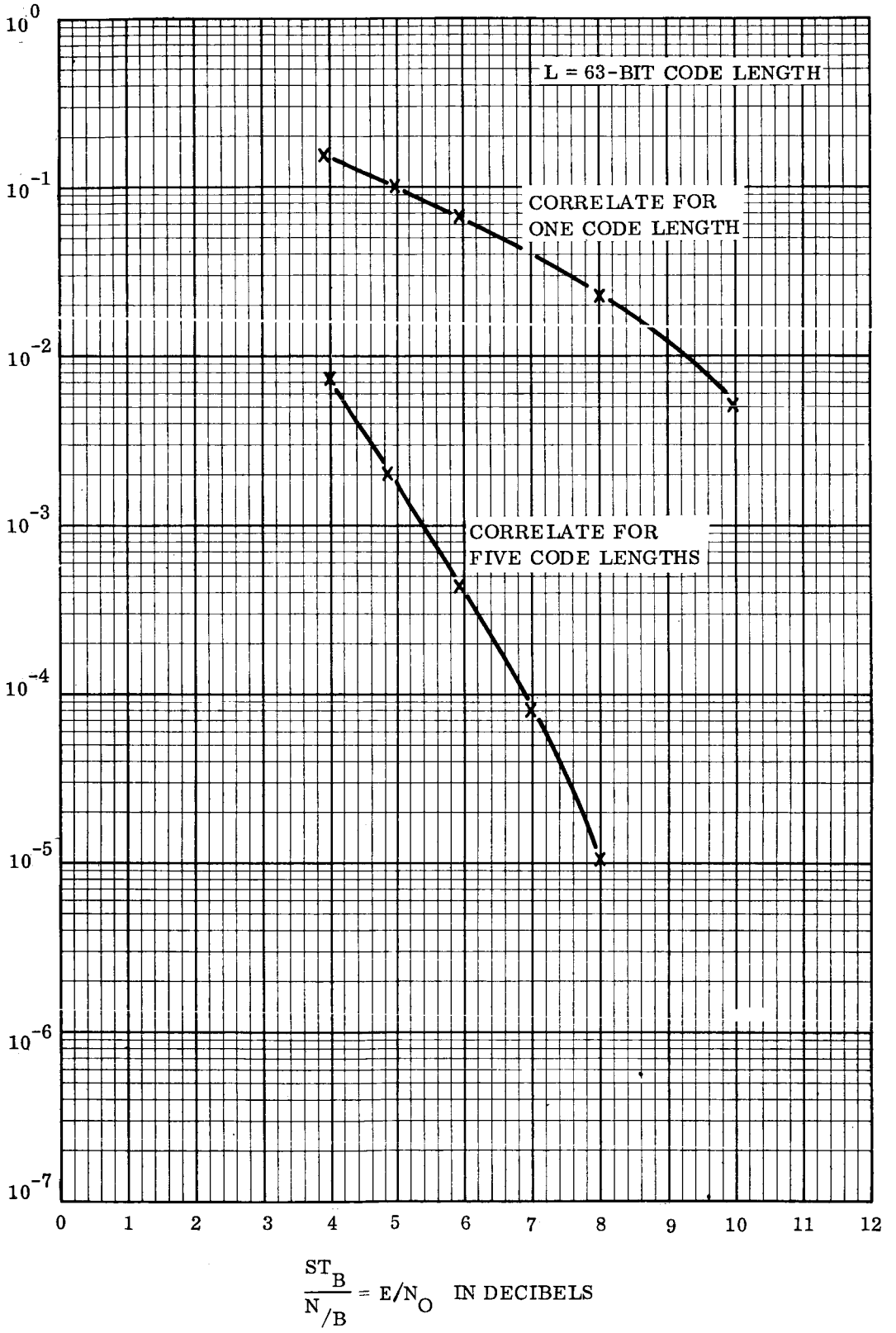

Figure VI-6. B-Type Error for Single-Channel Code Correlator

The input signal-to-noise ratio of the multiplier is defined as

$$(S/N)_{in} = A^2/K^2$$

Substituting the expression for the input SNR into the expression for BW_N we have

$$BW_N = 2B_1 \left\{ \frac{(3/8) + (S/N)_{in}}{(1 + 2(S/N)_{in})} \right\}$$

Inserting the value for BW_N into the expression for the noise density, N_o, we have

$$N_o = (K^4/2B_1)\ (1 + 2(S/N)_{in})$$

where B_1 is the bandwidth of the bandpass filters, BPF-1 and BPF-2.

The bandwidth of the bandpass filter that follows the multiplier will be defined as B_2; therefore, the noise power at the output of this filter is

$$N = N_o B_2 = (B_2/2B_1)K^4\ (1 + (S/N)_{in}) = \sigma_N^2 = VAR(X)$$

If we let X be the output of the bandpass filter that follows the multiplier, the variance of X, VAR(X), is given by the noise power, N. In deriving this output spectrum it was assumed that the bandwidths of the parallel channel bandpass filters did not overlap in frequency. This assumption allows us to consider the noise samples as independent random random variables. When the noise samples from both channels are independent, the mean output of the bandpass filter that follows the multiplier (Reference 4) is:

$$\overline{X} = A^2/\sqrt{2}$$

To continue the derivation, we will assume that X is the input to the integrate and dump network of the code correlator, and again use the sampling approach that was employed in the double channel code correlator. To obtain independent samples of X, we must space the samples at least $1/B_2$ apart in time where B_2 is the bandwidth of the bandpass filter at the output of the multiplier. When this is done, the output, Z, of the code correlator can be represented by

$$Z = X_1 + X_2 + X_3 + X_4 + \cdots + X_n$$

where, n, is the number of samples taken before the dump occurs.

Whatever the distribution of the independent random variable, X_i, subject to certain very general conditions, the sum $Z = X_1 + X_2 + X_3 + \cdots X_n$ is asymptotically normal $N(\mu_o, \sigma_o^2)$ where μ_o and σ_o^2 are given by

$$\mu_o = n\overline{X}$$

$$\sigma_o^2 = n\sigma_N^2 = n\,VAR(X)$$

This relationship follows from the Central Limit Theorem of mathematical statistics.

If we let $B_2 = R$, then for a 63 bit PN code only 7 samples per code length can be taken and still insure independency between samples. The period of the PN code T_{PN} is

$$T_{PN} = L/2f_s = L/9R$$

The number of samples, n, that can be taken during a code length is the ratio of the PN code period to the sample period

$$n = LB_2/9R$$

where $1/B_2$ is the sample period. Therefore, the mean and the variance of the output probability density function for the correlator is asymptotically normal $N(\mu_o, \sigma_o^2)$ with the mean and variance given by

$$\mu_o = \frac{k\,L\,B_2}{9R}\,\overline{X}$$

$$\sigma_o^2 = \frac{k\,L\,B_2}{9R}\,VAR(X) = \frac{k\,L\,B_2}{9R}\,\sigma_N^2$$

where

k = number of code lengths used in the correlation time

L = the code length in PN bits

Substituting in the values for $\overline{X}$ and VAR(X), the mean and variance for the normal distribution p(Z) that describes the output of the single channel code correlator for the in-sync condition of the codes, we have

$$\mu_o = \frac{k\,L\,B_2}{9R}\left(\frac{A^2}{\sqrt{2}}\right)$$

$$\sigma_o^2 = \left(\frac{k\ L\ B_2}{9R}\right) \left(\frac{B_2}{2B_1}\right) K^4 \left(1 + 2(S/N)_{in}\right)$$

From the normal probability density function the probability of a β type error is

$$\beta = \frac{1}{\sqrt{2\pi}\,\sigma_o} \int_{-\infty}^{Z_T} \mathrm{EXP}\left[-\frac{(Z - \mu_o)^2}{2\sigma_o^2}\right] dZ$$

This can be expressed in terms of error functions (erf(x)) as

$$\beta = \frac{1}{2}\left\{1 - \mathrm{erf}\left(\frac{\mu_o - Z_T}{\sqrt{2}\sigma_o}\right)\right\}$$

Since we have no knowledge of the out-of-sync distribution it will be impossible to make $\alpha = \beta$ as we did for the double channel analysis by selecting the appropriate threshold setting Z_T. However, in the double channel analysis, the threshold for $\alpha = \beta$ was set at approximately one-half the mean of the in-sync distribution. We will use the same setting for the present analysis knowing that as Z_T increases α decreases and β increases. Thus, when $Z_T = \mu_o/2$ the expression for β reduces to

$$\beta = \frac{1}{2}\left\{1 - \mathrm{erf}\left(\frac{\mu_1}{2\sqrt{2}\sigma_o}\right)\right\}$$

where

$$\frac{\mu_o}{2\sqrt{2}\sigma_o} = \frac{\sqrt{2}}{4}\sqrt{\frac{k\ 7\ B_1}{R}}\left\{\frac{(S/N)_{in}}{\sqrt{1 + 2(S/N)_{in}}}\right\}$$

The bandwidth of B_1 must be sufficiently large to pass most of the data spectrum, therefore, $B_1 = 2R$. When this is done, the argument of the error function becomes

$$y = \frac{\mu_o}{2\sqrt{2}\sigma_o} = \frac{\sqrt{k\ 7}}{2} \cdot \frac{(S/N)_{in}}{\sqrt{1 + 2(S/N)_{in}}}$$

The term $(S/N)_{in}$ is the input signal-to-noise ratio of the multiplier of the code acquisition network Figure VI-4. This can be related to E/N_o needed at the data detector by taking into account the gain of the bandpass filters due to decrease in input bandwidth, and the loss in the filters caused by passing only the fundamental of $2f_s$ square-wave subcarrier. This loss is approximately 0.9 decibel.

The signal-to-noise ratio into the 36R input bandwidth of the subcarrier demodulator is

$$\alpha_1 = \frac{1}{36}\left(\frac{E}{N_o}\right)$$

If we classify the loss in the bandpass filter as F_L and let the filter bandwidth be 2R (R is the data rate), then the signal-to-noise ratio at the input of the multiplier, $(S/N)_{in}$, can be represented by

$$(S/N)_{in} = \left(\frac{1}{2}\right)\left(\frac{E}{N_o}\right)\left(\frac{1}{F_L}\right)$$

Inserting this relationship into the expression for the argument of the error function that defines the beta error probability we have for this argument

$$y = \left\{\frac{(E/N_o)\left(\frac{1}{F_L}\right)(1/2)}{\sqrt{1 + (E/N_o)(1/F_L)}}\right\}\frac{\sqrt{k\,7}}{2}$$

where

$$\beta = \frac{1}{2}\left\{1 - \text{erf}\,(y)\right\}$$

In Figure VI-6, the β error probability is plotted as a function of E/N_o needed at the data detector for two different values of k, the number of code lengths taken in the correlation process, k = 1 and k = 5. Notice that a large reduction in the β error probability can be obtained when more than one code length is integrated before an in-sync or out-of-sync decision is made.

VI.4 REFERENCES

1. Roe, G.M., and White, G.M., "Probability Density Function for Correlators with Noisy Reference Signals," IRE Transaction on Information Theory, Vol. IT-7, pp. 13-18, January 1961.

2. McBride, Alan L., "Probability Density Function for Synchronization Correlators with Noisy Received Goods," Texas Instrument Internal Report, 1963.

3. Springett, T., "Telemetry and Command Techniques for Planetary Spacecraft," Advances in Communications Systems, Vol. 1, pp. 77-127, Academic Press, New York, 1965.

4. Copper, D. C., "The Probability Density Function for the Output of a Correlator with Band-Pass Input Waveforms," IEEE Transactions on Information Theory, Vol. IT-11, No. 2, p. 190, April 1965.

APPENDIX VII.0

ANALYSIS OF ACQUISITION OF WORD AND FRAME SYNC

In devices where either a yes or no decision has to be made in the presence of noise, two types of errors are possible; the false alarm error (α type error) and the false dismissal error (β type error). The probability α_1 of a false alarm is the probability that the condition is not satisfied but the equipment indicates (due to noise) that the condition is satisfied. Similarly, the probability, β, of a false dismissal is the probability that the condition is satisfied but the equipment (due to noise) fails to indicate this.

In detecting frame sync, the probability β is the probability that frame sync is actually present, but due to noise or some other random occurrence the equipment fails to indicate frame sync. This will cost us in frame sync acquisition time since the equipment must continue its search for frame sync until its next occurrence in the data. At this point it must again make a decision. It will make the correct decision that frame sync is actually present with probability of $(1 - \beta)$ or make a false decision with probability β and continue the search.

When frame sync is actually not present, the equipment can falsely indicate its presence with probability α (generate a false alarm) or continue with the search with probability $(1 - \alpha)$. When a false alarm is generated, the equipment will assume that the proper frame sync has occurred and will start to decode information. If the equipment continuously monitors the frame sync indication eventually an indication of the erroneous decision will occur. The search for frame sync will again commence.

Both of these errors cost us in decoded data, and will use up a portion of the available transmission time. To show that we can enhance the detection of frame sync if we first correctly obtain word sync we will evaluate these α and β error probabilities for both situations; knowing word sync and not knowing word sync.

VII.1 α AND β ERROR PROBABILITIES WITH KNOWN WORD SYNC

When the word location is correctly known, the errors associated with acquiring frame sync depend only on the probability of detecting the transmitted data correctly, i.e., depend on the probability of bit error, P_B.

Since our data format calls for a 7-bit data word, the probability that the 7-bit frame sync word being erroneously detected as not being frame sync is one minus the probability of it being detected correctly. The probability that one data bit will be detected correctly is $(1 - P_B)$, therefore, the probability that all 7 data bits will be detected correctly is

$$(1 - P_B)^7$$

Then, the probability that these seven bits will not be detected correctly is the probability of false dismissal, β_F, and is

$$\beta_F = 1 - (1 - P_B)^7$$

Therefore, any time the seven bit frame sync word is sent the probability that it will not be detected correctly is given by β_F. For $P_B = 5 \times 10^{-3}$, β_F reduces to

$$\beta_F = 0.03448$$

In a similar manner we can also derive the probability of a false alarm, α_F, or the probability that a data word will be erroneously detected as a frame sync word. First of all, there are 127 data words out of the possible 128 words that can be falsely identified as the frame sync word. If "x" bits in error will cause an erroneous frame sync indication, the probability that exactly "x" bits out of the 7 bits will be in error is given by the binomial distribution as

$$\binom{7}{x} P_B^x (1 - P_B)^{7-x}$$

Therefore, the probability that any one of the 127 data words could be erroneously decoded as a frame sync word is α_F and is given by the sum of the binomial distribution for x = 1, . . . , 7

$$F = \sum_{x=1}^{7} \binom{7}{x} P_B^x (1 - P_B)^{7-x}$$

which reduces to

$$\alpha_F = 1 - (1 - P_B)^7 = \beta_F$$

Before we can evaluate the effect on the frame sync detection process caused by these errors we need to know the cost function associated with these errors which requires knowledge of the tactics employed in the OSE to handle frame sync as well as those tactics employed in the spacecraft in formatting frame sync. Regardless of the cost function associated with these errors, we know that the nature of cost functions yield an increasing cost as both α and β errors increase. Therefore, we now need to evaluate the errors associated with detecting frame sync without prior knowledge of word sync and then compare the errors for both frame sync detection schemes. The scheme that has the smallest errors will be the better detection scheme; how much better depends on the cost functions. (This statement that the scheme that produces the smallest errors is the better scheme is only valid if both α and β errors of one scheme are smaller than the α and β errors of the other scheme. Fortunately, for the schemes we consider both errors are equal and the judgment can be

based on the evaluation of the α errors.) Now, let us investigate the α and β error probabilities associated with the detection of frame sync when word sync is not known.

VII.2 α AND β ERROR PROBABILITIES WITH WORD SYNC UNKNOWN

When the word location is not known, any sequence of 7-bits is just as likely to be the frame sync indicator word as any other sequence of 7-bits. However, the false dismissal error, β'_F, can only occur when the proper 7-bits are being tested. Therefore, β'_F, remains the same for both detection schemes and is

$$\beta'_F = 1 - (1 - P_B)^7 = 0.03448$$

In the frame detection scheme where previous knowledge of word sync is known, the false alarm error could only be caused by the noisy channel which caused errors to occur in the transmitted bits. For the frame sync detection scheme that does not use prior knowledge of word sync, the false alarm error can now be caused by channel noise as well as by the random nature of the transmitted data. That is, it is now possible for the ending of one 7-bit word and the beginning of another word to make up the 7-bit word we are testing for frame sync. When this happens, the detection scheme is no longer protected by only allowing the frame sync indicator to occur for frame sync and not as data. Furthermore, if a false alarm should occur due to overlapping data words, there is a very good chance that on the next pass by this word this false alarm will be verified as the correct frame sync. This situation exists due to the nature of the data being transmitted from the spacecraft-particularly the engineering data. It usually remains constant over long intervals of time. Thus, the erroneous frame sync word could occur for many frames of data.

A numerical evaluation of this false alarm error is rather complicated since it requires evaluating the erroneous indication that could occur for a sequence of 7-bits when they are in proper word sync and the six conditions when they are not in the proper word sync. These six out-of-word sync indications must be evaluated for two consecutive words not being the frame sync and when the latter of these words is the frame sync indicator. Since the evaluation of the false alarm probability for the case when the 7-bits are in word sync will give the same value that was obtained in the previous scheme with word sync known, it is obvious that the false alarm probability, α'_F, for this unknown word sync situation will be greater than that obtained for the known word sync situation. Therefore, since the β errors are the same for both schemes and the false alarm probability, α'_F, for the unknown word sync scheme is greater than α'_F, the false alarm probability for the known word sync scheme, the scheme that uses prior knowledge of word sync to acquire frame sync, is the better scheme.

We could decrease the false alarm rate in the acquisition of frame sync when prior knowledge of word sync is not available by increasing the amount of frame sync information contained in the data. One method would be to send the 7-bit frame sync word

twice. The optimum way though would be to use a correlation technique for obtaining frame sync. This, however, would necessarily increase the time required to obtain frame sync - particularly since frame sync does not occur too often. A better way would be to acquire word sync by correlation techniques since word sync occurs much more often than frame sync and it could be acquired faster. Once word sync is acquired, frame sync could be acquired by searching the incoming data a word at a time. The probability of obtaining consecutive erroneous frame sync indications approaches zero quite rapidly when the knowledge of word sync is used in the acquisition process. Thus, we conclude that acquiring word sync prior to acquiring frame sync appears to be the better approach to take.

APPENDIX VIII

EFFICIENCY COMPARISON OF SINGLE AND DOUBLE CHANNEL SYSTEMS

The determination of the efficiency of the double and single channel system was done in the following manner:

VIII. 1 LOW DATA RATE

a. The E/N required in the single channel system to maintain BEP of 5×10^{-3} is 8.0 db (6.31).

b. The average time required to sync at the low data rate will be constrained to be no more than 1.5 minutes.

c. The average error free sync time for R = 3 1/3 bps is

$$t_1 = \left| \frac{LT_o}{2} \right| = 1.1 \text{ minute}$$

For 1 = 63 PN bits per code length

$$T_o = L/2f_s = 7/R$$

d. The maximum number of code lengths that can be correlated in the sync acquisition for the low data rate is no more than one code length and still stay within the limitations of 1.5 minutes.

e. The β error probability for E/N_o = 8 db, T_o = one code length, $\alpha = \beta$ is: β = 0.025 (See Figure VI-6)

f. For the single and double channel code acquisition to have identical performance they need to have the same beta error probabilities. To maintain $\beta = 0.025$, the double channel correlation requires that the PN channel have

-3.0 db into 4.5 R bandwidth

This value was obtained from the curve of β probability error versus the input signal-to-noise ratio of the double channel correlator, Figure VI-3. The SNR per 1 cps of noise bandwidth is $(S/N_o)_{sync} = (0.5)(4.5)$ R.

g. The sync efficiency E_s is defined as

$$E_s = \frac{(E/N_o)\ R}{(E/N_o)\ R + (S/N_o)_{sync}}$$

$$E_s = \frac{6.31}{6.31 + 2.25} = 74\%$$

E_s (Double Channel) = 74%

E_s (Single Channel) = 100%

h. The modulation efficiency, EM, is defined as the ratio of the power in the data P_d to the power in the carrier P_c, plus the data, P_d, plus the sync, P_s.

$$E_M = \frac{P_d}{P_c + P_s + P_d}$$

For the low data rate system, 70% of the total power is in the carrier and 30% in the subcarrier.

$$P_T = K_1 (P_d + P_s + P_c)$$

$$P_d + P_s = 0.3 k_1$$

$$P_c = 0.7 k_1$$

where

K_1 = total power.

i. Transmitter Power required:

VIII.1.1 DOUBLE CHANNEL: $(P_s + P_d = 0.3K_1)$

Of the $0.3K_1$ transmitter power in the subcarrier, approximately 74% is in the data and 26% is in the sync.

$$P_d = (0.74)(0.3K_1) = 0.222K_1$$

$$P_s = (0.26)(0.3)K_1 = 0.078K_1$$

The modulation efficiency for the double channel system is

$$E_M = \frac{P_d}{P_d + P_s + P_c} = \frac{0.222K_1}{K_1} = 22.2\% \text{ (double channel)}$$

For the single channel system, no power is needed in the sync and all the available power can be placed in the data, therefore, the modulation efficiency for the single channel system is

$$EM = \frac{P_d}{P_d + P_c} = \frac{0.3K_1}{K_1} = 30\%$$

VIII.2 HIGH DATA RATES

In a similar fashion, the sync and modulation efficiencies can be obtained for the high data rate systems. For these systems the $E/N_o = 5.9$ db and we will assume that we integrate over 5 code lengths. For $E/N_o = 5.9$ db and integrating over 5 code periods, the β error probability for the single channel system is obtained from the curve, of Figure VI-6:

$$\beta = 5 \times 10^4$$

For the double channel system to obtain the same β error probability, the input signal-to-noise ratio of the correlator must be, from Figure VI-3:

$$-7 \text{ db into } 4.5R \text{ bandwidth} = (0.2)\,4.5R = (S/N_o) \text{ sync}$$

The Sync Efficiency is

$$E_s = \frac{(E/N_o)\,R}{(E/N_o)\,R + (S/N_o)_{\text{sync}}} = 81.5\%$$

In the high data rate systems 0.7 of the total power is available for the subcarrier with the other 0.3 in the carrier. Therefore, the modulation efficiency for the double channel system at the high data rates is

$$E_M\,(\text{2-channel}) = \frac{P_d}{P_d + P_s + P_c} = 57\%$$

For the single channel system, the modulation efficiency is

$$E_M\,(\text{1-channel}) = 70\%.$$

APPENDIX IX

ERROR CONTROL CODING

IX.0 THE DERIVATION OF THE ENCODING AND DECODING LOGIC FOR A (15,7) BOSE-CHAUDHURI CODE

IX.1 INTRODUCTION

Bose-Chaudhuri codes have been recognized as one of the most promising types of algebraic cyclic codes for digital detection and correction of multiple, independent bit errors. This is due to the inherent simplicity in their encoder/decoder implementation and operation. Bose and Chaudhuri [1] have shown that an (n, k) linear or group code may be devised having a minimum Hamming distance of 2t + 1 which will detect 2t or fewer errors or, alternately, will perform t-error correction. They have shown that for every m and t there exists a t-error-correcting (n, k) code in which

$$n = 2^m - 1 = \text{length of code word, and}$$

$$k \geqq 2^m - 1 - mt = \text{number of information bits}$$

In applications where $n \neq 2^m - 1$, Bose and Chaudhuri proposed shortened cyclic codes of the form (n-c, k-c).

For the Voyager, Bose-Chaudhuri codes having a relatively short encoder shift register and, hence, a relatively simple decoder configuration were considered in order to keep the spacecraft encoder equipment down to the comparable complexity of an orthogonal type encoder having approximately the same (or better) improvement in signal efficiency. In particular, the main work in this appendix has been directed toward the (15, 7) Bose-Chaudhuri double-error-correcting code since the 7 information bits corresponds to the assumed data word size in a typical telemetry channel and the redundancy of 8/15 seems to be tolerable. Furthermore, the detailed decoder design reported herein made it possible to determine the feasibility of using a high speed, general purpose computer to perform the decoding functions.

The material which follows treats the manner of determining the characteristic or generator polynomial $\varphi(x)$ for the code, the implementation of the encoder, the derivation of the encoding and decoding equations, and the implementation of the decoder.

IX-2. THE CHARACTERISTIC OR GENERATOR POLYNOMIAL

For a given m and t, the characteristic or generator polynomial for a t-error-correcting Bose-Chaudhuri code has been determined to be

$$\varphi(x) = \prod_{i=1}^{t} \varphi_i(x) \tag{1}$$

where $\varphi_1(x)$ is of degree m, primitive and the characteristic polynomial of the corresponding generator T-matrix. For $1 < i \leq t$ the $\varphi_i(x)$ are the characteristic polynomials of the matrices T^{2i-1}, i.e.,

$$\varphi_i(x) = \left| T^{2i-1} - xI \right| \tag{2}$$

By a fundamental theorem in matrix algebra a T-matrix satisfies its own characteristic polynomial; hence,

$$\varphi_i(T^{2i-1}) = 0 \tag{3}$$

for i= 0, 1, ---, t.

For the (15, 7) code, m = 4 in order that

$$n = 2^m - 1 = 15$$

be satisfied. Therefore, a primitive polynomial of degree 4 is chosen from the two available (see Peterson 2, Appendix C) to be

$$\varphi_i(x) = x^4 + x + 1 \tag{4}$$

The associated generator T-matrix is

$$T = \begin{Bmatrix} 0011 \\ 1000 \\ 0100 \\ 0010 \end{Bmatrix}$$

and, for i = 2,

$$T^{2i-1} = T^3 = \begin{Bmatrix} 1100 \\ 0110 \\ 0011 \\ 1000 \end{Bmatrix}$$

Consequently,

$$\varphi_2(x) = \left| T^3 - xI \right| = \begin{vmatrix} 1-x & 1 & 0 & 0 \\ 0 & 1-x & 1 & 0 \\ 0 & 0 & 1-x & 1 \\ 1 & 0 & 0 & -x \end{vmatrix}$$

$$= X^4 + X^3 + X^2 + X + 1 \tag{5}$$

By use of equations (1), (4), and (5)

$$\varphi(X) = \varphi_1(X) \cdot \varphi_2(X) = X^8 + X^7 + X^6 + X^4 + 1 \tag{6}$$

which is implemented with a simple shift register generator shown in Figure IX-1. Note that a characteristic polynomial of degree n (which does not have x as a factor) may be written in the form

$$\varphi(X) = X^n + X^{j_1} + X^{j_2} + \text{----------} + X^\circ \tag{7}$$

and the shift register generator which implements it has feedback connections into a mod 2 adder denoted by

$$(n - 0, ---, n - j_2, n - j_1, n - n) \tag{8}$$

as indicated in Birdsall and Ristenbatt[3]. In other words, stages n, ---, $n - j_2$, $n - j_1$ are added together modulo 2 to form the feedback bit which is fed into the first stage.

IX.3 IMPLEMENTATION OF THE ENCODER

There are several alternative ways to implement the encoder. For this report an encoder similar to the shift register generator in Figure IX-1 is utilized to provide the 128, 15-bit code words. The logic for the encoder is based on the feedback logic of the above shift-register generator, viz:

$$a_{i+1} \oplus a_{i+5} \oplus a_{i+7} \oplus a_{i+8} = 0$$

This is called the parity check equation where $a_1, a_2, ---, a_7$ represent the independent information bits and $a_8, a_9, ---, a_{15}$ are the dependent parity check bits. By adding a_{i+8} to both members of equation (7) and rearranging we have

$$a_{i+8} = a_{i+7} \oplus a_{i+5} \oplus a_{i+1}$$

which represents the recursion formula for the feedback logic of a seven stage encoder indicated in Figure IX-2. Note that i = 0, 1, ---, 7 for the (15,7) code. The encoder may receive the data in parallel or serially whereas the output is generally taken out serially from the seventh stage.

For convenience of mathematical manipulations, let C_1, C_2, ---, C_{15} represent the 15 bit output code word; then C_1, C_2, ---, C_7 are identical respectively to a_1, a_2, ---, a_7 while C_8, C_9, ---, C_{15} are mod 2 functions of at least 3 of the information bits a_1, a_2, ---, a_7. Table IX-1 lists all the encoded bits as functions of the information bits. From this Table an encoder parity check matrix of 8 x 7 dimension may be formed (from equations for C_8, ---, C_{15}) as follows:

$$C = \begin{Bmatrix} 1000101 \\ 1100111 \\ 1110110 \\ 0111011 \\ 1011000 \\ 0101100 \\ 0010110 \\ 0001011 \end{Bmatrix} \qquad (11)$$

The first row of matrix C has a 1 or 0 to correspond with the coefficients of the a_1 (ascending order) in the parity check equation for C_8; the second row ---- for C_9; etc.

The 8-bit parity check word may be written in matrix notation as

$$\begin{bmatrix} C_9 \\ C_{10} \\ \cdot \\ \cdot \\ \cdot \\ C_{15} \end{bmatrix} = C \begin{bmatrix} a_1 \\ a_2 \\ \cdot \\ \cdot \\ \cdot \\ a_7 \end{bmatrix}$$

IX.4 IMPLEMENTATION OF THE DECODER

There are several decoder configurations for the (15,7) code. The one to be described is based on five decoding equations derived from the 15 encoder equations for the c_1. The resulting implementation is identical to that described by Mitchell (4) wherein a majority decision is made on five decoding modulo 2 logic gates to provide double error correction on the information bits.

Proceeding with the derivation of the decoding equations, an inspection of the 15 encoder equations indicates the information bit a_1 appears in C_1, C_8, C_9, C_{10}, and C_{12}.

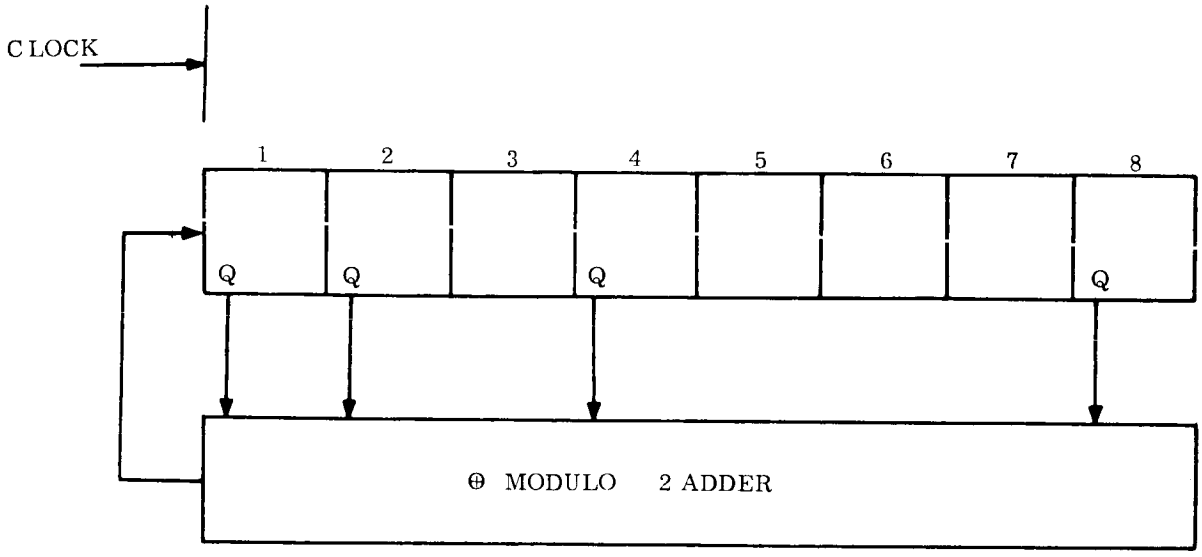

Figure IX-1. Simple Shift Register Generator Implementing the Characteristic Polynomial $\Phi(X) = X^8 + X^7 + X^6 + X^4 + 1$

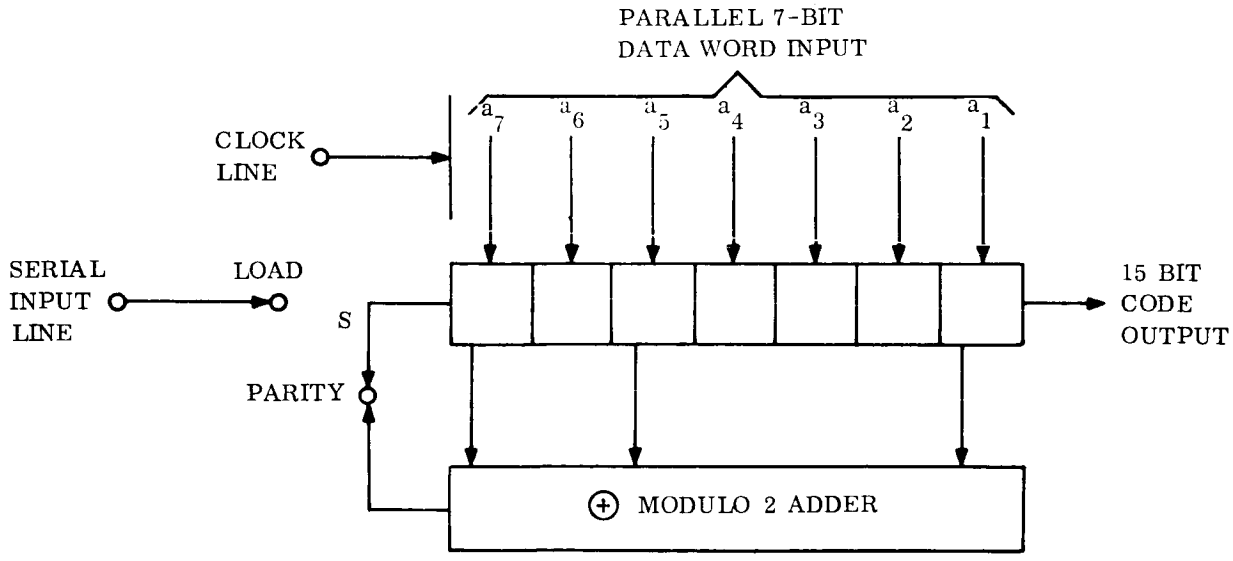

Figure IX-2. Shift Register Generator Encoder for (15, 7) Base-Chandhuri Double-Error-Correcting Code

Table IX-1. Encoder Equations

Encoded Bits		Encoded Bits as a Function of Information Bits						
		1	2	3	4	5	6	7
$C_1 = a_1$	=	a_1						
$C_2 = a_2$	=		a_2					
$C_3 = a_3$	=			a_3				
$C_4 = a_4$	=				a_4			
$C_5 = a_5$	=					a_5		
$C_6 = a_6$	=						a_6	
$C_7 = a_7$	=							a_7
$C_8 = a_1 \oplus a_5 \oplus a_7$	=	a_1				$\oplus a_5$		$\oplus a_7$
$C_9 = a_2 \oplus a_6 \oplus C_8$	=	a_1	$\oplus a_2$			$\oplus a_5$	$\oplus a_6$	$\oplus a_7$
$C_{10} = a_3 \oplus a_7 \oplus C_9$	=	a_1	$\oplus a_2$	$\oplus a_3$		$\oplus a_5$	$\oplus a_6$	
$C_{11} = a_4 \oplus C_8 \oplus C_{10}$	=		a_2	$\oplus a_3$	$\oplus a_4$		$\oplus a_6$	$\oplus a_7$
$C_{12} - a_5 \oplus C_9 \oplus C_{11}$	=	a_1		$\oplus a_3$	$\oplus a_4$			
$C_{13} = a_6 \oplus C_{10} \oplus C_{12}$	=		a_2		$\oplus a_4$	$\oplus a_5$		
$C_{14} = a_7 \oplus C_{11} \oplus C_{13}$	=			a_3		$\oplus a_5$	$\oplus a_6$	
$C_{15} = C_8 \oplus C_{12} \oplus C_{14}$	=				a_4		$\oplus a_6$	$\oplus a_7$

We wish to manipulate these 5 equations so that a_1 may be written as a function of the C_i; viz:

$$a^j_i = \alpha^j_1 \cdot C_1 + \alpha^j_2 \cdot C_2 + \text{-------} + \alpha^j_{15} \cdot C_{15}$$

$$= \sum_{i=1}^{15} \alpha^j_i \cdot C_i \qquad (13)$$

where

α^j_i = 0, 1 and the j = 1, 8, 9, 10 and 12 corresponding to the respective encoder equation.

Starting with the most obvious solutions:

(1) From C_1 we have

$$a^1_1 = C_1 \qquad (14)$$

(2) From C_8 we have by adding $a_5 \oplus a_7$ to both members

$$a^8_1 = C_8 \oplus a_5 \oplus a_7$$

or rearranged and substituting $C_5 = a_5$ and $C_7 = a_7$ we have

$$a^8_1 = C_5 \oplus C_7 \oplus C_8 \qquad (15)$$

(3) From C_{12} we have by adding $a_3 \oplus a_4$ to both members

$$a^{12}_1 = C_{12} \oplus a_3 \oplus a_4$$

or by rearranging and substituting it becomes

$$a^{12}_1 = C_3 \oplus C_4 \oplus C_{12} \qquad (16)$$

(4) From C_{10}

$$a^{10}_1 = C_{10} \oplus a_2 \oplus a_3 \oplus a_5 \oplus a_6$$

or

$$a_1^{10} = C_2 \oplus C_{10} \oplus C_{14} \tag{17}$$

since $C_2 = a_2$ and $C_{14} = a_3 \oplus a_5 \oplus a_6$

(5) From C_9,

$$a_1^9 = C_9 \oplus a_2 \oplus a_5 \oplus a_6 \oplus a_7$$

or,

$$a_1^9 = C_9 \oplus C_{13} \oplus C_{15} \tag{18}$$

since $C_{13} = a_2 \oplus a_4 \oplus a_5$ and $C_{15} = a_4 \oplus a_6 \oplus a_7$

If no errors exist in the received code word, then all the a_i^j equations (14) - (18) will decode correctly the information bit a_1. Since each decoding equation has a unique set of the C_i, a single error in any C_i causes only its corresponding a_i^j to be in error; consequently, a majority decision on the a_i^j provides the correct decoding. Similarly, two errors in the C_i cause at most only two of the a_i^j to be in error and a majority decision will decode the a_1 bit correctly. A simplified block diagram of the decoder is shown in Figure IX-3.

Notice that an even number of errors in a decoding equation still provides the correct answer for the equation; hence, some distributions of error patterns containing more than 2 errors will still be decoded correctly. Table IX-2 (taken from Mitchell 5) shows the error-correcting capability of the (15, 7) code for code words received with more than 2 errors.

Because of the cyclic structure of the code, a 15-stage shift register and decoding logic based on the a_i^j will also decode the remaining information bits a_2, a_3, ---, a_7 provided the a_j are recirculated back into the shift register, preferably after being corrected (as configured in the block diagram). Referring to Figure IX-3, assume that a_1 has been decoded and the shift register has shifted once to the right. Let A^1, A^8, A^9, A^{10}, and A^{12} represent the inputs to the majority gate corresponding to the decoding equations a^1, a^8, a^9, a^{10}, and a^{12}.

Then, for the moment assuming no errors in the received code word, we have

$$A^1 = C_2 = a_2$$

$$A^8 = C_6 \oplus C_8 \oplus C_9 = a_6 \oplus (a_1 \oplus a_5 \oplus a_7) \oplus (A_1 \oplus a_2 \oplus a_5 \oplus a_6 \oplus a_7)$$

$$= a_2$$

Table IX-2. Error-Correcting Capability of the (15, 7) Code

Number of Code Digits in Error	Number of Correctable Error Patterns	Fraction of Error Patterns Correctable
e	N(e)	F(e)
0	1	1.00000
1	15	1.00000
2	105	1.00000
3	74	0.16264
4	46	0.03370
5	9	0.00300
6	5	0.00100
7	1	0.00016
	N(e) = 0, e 7	

Similarly,

$$A^9 = C_{10} \oplus C_{14} \oplus a_1$$

$$= (a_1 \oplus a_2 \oplus a_3 \oplus a_5 \oplus a_6) \oplus (a_3 \oplus a_5 \oplus a_6) \oplus a_1$$

$$= a_2$$

$$A^{10} = C_3 \oplus C_{11} \oplus C_{15}$$

$$= a_3 \oplus (a_2 \oplus a_3 \oplus a_4 \oplus a_6 \oplus a_7) \oplus (a_4 \oplus a_6 \oplus a_7)$$

$$= a_2$$

and

$$A^{12} = C_4 \oplus C_5 \oplus C_{13}$$

$$= a_4 \oplus a_5 \oplus (a_2 \oplus a_4 \oplus a_5)$$

$$= a_2$$

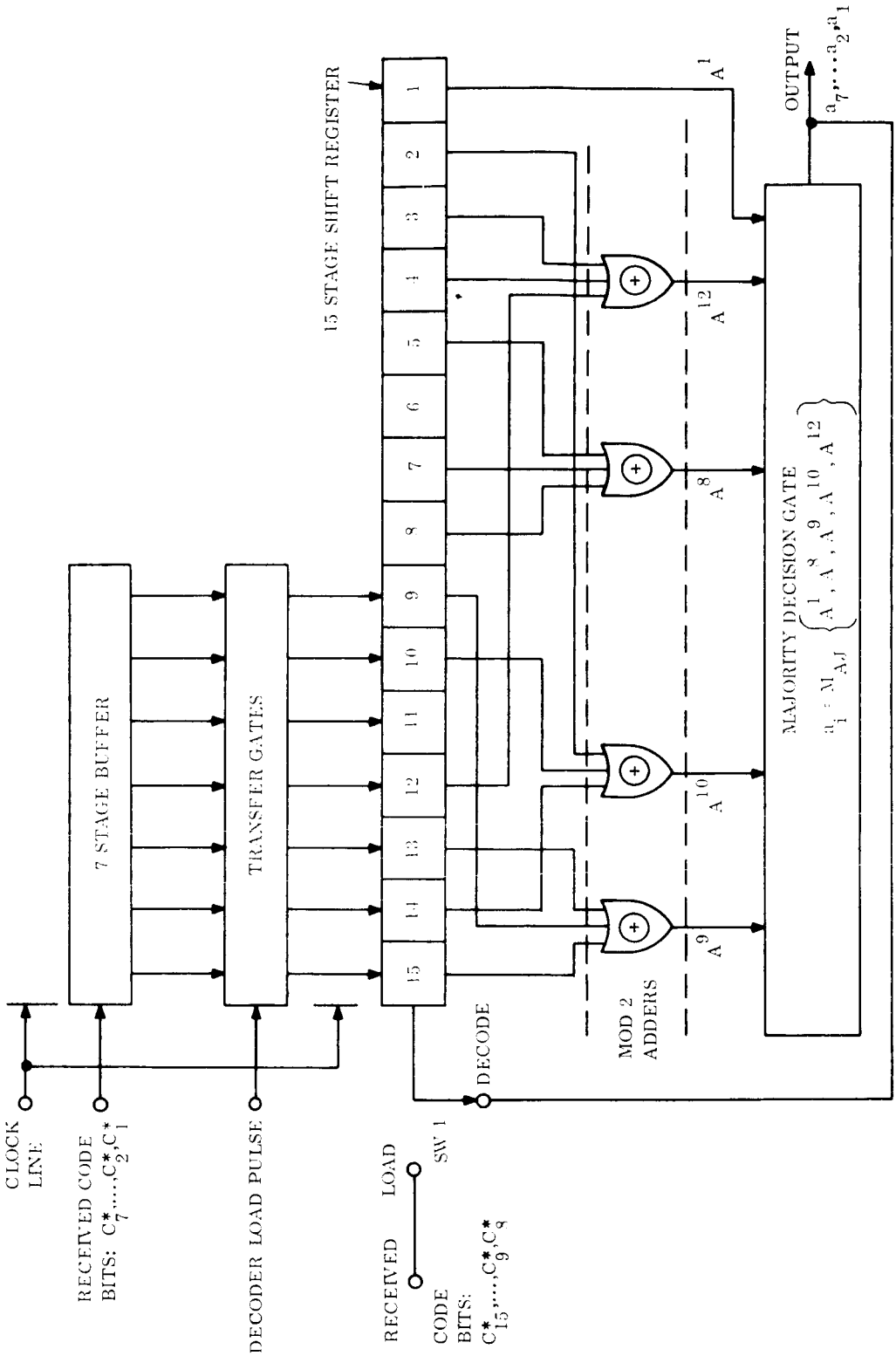

Figure IX-3. Block Diagram (Simplified) of the (15, 7) Decoder

The remaining information bits are likewise decoded with the same logic.

Since the decoder requires 7 clock pulse intervals to perform decoding on the 7 information bits, the first 7 bits of the subsequent word must be stored temporarily in a 7-stage buffer, then transferred in parallel into the decoder register. The remaining 8 received code bits are shifted serially directly into the decoder register, after which decoding commences and continues for 7 bit intervals while the first 7 bits of the next word are being stored in the buffer. Switch SW1 is in the "DECODE" position for the first 7 clock pulses and in the "LOAD" position for the remaining 8 clock pulses.

IX.5 REFERENCES

1. R.C. Bose and D.K. Ray-Chaudhuri, "On a Class of Error-Correcting Binary Group Codes," Information and Control, Vol. 3, pp. 68-79, March 1960.

2. W.W. Peterson, Error-Correcting and Error-Detecting Codes, M.I.T. Press, Cambridge, Massachusetts, and John Wiley and Sons, Inc., New York, New York, 1961.

3. T.G. Birdsall, and M.P. Ristenbatt, "Introduction to Shift-Register Generated Sequences," University of Michigan Research Institute, Technical Report No. 90, October 1958. (ASTIA AD 225-380).

4. M.E. Mitchell, "Simple Decoders and Correlators for Cyclic Error-Correcting Codes," IRE Transactions on Communication Systems, Vol. CS-10, No. 3, pp. 284-290, September 1962.

5. "Performance of Error-Correcting Codes," Advanced Electronics Center, Ithaca, New York, General Electric Report No. R61ELC78, November 1961.

APPENDIX X

ERROR CONTROL CODING

X.0 THE (73, 45) BOSE-CHAUDHURI ERROR CONTROL ENCODER AND DECODER*

X.1 THE ENCODING SUBSYSTEM

The encoding subsystem consists of an encoder for the (73, 45) code, and an encoder timer, as shown in Figure X-1. The (73, 45) encoder performs the function of transforming a sequence of 45 data bits into a 73-digit code word. The encoder consists of the 28 stage shift register and associated logic shown in Figure X-2.

The encoder is sequenced through two modes during encoding of a (73, 45) code word. In the first mode, the sequence of 45 data bits is transmitted, and at the same time is also read into the encoder logic to establish the proper "initial condition". In the second mode the encoder sequentially computes the 28 redundant code digits (called "check digits") from the initial condition, and simultaneously reads them out to the transmitter. The encoder timer consists of a novel preset (45-bit) counter and the associated logic shown in Figure X-3. It performs two functions which may be described as follows.

The encoder timer first of all performs the function of deriving a burst of 45 consecutive "data sampling pulses" from the word sync pulse train (at f_W PPS) and the clock pulse train (at $f_C = 73\ f_W$ PPS) as indicated in Figure X-4. This burst of sampling pulses consists of clock pulses 1 through 45 from each block of 73. The sampling pulse burst is fed back to the sampling gate located in the data generation system, as indicated in Figure X-1.

A second function of the encoder timer is to sequence the encoder through its (repetitive) cycle of first transmitting a block of 45 information bits, and then transmitting the corresponding block of 28 redundant code digits of the 73 digit code word. The output of flip-flop M of the encoder timer controls the operating mode (information or redundant half-cycle) of the encoder as indicated.

X.2 DECODING SUBSYSTEM

The decoding subsystem consists of a 45-stage buffer, a (73,45) decoder, a decoder timer, and the interconnecting gates shown in Figure X-5.

The (73, 45) decoder performs the function of transforming a received 73-digit code word, with any of its correctable errors, into a sequence of 45 data bits identical to that read into the encoder. The decoder consists of a 73-stage shift register, a block of mod 2 adders, and a majority decision element, as shown in Figure X-6.

---

*This material appeared originally in the GE Final Report (Voyager).

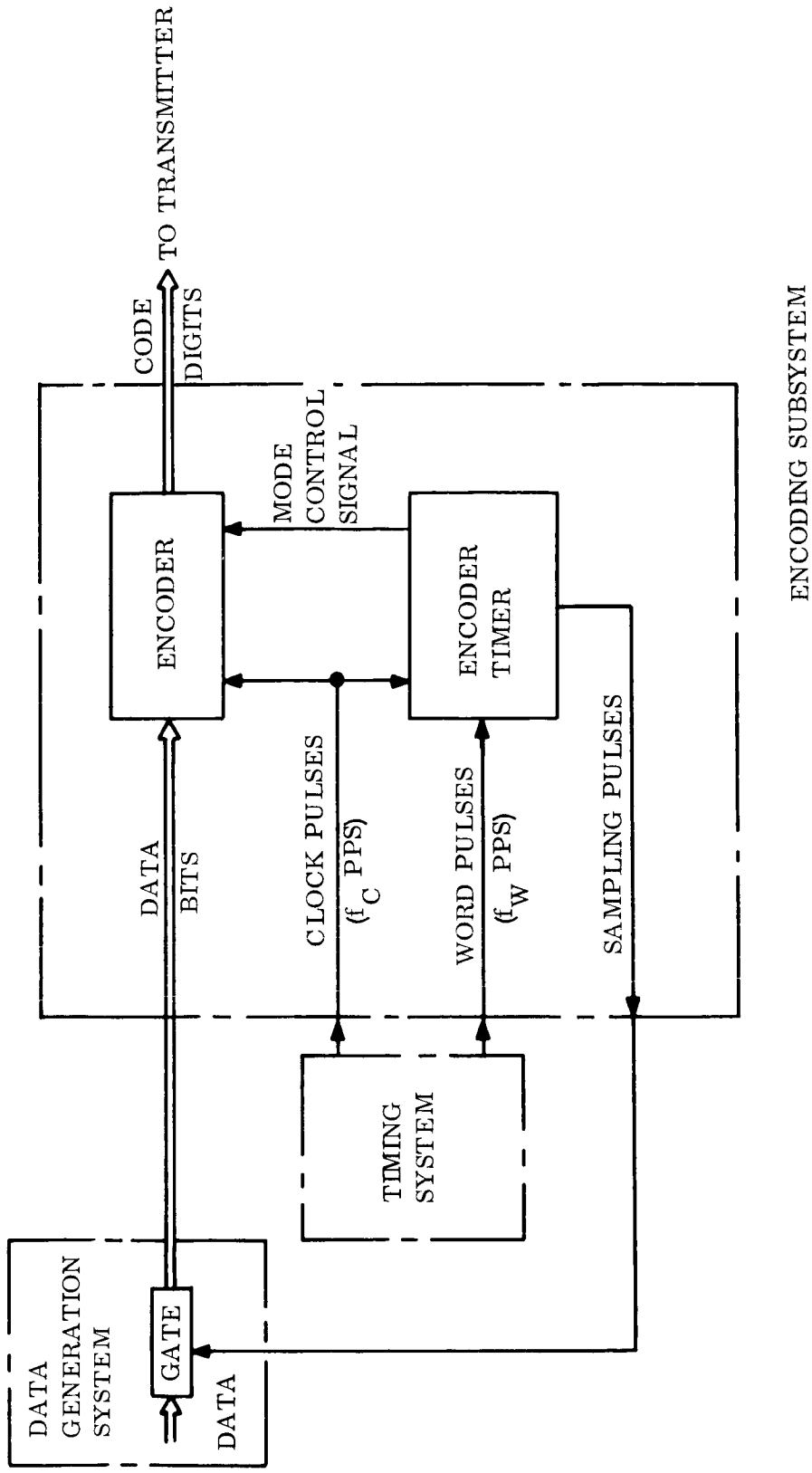

Figure X-1. Encoding Subsystems

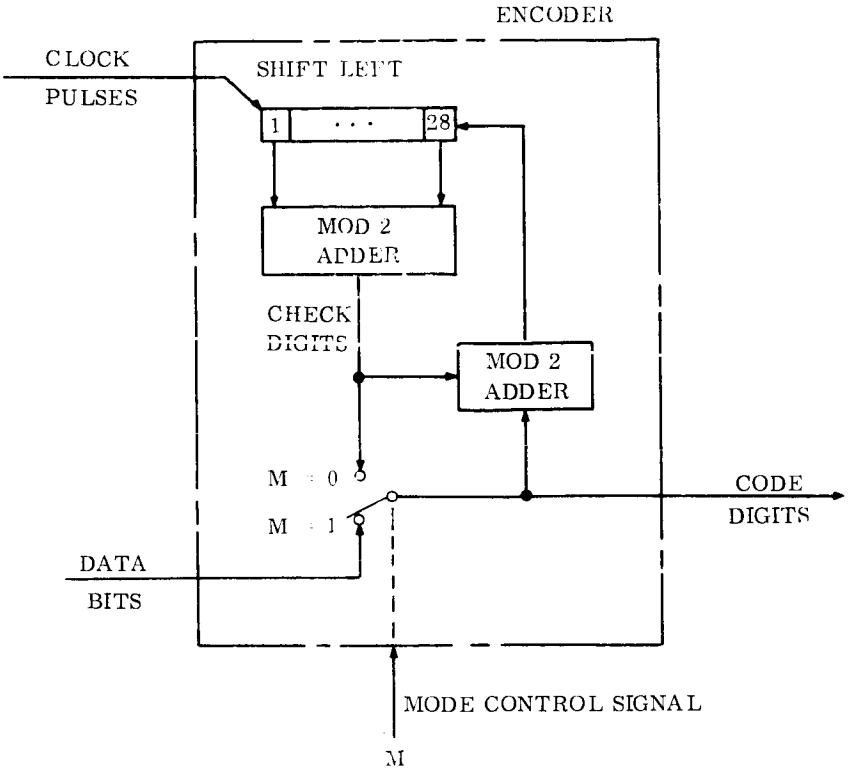

Figure X-2. (73, 45) Encoder

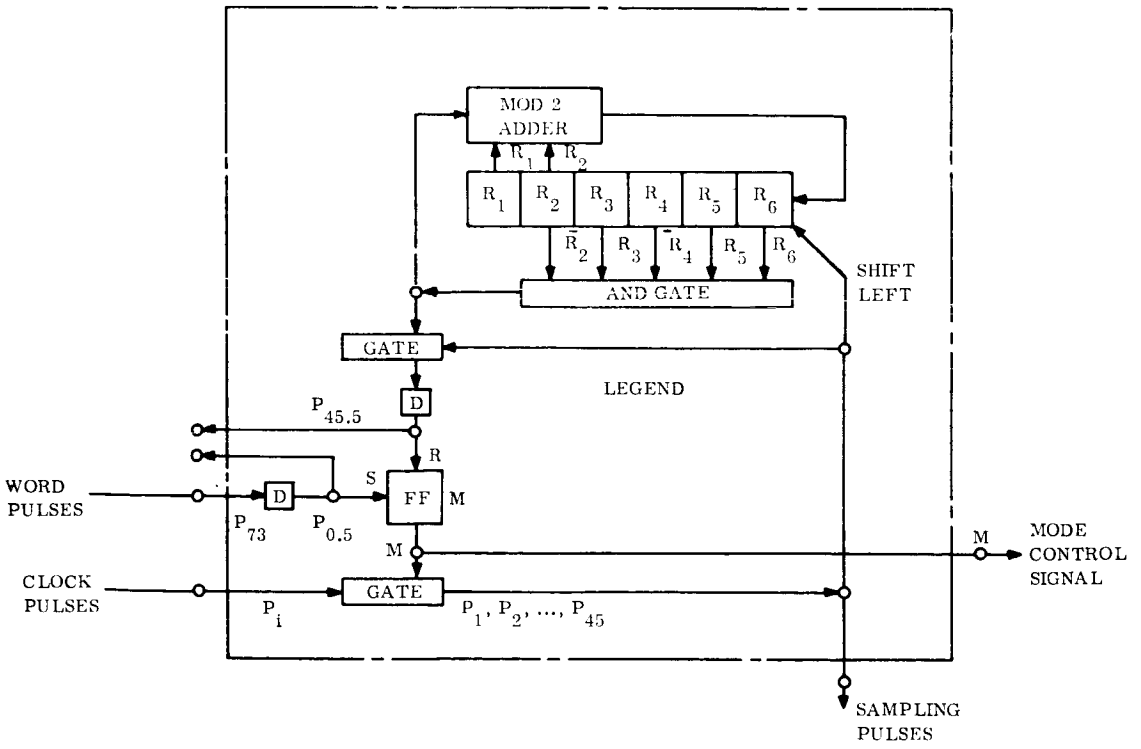

Figure X-3. Encoder Timer

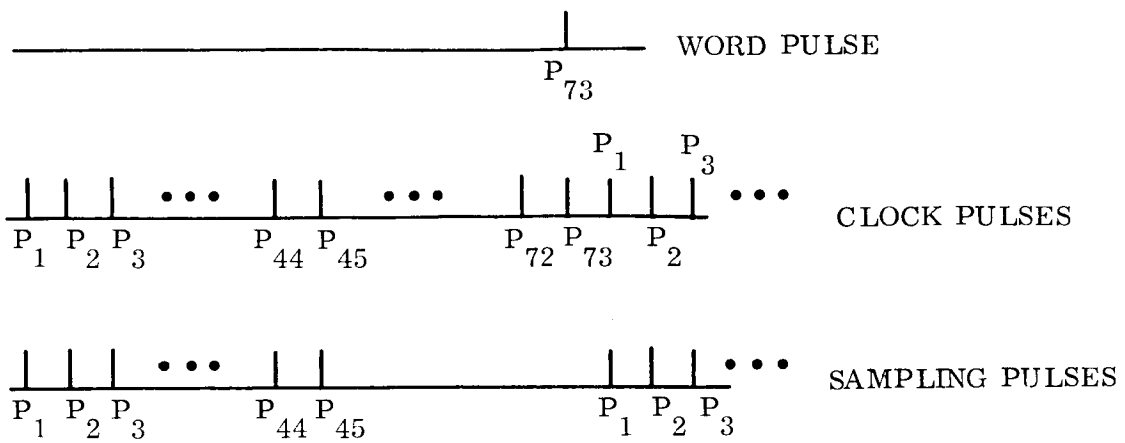

Figure X-4. Timing

The 45-stage buffer is merely a 45-stage shift register with serial input and parallel output. The buffer is used to accumulate received digits while the 45-data bits of the previously received 73 digit word are being decoded.

The decoding subsystem sequences through four modes during each complete 73-digit cycle of its operation. Assuming that a sequence of (73, 45) code words A_1, A_2 ---, A_j, --- is transmitted, and that each A_j is received as B_j, the operation of the decoding subsystem can be summarized as follows:

MODE 1 (Clock times t = 1, 2, ..., 45)
A. Decode B_j into 45 decoded data bits
B. Read first 45 digits of B_{j-1} into the 45-stage buffer.

MODE 2 (Clock time t = 45.5)
Transfer (in parallel) first 45 digits of B_{j-1} from 45-stage buffer into first 45 stages of 73-stage decoding register, and switch the input of the 73-stage decoding register from the output of the majority element to the decoding subsystem input terminal.

MODE 3 (Clock times t = 46, 47, ..., 73)
Read digits 46-73 of B_{j-1} into 73-stage decoding buffer.

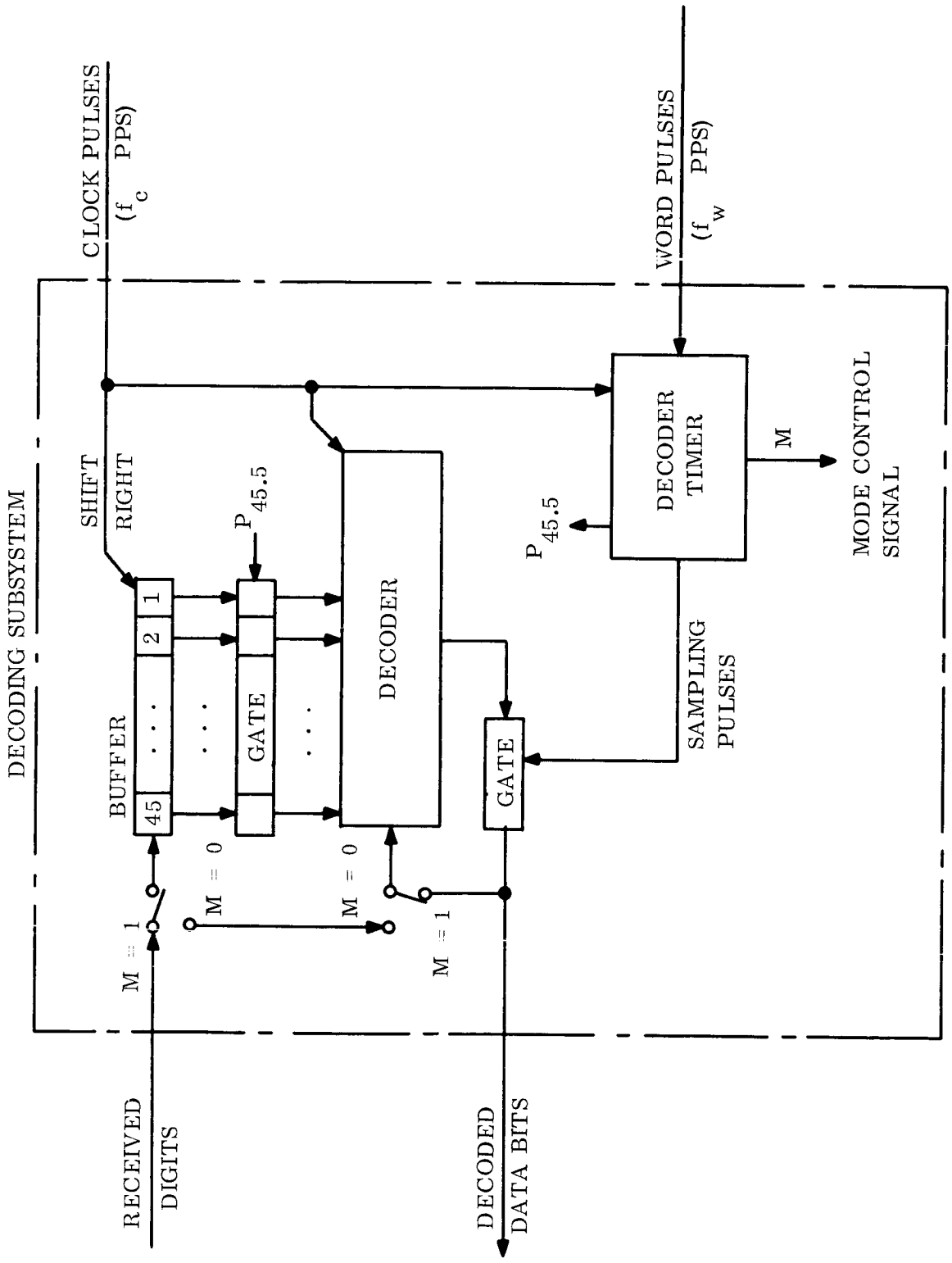

Figure X-5. Decoding Subsystems

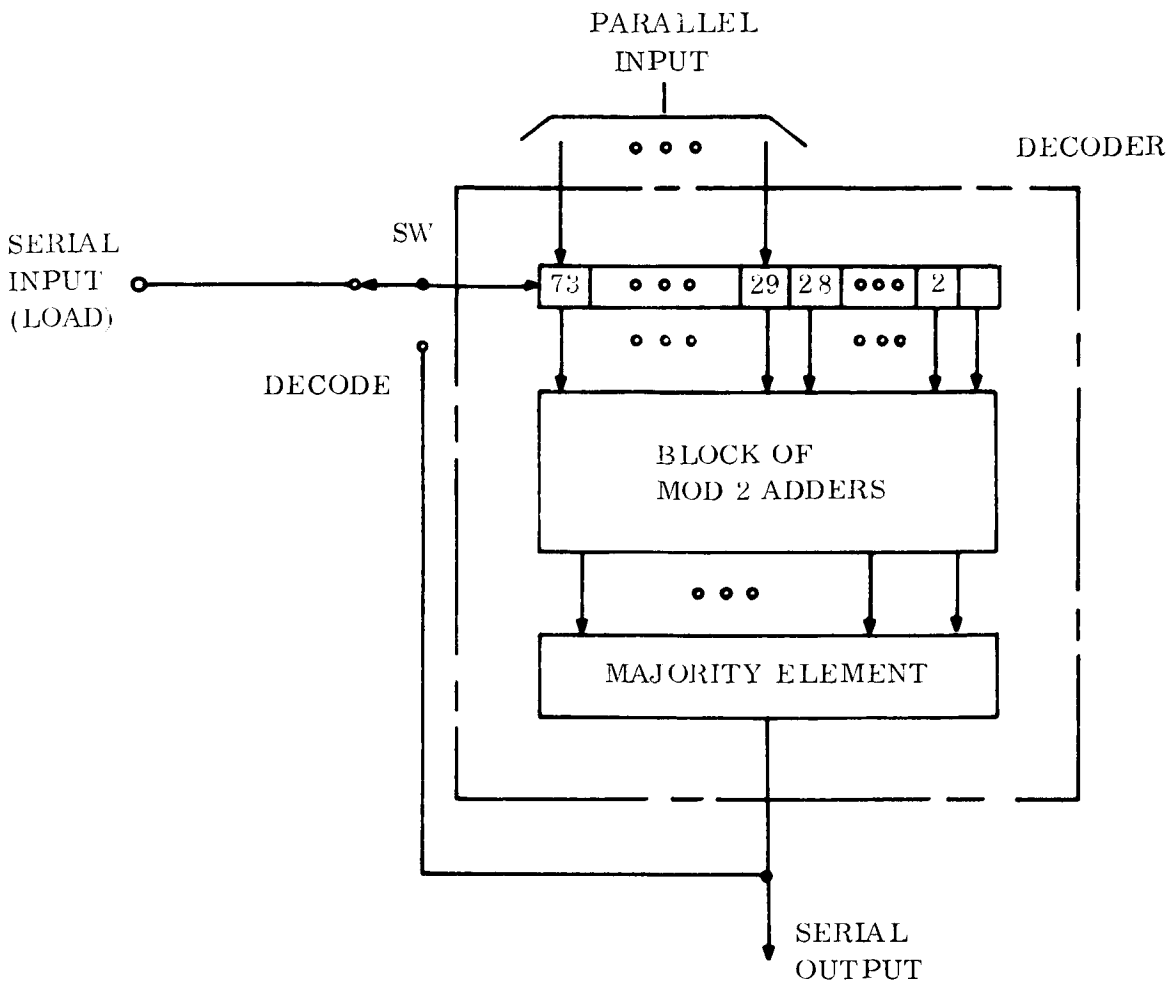

Figure X-6. (73, 45) Decoder

MODE 4 (Clock time t = 0.5)
Switch input of 73-stage decoding register from input terminal to output of majority element, and switch decoding subsystem input terminal to input of 45-stage buffer.

The decoder timer is identical to that for the encoder just discussed. However, its outputs are used somewhat differently. One difference is that the 45-bit sampling burst is used for output rather than input gating, and the output of flip-flop M controls the decoder mode switches (instead of the encoder mode switch). A second difference is the use of the special pulse $P_{45.5}$ generated in Mode 4, as indicated.

APPENDIX XI

ERROR CONTROL CODING

XI.0 THE (15, 5) BI-TRANSORTHOGONAL CODE

XI.1 INTRODUCTION

A close approximation to the (16, 5) bi-orthogonal code is a code consisting of two sets of words: a (15, 4) transorthogonal code set and its complementary code set. This double set is defined herein as a (15, 5) bi-transorthogonal code and is selected over the (16, 5) bi-orthogonal code because the cyclic nature of the former permits a simpler mechanization of the correlation decoder.

XI.2 PROPERTIES OF THE BI-TRANSORTHOGONAL CODE

Table XI-1 shows an example of a transorthogonal code set and complement set derived from a 7-bit pseudorandom sequence. At the top of the table is seen two periods of the sequence while below it are the two sets A and B, each containing eight 7-bit words. Note that the corresponding words in each set are complements of each other; for example, the first word of set A, all zeros, is a complement of the first word of set B, all ones.

Let S_i and S_j be any two words taken from either set, and let the zeros in the table be replaced by -1, then the cross correlation between the two code words is given by the following equation.

$$\varphi_{ij}(S_i, S_j) = \frac{1}{T} \int_0^T S_i(t)\, S_j(t)\, dt = \begin{cases} -\dfrac{1}{2^N - 1} & \text{for code words in the same set and } i \neq j \\[2ex] +\dfrac{1}{2^N - 1} & \text{for code words \underline{not} in the same set and } i \neq j \\[2ex] -1 & \text{for code words \underline{not} in the same set and } i = j \\[2ex] +1 & \text{for code words in the same set and } i = j \end{cases} \qquad (1)$$

where

N is the number of stages in the maximal length shift register generator.

Table XI-1. Transorthogonal Code Set and Complementary Set

	Two Periods of Pseudorandom Sequence (N = 3)	
	1 1 1 0 0 1 0	1 1 1 0 0 1 0
S_i	Set A	Set B
1	0 0 0 0 0 0 0	1 1 1 1 1 1 1
2	1 1 1 0 0 1 0	0 0 0 1 1 0 1
3	0 1 1 1 0 0 1	1 0 0 0 1 1 0
4	1 0 1 1 1 0 0	0 1 0 0 0 1 1
5	0 1 0 1 1 1 0	1 0 1 0 0 0 1
6	0 0 1 0 1 1 1	1 1 0 1 0 0 0
7	1 0 0 1 0 1 1	0 1 1 0 1 0 0
8	1 1 0 0 1 0 1	0 0 1 1 0 1 0

The only difference between this transorthogonal code set and complement and a biorthogonal code set is that the first two correlations shown in the above equations are zero when the latter code set is used. Note, however, that as N gets larger the value of these two correlations become very small and therefore may be neglected for all practical purposes. In the proposed (15, 5) code, N = 4.

XI.3 ENCODER

Figure XI-1 shows a simplified block diagram of the (15, 5) encoder. It consists primarily of a 4-stage maximal length shift register generator with a switch in its feedback loop. The first four bits of a 5-bit data group (b_1, b_2, b_3, b_4) are shifted serially through the switch in the LOAD position into the shift register, after which the switch is changed to the ENCODE position and the fifth data bit is loaded into the extra flip-flop. At the next clock pulse the first bit of the 15-bit code is shifted out of the shift register through the Mod 2 adder to the modulator. The process continues for the next 10 clock pulses at which time the switch is changed to the LOAD position and remains there for the next 4 clock pulses, etc. Data bit b_5 determines whether the output of the generator is complemented or not.

In summary, the 4 bits entering the shift register generator initialize it and enables it to produce 16 distinct 4-bit word entering the generator. The fifth bit selects the straight sequence or its complement.

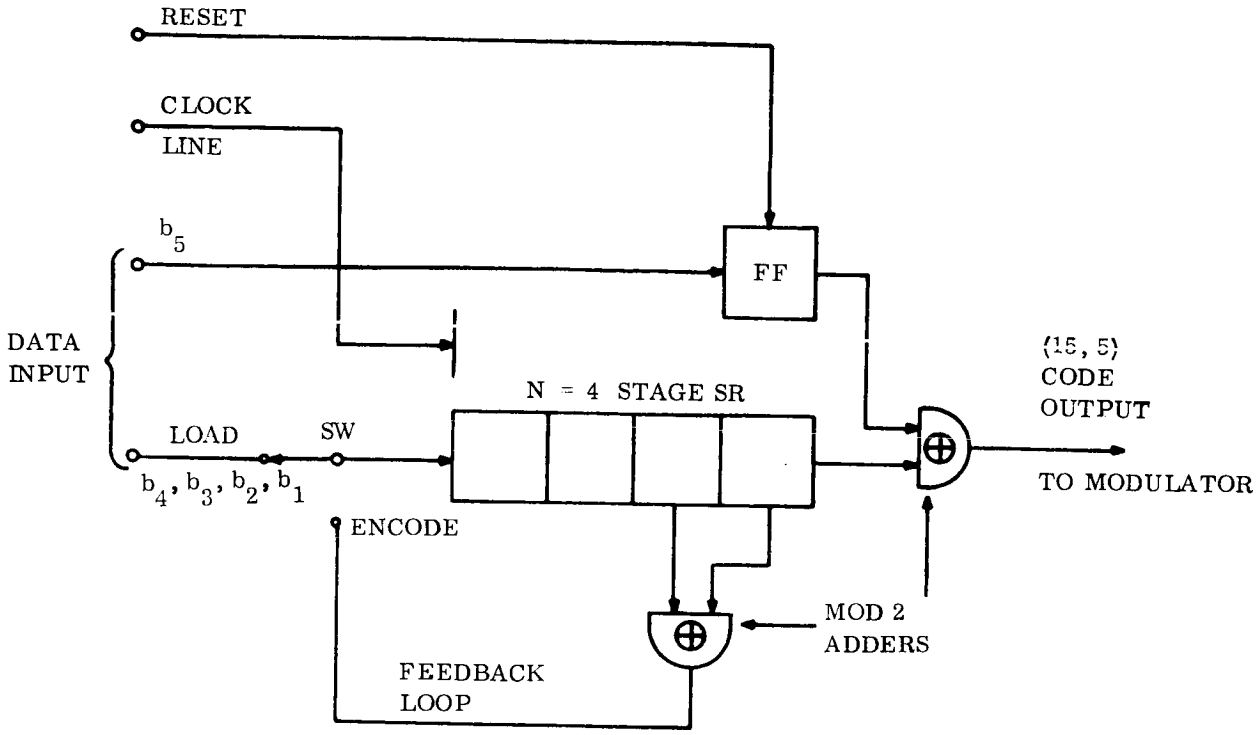

Figure XI-1. Encoder for (15, 5) Bi-Transorthogonal Code

XI.4 DECODER

Essentially, the main problem of the orthogonal category of codes is that the decoder must make multiple correlations on each received signal or code word, then select the correlation which is highest to determine which of the code words was "most likely" transmitted. In short, a "greatest-of" decision must be made.

In the literature on orthogonal and biorthogonal systems the usual way shown for implementing the decoder is to employ multiple correlators, one for each code word in the set, and operate them in parallel. At word sync time, each integrator is sampled to determine which has the highest value. This method may be described as one in which all correlations are performed serially on the incoming signal by each individual correlator and with all correlators working in parallel. An alternative method of implementation is one in which the correlation coefficient between the received signal and each local replica is produced in parallel (within one bit period of the code) and the process repeated with a different replica until all correlation coefficients for the received signal have been produced.

This latter technique requires one relatively large parallel hybrid correlator which produces sequentially the correlation coefficients between the received signal or code and each of the code words in the set. It has been chosen for implementation of the

bi-transorthogonal decoder because it is primarily a digital system and in several ways is simpler than the other approaches. It may be designed to approximate the first alternative mentioned to any degree desired.

The overall block diagram of the hybrid correlator used to decode the transorthogonal code set and complement is shown in Figure XI-2. The following are the essential functions performed by the correlator.

- After bit sync has been acquired a product detector works in conjunction with an integrate and dump circuit to produce an analog signal level which is proportional to the correlation coefficient between the received bit and the locally generated replica, thus, indicating how "good" of a "one" or "zero" it is.

- The analog signal level coming from the integrate and dump circuit is digitized to K bits in the analog-to-digital converter.

- The K bits are stored in a buffer shift register until all digitized bits of the code are contained in the buffer register.

- Parallel word correlation begins when the contents of the buffer shift register, being full, are transferred into the front half of the correlator shift register. The analog summing network immediately produces a voltage which corresponds to the correlation coefficient between the received code word and the first permutation of the pseudorandom sequence. With each bit sync pulse on the shift line the received code word is shifted to a new position on the correlator and a new correlation coefficient is produced corresponding to the permutation in that position. Precisely $2^N - 1$ correlations are made before the buffer shift register is completely loaded again and ready to transfer in the subsequent word that has been received. Thus, as a new quantized code word is transferred to the front end of the correlator register, the second half of the correlator register is cleared by the reset line shown on the diagram.

- The output of the analog summing network is routed over to a "greatest-of" and a "least-of" circuit, the purpose of which is to detect which correlation has the "greatest" and which has the "least" value, respectively.

- A word sync, or READ signal, is used to read out the value being held in the holding register of either of the two circuits. Also a special integrate and dump circuit is sampled with a dual threshold at this time to determine if the code word received were all "zero" or all "ones" rather than a permutation of the pseudorandom sequence.

The bit and word sync recovery system employed in the correlator is essentially the same as that used in the standard single channel demodulator with the exception that the pseudorandom code used for synchronization is selected so that its period is a multiple

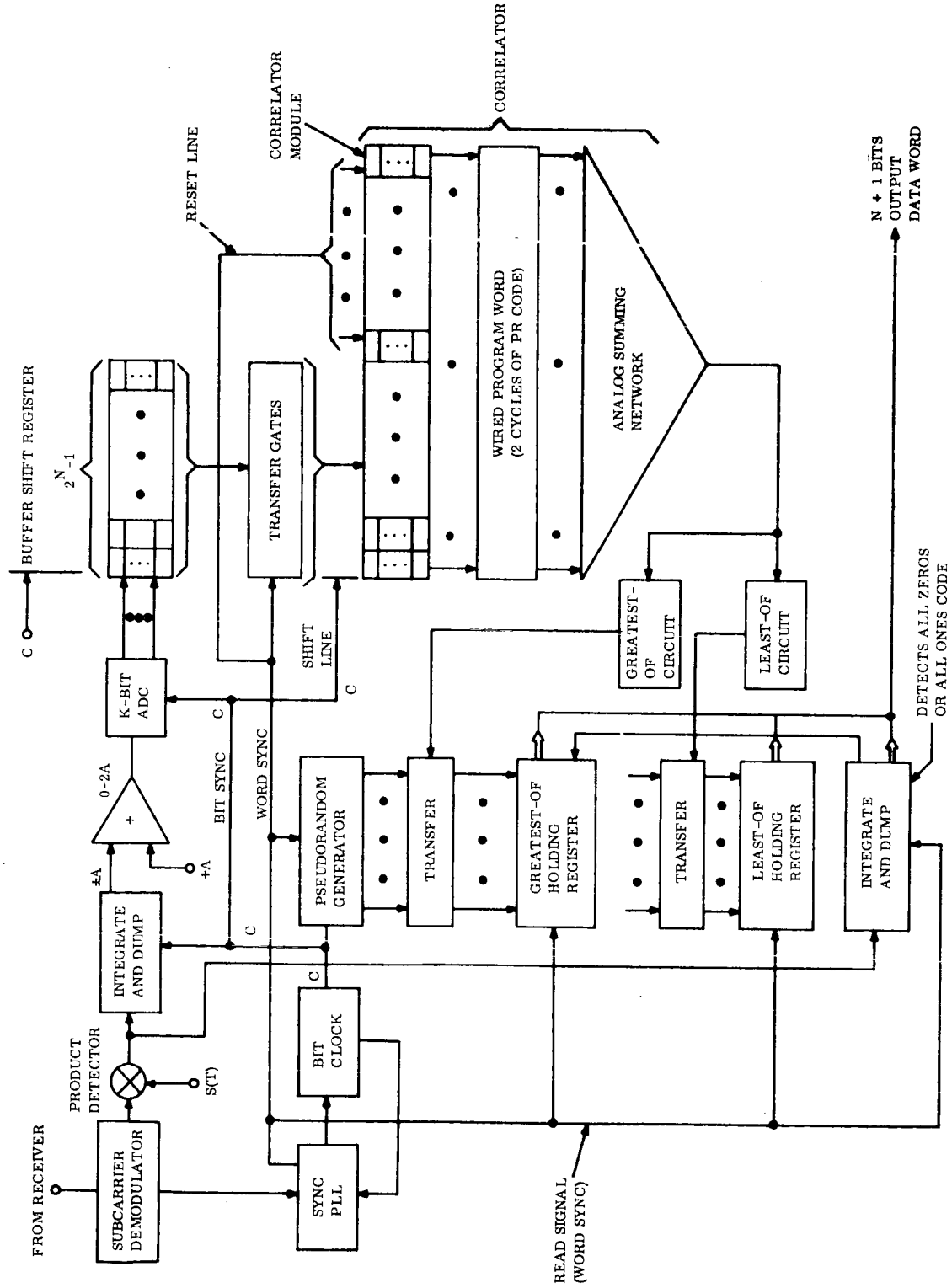

Figure XI-2. Parallel Hybrid Correlator

of the length of the transorthogonal code set used. For example, when a 15-bit transorthogonal code set and complement are used, the pseudorandom sequence used for synchronization in the single channel operation would have a period of 255 bits.

The product detector and integrate and dump circuit used for detection of the individual bits in the transorthogonal code is standard although the output of the integrate and dump circuit is fed into an amplifier which translates its range so that it becomes a unipolar signal.

Quantization of each of the transorthogonal code bits is performed by the analog-to-digital converter where a typical value for K may be 3, 4, or 5. Therefore, the number of stages in the buffer shift register is equal to K times the length of the transorthogonal code. The number of stages in the correlator shift register is double that value. The correlator program is wired with two cycles of the pseudorandom transorthogonal code in such a way that all of the permutations of the pseudorandom sequence set (set A) will appear somewhere within the length of the two cycles of the sequence, a property which may be observed by referring to Table 1.

The "greatest-of" circuit is designed so that it is sensitive only to levels which are above a prescribed upper threshold, whereas the "least-of" circuit is designed to be sensitive only to levels which are below a certain threshold. Hence, if the all "ones" or all "zeros" code on the transorthogonal code set is received, then neither the "greatest-of" nor the "least-of" circuit will have caused a word to be transferred to their respective hold registers. A special integrate and dump circuit is designed to detect the all ones or the all zeros code and will produce no output or indication under normal operation when any permutation of the pseudorandom code is received since the integrator value would thereby be at or near the mean or zero voltage level rather than some highly positive or negative level.

To aid in an understanding of the operation of the correlator, a diagram of a typical correlator module is shown in Figure XI-3. The number of these modules required on the hybrid correlator is equal to twice the number of bits in the transorthogonal code.

The module is shown with a K = 3 so that the 3 bits representing the quantized level of the received code bit may be transferred in parallel into the three flip-flops shown on the diagram. The resistors are wired to the output of the flip-flops according to the position of the module on the two cycles of the transorthogonal code. Specifically, if the module is at a position which is programmed for a "one," then the resistors are wired as shown; however, if the position is such that a "zero" is to be detected, then the resistors will be wired to the $\overline{Q}$ side of the flip-flop outputs. In this fashion, the three bits produced by the analog-to-digital converter are correlated in each position and an equivalent voltage is contributed to the summing line so that the sum of all module contributions produces the correlation coefficient between the received code being correlated and the permutation of the transorthogonal code at that instant.

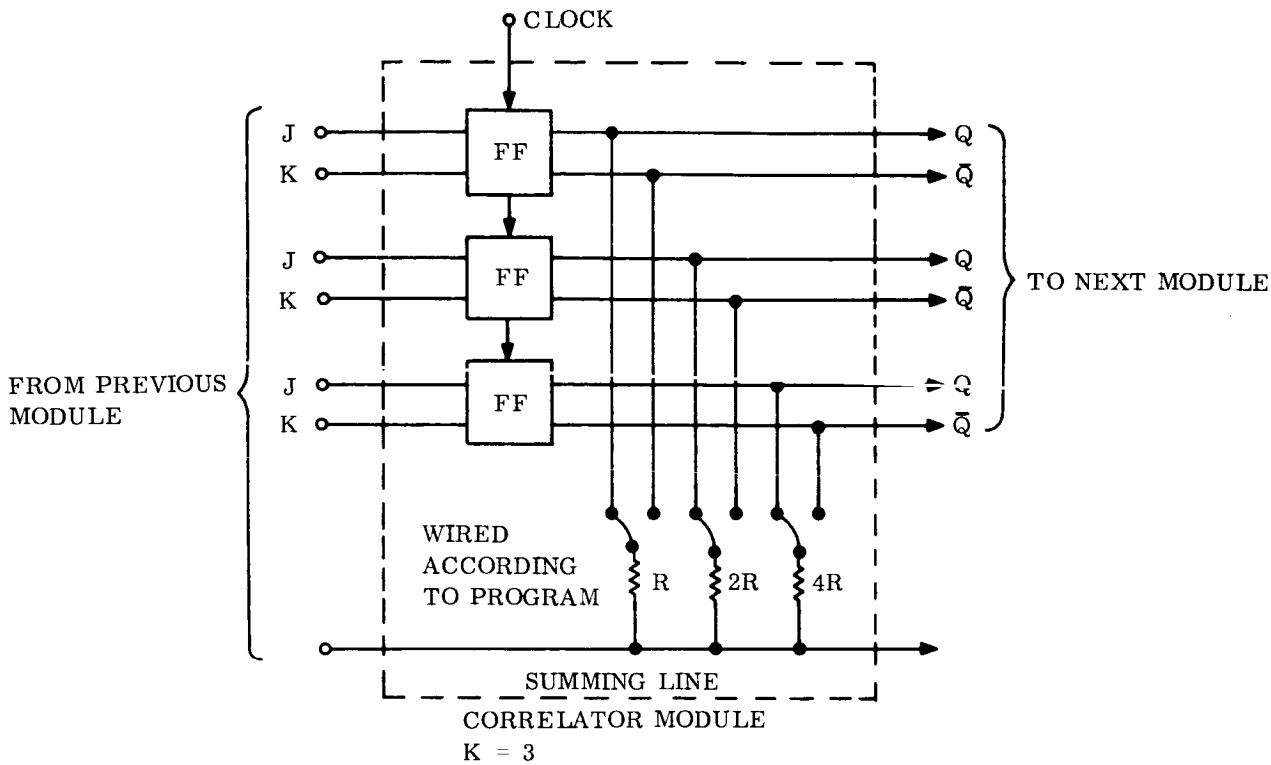

Figure XI-3. Correlator Module (K = 3)

While the received quantized code word is shifting across the correlator, it is preceded and followed by all zeros on each of the correlator modules which are not being used. Because of the structure of the two cycles of the transorthogonal code, the contribution due to the zeros before and after a received code will be a constant value (or bias) during the series of correlations and therefore is easily compensated for in the decision circuits.

A circuit which is typical of both the "greatest-of" circuit and the "least-of" circuit is that indicated in Figure XI-4. Whenever the correlator output is above or below the prescribed threshold mentioned earlier, the level goes into a differential amplifier where it is compared with that which is being stored on the holding capacitor shown in the diagram. If a subsequent output from the correlator is greater than that being stored on the capacitor, a voltage appears on the output of the differential amplifier which is used to transfer, at that bit period, the contents of the pseudorandom shift register generator into the holding register. In this manner the correlator output which was the greatest over the $2^N - 1$ trials will be stored on the holding capacitor and the state of the pseudorandom generator shift register which corresponds to that particular correlation is held in the holding register for transfer out at the appropriate time.

It should be noted that the pseudorandom generator shown on the diagram is identical to that which was used in the encoder and is synchronized so that it provides a relatively simple means of providing instantaneously the proper decision at the end of the $2^N - 1$ trials.

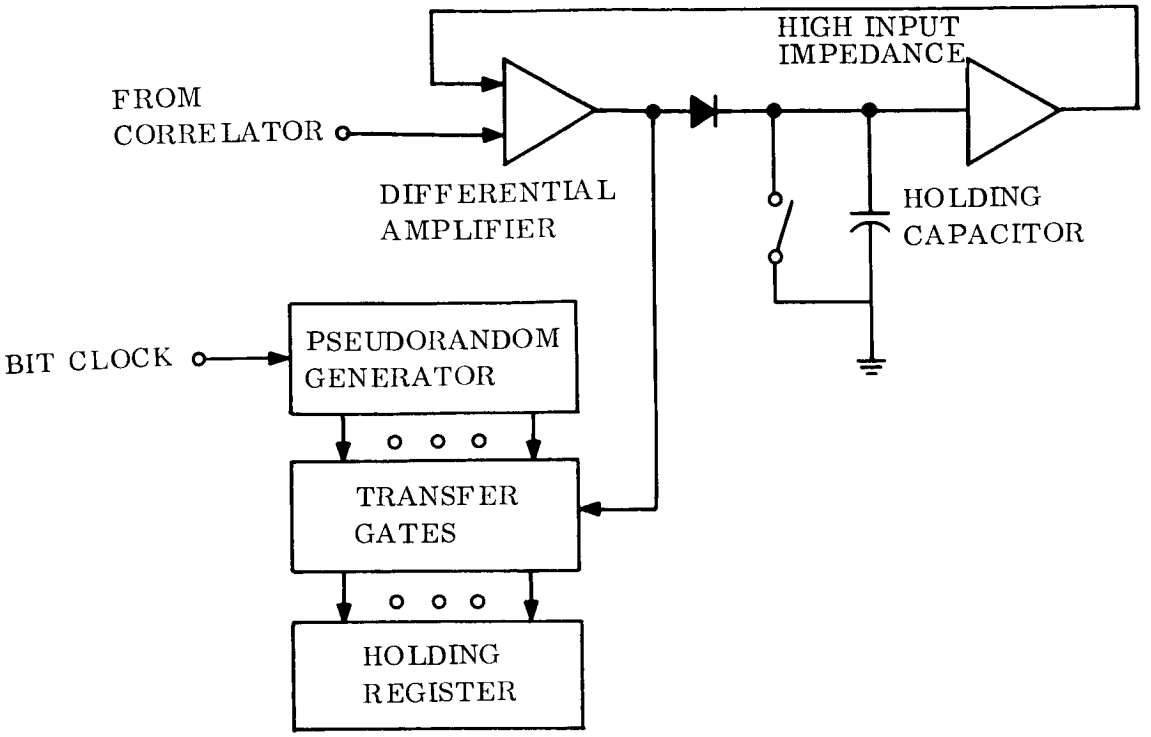

Figure XI-4. "Greatest of" Decision Circuit

CII - VB233AA107

ALTERNATE SUBSYSTEM MECHANIZATIONS CONSIDERED

DATA STORAGE

Index

1	Scope
2	Applicable Documents
3	General
4	Development of a Minimum Data Storage Subsystem
5	Preferred Design of Voyager Data Storage Subsystem
6	Alternate and Backup Operations Available for Preferred Design
7	An Alternate Storage Configuration
8	Selection of High-Capacity Storage Components
9	Selection of Magnetic Tape Recorder Configuration
10	Selection of Non-Bulk Storage Components

1.0 SCOPE

The following sections justify the selection of the preferred Data Storage (D/S) Subsystem configuration described in Volume VB233FD107. A basic minimum system is developed on functional grounds, with no reference to implementation considerations, and used as a basis of comparison for the preferred design. This comparison demonstrates the operational flexibility, reliability, and minimum implementation cost features of the preferred system.

Following this comparison, several variations on the preferred design are considered and evaluated. Finally, a basically different configuration is presented and compared with the preferred design.

2.0 APPLICABLE DOCUMENTS

VB220SR101	Design Characteristics
VB220SR102	Design Restraints
VB220FD106	Capsule Interface
VB220FD108	Science Interface
VB233FD107	Data Storage Subsystem
VB233FD105	Data Handling and Storage
VB233TA105	Data Handling and Storage

3.0 GENERAL

The Data Storage (D/S) Subsystem provides for storage of binary digital data as required by the mission data handling requirements. Justification of the preferred design and alternates considered are discussed in the following sections:

a. Minimum D/S Requirements

b. Preferred Configuration of Voyager D/S Subsystem

c. Alternate and Back-up Operations Available For the Preferred Design.

d. An alternate Bulk Storage Configuration

e. Selection of High Capacity Storage Components

f. Selection of Magnetic Tape Recorder Configuration

g. Selection of Non-Bulk Storage Components.

4.0 DEVELOPMENT OF A MINIMUM DATA STORAGE SUBSYSTEM

The requirements for data storage are generated by the mission data handling sequence developed and presented in Volumes VB233FD105 and VB233AA105. This development indicates a requirement for three basically different sections of the D/S subsystem. These sections are a low capacity (98 bit max) capsule data buffer, a medium capacity (approximately 50 k bit) storage for various data types, and a high (6×10^8 bit) capacity store for planet scan data. For reasons discussed in Sections 8 and 9 of this volume, these requirements are to be satisfied with, respectively, integrated circuit registers, designated as Capsule Relay Buffers (CRB's); ferrite core memories, designated as Magnetic Core Memories (MCM's); and tape recorders, designated as Magnetic Tape Recorders (MTR's). The following discussion develops the minimum basic D/S subsystem configuration. It is organized on the basis of the three major D/S sections defined above, and employs the various mission sequence requirements to determine capacity and rate requirements.

4.1 CAPSULE RELAY BUFFERS

Throughout the mission until capsule impact, data is received from the capsule in a uniform 10.16 bps stream. Since the capsule clock is not synchronized with the bus clock, the data must be phase buffered to allow resynchronization with the bus clock. In addition, groups of 70 or 98 capsule data bits, depending on the transmission format, must be accumulated for synchronous block insertion into the transmission bit stream. Since the dumping of a 70 or 98 bit group at the normal 106.67 bps transmission spans several capsule bit times, a minimum of two 98 bit CRB registers with a toggled input/output switch are required to avoid data loss.

4.2 MAGNETIC CORE MEMORIES

The primary requirement for MCM storage is the buffering of engineering and non-scan science data in orbit to permit its multiplexing with the playback of planet scan data from the MTR units. The capacity required for this operation is 49.14 kbits (See Table 4-1). Since this data is supplied as 7 bit words that have no word sync information until PN encoded, the MCM store should be word rather than serial bit organized to allow the easy maintenance of word sync in storage. For simplicity, it would be desirable that the word length be some multiple of the 7 bit data word length.

The loss of the high gain transmission link during spacecraft maneuver turns requires that engineering and capsule data be stored to avoid its loss. The nominal capacities required for these operations are 62,180 bits (102 min x 10.16 ps) of capsule data and 22,400 bits (102 min x 3.33 bps) of maneuver engineering data.

Table 4-1. Data Storage Subsystem Functional Requirements and Operating Configurations

I	II	III	IV	V	VI
Mission Phase	Requirements on Storage Subsystem	Input Rates	Output Rates	Capacity Required	Description of Storage Subsystem Operating Configuration
Normal Cruise	Buffer Capsule Umbilical data to allow insertion into transmission format. No other storage required	10.1 bps continuous buffering	At transmission rate in bursts to fit format	70 bits	Capsule Relay Buffers CRB1 and CRB2 alternately load 70 bits (10 words) of data and read out to DE input. Magnetic Core Memory (MCM) section on standby. Magnetic Tape Recorder (MTR) section not required until orbit phase.
Science Flare in Cruise	Store flare science data from DAE at high rate	As high as practical	NA	As large as practical	MCM1, MCM2, MCM3 cascaded to store flare data in any format and at any rate < 100 Kbps. Maximum storage is 85,939 bits + 56-bit preamble. If not dumped, may be overwritten by maneuver data.
Spacecraft Maneuvers	Store capsule data during maneuver. Store engineering data in parallel with transmission	10.1 bps capsule	NA	As required by duration of maneuver	MCM1, MCM2 cascaded to store capsule data from relay or umbilical link at 10.16 bps for a maximum of 5640.4 sec. (57,274 bits + 56 bit preamble.)
		3.33 bps engineering	NA	As required by duration of maneuver	MCM3 stores maneuver data at 3.33 bps for a maximum of 8597.5 sec. (28,609 bits + 56-bit preamble)
Core Memory Dump	Dump out stored maneuver, capsule, or flare data for high rate transmission	NA	Matched to transmission rate	NA	MCM1, MCM2 dump contents in cascade 3 times: then MCM3 dumps 3 times, all at transmission rate (usually 2.133 Kbps). Dump duration is (257,985/Rate): e.g. 120.9 sec at 2.133 Kbps.
Capsule Cruise	Buffer capsule relay data to allow insertion into transmission format	10.1 bps continuous buffering	Transmission rate in bursts to fit format	70 bits or 98 bits	Capsule Relay Buffer Registers CRB1 and CRB2 alternately load 70 bits or 98 bits of data and readout to DE input.
Capsule Entry	Provide storage of entry data from capsule relay as backup to simultaneous transmission	10.1 bps	NA	18,285 bits	MCM1, MCM2 store (in cascade) capsule relay data for a maximum of 5640.4 sec. (57,274 bits + 56-bit preamble) CRB section functions as during capsule cruise.
Normal Orbit (A)	Provide high capacity storage for planet scan data at a 50 Kbps rate: buffer non-scan science and engineering playback scan data multiplexed with non-scan science and engineering	50 Kbps scan data + 426.67 bps engineering and non-scan science data	Transmission rate	6×10^8 bits (Nominal) + buffering capacity	Recorders MTR1, MTR2, and MTR3 cascaded to store 6×10^8 bits of planet scan data at an input rate of 50 Kbps. The data is recorded in data blocks of 10^6 bits or less followed by 56 bit identification blocks and separated by one second data-free gaps or MTR stop/stop operations. The playback is bit synchronous with the transmission rate and is continuous. During playback, MCM1 and MCM2 are cascaded to store 39 frames (49, 140 bits) of non-scan science and engineering during the transmission of a scan frame. (115.17 sec at 8.533 Kbps). This data is dumped (bit synchronous) into the transmission stream during the passing of each data-free gap or stop/start blank over the MTR playback head. (5.759 sec at 8.533 Kbps) The playback continues until all scan data is exhausted.
(B)	Scan data exhausted Scan not in process.	NA	NA	NA	No storage required.
(C)	Scan data exhausted from previous scan. Scan data being generated.	Scan 50 Kbps	NA	6×10^8 bit (Nominal)	MTR1 records until filled, then playback begins. MTR1 will begin playback as MTR2 and MTR3 record scan data. MCM units do not function until playback begins, as in Normal Orbit (A).
I	II	III	IV	V	VI
Mission Phase	Requirements on Storage Subsystem	Input Rates	Output Rates	Capacity Required	Description of Storage Subsystem Operating Configuration

The total MCM storage required for this purpose is therefore 84,580 bits, which is somewhat more than that required for the orbital buffering operations. The other requirements for MCM storage of capsule entry and cruise science flare data require no more capacity than maneuver data. They do, however, create requirements for an MCM input selector control that can, either on command or by internal priority decision, select the proper input at the proper times. This control would function, for example, to initiate storage of flare data when required, and to prevent its storage during maneuver intervals.

4.3 MAGNETIC TAPE RECORDER

The required capacity of the planet scan data storage is nominally 6×10^8 bits. Data must be accepted at a 50 Kbps rate and replayed at 8.533; 4.267, 2.133, and 0.533 kbps. A control section would also be required to start and stop the recorder and to control record or playback functions.

4.4 MINIMUM D/S SUBSYSTEM CONFIGURATION

The minimum D/S Subsystem is shown in Figure 4-1 consists of two 98-bit CRB registers with their input/output toggle switch, one 84,580 bit MCM unit with its control, and one 6×10^8 bit MTR and its associated function control. The data handling sequence requirements discussed above are summarized in Table 4-1, columns II, III, IV and V. Column VI of that table is a summary description of the response of the preferred system to the stated requirements, and will be discussed in the following sections.

5.0 PREFERRED DESIGN OF VOYAGER DATA STORAGE SUBSYSTEM

The preferred Voyager D/S Subsystem configuration, described in detail in Volume VB233FD107, is shown in block diagram form in Figure 5-1. This configuration consists of three 99-bit CRB registers, three 28,665-bit 4095 word MCM stores, three 2×10^8 bit capacity MTR units, their associated control sections, and a central power supply. It may be seen that, as discussed below, it differs in detail rather than concept from the minimum configurations developed in the preceding sections. The differences are based on requirements for redundancy and operational flexibility, and for minimized implementation costs. The preferred and minimum configurations are compared on these bases in the following sections.

5.1 CONFIGURATION COMPARISON

The following discussion is organized on the basis of the three major sections of the D/S subsystem.

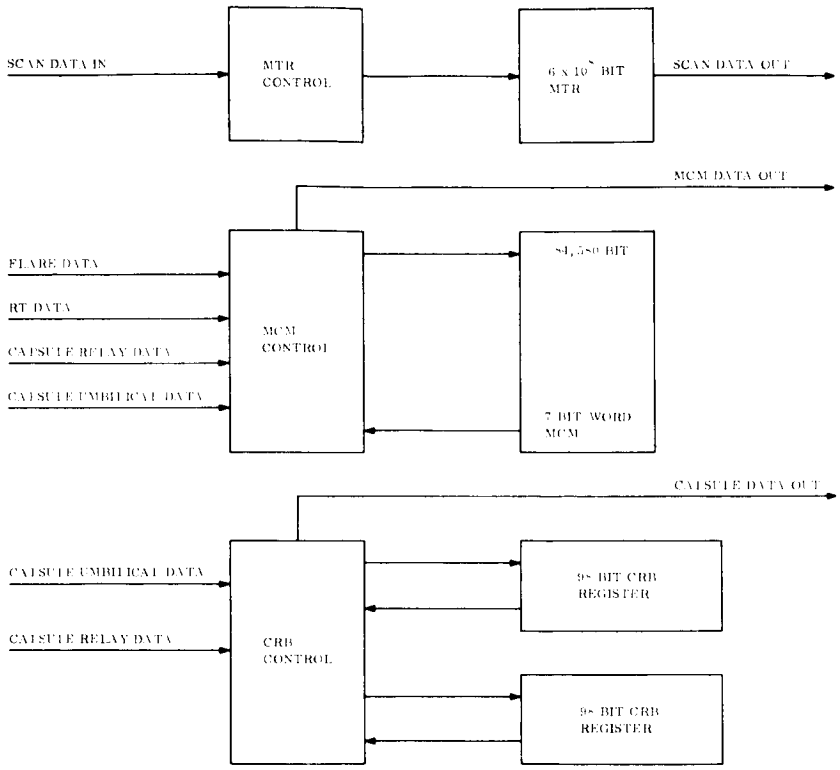

Figure 4-1. Basic Minimum D/S Configuration

5.1.1 CRB SECTION

The preferred CRB section configuration varies in two ways from the basic required system. First, a third CRB register, which may replace either of the other two, has been added for the sake of increased reliability, as shown by Table 5-1. Second, the size of the CRB register has been increased from 98 to 99 bits for the purpose of a more simple implementation of "register filled" signal generation required to toggle the input/output control switch. The selection of the CRB register components is described in Section 10 of this volume, where the results of more extensive reliability calculations are presented.

Table 5-1. Effect of CRB Register Redundancy on Survival Probability

Configuration	Probability of Survival until capsule impact
2 registers only	0.9663
3 registers with one redundant	0.9995

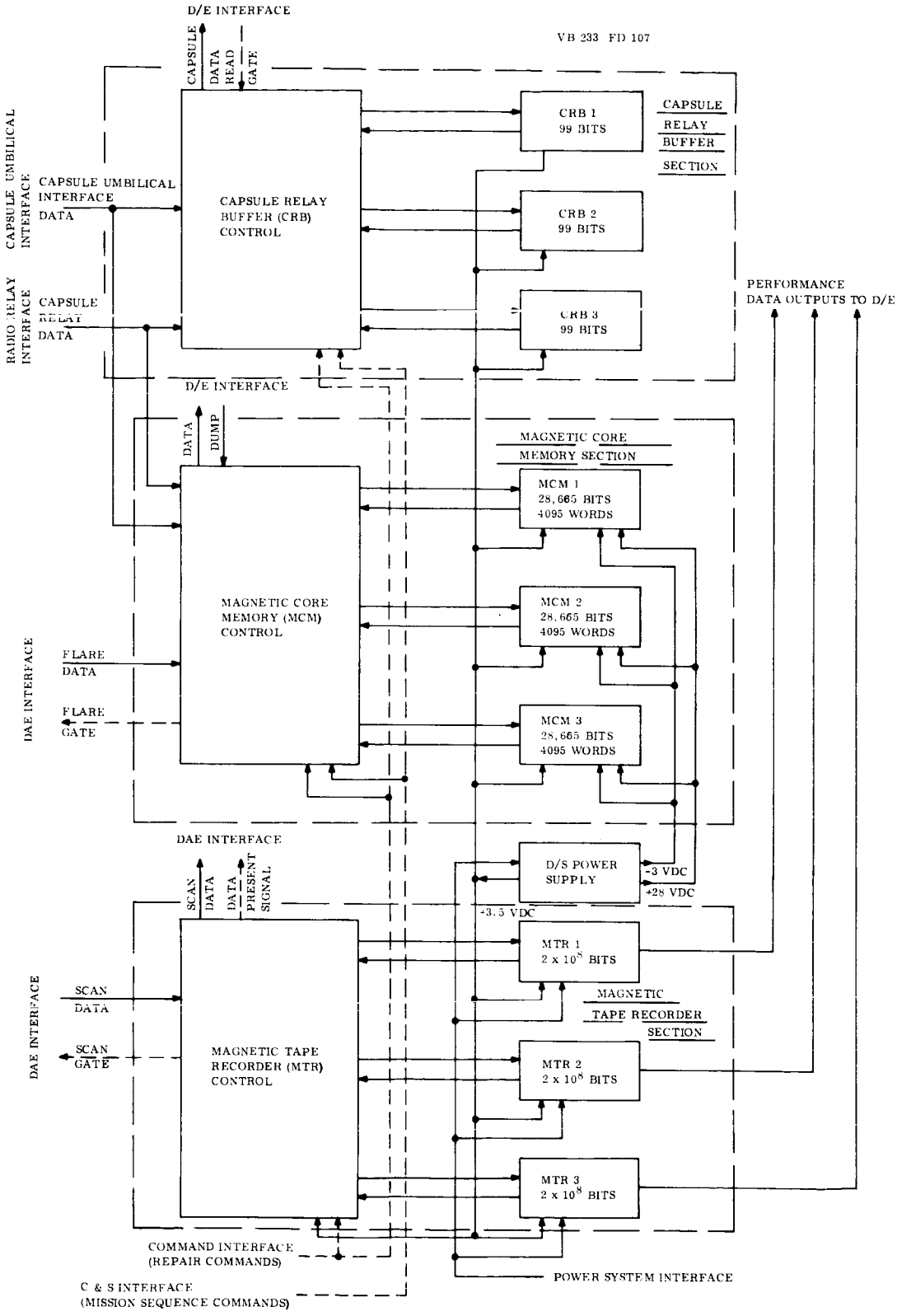

Figure 5-1. Data Storage Subsystem

Detailed discussion of the functioning of the CRB section may be found in Volume VB233FD107 (Data Storage). A summary of these operations is given in Section 6.0 below.

5.1.2 MCM SECTION

The preferred MCM section configuration employs three 28,665-bit, 4095-word stores instead of the one 84,580-bit unit required by the minimum system. The capacity of the units was determined on the basis of three factors. First, the 4095 word count is compatible with a 5 x 7 x 9 x 11 four-way access switch configuration. Second, as discussed in Section 10, the 4095 word size is near the maximum compatible with the nominal allowable bits/sense line figure of 4000. Finally, organization on a 7 bit/word basis yields 28,665 bits.

This capacity is large enough to permit the use of only two MCM units in normal orbital operations, allowing the third to function as a redundant standby. The increase in reliability over a single MCM unit is shown in Table 5-2. In maneuver operations, capsule data can be stored in two cascaded MCM units while maneuver engineering is stored in the third. This operation removes the necessity for onboard multiplexing and ground separation of the two data types.

Table 5-2. Effect of MCM Redundancy on Survival Probability

Configuration	Probability of Survival Through 6-Month Orbit (5352 hours total operation)
1 - 84,580-bit MCM	0.8100
2 out of 3 28,665 bit MCM units (68,000 hr MTBF)	0.9917

Three identical MCM units are employed for two reasons. The uniformity simplifies the redundancy switching of the spare unit, and the development, production and spares costs are minimized by having only one size unit to design and produce.

A detailed discussion of the functioning of the MCM section may be found in Volume VB233FD107, (Data Storage). Details of these operations are also summarized in Section 6.0.

5.1.3 MTR SECTION

The preferred design differs from the basic system in that it employs three 2×10^8 bit recorders rather than one large unit. The desirability of limiting the individual MTR capacity to this value is discussed in Section 9. The system reliability is enhanced by this division of the MTR storage, in the sense that the probability of maintaining reduced capacity operations is increased. This is demonstrated in Table 5-3, where the preferred system is compared with the use of one 6×10^8-bit MTR.

Table 5-3. Effect of MTR Redundancy of Survival Probability
Probability of Survival, 6-Month Orbit

	6×10^8 bits	(4321 hours) 4×10^8 bits	2×10^8 bits
1 - 6×10^8-bit MTR (Est. MTBF = 7000 hrs)	.5395	.5395	.5395
3 - 2×10^8-bit MTR's (MTBF = 10000 hrs)	.2740	.7890	.9568

The operation of the MTR section of the D/S Subsystem is summarized in Section 6.0.

5.1.4 D/S SUBSYSTEM POWER SUPPLY

On the basis of previous experience, all power supplies except some special MTR units were centralized and combined into the single unit shown in Figure 5-2. Preliminary calculations indicated that substantial savings of size and weight could be made by employing this design rather than distributed individual unit or section supplies. Any reduction in reliability was negligible when compared with the failure rates of the serial reliability chains of which it is an element. Table 5-4 compares the centralized supply to a distributed type on the basis of estimated size and weight. Both are considered to be doubly redundant systems. The use of component and system redundancy illustrated in Figure 5-2 also qualifies it for use under a single critical failure criterion.

Table 5-4. Comparison of Power Supply Characteristics

	Volume (in.)	Weight (lb)
Centralized (Preferred) Design	220	5.0
Distributed Design (Total)	350	8.0

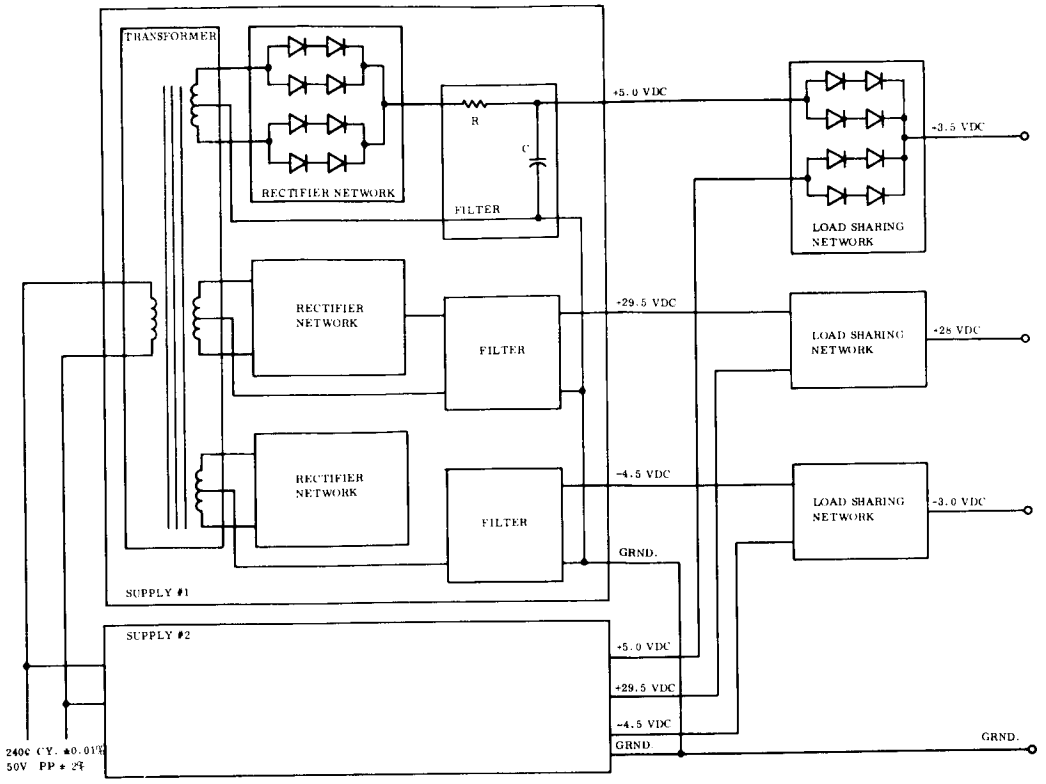

Figure 5-2. Data Storage Power Supply, Functional Blocks

5.2 GENERAL FEATURES OF PREFERRED DESIGN

The following justifies design features common to all sections of the D/S Subsystems.

5.2.1 CYCLIC FUNCTION EXCHANGE

The repair functions available in the CRB, MCM, and MTR sections are implemented as cyclic permutations of control output channels and storage units. Since only three storage units are employed in any section, this cyclic function permits the placing of any one or two malfunctioning units in unused or low priority operational positions. This technique is employed because it requires only slightly more implementation than a simple function transfer switch and allows the use of only one command line per section.

5.2.2 DIRECT ACCESS LEADS

The D/S Subsystem direct access interface connections listed in Volume VB233FD107 were chosen as the functions most useful in evaluating system performance.

6.0 ALTERNATE AND BACKUP OPERATIONS AVAILABLE FOR PREFERRED DESIGN

There are a number of alternate modes of operation available for the preferred design, some of which might be implemented as degraded capability backups to normal operations. These are discussed in the following sections, where the normal mission operation is summarized to provide a basis of reference. A quick reference summary is also provided in column VI of Table 4-1.

6.1 NORMAL CRUISE OPERATION

In normal cruise operation, the MTR sections may be totally disabled, but the MCM section must be capable of responding rapidly to a science flare occurrence, requiring storage of data. The CRB functions continuously until capsule impact.

6.2 SCIENCE FLARE OPERATION

When a science flare event occurs, the 3 MCM's are connected in cascade to form an 85,995-bit store which will accept data at any rate below 100 kbps until the store is filled. The data stored during flare intervals is tagged with a 56-bit preamble for source identification, leaving 85,939 bits for data storage. After storage of flare data, its presence is indicated as an engineering data signal, and further input to the MCM section is inhibited until a data dump has been completed. The exception to this rule is maneuver data, which may be written over flare storage. In case of failure of the storage of flare data in MCM units, storage could alternately be done by one of the MTR stores.

The performance would be degraded by the 1-second start time requirement and the fixed 50 Kb input rate. The former would entail the loss of the first second of flare event data, and the latter would result in high inefficiencies in data storage packing and transmission densities. A commanded recorder dump mode would also be required to enable recovery of this data, unless it could wait until the first orbital transmission period.

6.3 SPACECRAFT MANEUVERS

During bus maneuvers, capsule output data is stored for later transmission, and bus engineering is stored in parallel with its low-rate transmission. The capsule data is stored in two cascaded MCM's (MCM 1, MCM 2) to a limit of 57,274 bits plus a 56-bit identifying preamble. The maximum duration of this storage is 5635.8 seconds at the 10.16-bps capsule rate. Maneuvers engineering is stored in MCM 3 to a limit of 28,609 bits plus 56-bit preamble. The maximum maneuver storage is 8589 seconds at 3.33 bps. After storage of maneuver data, all further input is inhibited until a dump or another maneuver interval occurs.

Again, in case of failure of the MCM section, an MTR could be employed as the storage component. Although the start time characteristics of the MTR are no problem in this application, the data packing efficiency would be only ((14) (10.16)/ 5×10^4) x 100 = 0.028% the normal 50 kbps record rate, and the transmission of the nominal 58 kbit of maneuver data would require approximately 12 hours at the highest transmission rate.

6.4 CORE MEMORY DUMP

The MCM dump operation is always automatically initiated after completion of a maneuver and may be commanded in case of a flare storage or C&S malfunction after maneuver. The dump proceeds in two stages. First, MCM 1 and MCM 2 are dumped in cascade for three full cycles in synchronism with the transmission of the data. The MCM 3 is dumped three times at the transmission rate. All readout is non-destructive and a dump may be repeated if not properly received. Dumps normally occur at the 2.133 kbps transmission rate.

6.5 CAPSULE RELAY BUFFERING AND ENTRY STORAGE

Throughout the mission, prior to capsule impact, all capsule relay data is phase and rate buffered by the CRB section for insertion into the bus transmission format. The CRB registers alternately accumulate 70 bits (10 words) or 98 bits (14 words) of capsule relay data, depending on the transmission format, and dump them at the transmission rate when called for by the Data Encoder. The input/output functions are toggled so that one CRB is always loading while the other may be reading out. During the nominally 60-minute entry period preceding capsule impact, the relay data is stored in cascade in MCM 1 and MCM 2, and is simultaneously transmitted after processing by the CRB section. The maximum storage is 57,274 bits or 5635.8 seconds. A 56-bit preamble is also provided. A commanded interlock may prevent the replacement of this data by any other until another ground command is received signifying that the data transmission has been successful.

In case of the failure of the CRB section during cruise, two MCM units could be employed to alternately gather and dump data in the same fashion as the normal CRB operation. This system has the disadvantage that the storage of entry data could not be conducted in parallel with the buffering operation unless only one MCM stored the entry data while two acted as CRB replacement, thus reducing the storage capacity to 28,609 bits or 2817.9 seconds.

6.6 ORBITAL OPERATIONS

The normal orbital operation involves storage and replay of planet scan data, as well as insertion of non-scan DAE science and bus engineering data in the transmission format. The scan data is stored in the MTR Section to a limit of 6×10^8 bits. The DAE interface is constrained to supply this data in no larger than 10^6-bit blocks at a fixed 50 kbps rate. The blocks must be separated by at least 1-second intervals. If

the interval is to exceed 1 second, the DAE indicates this and the recorder stops and restarts for the next block, requiring a 1 second start time before data may be accepted.

Each stored scan data block is preceded by a 56-bit preamble. Storage of data continues until the capacity of 600 blocks is exhausted or the scan interval terminates. While scan data is being stored, and before playback begins, non-scan science and engineering data is transmitted in real time and no other storage is required.

When playback begins, the scan data is transmitted as the MTR plays it out in bit synchronism with the transmitter. Real-time data is accumulated in MCM 1 and MCM 2 (cascaded) during the transmission of each scan block at a rate allowing the storage of 39 frames (49,252 bits, 7036 words). As the data-free gap caused by stop/start or scan frame spacing reaches the play-back head, this is detected by the MTR data validity detector. The modulator input is then connected to the MCM output line by the Data Encoder, and the contents of the buffers are dumped once in this gap. After the dump is completed, bit sync is maintained by a string of "zeros" until the next valid scan data block is detected at which time the modulator is reconnected to the MTR output.

Playback continues until the scan data is exhausted or the next scan period requires that the recorder playing back be readied for recording new data.

If storage of science flare data during orbital operations were required, it could pre-empt the MCM storage normally assigned to real-time buffering functions. The accumulated data could be multiplexed with scan data in the same way that the real-time data would be in normal operation.

Operations after multiple-MCM failures in the orbital mode could be conducted by operating the Data Multiplexer at the transmission rate during the gaps between scan data frames. This, in effect, leads to burst sampling of the engineering and DAE science channels with a repetition rate equal to the inverse of the scan frame transmission time interval.

The only feasible backup to total failure of the MTR system is real-time transmission of scan data, since no significant amount of scan data could be stored in the MCM units. The MCM units could, if required, be employed to rate buffer 85,995 bit blocks by operating alternately in store and dump modes. The transmission capacity would, however, be reduced to the product of the scan interval and the maximum transmission rate; e.g., (8 kbps x 2·hrs) $\doteq 6 \times 10^7$ bits.

7.0 AN ALTERNATE STORAGE CONFIGURATION

An unattractive feature of the preferred D/S subsystem is the relative inflexibility of the interface requirements on the DAE scan data inputs. The restriction to 10^6 bit maximum frame size, the one second minimum frame spacing, and the fixed 50 kbps input rate of the MTR system place severe restraints on the DAE. The alternate D/S configuration of Figure 7-1 was developed to permit the relaxing of these requirements. It differs physically from the preferred configuration in that it employs two 10^5-bit MCM units. It was found that, as described below, the implementation requirements were beyond the capabilities of the present state of the art for the MTR storage components. It was therefore rejected as a useful replacement for the preferred system.

7.1 OPERATING SEQUENCE

The operation of this configuration is identical to that of the preferred system except in its handling of recorded planet scan data. During the planet scan period when data is being generated, the 10^5-bit MCM units alternately collect data at any rate below 50 kbps and in any format or frame size. The contents of each MCM is recorded on an MTR after a 10^5 block has been accumulated. The record function sequence is shown in Figure 7-2. The effect of this operation is that the DAE output may have any format and rate, restricted only to rates less than 50 kbps. The MCM format in the data for block storage on the MTR in 10^5-bit blocks separated by a stop/start or equivalent dataless gap. Playback occurs as shown in Figure 7-3. Blocks of MTR data are alternately loaded into the MCM units as required, with each transfer separated by an MTR stop/start operation. MCM output may be at any rate and any format, so that real time data could easily be multiplexed with the scan data playback.

7.2 ANALYSIS OF TRADEOFFS

The principle objection to the use of this configuration is the implementation requirements. The MCM capacity and the maximum required number of MTR stop/start operations per orbit, n, interact to make either a highly reliable or a physically small system impossible to obtain. The equation $\frac{n}{2} = \frac{6 \times 10^8}{c}$ described this relation. For the nominal $c = 10^5$ bits, which is already a large MCM capacity for spacecraft applications, the number of stop/start operations is 6000 per orbit, or nominally 6000/24 hrs. The results of Section 9 indicate that this is far in excess of the allowable number of such operations for a high-reliability system. The problem is further aggravated by the high record rates (100 kbps) and the less efficient uses of the tape for data storage (only 50% for 10^5-bit block size). Expansion of the block size to higher limits results in a decreased reliability due to the increased MCM size required. For this reason, consideration of the configuration was abandoned.

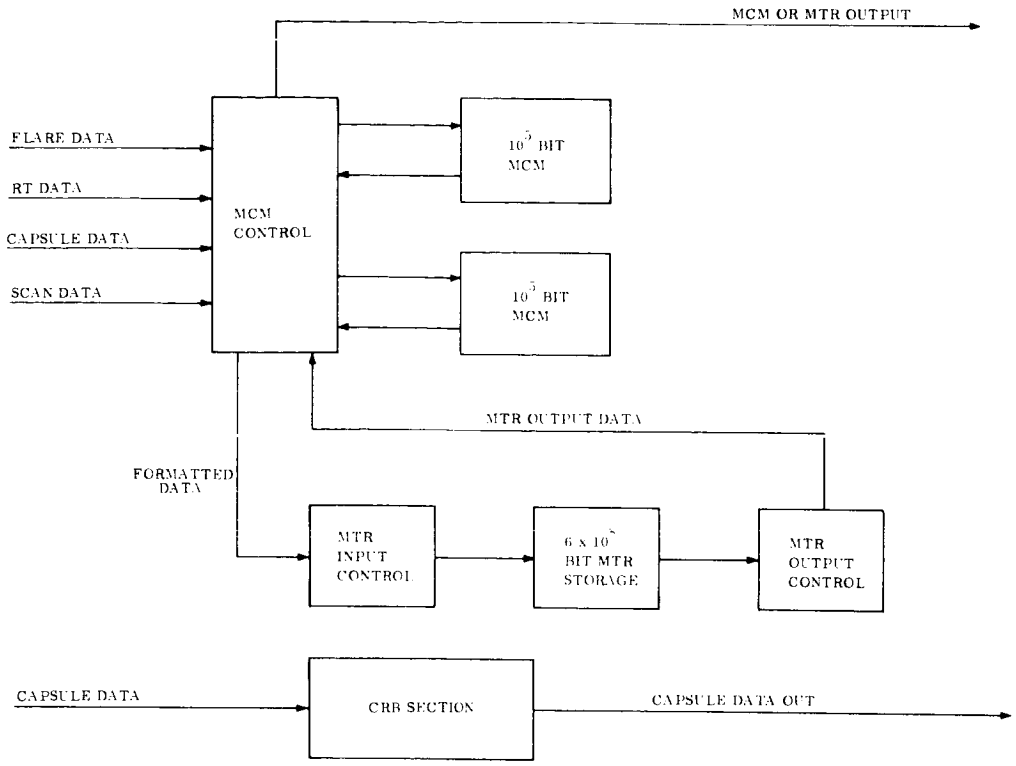

Figure 7-1. Alternative D/S Subsystem Configuration

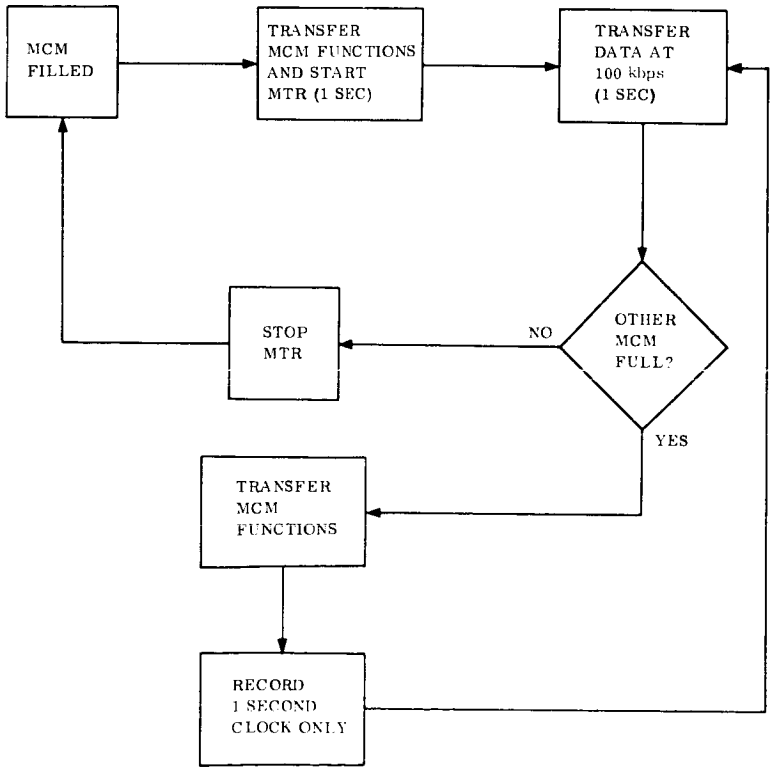

Figure 7-2. Record Operation Sequence for Alternate D/S

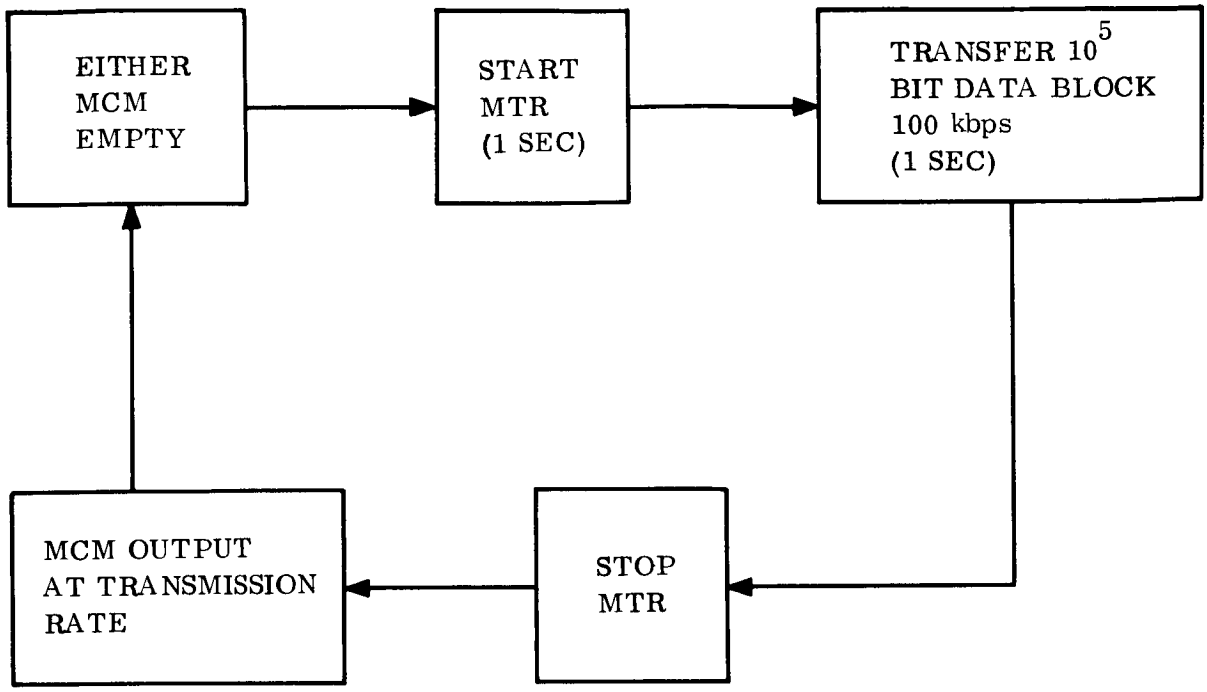

Figure 7-3. Playback Operation Sequence for Alternate D/S

8.0 SELECTION OF HIGH-CAPACITY STORAGE COMPONENTS

8.1 SCOPE

The following subsections detail the steps leading to the selection of magnetic tape recording as the high capacity data storage component for Voyager. This selection is justified from the results of literature and vendor surveys. Justification is also given, again on the basis of information obtained in vendor and user questionnaires and visitations, for the selection of the parallel track, peripheral drive recorder described in Volume VB-233-FD-107 (Data Storage). Competing alternatives to the preferred components and techniques are given, and the possible tradeoffs are discussed, as well as points requiring further investigation and evaluation. It should be noted that the conclusions of this section are based on the best information presently available. It is hoped that information gained in presently funded JPL studies of magnetic recording will be available before design finalization.

8.2 FUNCTIONAL OBJECTIVES AND CHARACTERISTICS

The primary function of the high-capacity section of the Voyager Data Storage Subsystem is the storage of orbital planet scan data generated by the DAE. Three principal characteristics of this data type are important in the choice of a storage technique. They are:

8.2.1 CAPACITY

Assuming that all the data is collected in a relatively short scan period and transmitted over the remainder of the orbit, the nominal storage capacity required is 6×10^8 binary bits (8.533 Kbps x 20 hour orbit period).

8.2.2 DATA CHARACTERISTICS

In the usual format, the planet scan data consists of "frames", which directly correspond to still video images or IR scanner outputs. Although the bit equivalent site of these frames may vary, a typical maximum value is 1×10^6 bits.

8.2.3 LIFETIME-TOTAL DATA THROUGHPUT

The Voyager mission characteristics and design goals indicate that the high capacity storage system should have a total lifetime of approximately 14 months, divided into an 8-month inoperative period during cruise and a 6 month operational orbital life. During the operational phase, the total data throughput will be nominal 7.2×10^{10} bits, or 7.2×10^4 images at 10^6 bits/image.

8.3 APPROACHES CONSIDERED

A number of basically different binary data storage methods with capacity capabilities in the 6×10^8-bit range are available, and of these, several are conceivably adaptable to spacecraft applications. The latter were considered for inclusion in the Voyager system. In addition to these, two techniques presently used for direct image storage were analyzed for applicability to the Voyager mission. The storage techniques considered were:

a. Magnetic Tape Recorders

b. Magnetic Discs and Drums

c. Thermoplastic Recorders

d. Cryogenic Storage Systems

e. Image Storage

1. Dielectric Film

2. Photographic

8.4 INITIAL EVALUATION

The majority of the various storage techniques listed above were eliminated from consideration on the basis of the simple initial criteria given below:

8.4.1 RELIABILITY - STATE OF DEVELOPMENT

The predominant consideration in the initial selection evaluation was the state-of-the-art and history of performance, if any, in spacecraft systems for each technique. Closely related to these considerations were the questions of the probable reliability characteristics of the system and how well this reliability figure could be backed by actual system test data.

The state-of-the-art was also an important consideration from the standpoint of cost and lead time for the initial procurement of the storage system. Due to the time schedule required by the '69 and '71 missions, extensive development programs were not feasible, particularly if any doubt existed about the ultimate feasibility of implementing the technique for spacecraft.

8.4.2 SPACECRAFT SYSTEM REQUIREMENT AND INTERACTIONS

The requirements made on the total spacecraft system by the memory store were a secondary initial selection criteria. These effects fell into two basic classes.

The size, weight, power, and thermal characteristics of the memory store must be compatible with the nominal Voyager spacecraft system, and the operation of the memory store must not interfere with the proper spacecraft system functions; e.g., high angular momenta or RFI noise levels would be prohibited.

8.5 APPROACHES ELIMINATED

8.5.1 MAGNETIC DISCS AND DRUMS

These systems were eliminated because of the high angular momenta and reliability liability inherent in the mechanical complexity of the systems.

8.5.2 THERMOPLASTIC RECORDERS

The TPR systems were eliminated because their state of development leaves serious doubt about the possibility of implementing a useable spacecraft system for the Voyager Schedule.

8.5.3 CRYOGENIC SYSTEMS

The special cryogenic cooling requirements of such systems make them impractical for spacecraft system. In addition, systems of this capacity range have not been presently implemented.

8.5.4 PLATED WIRES

At the present state of development, stores of the order of 10^8 bits have not been constructed, and would be physically too large for spacecraft systems if they were available.

8.6 FINAL SELECTION

The three approaches not initially eliminated were magnetic tape recorders, dielectric film storage, and photographic film storage. These were further evaluated on the basis of information obtained from vendors and users of these systems, as well as consideration of the more detailed requirement and design constraints of the Voyager system. The results of this evaluation are discussed below.

8.6.1 PHOTOGRAPHIC FILM STORAGE

The photographic film storage technique was eliminated for three reasons:

a. The photographic systems presently implemented for spacecraft applications are designed solely for image storage. Although programs of this type are in progress, storage of other than visual images would require an extensive development program.

b. The total storage requirement of 7.2×10^4 frames implies a film capacity much larger than any presently available. In addition, the one-shot nature of the film implies that the maximum useful life of the storage system would be set by the film pack size rather than being open-ended as in the case of a reuseable recording medium.

c. The resistance of photographic film to environmental effects is lower than the other methods considered, particularly the susceptibility to permanent radiation damage of the storage medium.

8.6.2 DIELECTRIC TAPE STORAGE

A dielectric tape storage system, such as that developed for Nimbus, has advantages over the photographic technique in that the medium is indefinitely reusable and is insensitive to radiation damage. It, however, has two basic disadvantages that disqualified it for Voyager application:

a. As in the case of photographic systems, dielectric tape storage has been implemented for image storage alone. The requirement for high-capacity storage of non-image scan data would necessitate a large development program to implement a digital storage system for this type.

b. Although a flight model of a dielectric image storage system has been developed for the Nimbus program and has been partially flight qualified, no firm date for system flight is available. It is therefore unlikely that any significant inflight reliability data could be obtained prior to the Voyager design freeze.

8.6.3 MAGNETIC TAPE RECORDERS

The remaining alternative, magnetic tape recording, has both the digital storage and space flight experience lacking in the other choices. Despite its mechanical nature, with the proper choice of configuration the recorder reliability can be made to approach that of other components of the spacecraft; while its size, weight, and power consumption are within the range allowable for spacecraft applications. Magnetic tape recording is therefore the selected high capacity storage component for the Voyager data storage subsystem.

9.0 SELECTION OF MAGNETIC TAPE RECORDER CONFIGURATION

9.1 CONFIGURATION SELECTION CRITERIA

The selection criteria for the Voyager Magnetic Tape Recorder (MTR) configuration originated from two sources. The first source was the functional requirements on the high capacity store generated by the overall Data Handling and Storage Subsystem design. Inputs from this source were in the nature of operational requirements such as record rates, playback rates, capacity, etc. The second source for the configuration selection parameters was an intensive survey of major MTR vendors and users that had as its aim the determination of the state-of-the-art in MTR technology. Both questionnaires and plant visits were employed to obtain the required information. A summary of the responses of the various vendors to basic questions is shown in Table 9-1. The combination of information from both sources was employed to establish the most reliable system embodying the minimum complexity necessary to meet the functional requirements.

Vendor	Size ($in.^3$)	Weight (lb)	Power (watt)	1 in. Tape (ft)	Tracks	Type	Tape Speed (ips)
Astro-Science		17	15			P	10
Borg-Warner	900 70	30 5	50 r 20 pb	600'	14	P	7
CEC	600	7-8	1.5r 1.5pb	500'	16	P	7
Cook							
Kinelogic	126 +30% for electronics	5.4	3.5r 1.5p +50% for electronics	200'	25	P	4
Leach	600	34	33	600'	16	P	7
Lockheed		5	2r 0.75pb	1/4" tape	8 on 1/4"	P	40
Parsons	215	7-1/2	10r 5pb	940'	5 / 16-20 max.	P	22
RCA	400	14.5	12r 8pb	1/2" tape 2400'	2 Serial	S	40
Raymond	500 -1000	18 -36	15r "much less p.b."		16	P	7
T.I.	Kinelogic Model E transport				25	S	4

Table 9-1. Responses of Recorder Vendors

Max. Safe Tape Speed	Use of Integ. Electronics	Drive Type	Oper. Temp. Range (°C)	Present Systems and Experience	Development		Comments
					Time (mo)	Cost (K$)	
	"some"	D.C. reel motors and capstan drive			9	NA	Primary experience in systems for operation in severe environments.
120	Playback and Logic now.	Diff. capstan and negator spring	-15° to + 50°	R150 recorder	9-12	250	
120	No-but would like to use	Mylar belt phase lock servo	0° - 65° 120° max non-oper.	Courier, Discoverer, Prototype Surv.	9	NA	
	No exp.	Doesn't like the idea of negator springs	Keep cool	NONE	9-12	NA	Little or no experience in space systems.
30	TI presently doing some for their transport	Isoelastic drive with open loop speed control	-20° to +65°	Mariner backup. Much NASA exp. Lunar Exp. record	9-12	100-200	
	Some exp. but not in tape recorders.	Straight capstan and coaxial negat. springs - Hyster. synch. motors	Have exp. with metal tapes.	150-200 spacecraft recorders - Presently on Apollo	12	300-600	Predict 90% confidence for 2 yrs. on basis of Minuteman studies.
	Using digital now-developing linear types.	Mylar belt with separate reel drive coplanar	75°c max. Working with Goddard on high temp. system.	Nimbus and other NASA programs	12	300	Experience in brushless d.c. motors. Modular design for reliability.
	Yes in digital circuits	Dual differential capstans coaxial negator springs	-20 to +60° max. 85° 125° with metal tape	Purpose "off the shelf" SIR900 Satellite recorder	5-6	125	
	No, but think its feasible	Capstan and negator spring coaxial	Max 120° non oper. Have H film experience	TIROS, Gemini Many others proposed	6-8	100 for dev. 35 ea. record	
50 20 for reliab.	No, but want to, if funded-estimate 60% reduction in size and weight	Peripheral mylar belt (isoelastic) Phase lock servo	Max 70% cap. 120° nonop. Have ster. H.film tape at 135°c	2-OSO, TIROS, Nimbus, UK1, S15. Mariner C.	6-10	100-200	Remarked that, "must carefully consider the test requirements-can double the size, weight, power, and cost." 50% confid. 2 yrs. 90% confid. 1 yr.
	Developing integ. and film circuits					est. 100 recorder 30 electronics	

2

9.2 FUNCTIONAL REQUIREMENTS

The following are the functions required of the MTR by the preferred configuration.

a. Record Rate: 50 kbps fixed.

b. Playback Rates: 8.533, 4.267, 2.133, 0.533 kbps.

c. Synchronous Playback: The playback output from the MTR section must be bit and word synchronous with the transmission rate.

d. Stop/Start: The start/stop tape length should nominally be equal to 50 k bits at the playback speed. The number of stop/start operations per MTR per day is approximately 200, with total accumulation of 3.6×10^4 operations in 6 months.

e. Data Validity Detection: The recorder must be able to detect the presence or absence of recorded scan data during playback to allow the Data Encoder to multiplex in buffered real time data in the gaps between scan frames.

9.3 MTR CHARACTERISTICS

The following are summaries of the opinions obtained during the vendor survey on a number of topics concerning the design and operation of magnetic tape recorders. The tradeoffs between configuration alternatives are also discussed.

a. Serial vs. Parallel Recording - The important points of difference between serial multitrack and parallel multitrack recording are the amounts of electronics required, the tape speeds required for given data rates, and the amounts of tape and number of tape passes required for a given storage capacity.

   This last point is related to the allowable bit packing densities for the two techniques which are discussed in the following section. In addition to these factors, other points of difference exist for the Voyager application. These are discussed in detail in Section 9.4.

b. Storage Packing Densities - Two factors determine the maximum bit packing densities obtainable on magnetic tape. The first of these in the linear packing density in (bits/track/in). In the case of serial recording, this density is limited essentially by the resolution characteristics of the heads and tape. Although densities of 4×10^3 bit/in have been achieved under laboratory conditions, the accepted maximum is 2500 bit/in for reliable operations under varying ambient conditions. Linear packing in parallel systems is limited by head-tape skew, which causes non-coincidence in the detection of all bits of a parallel word. The state-of-the-art reliable operating range is centered at 1000 (bits/in), although densities twice that high have been achieved.

The second factors determining the bit density of MTR storage is the track packing density in (tracks/in tape width). For a given tape speed, this is virtually independent of whether serial or parallel recording is used, and depends primarily on the head structure and the required magnitude of playback signal. If tracks become too narrow, it becomes impossible to put enough turns on the playback head for proper signal-to-noise performance. Since the signal amplitude also is a linear function of the track width, the signal decreases more than linearly as high track densitites are reached. A good state-of-the-art limit for track density was agreed to be 16 (tracks/in) for reliable operation, although as many as 40 (tracks/in) have been employed. The use of Hall effect heads would allow higher densities but their other characteristics are much less desirable than conventional heads. Combining the two factors discussed above, the maximum parallel packing density is 1.6×10^4 bits/in^2 while serial multitrack operation might employ 4×10^4 bit/in^2.

c. Transport Reel Configuration - Three transport reel configurations may be employed in an MTR:coaxial reel-to-reel, planar reel-to-reel, and endless loop. Endless loop techniques are presently limited to relatively short lengths of narrow tape, and in general, are the least mechanically reliable of the three configurations. The difference between types of reel-to-reel transports is less from a reliability standpoint, although the planar system places fewer stresses on the tape. Unless wearout is a problem however, packaging considerations might outweigh this minor factor. The choice of configuration may also depend on the choice of tape drive system.

d. Tape Drive - Although a number of tape drive systems are in use by various vendors, two principal types pre-dominate. The first of these is a differential capstan drive with negator spring tensioning such as was used in the Gemini and Tiros MTR systems, and the second is the dual-capstan peripheral mylar belt drive. Both systems have been employed in flight or prototype spacecraft MTR's. The peripheral drive has the advantages of fewer moving parts, smaller and lighter weight mechanism due to the use of flangeless reels, and uniform end-to-end tape tensioning. It does not, however, operate as well in severe mechanical environments as the negator-spring system. The peripheral drive is constrained to operate in a co-planar reel-to-reel configuration, while negator spring drive may be implemented as either coaxial or co-planar systems.

e. Motor Types - Two basic types of drive motors are presently employed in MTR systems - conventional dc motors with brushes and hysteresis synchronous ac motors. In addition, presently under development are "brushless" dc motors with semiconductor commutation. Brush type dc motors have limited life and reliability due to the presence of the brushes. They are, however, efficient and have the high blocked rotor torques necessary for fast starts. Synchronous motors are much more reliable and and have long lifetime compared to the brush type dc motors, but are less

efficient and have lower starting torques. Present laboratory models of brushless dc motors indicate that they combine the good features of both the other types. No MTR systems have, however, been implemented with this type motor, and actual long term performance data is lacking.

f. Speed Range Control - A requirement for speed range changes in an MTR may be met in several ways. Most simply and reliably, multiple winding may be employed in a synchronous motor; but this technique is usually limited to two speeds for one motor.

Alternately, the frequency and voltage input to a synchronous motor may be varied to vary motor speed. Changes by this method yield continuously variable speed control without serious variations in input power requirements, but the practical range is limited to about 8:1 variations by motor hunting or cogging effects. For larger speed changes, electromechanical clutches and alternate speed ratio drive trains must be employed. This is the least reliable of the methods from a mechanical standpoint and requires about 1 watt of power for continuous clutch activation. Saturable impulse switched hysteresis clutches are, however, presently under development.

g. Data Output Synchronization - The extent to which the data output stream from an MTR can be externally synchronized depends on two factors, tape speed control and output buffering. With an open-loop frequency-stabilized drive motor control, the end-to-end tape speed variations may be as high as 1%, the effect of which must be nullified by an external buffer store large enough to accommodate the integrated bit rate fluctuations due to tape speed, both long and short term.

As an alternative, a phase locked loop (PLL) servo may be employed to control the motor speed and hence the tape speed, to the extent that a short buffer is sufficient for absolute synchronization. The implementation cost of the PLL is usually small compared to that of the large buffer store.

h. Stop/Start Operations - The time and tape length utilized for an MTR stop/start operation is directly dependent on the tape speed and to a lesser extent on the size of the tape pack. With motor reversal or some other braking for stopping torque, stop/start operations can be made uniform ±10% over the tape pack length. The time required for a start or stop at tape speeds below about 7 ips is generally constrained to be above 0.5 sec for machines without spring-load idler loops or other special devices. At higher speed (above about 20 ips) the start/stop time and tape length requirements increase with the speed, and the maintenance of a 1 second start/stop time requires a clutched start with continuously running motor and solenoid-actuated brakes with attendant decrease in mechanical reliability. The effect of the frequency of stop/start operations on the reliability of a

MTR is not well understood. It is known, however that parts stresses are at least doubled during these periods, with consequent increases in failure probability. On the basis of engineering experience, most vendors expressed the opinion that up to about 400 stop/start operations a day for 6 months could be done, but that as the number approached 1000/day, they would expect a significant decrease in the MTBF of the recorder due to mechanical causes.

i. Tape Types - Three types of recording tapes are presently available for use in recorders of the Voyager type. They are the conventional oxide-Mylar type, the "H" film backed oxide type, and the NiCo plated metal foil type. Of these, only the Mylar tape has presently been used in any operational system, although the other types have been extensively tested by MTR vendors. Mylar is presently limited to operating temperature below 65-70 °C, while H film has been operated to 100 °C and metallic foils to 125 °C. The primary objection to the use of H film tapes is that the quality of the recording medium is presently well below that of Mylar, although this is probably due to the lack of incentive for improvement provided the H film tape manufacturers. The metallic foil appears to have excellent recording characteristics, but is relatively mass density, leading to a heavy tape pack with high inertia.

j. Tape Motion Sensors - In general, it is desirable to sense the motion of the tape for two reasons. Primarily, it may be employed to detect the attaining of record speed after a start operation in the record mode. This signal may also be employed as a valuable engineering data output to describe the MTR system condition. Used in this way, it allows discrimination between electronic and mechanical malfunctions in the MTR system.

The simplest and most reliable means of sensing tape motion is an optical system employing neon bulb sources and solid state detectors. Its primary advantages lie in its simplicity and reliability and in the fact that no mechanical connection to the MTR tape transport is required.

k. Data Validity Detection - Data free gaps in the playback bit stream may be detected in two basically different ways. The first of these is the method employed on Mariner C, the detection of clock output from the biphase modulated data stream. Alternatively, a parallel "data validity" track may be employed to indicate the presence or absence of data. The first method has the advantage, particularly for serial recording, of not requiring the parallel validity track. Its disadvantage lies in the time and bit loss inherent in the decision interval required to determine whether or not the bi-phase signal is present and to synchronize the playback stream. In parallel recording with separate clocking, this problem may be eliminated.

l. Launch and Cruise Exercise - Although quantitative data on the subject is lacking, most MTR vendors feel that the tape transport should be exercised during launch. This is said to prevent bearing damage and tape spillage.

There is some question, however, in the case of peripheral drive systems, since the edges of the tape pack might be damaged if launch operations were employed. A similar uniformity of vendor opinion exists in favor of periodic cruise exercise of MTR systems. This is said to prevent bearing and belt set, remove head oxidation, relieve pack stresses, etc., although, again, no data is available to support these opinions.

m. Capacity - The present state-of-the-art capacity limit in MTR systems for space applications is in the vicinity of 2×10^8 bits. This limit is determined by the tape packing densities and tape pack sizes that have been employed to date. It is the opinion of vendors that a 2×10^8 bit capacity can, however, be implemented with high reliability and without extensive development programs.

n. Vacuum Encapsulation - All the present spacecraft MTR systems require a pressurized container for operation, primarily due to the lubrication loss which would occur in vacuum. In the opinion of MTR vendors, however, the development of a vacuum operational MTE is not warranted since the encapsulation requires a relatively small increase in the normal structure required for the protection and rigidity of the MTR.

Various techniques are presently employed in obtaining seals for MTR's. Most used however, is an "O" ring seal; with the highest leak rates indicating seal lifetime of 5 years or more.

o. Reliability - Accurate reliability information on such complex and specialized systems as MTR's is difficult to obtain, particularly because too few units can be produced and tested to yield statistically valid results. Reliability calculations for a particular MTR therefore, must be made on the basis of component reliability information obtained from vendors or previous experience with similar MTR systems. Preceding on this basis, MTR vendors indicated that the present state-of-the-art could produce MTBF's of approximately 10^4 hours for an MTR systems capable of satisfying Voyager specifications.

Of this, approximate 60-70% of failure were attributed to electronic components and 30-40% to mechanical components. Since the electronic sections are the chief reliability factors, it is certain that the use of integrated circuits and high reliability conventional components could substantially increase the total MTBF.

9.4 SELECTION OF THE PREFERRED MTR CONFIGURATION

The selected Voyager MTR is a 16 track parallel type with peripherial drive. Functional block diagrams of the MTR and the MTR control are shown in Figures 9-1 and 9-2. A summary of the Voyager MTR characteristics and specifications are given in Table 9-2. A detailed discussion of its major physical elements and their functions may be found in Volume VB233FD107, Section 3.4.

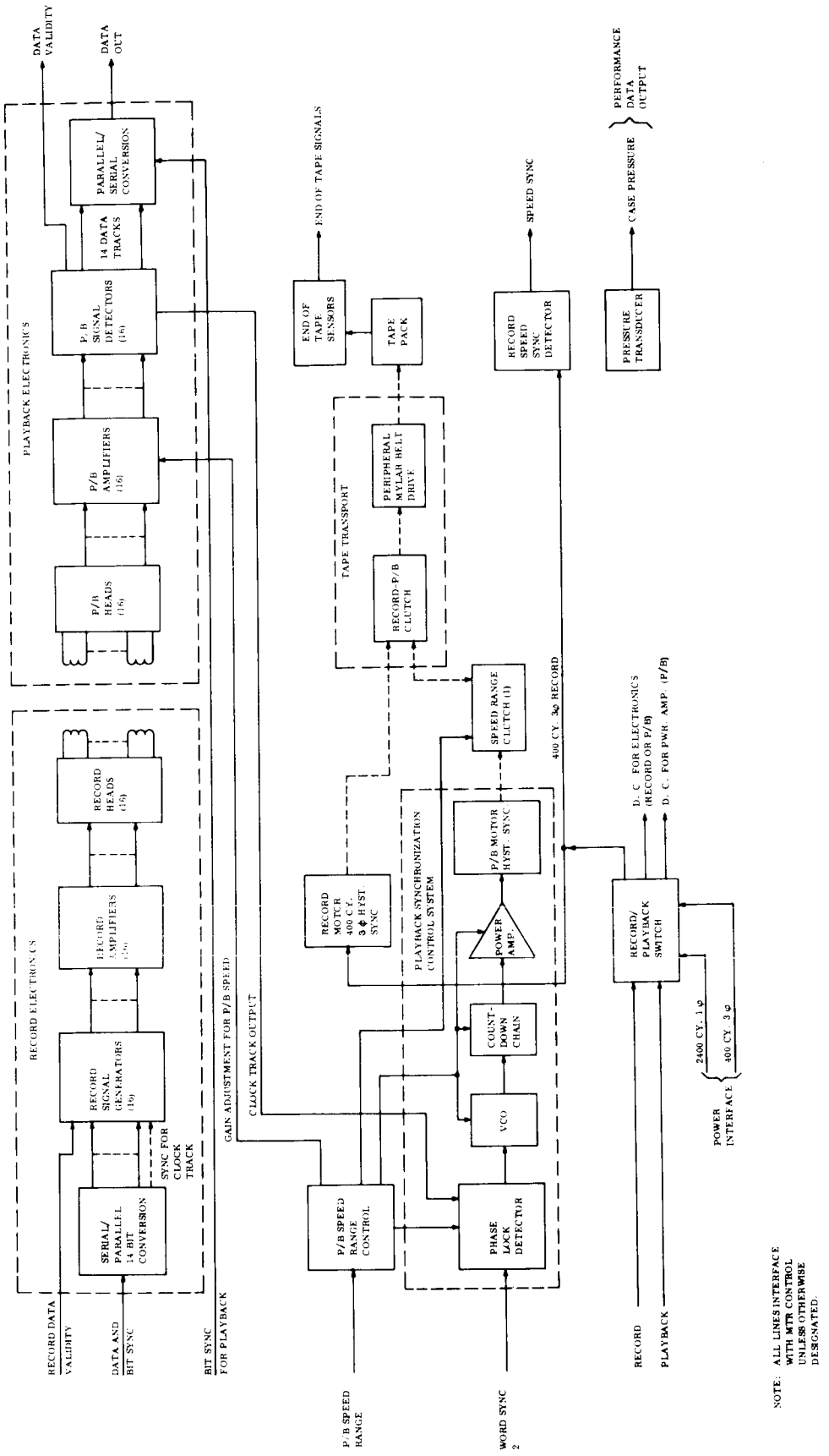

Figure 9-1. Voyager Magnetic Tape Recorder Function Blocks

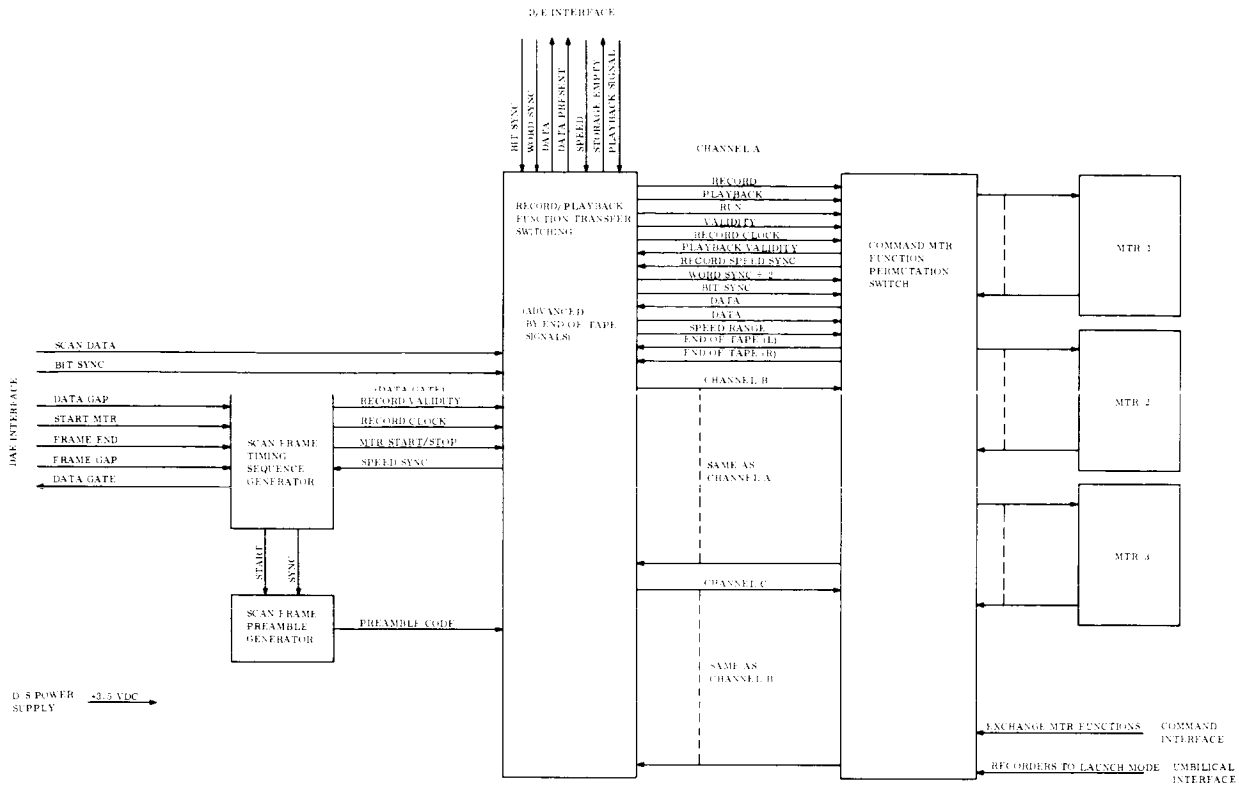

Figure 9-2. Voyager Magnetic Tape Control Functional Blocks

The following paragraphs justify the selection of the major elements of the preferred configuration on the basis of the functional requirement stated in Sections 9.1 and 9.2. Again, it should be emphasized that this selection is based on the best present information and is subject to modification on the basis of new developments or information.

Table 9-3 summarizes the characteristics of a serial and a parallel 2×10^8 bit recorder with capacities and speeds calculated for the Voyager requirements. Figures for the serial type are based on the RCA Gemini MTR, while those for the parallel type are based on information from Raymond and Kinelogic Corporations. Size, weight, and power are not shown because both types have approximately the same characteristics, as shown in Table 9-1. The parallel recorder was selected primarily because of its history of performance in long life space systems and because of lower tape speeds and correspondingly lower mechanical stresses inherent in its operation. It also has the advantage that the stored data can easily be word organized to enable the maintenance of word sync for frame identification patterns. Finally, it was selected on the basis of requiring fewer total head passes and one-way record/reversed playback which allows simplification of the drive system.

Table 9-2. Summary of Characteristics of Voyager MTR

Type:	Parallel - 14 data tracks + clock track + data validity track.
Transport:	Reel-to-reel, co-planar, peripheral drive.
Bit Packing:	1000 bits/in/track
Drive type:	Mylar belt.
Motors:	2 Hysteresis Synchronous
Record Rate:	50 kbps (3.57 ips)
Playback rate:	8.533 kbps (0.610 ips)
	4.267 kbps (0.305 ips)
	2.133 kbps (0.152 ips)
	0.533 kbps (0.038 ips)
Speed Range Control:	Motor drive voltage and frequency changes for 8, 4, 2 kbps + clutch for 0.5 kbps.
Speed Sync Control:	Phase locked loop.
Size: 500 in^3	
Weight: 15 lbs.	
Power Consumption:	7 w record 3 w playback
Capacity: 2×10^8 bits - 1325 of 1" tape	

9.4.1 PERIPHERAL DRIVE

Because operation is required only in periods of negligible mechanical stress, and because of its lower weight and complexity, the peripheral drive was selected over the negator spring type. Vendor response also indicated that a more reliable system could be constructed with this drive type.

9.4.2 PACKING DENSITY

The packing densities of 1000 bit/in/track and 16 track/in were selected as representing the present maximum limits for reliable parallel track MTR.

Table 9-3. Comparison of Serial and Parallel MTR Configurations

Topic			
50 Kbps Record speed	3.57 ips	20 ips	The higher serial speed makes rapid start/stop more difficult. Record motor would run continuously with clutched start.
Minimum Playback Speed	0.38 ips	0.2 ips	The low parallel speed requires sensitive amplifiers and short low level paths.
Packing Density Bits/track/in	1000	2500	
Track Density (tracks/in tape)	16	16	1 inch tape width
Total density (bits/in^2)	16,000	40,000	Density = (no. of tracks) (bit/in/track)
Data tracks	14	16	Serial requires no validity tracks. Parallel 1 validity track and 1 clock track.
Total Data Density (bit/in^2)	14,000	40,000	
Minimum Tape Pack required (1" tape)	1250 ft / 1.5 lb	440 / 0.5 lb	Serial has approximately 1/3 the tape required by the parallel machine.
Electronics	16 channels	1 channel w/ switching or 16 channels	
Tape Passes	2	16	Parallel records one-way. Plays back in reverse.
Data Gap detection	Separate validity track	Biphase signal detector	Some serial data loss due to detection lag.

9.4.3 REEL-TO_REEL CONFIGURATION

This type of configuration is the only one presently available in peripheral drive systems.

9.4.4 SYNCHRONOUS MOTORS

Hysteresis synchronous motors were selected as being the most reliable type available, and because they allow open loop record speed control without the necessity for an inverter power supply.

9.4.5 SPEED RANGE CONTROL

The voltage-frequency control for playback speeds was chosen because of its reliability, and because the top three playback rates are within its 8:1 speed range capability. The technique is also compatible with the PLL speed control.

9.4.6 PHASE-LOCKED SPEED CONTROL

Phase locked control was chosen because of the stringent requirement for synchronous playback, and because it requires much less implementation than output buffering.

9.4.7 STOP/START DURATION

The stop/start duration was established at 1 second because this was indicated to be a conservative figure for reliable implementation.

10.0 SELECTION OF NON-BULK STORAGE COMPONENTS

10.1 SCOPE

The following section justifies the selection of the preferred non-bulk storage components for the Voyager system. Competing alternatives are described and comparison made on the basis of size, weight, power, and reliability estimates. As in the case of the high capacity storage; both quantitative and qualitative information is in part based on the results of an extensive survey of the vendors and users of spacecraft memory systems.

10.2 FUNCTIONAL OBJECTIVES

As discussed below, the non-bulk storage components of the Voyager Data Storage Subsystem are required to perform two basically different classes of operations, each with its associated capacity requirement.

a. Capsule Relay Buffering - Throughout the mission until capsule impact, the data stream received from the capsule is inserted into the bus transmission format in real time. Since the capsule clock is not synchronized with the bus system, phase and rate buffering is required to synchronize the relay data to the bus system. In addition, 70 or 98 bit capsule data groups depending on the format, must be accumulated at the 10.16 bps rate for burst insertion into the transmission format at 106.67 bps.

b. Medium Capacity Storage - The Data Storage Subsystem is also required to buffer the non-scan science and engineering data stream for burst insertion into the orbital transmission format. In addition, it should provide storage for science flare, maneuver engineering and capsule data during pre-orbital operations. The storage operates in periods when the data generation rate exceeds the transmission rate, to low rate transmissions during maneuvers.

The capacities and data rates nominally required for these operations are shown in Table 4-1 columns V and VI respectively.

10.3 APPROACHES CONSIDERED

A large number of basically different storage techniques are available for use in the capacity ranges required. Those that could conceivably be adapted to spacecraft applications were considered for inclusion in the Voyager system. The elements considered for the capsule relay buffers (CRB) and the medium capacity storage (MCS) are listed below.

a. CRB Alternatives - The low capacity buffering functions required by the CRB may be implemented by the following elements:

1. Integrated Circuit Shift Register (SIC)
2. Conventional Component Shift Register
3. Hybrid Magnetic/Semiconductor Shift Register
4. Memory-Organized Ferrite Core Register
5. Monolithic Semiconductor Shift Register
6. Thin Film or Plated Wire Shift Register

b. MCM Alternatives - Memory systems employing the following memory storage elements have been developed and were considered for the Voyager MCM application.

1. Ferrite Cores
2. Ferrite Multiaperature Devices

3. Ferrite Continuous Structures

4. Plated Wires

5. Thin Films

6. Cryogenic Elements

7. Ferroelectric Elements

8. Monolithic Semiconductor Memory Blocks

10.4 INITIAL EVALUATION

The majority of the various storage techniques listed above were eliminated from consideration on the basis of the simple initial criteria given below:

a. Reliability - State of Development - The predominant consideration in the initial selection evaluation was the state-of-the-art and history of performance, if any, in spacecraft systems for each technique. Closely related to these considerations were the questions of the probable reliability characteristics of the system and how well this reliability figure could be backed by actual system test data.

   The state-of-the-art was also an important consideration from the standpoint of cost and lead time for the initial procurement of the storage system. Due to the time schedule required by '69 and '71 missions, extensive development programs were not feasible, particularly if any doubt existed about the ultimate feasibility of implementing the technique.

b. Spacecraft System Requirement and Interactions - The requirements made on the total spacecraft system by the memory store were a second initial selection criteria. The effects fall into two basic classes. The sizes, weight, power and thermal characteristics of the memory store must be compatible with the nominal Voyager spacecraft system, and the operation of the memory store must not interfere with the proper spacecraft system functions, e.g. the generation of high RFI noise levels would be prohibited.

10.5 APPROACHES ELIMINATED

10.5.1 CRB COMPONENTS

Thin film, plated wire, and monolithic semiconductor registers were eliminated on the basis of their stage of development. None of them have been implemented for spacecraft systems and none has sufficient inherent advantages over other alternatives to justify a development program.

Since the Voyager requirement was for only 98 bits of buffering, the use of memory organized ferrite cores was eliminated on the basis of information from memory vendors indicating that the reliability break point for transition from hybrid magnetic register to memory organized stores was above 150 bits.

10.5.2 MCM COMPONENTS

The use of cryogenic elements was eliminated because these elements have not been developed for any application and; in fact, the development of such a system for spacecraft may be impossible because of the requirement for cryogenic cooling.

Similarly, ferroelectric and monolithic semiconductor stores were eliminated because neither of the systems is presently in a state of development to warrant consideration for inclusion in the Voyager. Continuous ferrite structures such as the "apertured plate" or "flute" do not have a background of experience necessary to qualify them for Voyager systems. In addition, their primary advantage over other ferrite structures is their mass production capability, which is not required in this application.

10.6 FINAL SELECTION OF CRB COMPONENTS

The following are the analysis parameters considered in the selection of the preferred CRB components.

a. The size and weight of the CRB components were weighted least in the tradeoff analysis, since the CRB is such a small element that variations in its size and weight effect the Data Storage Subsystem totals very little.

b. The power consumption of the CRB was weighted more heavily than the size and weight, since in some cases it exceeds that required by the MCM system.

c. In keeping with the Voyager design philosphy, the component reliability was by far the most heavily weighted analysis parameter.

Table 10-1 lists the volume, weight, power, and reliability values calculated for the three competing CRB alternatives. These figures are based on values established by vendors and users of such equipment, and are calculated for a 98 bit register without enclosure, connections, etc. The volume and weight are estimated relative values with the SIC register arbitrarily = 1. The power calculation is based on a 10 bps rate and does not include any power supply efficiency. The power consumption of the conventional component register was established as 1 mw/stage on the basis of prior experience in the design of such circuits.

The integrated circuit register was selected for use in the Voyager system primarily because of its low failure rate. In addition, it has the advantage of direct compatibility and standardization with the integrated logic utilized by all the spacecraft systems with which it interfaces.

Table 10-1. CRB Alternatives

	Volume	Weight	Power (MW)	Failure Rate (%/10^3 hr)
Magnetic Shift Register	30	30	15	0.882
Integrated Circuit (SIC) Shift Register	1	1	294	0.490
Conventional Component Shift Register	10	15	98	1.64

A functional block diagram of the preferred CRB system and its control is shown in Figure 10-1. Total size, weight, power and reliability for the system are given in Table 10-2.

The operating system total include the redundancy effect of the third (standby) register, the size and weight of packaging and the power supply efficiency.

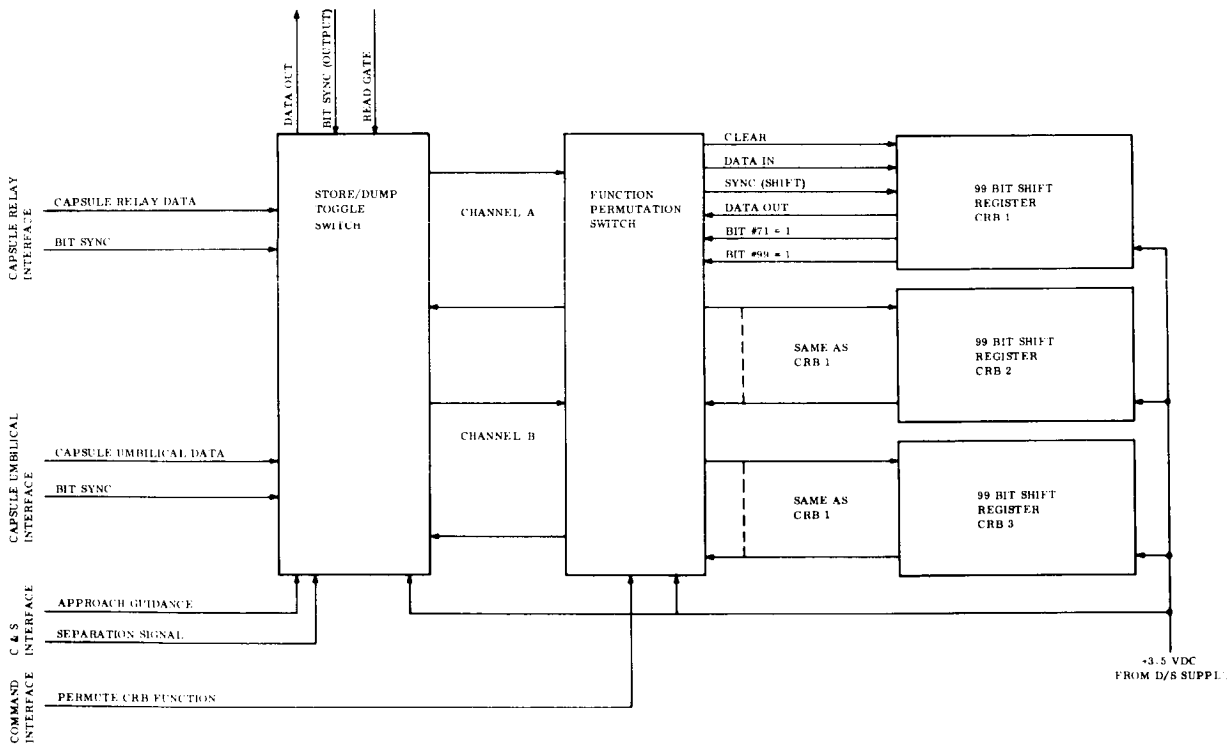

Figure 10-1. Capsule Relay Buffers and Control Functional Blocks

Table 10-2. Preferred CRB Design

	Size (in^3)	Weight (lb)	Power (mw)	Failure Rate (%/103 hrs.)
CRB Control			75	.125
Each Register (99 stages + 5 shift drivers)			297	.520
Operating System totals (3 registers and control)	80	1.5	1450	.150

10.7 FINAL SELECTION OF MCM COMPONENTS

The quantitative analysis parameters for the MCM store were again size, weight, power and reliability; however, the final selection was made on the basis of proven capability in spacecraft systems, and the amount of development that would be required to implement such a system.

Table 10-3 lists the average size, weight, power and reliability estimates for 10^5 bit memories employing ferrite core, thin film, and plated wire storage elements. Also included is a summary of the experience background of the three types of memories, and statements of the relative time and dollar cost of developing a spacecraft system. All of this information represents a summary of responses from vendors of the particular vendors of the particular system types. A list of the vendors and their responses to survey questions is given in Table 10-4.

Since neither of the two competing systems offer any substantial advantages for the capacity and operating speed ranges required, the ferrite core memory was selected for use in the Voyager system primarily on the basis of its background of experience in spacecraft systems. The plated wire system would be the first alternative selection, and its appeal would increase rapidly if the capacity and rate requirements were increased, since it appears more suited to capacities above 10^5 bits. In particular, as the capacity approached 10^6 bits, plated wire systems would become much more attractive than core systems.

10.8 PREFERRED MAGNETIC CORE MEMORY DESIGN

Functional block diagrams of the preferred magnetic core memory (MCM) configuration and control system are shown in Figures 10-2 and 10-3 respectively. The size, weight, power and reliability for the individual MCM's and the MCM system are shown in Table 10-5.

Table 10-3. Characteristics of MCM Competing Alternatives - 10^5 Bit Memory

	Size (in^3)	Weight (lb)	Power (w) at 8 kbps	Probability of Success for 1 year	Spacecraft Experience and Development Costs
Ferrite Cores	125	6	0.6-0.8	0.93	The only type of memory flown in the spacecraft to date. Reliability confidence level high because of base of experience in testing of such system. Development relatively inexpensive -- based on present models. Short lead time.
Plated Wire	130	6	1.0w	"greater than 0.9"	No spacecraft system flown. First flight in 1966 (scheduled). One model has passed flight tests. Reliability figures based primarily on component testing. Development cost higher and lead time 50% more than ferrite system.
Thin Film	125	8	1.0w	0.83 Simplex System	No spacecraft systems flown. Development would require a program costing twice the time and money of ferrite core system.

Detailed discussions of the characteristics and operations of this MCM system may be found in Volume VB233FD107 (Data Storage).

The following sections discuss several design features that were indicated as being critical factors by MCM vendors, and that were considered in the selection of the preferred MCM configuration.

The maximum bit plane capacity served by one sense line in a coincident current system is 4,000 to 4,500 bits. This limitation exists because of delta noise generated in non-selected cores by the half-select currents.

Table 10-4. Buffer and Program Storage System Vendors' Responses - $10.^5$ Bit Capacity

Vendor	Memory Element	Size (in^3)	Weight (lb)	Power Watt	Logic Type	NDRO	Operating Temperature (°C)	Present Systems and Experience	Development Cost ($\$x10^3$)	Development Time (MO)	Comments
DI/AN	30 mil ferrite cores	150	6 - 7	8-10 Prop. to speed	Mag.	Full cy. read/re-write	50° to + 75° maybe less at 100 KC	Pegasus, AOSO, Other NASA	100 for first 25 each after	4.5	They are working on plated wire. (Confidence 0.93 for 1 year.) Priced for Minuteman parts.
EMI	"Isodrive" cores	100	5	6-prop to spd.	Mag.	Full cy. read/re-write	Have done 150° steril	Pioneer, IRLS, LOM, Surveyor	150-1st prototype 10^3 bits 65 K $	7 max. 4-5	Have advanced packaging, connection, and encapsulation techniques.
FABRITEK											Do not presently make space systems.
IBM	Coupled Thin films Also do cores	125	8	2-little speed depend	Inte.	Inherent NDRO	0° -65°	OAO processor, Gemini, Saturn V (Mars NDRO) (core)		18	Price probably high because they are system rather than memory subsystem oriented. Confidence limit 0.7 for 24 months.
LIBRAS-COPE	Woven Plated Wire	200	5		Inte.	Inher. NDRD	60° to +150° for memory planes	Presently develop-ing first prototype models-due this summer	22		Cost estimate very low, particularly in light of extent of development required.
LOCKHEED	MAD	100 to 200			Semi Cond.	Read/ Restore	0° to 95° c		100	7-9	
RAYTHEON	Biax				Semi Cond.	Inherent NDRO	-60° to +125	No space systems. Beginning air-borne program	350	18-24	
T.I.	Films										Presently doing only large, fast ground-based computer memories. Extensive de-velopment would be required for any spacecraft systems.
UNIVAC (Bluebell)	Plated Wire	180 130	6 5	0.54 2.2	Disc. comp. Integ.	Inherent NDRO	-20° to 100° 0° to 65° "easy"	3×10^6 bit memory to NASA Goddard for flight testing.	100 +25 ea. after 1st	6-8	Reliability: .9 with minuteman parts for 12 mo. Majority of failures in connections.
UNIVAC (St. Paul)	Thin films and cores										No response to survey

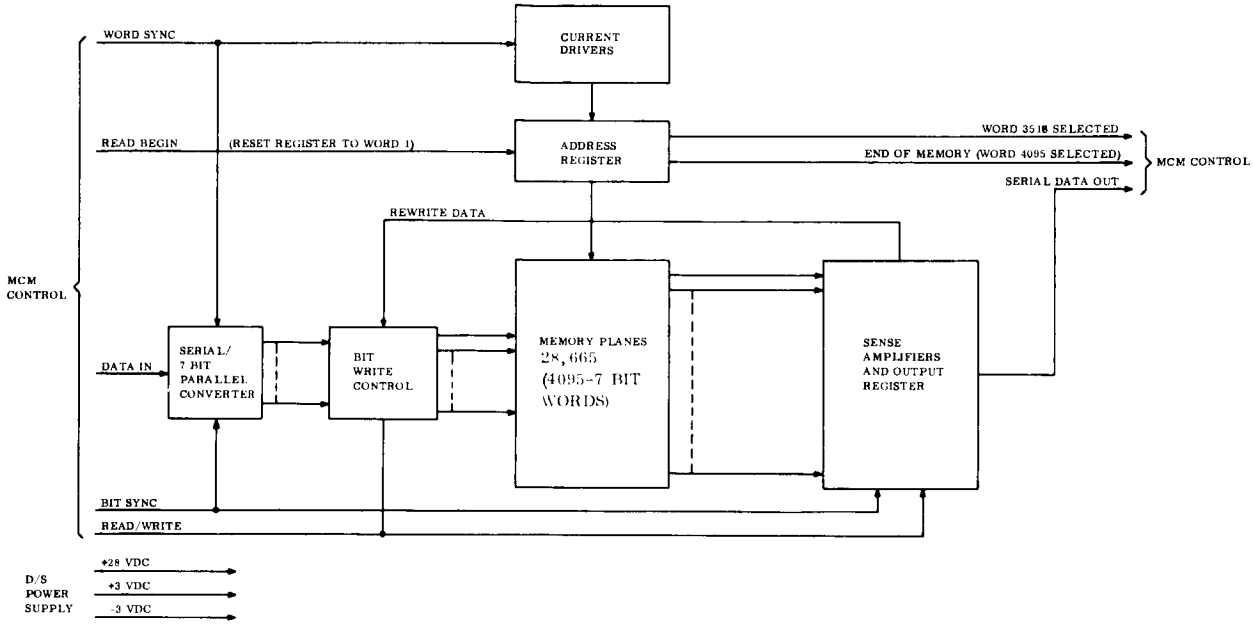

Figure 10-2. Magnetic Core Memory - Functional Blocks

Table 10-5. Characteristics of MCM System

	Size in^3	Weight (lb)	Power (w)			Effective Failure Rate ($\%/10^3$ hrs)
			100 cps	8kc	100kc	
MCM Control			0.6	0.6	0.6	0.805
Each MCM			0.05	0.65	8w	1.47
Operating System Total	240	13	0.65	1.25	10.6	Probability of Survival .956 for 1 mo. orbit .924 for 6 mo. orbit
System Total						

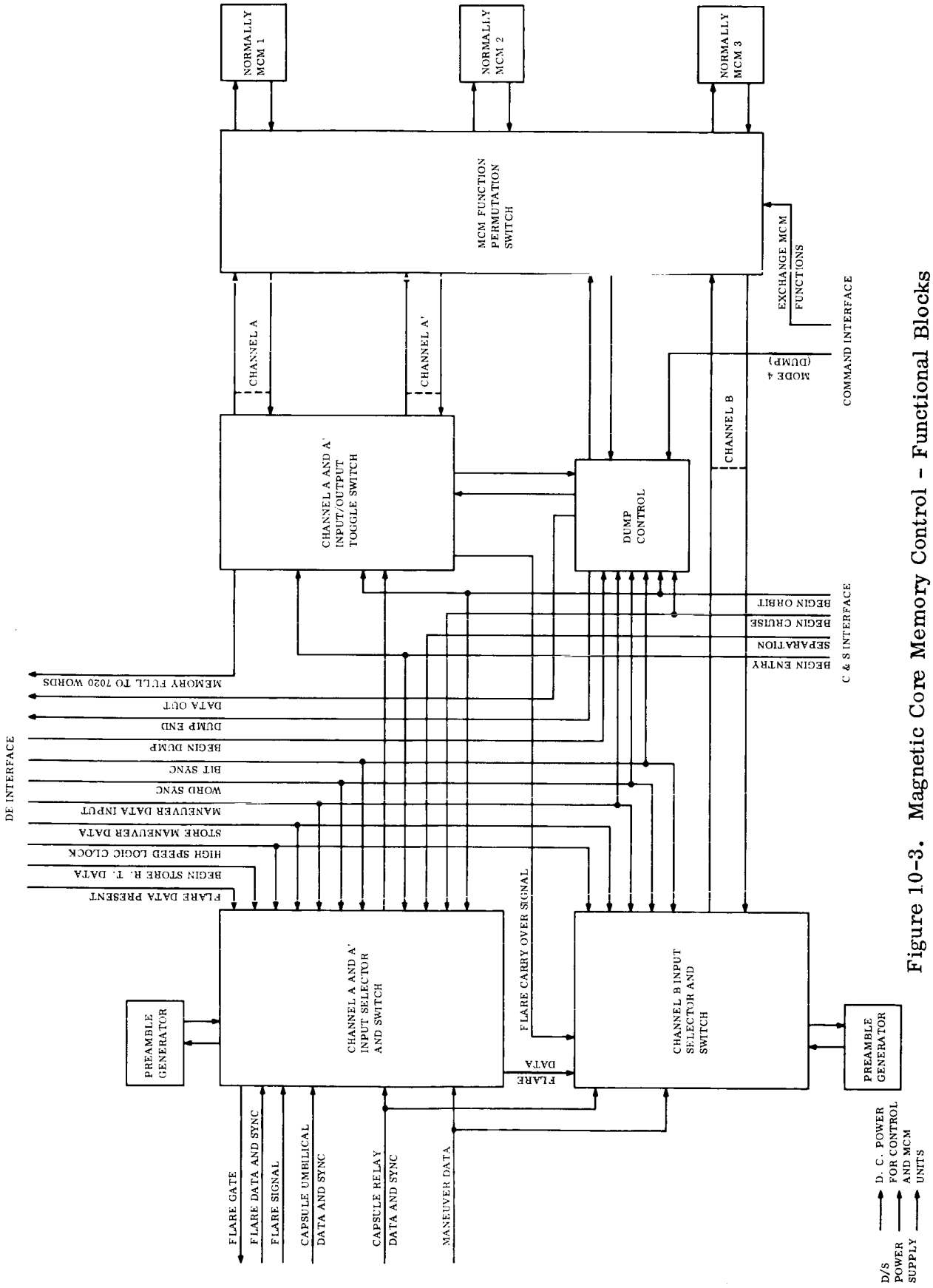

Figure 10-3. Magnetic Core Memory Control - Functional Blocks

Sequential addressing of memory locations may best be done by self-commutating magnetic switches, particularly at speeds below 25 x 10^3 word cycles per second. This is particularly true because the standby power requirements of the switch is negligible. The switches may be of either the current sterring or the two-core-per-stage magnetic shift register type. In either case, a four coordinate switch coincident current system is employed for minimum part requirement.

True non-destructive readout operations in ferrite core systems have not yet been developed to the point of reliable implementation. The accepted and time-tested technique of two phase (full cycle) read/write operation is suited to the characteristics of the magnetic accessing switches and is the one recommended for the Voyager system.

The power requirements of the MCM may be minimized by the use of power strobing to the sense amplifier. This technique has been used long enough to have a background of experience to qualify it for the Voyager system. The use of discrete component sense amplifiers is also presently desirable from a power consumption standpoint, since integrated types have not yet been able to function at low power levels as have discrete types. In addition, discrete component types can be more easily changed to adapt to any requirements peculiar to the spacecraft system.

The primary problem area in magnetic core memory failure is the number of internal connections required in their fabrication. The appropriate choice of welding or soldering, depending on the connection characteristics can, however, minimize this problem. Encapsulation of the memory planes must also be done properly to avoid thermal and magneto-strictive forces detrimental to reliability. Calculations based on component and system values obtained for the AOSO program indicate a minimum MTBF of 68,000 hours could be obtained for the 28,665 bit system chosen for Voyager. Vendor responses indicate that this figure is conservative.

The responses of MCM vendor indicate that it is possible to build units that conform to the Voyager magnetic specification. In general, the closed toroidal flux structures contained in the memory and logic do not materially affect the external field, and the primary difficulty arises from d.c. currents and structural members. Both these latter problems may be overcome by power gating techniques and the appropriate choice of construction materials.

VOLUME B

BOOK 2

VB233AA105

1. Page 11 of 35, Table 3-2, Column 3, Line 3. Change 77.4 to 78.4.

2. Page 13 of 35, Paragraph 3.2, Line 12. Change 20.6 bps to 426.6 bps.

3. Page 16 of 35, Table 3-3. Approach Guidance Engineering Data Handling change 16.7 bps to 27.6 bps.

CII-VB233AA106

1. Page 78 of 89, Equation (6). Change F (j/u) = to F (j|u) =

2. Page 78 of 89, Line 9. Change N (j/u) = to N (j|u) =

3. Appendix IX, Page IX-9 of 11, Table IX-2. Number of Correctable Error Patterns, change e #7 to e ≥ 7.

4. Appendix IX, Page IX-11 of 11, Reference 5. Add M.E. Mitchell before "Performance"

CII-VB233AA107

1. Page 26 of 42, Section 1, Last two lines. Should read but has relatively high mass density instead of but is relatively mass density.

2. Page 31 of 42, Table 9-3. Column should be headed Parallel and Serial. Row heading Min. playback speed should be followed by (533 bps). The parallel entry in that row should be 0.038 bps rather than 0.38.

BOOK 2 OF 3

CII-VB233AA106

1. Page 71 of 89, First equation. The symbols under the radical should be $\frac{KL}{2}$ instead of $\frac{K_L}{2}$

2. Page 71 of 89, third equation. The radical sign should not extend over the Greek letter σ_o . This is also true in the nex expression.

3. Page III-3 of 8, Last equation. Remove the line above the equation.

4. Page III-4 of 8, Second equation from top of page. Change $(SIN)_{IN}$ to $(S/N)_{IN}$.

5. Page III-6 of 8, last equation, bottom of page. The first term $P_{So}(f)$ should be added to the next term, not multiplied as shown.

6. Page IV-1 of 10, last equation, bottom of page. Should read

$$\beta = \int_{\infty}^{Z_T} P_I(Z)\, dZ$$

7. Page IV-2 of 10, under method c . Should read: "of the game by differentiation".

8. Page IV-3 of 10, next to last paragraph, last word. Should read $\frac{\alpha}{10}$ and not α_Z as shown.

9. Page IV-5 of 10, Figure IV-3. Brackets are left off in the equations:

   Eq. 1 - brackets [ ] should enclose all terms following the first $(1 - \alpha)Z$

   Eq. 3 - brackets should enclose all terms following $(1-P_1)$

   Eq. 4 - brackets should enclose all terms following $(1-P_1)$

10. Page IV-6 of 10, Equation for T(Z) in middle of the page. The L-1 term in the denominator of the equation is supposed to be the exponent for the [H(Z)] term.

11. Page V-1 of 2, Center of page. "For S/N ≥ decibels" should read For S/N ≥ 10 decibels

12. Page V-1 of 2, Lower portion of the page. The sentence that starts with "For an arbitrary. . ." the Greek letter δ should be replaced with a θ^1 .

VOLUME B (Continued)

BOOK 2 of 3

13. Page VI-3 of 13, Second equation from top of the page. The radical sign does not include the Greek letter σ_N .

14. Page VI-13 of 13, References, Reference #2. The last word of the title should be "Codes".

15. Page VII-2 of 4, Fourth equation from top. Should read α_F = instead of F= .

16. Page VIII-3 of 3, Under VIII-2 High Data Rates.

$$\beta = 5 \times 10^{-4}$$